PROTEOGLYCANS AS MEDIATORS OF CELL BEHAVIOR

EDITED BY: Larisa M. Haupt, Rachel K. Okolicsanyi and Jeremy Turnbull
PUBLISHED IN: Frontiers in Cell and Developmental Biology

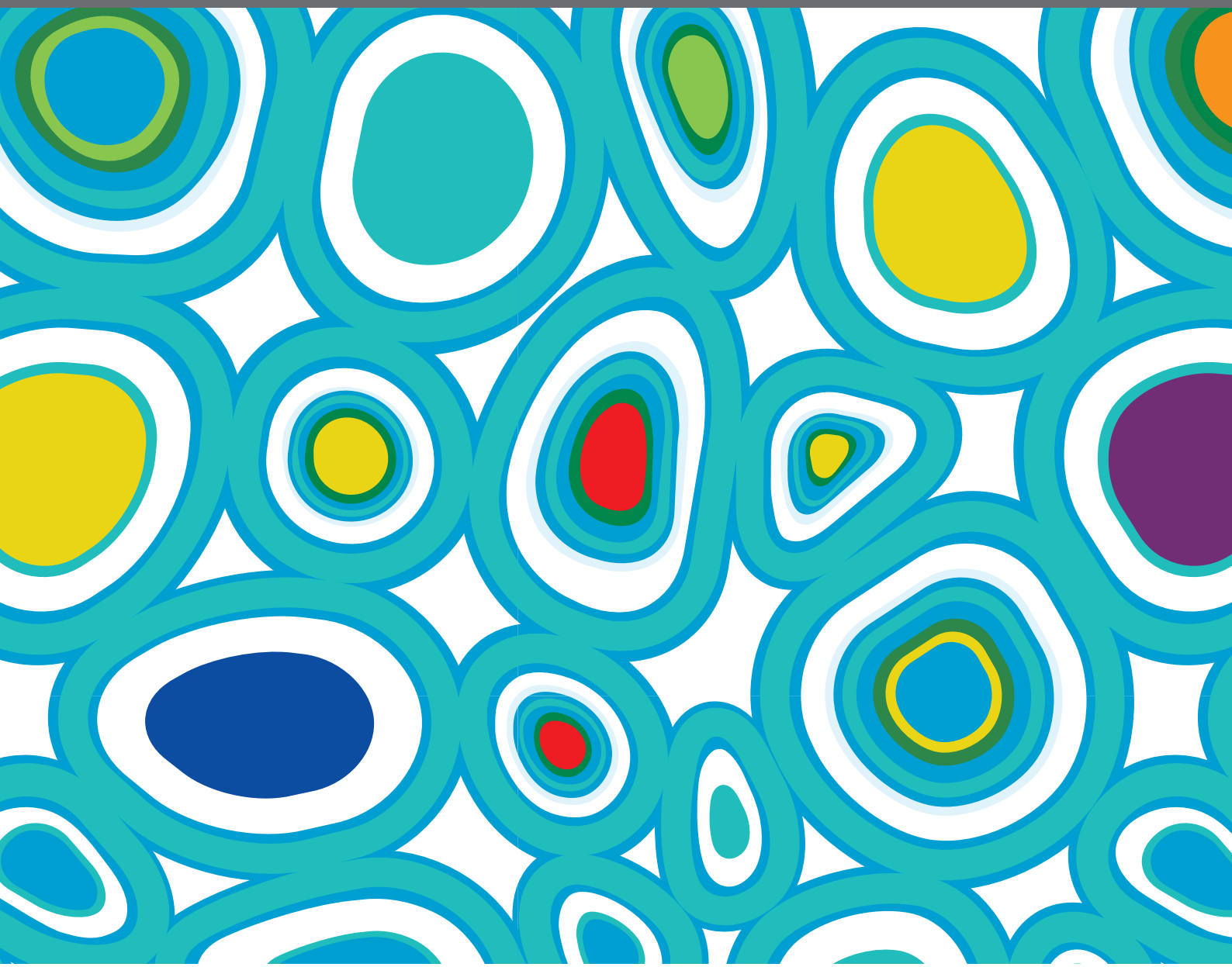

frontiers Research Topics

frontiers

ISSN 1664-8714
ISBN 978-2-88971-644-9
DOI 10.3389/978-2-88971-644-9

About Frontiers

Frontiers is more than just an open-access publisher of scholarly articles: it is a pioneering approach to the world of academia, radically improving the way scholarly research is managed. The grand vision of Frontiers is a world where all people have an equal opportunity to seek, share and generate knowledge. Frontiers provides immediate and permanent online open access to all its publications, but this alone is not enough to realize our grand goals.

Frontiers Journal Series

The Frontiers Journal Series is a multi-tier and interdisciplinary set of open-access, online journals, promising a paradigm shift from the current review, selection and dissemination processes in academic publishing. All Frontiers journals are driven by researchers for researchers; therefore, they constitute a service to the scholarly community. At the same time, the Frontiers Journal Series operates on a revolutionary invention, the tiered publishing system, initially addressing specific communities of scholars, and gradually climbing up to broader public understanding, thus serving the interests of the lay society, too.

Dedication to Quality

Each Frontiers article is a landmark of the highest quality, thanks to genuinely collaborative interactions between authors and review editors, who include some of the world's best academicians. Research must be certified by peers before entering a stream of knowledge that may eventually reach the public - and shape society; therefore, Frontiers only applies the most rigorous and unbiased reviews.
Frontiers revolutionizes research publishing by freely delivering the most outstanding research, evaluated with no bias from both the academic and social point of view. By applying the most advanced information technologies, Frontiers is catapulting scholarly publishing into a new generation.

What are Frontiers Research Topics?

Frontiers Research Topics are very popular trademarks of the Frontiers Journals Series: they are collections of at least ten articles, all centered on a particular subject. With their unique mix of varied contributions from Original Research to Review Articles, Frontiers Research Topics unify the most influential researchers, the latest key findings and historical advances in a hot research area! Find out more on how to host your own Frontiers Research Topic or contribute to one as an author by contacting the Frontiers Editorial Office: frontiersin.org/about/contact

PROTEOGLYCANS AS MEDIATORS OF CELL BEHAVIOR

Topic Editors:
Larisa M. Haupt, Queensland University of Technology, Australia
Rachel K. Okolicsanyi, Queensland University of Technology, Australia
Jeremy Turnbull, University of Liverpool, United Kingdom

Citation: Haupt, L. M., Okolicsanyi, R. K., Turnbull, J., eds. (2021). Proteoglycans as Mediators of Cell Behavior. Lausanne: Frontiers Media SA.
doi: 10.3389/978-2-88971-644-9

Table of Contents

frontiers in Cell and Developmental Biology

MINI REVIEW
published: 14 July 2020
doi: 10.3389/fcell.2020.00631

Heparan Sulfate Proteoglycan Clustering in Wnt Signaling and Dispersal

Yusuke Mii[1,2,3,4]* *and Shinji Takada*[1,2,3]*

[1] National Institute for Basic Biology, National Institutes of Natural Sciences, Okazaki, Japan, [2] Exploratory Research Center on Life and Living Systems, National Institutes of Natural Sciences, Okazaki, Japan, [3] Department of Basic Biology, Graduate University for Advanced Studies (SOKENDAI), Okazaki, Japan, [4] Japan Science and Technology Agency, PRESTO, Saitama, Japan

Wnt, a family of secreted signal proteins, serves diverse functions in animal development, stem cell systems, and carcinogenesis. Although Wnt is generally considered a morphogen, the mechanism by which Wnt ligands disperse is still debated. Heparan sulfate proteoglycans (HSPGs) are extracellular regulators involved in Wnt ligand dispersal. *Drosophila* genetics have revealed that HSPGs participate in accumulation and transport of Wnt ligands. Based on these findings, a "restricted diffusion" model, in which Wnt ligands are gradually transferred by repetitive binding and dissociation to HSPGs, has been proposed. Nonetheless, we recently found that HSPGs are not uniformly distributed, but are locally clustered on cell surfaces in *Xenopus* embryos. HSPGs with *N*-sulfo-rich HS chains and those with *N*-acetyl-rich unmodified HS chains form different clusters. Furthermore, endogenous Wnt8 ligands are discretely accumulated in a punctate fashion, colocalized with the *N*-sulfo-rich clusters. Based on these lines of evidence, here we reconsider the classical view of morphogen spreading controlled by HSPGs.

Keywords: HSPG, glypican, HS cluster, *N*-sulfation, NDST, Wnt, signaling, morphogen gradient

OPEN ACCESS

Edited by:
Rachel K. Okolicsanyi, Queensland University of Technology, Australia

Reviewed by:
Sally Ann Moody, The George Washington University, United States
Dalit Sela-Donenfeld, The Hebrew University of Jerusalem, Israel

***Correspondence:**
Yusuke Mii
mii@nibb.ac.jp
Shinji Takada
stakada@nibb.ac.jp

Specialty section:
This article was submitted to Signaling, a section of the journal Frontiers in Cell and Developmental Biology

Received: *08 May 2020*
Accepted: *23 June 2020*
Published: *14 July 2020*

Citation:
Mii Y and Takada S (2020) Heparan Sulfate Proteoglycan Clustering in Wnt Signaling and Dispersal. Front. Cell Dev. Biol. 8:631. doi: 10.3389/fcell.2020.00631

INTRODUCTION

It is generally recognized that functions of secreted signaling proteins, or morphogens, are affected by heparan sulfate proteoglycans (HSPGs). Some of the greatest contributions to this view have come from genetic research involving *Drosophila* (Yan and Lin, 2009). Historically, genes responsible for segment polarity cuticle phenotypes, which are similar to the phenotypes of *wingless* (*wg; Drosophila* ortholog of *Wnt1*), and *hedgehog* mutant embryos, were identified as genes involved in glycogenesis of heparan sulfate (HS) chains (Binari et al., 1997; Hacker et al., 1997; Haerry et al., 1997; Lin and Perrimon, 1999). Furthermore, genes encoding core proteins of HSPGs, such as glypicans (Filmus et al., 2008) and enzymes for glycosaminoglycan (GAG) chains, such as EXTs (Busse-Wicher et al., 2014), regulate signal transduction and extracellular trafficking of morphogen proteins. In parallel with genetic research, biochemical studies have shown that HS chains have high affinity for many kinds of morphogens, including FGF (Esko and Selleck, 2002) and Wnt (Gao et al., 2016). Based on these studies, interactions between morphogens and HSPGs have been considered crucial for generation and maintenance of signaling (Sarrazin et al., 2011).

Interestingly, HSPGs show variable GAG chain composition and core protein structure. GAG chains are especially highly modified by *N*- and *O*-sulfation and the extent of these modifications is variable (Esko and Selleck, 2002). This variation has been recognized for a long time, but it was

unclear whether modifications of individual HS chains vary within individual cells. However, our recent studies have revealed that *N*-sulfo-rich and *N*-acetyl-rich HSPGs form different clusters on individual cells (Mii et al., 2017). This new finding suggests that distinct clusters of HSPGs regulate Wnt signaling differently and that distribution of these clusters may govern dispersal of signaling proteins and may define the signaling range (distance) of morphogens. In this review, we will first provide a general understanding of the structural and functional diversity of HSPGs. Then we will document the clustering of specifically modified HSPGs and propose a model by which Wnt signaling is governed via interaction with clusters of HSPGs.

WNT SIGNALING AND INTERCELLULAR DELIVERY

Wnt ligands activate several distinct cellular signaling pathways, including the Wnt/β-catenin and Wnt/JNK pathways (Niehrs, 2012). Upon activation of the Wnt/β-catenin pathway, Wnt ligands promote assembly of signaling complexes called "signalosomes," which involve Frizzled (Fz) receptors, Lrp5/6 coreceptors, and cytoplasmic components Dishevelled (Dvl) and Axin (Bilic et al., 2007; Kikuchi et al., 2009). Formation of signalosomes results in stabilization of cytosolic β-catenin, thereby activating Tcf transcription factors and their target genes (Kikuchi et al., 2009). In contrast, the Wnt/JNK pathway requires Fz receptors and Dvl, and it activates small GTPases, such as Rho and Rac, and the protein kinase, JNK (Niehrs, 2012). In humans and mice, 19 Wnt ligands have been identified, and some of them, Wnt1, Wnt3a, and Wnt8, preferentially activate Wnt/β-catenin whereas others, Wnt5a and Wnt11, activate mainly the Wnt/JNK pathway.

Most Wnt ligands are modified with palmitoleic acid and delivered to neighboring cells (Takada et al., 2006). A number of mechanisms have been proposed to explain Wnt delivery (Takada et al., 2017). For instance, extracellular vesicles, like exosomes (Gross et al., 2012), lipoprotein particles (Panakova et al., 2005), and filopodia-like cellular processes called cytonemes (Stanganello et al., 2015; Stanganello and Scholpp, 2016) have been shown to mediate Wnt delivery. In contrast, secreted Wnt does not appear to exist as a monomer, because no monomeric form was detected in the culture medium of Wnt3a-expressing mouse L cells (Takada et al., 2018). Rather, Wnt3a protein forms heteromeric complexes with partner proteins or assembles itself into high-molecular-weight complexes, which are less diffusible and which easily dissociate to form complexes with Fz receptors (Takada et al., 2018). In embryos, some Wnt-binding proteins facilitate Wnt delivery. Some secreted Frizzled-related proteins (sFRP), sFRP2 and Frzb, form heteromeric complexes with Wnt so as to enhance their delivery in *Xenopus* embryos (Mii and Taira, 2009; Takada et al., 2018). Similarly, swim, a member of the Lipocalin family of extracellular transport proteins, facilitates Wg diffusion in *Drosophila* imaginal disks (Mulligan et al., 2012).

In addition to these delivery systems, HSPGs are also involved in Wnt delivery. Genetic studies in *Drosophila* suggest that HSPGs either enhance signaling by Wnt ligands or delivery of Wnt ligands to neighboring cells in a context-dependent manner (Han et al., 2004b; Franch-Marro et al., 2005; Yan and Lin, 2009). It has been proposed that HSPGs mediate Wnt delivery by a restricted-diffusion mechanism, in which Wnt ligands are transported in a "bucket brigade" manner by repeated association and dissociation with HSPGs on cell membranes (Yan and Lin, 2009). The restricted diffusion model has been adopted to explain the mechanism of delivery of several secreted signal proteins, including Wnt. However, results of recent quantitative analyses do not appear to support this model. For instance, Dpp diffuses freely in *Drosophila* wing disks (Zhou et al., 2012). Similarly, freely diffusing forms of Wnt8 have also been detected in *Xenopus* embryos (Mii et al., 2020). These examples imply that the restricted diffusion model should be carefully reconsidered.

CHARACTERISTICS OF CORE PROTEINS AND SUGAR CHAINS OF HSPGS

HSPGs are composed of core proteins with attached heparan sulfate (HS) GAG chains. Approximately 20 core proteins have been identified and are classified into several families, based upon their structures (Sarrazin et al., 2011). Proteins of the two major families, the glypican and syndecan families, are attached to cell membranes (Bernfield et al., 1999). Glypican family proteins, including GPC1-6 in vertebrates and Dally and Dally like protein (Dlp) in *Drosophila*, are linked to the membrane by glycerophosphatidylinositide (GPI)-anchors. These glypicans can be divided into two subgroups based upon amino acid sequence homology. GPC1/2/4/6 and Dlp form one group, while GPC3/5 and Dally form the other (Filmus et al., 2008). Evidence suggests some functional differences among glypicans, but it remains to be seen whether such differences result from structural differences between the subfamilies (Han et al., 2004b; Franch-Marro et al., 2005; Yan and Lin, 2009). Glypican family proteins commonly have a cysteine-rich domain at their N-termini and several HS attachment sites close to the membrane anchoring site. Interestingly, the structure of this cysteine-rich domain is similar to that of Fz and it mediates Wnt binding (Topczewski et al., 2001). On the other hand, syndecan family members (SDC1-4 in vertebrates and a single syndecan in *Drosophila*) are transmembrane proteins. Syndecans bear HS chains at their N-termini and some SDCs also bear chondroitin sulfate (Gondelaud and Ricard-Blum, 2019). In addition to these two types of cell surface HSPGs, secreted HSPGs (perlcan, agrin, and collagen type XVIII in vertebrates and terribly reduced optic lobes (trol) in *Drosophila*), have also been identified. Secreted HSPGs are mainly found in the extracellular matrix (Sarrazin et al., 2011).

HS chains are linear polysaccharides that contain 20–150 repeating disaccharide units of *N*-acetylglucosamine (GlcNAc) and either uronic acid [glucuronic acid (GlcA) or iduronic acid (IdoA)] (Sarrazin et al., 2011). These chains are synthesized in the Golgi by sequential actions of glycosyl transferases and modification enzymes (Esko and Selleck, 2002). HS chain synthesis is initiated by adding tetrasaccharide linkers to serine residues in the core proteins. Then, a number of

disaccharide units are sequentially attached to HS chains by co-polymerases known as Ext1 and Ext2 [*Tout-velu* (*Ttv*) and *Sister of ttv* (*Sotv*) in *Drosophila*]. Following this polymerization process, elongated HS chains are extensively modified by sulfotransferases and an epimerase. For instance, GlcNAc *N*-deacetylase/*N*-sulfotransferase [NDST1-4, or *sulfateless* (*sfl*) in *Drosophila*] catalyzes GlcNAc *N*-deacetylation and *N*-sulfation (**Figure 1A**), and C5 epimerase converts GlcA to IdoA. In addition, 2-*O*-Sulfotransferase, 6-*O*-Sulfotransferases, and 3-*O*-Sulfotransferases variously catalyze *O*-sulfation at C2 of uronic acid, at C6 of *N*-acetyl- and *N*-sulfo-glucosamine, and at C3 of glucosamine, respectively. Notably, these reactions do not proceed to completion in the Golgi, resulting in structural diversity of HS chains. Domains rich in *N*-sulfated disaccharides and those rich in unmodified disaccharides, that is, *N*-acetyl disaccharides, exist on HS chains (NS or NA domains, respectively, **Figure 1B**; Gallagher and Walker, 1985; Maccarana et al., 1996; Bernfield et al., 1999). In the *N*-sulfated rich domain, *O*-sulfation is also frequently detected. Thus, these modifications appear to occur commonly among adjacent disaccharides in HS synthesis.

INVOLVEMENT OF GLYPICANS IN WNT SIGNALING AND DISTRIBUTION

Genetic studies using *Drosophila* illustrate the importance of HSPGs in Wnt signaling. For instance, loss-of-function of glypican, Dally or Dlp, results in reduction of Wg signaling and extracellular Wg levels in wing disks (Franch-Marro et al., 2005; Han et al., 2005). Similarly, Wg signaling and the extracellular distribution of Wg are reduced in cells deficient in genes required for biosynthesis of HS chains, including *sugarless* (UDP-glucose dehydrogenase) (Hacker et al., 1997; Haerry et al., 1997), *sfl* (NDST) (Lin and Perrimon, 1999; Baeg et al., 2004), and *Ttv* and *Sotv* (EXTs) (Han et al., 2004a; Takei et al., 2004). Thus, HSPGs are essential for proper signaling and distribution in fly development.

In vertebrates, HSPGs may modulate various extracellular signaling proteins, but several lines of evidence confirm their involvement in Wnt signaling. For instance, in zebrafish and *Xenopus*, disruption of *gpc4/knypek* function causes defects in convergent extension movement, which is modulated by Wnt/JNK signaling, during gastrulation (Topczewski et al., 2001; Ohkawara et al., 2003). Mouse embryos lacking *Gpc3* show reduced Wnt/JNK signaling (Song et al., 2005). Cell culture studies indicate that glypicans appear to modulate β-catenin-dependent and -independent pathways in vertebrate cells, depending on different membrane microdomains (Sakane et al., 2012). In addition to glypicans, other HSPG core proteins, syndecan and perlecan, are involved in Wnt signaling, but will not be considered here.

One of the important issues regarding Wnt binding is whether HSPG core proteins or GAG chains are required. Since Gpc3 lacking GAG chains can bind to several Wnt ligands and can positively regulate canonical Wnt signaling (Capurro et al., 2005), glypican core protein appears sufficient for Wnt binding. In contrast, involvement of GAG chains for interaction with Wnt has also been reported. Wnt8 accumulation upon overexpression of Gpc4 or Gpc5 appears to be HS chain-dependent, because ΔGAG mutants of these glypicans do not accumulate Wnt8 (Mii et al., 2017). Furthermore, *Drosophila* mutants with impaired HS chains suggest essential roles for HS chains in Wg binding and regulation (Lin and Perrimon, 1999; Baeg et al., 2004; Takei et al., 2004). Thus, in addition to core protein, HS chains appear to be required for Wnt signaling *in vivo*.

HS CLUSTERS AND WNT SIGNALING

Assembly of HSPGs With Similarly Modified HS Chains

For better understanding of HSPG-mediated Wnt signaling and dispersal, it is important to understand the spatial distribution of HSPGs in tissues or cells. Given the variability in core proteins and HS chain composition, it is important to examine the expression pattern of each core protein and fine localization patterns of HS chain modifications. Using two monoclonal antibodies, HepSS-1 (Kure and Yoshie, 1986; van den Born et al., 2005) and NAH46 (Suzuki et al., 2008), which recognize HS chains of *N*-sulfated $(GlcA\text{-}GlcNS)_n$ and unmodified *N*-acetylated $(GlcA\text{-}GlcNAc)_n$ structures, respectively, distributions of differently modified HS chains were examined in *Xenopus* embryos at gastrula stage. At this stage, Wnt8 is expressed in the ventral and lateral marginal zone and participates in ventral mesodermal patterning. Immunostaining with either of these two antibodies showed that HSPGs that react with these antibodies are not uniformly distributed on cell surfaces. Instead, they aggregate locally to form discrete clusters (**Figures 1C,D**). Increased or decreased expression of NDST1, which catalyzes *N*-sulfation of HS disaccharides, showed that HepSS-1 and NAH46 clusters actually represent *N*-sulfo- or *N*-acetyl-rich clusters, respectively. These results suggest that HSPGs with *N*-sulfo-rich or *N*-acetyl-rich HS chains form discrete clusters, designated "HS clusters" on the cell surface (Mii et al., 2017).

Distinct Roles of HS Clusters in Wnt Signaling and Dispersal

These two types of clusters show different specificities for secreted signal proteins. First, Wnt ligands are specifically colocalized with *N*-sulfo-rich clusters. In *Xenopus* embryos, endogenous, as well as overexpressed Wnt8 ligands, are also distributed in a punctate pattern on cell surfaces. Most of these dots overlap with *N*-sulfo-rich clusters (**Figure 1E**). This interaction between Wnt8 and *N*-sulfo-rich HSs is dependent on *N*-sulfation, because overexpression of *ndst1* increases *N*-sulfation levels and Wnt8 accumulation, and vice versa. Thus, *N*-sulfo-rich HS clusters serve as major scaffolds where Wnt8 ligands are trapped in *Xenopus* embryos (Mii et al., 2017). On the other hand, *N*-acetyl-rich HS clusters serve as scaffolds for Frzb (Leyns et al., 1997; Wang et al., 1997), a member of the secreted Frizzled-related protein (sFRP) family (Bovolenta et al., 2008; Mii and Taira, 2011).

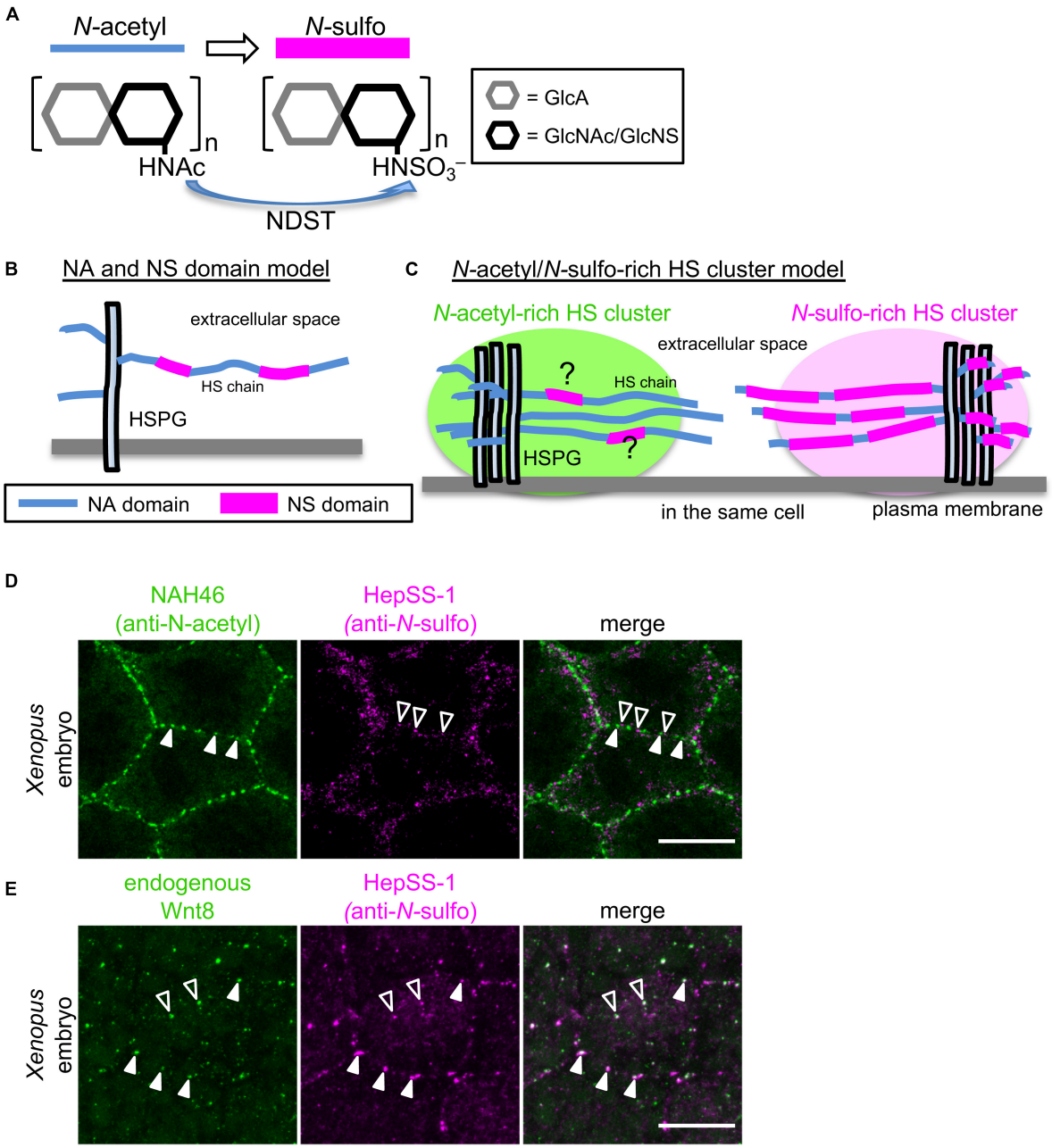

FIGURE 1 | Models explaining the diversity of HS chain modification of HSPGs. **(A)** *N*-sulfation of GlcA-GlcNAc units of HS chains by NDST. HS chains are synthesized by sequential actions of glycosyl transferases and modification enzymes. After polymerization of disaccharide units, elongated HS chains are extensively modified by sulfotransferases, including GlcNAc *N*-deacetylase/*N*-sulfotransferase (NDST), which catalyzes *N*-sulfation of GlcA-GlcNAc units of HS chains. **(B)** NA and NS domain model. Analysis of the oligosaccharides of HS chains obtained by digestion under conditions in which *N*-sulfated GlcA-GlcNAc units are selectively attacked, showed that various heparan sulfate samples all contained regions of consecutive *N*-sulfated GlcA-GlcNAc units, as well as contiguous *N*-acetylated ones (Gallagher and Walker, 1985; Maccarana et al., 1996; Bernfield et al., 1999). These findings suggest that modifications occur in clusters of variable length (*N*-sulfated or NS domains), which are interspersed among unmodified domains (*N*-acetylated or NA domains). It has been proposed that these two domains coexist on single HS chains. **(C)** *N*-acetyl-rich and *N*-sulfo-rich HS cluster model. Recently, Mii et al. found that *N*-sulfo-rich and *N*-acetyl-rich HSPGs are clustered independently on cell membranes of *Xenopus* embryos and on cultured cells (Mii et al., 2017). This new finding strongly suggests that NS and NA domains do not exist randomly on individual HS chains. Rather, the extent of *N*-sulfation appears to vary between HSPG clusters. Although *N*-sulfo-rich and *N*-acetyl-rich clusters rarely overlap on the cell surface, it cannot be excluded that HS chains in *N*-sulfo-rich and *N*-acetyl-rich HS clusters may contain some NA and NS domains, respectively. **(D)** *N*-acetyl-rich and *N*-sulfo-rich HS clusters in a *Xenopus* embryo. Double color immunostaining with direct-labeled NAH46 (anti-*N*-acetyl subunits) and HepSS-1 (anti-*N*-sulfo subunits) antibodies shows clustered distributions of HS chains recognized by these antibodies (Mii et al., 2017). Notably, NAH46 and HepSS-1 staining do not largely overlap, but rather show distinct distributions. **(E)** Endogenous Wnt8 colocalized with *N*-sulfo rich HS clusters. Double color immunostaining with anti-Wnt8 and HepSS-1 antibodies shows that Wnt8 staining mostly overlaps with HepSS-1 staining. Colocalization is indicated with closed (cell boundary) and open (inside cells) arrowheads. Scale bars, 20μm.

Wnt ligands trigger formation of signalosomes (Bilic et al., 2007), which are subsequently internalized by caveolin-mediated endocytosis (Yamamoto et al., 2006; Kikuchi et al., 2009). In signalosomes, Fz receptors, LRP5/6 coreceptors, and cytoplasmic components, including Dvl and Axin, are assembled to facilitate phosphorylation of LRP5/6, which is essential for activation of canonical Wnt signaling (Bilic et al., 2007; Kikuchi et al., 2009). Notably, *N*-sulfo-rich HS clusters, but not *N*-acetyl-rich HS clusters, are frequently internalized (Mii et al., 2017). In the presence of Wnt8, phosphorylated LRP6 is preferentially detected at *N*-sulfo-rich HS clusters, but NDST1 knockdown reduces LRP6 phosphorylation and also Wnt/β-catenin signaling. Consistent with these results, NDST1 knockdown inhibits secondary axis formation caused by ventral injection of *wnt8* mRNA in *Xenopus* embryos. It was also shown that Wnt3a and signalosome components are localized with *N*-sulfo-rich HS in HeLa cells. These results suggest that *N*-sulfo-rich HS clusters are required for Wnt/β-catenin signaling and signalosome formation in *Xenopus* embryos and cultured cells. Because *N*-sulfo-rich HS clusters form independently of Wnt ligand, it seems probable that *N*-sulfo-rich HS clusters serve as pre-existing scaffolds to assemble signalosomes (Mii et al., 2017).

As described above, Wnt8 associates with *N*-sulfo-rich HS clusters in *Xenopus* embryos. However, when Frzb is overexpressed, Wnt8 association with *N*-sulfo-rich HS clusters decreases, and Wnt8 then associates with *N*-acetyl-rich clusters via Frzb (Mii et al., 2017). Given that Wnt8 forms a heteromeric complex with Frzb (Leyns et al., 1997; Wang et al., 1997), Wnt8 that forms these heteromeric complexes probably associates with *N*-acetyl-rich clusters. In contrast, other forms of Wnt8, such as Wnt8 in extracellular vesicles or in homomeric complexes (Takada et al., 2018), as indicated above, may associate with *N*-sulfo-rich clusters. In *Xenopus* embryos, ectopically expressed Wnt8 shows only a short distribution range, but this range can be expanded if Frzb, which shows a much longer one, is coexpressed with Wnt8 (Mii and Taira, 2009). Thus, in this context, it seems probable that *N*-acetyl-rich HS clusters serve as scaffolds that enable more long-range delivery of Wnt8/Frzb complexes.

We recently found that some Wnt8 diffuses freely, but that the majority of it is bound to cell surface scaffolds, probably HSPG clusters (Mii et al., 2020). Interestingly, Wnt8 molecules bound to scaffolds seem to be released occasionally, but diffusing away rather than being trapped on the adjacent cell surface. Thus, in contrast to predictions by the restricted diffusion model (**Figure 2A**), "bucket-brigade"-type transfer of Wnt8 was not detectable on cell surfaces (Mii et al., 2020). Given that scaffolds are scattered on cell membranes, Wnt8 molecules, probably associating with Frzb, are likely to be delivered over long distances by jumping between the scaffolds, probably provided by *N*-acetyl-rich clusters (**Figure 2B**; Mii and Taira, 2009; Mii et al., 2017).

Specificity of Glypicans for Distinct HS Clusters

Evidence suggests that glypicans are the major core proteins of these HS clusters. PI-PLC treatment and cholesterol removal with methyl-β-cyclodextran reduced HS clusters, suggesting that GPI-anchored proteins, most probably glypicans, are involved in clustering. Among glypicans, Gpc4 and Gpc5 are highly expressed in *Xenopus* gastrulae. We demonstrated that Gpc5, an ortholog of *Drosophila* Dally, bears mainly *N*-sulfo-rich HS, whereas Gpc4, an ortholog of Dlp, bears both *N*-sulfo-rich and *N*-acetyl-rich HS (Mii et al., 2017). Thus, although glypican core proteins provide a molecular basis for clustering, composition of core proteins appears to differ between the two cluster types. On the other hand, it is still uncertain whether other core proteins, such as syndecans, are involved in formation of HS clusters.

Interestingly, Dally and Dlp appear to modulate Wg signaling and distribution differently in *Drosophila* wing disk (Franch-Marro et al., 2005; Han et al., 2005). Dally enhances Wg signaling through DFz2 receptors and internalization of receptor complexes. On the other hand, Dlp exhibits biphasic activity in Wg signaling and distribution. While Dlp acts as a positive regulator in regions distal from Wg-producing cells, it also acts as a negative regulator proximally. This biphasic behavior can be explained if Dlp delivers captured Wg to Fz receptors on the same cell or passes it to neighboring cells, depending on the cellular context. In view of phylogenetic relationships of these *Drosophila* glypicans to Gpc5 and Gpc4, as shown above, we propose that the specificity of the two glypican subfamilies in Wnt signaling and distribution is consistent among invertebrates and vertebrates.

Mechanisms by Which Discrete HS Clusters Are Formed

It remains to be determined how these two distinct types of clusters are generated. To answer this question, understanding the regulation of HS modifications in the ER and/or the Golgi seems to hold the key. Interestingly, it has been suggested that NDST1 is associated with Ext1 or Ext2 in the Golgi, forming an HS biosynthesis complex called a GAGosome (Esko and Selleck, 2002). The stoichiometry and composition of these enzymes in GAGosomes may affect modifications of HS chains, such as *N*-sulfation (Presto et al., 2008). Given that some types of GAGosomes are localized in particular regions in the Golgi, this spatial heterogeneity may generate differential *N*-sulfation even within a single cell. Consistent with this idea, *sulfateless*, *Drosophila* NDST localizes in a specific sub-compartment of the Golgi apparatus (Yano et al., 2005). On the other hand, biosynthesis and transport of 3′-phosphoadenyl 5′-phosphosulfate (PAPS), a sulfuryl group donor, are required for proper sulfation reactions (Kurima et al., 1998; Esko and Selleck, 2002; Kamiyama et al., 2003). If local abundance or absence of PAPS exists in Golgi, this could be a mechanism generating distinct modifications of HS clusters.

PERSPECTIVES

In this review, we proposed that novel types of HSPGs, *N*-sulfo- and *N*-acetyl-rich HS clusters, provide insight into regulation of secreted signaling proteins, such as Wnt. HS clusters enable cells to regulate Wnt8 and its binding protein, Frzb, in a controlled

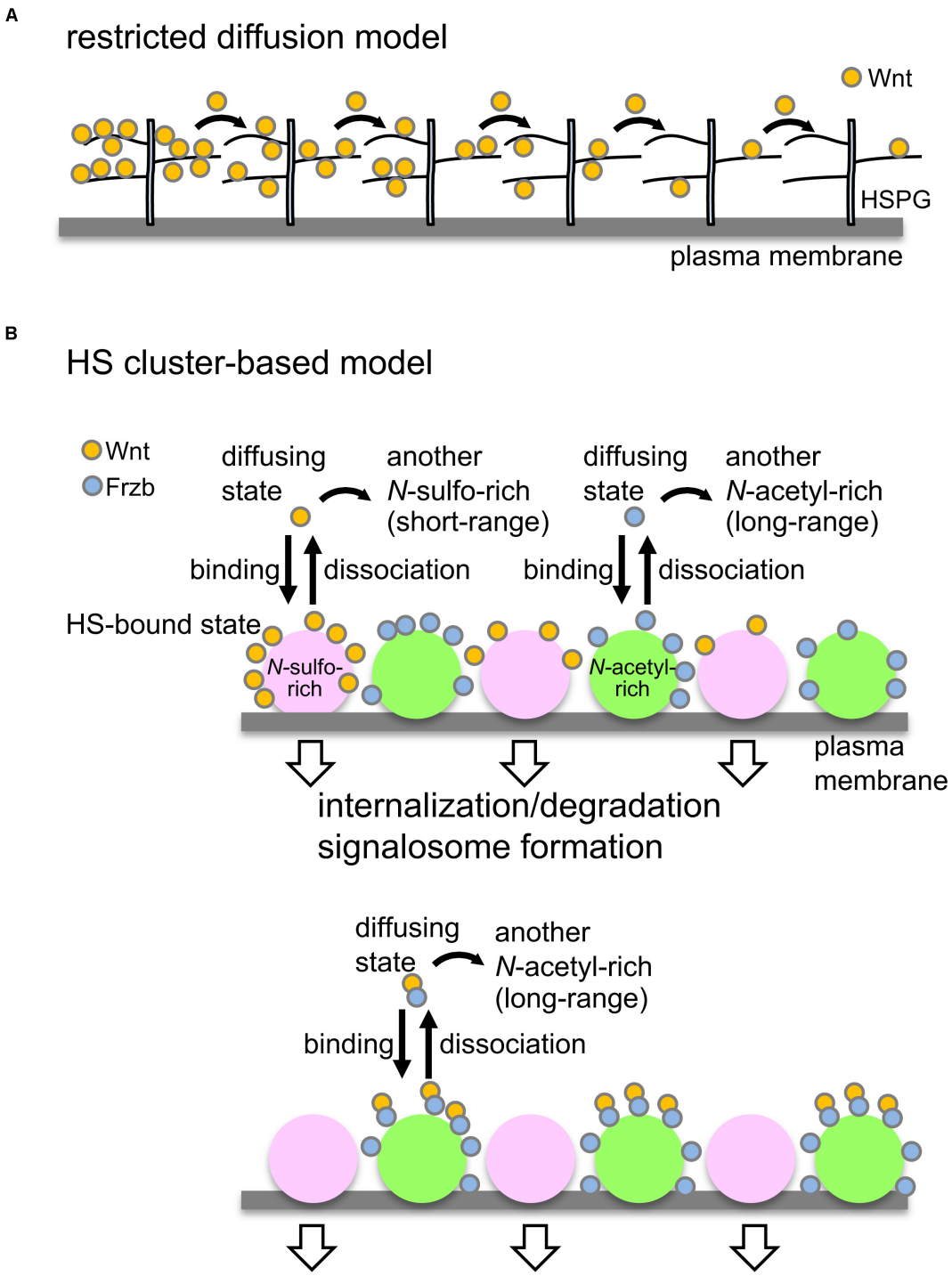

FIGURE 2 | Models to control Wnt signaling and dispersal by HSPGs. **(A)** Restricted diffusion model. Based on genetic studies in *Drosophila*, it has been proposed that HSPGs mediate Wnt delivery by a restricted-diffusion mechanism, in which Wnt ligands are transported in a "bucket brigade" manner by repeated association and dissociation with HSPGs on cell membranes (Yan and Lin, 2009). **(B)** Model to explain Wnt signaling and delivery by clustering of HSPGs. Wnt8 preferentially binds to *N*-sulfo-rich HS clusters and Frzb binds to *N*-acetyl-rich clusters (upper; Mii et al., 2017). Accumulation of Wnt8 on *N*-sulfo-rich HS clusters leads to signalosome formation and internalization of Wnt8, which may contribute to degradation of Wnt8. When Frzb is abundant (lower), Wnt8-Frzb complexes bind to *N*-acetyl-rich HS clusters, which may reduce degradation of Wnt8 (Mii et al., 2017). Given that these two clusters are not distributed uniformly on the cell surface, it seems unlikely that Wnt ligands are transported in a "bucket brigade" manner between these clusters. Since *N*-sulfo-rich HS clusters are frequently internalized, this cluster appears to shorten the distribution range of Wnt8 (Mii and Taira, 2009). On the other hand, *N*-acetyl-rich HS clusters tend to remain on the cell surface, resulting in long-range distributions of Frzb as well as Wnt8-Frzb complexes (Mii and Taira, 2009). One possible model is that the balance of Wnt interactions between *N*-sulfo-rich HS clusters and *N*-acetyl-rich HS clusters may regulate Wnt signaling range in tissues.

manner. Although organization of HSPGs is difficult to analyze by biochemical methods, we assume that various types of HS clusters could be involved in many aspects of embryogenesis and homeostasis. Hypothetical HS clusters with various modifications could serve as specific platforms on cell surfaces for various secreted proteins, as exemplified by combinations of Wnt8-*N*-sulfo-rich HS clusters and Frzb-*N*-acetyl-rich HS clusters (Mii et al., 2017). Future studies will focus on the generality of this finding, especially in other biological systems and with other modifications of HS chains. Given that HSPGs modulate Wnt signaling in various diseases (Capurro et al., 2005; Zittermann et al., 2010; Lund et al., 2020), HS modification and clustering could influence disease progression.

AUTHOR CONTRIBUTIONS

YM and ST conceived and wrote the review together, and approved the submitted version.

FUNDING

This work was supported by the following programs: Grants-in-Aid for Scientific Research (B), 23370094 and 18H02454 to ST, Grant-in-Aid for challenging Exploratory Research, 17K19418 to ST, Grants-in-aid for Scientific Research on Innovative Areas, 24111002 to ST, and Grant-in-Aid for Early Career Scientists, 18K14720 to YM from the Japan Society for the Promotion of Science; PRESTO (JPMJPR194B) to YM from Japan Science and Technology Agency. Additional support came from grants from the National Institutes of Natural Sciences (NINS Joint Research Program by Young Researchers to YM and NINS Joint Research Program to ST), and Daiko Foundation (to ST).

ACKNOWLEDGMENTS

We thank Dr. Steven D. Aird for his support in editing the manuscript.

REFERENCES

Baeg, G. H., Selva, E. M., Goodman, R. M., Dasgupta, R., and Perrimon, N. (2004). The Wingless morphogen gradient is established by the cooperative action of Frizzled and Heparan Sulfate Proteoglycan receptors. *Dev. Biol.* 276, 89–100. doi: 10.1016/j.ydbio.2004.08.023

Bernfield, M., Gotte, M., Park, P. W., Reizes, O., Fitzgerald, M. L., Lincecum, J., et al. (1999). Functions of cell surface heparan sulfate proteoglycans. *Annu. Rev. Biochem.* 68, 729–777. doi: 10.1146/annurev.biochem.68.1.729

Bilic, J., Huang, Y. L., Davidson, G., Zimmermann, T., Cruciat, C. M., Bienz, M., et al. (2007). Wnt induces LRP6 signalosomes and promotes dishevelled-dependent LRP6 phosphorylation. *Science* 316, 1619–1622. doi: 10.1126/science.1137065

Binari, R. C., Staveley, B. E., Johnson, W. A., Godavarti, R., Sasisekharan, R., and Manoukian, A. S. (1997). Genetic evidence that heparin-like glycosaminoglycans are involved in wingless signaling. *Development* 124, 2623–2632.

Bovolenta, P., Esteve, P., Ruiz, J. M., Cisneros, E., and Lopez-Rios, J. (2008). Beyond Wnt inhibition: new functions of secreted Frizzled-related proteins in development and disease. *J. Cell Sci.* 121, 737–746. doi: 10.1242/jcs.026096

Busse-Wicher, M., Wicher, K. B., and Kusche-Gullberg, M. (2014). The exostosin family: proteins with many functions. *Matrix Biol.* 35, 25–33. doi: 10.1016/j.matbio.2013.10.001

Capurro, M. I., Xiang, Y. Y., Lobe, C., and Filmus, J. (2005). Glypican-3 promotes the growth of hepatocellular carcinoma by stimulating canonical Wnt signaling. *Cancer Res.* 65, 6245–6254. doi: 10.1158/0008-5472.can-04-4244

Esko, J. D., and Selleck, S. B. (2002). ORDER OUT OF CHAOS: assembly of Ligand Binding Sites in Heparan Sulfate. *Annu. Rev. Biochem.* 71, 435–471. doi: 10.1146/annurev.biochem.71.110601.135458

Filmus, J., Capurro, M., and Rast, J. (2008). Glypicans. *Genome Biol.* 9:224.

Franch-Marro, X., Marchand, O., Piddini, E., Ricardo, S., Alexandre, C., and Vincent, J. P. (2005). Glypicans shunt the Wingless signal between local signalling and further transport. *Development* 132, 659–666. doi: 10.1242/dev.01639

Gallagher, J. T., and Walker, A. (1985). Molecular distinctions between heparan sulphate and heparin. Analysis of sulphation patterns indicates that heparan sulphate and heparin are separate families of N-sulphated polysaccharides. *Biochem. J.* 230, 665–674. doi: 10.1042/bj2300665

Gao, W., Xu, Y., Liu, J., and Ho, M. (2016). Epitope mapping by a Wnt-blocking antibody: evidence of the Wnt binding domain in heparan sulfate. *Sci. Rep.* 6:26245.

Gondelaud, F., and Ricard-Blum, S. (2019). Structures and interactions of syndecans. *FEBS J.* 286, 2994–3007. doi: 10.1111/febs.14828

Gross, J. C., Chaudhary, V., Bartscherer, K., and Boutros, M. (2012). Active Wnt proteins are secreted on exosomes. *Nat. Cell Biol.* 14, 1036–1045. doi: 10.1038/ncb2574

Hacker, U., Lin, X., and Perrimon, N. (1997). The Drosophila sugarless gene modulates Wingless signaling and encodes an enzyme involved in polysaccharide biosynthesis. *Development* 124, 3565–3573.

Haerry, T. E., Heslip, T. R., Marsh, J. L., and O'Connor, M. B. (1997). Defects in glucuronate biosynthesis disrupt Wingless signaling in Drosophila. *Development* 124, 3055–3064.

Han, C., Belenkaya, T. Y., Khodoun, M., Tauchi, M., and Lin, X. (2004a). Distinct and collaborative roles of Drosophila EXT family proteins in morphogen signalling and gradient formation. *Development* 131, 1563–1575. doi: 10.1242/dev.01051

Han, C., Belenkaya, T. Y., Wang, B., and Lin, X. (2004b). Drosophila glypicans control the cell-to-cell movement of Hedgehog by a dynamin-independent process. *Development* 131, 601–611. doi: 10.1242/dev.00958

Han, C., Yan, D., Belenkaya, T. Y., and Lin, X. (2005). Drosophila glypicans Dally and Dally-like shape the extracellular Wingless morphogen gradient in the wing disc. *Development* 132, 667–679. doi: 10.1242/dev.01636

Kamiyama, S., Suda, T., Ueda, R., Suzuki, M., Okubo, R., Kikuchi, N., et al. (2003). Molecular cloning and identification of 3'-phosphoadenosine 5'-phosphosulfate transporter. *J. Biol. Chem.* 278, 25958–25963. doi: 10.1074/jbc.m302439200

Kikuchi, A., Yamamoto, H., and Sato, A. (2009). Selective activation mechanisms of Wnt signaling pathways. *Trends Cell Biol.* 19, 119–129. doi: 10.1016/j.tcb.2009.01.003

Kure, S., and Yoshie, O. (1986). A syngeneic monoclonal antibody to murine Meth-A sarcoma (HepSS-1) recognizes heparan sulfate glycosaminoglycan (HS-GAG): cell density and transformation dependent alteration in cell surface HS-GAG defined by HepSS-1. *J. Immunol.* 137, 3900–3908.

Kurima, K., Warman, M. L., Krishnan, S., Domowicz, M., Krueger, R. C. Jr., Deyrup, A., et al. (1998). A member of a family of sulfate-activating enzymes causes murine brachymorphism. *Proc. Natl Acad. Sci. U.S.A.* 95, 8681–8685. doi: 10.1073/pnas.95.15.8681

Leyns, L., Bouwmeester, T., Kim, S. H., Piccolo, S., and De Robertis, E. M. (1997). Frzb-1 is a secreted antagonist of Wnt signaling expressed in the Spemann organizer. *Cell* 88, 747–756. doi: 10.1016/s0092-8674(00)81921-2

Lin, X., and Perrimon, N. (1999). Dally cooperates with Drosophila Frizzled 2 to transduce Wingless signalling. *Nature* 400, 281–284. doi: 10.1038/22343

Lund, M. E., Campbell, D. H., and Walsh, B. J. (2020). The Role of Glypican-1 in the Tumour Microenvironment. *Adv. Exp. Med. Biol.* 1245, 163–176. doi: 10.1007/978-3-030-40146-7_8

Maccarana, M., Sakura, Y., Tawada, A., Yoshida, K., and Lindahl, U. (1996). Domain structure of heparan sulfates from bovine organs. *J. Biol. Chem.* 271, 17804–17810. doi: 10.1074/jbc.271.30.17804

Mii, Y., Nakazato, K., Pack, C. G., Sako, Y., Mochizuki, A., Takada, S., et al. (2020). Quantitative analyses reveal extracellular dynamics of Wnt ligands in Xenopus embryos. *bioRxiv [Preprint]* doi: 10.1101/2020.02.20.957860

Mii, Y., and Taira, M. (2009). Secreted Frizzled-related proteins enhance the diffusion of Wnt ligands and expand their signalling range. *Development* 136, 4083–4088. doi: 10.1242/dev.032524

Mii, Y., and Taira, M. (2011). Secreted Wnt "inhibitors" are not just inhibitors: regulation of extracellular Wnt by secreted Frizzled-related proteins. *Dev. Growth Differ.* 53, 911–923. doi: 10.1111/j.1440-169x.2011.01299.x

Mii, Y., Yamamoto, T., Takada, R., Mizumoto, S., Matsuyama, M., Yamada, S., et al. (2017). Roles of two types of heparan sulfate clusters in Wnt distribution and signaling in Xenopus. *Nat. Commun.* 8:1973.

Mulligan, K. A., Fuerer, C., Ching, W., Fish, M., Willert, K., and Nusse, R. (2012). Secreted Wingless-interacting molecule (Swim) promotes long-range signaling by maintaining Wingless solubility. *Proc. Natl Acad. Sci. U.S.A.* 109, 370–377. doi: 10.1073/pnas.1119197109

Niehrs, C. (2012). The complex world of WNT receptor signalling. *Nat. Rev. Mol. Cell Biol.* 13, 767–779. doi: 10.1038/nrm3470

Ohkawara, B., Yamamoto, T. S., Tada, M., and Ueno, N. (2003). Role of glypican 4 in the regulation of convergent extension movements during gastrulation in *Xenopus laevis*. *Development* 130, 2129–2138. doi: 10.1242/dev.00435

Panakova, D., Sprong, H., Marois, E., Thiele, C., and Eaton, S. (2005). Lipoprotein particles are required for Hedgehog and Wingless signalling. *Nature* 435, 58–65. doi: 10.1038/nature03504

Presto, J., Thuveson, M., Carlsson, P., Busse, M., Wilen, M., Eriksson, I., et al. (2008). Heparan sulfate biosynthesis enzymes EXT1 and EXT2 affect NDST1 expression and heparan sulfate sulfation. *Proc. Natl Acad. Sci. U.S.A.* 105, 4751–4756. doi: 10.1073/pnas.0705807105

Sakane, H., Yamamoto, H., Matsumoto, S., Sato, A., and Kikuchi, A. (2012). Localization of glypican-4 in different membrane microdomains is involved in the regulation of Wnt signaling. *J. Cell Sci.* 125, 449–460. doi: 10.1242/jcs.091876

Sarrazin, S., Lamanna, W. C., and Esko, J. D. (2011). Heparan sulfate proteoglycans. *Cold Spring Harb. Perspect. Biol.* 3:a004952.

Song, H. H., Shi, W., Xiang, Y. Y., and Filmus, J. (2005). The loss of glypican-3 induces alterations in Wnt signaling. *J. Biol. Chem.* 280, 2116–2125. doi: 10.1074/jbc.m410090200

Stanganello, E., Hagemann, A. I., Mattes, B., Sinner, C., Meyen, D., Weber, S., et al. (2015). Filopodia-based Wnt transport during vertebrate tissue patterning. *Nat. Commun.* 6:5846.

Stanganello, E., and Scholpp, S. (2016). Role of cytonemes in Wnt transport. *J. Cell Sci.* 129, 665–672. doi: 10.1242/jcs.182469

Suzuki, K., Yamamoto, K., Kariya, Y., Maeda, H., Ishimaru, T., Miyaura, S., et al. (2008). Generation and characterization of a series of monoclonal antibodies that specifically recognize [HexA(± 2S)-GlcNAc]n epitopes in heparan sulfate. *Glycoconj. J.* 25, 703–712. doi: 10.1007/s10719-008-9130-z

Takada, R., Mii, Y., Krayukhina, E., Maruyama, Y., Mio, K., Sasaki, Y., et al. (2018). Assembly of protein complexes restricts diffusion of Wnt3a proteins. *Commun. Biol.* 1:165.

Takada, R., Satomi, Y., Kurata, T., Ueno, N., Norioka, S., Kondoh, H., et al. (2006). Monounsaturated fatty acid modification of Wnt protein: its role in Wnt secretion. *Dev. Cell* 11, 791–801. doi: 10.1016/j.devcel.2006.10.003

Takada, S., Fujimori, S., Shinozuka, T., Takada, R., and Mii, Y. (2017). Differences in the secretion and transport of Wnt proteins. *J. Biochem.* 161, 1–7. doi: 10.1093/jb/mvw071

Takei, Y., Ozawa, Y., Sato, M., Watanabe, A., and Tabata, T. (2004). Three Drosophila EXT genes shape morphogen gradients through synthesis of heparan sulfate proteoglycans. *Development* 131, 73–82. doi: 10.1242/dev.00913

Topczewski, J., Sepich, D. S., Myers, D. C., Walker, C., Amores, A., Lele, Z., et al. (2001). The zebrafish glypican knypek controls cell polarity during gastrulation movements of convergent extension. *Dev. Cell* 1, 251–264. doi: 10.1016/s1534-5807(01)00005-3

van den Born, J., Salmivirta, K., Henttinen, T., Ostman, N., Ishimaru, T., Miyaura, S., et al. (2005). Novel Heparan Sulfate Structures Revealed by Monoclonal Antibodies. *J. Biol. Chem.* 280, 20516–20523. doi: 10.1074/jbc.m502065200

Wang, S., Krinks, M., Lin, K., Luyten, F. P., Moos, M. Jr. (1997). Frzb, a secreted protein expressed in the Spemann organizer, binds and inhibits Wnt-8. *Cell* 88, 757–766. doi: 10.1016/s0092-8674(00)81922-4

Yamamoto, H., Komekado, H., and Kikuchi, A. (2006). Caveolin is necessary for Wnt-3a-dependent internalization of LRP6 and accumulation of beta-catenin. *Dev. Cell* 11, 213–223. doi: 10.1016/j.devcel.2006.07.003

Yan, D., and Lin, X. (2009). Shaping morphogen gradients by proteoglycans. *Cold Spring Harb. Perspect. Biol.* 1:a002493. doi: 10.1101/cshperspect.a002493

Yano, H., Yamamoto-Hino, M., Abe, M., Kuwahara, R., Haraguchi, S., Kusaka, I., et al. (2005). Distinct functional units of the Golgi complex in Drosophila cells. *Proc. Natl Acad. Sci. U.S.A.* 102, 13467–13472. doi: 10.1073/pnas.0506681102

Zhou, S., Lo, W. C., Suhalim, J. L., Digman, M. A., Gratton, E., Nie, Q., et al. (2012). Free extracellular diffusion creates the Dpp morphogen gradient of the Drosophila wing disc. *Curr. Biol.* 22, 668–675. doi: 10.1016/j.cub.2012.02.065

Zittermann, S. I., Capurro, M. I., Shi, W., and Filmus, J. (2010). Soluble glypican 3 inhibits the growth of hepatocellular carcinoma in vitro and in vivo. *Int. J. Cancer* 126, 1291–1301.

Conflict of Interest: The authors declare that the research was conducted in the absence of any commercial or financial relationships that could be construed as a potential conflict of interest.

frontiers in Cell and Developmental Biology

ORIGINAL RESEARCH
published: 14 July 2020
doi: 10.3389/fcell.2020.00599

Heparanase Promotes Syndecan-1 Expression to Mediate Fibrillar Collagen and Mammographic Density in Human Breast Tissue Cultured *ex vivo*

Xuan Huang[1,2,3], Gina Reye[1,2,3], Konstantin I. Momot[1,4], Tony Blick[1,2,3], Thomas Lloyd[5], Wayne D. Tilley[6], Theresa E. Hickey[6], Cameron E. Snell[7,8], Rachel K. Okolicsanyi[1,3,9], Larisa M. Haupt[1,3,9], Vito Ferro[10], Erik W. Thompson[1,2,3†] and Honor J. Hugo[1,2,3*†]*

[1] Institute of Health and Biomedical Innovation, Queensland University of Technology, Kelvin Grove, QLD, Australia, [2] Translational Research Institute, Woolloongabba, QLD, Australia, [3] School of Biomedical Science, Queensland University of Technology, Brisbane, QLD, Australia, [4] Faculty of Science and Engineering, Queensland University of Technology, Brisbane, QLD, Australia, [5] Radiology Department, Princess Alexandra Hospital, Woolloongabba, QLD, Australia, [6] Dame Roma Mitchell Cancer Research Laboratories, Adelaide Medical School, University of Adelaide, Adelaide, SA, Australia, [7] Cancer Pathology Research Group, Mater Research Institute, The University of Queensland, Brisbane, QLD, Australia, [8] Mater Pathology, Mater Hospital Brisbane, South Brisbane, QLD, Australia, [9] Genomics Research Centre, School of Biomedical Sciences, Institute of Health and Biomedical Innovation, Queensland University of Technology, Kelvin Grove, QLD, Australia, [10] School of Chemistry and Molecular Biosciences, The University of Queensland, Brisbane, QLD, Australia

OPEN ACCESS

Edited by:
José Lozano, University of Malaga, Spain

Reviewed by:
Qi Cao, University of Maryland, Baltimore, United States
Wei-Hsiung Yang, Mercer University, United States

***Correspondence:**
Erik W. Thompson
e2.thompson@qut.edu.au
Honor J. Hugo
honor.hugo@qut.edu.au

†These authors share last authorship

Specialty section:
This article was submitted to Signaling, a section of the journal Frontiers in Cell and Developmental Biology

Received: *22 April 2020*
Accepted: *19 June 2020*
Published: *14 July 2020*

Citation:
Huang X, Reye G, Momot KI, Blick T, Lloyd T, Tilley WD, Hickey TE, Snell CE, Okolicsanyi RK, Haupt LM, Ferro V, Thompson EW and Hugo HJ (2020) Heparanase Promotes Syndecan-1 Expression to Mediate Fibrillar Collagen and Mammographic Density in Human Breast Tissue Cultured ex vivo. Front. Cell Dev. Biol. 8:599. doi: 10.3389/fcell.2020.00599

Mammographic density (MD) is a strong and independent factor for breast cancer (BC) risk and is increasingly associated with BC progression. We have previously shown in mice that high MD, which is characterized by the preponderance of a fibrous stroma, facilitates BC xenograft growth and metastasis. This stroma is rich in extracellular matrix (ECM) factors, including heparan sulfate proteoglycans (HSPGs), such as the BC-associated syndecan-1 (SDC1). These proteoglycans tether growth factors, which are released by heparanase (HPSE). MD is positively associated with estrogen exposure and, in cell models, estrogen has been implicated in the upregulation of HPSE, the activity of which promotes SDC expression. Herein we describe a novel measurement approach (single-sided NMR) using a patient-derived explant (PDE) model of normal human (female) mammary tissue cultured *ex vivo* to investigate the role(s) of HPSE and SDC1 on MD. Relative HSPG gene and protein analyses determined in patient-paired high vs. low MD tissues identified SDC1 and SDC4 as potential mediators of MD. Using the PDE model we demonstrate that HPSE promotes SDC1 rather than SDC4 expression and cleavage, leading to increased MD. In this model system, synstatin (SSTN), an SDC1 inhibitory peptide designed to decouple SDC1-ITGαvβ3

parallel collagen alignment, reduced the abundance of fibrillar collagen as assessed by picrosirius red viewed under polarized light, and reduced MD. Our results reveal a potential role for HPSE in maintaining MD via its direct regulation of SDC1, which in turn physically tethers collagen into aligned fibers characteristic of MD. We propose that inhibitors of HPSE and/or SDC1 may afford an opportunity to reduce MD in high BC risk individuals and reduce MD-associated BC progression in conjunction with established BC therapies.

Keywords: mammographic density, breast cancer, heparanase, syndecan-1, NMR

INTRODUCTION

In Australia, mammographic screening reduces mortality by around 50% for screening participants (Roder et al., 2008; Nickson et al., 2012). However, mammographic test sensitivity is impaired in women who have high mammographic density (HMD), where the dense area on the mammogram can mask BC-associated features, contributing to an increase in "interval cancers" that arise within 1–2 years of a "clear" mammogram, and an increase in false negative and false positive screens (Nelson et al., 2016). HMD is therefore an important impediment to effective screening.

After adjusting for age and body mass index (BMI), on a population basis HMD is also one of the strongest risk factors for BC. Breast cancer is currently diagnosed in 1 in 8 Australian women over their lifetime, and accounts for ∼19,500 cases and 3,000 deaths annually (AIHW, 2019), making BC the major cause of female cancer-associated death in Australia. HMD is common; ∼43% of women aged between 40 and 74 have heterogeneously or extremely dense breasts, wherein HMD regions represent greater than 50% of the total area (Sprague et al., 2014). An underappreciated fact is that HMD-associated BC risk is more impactful than other known risk factors, including the BRCA1/2 BC predisposition genes, when considered on a population-wide basis (Hopper, 2015). In addition to increased BC risk, evidence is also emerging that HMD is associated with increased BC recurrence (Hwang et al., 2007; Cil et al., 2009; Shawky et al., 2015, 2019; Huang et al., 2016) and treatment resistance (Elsamany et al., 2015). Thus, interventions that reduce MD may offer new avenues for the prevention, diagnosis and treatment of BC.

A standout molecular feature of HMD is the preponderance of extracellular matrix (ECM), largely comprised of collagen fibers and proteoglycans (PGs), which are carbohydrate-coated proteins (Huo et al., 2014; Shawky et al., 2015). Abnormalities in ECM have been implicated in many pathologies, including cancer (Lu et al., 2012). Importantly, targeting ECM components has proven efficacious for the treatment of some diseases (Jarvelainen et al., 2009; Ferro et al., 2012). In the breast, increased abundance and organization of collagen is associated with HMD (Boyd et al., 2010; Huo et al., 2015; McConnell et al., 2016) and our LMD vs HMD "within breast" comparative data have confirmed that collagen-rich ECM is the most discriminatory feature of HMD (Lin et al., 2011; Huo et al., 2015). Accumulation of collagen can influence mammary malignancy both *in vitro* (Provenzano et al., 2008; Levental et al., 2009) and *in vivo* (Provenzano et al., 2009), and the collagen profile of HMD predicts poor survival in BC (Conklin et al., 2011). Although dense collagen is undoubtedly a major feature of HMD-associated ECM, it forms a scaffold for a wide range of around 350 distinct ECM proteins, collectively called the "Matrisome," which includes many PGs (Naba et al., 2012). HMD stroma has many similarities with BC-associated stroma, where both promote the progression of malignancy. To date, the specific components of HMD ECM that promote BC are unknown. One candidate of interest, SDC1, has been positively associated with both HMD and BC (Shawky et al., 2015). HMD is ∼60% genetically inherited (Boyd et al., 2002), and GWAS studies have identified single nucleotide polymorphisms (SNPs) in several PGs and in PG-modifying enzymes that correlate with increased BC risk (Shawky et al., 2015). In particular, we have identified SDC1 and SDC4 SNPs in BC (Okolicsanyi et al., 2015).

The heparan sulfate proteoglycan (HSPG) family of glycoproteins include membrane bound proteins SDC1 and SDC4, glypican (GPC 1-6), beta-glycan, neuropilin-1 and CD44 (hyaluronic acid receptor), secreted extracellular matrix components (agrin, perlecan, type XVIII collagen), and the secretory vesicle molecule, serglycin (Sarrazin et al., 2011). HSPGs are widely involved in biological activities, including cell signaling, cell adhesion, ECM assembly, and growth factor storage (reviewed in Nagarajan et al., 2018). HSPGs display primarily heparan sulfate-containing glycosaminoglycan (GAG) side chains that bind growth factors, which are in turn released by the action of HPSE (Shawky et al., 2015). This enzyme trims HS GAG chains from HSPGs (including SDC1), allowing the PG core proteins to be cleaved by enzymes such as MMP-9. For SDC1, this results in release from the cell membrane. Furthermore, a positive feedback loop occurs whereby SDC1 shedding stimulates its own expression (Ramani et al., 2012). Shed SDC1 is also taken up by BC cells to promote proliferation (Su et al., 2007), and has been shown to be important in Wnt signaling, contributing to tumorigenesis (Alexander et al., 2000).

HPSE expression strongly correlates with poor survival in BC (Sun et al., 2017) and serum levels of shed SDC1 have been identified to be informative in regards to progression of several cancers including breast (Joensuu et al., 2002; Vassilakopoulos et al., 2005; Szarvas et al., 2016). Shed SDC1 abundance detected in serum has been associated with BC size (Malek-Hosseini et al., 2017), and to be a result of chemotherapy (Ramani and Sanderson, 2014). SDC1 gene expression in BC can be prognostic

(Cui et al., 2017), with its induction in stromal fibroblasts identified in invasive BC (Yang et al., 2011; Vlodavsky et al., 2012). Of relevance to BC, HPSE action to deglycanate SDC1 is essential for the binding of the core protein of SDC1 with lacritin, a protein known to be expressed in the breast, enabling mitogenic signaling (Weigelt et al., 2003; Ma et al., 2006).

Recent data identifying a positive association of HMD with lifetime exposure to estrogens is also a key finding to our understanding of MD in BC (Huo et al., 2015). Estrogen unequivocally promotes MD, as evidenced by data showing alterations of MD with hormone contraceptives, hormone replacement therapy (Greendale et al., 1999; Byrne et al., 2017), menopause (Stone et al., 2009), and treatment with anti-estrogenic drugs (Chew et al., 2014; Shawky et al., 2017). Estrogen also influences cells within the tumor microenvironment, causing immunosuppression (Rothenberger et al., 2018). However, the mechanistic basis of estrogen promotion of MD is, as yet, unknown. Crucially, however, estrogen can directly upregulate HPSE in MCF-7 cells (Elkin et al., 2003; Xu et al., 2007), and thus the E2/HPSE/SDC1 axis has strong potential as the mediator of MD effects on BC through autocrine/paracrine pro-malignant actions.

We hypothesized that estrogen promotes HMD by up-regulating HPSE and SDC1 as part of its pro-oncogenic effects. Using anti-estrogens as well as HSPE inhibitors developed for cancer treatment and in use in clinical trials, and the SDC1 specific inhibitor SSTN, we investigated their effects in patient-derived explants of normal mammary tissue cultured over a 2 week period. Our data identified that MD change was detectable and linked to the estrogen-HPSE-SDC1 axis.

MATERIALS AND METHODS

Patient Cohort

Human breast tissue specimens with no evidence of malignancy, and surplus to pathology needs, were accrued from prophylactic mastectomy surgeries, primarily in women with high BC risk, as determined by family history of breast cancer and/or with contralateral benign or malignant disease. Tissue from patients on recent (<6 months) hormone-based therapies or patients who carried BRCA1/2 mutations were excluded from the study. The demographics of the patients who donated their breast tissue for this study are detailed in **Table 1**. The study was approved by the Metro South Hospital and Health Services, Queensland (HREC/16/QPAH/107). Resected breast tissue was placed on ice and taken to the Pathology Department at the respective hospital, cut into 1–1.5 cm thick slices and checked for lesions. Up to 3 slices were then obtained and used in this project. Some tissues were processed for downstream analyses and some HMD regions were delegated to culture as patient-derived explants.

TABLE 1 | Patient demographics from which tissue was examined for this study.

Patient ID	Age	Menopausal status	BIRADs density score
GPH008M	30	Pre	3
MPRIV015R	29	Pre	1
MPRIV022M	41	Pre	4
PAH001R	41	Pre	2
PAH005M	41	Pre	2
PAH010M	34	Pre	2
PAH021M	23	Pre	1
PAH025M	34	Pre	1
PAH033M	41	Pre	4
907	–	–	–
P15800	–	–	–
MATER004M	–	–	–
UR933036	48	Peri	2
GPH012M	53	Post	2
GPH019M	43	Post	2
PAH032M	48	Post	3
PAH040M	48	Post	4

RNA Extraction and RT-qPCR

RNA was extracted from human breast tissue after homogenization into TRIzol (Ambion, Life Technologies) using Qiagen Tissue Lyser II with metal beads. At the 1:1 isopropanol: sample step, the solution was added to a Bioline RNA extraction column (Catalog no BIO-52075) to purify RNA according to manufacturer's instructions. RT-qPCR was performed as previously described (Hugo et al., 2013). Primer sequences are detailed in **Table 2**.

Immunohistochemistry

Cut sections of HMD vs. LMD, were fixed overnight in 4% paraformaldehyde made up in PBS at 4 degrees, processed to paraffin, sectioned and stained with various primary antibodies (detailed in **Table 3**) on an automated system (Ventana Discovery Ultra, Roche, Switzerland). "Intensity" (as specified on Y axes in **Figures 1A–E**) represents per cent DAB positivity per tissue area, and was determined using ImageJ, where DAB brown positive tissue regions were separated using a Color Deconvolution plugin (H DAB), a threshold applied, and percentage positive area quantified.

Patient-Derived Explants of Normal Breast Tissue

Briefly, ∼2 cm^3 sized pieces of breast tissue excised from high, medium or low MD regions, determined from a slice mammogram by a radiologist (TL), were cut into smaller pieces of ∼0.5 cm^3 in size and placed onto a gelatin sponge scaffold submerged in media inside a well of a 24-well culture plate. Viability of this tissue was then maintained for up to 2 weeks in 24 well plates, submerged in basal media as previously described (Centenera et al., 2018) to sustain tissue viability and hormone responsiveness. For HPSE inhibitor treatment, this basal media comprised of RPMI containing 10% FBS (Thermofisher Scientific, Australia), 1 x penicillin and streptomycin (Merck, Australia), 100 μg/mL hydrocortisone (Merck, Australia) and 100 μg/mL insulin (Merck, Australia) was supplemented either one of the following: 100 μM

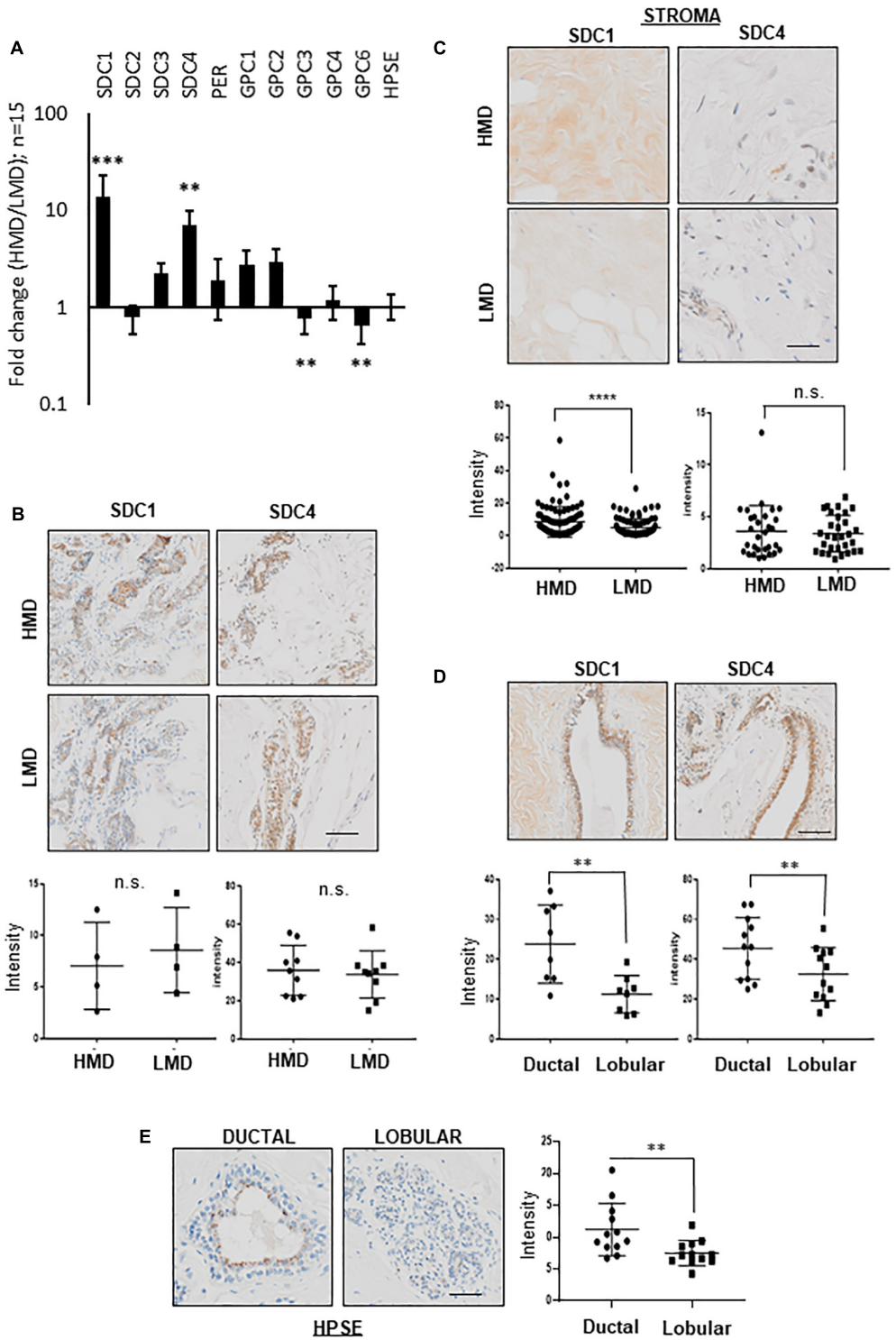

FIGURE 1 | PGs expression in HMD vs. LMD. **(A)** RT-qPCR for various HSPG proteins and HPSE (HPSE) in HMD vs. LMD paired patient tissue. Fold change (HMD/LMD) gene expression from 15 patients, plotted on a logarithmic Y-axis. Delta CT values were obtained using L32 as the housekeeper gene, then converted to ddCT (2^{CT}) for all fold change calculations. Student's paired t test was used to determine significance, where $^{**}p < 0.001$ and $^{***}p < 0.0001$. Significance was achieved after adjustment for multiple testing. **(B)** Assessment of SDC1 and SDC4 protein expression in HMD vs. LMD tissues. Representative IHC images are displayed with intensity data (% DAB positivity per tissue area) plotted underneath. Lobular epithelium, $n = 4$ pairs for SDC1, $n = 9$ pairs for SDC4; **(C)** Stromal regions, $n = 35$ pairs for SDC1, $n = 30$ for SDC4. **(D)** Ductal vs. lobular epithelium (HMD only shown) for SDC1 or SDC4, $n = 8$ pairs for SDC1 and $n = 12$ for SDC4. **(E)** Ductal vs. lobular epithelium (HMD only shown) for HPSE, $n = 12$ pairs analyzed. Student's paired T-test was used to determine significance, where $p < 0.001$ is indicated by ** and $p < 0.0001$ is indicated by ***. All images were captured at 10x magnification, scale bar = 50 μM.

TABLE 2 | Sequences of RT-qPCR primers used in this study.

Gene	Sequence
L32 Fwd	GATCTTGATGCCCAACATTGGTTATG
L32 Rev	GCACTTCCAGCTCCTTGACG
SDC1 Fwd	CTGGGCTGGAATCAGGAATATTT
SDC1 Rev	CCCATTGGATTAAGTAGAGTTTTGC
SDC2 Fwd	AGCTGACAACATCTCGACCACTT
SDC2 Rev	GCGTCGTGGTTTCCACTTTT
SDC3 Fwd	CTTGGTCACACTGCTCATCTATCG
SDC3 Rev	GCATAGAACTCCTCCTGCTTGTC
SDC4 Fwd	CCACGTTTCTAGAGGCGTCACT
SDC4 Rev	CTGTCCAACAGATGGACATGCT
HPSE Fwd	TCACCATTGACGCCAACCT
HPSE Rev	CTTTGCAGAACCCAGGAGGAT
GPC1 Fwd	GGACATCACCAAGCCGGACAT
GPC1 Rev	GTCCACGTCGTTGCCGTTGT
GPC2 Fwd	TGATCAGCCCCAACAGAGAAA
GPC2 Rev	CCACTTCCAACTTCCTTCAAACC
GPC3 Fwd	GATACAGCCAAAAGGCAGCAA
GPC3 Rev	GCCCTTCATTTTCAGCTCATG
GPC4 Fwd	GGTGAACTCCCAGTACCACTTTACA
GPC4 Rev	GCTTCAGCTGCTCCGTATACTTG
GPC6 Fwd	CAGCCTGTGTTAAGCTGAGGTTT
GPC6 Rev	GATGTGTGTGCGTGGAGGTATGT
MMP2 Fwd	CTCCTGACATTGACCTTGGCA
MMP2 Rev	ATCAAGGGCATTCAGGAGCTC
MMP9 Fwd	GGACGGCAATGCTGATGGGAAA
MMP9 Rev	CGCCGCCACGAGGAACAAA
MMP14 Fwd	GCAAAGCTGATGCAGACACCATGAA
MMP14 Rev	CTCTCCCACACGCGGAAC
TFF-1 Fwd	GCAATGGCCACCATGGAGAACAA
TFF-1 Rev	GAGGGCGTGACACCAGGAAAA

TABLE 3 | Primary antibodies used in this study for Immunohistochemistry.

Antigen	Antibody	Dilution	Supplier
SDC1	Monoclonal Rabbit Anti-Human	1:100	Abcam (ab130405)
SDC4	Polyclonal Rabbit Anti-Human	1:100	Abcam (ab24511)
TFF1	Polyclonal Rabbit Anti-human	1:1000	Invitrogen (PA5-31863)
HPSE (Hpa)	Monoclonal Mouse Anti-Human	1:100	ThermoFisher Scientific (MA5-16130)

fondaparinux (sourced from Princess Alexandra Hospital Pharmacy), 100 μM PI-88, 10 μM PG545 control or 10 μM PG545 (provided by V. Ferro). For estrogen (1nM Estradiol, Merck, Australia) and tamoxifen (1 μM 4-hydroxy-tamoxifen, Merck, Australia) treatments, phenol red-free RPMI was supplemented with 10% charcoal-stripped FBS (Thermofisher Scientific, Australia), with all other supplements the same as for the HI experiments. For all treatments, media within 24 well plates was replenished twice weekly.

NMR Measurements

The individual breast explants were removed from the underlying sponge and placed in a well within a dry 24 well plate for Portable NMR measurements. For PG545 and E2 treatments, NMR T1 values of the samples were measured using saturation-recovery pulse sequence on a PM5 NMR-MOUSE instrument (Magritek, Wellington, New Zealand) as previously described (Tourell et al., 2018; Huang et al., 2019). All saturation-recovery curves exhibited mono-exponential recovery. The curves were least-squares fitted with a three-parameter exponential fitting function, and the time constants of the recovery were taken as the respective T1 values. For SSTN treated explants,% water was measured using two approaches: (1) Carr-Purcell-Meiboom-Gill (CPMG) decay followed by an inverse Laplace transform, as described in Ali et al. (2019). This approach yielded T2 relaxation spectra with two peaks (Fat and Water), whose relative areas were taken as the content of the respective chemical component within the tissue; (2) Diffusion NMR measurements followed by two-component least-squares fitting of the diffusion attenuation plot (Huang et al., 2019). The amplitudes of the two components of the fit (Fat and Water) were taken as the content of the respective chemical component within the tissue.

Picrosirius Red (PSR) Staining and Analysis Under Polarized Light

PSR staining of human breast tissues to detect fibrillar collagen (collagen I) was performed as previously described (Kiraly et al., 1997). Quantification of staining was performed using specific ImageJ macros written to identify and quantify red color in PSR-stained sections illuminated with polarized light to visualize thick fibrillar collagens.

ELISA for Shed SDC1 and SDC4 in Explant Media

SDC1 and SDC4 proteins shed into the conditioned media surrounding explanted normal mammary tissue at experimental endpoint (day 14) were quantified using the SDC1 and SDC4 ELISA kits (Raybiotech, United States) according to the manufacturer's instructions, following dilution of the conditioned media 1:4 with the kit dilution buffer.

Statistics

Pearson's r coefficients and respective p-values and the Student's T-test (used to assess the differences in MD changes and gene expression levels between the different treatment groups) were calculated using GraphPad Prism 8.

RESULTS

HMD vs. LMD Pairwise ECM Gene and Protein Expression Analysis

RT-qPCR Data

As shown in **Figure 1**, RT-qPCR assessment of a range of HSPGs showed that mRNA levels of SDC1 and SDC4 were significantly more abundant, 14 and 7-fold higher, respectively, in HMD

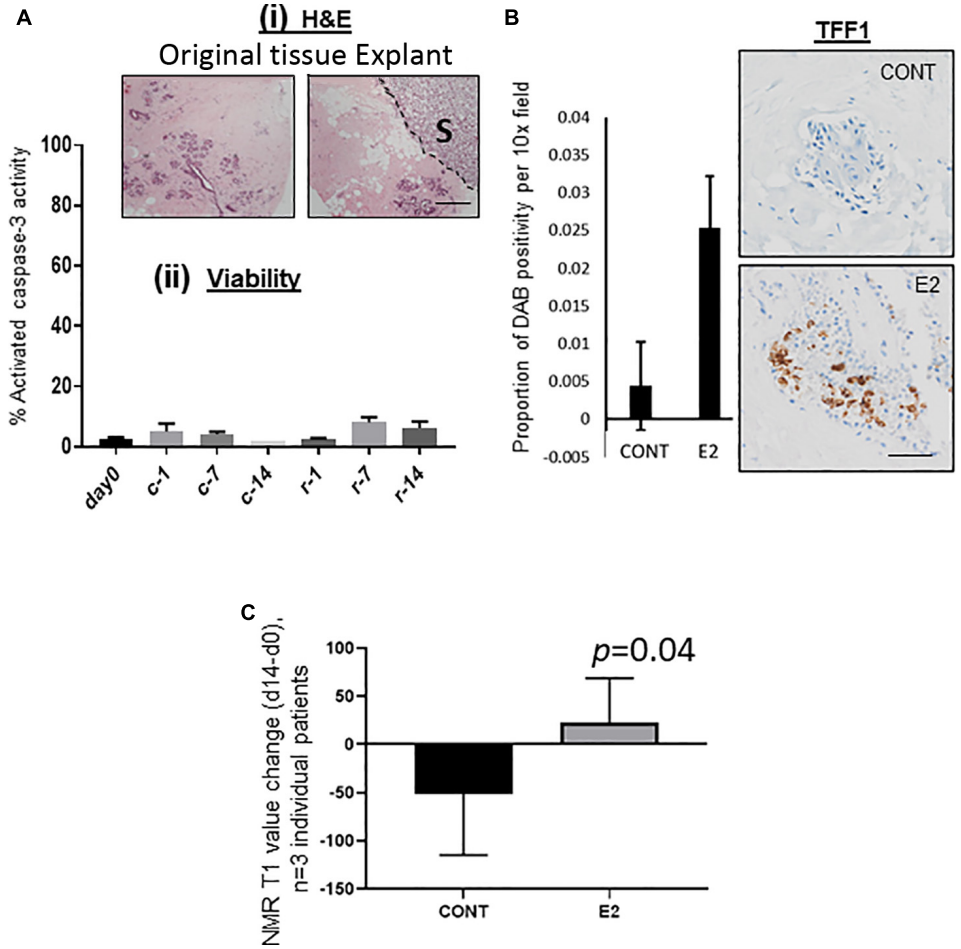

FIGURE 2 | (A) (i) Morphological comparison of original tissue at $t = 0$ and following 14 days as explant culture. S denotes position of the sponge, delineated from the explant tissue by a dotted line. (ii) Viability of explanted tissue up to 14 days as assessed by% activated caspase 3 activity as measured by IHC. C, clear media (Phenol-red free); r, red media (Phenol-red containing). **(B)** 1nM Estradiol treatment of PDEs led to a clear upregulation of the E2-signaling pathway protein TFF-1, images and quantification are typical representative data of 3 individual patients. **(C)** Mammographic density change (d14–d0) in E2 treated mammary tissue explants as measured by the change in NMR T1 values. For part **(C)** only, Student's paired *T*-test was used to determine significance, with *p*-values displayed on graph, $n = 3$ individual patient tissue tested. For all images shown, 10x magnification was used, scale bar = 50 μM.

vs. LMD paired tissue from 15 women. In contrast, levels of GPC3 and GPC6 were significantly decreased by 0.8- and 0.65-fold, respectively. Significance was achieved after adjustment for multiple testing. The proteins coded by these mRNAs are substrates for HPSE. We did not find any difference in HPSE expression between HMD and LMD. Given that increased stroma is characteristic of HMD (Huo et al., 2015), postulated in this study to be driven by HSPG abundance, SDC1 and SDC4 were thus taken forward for further analysis.

Localization of SDC1 and SDC4 in Normal Mammary Tissue

Stromal, not epithelial, localization of SDC1 protein has been implicated in promoting breast density and breast cancer (Lundstrom et al., 2006). Therefore, we performed a detailed IHC investigation of SDC1 and SDC4 PGs in epithelial and stromal compartments of paired HMD vs. LMD tissues (**Figures 1B–E**). No significant difference was observed for epithelial SDC1 or SDC4 protein expression in HMD vs. LMD (**Figure 1B**), however SDC1 expression was higher in stromal regions derived from HMD compared with LMD (**Figure 1C**). This was not observed for SDC4, suggesting SDC1 abundance may drive HMD. Both SDC1 and SDC4 protein levels appeared more abundant in ductal rather than in lobular epithelia, irrespective of MD status (**Figure 1D**). No difference in HMD vs. LMD epithelial vs. stromal regions were observed for HPSE *(data not shown),* however HPSE displayed the same expression pattern as for SDC1 and SDC4 in that it was higher in ductal vs. lobular epithelium (**Figure 1E**).

Establishment of a Patient-Derived Explant Model to Assess MD Change

All published reports that have examined MD change have been longitudinal and in human population cohorts

(Junkermann et al., 2005; Cuzick et al., 2011; Jacobsen et al., 2017). We sought a means to test the effect of exogenous agents on MD in a culture setting using intact mammary tissue, and adopted a whole-tissue explant model (patient-derived explant, PDE), originally designed for the study of human cancers *ex vivo* (Centenera et al., 2018). These original studies describe the culture of cancer tissue for periods of time measured in days, however we hypothesized that to observe any measurable change in density in normal tissue, treatment times would need to be extended to weeks. Initial concern in adopting this extended treatment time was that tissue viability would be compromised. However, as shown in **Figure 2Ai**, morphology of the PDEs after 2 weeks was comparable to tissue at day 0, and we found minimal activated caspase-3 activity in medium MD explant tissue cultured for 2 weeks, indicating that apoptosis was not a major event in these tissues during this time (**Figure 2Aii**).

Increase in MD With Estradiol Treatment of PDEs

We then treated our medium MD PDEs with 1nM estradiol for 14 days, as estrogen is an implicated driver of MD (Greendale et al., 1999; Byrne et al., 2017). After 14 days, we found the estrogen receptor signaling pathway mediator TFF-1 protein to be upregulated in comparison to the control (**Figure 2B**).

We have demonstrated that NMR T1 (and to a lesser extent, T2) values correlate strongly with microCT-derived% HMD in *ex vivo* explants, such that T1 values may be used as a surrogate marker for MD (Huang et al., 2019). We therefore chose to measure T1 as a surrogate marker of MD in our PDE model at $t = 0$ and $t = 14$, to determine MD change. As shown in **Figure 2C**, in all three experiments in which tissue from women was tested, estrogen increased MD change (d14–d0) compared to control treated ($p = 0.04$). In another patient, tamoxifen negated estradiol-mediated MD increases over the experimental period (14 days, **Supplementary Figure S1**).

Coupling of HPSE With SDC1 and SDC4 Induction With ERα Pathway Activation

Since it is known that estrogen upregulates HPSE mRNA (Elkin et al., 2003), that HPSE is a key modulator of both SDC1 and SDC4 abundance in the breast reviewed in Sarrazin et al. (2011), and that cleavage of SDC1 leads to SDC1 mRNA induction (Ramani et al., 2012), we investigated whether the E2-HPSE-SDC1 axis could be relevant in our human mammary tissue explants. As shown in **Figure 3A**, significant correlations were observed for both SDC1 and SDC4 with HPSE in E2-treated explants. Each of the data points shown in this Figure represent the average of 3 explants from 1 patient (independent biological replicates), and in **Figure 3A**, data from 8 individual patients was analyzed. The correlation observed in **Figure 3A** was lost when tissue explants were either treated with tamoxifen alone (**Figure 3B**) or co-treated with E2 and tamoxifen (**Figure 3C**), where 6 individual patient's explant tissue was examined. Furthermore, HPSE protein was found to be more abundant in E2-treated PDEs (**Supplementary Figure S2A**). These findings suggest a coupling of HPSE with SDC1 and SDC4 induction where the ERα pathway was activated, however, further studies with larger numbers are required to confirm this, including a more thorough examination of *in vitro* and *in vivo* tissues.

Effect of HPSE Inhibition in PDEs

Given that we were able to detect an increase in MD in the PDE model with estradiol, and that HPSE regulation of SDC may be implicated in mediating this change, we decided to use the PDE model to inhibit HPSE specifically and assess the effect on MD and gene expression outputs.

HPSE Inhibition Reduced MD

We examined the effect of the HS mimetic PG545 (Chhabra and Ferro, 2020) in the PDEs for the same period of time as for estradiol (14 days). IHC assessment of HPSE revealed that it was predominantly located around glandular epithelia, and 10 μM PG545 led to the strongest proportional reduction in peri-glandular HPSE protein content (**Supplementary Figure S1A**). Therefore, 10 μM was used in further studies. As shown in **Figure 4A**, in all three experiments in which breast tissue from women was tested, PG545 decreased MD relative to the respective control, as indicated by NMR T1 change (d14–d0, $p = 0.02$).

Gene Expression Changes Following HPSE Inhibitor Treatment in PDEs

Analysis of the effects of HPSE inhibition on various HSPG mRNA levels in explanted tissue at endpoint (14d) by RT-qPCR revealed a significant reduction in SDC1 expression, but not in SDC4 or other HSPGs (**Figure 4B** and **Supplementary Figure S3**), again indicating a complex transcriptional interplay between HSPG and SDC1. Given that HPSE activity has also been shown to positively influence MMP14 expression (Gomes et al., 2015) and is associated with MMP9 (Abu El-Asrar et al., 2016) we also examined MMP expression in the control vs. treated tissues. Of the MMPs that displayed expression above baseline (MMP-2, -9 and -14), MMP2 and MMP14 showed a significant increase after HPSE inhibitor (HI) treatment (**Figure 4B**).

Effect of HPSE Inhibitor Treatment on Shed SDC1 and SDC4

The abundance of SDC1 or SDC4 protein was examined in the conditioned media of PDEs at $t = 14$, as an indicator of HPSE activity, given that the form of the protein detected by this means has been shed from the cell membrane (Yang et al., 2007).

As shown in **Figure 4C**, there was, on average, 2 to 8-fold more SDC1 than SDC4 protein shed into the media, and only SDC1 displayed a significant reduction in abundance with HPSE inhibition ($p < 0.05$).

SDC1-Specific Inhibition Using SSTN Reduced Fibrillar Collagen and MD

Given that gene expression and shedding for SDC1 (but not SDC4) was significantly reduced with heparanase inhibition, we hypothesized that SDC1 was mediating the observed MD change shown in **Figure 4A**. But how could SDC1 mediate MD? McConnell and colleagues found that peri-ductally aligned collagen is correlated with MD (McConnell et al., 2016), and

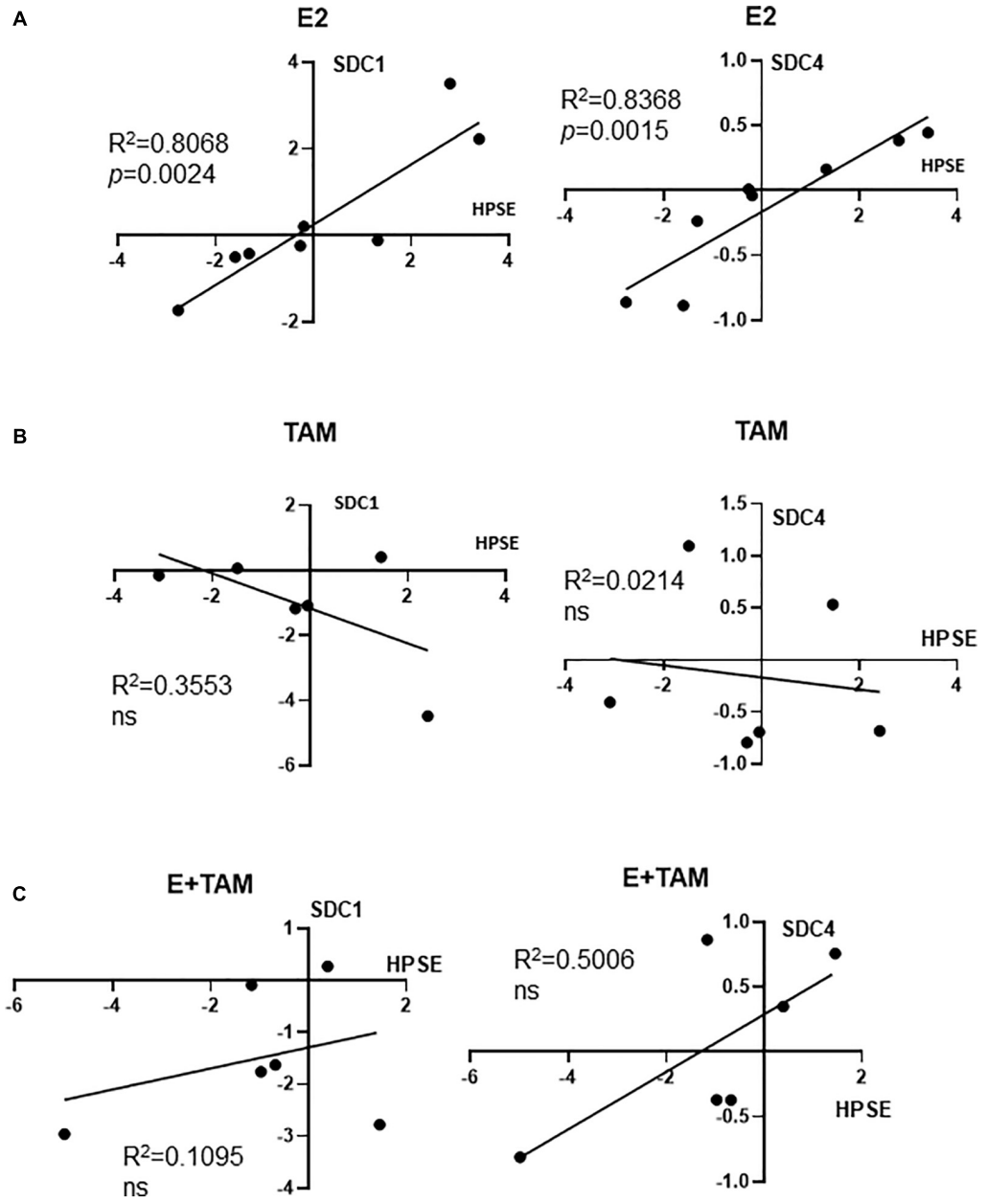

FIGURE 3 | RT-qPCR data from hormone treated explants: Correlation of HPSE with SDC1 or SDC4 in E2 **(A)**, Tamoxifen **(B)**, and E2 + Tamoxifen **(C)** treated explants. Expression data shown is normalized to control-treated explant mRNA control (ddCT). Each data point represents the average expression from 3 explants from 1 patient, where $n = 8$ for part **(A)**, $n = 6$ for parts **(B,C)**. Pearson's r coefficient is shown and where p-values stated where $p < 0.05$; ns, not significant.

a direct role for membrane-bound SDC1 in physically aligning collagen fibers has been described (Yang and Friedl, 2016). We therefore decided to interrogate the connection between SDC1 and collagen and MD in our PDE model.

SSTN is a peptide designed and validated to block SDC1-binding to ITGαvβ3, and hence ITGαvβ3 binding to peri-ductal collagen, but also with Insulin-like growth factor 1 receptor (IGF1R) (Rapraeger, 2013). First, we validated its effectiveness in our own hands to block MDA-MB-231 breast cancer cell binding to vitronectin, an interaction that specifically requires SDC1-ITGαvβ3 complexes. As shown in **Supplementary Figure S4**, 30 μM of SSTN reduced MDA-MB-231 cell binding and this concentration was therefore carried forward into our PDE experiments.

As shown in **Figure 5A**, SSTN significantly decreased MD relative to the respective control, as indicated by% water change determined by NMR (d14–d0, $n = 3$ individual patients, $p = 0.02$). PSR staining enhances the natural birefringence of collagen bundles. When visualized under polarized light, PSR-stained collagen I appears red while

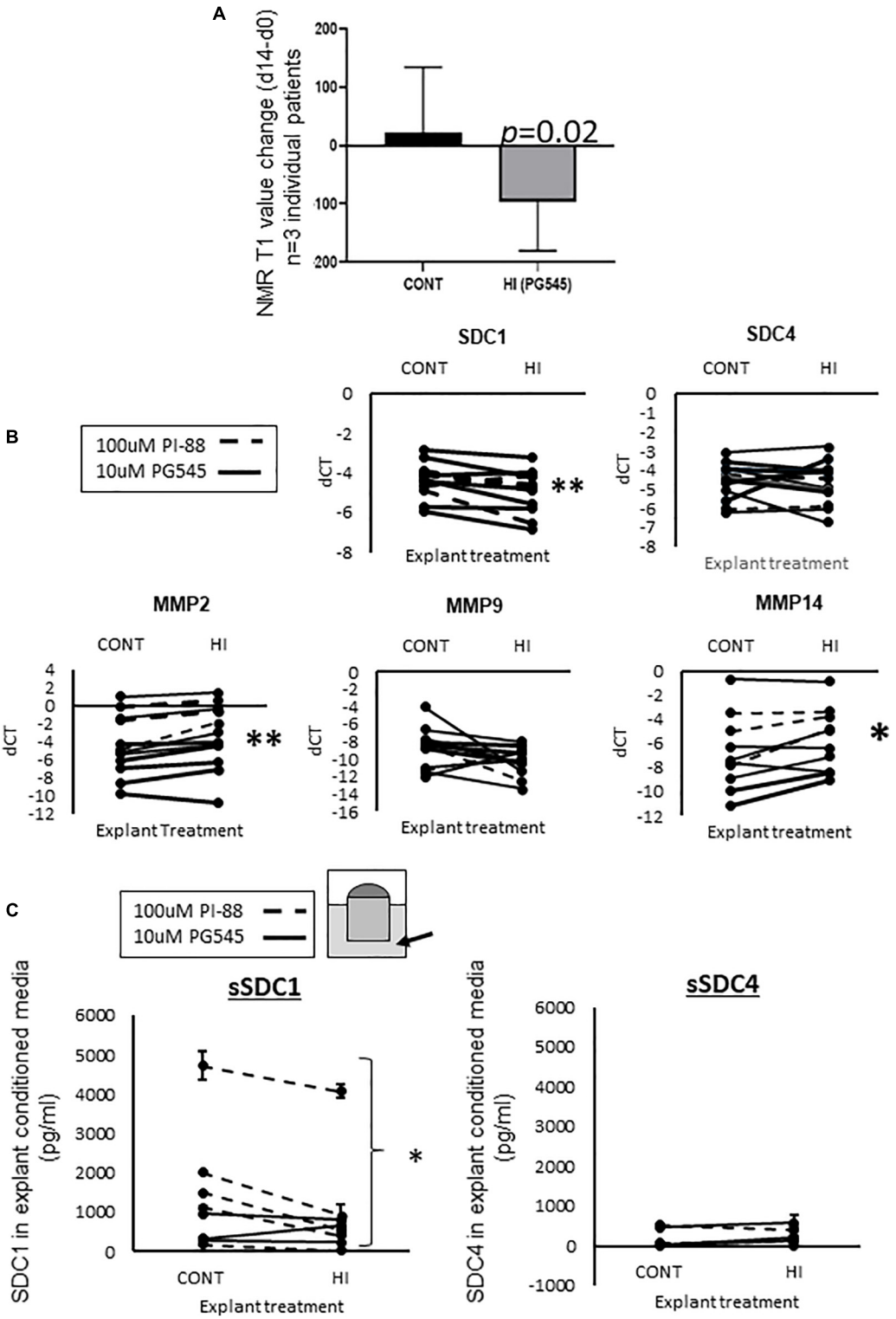

FIGURE 4 | (A) MD change (d14–d0) in PG545 treated mammary tissue explants as measured by the change in NMR T1 values, Student's paired *T*-test was used to determine significance, with *p*-values displayed on graph, $n = 3$ individual patient tissue tested. **(B)** RT-qPCR data from HI treated explants. Dotted line denotes 100 μM PI-88 treated explants, where control is 100 μM Fondaparinux; solid line denotes 10 μM PG545 treatment, where control is media alone. More gene expression data is found in **Supplementary Figure S3**. Delta CT values are plotted, determined using using L32 as the housekeeper gene. **(C)** Inhibition of HPSE led to a decrease in the abundance of shed SDC1 in explant conditioned media (Student's paired *T*-test used to determine significance, *denotes $p < 0.05$). Dotted line: PI-88, solid line: PG545. For SDC1, $n = 8$ pairs, for SDC4, $n = 6$.

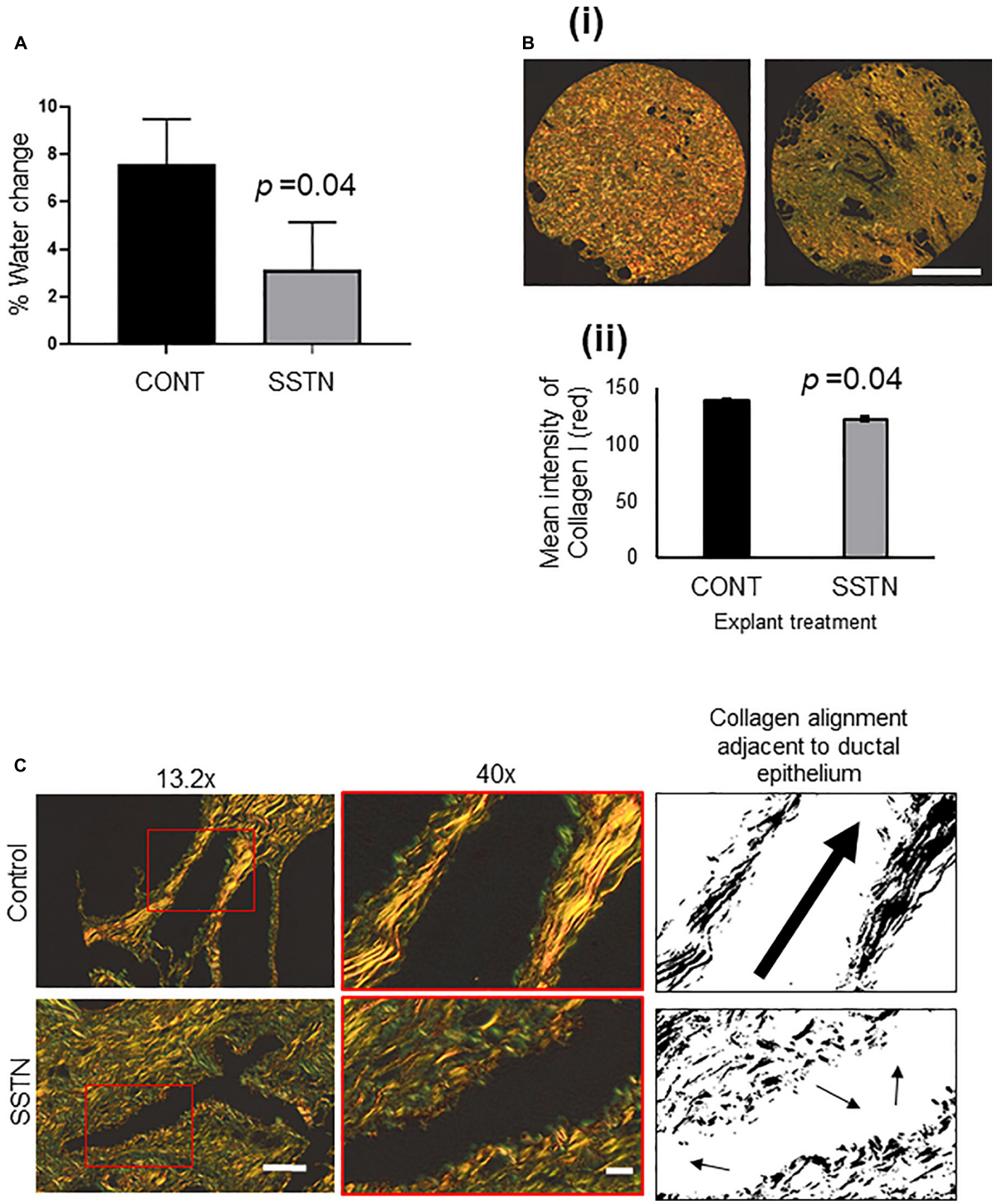

FIGURE 5 | (A) MD change (d14–d0) in SSTN treated mammary tissue explants as measured by the change in % water diffusion values as determined by single-sided NMR. **(B)** (i) Picrosirius red staining of PDE tissue microarray and imaging with polarized light to visualize dense collagen fibers; (ii) quantification of dense collagen represented as the mean intensity of red fibers visualized by polarized light (data from $n = 3$ patients, 3 explants quantified per patient). Results are the mean and error bars represent standard error. *P*-value was determined using Student's paired *T*-test. Images captured at 4x magnification, scale bar = 200 mm. **(C)** Picrosirius red images, enlarged region of image on left is within red box, then black and white thresholded image to highlight changes to alignment of collagen adjacent to ductal epithelium after treatment with Synstatin. Images captured at 13.2 × magnification, scale bar = 100 μM, 40 × magnification, scale bar = 20 μM.

collagen III appears green, and thus PSR staining can be used to determine collagen I/III content (Vogel et al., 2015). SSTN led to a visible reduction in dense collagen, or fibrillar collagen content, as measured by PSR visualized under polarized light (**Figure 5Bi,ii**). Upon closer inspection, the arrangement of collagen adjacent to ductal epithelium in SSTN treated explants exhibited reduced alignment compared to the control (**Figure 5C**).

DISCUSSION

We show for the first time that MD change can be measured *ex vivo*. This significant finding has enabled a dissection of molecules involved in the maintenance of MD. Our studies illustrate a key role for HPSE in maintaining MD, with SDC1 and possibly SDC4 implicated in this process. We have previously shown that stroma is the key differentiator between high vs. low MD (Huo et al., 2015), and we show in the current study that SDC1 and -4 are both more abundant in HMD vs. LMD (**Figure 1A**), and that SDC1, but not SDC-4, was more abundant in the HMD stroma (**Figure 1C**). Although the E2-HPSE-SDC induction pathway induced SDC1 and 4 in a relatively equal manner (**Figure 3A**), in HPSE inhibitor-treated explant tissue, SDC1, but not SDC4, gene expression was significantly reduced (**Figure 4B**), and shedding of SDC1, but not SDC4, was reduced (**Figure 4C**). Finally, our results indicate that fibrillar collagen is important in the maintenance of MD, and that SDC1 plays a direct role in mediating this effect, as SSTN reduced MD and fibrillar collagen abundance (**Figure 5**).

Despite both SDC1 and SDC4 mRNA being more abundant in HMD vs. LMD (**Figure 1A**), HPSE modulation had a more significant, and hence functional effect on SDC1 rather than SDC4. Interestingly, SDC1 (not SDC4) is implicated in both MD and BC (reviewed in Shawky et al. (2015) where SDC1 is informative as to BC staging (Cui et al., 2017). Our work highlights that SDC1 may be a key molecular target in efforts to reduce mammographic density as a means to reduce the associated BC risk.

Shed SDC1 has a number of potential effects in promoting tumorigenesis: growth factors bound to the extracellular domain can be carried into the nucleus and potentiate proliferation (Stewart et al., 2015) and also increase wnt signaling (Alexander et al., 2000). HPSE induces SDC4 shedding, as we observed in the conditioned medium of our PDEs (**Figure 4C**), however the pathological significance of SDC4 shedding is in cardiac disease (Strand et al., 2015). Given that shed SDC1 in the serum is a prognostic factor in several cancers (Joensuu et al., 2002; Vassilakopoulos et al., 2005; Szarvas et al., 2016) it is likely that there are several other pro-tumorigenic effects of shed SDC1 into the microenvironment that are yet to be discovered. SDC1 shedding itself increases SDC1 expression in the cell (Ramani et al., 2012), but may also increase SDC1 expression in neighboring cells, such as fibroblasts in the stroma, a mechanism through which stromal SDC1, particularly in HMD, may be potentiated, as we have observed (**Figure 1C**).

We found that SDC1, SDC4, and HPSE were significantly more abundant in ductal epithelium compared with lobular epithelium (**Figures 1D,E**). The basis of this expression pattern is not clear, however, it may be related to differing mechanical pressure placed on ductal vs. lobular epithelia. McConnell and colleagues (McConnell et al., 2016) found significant correlations between MD and localized PSR enhanced collagen birefringence located around breast ducts ($R^2 = 0.86$, $p < 0.0001$), but not around lobules or within distal stromal regions ($R^2 = 0.1$, $p = 0.33$; $R^2 = 0.24$, $p = 0.14$, respectively). The presence of this restrictive collagen lining may create a greater force on the cells underlying it. In the same way that increased load in cartilage due to exercise leads to an increase in proteoglycan content (Bird et al., 2000), perhaps this force is responsible for the observed SDC1 and SDC4 expression patterns. Indeed, we see the expression of all syndecan family members increase in human mammary epithelial cells cultured on stiff vs. soft 2D surfaces (6 kPa vs. 400 Pa, *unpublished observations*).

We observed an increase in MMP2 and MMP14 in HPSE inhibitor treated explants (**Figure 4B**). Similarly, HPSE knockout mice have been reported to display an upregulation of MMP2 and MMP14, where these metalloproteinases are thought to compensate for the loss of HPSE (Zcharia et al., 2009). Although decreased, SDC1 shedding was not eliminated in HPSE inhibitor-treated explants (**Figure 4C**). In light of the Zcharia study (Zcharia et al., 2009), this suggests that some SDC1 shedding was possible in the HPSE inhibitor-treated explants due to a MMP2 and -14 compensatory mechanism.

This study has demonstrated that the HPSE inhibitors PG545 and PI-88 are useful to interrogate the mechanistic effects of HPSE in tissue samples on MD. However, these inhibitors have undesirable anti-angiogenic and other off-target effects when used systemically (Chhabra and Ferro, 2020) and thus are unlikely MD-reducing agents to take forward to clinical trials. Tamoxifen reduces MD (Shawky et al., 2017), however, its long-term use is associated with a wide range of potential side effects, some of which are intolerable (Thorneloe et al., 2020). Both of these approaches are therefore potentially not feasible for MD reduction, although their mechanism of action provides important insight into how MD is governed, as our work alludes to, via the action of HPSE. We have uncovered a more targeted approach to MD reduction, discovered by teasing apart the connection between SDC1 and collagen. We believe this work will pave the way forward for other kinds of targeted approaches to be developed with aim to reduce MD and thus breast cancer risk.

DATA AVAILABILITY STATEMENT

All datasets presented in this study are included in the article/**Supplementary Material**.

ETHICS STATEMENT

The studies involving human participants were reviewed and approved by the Metro South Hospital and Health Services,

Queensland (HREC/16/QPAH/107). The patients/participants provided their written informed consent to participate in this study.

AUTHOR CONTRIBUTIONS

HH and ET equally conceived the study design and managed its progress. XH, GR, and HH obtained human breast tissue from respective Pathology Departments of the Princess Alexandra Hospital and Mater Private Hospital and set up human breast tissue explants for 2 week culture. XH and HH maintained explant cultures, performed gene expression and together with GR, performed IHC intensity quantification. HH performed ELISA for SDC1 and SDC4. XH and KM obtained NMR T1 measurements and KM performed analyses on this data. CS provided advice on estradiol concentrations and signaling outputs. RO performed RT-qPCR data for **Figure 1A**. TB provided input as to the correct statistical method to use. TL assessed breast tissue slice mammograms, and determined valid areas of HMD vs. LMD for excision. WT and TH provided hormonal reagents and technical advice on explant culture. LH provided HSPG primers and antibodies and advice in IHC interpretation. VF provided HPSE inhibitors used in explant culture, and advice in concentration optimization. All authors reviewed the manuscript prior to submission.

FUNDING

This research was supported by the Princess Alexandra Hospital Research Foundation (PARF) Research Innovation Award (2018–2020).

ACKNOWLEDGMENTS

We thank the Translational Research Institute Histology Core for performing IHC contained in this manuscript, but also Dr. Jason Northey for sharing the code he wrote for ImageJ to enable quantification of picrosirius red images for collagen I content. We thank Ms. Gillian Jagger for her central role in recruiting, obtaining consent and co-ordinating the collection of breast tissue from the study participants. Finally, we thank the ladies who donated their tissue that enabled this study be performed.

SUPPLEMENTARY MATERIAL

The Supplementary Material for this article can be found online at: https://www.frontiersin.org/articles/10.3389/fcell.2020.00599/full#supplementary-material

FIGURE S1 | (A) Dilution series (0–20 μM) of the heparan sulfate mimetic (heparanase inhibitor) PG545 and its effect on HPSE protein abundance, after 14 days treatment, as determined by IHC. Magnification 10x, scale bar = 50 μM. (B) Percentage water diffusion change data from 1 patient showing that the combination of tamoxifen with estrogen ameliorated MD increase over the treatment period (14 days).

FIGURE S2 | HPSE protein abundance as measured by IHC in A. PI-88 (HPSE inhibitor) and B. E2 treated explants.% DAB positivity was quantified from at least 5 10x microscope fields. Magnification 10x, scale bar = 50 μM.

FIGURE S3 | (A) RT-qPCR data derived from HI treated explants for the various other HSPG family members where no change in expression was observed.

FIGURE S4 | MDA MB 231 adherence to two-dimensional, Vitronectin coated substrates in the presence of increasing concentration of the SDC1 inhibitor SSTN. **(A)** Cellular morphology and **(B)** Percentage adherence calculations from images shown in **(A)**. Magnification 20x, scale bar = 50 μM.

REFERENCES

Abu El-Asrar, A. M., Siddiquei, M. M., Nawaz, M. I, De Hertogh, G., Mohammad, G., Alam, K., et al. (2016). Coexpression of heparanase activity, cathepsin L, tissue factor, tissue factor pathway inhibitor, and MMP-9 in proliferative diabetic retinopathy. *Mol. Vis.* 22, 424–435.

AIHW (2019). *Cancer In Australia*. Canberra: AIHW.

Alexander, C. M., Reichsman, F., Hinkes, M. T., Lincecum, J., Becker, K. A., Cumberledge, S., et al. (2000). Syndecan-1 is required for Wnt-1-induced mammary tumorigenesis in mice. *Nat. Genet.* 25, 329–332. doi: 10.1038/77108

Ali, T. S., Tourell, M. C., Hugo, H. J., Pyke, C., Yang, S., Lloyd, T., et al. (2019). Transverse relaxation-based assessment of mammographic density and breast tissue composition by single-sided portable NMR. *Magn. Reson. Med.* 82, 1199–1213.

Bird, J. L., Platt, D., Wells, T., May, S. A., and Bayliss, M. T. (2000). Exercise-induced changes in proteoglycan metabolism of equine articular cartilage. *Equine Vet. J.* 32, 161–163. doi: 10.2746/042516400777591624

Boyd, N. F., Dite, G. S., Stone, J., Gunasekara, A., English, D. R., McCredie, M. R., et al. (2002). Heritability of mammographic density, a risk factor for breast cancer. *N. Engl. J. Med.* 347, 886–894.

Boyd, N. F., Martin, L. J., Bronskill, M., Yaffe, M. J., Duric, N., and Minkin, S. (2010). Breast tissue composition and susceptibility to breast cancer. *J. Natl. Cancer Inst.* 102, 1224–1237.

Byrne, C., Ursin, G., Martin, C. F., Peck, J. D., Cole, E. B., Zeng, D., et al. (2017). Mammographic density change with estrogen and progestin therapy and breast cancer risk. *J. Natl. Cancer Inst.* 109:djx001.

Centenera, M. M., Hickey, T. E., Jindal, S., Ryan, N. K., Ravindranathan, P., Mohammed, H., et al. (2018). A patient-derived explant (PDE) model of hormone-dependent cancer. *Mol. Oncol.* 12, 1608–1622. doi: 10.1002/1878-0261.12354

Chew, G. L., Huo, C. W., Huang, D., Blick, T., Hill, P., Cawson, J., et al. (2014). Effects of Tamoxifen and oestrogen on histology and radiographic density in high and low mammographic density human breast tissues maintained in murine tissue engineering chambers. *Breast Cancer Res. Treat.* 148, 303–314. doi: 10.1007/s10549-014-3169-2

Chhabra, M., and Ferro, V. (2020). "PI-88 and related heparan sulfate mimetics," in *Heparanase: From Basic Research to Clinical Applications*, eds I. Vlodavsky, R. D. Sanderson, and N. Ilan (Cham: Springer).

Cil, T., Fishell, E., Hanna, W., Sun, P., Rawlinson, E., Narod, S. A., et al. (2009). Mammographic density and the risk of breast cancer recurrence after breast-conserving surgery. *Cancer* 115, 5780–5787. doi: 10.1002/cncr.24638

Conklin, M. W., Eickhoff, J. C., Riching, K. M., Pehlke, C. A., Eliceiri, K. W., Provenzano, P. P., et al. (2011). Aligned collagen is a prognostic signature for survival in human breast carcinoma. *Am. J. Pathol.* 178, 1221–1232. doi: 10.1016/j.ajpath.2010.11.076

Cui, X., Jing, X., Yi, Q., Long, C., Tian, J., and Zhu, J. (2017). Clinicopathological and prognostic significance of SDC1 overexpression in breast cancer. *Oncotarget* 8, 111444–111455. doi: 10.18632/oncotarget.22820

Cuzick, J., Warwick, J., Pinney, E., Duffy, S. W., Cawthorn, S., Howell, A., et al. (2011). Tamoxifen-induced reduction in mammographic density and breast

cancer risk reduction: a nested case-control study. *J. Natl. Cancer Inst.* 103, 744–752. doi: 10.1093/jnci/djr079

Elkin, M., Cohen, I., Zcharia, E., Orgel, A., Guatta-Rangini, Z., Peretz, T., et al. (2003). Regulation of heparanase gene expression by estrogen in breast cancer. *Cancer Res.* 63, 8821–8826.

Elsamany, S., Alzahrani, A., Abozeed, W. N., Rasmy, A., Farooq, M. U., Elbiomy, M. A., et al. (2015). Mammographic breast density: predictive value for pathological response to neoadjuvant chemotherapy in breast cancer patients. *Breast* 24, 576–581. doi: 10.1016/j.breast.2015.05.007

Ferro, V., Liu, L., Johnstone, K. D., Wimmer, N., Karoli, T., Handley, P., et al. (2012). Discovery of PG545: a highly potent and simultaneous inhibitor of angiogenesis, tumor growth, and metastasis. *J. Med. Chem.* 55, 3804–3813. doi: 10.1021/jm201708h

Gomes, A. M., Bhat, R., Correia, A. L., Mott, J. D., Ilan, N., Vlodavsky, I., et al. (2015). Mammary branching morphogenesis requires reciprocal signaling by heparanase and MMP-14. *J. Cell. Biochem.* 116, 1668–1679. doi: 10.1002/jcb.25127

Greendale, G. A., Reboussin, B. A., Sie, A., Singh, H. R., Olson, L. K., Gatewood, O., et al. (1999). Effects of estrogen and estrogen-progestin on mammographic parenchymal density. postmenopausal estrogen/progestin interventions (PEPI) investigators. *Ann. Intern. Med.* 130(4 Pt 1), 262–269.

Hopper, J. L. (2015). Odds per adjusted standard deviation: comparing strengths of associations for risk factors measured on different scales and across diseases and populations. *Am. J. Epidemiol.* 182, 863–867. doi: 10.1093/aje/kwv193

Huang, X., Ali, T. S., Nano, T., Blick, T., Tse, B. W., Sokolowski, K., et al. (2019). Quantification of breast tissue density: correlation between single-sided portable NMR and micro-CT measurements. *Magn. Reson. Imaging* 62, 111–120. doi: 10.1016/j.mri.2019.06.006

Huang, Y. S., Chen, J. L., Huang, C. S., Kuo, S. H., Jaw, F. S., Tseng, Y. H., et al. (2016). High mammographic breast density predicts locoregional recurrence after modified radical mastectomy for invasive breast cancer: a case-control study. *Breast Cancer Res.* 18:120.

Hugo, H. J., Pereira, L., Suryadinata, R., Drabsch, Y., Gonda, T. J., Gunasinghe, N. P., et al. (2013). Direct repression of MYB by ZEB1 suppresses proliferation and epithelial gene expression during epithelial-to-mesenchymal transition of breast cancer cells. *Breast Cancer Res.* 15:R113.

Huo, C. W., Chew, G., Hill, P., Huang, D., Ingman, W., Hodson, L., et al. (2015). High mammographic density is associated with an increase in stromal collagen and immune cells within the mammary epithelium. *Breast Cancer Res.* 17:79.

Huo, C. W., Chew, G. L., Britt, K. L., Ingman, W. V., Henderson, M. A., Hopper, J. L., et al. (2014). Mammographic density-a review on the current understanding of its association with breast cancer. *Breast Cancer Res. Treat.* 144, 479–502. doi: 10.1007/s10549-014-2901-2

Hwang, E. S., Miglioretti, D. L., Ballard-Barbash, R., Weaver, D. L., and Kerlikowske, K. (2007). Association between breast density and subsequent breast cancer following treatment for ductal carcinoma in situ. *Cancer Epidemiol. Biomarkers. Prev.* 16, 2587–2593. doi: 10.1158/1055-9965.epi-07-0458

Jacobsen, K. K., Lynge, E., Tjonneland, A., Vejborg, I., von Euler-Chelpin, M., and Andersen, Z. J. (2017). Alcohol consumption and mammographic density in the Danish Diet, Cancer and Health cohort. *Cancer Causes Control* 28, 1429–1439. doi: 10.1007/s10552-017-0970-3

Jarvelainen, H., Sainio, A., Koulu, M., Wight, T. N., and Penttinen, R. (2009). Extracellular matrix molecules: potential targets in pharmacotherapy. *Pharmacol. Rev.* 61, 198–223. doi: 10.1124/pr.109.001289

Joensuu, H., Anttonen, A., Eriksson, M., Makitaro, R., Alfthan, H., Kinnula, V., et al. (2002). Soluble syndecan-1 and serum basic fibroblast growth factor are new prognostic factors in lung cancer. *Cancer Res.* 62, 5210–5217.

Junkermann, H., von Holst, T., Lang, E., and Rakov, V. (2005). Influence of different HRT regimens on mammographic density. *Maturitas* 50, 105–110. doi: 10.1016/j.maturitas.2004.04.008

Kiraly, K., Hyttinen, M. M., Lapvetelainen, T., Elo, M., Kiviranta, I., Dobai, J., et al. (1997). Specimen preparation and quantification of collagen birefringence in unstained sections of articular cartilage using image analysis and polarizing light microscopy. *Histochem. J.* 29, 317–327.

Levental, K. R., Yu, H., Kass, L., Lakins, J. N., Egeblad, M., Erler, J. T., et al. (2009). Matrix crosslinking forces tumor progression by enhancing integrin signaling. *Cell* 139, 891–906. doi: 10.1016/j.cell.2009.10.027

Lin, S. J., Cawson, J., Hill, P., Haviv, I., Jenkins, M., Hopper, J. L., et al. (2011). Image-guided sampling reveals increased stroma and lower glandular complexity in mammographically dense breast tissue. *Breast Cancer Res. Treat.* 128, 505–516. doi: 10.1007/s10549-011-1346-0

Lu, P., Weaver, V. M., and Werb, Z. (2012). The extracellular matrix: a dynamic niche in cancer progression. *J. Cell Biol.* 196, 395–406. doi: 10.1083/jcb.201102147

Lundstrom, E., Sahlin, L., Skoog, L., Hagerstrom, T., Svane, G., Azavedo, E., et al. (2006). Expression of Syndecan-1 in histologically normal breast tissue from postmenopausal women with breast cancer according to mammographic density. *Climacteric* 9, 277–282. doi: 10.1080/13697130600865741

Ma, P., Beck, S. L., Raab, R. W., McKown, R. L., Coffman, G. L., Utani, A., et al. (2006). Heparanase deglycanation of syndecan-1 is required for binding of the epithelial-restricted prosecretory mitogen lacritin. *J. Cell Biol.* 174, 1097–1106. doi: 10.1083/jcb.200511134

Malek-Hosseini, Z., Jelodar, S., Talei, A., Ghaderi, A., and Doroudchi, M. (2017). Elevated Syndecan-1 levels in the sera of patients with breast cancer correlate with tumor size. *Breast Cancer* 24, 742–747. doi: 10.1007/s12282-017-0773-0

McConnell, J. C., O'Connell, O. V., Brennan, K., Weiping, L., Howe, M., Joseph, L., et al. (2016). Increased peri-ductal collagen micro-organization may contribute to raised mammographic density. *Breast Cancer Res.* 18:5.

Naba, A., Clauser, K. R., Hoersch, S., Liu, H., Carr, S. A., and Hynes, R. O. (2012). The matrisome: in silico definition and in vivo characterization by proteomics of normal and tumor extracellular matrices. *Mol. Cell. Proteomics* 11:M111014647. doi: 10.1016/j.matbio.2017.07.001

Nagarajan, A., Malvi, P., and Wajapeyee, N. (2018). Heparan sulfate and heparan sulfate proteoglycans in cancer initiation and progression. *Front. Endocrinol.* 9:483. doi: 10.3389/fendo.2018.00483

Nelson, H. D., O'Meara, E. S., Kerlikowske, K., Balch, S., and Miglioretti, D. (2016). Factors associated with rates of false-positive and false-negative results from digital mammography screening: an analysis of registry data. *Ann. Intern. Med.* 164, 226–235.

Nickson, C., Mason, K. E., English, D. R., and Kavanagh, A. M. (2012). Mammographic screening and breast cancer mortality: a case-control study and meta-analysis. *Cancer Epidemiol. Biomarkers. Prev.* 21, 1479–1488. doi: 10.1158/1055-9965.epi-12-0468

Okolicsanyi, R. K., Buffiere, A., Jacinto, J. M., Chacon-Cortes, D., Chambers, S. K., Youl, P. H., et al. (2015). Association of heparan sulfate proteoglycans SDC1 and SDC4 polymorphisms with breast cancer in an Australian Caucasian population. *Tumour Biol.* 36, 1731–1738. doi: 10.1007/s13277-014-2774-3

Provenzano, P. P., Eliceiri, K. W., and Keely, P. J. (2009). Multiphoton microscopy and fluorescence lifetime imaging microscopy (FLIM) to monitor metastasis and the tumor microenvironment. *Clin. Exp. Metastasis* 26, 357–370. doi: 10.1007/s10585-008-9204-0

Provenzano, P. P., Inman, D. R., Eliceiri, K. W., Knittel, J. G., Yan, L., Rueden, C. T., et al. (2008). Collagen density promotes mammary tumor initiation and progression. *BMC Med.* 6:11. doi: 10.1186/1741-7015-6-11

Ramani, V. C., Pruett, P. S., Thompson, C. A., DeLucas, L. D., and Sanderson, R. D. (2012). Heparan sulfate chains of syndecan-1 regulate ectodomain shedding. *J. Biol. Chem.* 287, 9952–9961. doi: 10.1074/jbc.m111.330803

Ramani, V. C., and Sanderson, R. D. (2014). Chemotherapy stimulates syndecan-1 shedding: a potentially negative effect of treatment that may promote tumor relapse. *Matrix Biol.* 35, 215–222. doi: 10.1016/j.matbio.2013.10.005

Rapraeger, A. C. (2013). Synstatin: a selective inhibitor of the syndecan-1-coupled IGF1R-alphavbeta3 integrin complex in tumorigenesis and angiogenesis. *FEBS J.* 280, 2207–2215. doi: 10.1111/febs.12160

Roder, D., Houssami, N., Farshid, G., Gill, G., Luke, C., Downey, P., et al. (2008). Population screening and intensity of screening are associated with reduced breast cancer mortality: evidence of efficacy of mammography screening in Australia. *Breast Cancer Res. Treat.* 108, 409–416. doi: 10.1007/s10549-007-9609-5

Rothenberger, N. J., Somasundaram, A., and Stabile, L. P. (2018). The role of the estrogen pathway in the tumor microenvironment. *Int. J. Mol. Sci.* 19:611. doi: 10.3390/ijms19020611

Sarrazin, S., Lamanna, W. C., and Esko, J. D. (2011). Heparan sulfate proteoglycans. *Cold Spring Harb. Perspect. Biol.* 3:a004952.

Shawky, M. S., Huo, C. W., Henderson, M. A., Redfern, A., Britt, K., and Thompson, E. W. (2019). A review of the influence of mammographic density on breast cancer clinical and pathological phenotype. *Breast Cancer Res. Treat.* 177, 251–276. doi: 10.1007/s10549-019-05300-1

Shawky, M. S., Martin, H., Hugo, H. J., Lloyd, T., Britt, K. L., Redfern, A., et al. (2017). Mammographic density: a potential monitoring biomarker for adjuvant and preventative breast cancer endocrine therapies. *Oncotarget* 8, 5578–5591. doi: 10.18632/oncotarget.13484

Shawky, M. S., Ricciardelli, C., Lord, M., Whitelock, J., Ferro, V., Britt, K., et al. (2015). Proteoglycans: potential agents in mammographic density and the associated breast cancer risk. *J. Mammary Gland Biol. Neoplasia* 20, 121–131. doi: 10.1007/s10911-015-9346-z

Sprague, B. L., Gangnon, R. E., Burt, V., Trentham-Dietz, A., Hampton, J. M., Wellman, R. D., et al. (2014). Prevalence of mammographically dense breasts in the United States. *J. Natl. Cancer Inst.* 106:dju255.

Stewart, M. D., Ramani, V. C., and Sanderson, R. D. (2015). Shed syndecan-1 translocates to the nucleus of cells delivering growth factors and inhibiting histone acetylation: a novel mechanism of tumor-host cross-talk. *J. Biol. Chem.* 290, 941–949. doi: 10.1074/jbc.m114.608455

Stone, J., Warren, R. M., Pinney, E., Warwick, J., and Cuzick, J. (2009). Determinants of percentage and area measures of mammographic density. *Am. J. Epidemiol.* 170, 1571–1578. doi: 10.1093/aje/kwp313

Strand, M. E., Aronsen, J. M., Braathen, B., Sjaastad, I., Kvaloy, H., Tonnessen, T., et al. (2015). Shedding of syndecan-4 promotes immune cell recruitment and mitigates cardiac dysfunction after lipopolysaccharide challenge in mice. *J. Mol. Cell Cardiol.* 88, 133–144. doi: 10.1016/j.yjmcc.2015.10.003

Su, G., Blaine, S. A., Qiao, D., and Friedl, A. (2007). Shedding of syndecan-1 by stromal fibroblasts stimulates human breast cancer cell proliferation via FGF2 activation. *J. Biol. Chem.* 282, 14906–14915. doi: 10.1074/jbc.m611739200

Sun, X., Zhang, G., Nian, J., Yu, M., Chen, S., Zhang, Y., et al. (2017). Elevated heparanase expression is associated with poor prognosis in breast cancer: a study based on systematic review and TCGA data. *Oncotarget* 8, 43521–43535. doi: 10.18632/oncotarget.16575

Szarvas, T., Reis, H., Vom Dorp, F., Tschirdewahn, S., Niedworok, C., Nyirady, P., et al. (2016). Soluble syndecan-1 (SDC1) serum level as an independent pre-operative predictor of cancer-specific survival in prostate cancer. *Prostate* 76, 977–985. doi: 10.1002/pros.23186

Thorneloe, R. J., Hall, L. H., Walter, F. M., Side, L., Lloyd, K. E., and Smith, S. G. (2020). Knowledge of potential harms and benefits of tamoxifen among women considering breast cancer preventive therapy. *Cancer Prev. Res.* 13, 411–422. doi: 10.1158/1940-6207.CAPR-19-0424

Tourell, M. C., Ali, T. S., Hugo, H. J., Pyke, C., Yang, S., Lloyd, T., et al. (2018). T1 -based sensing of mammographic density using single-sided portable NMR. *Magn. Reson. Med.* 80, 1243–1251. doi: 10.1002/mrm.27098

Vassilakopoulos, T. P., Kyrtsonis, M. C., Papadogiannis, A., Nadali, G., Angelopoulou, M. K., Tzenou, T., et al. (2005). Serum levels of soluble syndecan-1 in Hodgkin's lymphoma. *Anticancer Res.* 25, 4743–4746.

Vlodavsky, I., Beckhove, P., Lerner, I., Pisano, C., Meirovitz, A., Ilan, N., et al. (2012). Significance of heparanase in cancer and inflammation. *Cancer Microenviron.* 5, 115–132. doi: 10.1007/s12307-011-0082-7

Vogel, B., Siebert, H., Hofmann, U., and Frantz, S. (2015). Determination of collagen content within picrosirius red stained paraffin-embedded tissue sections using fluorescence microscopy. *MethodsX* 2, 124–134. doi: 10.1016/j.mex.2015.02.007

Weigelt, B., Bosma, A. J., and van 't Veer, L. J. (2003). Expression of a novel lacrimal gland gene lacritin in human breast tissues. *J. Cancer Res. Clin. Oncol.* 129, 735–736. doi: 10.1007/s00432-003-0514-y

Xu, X., Ding, J., Rao, G., Shen, J., Prinz, R. A., Rana, N., et al. (2007). Estradiol induces heparanase-1 expression and heparan sulphate proteoglycan degradation in human endometrium. *Hum. Reprod.* 22, 927–937. doi: 10.1093/humrep/del483

Yang, N., and Friedl, A. (2016). Syndecan-1-induced ECM fiber alignment requires integrin alphavbeta3 and syndecan-1 ectodomain and heparan sulfate chains. *PLoS One* 11:e0150132. doi: 10.1371/journal.pone.0150132

Yang, N., Mosher, R., Seo, S., Beebe, D., and Friedl, A. (2011). Syndecan-1 in breast cancer stroma fibroblasts regulates extracellular matrix fiber organization and carcinoma cell motility. *Am. J. Pathol.* 178, 325–335. doi: 10.1016/j.ajpath.2010.11.039

Yang, Y., Macleod, V., Miao, H. Q., Theus, A., Zhan, F., Shaughnessy, J. D. Jr., et al. (2007). Heparanase enhances syndecan-1 shedding: a novel mechanism for stimulation of tumor growth and metastasis. *J. Biol. Chem.* 282, 13326–13333. doi: 10.1074/jbc.m611259200

Zcharia, E., Jia, J., Zhang, X., Baraz, L., Lindahl, U., Peretz, T., et al. (2009). Newly generated heparanase knock-out mice unravel co-regulation of heparanase and matrix metalloproteinases. *PLoS One* 4:e5181. doi: 10.1371/journal.pone.0005181

Conflict of Interest: The authors declare that the research was conducted in the absence of any commercial or financial relationships that could be construed as a potential conflict of interest.

frontiers in Cell and Developmental Biology

CORRECTION
published: 31 March 2021
doi: 10.3389/fcell.2021.678589

Corrigendum: Heparanase Promotes Syndecan-1 Expression to Mediate Fibrillar Collagen and Mammographic Density in Human Breast Tissue Cultured *ex vivo*

Xuan Huang[1,2,3], Gina Reye[1,2,3], Konstantin I. Momot[1,4], Tony Blick[1,2,3], Thomas Lloyd[5], Wayne D. Tilley[6], Theresa E. Hickey[6], Cameron E. Snell[7,8], Rachel K. Okolicsanyi[1,3,9], Larisa M. Haupt[1,3,9], Vito Ferro[10], Erik W. Thompson[1,2,3†] and Honor J. Hugo[1,2,3*†]*

[1] Institute of Health and Biomedical Innovation, Queensland University of Technology, Kelvin Grove, QLD, Australia, [2] Translational Research Institute, Woolloongabba, QLD, Australia, [3] School of Biomedical Science, Queensland University of Technology, Brisbane, QLD, Australia, [4] Faculty of Science and Engineering, Queensland University of Technology, Brisbane, QLD, Australia, [5] Radiology Department, Princess Alexandra Hospital, Woolloongabba, QLD, Australia, [6] Dame Roma Mitchell Cancer Research Laboratories, Adelaide Medical School, University of Adelaide, Adelaide, SA, Australia, [7] Cancer Pathology Research Group, Mater Research Institute, The University of Queensland, Brisbane, QLD, Australia, [8] Mater Pathology, Mater Hospital Brisbane, South Brisbane, QLD, Australia, [9] Genomics Research Centre, School of Biomedical Sciences, Institute of Health and Biomedical Innovation, Queensland University of Technology, Kelvin Grove, QLD, Australia, [10] School of Chemistry and Molecular Biosciences, The University of Queensland, Brisbane, QLD, Australia

Keywords: mammographic density, breast cancer, heparanase, syndecan-1, NMR

OPEN ACCESS

Approved by:
Frontiers Editorial Office, Frontiers Media SA, Switzerland

***Correspondence:**
Erik W. Thompson
e2.thompson@qut.edu.au
Honor J. Hugo
honor.hugo@qut.edu.au

†These authors share last authorship

Specialty section:
This article was submitted to Signaling, a section of the journal Frontiers in Cell and Developmental Biology

Received: *10 March 2021*
Accepted: *11 March 2021*
Published: *31 March 2021*

Citation:
Huang X, Reye G, Momot KI, Blick T, Lloyd T, Tilley WD, Hickey TE, Snell CE, Okolicsanyi RK, Haupt LM, Ferro V, Thompson EW and Hugo HJ (2021) Corrigendum: Heparanase Promotes Syndecan-1 Expression to Mediate Fibrillar Collagen and Mammographic Density in Human Breast Tissue Cultured ex vivo. Front. Cell Dev. Biol. 9:678589. doi: 10.3389/fcell.2021.678589

A Corrigendum on

Heparanase Promotes Syndecan-1 Expression to Mediate Fibrillar Collagen and Mammographic Density in Human Breast Tissue Cultured *ex vivo*

by Huang, X., Reye, G., Momot, K. I., Blick, T., Lloyd, T., Tilley, W. D., et al. (2020). Front. Cell Dev. Biol. 8:599. doi: 10.3389/fcell.2020.00599

In the original article, there was an error. The last author in the authorlist is shown as Honor J. Hugo when acknowledgment needs to be made of equal last authorship for Honor J. Hugo and Erik W. Thompson.

A correction has been made to the authorship section.

Xuan Huang[1,2,3], Gina Reye[1,2,3], Konstantin I. Momot[1,4], Tony Blick[1,2,3], Thomas Lloyd[5], Wayne D. Tilley[6], Theresa E. Hickey[6], Cameron E. Snell[7,8], Rachel K. Okolicsanyi[1,3,9], Larisa M. Haupt[1,3,9], Vito Ferro[10], Erik W. Thompson[1,2,3†] and Honor J. Hugo[1,2,3†]

Note: †These authors share last authorship.

The authors apologize for this error and state that this does not change the scientific conclusions of the article in any way. The original article has been updated.

frontiers in Cell and Developmental Biology

ORIGINAL RESEARCH
published: 31 July 2020
doi: 10.3389/fcell.2020.00730

Syndecan-4$^{-/-}$ Mice Have Smaller Muscle Fibers, Increased Akt/mTOR/S6K1 and Notch/HES-1 Pathways, and Alterations in Extracellular Matrix Components

*Sissel Beate Rønning[1†], Cathrine Rein Carlson[2†], Jan Magnus Aronsen[2,3], Addolorata Pisconti[4], Vibeke Høst[1], Marianne Lunde[2], Kristian Hovde Liland[1,5], Ivar Sjaastad[2,6], Svein Olav Kolset[7], Geir Christensen[2,6] and Mona Elisabeth Pedersen[1]**

[1] Nofima AS, Ås, Norway, [2] Institute for Experimental Medical Research, Oslo University Hospital and University of Oslo, Oslo, Norway, [3] Bjørknes College, Oslo, Norway, [4] Department of Biochemistry and Cell Biology, Stony Brook University, Stony Brook, NY, United States, [5] Faculty of Sciences and Technology, Norwegian University of Life Sciences, Ås, Norway, [6] K.G. Jebsen Center for Cardiac Research, University of Oslo, Oslo, Norway, [7] Department of Nutrition, Institute of Basic Medical Sciences, University of Oslo, Oslo, Norway

Background: Extracellular matrix (ECM) remodeling is essential for skeletal muscle development and adaption in response to environmental cues such as exercise and injury. The cell surface proteoglycan syndecan-4 has been reported to be essential for muscle differentiation, but few molecular mechanisms are known. Syndecan-4$^{-/-}$ mice are unable to regenerate damaged muscle, and display deficient satellite cell activation, proliferation, and differentiation. A reduced myofiber basal lamina has also been reported in syndecan-4$^{-/-}$ muscle, indicating possible defects in ECM production. To get a better understanding of the underlying molecular mechanisms, we have here investigated the effects of syndecan-4 genetic ablation on molecules involved in ECM remodeling and muscle growth, both under steady state conditions and in response to exercise.

Methods: Tibialis anterior (TA) muscles from sedentary and exercised syndecan-4$^{-/-}$ and WT mice were analyzed by immunohistochemistry, real-time PCR and western blotting.

Results: Compared to WT, we found that syndecan-4$^{-/-}$ mice had reduced body weight, reduced muscle weight, muscle fibers with a smaller cross-sectional area, and reduced expression of myogenic regulatory transcription factors. Sedentary syndecan-4$^{-/-}$ had also increased mRNA levels of syndecan-2, decorin, collagens, fibromodulin, biglycan, and LOX. Some of these latter ECM components were reduced at protein level, suggesting them to be more susceptible to degradation or less efficiently translated when syndecan-4 is absent. At the protein level, TRPC7 was reduced, whereas activation of the Akt/mTOR/S6K1 and Notch/HES-1 pathways were increased. Finally,

OPEN ACCESS

Edited by:
Jeremy Turnbull, University of Liverpool, United Kingdom

Reviewed by:
Ole-Morten Seternes, Arctic University of Norway, Norway
Francisco Iñesta-Vaquera, University of Dundee, United Kingdom

***Correspondence:**
Mona Elisabeth Pedersen
mona.pedersen@nofima.no

† These authors share first authorship

Specialty section:
This article was submitted to Signaling, a section of the journal Frontiers in Cell and Developmental Biology

Received: *06 May 2020*
Accepted: *15 July 2020*
Published: *31 July 2020*

Citation:
Rønning SB, Carlson CR, Aronsen JM, Pisconti A, Høst V, Lunde M, Liland KH, Sjaastad I, Kolset SO, Christensen G and Pedersen ME (2020) Syndecan-4$^{-/-}$ Mice Have Smaller Muscle Fibers, Increased Akt/mTOR/S6K1 and Notch/HES-1 Pathways, and Alterations in Extracellular Matrix Components. Front. Cell Dev. Biol. 8:730. doi: 10.3389/fcell.2020.00730

although exercise induced upregulation of several of these components in WT, a further upregulation of these molecules was not observed in exercised syndecan-4$^{-/-}$ mice.

Conclusion: Altogether our data suggest an important role of syndecan-4 in muscle development.

Keywords: skeletal muscle, syndecan, exercise, myogenesis, Notch, decorin, Akt, ECM

INTRODUCTION

Skeletal muscle is a highly dynamic tissue, responding to physiological stimuli during development and exercise. It is composed of muscle cells (myofibers) collected in bundles. Both the individual myofibers and the myofiber bundles are surrounded by extracellular matrix (ECM). It was demonstrated more than 50 years ago that the satellite cells, the skeletal muscle stem cells (MuSCs), which are located between the basal lamina and sarcolemma (plasma membrane) of the skeletal muscle fibers and normally quiescent in adult muscle, become activated upon exercise, injury or disease, and are involved in the skeletal muscle regeneration (Mauro, 1961). More recently, several reports have identified MuSCs as the primary contributors to the postnatal growth, maintenance and regeneration of skeletal muscles. These cells have a remarkable ability to self-renew, expand, or undergo myogenic differentiation to fuse and restore damaged muscle (Tsivitse, 2010). The activation, proliferation and differentiation of MuSCs in adult muscle are mainly controlled by myogenic regulatory transcription factors (MRFs) such as myoblast determination protein (MyoD), myogenin, myogenic factor 5 (myf5) and 6 (myf6/mrf4). MuSCs express MyoD when they are activated and start to proliferate (Zammit et al., 2004), whereas myogenin is crucial for later stages of myogenic differentiation (Sabourin and Rudnicki, 2000).

The ECM, a complex network of collagens, in addition to glycoproteins and proteoglycans, is the niche of MuSCs and the myofibers. The small leucine rich proteoglycans (SLRPs) decorin, fibromodulin and biglycan, regulate collagen fibrillogenesis and crosslinking (Kalamajski and Oldberg, 2010; Kalamajski et al., 2014; Christensen et al., 2018). The ECM composition is highly dynamic and promotes skeletal muscle adaption in response to environmental forces during, e.g., exercise and regeneration, and during muscle growth and development. The ECM network also builds a scaffold for muscle cells to adhere, grow and differentiate, and functions as a storage and presenter of relevant muscle tissue growth factors and different cytokines during development (Thomas et al., 2015).

Previous work has also identified syndecans to be important for muscle development, maintenance and regeneration (Pisconti et al., 2012, 2016; Pawlikowski et al., 2017; Velleman and Song, 2017). The syndecans belong to a group of transmembrane proteoglycans, which consists of four members in mammals (Velleman et al., 2012). The syndecans are characterized by a large diverse extracellular domain with glycosaminoglycan (GAG) attachment sites, a conserved transmembrane domain and a short cytoplasmic domain with a unique variable domain differing between each syndecan. Syndecans have a wide spectrum of biological functions, and regulate calcium ion channels, polarization of epithelial cells, cell adhesions, and migration (Couchman et al., 2015). They also function as co-receptors of various growth factors and transduce signals into the cell through their cytoplasmic domains (Couchman, 2010). All four syndecans are expressed in developing muscles (Cornelison et al., 2001; Olguin and Brandan, 2001) and in proliferating myoblasts, but their expression is progressively lost during myogenesis (Brandan and Gutierrez, 2013). Syndecan-2 is reported to be highly expressed in early-differentiated myoblasts (Do et al., 2015). Syndecan-1 is not detected in postnatal muscle, while syndecan-3 and syndecan-4 are present and restricted to MuSCs and vascular cells (Cornelison et al., 2001; Cornelison et al., 2004). Syndecan-4 as well as syndecan-3 have roles in development and regeneration. Both are highly expressed in myoblasts and around early embryonal myotubes but are reduced around myotubes postnatally and restricted to MuSCs in young adults (Cornelison et al., 2001). Syndecan-3 regulates muscle progenitor cell homeostasis by promoting MuSC self-renewal. Syndecan-3$^{-/-}$ mice show improved muscle regeneration upon repeated muscle injuries, and reduced muscle pathology in dystrophic mice (Pisconti et al., 2016). Syndecan-4$^{-/-}$ mice are unable to regenerate damaged muscle and display deficient MuSC activation, proliferation, myoD expression and differentiation (Cornelison et al., 2004). Interestingly, a reduced myofiber basal lamina has also been reported in syndecan-4$^{-/-}$ muscle (Cornelison et al., 2004), indicating possible defects in ECM biosynthesis and turnover.

Limited knowledge on molecular mechanisms of syndecan-4 in skeletal muscle exist. To get a better understanding of the role of syndecan-4 in skeletal muscle and the underlying molecular mechanisms, we have here investigated the effects of syndecan-4 genetic ablation in tibialis anterior (TA), and analyzed molecules involved in ECM remodeling and muscle growth, both under steady state conditions and in response to exercise. Reduced muscle growth, changes in multiple signaling molecules and ECM components were found when syndecan-4 was absent. These molecular changes were mostly not affected further by exercise.

Abbreviations: Dvl, disheveled; ECM, extracellular matrix; ET: exercised trained; GAG glycosaminoglycan; IGF1R, insulin-like growth factor I receptor; LOX, Lysyl oxidase; LRP6, low-density lipoprotein receptor-related protein 6; MRFs, myogenic regulatory transcription factors; MuSC, skeletal muscle stem cells; Myf, myogenic factor; MyoD, myoblast determination protein 1; PKC, protein kinase C; RPS6, ribosomal protein 6; SED, sedentary; SK61, ribosomal protein S6 kinase 1; SLRPs, small leucine-rich proteoglycans; TA, tibialis anterior; TRPC7, Transient Receptor Potential Cation Channel Subfamily C Member 7; WT, wild type.

MATERIALS AND METHODS

Animal Experiments

All animal experiments were performed in accordance with the National Regulation on Animal Experimentation in accordance with an approved protocol (ID#2845 and 7696) and the Norwegian Animal Welfare Act and conform the NIH guidelines (2011). Female syndecan-$4^{-/-}$ mice (KO) (Echtermeyer et al., 2001) were compared to either C57Bl/6j mice or syndecan-$4^{+/+}$ bred from the same genetic background to study syndecan-4 dependent effects. Up to six mice per cage were housed in a temperature-regulated room with a 12:12-h light dark cycle, and access to food and water *ad libitum*. Animals were sacrificed by cardiac excision in deep surgical anesthesia.

Exercise Training Protocol

Exercise training was performed on female syndecan-$4^{-/-}$ mice (KO) and syndecan-$4^{+/+}$ mice (WT) bred from the same genetic background with a treadmill for rodents (Columbus Instruments, OH, United States) with a 30-degree inclination. The mice were adapted 2 days to the treadmill, before exercise training was performed for 60 min per day for 14 days (1 day rest without training) on a treadmill with moderate intensity. All mice had 3 min of warmup before each running session that consisted of six times 8 min of running followed by 2 min rest. Running speed was set to 14–18 m per minute. Mice that were not able to complete the training protocol were excluded from the study. Animals were sacrificed by cardiac excision in deep surgical anesthesia.

Real-Time PCR

Tibialis anterior muscle was collected from WT and syndecan-$4^{-/-}$ mice, exercised and sedentary mice, and snap-frozen in liquid nitrogen. Tissue samples were homogenized in lysis RLT-buffer of RNeasy minikit (#74104, Qiagen, Hilden, Germany) using a Precellys24 (#74106, Bertin Technologies, Villeurbanne, France) at 5500 rpm for 2 × 20 s, and RNA further purified following the manufacturer's protocol of the RNeasy minikit including a DNase treatment on column according to the manufacturer's protocol. cDNA was generated from ∼400 ng mRNA using TaqMan® Reverse Transcription Reagents (Invitrogen, Carlsbad, CA, United States) according to the manufacturer's protocol. The cDNA was diluted four times before aliquots (in duplicates) were subjected to real-time PCR analysis using an ABI Prism 7700 Sequence Detection system (Applied Biosystem, United Kingdom), and TaqMan® primer/probe assays (see **Table 1** for primer/probes used) according to manufacturer's protocol. The efficiency of each set of primers was always higher than 96%. Amplification of cDNA by 40 two-step cycles (15 s at 95°C for denaturation of DNA, 1 min at 60°C for primer annealing and extension) was used, and cycle threshold (Ct) values were obtained graphically (Applied Biosystem, Sequence Detection System, Software version 2.2). ΔCt values and ΔΔCt values were calculated according to the MIQE guidelines (Bustin et al., 2010). Comparison of the relative gene expression (fold change) was derived by using the comparative Ct method. In short, values were generated by subtracting ΔCt values between two samples which gives a ΔΔCt value. The relative gene expression (fold change) was then calculated by the formula $2^{-\Delta\Delta Ct}$ (Schmittgen and Livak, 2008). Statistical analyses were performed using the ΔΔCt-values.

Immunofluorescence

TA muscles ($n = 4$) were collected from WT and syndecan-$4^{-/-}$ mice, embedded in OCT compound (Tissue Tek, Sakura Finetek, CA, United States) and then snap-frozen. Five micrometer-thick sections were cut on a cryostat and mounted on poly-L-lysine coated glass slides. The sections were air-dried for 5 min, before fixation using ice-cold acetone for 5 min. The sections were washed briefly twice in PBS, permeabilized using 0.5% Triton-X in PBS and incubated with 5% non-fat dry milk for 30 min before incubation with primary antibody for 1 h. Subsequent incubation with secondary antibodies was performed for 30 min before mounting using Dako fluorescent mounting medium (Glostrup, Denmark). Antibodies used were: Rabbit anti-Collagen 1 (ab34710, Abcam, Cambridge, United Kingdom), anti-pSer473-Akt (#9271, Cell Signaling, United States) and Alexa 488-goat anti-rabbit (#A-11078 Thermo Fisher Scientific, MA, United States). To quantify myofiber number sections were air-dried for 30 min and incubated with P-Block (5% goat serum, 1% Triton-X, 0.012% BSA, 0.012% non-fat dry-milk in PBS) for 1h. The sections were washed briefly four times with P-Block before incubation with primary antibody over night at 4°C. Subsequent washing was performed twice with PBS before incubation with secondary antibody in P-Block for 1 h. The sections were washed briefly three times with P-Block, twice with PBS for 5 min each, rinsed in water before mounted using Dako fluorescent mounting medium. The total number of fibers in WT and KO TA muscles were quantified based on Laminin staining, using the ImageJ Cell counter plugin. Antibodies used were: Rabbit anti-Laminin (PA5-16287, Thermo Fisher Scientific, MA, United States). DyLight 549 mouse anti-rabbit were from Jackson Immunoresearch Cambridgeshire, United Kingdom. The sections were examined by fluorescence microscopy analysis

TABLE 1 | Gene target and TaqMan® primer/probe assays.

Gene target	TaqMan® primer/probe assays
Decorin	Mm00514535_m1
Fibromodulin	Mm00491215_m1
Lumican	Mm00500510_m1
Biglycan	Mm00455918_m1
Collagen 1a2	Mm00483888_m1
Collagen 3a1	Mm00802331_m1
Lox	Mm00495386_m1
Syndecan-2	Mm00484718_m1
Syndecan-4	Mm00488527_m1
Syndecan-3	Mm01179833_m1
MyoD	Mm01203489_g1
Desmin	Mm00802455_m1
Myogenin	Mm00446195_g1
Ribosomal protein gene RP132	Mm02528467_g1

(apotome mode) (ZEISS Axio Observer Z1 microscope, Jena, Germany), and images were processed using Adobe Photoshop CS3. If needed, brightness and contrast were adjusted manually across the entire image. Myofiber cross-sectional area in WT and KO TA muscles were quantified based on collagen staining. A minimum of 1,000 myofibers and four sections were analyzed per biological replica. Hoechst (Hoechst 33342, 10 μg/ml) was from Thermo Fisher Scientific. For assessment of connective tissue, sections were incubated with WGA Alexa Fluor™ 546 Conjugate (Thermo Fisher Scientific, MA, United States).

Western Blotting

Protein extracts from TA muscle were prepared using ice-cold lysis buffer (20 mm Hepes, pH 7.5, 150 mm NaCl, 1 mm EDTA, 0.5% Triton) supplemented with Complete EDTA-free protease inhibitor cocktail (#5056489001, Roche Applied Science, Merck, Darmstadt, Germany) and PhosSTOP (#4906837001, Roche Applied Science). Tissue samples were homogenized three times for 1 min on ice with a Polytron 1200 homogenizer and centrifuged at 14,000 × *g* for 10 min at 4°C. Supernatants were collected and stored at −70°C. Protein concentrations were determined using the Micro BCA protein assay kit (#23235, Pierce). An equal amount of protein was loaded per lane (40 μg/μl). The protein extracts were resolved on 4–15% Criterion™ Tris-HCl precast gels (#3450029, Bio-Rad Laboratories, CA, United States) and blotted onto PVDF membranes (#1704157, Trans-Blot Turbo Transfer Pack, Bio-Rad) using the Trans-Blot Turbo system (Bio-Rad) or tank blotting. The PVDF membranes were blocked in 5% non-fat dry milk, 1% casein or 3% BSA in TBS-T for 60 min at room temperature, followed by incubation with primary antibodies overnight at 4°C. Membranes were washed two times for 10 min each in TBS-T, incubated with a horseradish-peroxidase-conjugated secondary antibody and thereafter washed two times for 10 min and one time for 5 min in TBS-T. Blots were developed using ECL Prime (RPN 2232, GE Healthcare, IL, United States). The chemiluminescence signals were detected by Las-4,000 (GE Healthcare). Membranes were re-probed after stripping using the Restore Western Blot Stripping buffer for 5 min at room temperature (21059, Thermo Fisher Scientific, MA, United States).

Antibodies and conditions were: anti-pSer235/236-RPS6 (1:1000, 5% BSA, #4858, Cell Signaling, MA, United States), anti-RPS6 (1:1000, 5% BSA, #2217, Cell Signaling), anti-HES-1 (1:500, 1% casein, #AB5702, Millipore, Merck, Darmstadt, Germany), anti-LRP6 (1:1000, 1% casein, #2560, Cell Signaling), anti-Dvl (1:1000, 1% casein, #3224, Cell Signaling), anti-β-catenin (1:5000, 1% casein, ab32572, Abcam, Cambridge, United Kingdom), anti-Frizzled-7 (1:1000, 1% casein, #ab64636, Abcam), anti-Cleaved Notch1 (1:1000, 5% BSA, #4147, Cell Signaling), anti-Wnt4 (1:1000, 1% casein, ab91226, Abcam), anti-TRPC7 (1:500, 1% casein, #SAB5200051, Sigma-Aldrich), anti-PKC (1:250, 1% casein, sc-208, Santa Cruz, TX, United States), anti-DSCR1/RCAN1.4 (1:500, 5% milk, #D6694, Sigma-Aldrich), anti-pSer240/244-RPS6 (1:1000, 5% BSA, #5364 Cell Signaling), anti-pSer473-Akt (1:500, 5% BSA, #9271, Cell Signaling), anti-pThr308-Akt (1:500, #5106, 5% BSA, Cell Signaling), anti-Akt (1:500, 1% casein, #9272, Cell Signaling), anti-fibromodulin (1:500, 1% casein, sc-33772, Santa Cruz), anti-pSer2448-mTOR (1:1000, #2971, 5% BSA, Cell Signaling), anti-mTOR (1:1000, #2983, 5% BSA, Cell Signaling), anti-Pax-7 (1:500, sc-81648, 1:500, 1x casein, Santa Cruz) anti-decorin (1:500, 1% casein, AF1060, R&D Systems, MN, United States), anti-biglycan (1:500, 1% casein, ab49701, Abcam) and anti-LOX (1:500, 1% casein, sc-32409, Santa Cruz). Anti-rabbit IgG HRP (NA934V) affinity-purified polyclonal antibody, anti-mouse IgG HRP (NA931V) (both from GE Healthcare) and anti-goat IgG HRP (HAF109, R&D Systems, MI, United States) were used as secondary antibodies. Since housekeeping genes like vinculin and beta-tubulin were regulated across the four groups, ProBlueSafeStain (Coomassie) (#G00PB001, Giotto Biotech, FI, Italy) was used to verify equal protein loading. Two or three distinct Coomassie stained bands, mostly in the 75–100 kDa region, was used to show equal loading of the samples.

Statistics

All data were expressed as mean ± SEM. Comparisons between two groups were analyzed using Mann–Whitney *U* test (GraphPad Prism version 8.0.1, La Jolla, CA, United States). A p-value of <0.05 was considered statistically significant. Comparison of fiber area sizes was performed using analysis of variance where each fiber's estimated area was used as a sample, WT/KO was used as a fixed effect (the effect of interest) and magnification and muscle image number were included as random effects. The reason for including magnification was that image generation and fiber identification could be affected by the magnification. Muscle image was included to separate individual mouse effects from the true fiber area effects. Analyses were conducted in MATLAB 2015a, The MathWorks, Inc., Natick, MA, United States.

RESULTS

Syndecan-4$^{-/-}$ Mice Have Reduced Body Weight, Smaller Muscle Fibers and Reduced myoD and Myogenin mRNA Levels

To investigate the skeletal muscle of syndecan-4$^{-/-}$ mice, we analyzed the TA muscles from adult female mice of 12–22 weeks. The syndecan-4$^{-/-}$ mice were viable and showed no obvious postnatal abnormalities, however, they had a significantly lower body weight and TA weight compared to WT (**Figures 1A,B**, respectively). Closer inspection showed that the syndecan-4$^{-/-}$ muscle fibers had smaller cross-sectional area compared with those of the WT mice (**Figure 1C**). More specifically, a larger fraction of the syndecan-4$^{-/-}$ muscle fibers scored less than 2000 μm^2 and there were hardly any larger muscle fibers (6000 μm^2 and over) (**Figure 1D**). Statistical analyses showed that the average size of the syndecan-4$^{-/-}$ muscle fibers was 468 μm^2 smaller compared to WT (p = 0.0009), which was not accompanied by a change in total number of myofiber per muscle section (**Figure 1E**). As previously

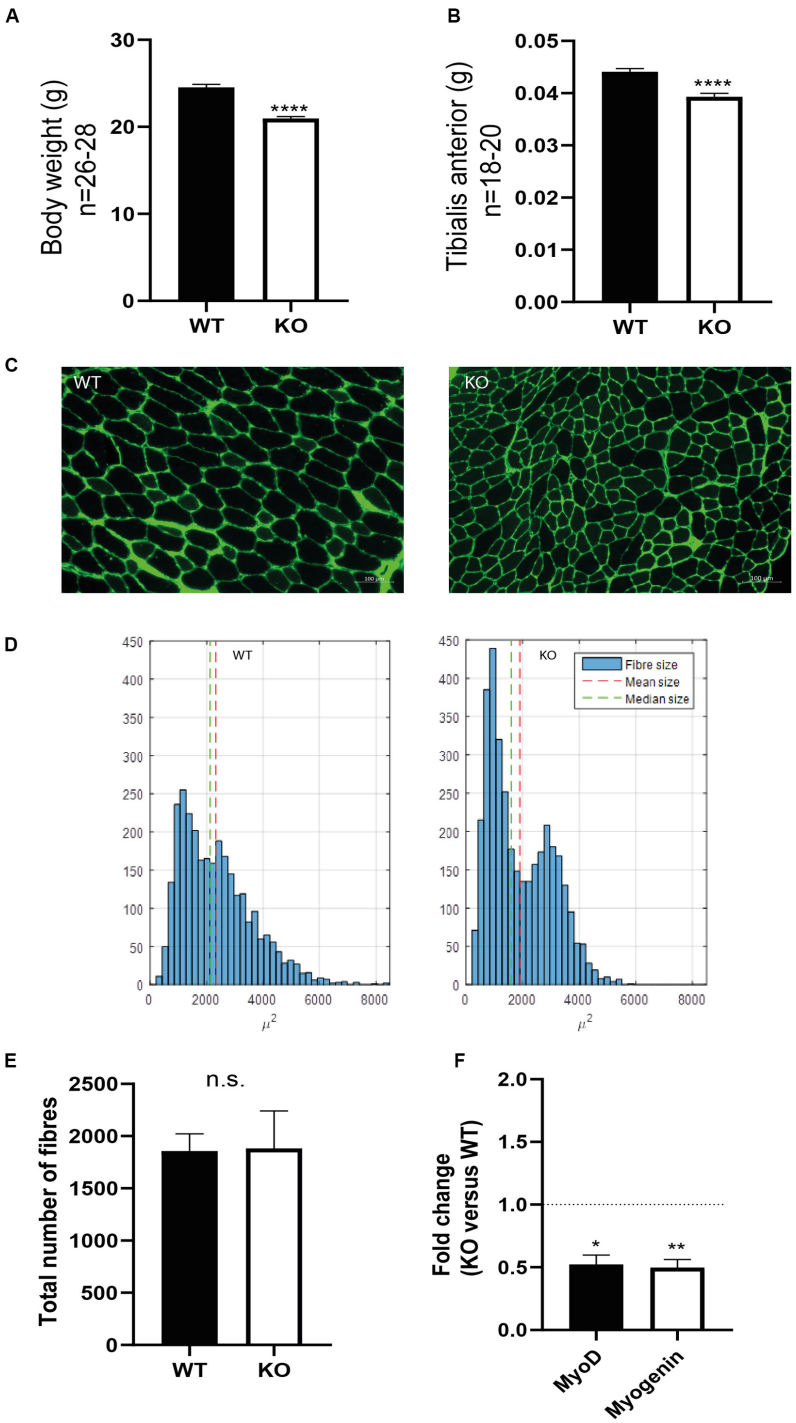

FIGURE 1 | Syndecan-4$^{-/-}$ mice have reduced body weight, smaller muscle fibers and reduced myoD and myogenin mRNA levels. Bars show **(A)** bodyweight and **(B)** tibialis anterior (TA) wet weight in syndecan-4$^{-/-}$ mice compared to WT. The data are presented as average ± SEM. Asterisks denote significant differences (***$p < 0.001$) between syndecan-4$^{-/-}$ and WT using un-paired two-tailed *t*-test. **(C)** Cross-sections of TA muscles from WT (left panel) and syndecan-4$^{-/-}$ mice (right panel) were cryo-sectioned and stained with rabbit-anti collagen 1 (green), followed by Alexa Fluor 488-conjugated goat anti-rabbit before fluorescence microscopy analysis. **(D)** Quantification of images in **(C)** show fiber size distribution with a shift toward more fibers of low cross-sectional area (right panel) in syndecan-4$^{-/-}$ compared to WT (left panel). Differences were tested using an analysis of variance with random effects. **(E)** Quantification of number of fibers in WT and syndecan-4$^{-/-}$. The data are presented as average ± SEM. Differences were tested using un-paired two-tailed *t*-test (ns; non-significant). **(F)** Bars show relative gene expression levels (fold change) in syndecan-4$^{-/-}$ versus WT (young mice, aged 12–22 weeks, $n = 12$) ± SEM. The values of the bars are presented as fold change (in ΔΔCT) of syndecan-4$^{-/-}$ related to WT (the latter is set to 1 and is represented as dotted line). Asterisk indicate significant differences, statistics assessed for ΔΔCT values by unpaired two-tailed *t*-test (*$p < 0.05$, **$p < 0.01$).

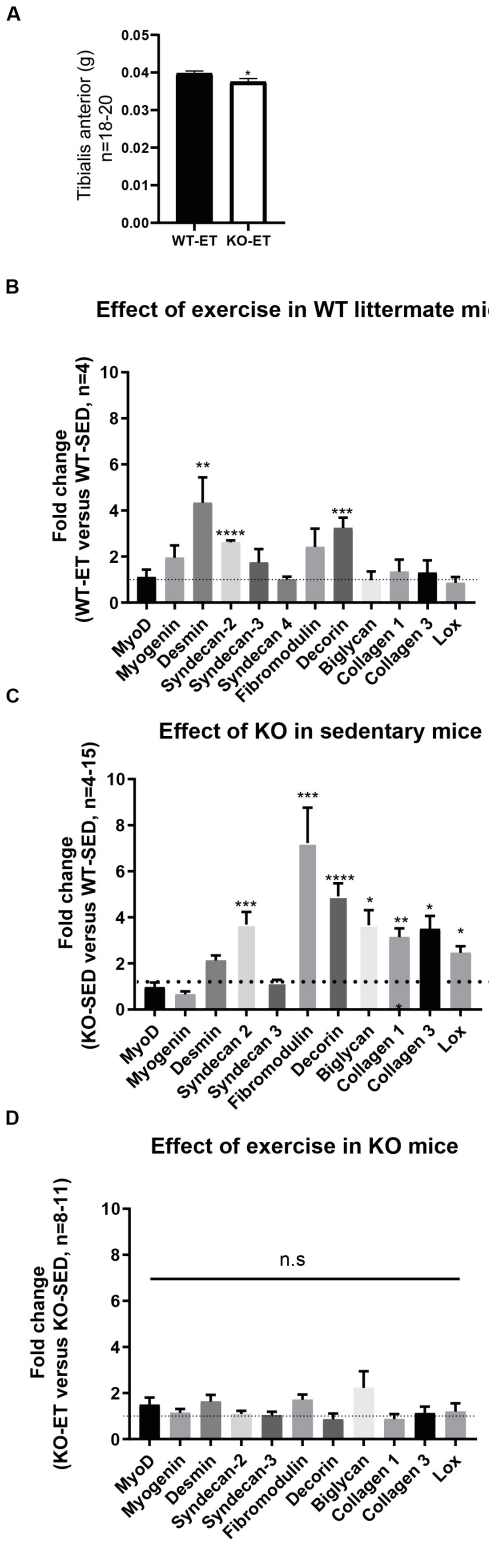

FIGURE 2 | The syndecan-$4^{-/-}$ muscle has increased mRNA levels of several ECM components. **(A)** Bars show tibialis anterior (TA) wet weight from exercised WT littermates (WT-ET) and syndecan-$4^{-/-}$ mice (KO-ET) (10–12 weeks at harvest). The data is presented as the average ± SEM.

(Continued)

FIGURE 2 | Continued

Comparisons between the groups were analyzed using Mann–Whitney *U* test (*$p < 0.05$). Bars show relative mRNA levels in TA muscle from **(B)** WT-ET versus WT-SED, **(C)** KO-SED versus WT-SED and **(D)** KO-ET versus KO-SED (10–12 weeks at harvest). The values of the bars are presented as fold change (ΔΔCT) in WT-ET/WT-SED, KO-SED/WT-SED and KO-ET/KO-SED in **(B–D)**, respectively. WT-SED is set to 1 in **(B,C)**, whereas KO-SED is set to 1 in **(D)** (represented as dotted lines). Statistics are based on ΔΔCT values using unpaired two-tailed *t*-test (*$p < 0.05$, **$p < 0.01$, ***$p < 0.001$).

reported (Cornelison et al., 2004), the mRNA levels of the muscle transcriptional activator myoblast determination protein (myoD) and myogenin (this study) were significantly lower in syndecan-$4^{-/-}$ compared to WT (**Figure 1F**). Consistent with the previous report (Cornelison et al., 2004), we did not observe any centrally nucleated myofibers in the syndecan-$4^{-/-}$ (**Supplementary Figure 1A**), a characteristic often associated with muscle disorders (Cornelison et al., 2004; Folker and Baylies, 2013) and impaired maintenance of MuSC quiescence (Pisconti et al., 2016). We did neither observe any differences in the protein levels of the paired box transcription factor Pax7, which is a marker of quiescent MuSCs (Seale et al., 2000) (**Supplementary Figure 1B**). This is in line with Cornelison et al. (2004), who demonstrated no difference in the number of MuSCs in syndecan-$4^{-/-}$ and WT.

The Syndecan-$4^{-/-}$ Muscle Has Several Changes in the ECM Components

To further investigate the role of syndecan-4, syndecan-$4^{-/-}$ and age-matched WT littermates were subjected to a 2 weeks-long treadmill exercise protocol (ET mice) (10–12 weeks at harvest). Sedentary syndecan-$4^{-/-}$ and WT littermates of same age were used as controls (SED mice). As shown in **Figure 2A**, the syndecan-$4^{-/-}$ TA muscles were still significantly smaller than those from WT littermates after exercise (WT-ET versus KO-ET).

To detect possible differences between syndecan-$4^{-/-}$ and WT at the molecular level, we measured mRNA and protein levels of different ECM and signaling molecules we hypothesized could have a role in exercise and syndecan-4-mediated signaling. The mRNA levels of desmin and the ECM component decorin were both upregulated in WT after exercise (**Figure 2B**, WT-ET versus WT-SED), which is consistent with a role of decorin and desmin in myoblast differentiation and fusion (Brandan and Gutierrez, 2013; Hnia et al., 2015). Syndecan-2 was also highly up-regulated in response to exercise, while no changes were seen in syndecan-3 and 4 (**Figure 2B**). Myogenin and fibromodulin showed a tendency to increase in WT after exercise, whereas myoD, biglycan, collagen 1, collagen 3 and the collagen cross-linking enzyme lysyl oxidase (LOX) were unchanged (**Figure 2B**). Consistently, although not significant, immunoblotting indicated a slight increased level of decorin and unchanged levels of fibromodulin, biglycan and LOX after exercise (**Figures 3A–D**, WT-SED versus WT-ET).

Similar to exercise, syndecan-$4^{-/-}$ loss led to increased mRNA levels of both syndecan-2 and decorin (**Figure 2C**, KO-SED versus WT-SED). However, in contrast to WT, exercise

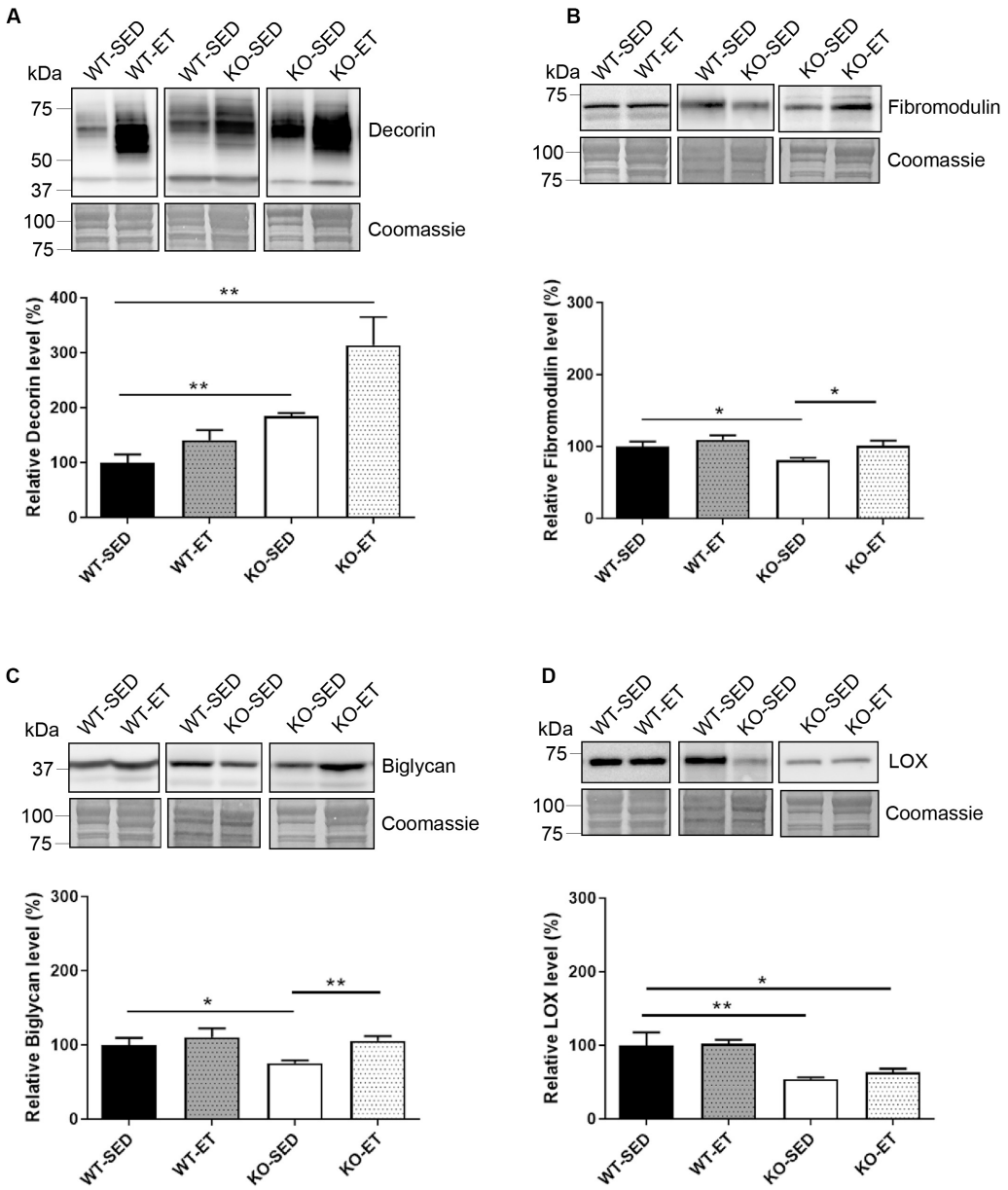

FIGURE 3 | The syndecan-4$^{-/-}$ muscle has changed protein levels of several ECM components. Immunoblot analyses of **(A)** decorin, **(B)** fibromodulin, **(C)** biglycan, and **(D)** LOX in WT-SED, WT-ET, KO-SED and KO-ET. The values are presented in percentage and are normalized to WT-SED (n = 4–10). Comparisons between the groups were analyzed using Mann–Whitney U test (*$p < 0.05$, **$p < 0.01$). ProBlue Safe Stain (Coomassie) was used as loading control.

failed to induce any further upregulation (**Figure 2D**, KO-ET versus KO-SED). Interestingly, syndecan-4 loss also led to increased mRNA levels of ECM components and modifiers such as fibromodulin, biglycan, collagen 1, collagen 3 and LOX (**Figure 2C**, KO-SED versus WT-SED). Consistently with the mRNA data, immunoblotting showed increased levels of decorin when syndcan-4 was absent (**Figure 3A**, KO-SED versus WT-SED), but surprisingly a reduction in the fibromodulin, biglycan and LOX protein levels (**Figures 3B–D**, KO-SED versus WT-SED). Notably, the biglycan and LOX protein levels increased in syndecan-4$^{-/-}$ mice in response to exercise (**Figures 3C,D**, KO-ET versus KO-SED), where fibromodulin and biglycan returned to the level observed in WT sedentary mice (**Figures 3B,C**, KO-ET versus WT-SED).

Taken together, the syndecan-4$^{-/-}$ muscle had increased mRNA levels of syndecan-2, collagen 1 and 3, decorin, fibromodulin, biglycan, and LOX. These three latter ECM components were reduced at protein level, suggesting that they might be more susceptible to degradation or less efficiently translated when syndecan-4 is absent. Although exercise induced upregulation of desmin, syndecan-2 and decorin in WT mice,

a further upregulation was not observed in exercised syndecan-$4^{-/-}$ mice.

The Syndecan-$4^{-/-}$ Muscle Has Increased Akt/mTOR/S6K1 and Notch-HES-1 Pathways

Next, we analyzed activation of the protein kinase Akt, which transduces decorin-insulin-like growth factor I receptor (IGF1R) signaling (Suzuki et al., 2013) and regulates muscle fiber growth and hypertrophy through the Akt/mTOR/S6K1 pathway (Schiaffino et al., 2013). Interestingly, the Akt/mTOR pathway associates also with syndecan-4 signaling (Elfenbein and Simons, 2013). Immunofluorescence data showed that pSer473-Akt localized to the skeletal muscle cell nuclei and to the ECM perimysium in WT where fibroblasts and resident immune cells are located (**Figure 4A**, upper panels). Visual inspection clearly showed an increased expression of pSer473 in syndecan-$4^{-/-}$ (**Figure 4A**, lower panels). Consistently, immunoblotting revealed that the pSer473-Akt levels were constitutively higher in both sedentary as well as exercised syndecan-$4^{-/-}$ mice compared to WT mice (**Figure 4B**, KO-SED and KO-ET versus WT-SED). Also the levels of pThr308-Akt/Akt and pSer2448-mTOR/mTOR showed a tendency to be increased in sedentary syndecan-$4^{-/-}$ mice (**Supplementary Figure 2A** and **Figure 4C**, KO-SED versus WT-SED). We also analyzed the phosphorylation levels of the 40S ribosomal protein S6 (RPS6), which is downstream of the Akt/mTOR/S6K1 signaling, and directly links to cell size control and myofiber growth (Ruvinsky et al., 2009; Meyuhas, 2015). Immunoblotting revealed that the pSer235/236-RPS6 levels were increased in WT muscles upon exercise (**Figure 4D**, WT-ET versus WT-SED), but also in sedentary and exercised syndecan-$4^{-/-}$ (**Figure 4D, KO-SED** and **KO**-ET versus WT-SED). The levels of pSer240/244-RPS6 were also slightly increased in syndecan-$4^{-/-}$ muscles, although the increase was not statistically significant (**Supplementary Figure 2B**, KO-SED versus WT-SED). No difference in the total RPS6 levels was observed between syndecan-$4^{-/-}$ and WT muscles (**Figure 4D**, WT-SED versus KO-SED, lower most panel).

We next analyzed Cleaved Notch, as Notch signaling associates with increased syndecan-2 levels (Zhao et al., 2012), and is known to increase upon exercise and be involved in myogenesis (Arthur and Cooley, 2012). Although our data indicated no significant changes of Cleaved Notch1 in WT (**Figure 5A**, WT-ET versus WT-SED), the Notch target gene HES-1 was increased in response to exercise (**Figure 5B**, WT-ET versus WT-SED). Surprisingly, both the Cleaved Notch and HES-1 levels were increased in sedentary syndecan-$4^{-/-}$ mice and did not further increase in response to exercise (**Figures 5A,B**, KO-SED versus WT-SED).

Finally, since syndecan-4 has been shown to associate with Wnt (Pataki et al., 2015), calcineurin-NFAT (Finsen et al., 2011) and protein kinase C (PKC) – transient receptor potential canonical 7 (TRPC7) signaling (Gopal et al., 2010), we also analyzed proteins in these pathways. Immunoblotting showed that the TRPC7 protein level was reduced in both sedentary and exercised syndecan-$4^{-/-}$ (**Figure 5C**, KO-SED and KO-ET versus WT-SED). However, no differences were detected in disheveled (Dvl), β-catenin, frizzled-7, low-density lipoprotein receptor-related protein 6 (LRP6) or Wnt4 in syndecan-$4^{-/-}$ versus WT, indicating no involvement of canonical Wnt/β-catenin or non-canonical Wnt signaling (**Supplementary Figures 2C–G**). Similarly, no differences in the PKC or RCAN4.1 (regulator of calcineurin and a target for NFAT) levels were detected (**Supplementary Figures 2H,I**).

Taken together, our data indicate that the syndecan-$4^{-/-}$ muscle had increased activation of the Akt/mTOR/S6K1 and Notch-HES-1 pathways and that these pathways were not induced any further by exercise. Except for an also reduced TRPC7 level, few other changes were observed.

DISCUSSION

In this study we have characterized the TA muscle from syndecan-$4^{-/-}$ mice and analyzed molecules involved in ECM remodeling and muscle growth, both under steady state conditions and in response to exercise. Compared to WT, we found that syndecan-$4^{-/-}$ mice had reduced body weight, reduced muscle weight, muscle fibers with a smaller cross-sectional area, and reduced expression of MRFs. The syndecan-$4^{-/-}$ mice had also increased activation of the Akt/mTOR/S6K1 and Notch-HES-1 pathways, a reduced TRPC7 level, increased syndecan-2 expression, and altered expression of several ECM components. These molecular changes were observed under steady state conditions, and in contrast to WT mice, were mostly not affected further by exercise.

Closer inspection of the syndecan-$4^{-/-}$ muscle showed that the muscle fibers were on average smaller than wild type (WT) fibers, which probably accounts for the reduced TA weight. Consistent with previous findings (Cornelison et al., 2004), we found that myoD and myogenin were reduced in syndecan-$4^{-/-}$ mice of 12–22 weeks. MyoD is required for MuSC activation, proliferation and differentiation (Asfour et al., 2018). Myogenin expression is upregulated during differentiation and directs differentiating myoblasts to become terminally differentiated (Asfour et al., 2018). Consistent with a role of syndecan-4 in myogenesis, we have previously also demonstrated that the cytoplasmic part of syndecan-4 plays an important role in the early fusion process of myoblasts *in vitro* (Rønning et al., 2015). Our findings of the reduced body weight, muscle weight, muscle fibers and MRFs in syndecan-$4^{-/-}$ are illustrated in **Figure 6A**.

Previous experiments have shown that both syndecan-3 and syndecan-4 are affected by exercise in humans. Syndecan-4 was reported up-regulated after acute exercise, whereas syndecan-3 was up-regulated after long-term exercise (Hjorth et al., 2015). However, in another study using rats, exercise did not change the syndecan-4 level (Eftestol et al., 2016). In our study using mice subjected to 2 weeks treadmill running, syndecan-2, but not syndecan-4 was increased, suggesting a potential involvement of syndecan-2 in the muscle response to exercise. Interestingly, we also observed higher levels of syndecan-2 in syndecan-$4^{-/-}$ compared to WT (illustrated in **Figure 6B**). Upregulation of

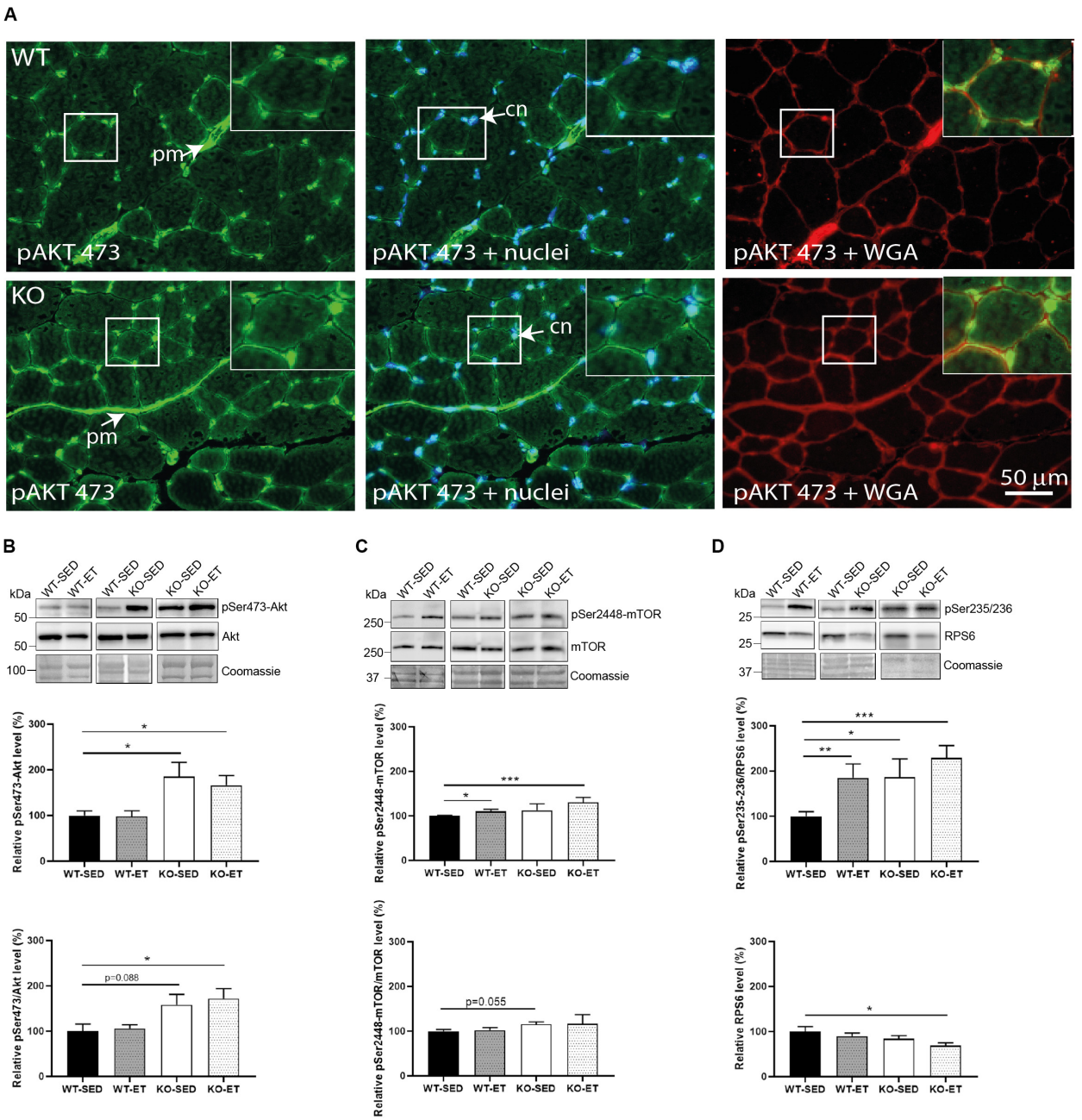

FIGURE 4 | The syndecan-4$^{-/-}$ muscle has an increased Akt/mTOR/S6K1 pathway. **(A)** Immunofluorescence of pSer473-Akt (green) in WT and syndecan-4$^{-/-}$ muscles. The cell nuclei were counterstained with Hoechst (blue). The connective tissue was stained with WGA (red). *cn* cell nuclei, *pm* perimysium, indicated with arrows. Inserts show magnification of boxed areas. Scalebar as indicated. Immunoblot analyses of **(B)** pSer473-Akt (upper panels) and Akt (middle panels), **(C)** pSer2448-mTOR (upper panels) and mTOR (middle panels), and **(D)** pSer235/236-RPS6 (upper panels) and RPS6 (middle panels) in WT-SED, WT-ET, KO-SED and KO-ET. The values are presented in percentage and are normalized to WT-SED (n = 6–10). Comparisons between the groups were analyzed using Mann–Whitney U test (*$p < 0.05$, **$p < 0.01$ and ***$p < 0.001$). ProBlue Safe Stain (Coomassie) was used as loading control (lower panels in **B–D**).

syndecan-2 has been reported as a compensatory mechanism during cartilage development in syndecan-4$^{-/-}$ (Bertrand et al., 2013). However, syndecan-2 was not higher in the left ventricle from syndecan-4$^{-/-}$ compared to WT (Strand et al., 2013), suggesting that compensatory upregulation of syndecan-2 is tissue dependent.

Although the mRNA levels of fibromodulin, decorin, biglycan, collagen 1, collagen 3 and the collagen cross-linking enzyme LOX were increased in syndecan-4$^{-/-}$ mice, the protein levels of fibromodulin, biglycan and LOX were reduced (illustrated in **Figure 6B**). This finding might suggest that some ECM components are more susceptible to degradation or less efficiently

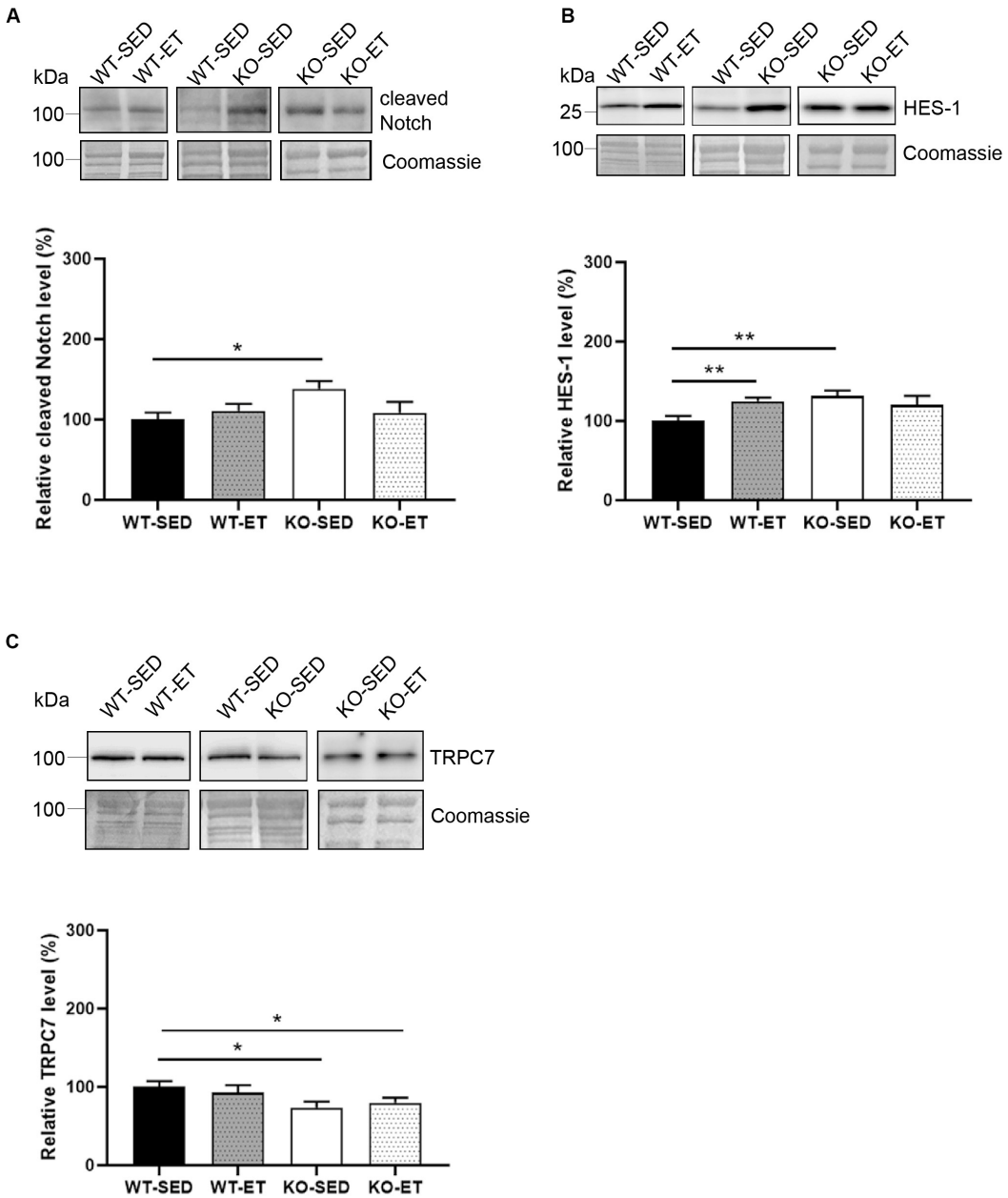

FIGURE 5 | The syndecan-4$^{-/-}$ muscle has an increased Notch/HES-1 pathway and a reduced TRPC7 level. Immunoblot analyses of **(A)** Cleaved Notch, **(B)** HES-1, and **(C)** TRPC7 in WT-SED, WT-ET, KO-SED, and KO-ET. The values are presented in percentage and are normalized to WT-SED (n = 6–10). Comparisons between the groups were analyzed using Mann–Whitney U test (*$p < 0.05$, **$p < 0.01$). ProBlue Safe Stain (Coomassie) was used as loading control (lower panels in **A–C**).

translated when syndecan-4 is absent. Indeed, proteins involved in the translational machinery have been identified in the cardiac syndecan-4 interactome (Mathiesen et al., 2019). It is also possible that syndecan-4 affects factors involved in post-transcriptional regulation of these proteins. Decorin is abundant in adult skeletal muscle and expressed during skeletal muscle differentiation (Brandan and Gutierrez, 2013), and consistent with our mice mRNA data, reported to be upregulated in rats after moderate treadmill running (Xu et al., 2018). Biglycan expression is reported highly upregulated during injury-induced regeneration, both in growing myotubes and in activated precursor cells, then the expression decreases again during maturation of muscle fibers (Casar et al., 2004; Brandan and Gutierrez, 2013). The relationship between biglycan and syndecan-4 in skeletal muscle is not known, however a recent publication using cultured vascular endothelial cells suggests biglycan as a regulatory molecule of the ALK5-Smad2/3-TGF-β1 signaling, with a direct negative impact on syndecan-4

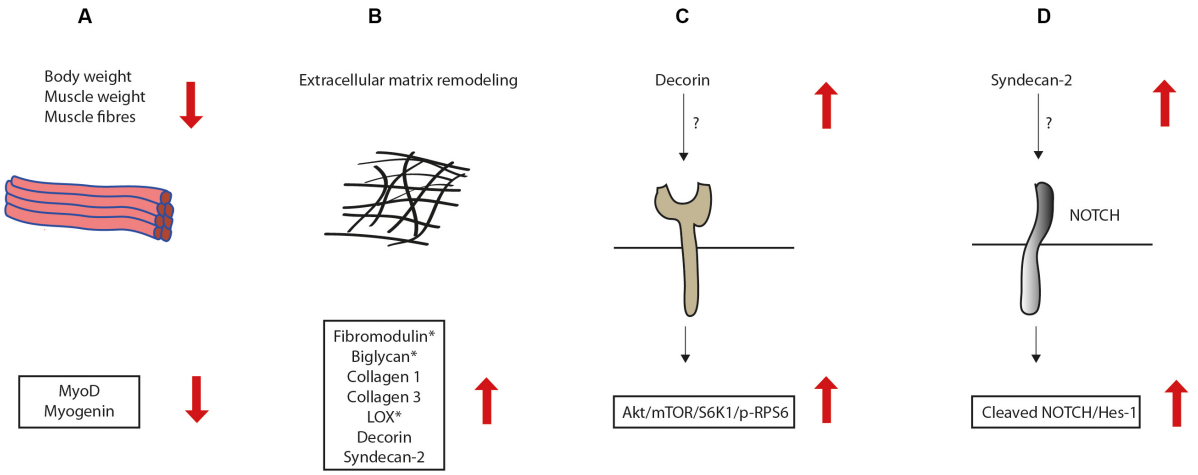

FIGURE 6 | Illustration of alterations in the syndecan-4$^{-/-}$ mice. **(A)** The syndecan-4$^{-/-}$ mice had reduced body weight, muscle weight, muscle fibers and expression of myogenic regulatory transcription factors. **(B)** The syndecan-4$^{-/-}$ muscle had increased mRNA levels of syndecan-2 and the ECM components decorin, fibromodulin, biglycan, collagen 1, collagen 3 and the collagen cross-linking enzyme lysyl oxidase (LOX). However, fibromodulin, biglycan and LOX were reduced at the protein level (denoted with star), suggesting that these ECM components are more susceptible to degradation or less efficiently translated when syndecan-4 is absent. The syndecan-4$^{-/-}$ muscle had also increased activation of the **(C)** Akt/mTOR/S6K1 and **(D)** Cleaved Notch1-HES-1 pathways.

expression (Takato et al., 2017). Further experiments are required to investigate whether the ALK5-Smad2/3-TGF-β1 pathway is also involved in the biglycan-syndecan-4 relationship in skeletal muscle. Fibromodulin is also central in the myogenic program and plays an important role in tissue repair (Lee et al., 2016). Specifically, fibromodulin triggers myoblast differentiation by preventing myostatin binding to its receptor; the activin receptor type-2B. Fibromodulin, biglycan and decorin are also suggested to regulate collagen fibrillogenesis and crosslinking, and thus ECM integrity and function of skeletal muscle (Kalamajski and Oldberg, 2010). Whether the increased mRNA expression of these ECM components, including collagens and LOX, represent a compensatory mechanism to improve ECM function and trigger myoblast differentiation in the syndecan-4$^{-/-}$ muscle, has to be determined in future work. In contrast to our findings, the syndecan-4$^{-/-}$ heart has rather reduced mRNA levels of collagen 1, collagen 3 and LOX following pressure overload, leading to an impaired cross-linking and collagen assembly (Herum et al., 2013, 2015). Our group has also previously shown that syndecan-4 is essential for cardiac myoblast differentiation (Herum et al., 2013) and that the syndecan-4$^{-/-}$ hearts do not develop concentric hypertrophy, but rather left ventricle dilatation and dysfunction following pressure overload (Finsen et al., 2011). Although a syndecan-4-calcineurin-NFAT pathway appeared essential for these events in the heart (Finsen et al., 2011; Herum et al., 2013, 2015), we found no changes in the calcineurin-NFAT pathway in the syndecan-4$^{-/-}$ TA muscle. Thus, although syndecan-4 is involved in both differentiation and cell growth of the heart and skeletal muscle, different pathways seem to be involved.

We also found higher levels of pSer473-Akt and pSer235/236-RPS6 in syndecan-4$^{-/-}$. The Akt/mTOR pathway is an important signaling pathway promoting muscle growth and fibrosis (Bodine et al., 2001; Li et al., 2013). Akt induces protein synthesis and hypertrophy by activating the serine/threonine kinase mTOR and the ribosomal protein S6 kinase 1 (SK61) (Schiaffino et al., 2013). SK61 is one of the main kinases phosphorylating ribosomal protein 6 (RPS6) (Meyuhas, 2015). Although RPS6 is primarily a structural protein of the ribosome, phosphorylation of RPS6 has been shown to be directly involved in cell size control (Meyuhas, 2015), and affects both translation as well as transcription efficiency. Our finding of an increased pSer235/236-RPS6 level in the syndecan-4$^{-/-}$ mice was quite surprising, since the smaller cell size and smaller cross-sectional area of myofibers rather links to a reduced pSer235/236-RPS6 level (Ruvinsky et al., 2009; Meyuhas, 2015). Our finding of the increased activation of the Akt/mTOR/S6K1 pathway in syndecan-4$^{-/-}$ is illustrated in **Figure 6C**. Notably, decorin, which was also increased in syndecan-4$^{-/-}$, has been shown to activate Akt downstream of IGF1R, in addition to increase myoD and myogenin expression and promote myoblast differentiation (Suzuki et al., 2013).

Our findings of higher levels of both Cleaved Notch and HES-1 in syndecan-4$^{-/-}$ mice, strongly suggest an increased Notch signaling when syndecan-4 is absent. HES-1 signaling was also higher in exercised compared to sedentary WT mice. Notch is a regulator of myogenesis and is increased upon physiological stimuli such as exercise (see review Arthur and Cooley, 2012; LaFoya et al., 2016). Notch signaling is indispensable for maintaining quiescence and self-renewal of MuSCs, and promotes proliferation of MuSCs by keeping low MyoD levels and prevents differentiation (Buas and Kadesch, 2010; Bi et al., 2016). Upon ligand binding, the intracellular domain of the Notch receptor is cleaved off (Cleaved Notch) and translocated to the nucleus where it activates the transcription factor CLS/RBPJ and induces expression of the transcriptional repressors of the HES and HEY family (Iso et al., 2003;

D'Souza et al., 2008). Interestingly, both syndecan-2 and 3 have been linked to Notch signaling pathways (Pisconti et al., 2010; LaFoya et al., 2016). Syndecan-3 interacts with Notch at the plasma membrane in the MuSC, and this interaction has been suggested to be important for Notch cleavage (Pisconti et al., 2010). Loss of syndecan-3 impairs Notch signaling, alters MuSC homeostasis and leads to progressively increased myofiber size, which is especially noticed in repeatedly injured and dystrophic mice (Pisconti et al., 2010, 2016). Syndecan-2 is reported highly abundant in early-differentiated myoblasts (Do et al., 2015). Interestingly, Cleaved Notch has been shown to induce syndecan-2 expression in smooth muscle cells, which again interacts with the Notch receptor at the surface membrane and promotes further Notch signaling (Zhao et al., 2012). Whether the increased Notch signaling we observed in syndecan-4$^{-/-}$ is due to the increased syndecan-2 level or *vice versa* has to be determined by future experiments (illustrated in **Figure 6D**).

Desmin was the only protein in our analyses that was increased in exercised WT, but neither changed in sedentary or exercised syndecan-4$^{-/-}$. Desmin is the most abundant intermediate filament protein in adult skeletal muscle, expressed at low levels in MuSCs and increased during myogenic commitment and differentiation (Hnia et al., 2015). Human heterozygous desmin mutations link to muscular weakness and different skeletal and cardiac myopathies. In line with this, the desmin$^{-/-}$ mouse model is also reported weaker; it fatigued more easily and showed an impaired performance on endurance tests (Haubold et al., 2003). Whether the syndecan-4$^{-/-}$ mice also fatigues more easily must be determined in larger endurance tests in future.

Conclusively, our data show that key molecular pathways involved in matrix remodeling and muscle growth were affected in syndecan-4$^{-/-}$ mice. These molecular changes were observed under steady state conditions, and in contrast to WT, were mostly not affected by exercise. Functional studies to elucidate the exact role of the ECM components in the syndecan-4$^{-/-}$ mice should be performed in future studies. In particular, compensatory effects of syndecan-2 and vice-versa is of particular interest in follow up-studies.

DATA AVAILABILITY STATEMENT

All datasets presented in this study are included in the article/**Supplementary Material**.

ETHICS STATEMENT

All animal experiments were performed in accordance with the National Regulation on Animal Experimentation in accordance with an approved protocol and the Norwegian Animal Welfare Act and conform the NIH guidelines.

AUTHOR CONTRIBUTIONS

SR, CC, and MP: conceptualization, investigation, methodology, visualization, and writing the original draft. JA: conceptualization, investigation, methodology, and review and editing the original draft. AP: conceptualization, visualization, review and editing the original draft. VH, ML, and KL: investigation, methodology, and review and editing the original draft. IS: methodology, review and editing the original draft, and funding acquisition. SK: conceptualization, investigation, review and editing the original draft. GC: conceptualization, investigation, review and editing the original draft, and funding acquisition. All authors contributed to the article and approved the submitted version.

FUNDING

This work was supported by grants from the Norwegian Fund for Research Fees for Agricultural Products, Stiftelsen Kristian Gerhard Jebsen, The Research Council of Norway, and Anders Jahre's Fund for the Promotion of Science University of Oslo. The funder had no role in study design, data collection and analysis, decision to publish, or preparation of the manuscript.

ACKNOWLEDGMENTS

We would like to thank Anita Kaupang for some of the immunoblot analysis and Marita Martinsen and Per Kristian Lunde for help with muscle dissection.

SUPPLEMENTARY MATERIAL

The Supplementary Material for this article can be found online at: https://www.frontiersin.org/articles/10.3389/fcell.2020.00730/full#supplementary-material

REFERENCES

Arthur, S. T., and Cooley, I. D. (2012). The effect of physiological stimuli on sarcopenia; impact of Notch and Wnt signaling on impaired aged skeletal muscle repair. *Int. J. Biol. Sci.* 8, 731–760. doi: 10.7150/ijbs.4262

Asfour, H. A., Allouh, M. Z., and Said, R. S. (2018). Myogenic regulatory factors: the orchestrators of myogenesis after 30 years of discovery. *Exp. Biol. Med.* 243, 118–128. doi: 10.1177/1535370217749494

Bertrand, J., Stange, R., Hidding, H., Echtermeyer, F., Nalesso, G., Godmann, L., et al. (2013). Syndecan 4 supports bone fracture repair, but not fetal skeletal development, in mice. *Arthritis Rheumatism.* 65, 743–752. doi: 10.1002/art.37817

Bi, P., Yue, F., Sato, Y., Wirbisky, S., Liu, W., Shan, T., et al. (2016). Stage-specific effects of Notch activation during skeletal myogenesis. *eLife* 5:e17355.

Bodine, S. C., Stitt, T. N., Gonzalez, M., Kline, W. O., Stover, G. L., Bauerlein, R., et al. (2001). Akt/mTOR pathway is a crucial regulator of skeletal muscle hypertrophy and can prevent muscle atrophy in vivo. *Nat. Cell Biol.* 3, 1014–1019. doi: 10.1038/ncb1101-1014

Brandan, E., and Gutierrez, J. (2013). Role of skeletal muscle proteoglycans during myogenesis. *Matrix Biol.* 32, 289–297. doi: 10.1016/j.matbio.2013.03.007

Buas, M. F., and Kadesch, T. (2010). Regulation of skeletal myogenesis by Notch. *Exp. Cell Res.* 316, 3028–3033. doi: 10.1016/j.yexcr.2010.05.002

Bustin, S. A., Beaulieu, J. F., Huggett, J., Jaggi, R., Kibenge, F. S., Olsvik, P. A., et al. (2010). MIQE precis: practical implementation of minimum standard guidelines for fluorescence-based quantitative real-time PCR experiments. *BMC Mol. Biol.* 11:74. doi: 10.1186/1471-2199-11-74

Casar, J. C., McKechnie, B. A., Fallon, J. R., Young, M. F., and Brandan, E. (2004). Transient up-regulation of biglycan during skeletal muscle regeneration: delayed fiber growth along with decorin increase in biglycan-deficient mice. *Dev. Biol.* 268, 358–371. doi: 10.1016/j.ydbio.2003.12.025

Christensen, G., Herum, K. M., and Lunde, I. G. (2018). Sweet, yet underappreciated: proteoglycans and extracellular matrix remodeling in heart disease. *Matrix Biol.* 76, 286–299. doi: 10.1016/j.matbio.2018.01.001

Cornelison, D. D., Filla, M. S., Stanley, H. M., Rapraeger, A. C., and Olwin, B. B. (2001). Syndecan-3 and syndecan-4 specifically mark skeletal muscle satellite cells and are implicated in satellite cell maintenance and muscle regeneration. *Dev. Biol.* 239, 79–94. doi: 10.1006/dbio.2001.0416

Cornelison, D. D. W., Wilcox-Adelman, S. A., Goetinck, P. F., Rauvala, H., Rapraeger, A. C., and Olwin, B. B. (2004). Essential and separable roles for Syndecan-3 and Syndecan-4 in skeletal muscle development and regeneration. *Genes Dev.* 18, 2231–2236. doi: 10.1101/gad.1214204

Couchman, J. R. (2010). Transmembrane signaling proteoglycans. *Annu. Rev. Cell Dev. Biol.* 26, 89–114. doi: 10.1146/annurev-cellbio-100109-104126

Couchman, J. R., Gopal, S., Lim, H. C., Nørgaard, S., and Multhaupt, H. A. B. (2015). Syndecans: from peripheral coreceptors to mainstream regulators of cell behaviour. *Int. J. Exp. Pathol.* 96, 1–10. doi: 10.1111/iep.12112

Do, M. K., Shimizu, N., Suzuki, T., Ohtsubo, H., Mizunoya, W., Nakamura, M., et al. (2015). Transmembrane proteoglycans syndecan-2, 4, receptor candidates for the impact of HGF and FGF2 on semaphorin 3A expression in early-differentiated myoblasts. *Physiol. Rep.* 3:e12553. doi: 10.14814/phy2.12553

D'Souza, B., Miyamoto, A., and Weinmaster, G. (2008). The many facets of Notch ligands. *Oncogene* 27, 5148–5167. doi: 10.1038/onc.2008.229

Echtermeyer, F., Streit, M., Wilcox-Adelman, S., Saoncella, S., Denhez, F., Detmar, M., et al. (2001). Delayed wound repair and impaired angiogenesis in mice lacking syndecan-4. *J. Clin. Invest.* 107, R9–R14.

Eftestol, E., Egner, I. M., Lunde, I. G., Ellefsen, S., Andersen, T., Sjaland, C., et al. (2016). Increased hypertrophic response with increased mechanical load in skeletal muscles receiving identical activity patterns. *Am. J. Physiol. Cell Physiol.* 311, C616–C629.

Elfenbein, A., and Simons, M. (2013). Syndecan-4 signaling at a glance. *J. Cell Sci.* 126(Pt 17), 3799–3804. doi: 10.1242/jcs.124636

Finsen, A. V., Lunde, I. G., Sjaastad, I., Ostli, E. K., Lyngra, M., Jarstadmarken, H. O., et al. (2011). Syndecan-4 is essential for development of concentric myocardial hypertrophy via stretch-induced activation of the calcineurin-NFAT pathway. *PLoS One* 6:e28302. doi: 10.1371/journal.pone.0028302

Folker, E. S., and Baylies, M. K. (2013). Nuclear positioning in muscle development and disease. *Front. Physiol.* 4:363. doi: 10.3389/fphys.2013.00363

Gopal, S., Bober, A., Whiteford, J. R., Multhaupt, H. A., Yoneda, A., and Couchman, J. R. (2010). Heparan sulfate chain valency controls syndecan-4 function in cell adhesion. *J. Biol. Chem.* 285, 14247–14258. doi: 10.1074/jbc.m109.056945

Haubold, K. W., Allen, D. L., Capetanaki, Y., and Leinwand, L. A. (2003). Loss of desmin leads to impaired voluntary wheel running and treadmill exercise performance. *J. Appl. Physiol.* 95, 1617–1622. doi: 10.1152/japplphysiol.00408.2003

Herum, K. M., Lunde, I. G., Skrbic, B., Florholmen, G., Behmen, D., Sjaastad, I., et al. (2013). Syndecan-4 signaling via NFAT regulates extracellular matrix production and cardiac myofibroblast differentiation in response to mechanical stress. *J. Mol. Cell. Cardiol.* 54, 73–81. doi: 10.1016/j.yjmcc.2012.11.006

Herum, K. M., Lunde, I. G., Skrbic, B., Louch, W. E., Hasic, A., Boye, S., et al. (2015). Syndecan-4 is a key determinant of collagen cross-linking and passive myocardial stiffness in the pressure-overloaded heart. *Cardiovasc. Res.* 106, 217–226. doi: 10.1093/cvr/cvv002

Hjorth, M., Norheim, F., Meen, A. J., Pourteymour, S., Holen, T., Jensen, J., et al. (2015). The effect of acute and long-term physical activity on extracellular matrix and serglycin in human skeletal muscle. *Physiol. Rep.* 3:e12473. doi: 10.14814/phy2.12473

Hnia, K., Ramspacher, C., Vermot, J., and Laporte, J. (2015). Desmin in muscle and associated diseases: beyond the structural function. *Cell Tissue Res.* 360, 591–608. doi: 10.1007/s00441-014-2016-4

Iso, T., Kedes, L., and Hamamori, Y. (2003). HES and HERP families: multiple effectors of the Notch signaling pathway. *J. Cell. Physiol.* 194, 237–255. doi: 10.1002/jcp.10208

Kalamajski, S., Liu, C., Tillgren, V., Rubin, K., Oldberg, A., Rai, J., et al. (2014). Increased C-telopeptide cross-linking of tendon type I collagen in fibromodulin-deficient mice. *J. Biol. Chem.* 289, 18873–18879. doi: 10.1074/jbc.m114.572941

Kalamajski, S., and Oldberg, A. (2010). The role of small leucine-rich proteoglycans in collagen fibrillogenesis. *Matrix Biol.* 29, 248–253. doi: 10.1016/j.matbio.2010.01.001

LaFoya, B., Munroe, J. A., Mia, M. M., Detweiler, M. A., Crow, J. J., Wood, T., et al. (2016). Notch: a multi-functional integrating system of microenvironmental signals. *Dev. Biol.* 418, 227–241. doi: 10.1016/j.ydbio.2016.08.023

Lee, E. J., Jan, A. T., Baig, M. H., Ashraf, J. M., Nahm, S. S., Kim, Y. W., et al. (2016). Fibromodulin: a master regulator of myostatin controlling progression of satellite cells through a myogenic program. *FASEB J.* 30, 2708–2719. doi: 10.1096/fj.201500133r

Li, H. Y., Zhang, Q. G., Chen, J. W., Chen, S. Q., and Chen, S. Y. (2013). The fibrotic role of phosphatidylinositol-3-kinase/Akt pathway in injured skeletal muscle after acute contusion. *Int. J. Sports Med.* 34, 789–794. doi: 10.1055/s-0032-1333284

Mathiesen, S. B., Lunde, M., Aronsen, J. M., Romaine, A., Kaupang, A., Martinsen, M., et al. (2019). The cardiac syndecan-4 interactome reveals a role for syndecan-4 in nuclear translocation of muscle LIM protein (MLP). *J. Biol. Chem.* 294, 8717–8731. doi: 10.1074/jbc.ra118.006423

Mauro, A. (1961). Satellite cell of skeletal muscle fibers. *J. Biophys. Biochem. Cytol.* 9, 493–495. doi: 10.1083/jcb.9.2.493

Meyuhas, O. (2015). Ribosomal Protein S6 phosphorylation: four decades of research. *Int. Rev. Cell Mol. Biol.* 320, 41–73. doi: 10.1016/bs.ircmb.2015.07.006

Olguin, H., and Brandan, E. (2001). Expression and localization of proteoglycans during limb myogenic activation. *Dev. Dyn.* 221, 106–115. doi: 10.1002/dvdy.1129

Pataki, C. A., Couchman, J. R., and Brabek, J. (2015). Wnt signaling cascades and the roles of syndecan proteoglycans. *J. Histochem. Cytochem.* 63, 465–480. doi: 10.1369/0022155415586961

Pawlikowski, B., Vogler, T. O., Gadek, K., and Olwin, B. B. (2017). Regulation of skeletal muscle stem cells by fibroblast growth factors. *Dev. Dyn.* 246, 359–367. doi: 10.1002/dvdy.24495

Pisconti, A., Banks, G. B., Babaeijandaghi, F., Betta, N. D., Rossi, F. M., Chamberlain, J. S., et al. (2016). Loss of niche-satellite cell interactions in syndecan-3 null mice alters muscle progenitor cell homeostasis improving muscle regeneration. *Skeletal Muscle* 6:34.

Pisconti, A., Bernet, J. D., and Olwin, B. B. (2012). Syndecans in skeletal muscle development, regeneration and homeostasis. *MusclesLigaments Tendons J.* 2, 1–9.

Pisconti, A., Cornelison, D. D. W., Olguin, H. C., Antwine, T. L., and Olwin, B. B. (2010). Syndecan-3 and Notch cooperate in regulating adult myogenesis. *J. Cell Biol.* 190, 427–441. doi: 10.1083/jcb.201003081

Rønning, S. B., Carlson, C. R., Stang, E., Kolset, S. O., Hollung, K., and Pedersen, M. E. (2015). Syndecan-4 regulates muscle differentiation and is internalized from the plasma membrane during myogenesis. *PLoS One* 10:e0129288. doi: 10.1371/journal.pone.0129288

Ruvinsky, I., Katz, M., Dreazen, A., Gielchinsky, Y., Saada, A., Freedman, N., et al. (2009). Mice deficient in ribosomal Protein S6 phosphorylation suffer from muscle weakness that reflects a growth defect and energy deficit. *PLoS One* 4:e5618. doi: 10.1371/journal.pone.0005618

Sabourin, L. A., and Rudnicki, M. A. (2000). The molecular regulation of myogenesis. *Clin. Genet.* 57, 16–25. doi: 10.1034/j.1399-0004.2000.570103.x

Schiaffino, S., Dyar, K. A., Ciciliot, S., Blaauw, B., and Sandri, M. (2013). Mechanisms regulating skeletal muscle growth and atrophy. *Febs J.* 280, 4294–4314. doi: 10.1111/febs.12253

Schmittgen, T. D., and Livak, K. J. (2008). Analyzing real-time PCR data by the comparative C(T) method. *Nat. Protoc.* 3, 1101–1108. doi: 10.1038/nprot.2008.73

Seale, P., Sabourin, L. A., Girgis-Gabardo, A., Mansouri, A., Gruss, P., and Rudnicki, M. A. (2000). Pax7 is required for the specification of myogenic satellite cells. *Cell* 102, 777–786. doi: 10.1016/s0092-8674(00)00066-0

Strand, M. E., Herum, K. M., Rana, Z. A., Skrbic, B., Askevold, E. T., Dahl, C. P., et al. (2013). Innate immune signaling induces expression and shedding of the heparan sulfate proteoglycan syndecan-4 in cardiac fibroblasts and myocytes, affecting inflammation in the pressure-overloaded heart. *Febs J.* 280, 2228–2247. doi: 10.1111/febs.12161

Suzuki, K., Kishioka, Y., Wakamatsu, J., and Nishimura, T. (2013). Decorin activates Akt downstream of IGF-IR and promotes myoblast differentiation. *Anim. Scie. J.* 84, 669–674. doi: 10.1111/asj.12055

Takato, H., Eiko, Y., Yasuhiro, S., Chika, Y., Yasuyuki, F., Yoshito, K., et al. (2017). Biglycan Intensifies ALK5–Smad2/3 Signaling by TGF-β1 and downregulates syndecan-4 in cultured vascular endothelial cells. *J. Cell. Biochem.* 118, 1087–1096. doi: 10.1002/jcb.25721

Thomas, K., Engler, A. J., and Meyer, G. A. (2015). Extracellular matrix regulation in the muscle satellite cell niche. *Connect. Tissue Res.* 56, 1–8. doi: 10.3109/03008207.2014.947369

Tsivitse, S. (2010). Notch and Wnt signaling, physiological stimuli and postnatal myogenesis. *Int. J. Biol. Sci.* 6, 268–281. doi: 10.7150/ijbs.6.268

Velleman, S. G., Shin, J., Li, X. H., and Song, Y. (2012). Review: the skeletal muscle extracellular matrix: Possible roles in the regulation of muscle development and growth. *Can. J. Anim. Sci.* 92, 1–10. doi: 10.4141/cjas2011-098

Velleman, S. G., and Song, Y. (2017). Development and growth of the avian pectoralis major (Breast) muscle: function of syndecan-4 and Glypican-1 in adult myoblast proliferation and differentiation. *Front. Physiol.* 8:577. doi: 10.3389/fphys.2017.00577

Xu, S. Y., He, Y. B., Deng, S. Y., Liu, S. Y., Xu, L., and Ni, G. X. (2018). Intensity-dependent effect of treadmill running on rat Achilles tendon. *Exp. Ther. Med.* 15, 5377–5383.

Zammit, P. S., Golding, J. P., Nagata, Y., Hudon, V., Partridge, T. A., and Beauchamp, J. R. (2004). Muscle satellite cells adopt divergent fates: a mechanism for self-renewal? *J. Cell Biol.* 166, 347–357. doi: 10.1083/jcb.200312007

Zhao, N., Liu, H., and Lilly, B. (2012). Reciprocal regulation of syndecan-2 and Notch signaling in vascular smooth muscle cells. *J. Biol. Chem.* 287, 16111–16120. doi: 10.1074/jbc.m111.322107

Conflict of Interest: The authors declare that the research was conducted in the absence of any commercial or financial relationships that could be construed as a potential conflict of interest.

frontiers in Cell and Developmental Biology

REVIEW
published: 07 August 2020
doi: 10.3389/fcell.2020.00731

Distribution and Function of Glycosaminoglycans and Proteoglycans in the Development, Homeostasis and Pathology of the Ocular Surface

*Sudan Puri[1], Yvette M. Coulson-Thomas[2], Tarsis F. Gesteira[1,3] and Vivien J. Coulson-Thomas[1]**

[1] College of Optometry, University of Houston, Houston, TX, United States, [2] Molecular Biology Section, Department of Biochemistry, Universidade Federal de São Paulo, São Paulo, Brazil, [3] Optimvia, LLC, Batavia, OH, United States

OPEN ACCESS

Edited by:
Jeremy Turnbull, University of Liverpool, United Kingdom

Reviewed by:
Jun Zhou, German Cancer Research Center (DKFZ), Germany
Rizaldy Paz Scott, Northwestern University, United States

***Correspondence:**
Vivien J. Coulson-Thomas
vcoulsonthomas@gmail.com; vjcoulso@central.uh.edu

Specialty section:
This article was submitted to Signaling, a section of the journal Frontiers in Cell and Developmental Biology

Received: *30 April 2020*
Accepted: *15 July 2020*
Published: *07 August 2020*

Citation:
Puri S, Coulson-Thomas YM, Gesteira TF and Coulson-Thomas VJ (2020) Distribution and Function of Glycosaminoglycans and Proteoglycans in the Development, Homeostasis and Pathology of the Ocular Surface. Front. Cell Dev. Biol. 8:731. doi: 10.3389/fcell.2020.00731

The ocular surface, which forms the interface between the eye and the external environment, includes the cornea, corneoscleral limbus, the conjunctiva and the accessory glands that produce the tear film. Glycosaminoglycans (GAGs) and proteoglycans (PGs) have been shown to play important roles in the development, hemostasis and pathology of the ocular surface. Herein we review the current literature related to the distribution and function of GAGs and PGs within the ocular surface, with focus on the cornea. The unique organization of ECM components within the cornea is essential for the maintenance of corneal transparency and function. Many studies have described the importance of GAGs within the epithelial and stromal compartment, while very few studies have analyzed the ECM of the endothelial layer. Importantly, GAGs have been shown to be essential for maintaining corneal homeostasis, epithelial cell differentiation and wound healing, and, more recently, a role has been suggested for the ECM in regulating limbal stem cells, corneal innervation, corneal inflammation, corneal angiogenesis and lymphangiogenesis. Reports have also associated genetic defects of the ECM to corneal pathologies. Thus, we also highlight the role of different GAGs and PGs in ocular surface homeostasis, as well as in pathology.

Keywords: cornea, wound healing, lumican, keratan sulfate, decorin

Abbreviations: ALK5, activin linked kinase 5; Asn, asparagines; Cmd, cartilage matrix deficiency; CS, chondroitin sulfate; CSPGs, chondroitin sulfate proteoglycans; DS, dermatan sulfate; DSPGs, dermatan sulfate proteoglycans; ECM, extracellular matrix; ERK, extracellular signal-regulated kinase; Ext1, exostosin glycosyltransferase 1; FAK, focal adhesion kinase; GAGs, glycosaminoglycans; Gal, galactose; GalNAc, *N*-acetylgalactosamine; GlcA, glucuronic acid; GlcNAc, *N*-acetylglucosamine; GlcNAc6ST, *N*-acetylglucosamine-6-*O*-sulfotransferase; GPCs, glypicans; GPI, glycosylphosphatidylinositol; HA, hyaluronan; HAS, hyaluronan synthase; HEP, heparin; HS, heparan sulfate; HSPGs, heparan sulfate proteoglycans; IdoA, iduronic acid; JNK, c-Jun N-terminal kinase; KS, keratan sulfate; KSPGs, keratan sulfate proteoglycans; LPS, lipopolysaccharides; MMP, matrix metalloproteinase; NDST, glucosaminyl *N*-deacetylase/*N*-sulfotransferase; PAPS, 3′-phosphoadenosine-5′-phosphosulfate; PGs, proteoglycans; PRG4, proteoglycan 4; Ser, serine; SLRPs, small leucine-rich proteoglycans; TGF-β, transforming growth factor beta; TGFBIP, TGF beta-induced protein; Thr, threonine; TLR4, toll-like receptor 4.

INTRODUCTION

The ECM components are not only space fillers, as believed for many decades, but are actually physiologically active components that play an important role in development, homeostasis and pathology (Badylak et al., 2009; Frantz et al., 2010; Clause and Barker, 2013). PGs and GAGs are ubiquitous components of the ECM and are particularly enriched in connective tissues (Varki et al., 1999). PGs are composed of a core protein covalently linked to at least one GAG side chain and can be classified into different groups based on their core protein and/or the composition of GAG side chains (Hardingham and Fosang, 1992; Iozzo, 1998). GAGs are unbranched polysaccharides with repeating disaccharide units composed of a hexosamine (D-GlcNAc or D-GalNAc) and a hexuronic acid (D-GlcA, L-IdoA, or D-Gal in the case of KS) (Anseth, 1969; Varki et al., 1999; Mikami and Kitagawa, 2017). Based on the composition of the repeating disaccharide unit, GAGs are subdivided into CS, DS, KS, HS/heparin (HEP) and HA (a stick representation of each GAG is shown in **Figure 1**) (Anseth, 1969; Varki et al., 1999). During biosynthesis, GAG chains undergo secondary modifications by the actions of sulfotransferase and epimerase enzymes (Mikami and Kitagawa, 2017). The spatiotemporally controlled expression of these enzymes enables cells to fine-tune sugar heterogeneity (Varki et al., 1999). Sulfotransferases use the universal sulfate donor PAPS to add 2-, 6- and 3-*O* sulfates to HS/HEP and 2-, 4-, and 6-*O* sulfates to CS/DS, while the epimerases convert GlcA to IdoA (Mencio et al., 2015). Thus, GAG biosynthesis is not template driven, which means there is significant variation in sulfation patterns and glucuronic/IdoA content among the synthesized GAGs, which are essential in determining their physical properties (Varki et al., 1999; Ohtsubo and Marth, 2006; Afratis et al., 2013). The presence of carboxylate and sulfate groups provides GAGs with highly negative charges and means they attract and retain water, which also directly correlates with their physiological properties (Rozario and DeSimone, 2010). These water molecules play an essential role in mediating interactions between GAG and protein binding sites (Warshel et al., 1986; Sarkar et al., 2016; Cui et al., 2018). In **Figure 1** we demonstrate the calculated water energy density distributions for the different GAGs, specifically the force with which each GAG interacts with water molecules. The representative tetrasaccharide unit of heparin has the highest solvation energy, while the tetrasaccharide unit in HA has the lowest. Recent studies have shown that GAG chains preferentially bind to ligands that will lower their desolvation energy and water molecules participate in many GAG-protein interactions within the binding site (Sarkar et al., 2016; Cui et al., 2018). **Figure 1** shows the solvent-solute energies of a representative tetrasaccharide for each GAG, calculated using the three-dimensional reference interaction site model (3D-RISM) theory. These energy maps function as a predictive of the specificity of the interaction of each GAG with their binding partners (Sugita et al., 2020).

Glycosaminoglycans and PGs have been shown to participate and/or regulate various signaling pathways, such as, the TGF-β, JNK/p38, FAK, and ERK pathways. TGF-β is a family of dimeric proteins with three isoforms – TGF-β1, TGF-β2, and TGF-β3 expressed by corneal and limbal epithelia, conjunctiva and stromal keratocytes (Saika et al., 2004; Chen et al., 2006). TGF-β receptor-III (betaglycan) is the most abundant membrane PG receptor containing HS and CS chains (Cheifetz et al., 1988; Chen et al., 2006). The HS regulates the binding of betaglycan to TGF-β and the deficiency or enzymatic removal of HS in epithelial cells reduces the degradation of TGF-β1 (Chen et al., 2006). TGF-β plays an important role in ocular surface homeostasis and pathology as it induces the synthesis and secretion of ECM components, promotes adhesion complex formation with corneal epithelial cells, increases protease inhibitor expression and recruits monocytes/neutrophils during

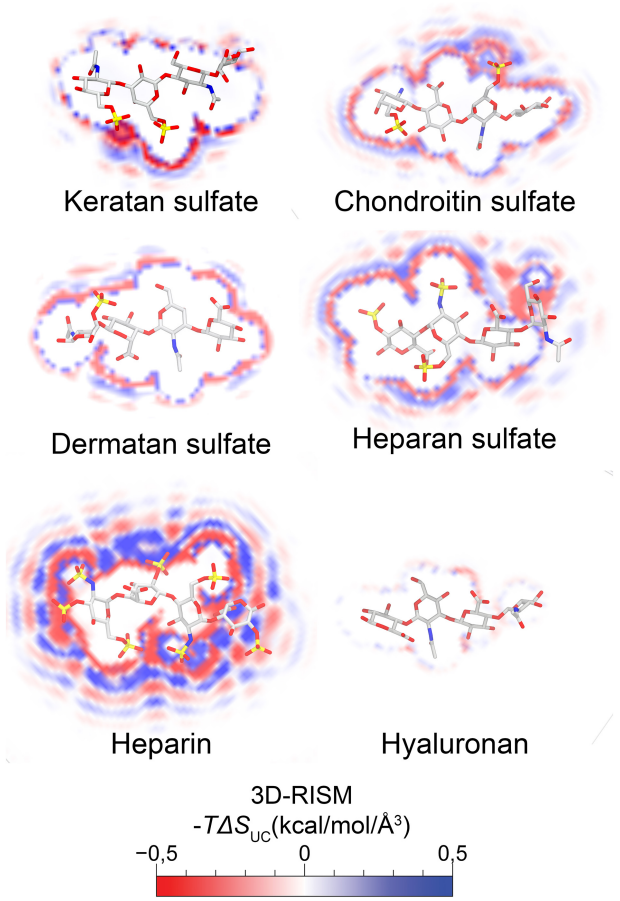

FIGURE 1 | Molecular reconstruction of thermodynamic maps of water entities around a representative tetrasaccharide of the different GAGs. Molecular reconstruction of thermodynamic maps of water entities were depicted additively by combining oxygen and hydrogen against a solute. Solute-solvent interaction description was calculated by 3D-RISM (three-dimensional reference interaction site model with Universal Correlation, UC) (Luchko et al., 2010; Nguyen et al., 2019). The displacement of water molecules favorably modulates the free energy of protein-ligand complex binding. A cross section at the center of mass is represented in the *x*-axis for each tetrasaccharide with a licorice representation of each GAG in an overlay. The thermodynamic maps of water entities can be directly correlated with the electrostatic charges of each tetrasaccharide unit and the specificity with which they bind to their binding partners.

inflammation (Gassner et al., 1997; Ljubimov and Saghizadeh, 2015). The TGF-β-receptor complex activates the Smad signaling pathway and other non-Smad pathways involving ras/MEK/ERK, RhoA, stress kinases (JNK and p38MAPK), and PI3K/AKT (Bhowmick et al., 2001; Santander and Brandan, 2006). The ERK signaling pathway requires the HSPG syndecan-4 for Cellular Communication Network Factor 2 and type I collagen expression (Leask , 2010; Nourian et al., 2019). TGF-β also induces the differentiation of fibroblasts to myofibroblasts via the FAK-MEKK1-JNK pathway (Liu et al., 2007). TGF-β activates FAK, which induces JNK-dependent actin stress fiber formation and expression of profibrotic genes in fibroblasts leading to ECM remodeling (Liu et al., 2007; Leask , 2010).

The ocular surface, including the cornea, corneoscleral limbus, conjunctiva, tear producing glands and tear film, form the interface between the external and internal environment of the eye. The unique organization of ECM components throughout the ocular surface is essential for maintaining healthy tissue, and therefore for enabling vision. The ocular surface is protected from external chemicals and microbes by mucin glycoproteins rich in *O*-glycans, which are synthesized by corneal and conjunctival epithelial cells (Brockhausen et al., 2018). Since the initial study of GAGs in corneal disorders in 1969 (Anseth, 1969), a plethora of studies have investigated the role of GAGs and PGs in the ocular surface of various species including humans. For example, HSPGs are constituents of cell-cell and cell-basement membrane junctions that are important for the barrier function of the corneal epithelium and endothelium, while small leucine-rich PGs (SLRPs) are necessary for the organization of collagen fibers within the stroma and are therefore necessary for maintaining corneal transparency (Varki et al., 1999). More recently, important roles have been suggested for the ECM in regulating limbal stem cells, corneal innervation, corneal inflammation, angiogenesis and lymphangiogenesis (Cursiefen et al., 2004; Gesteira et al., 2017; Pal-Ghosh et al., 2017; Sun et al., 2019). Moreover, ECM components have also been shown to be important constituents of the tear film (Baier et al., 1990; De Souza et al., 2006). Reports have also associated genetic defects to abnormalities in the ECM leading to corneal opacity and blindness (Clause and Barker, 2013). Herein, we will outline the roles of GAGs and PGs in the different compartments of the ocular surface and how they correlate with pathology.

KERATAN SULFATE PROTEOGLYCANS (KSPGs)

Keratan sulfate is composed of a repeating disaccharide unit made up of GlcNAc and a Gal, more specifically 3Galβ1-4GlcNAcβ1, and can be sulfated at carbon position 6 (C6) of the Gal or GlcNAc monosaccharides. Although all GAGs are bound to PGs via the tetrasaccharide linkage region Xyl-Gal-Gal-GlcNAc, KS is an exception and has a unique linkage region which gives rise to different types of KS, namely KS types I, II, and III (Funderburgh, 2000). More specifically, KS type I attaches to an Asn residue on the core protein via a complex N-linked branched oligosaccharide. KS type II attaches to a serine or threonine (Ser/Thr) amino acid on the core protein via an O-linked glycan (α-Gal-Ser/Thr). KS type III attaches to a Ser amino acid on the core protein via a mannose-Ser linkage (Funderburgh, 2000). The cornea is the tissue with the highest KS content and is the richest source of type I KSPGs, which were originally identified in the cornea in 1939 (Suzuki, 1939; Funderburgh, 2000; Quantock et al., 2010). Normal human corneas contain 15 μg of KS per mg dry weight with ∼14 disaccharides per chain consisting of ∼4% unsulfated, 42% monosulfated, and 54% disulfated disaccharides (Plaas et al., 2001). The enzymatic sulfation of KS by GlcNAc-6-*O*-sulfotransferase (GlcNAc6ST) is required for normal collagen matrix biosynthesis and organization in the cornea (Hayashida et al., 2006). Reduced activity of GlcNAc6ST, which catalyzes the transfer of sulfate to position 6 of terminal GlcNAc, results in low-sulfated KS synthesis and accumulation in macular corneal dystrophy (Hasegawa et al., 2000). In normal human corneas, KS is predominantly found in the central cornea and gradually decreases toward the limbus–sclera regions (Borcherding et al., 1975). Loss of KS in corneas of β-1,3-NAcetylglucosaminyltransferase-7 *null* mice leads to corneal thinning (Littlechild et al., 2018). Interestingly, KS deficient mice significantly up-regulate CS throughout the corneal stroma through a compensatory mechanism (Littlechild et al., 2018).

The KS in corneas is mostly bound to SLRPs such as lumican, keratocan, fibromodulin, and osteoglycin/mimecan, which have been shown to regulate corneal development, corneal transparency and wound healing. Lumican belongs to the SLRP family and has four N-linked glycosylation sites which can contain KS side chains in humans (Chakravarti et al., 1995). A representation of lumican containing four KS side chains is shown in **Figure 2**. The characteristic leucine-rich repeats in the protein core mediate binding to other extracellular components like collagen (Danielson et al., 1997; Chakravarti et al., 1998; Smith and Hassell, 2006). The structure of lumican is homologous to decorin; a superhelix with a horseshoe or arch-like structure having β-sheets at the concave surface and α-helices at the convex surface (Chakravarti et al., 1995; Weber et al., 1996; Iozzo, 1997). Our group has modeled the structure of lumican using decorin as a template and the location of KS attachment sites can be seen on the convex side of the molecule (**Figure 2**). This shape allows for accommodation of a collagen fibril within the concave surface of lumican (and other SLRPs), and the KS side chains that are bound to the convex side project outwards. These KS side chains, which due to their high anionic charge retain water, are important for the normal assembly and growth of collagen fibrils (Iozzo, 1997; Chakravarti et al., 1998). Immunostaining of human corneas with anti-lumican (green) and anti-KS (red) antibodies demonstrates how the KS side chains project outwards into the "empty" space (**Figure 3**). Specifically, a thin line of KS (represented in red) can be seen lining the outer surfaces of the stromal lamellae (**Figure 3**). In adult mouse corneas, immunohistochemistry shows an increasing concentration of lumican from low levels of non-specific staining in the epithelium to markedly increased levels in the posterior third of the stroma (**Figure 4**) (Chakravarti et al., 2000; Bouhenni et al., 2013). Studies in chick corneal

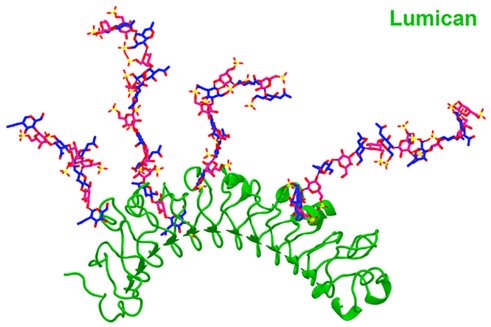

FIGURE 2 | A cartoon representation of the SLRP lumican containing four KS side chains. The structure of lumican was modeled on the crystalized structure of decorin and presented as a cartoon representation of human lumican (green). The KS side chains at the *N*-glycosilation sites at N88, N127, N160 and N252 are represented as a sticks (*N*-acetyl glucosamine in pink, galactose in blue, oxygen in red and sulfate in yellow).

development have shown that the switch from the glycoprotein form of lumican (containing polylactosamine – non-sulfated KS) side chains, at embryonic day 7 (E7) to the PG form of lumican (with sulfated KS side chains) after E15 is well correlated with development of corneal transparency (Cornuet et al., 1994; Dunlevy et al., 2000). Similarly, the switch to lumican containing KS side chains occurs concomitantly with corneal transparency and eye opening in mice (Ying et al., 1997). The important role lumican plays in maintaining corneal transparency came to light with the generation of lumican *null* mice (Chakravarti et al., 1998; Saika et al., 2004). These studies revealed that lumican is necessary for the correct alignment of collagen fibers and for maintaining interfibrillar collagen spacing (Chakravarti et al., 1998, 2000). Lumican *null* mice have collagen fibers with a larger fibril diameter, abnormal fibril packing, and irregular lamellar organization particularly in the posterior stroma (Chakravarti et al., 1998, 2000).

The role of lumican in corneal wound healing was evidenced by delayed closure of epithelial defects in lumican-*null* mice *in vivo* and slower scratch closure after addition of an anti-lumican antibody *in vitro* (Saika et al., 2000). Lumican expression during corneal wound healing contributes to important processes like epithelial cell migration and adhesion (Saika et al., 2000), neutrophil and macrophage recruitment (Funderburgh et al., 1997; Vij et al., 2004), proliferation and apoptosis of stromal keratocytes (Vij et al., 2004). Lumican is expressed by stromal keratocytes and not by the corneal epithelium in normal corneas; however, it is expressed transiently and ectopically by mouse corneal epithelial cells during the process of epithelial wound healing (Saika et al., 2000). Studies have suggested that the functions of lumican may be mediated by the interaction of lumican with Fas/Fas ligand (Vij et al., 2005), TLR4 (Lohr et al., 2012) or Transforming growth factor-β receptor 1 (ALK5) (Yamanaka et al., 2013). Recently, the cleavage of lumican, for example by matrix metalloproteinase 14 (MMP14), has been shown to generate physiologically active products that have been named lumikines by the Kao group (Yamanaka et al., 2013; Gesteira et al., 2017). Thus, upon wound healing, lumican throughout the cornea could serve as a storage pool of signaling molecules that are mobilized with the release of certain MMPs. A representation of MT1-MMP cleavage sites on the lumican core protein can be seen in **Figure 4**. Interestingly, a C-terminal product of lumican, which can be generated for example by MT1-MMP cleavage (**Figure 5**), has been shown to bind to ALK5 and promote corneal epithelial wound healing, increasing both epithelial cell migration and proliferation (Yamanaka et al., 2013; Gesteira et al., 2017). Although lumican expression is important during the process of wound healing, persistent up-regulation of lumican beyond wound closure can lead to reduced adhesion of corneal epithelial basal cells, as seen in streptozotocin-induced diabetic rats (Yamamoto et al., 2018).

Keratocan is another member of the SLRP family found in the corneal stroma, and has a protein sequence that is similar to lumican, containing putative KS side chains (Dunlevy et al., 1998). A representative image of keratocan (green) and KS (red) staining in the human cornea can be seen in **Figure 6**. In the cornea, keratocan is solely expressed by keratocytes, thus it is commonly used as a phenotypic marker for stromal keratocytes (**Figure 4**) (Kao and Liu, 2002). Because the expression of keratocan is restricted to stromal keratocytes, Keratocan-Cre (Kera-Cre) transgenic driver mice (not inducible) and, recently, the doxycycline inducible Keratocan-rtTA (KeraRT) driver mouse line have been generated to ablate genes specifically in stromal keratocytes (Kao, 2006; Zhang et al., 2017). Lumican has been shown to regulate the expression of keratocan. Specifically, lumican-*null* mice (*in vivo*) and lumican knockdown using siRNA in cells (*in vitro*) both present reduced keratocan expression (Carlson et al., 2005). Furthermore, keratocan transcriptional activity is increased after the expression of lumican is rescued in lumican-*null* mice (Carlson et al., 2005), and keratocan expression is increased at both protein and mRNA levels when lumican is overexpressed in wild-type mouse corneas (Carlson et al., 2005). During corneal wound healing, if keratocytes are activated into a fibroblast or myofibroblast phenotype by FGF-2/heparin sulfate (HS) or TGF-β1, the synthesis of keratocan and lumican is downregulated via activation of the Jun N-terminal kinase-signaling pathway (Chen et al., 2011). KS biosynthesis, chain length and sulfation are significantly reduced in these activated fibroblasts and myofibroblasts when compared to naïve keratocytes (Funderburgh et al., 2003).

Studies in a mouse model of LPS-induced keratitis have shown that lumican and keratocan can regulate the innate immune response. Lumican and keratocan double knockout mice receiving intrastromal LPS present a less intense increase in corneal thickness and cloudiness, and reduced stromal neutrophil invasion when compared to wild-type mice (Carlson et al., 2005). In contrast to lumican-*null* mice, keratocan-*null* mice have thin but clear corneal stromas with abnormal collagen fibril spacing (Carlson et al., 2005). Interestingly, mutations in the keratocan gene leading to a single amino acid substitution or a C-terminal truncation cause flattening of the anterior corneal curvature in humans, a condition called cornea plana (Pellegata et al., 2000).

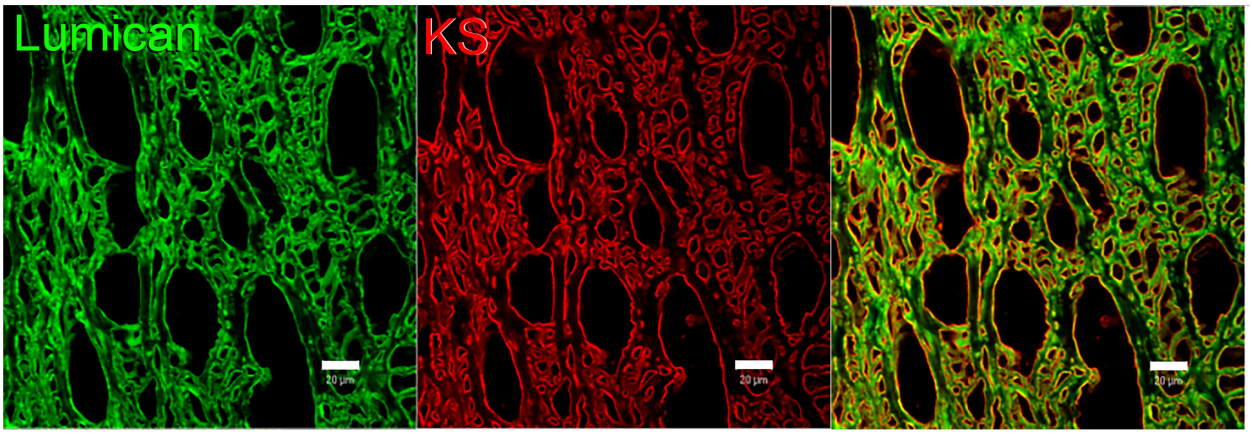

FIGURE 3 | Representative image of lumican and KS imunolocalized in human corneas. Lumican (green) and KS (red) were immunolocalized in a sagittal section of a normal human cornea. Lumican was detected with a monoclonal anti-lumican antibody, clone 1F12B10, produced by our group, and KS was detected using anti-KS clone 5D4, kindly provided by Prof. Bruce Caterson. Scale bar represents 20 μm.

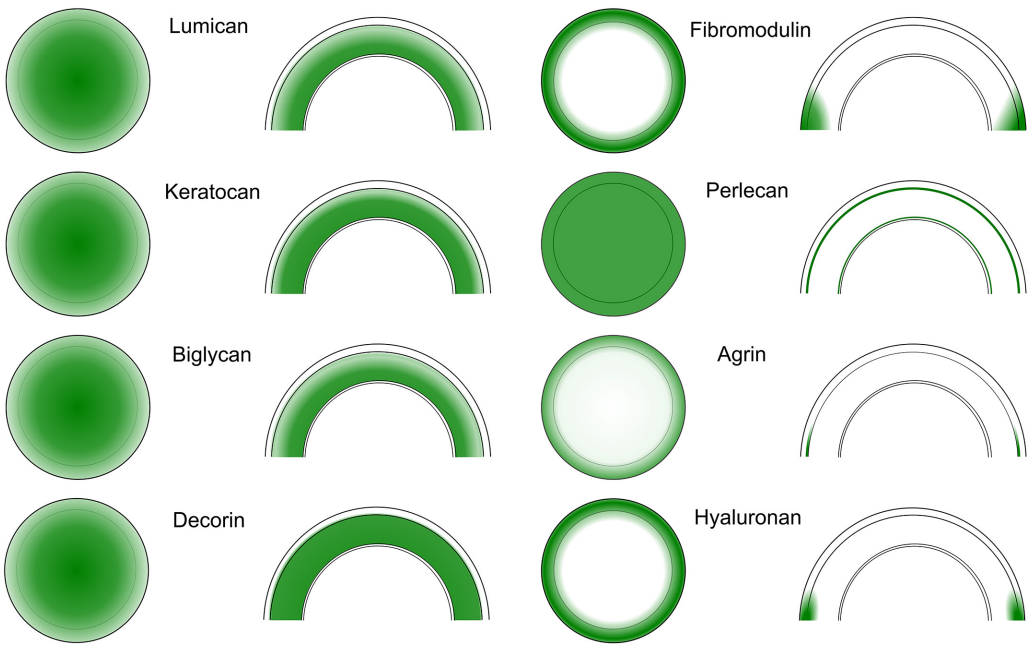

FIGURE 4 | Spatial distribution of SLRPs, HSPGs and HA in the cornea and limbal region. Spatial distribution maps showing the distribution of the SLRPs lumican, keratocan, decorin, biglycan, and fibromodulin, the HSPGs perlecan and agrin, and HA, all represented in green, in the cornea and limbal region. A frontal view of the whole cornea and limbal region is shown on the left of each panel, with the inner circle demarcating the cornea/limbus interface. The corresponding image on the right show a cross-sectional view of the cornea with the limbal regions toward the bottom. The lines demarcate the different layers of the cornea, specifically the upper line represents the intersection between the epithelium and the stroma, with the other line representing the intersection between the stroma and the endothelium. The intensity of the green color correlates with expression levels, with the darker color representing higher expression.

Fibromodulin, another SLRP with putative KS side chains, is also involved in regulating collagen fibrillogenesis in the peripheral cornea. It is expressed in the central cornea and limbus during development but becomes restricted to the limbus and sclera in adult mice (**Figure 4**) (Chen et al., 2010). This specific expression pattern during development is correlated with the change in corneal curvature and change in the axial length of the eye during the normal emmetropization process (Chen et al., 2010). Although fibromodulin-*null* mice have normal eye axial length, fibromodulin and lumican have synergistic effects during the emmetropization process in the region-specific regulation of collagen fibrils as shown in combined lumican/fibromodulin-*null* mice (Chakravarti et al., 2003).

Mimecan, another SLRP with putative KS side chains, exists in the corneal stroma as a KSPG and is mostly found in its non-sulfated form in other connective tissues (Funderburgh

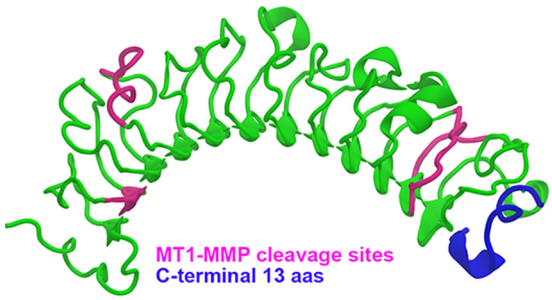

FIGURE 5 | A cartoon representation of the lumican core protein with indicated MT1-MMP cleavage sites. A cartoon representation of human lumican (green) modeled using the structure of decorin (pdbID 1XDC) as a scaffold. MT1-MMP cleavage sites are depicted in pink in order to represent the lumican products that would be produced upon MT1-MMP cleavage. The c-terminal 13 aas of lumican, which have been shown to promote corneal wound healing, have been shown in blue.

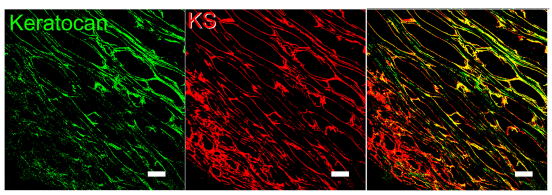

FIGURE 6 | Representative image of keratocan and KS imunolocalized in human corneas. Immunolocalization of keratocan (green) and KS (red) in a sagittal section of normal human cornea. Keratocan was detected with a monoclonal anti-keratocan antibody and KS was detected using anti-KS kindly provided by Prof. Bruce Caterson. Scale bar represents 20 μm.

et al., 1997). Unlike other SLRPs, mimecan seems to have minimal contribution toward the structure and organization of collagen fibrils in the mouse cornea (Beecher et al., 2005). Studies using mimecan-*null* mice found no significant changes in corneal thickness or clarity, but divergent results were found regarding the role of mimecan in regulating collagen fibril thickness (Tasheva et al., 2002; Beecher et al., 2005). On average, collagen fibrils in corneas of mimecan-*null* mice were thicker when compared to wild-type littermates using transmission electron microscopy ultrastructural analyses (Tasheva et al., 2002). However, a low-angle synchrotron x-ray diffraction study showed that the mean collagen fibril diameter, collagen fibril spacing and collagen fibril organization throughout the cornea of mimecan-*null* mice were comparable to those of wt mice (Beecher et al., 2005).

CHONDROITIN SULFATE PROTEOGLYCANS (CSPGs)

Chondroitin sulfate is composed of repeating disaccharide units of GlcA and GalNAc with sulfation at various positions. Chondroitin sulfate A (chondroitin-4-sulfate) is sulfated at carbon 4 of the GalNAc sugar, chondroitin sulfate C (chondroitin-6-sulfate) is sulfated at carbon 6 of the GalNAc sugar, chondroitin sulfate D (chondroitin-2,6-sulfate) is sulfated at carbon 2 of the GlcA and 6 of the GalNAc sugar, and chondroitin sulfate E (chondroitin-4,6-sulfate) is sulfated at carbons 4 and 6 of the GalNAc sugar (Mikami and Kitagawa, 2013). In the rat cornea, CS expression is high at birth and decreases with postnatal development (Koga et al., 2005). In normal human corneas there are 8 μg of CS/DS per mg dry weight with ∼40 disaccharides per chain, which decreases to ∼15 disaccharides in corneas affected by macular corneal dystrophies (Plaas et al., 2001). CSPGs are important ECM components with diverse functions in tissues, such as regulating cell adhesion, cell growth, neuronal plasticity, neuronal regeneration and cell migration, and form the bulk of the majority of connective tissues (Coulson-Thomas et al., 2008, 2016; Silver et al., 2013; Silver and Silver, 2014; Smith et al., 2015; Gesteira et al., 2016; Pai et al., 2018; Pudełko et al., 2019).

Lubricin, also known as proteoglycan 4 (PRG4) or superficial zone protein, acts as a boundary lubricant anti-adhesive component in tissues, protecting them against frictional forces (Bao et al., 2011). The lubricin in human synovial fluid consists of glycoprotein isoforms that may or may not have CS and/or KS side chains (Lord et al., 2012). Lubricin is produced by ocular surface epithelia, including the corneal and conjunctival epithelia, and the lacrimal and meibomian glands (Cheriyan et al., 2011; Schmidt et al., 2013). Lubricin reduces friction and protects the cornea and conjunctiva against significant shear forces generated by the eyelid during blinking. Hence, lubricin-*null* mice present a dry eye phenotype with ocular surface damage and positive corneal fluorescein staining due to lack of protective lubrication (Schmidt et al., 2013). A randomized clinical trial of recombinant human lubricin in moderate dry eye treatment produced significant improvement in signs and symptoms when compared to HA (Lambiase et al., 2017). Further studies with lubricin could provide promising management options for dry eye disease.

Aggrecan is a large bottlebrush-shaped PG of the lectican family which forms complexes with HA (Kiani et al., 2002; Ng et al., 2003). Aggrecan has three highly conserved globular domains and three less conserved extended domains in different species (Kiani et al., 2002). Aggrecan contains multiple CS side chains and few KS side chains in all species except in mice where aggrecan has a truncated core protein devoid of a KS-rich region (Watanabe et al., 1995). Because of the highly absorbent and lubricating properties of aggrecan, it acts as a shock absorber in cartilage (Chandran and Horkay, 2012). Aggrecan has been reported to be expressed during development as well as in adult corneas of Wistar rats (Koga et al., 2005). Similarly, in human corneas, aggrecan is immunolocalized mostly in the corneal and conjunctival epithelia, with weak staining in the anterior corneal stroma and moderate staining in the scleral stroma (Bouhenni et al., 2013). Although aggrecan is known to be expressed in the cornea, its function remains to be elucidated. To further understand the role of aggrecan in the ocular surface, cmd mice could be used, which are aggrecan knockout mouse models with a functional null mutation of the aggrecan gene (Watanabe et al., 1994).

Versican is another large CSPG of the lectican protein family, which undergoes alternative splicing and occurs as four isoforms, namely V0, V1, V2, and V3, where V0 is full length versican (Zimmermann and Ruoslahti, 1989; Ito et al., 1995). Versican has an HA-binding region at the N-terminus and several CS attachment regions where V0 has both CS-α and CS-β, V1 has CS-β, V2 has CS-α, and V3 does not have any CS attached (Ito et al., 1995). Versican is a major PG in the dermis and plays an important role in skin wound healing. In particular, the V3 isoform promotes normal dermal fibroblast-myofibroblast transition (Hattori et al., 2011). Studies have suggested that versican is involved in corneal development: in the rat cornea, versican isoforms are highly expressed at birth but larger isoforms (V0) are replaced by smaller isoforms during early postnatal development (P1–P14) and become undetectable in adulthood, while the V1 and V2 isoforms remain unchanged (Koga et al., 2005). Versican has been immunolocalized in the subepithelial region of the anterior limbus in human corneas (Schlötzer-Schrehardt et al., 2007). Although many studies have identified versican in the corneas of multiple species, a function has still to be attributed to it. Therefore, as is the case for aggrecan, further studies are needed to unveil the function of versican in the ocular surface.

DERMATAN SULFATE PROTEOGLYCANS (DSPGs)

Dermatan sulfate, previously known as chondroitin sulfate B, has the same basic composition as CS; however, the GlcA is epimerized to IdoA by glucuronyl C5-epimerase (Malmström and Fransson, 1975). Thus, similarly to CS, DS is a copolymer of alternating IdoA-GalNAc(4S) (iA unit), IdoA(2S)-GalNAc(4S) (iB unit), or IdoA-GalNAc(4S,6S) (iE unit) units (Maccarana et al., 2009). DS is predominantly present in the skin and plays an important role in wound healing (Penc et al., 1998). DSPGs present in the corneal stroma are involved in controlling the interfibrillar spacing and lamellar adhesion properties of corneal collagens (Maccarana et al., 2009).

Decorin is a member of the SLRP family with three potential GAG attachment sites, but generally only one DS/CS chain is linked to the serine residues in the N-terminal region (Weber et al., 1996). Interaction of decorin and its side chain with growth factors and other proteins helps in the regulation of various processes, such as collagen fibrillogenesis, angiogenesis, autophagy and wound healing (Gubbiotti et al., 2016). Decorin-deficient mice exhibit skin fragility, tendon weakness and lower lung airway resistance due to abnormal collagen fibrillogenesis (Danielson et al., 1997). Mice lacking decorin DS chains, due to mutation of the serine residue at the site of DS substitution, do not exhibit such anomalies (Moffatt et al., 2017). In the cornea, decorin is abundantly expressed in the stroma (**Figure 4**) and accumulation of a truncated form of decorin causes stromal opacity in congenital stromal corneal dystrophy (Bredrup et al., 2005, 2010; Rødahl et al., 2006). However, decorin-*null* mice present only a few large and irregular fibrils, therefore it has been proposed that decorin alone does not significantly affect corneal collagen fibril phenotype (Danielson et al., 1997; Zhang et al., 2009). Decorin inhibits TGF-β by binding to its core protein in the latent complex leading to inhibition of myofibroblast differentiation and scar formation (Ständer et al., 1999; Tandon et al., 2010). Decorin has been tested as an anti-fibrotic agent in the cornea significantly reducing corneal opacity in a murine model of *Pseudomonas* keratitis (Hill et al., 2018). The Chinnery group further investigated the use of exogenous decorin to promote corneal nerve regeneration after a corneal epithelial abrasion injury and found that human recombinant decorin promotes corneal nerve regeneration (Wu et al., 2020). It was hypothesized that decorin promotes corneal nerve regeneration via the activation of dendritic cells (Wu et al., 2020).

Biglycan is also a PG of the SLRP family with two DS/CS chains linked to serine residues in the protein core, homologous to the decorin protein (Fisher et al., 1989). Biglycan binds various growth factors to modulate cell signaling pathways, and disruption of the biglycan gene results in osteopenia with decreased growth and bone mass (Young et al., 2002). Biglycan is expressed throughout the corneal stroma (**Figure 4**) with high expression levels during early developmental stages, which decrease to very low levels in the mature cornea (Zhang et al., 2009). However, normal collagen fibrils and stromal structures are found in biglycan-*null* mice (Zhang et al., 2009). Since decorin and biglycan interact with a similar region on collagen when regulating lateral fibril growth, studies in decorin and biglycan double knockout mice have shown that decorin and biglycan have a synergistic effect producing abnormal fibril morphology resulting in additive deficiency in skin and bone (Young et al., 2002; Bi et al., 2005). Thus, there is a compensatory effect between decorin and biglycan with regard to regulating collagen fibril organization. Decorin and biglycan double knockout mice also show large irregular collagen fibrils throughout the corneal stroma, especially in posterior regions (Zhang et al., 2009), confirming compensatory expression in single decorin- or biglycan-*null* mice. Accordingly, in decorin-*null* mice there is higher than normal expression of biglycan in the cornea, although in biglycan-*null* corneas there is not a significant change in decorin expression (Zhang et al., 2009). This suggests that decorin has a primary role in corneal fibrillogenesis with some contribution from biglycan, which can compensate for the loss of decorin (Zhang et al., 2009).

HEPARAN SULFATE PROTEOGLYCANS (HSPGs)

Heparan sulfate and HEP are synthesized as a polymer made up of repeating disaccharide units composed of GlcA and GlcNAc polymerized by glycosyltransferase enzymes called exostosins (Exts). HS/HEP are sequentially modified during and shortly after biosynthesis. The NDST enzyme creates different degrees of sulfation by *N*-deacetylation and *N*-sulfation of GlcNAc, which creates domains of unmodified *N*-acetylated disaccharides (NA domains), *N*-sulfated disaccharide units (NS domains), and alternating *N*-acetylated and *N*-sulfated disaccharides (NS/NA domains) (Esko and Lindahl, 2001). These modifications

create binding sites for different proteins and also enable further enzymatic modification of the HS chain, such as C5-epimerization of GlcA to IdoA and *O*-sulfation of both residues (Esko and Lindahl, 2001; Ledin et al., 2004). Abnormalities in the biosynthesis of HS chains can lead to developmental defects ranging from embryonic lethality to tumor formation and altered organ-system development (Poulain and Yost, 2015).

In order to study the role of HS/HEP and HS/HEP sulfation *in vivo* and also understand how the various enzymes involved in HS biosynthesis and modifications are regulated, *null* and floxed mice have been generated for many of the biosynthetic enzymes. Many of these mice have been used in eye related studies. HS was ablated from corneal epithelial cells using a cytokeratin 14-rtTA (K14RtTA diver mouse);TetO-cre to remove exostosin 1 gene (*Ext1*), which resulted in defective corneal stratification and delayed wound healing due to loss of tight junctions (Coulson-Thomas et al., 2015). A similar phenotype was also observed in extracellular endosulfatase Sulf1-*null* mice (Maltseva et al., 2013). Studies have shown that the number and sulfation pattern of HS on HSPGs, such as syndecans, GPCs, perlecan and agrin, can modify their function (Mertens et al., 1996; Langford et al., 1998; Poulain, 2015).

Syndecans are a family of type-I transmembrane proteins that consists of syndecan-1, syndecan-2, syndecan-3 and syndecan-4. They are cell surface PGs that can carry three to five HS chains or CS chains and are involved in cell proliferation, migration and cell-matrix interactions (Bernfield et al., 1999). Syndecan-1 and syndecan-3 have GAG binding sites at both ends of the ectodomain, whereas syndecan-2 and syndecan-4 have them at the distal region only (Elenius and Jalkanen, 1994). Syndecan-1 is mostly expressed in the epithelium and syndecan-2 (fibroglycan) is expressed in vascular endothelium mediating angiogenic sprouting during development. Syndecan-3 (*N*-syndecan) is expressed in Schwann cells and on axons in neurons migrating along nerve bundles (Toba et al., 2002; Hienola et al., 2006). Syndecan-4 is expressed ubiquitously and plays a role in fibroblast migration, angiogenesis and wound healing (Morgan et al., 2007). In the cornea, syndecan-1 has been shown to play a role in corneal epithelial homeostasis, wound healing, and more recently, reinnervation (Pal-Ghosh et al., 2017). Syndecan-1-*null* mice with a BALB/c background are viable and fertile, with transparent corneas but altered intraepithelial corneal nerve morphology (Stepp et al., 2002). Loss of syndecan-1 causes delayed wound healing in skin and cornea due to defective migration and integrin expression in epithelial cells (Stepp et al., 2002). Altered integrin activity and TGFβ1 signaling makes epithelial cells isolated from syndecan-1-*null* mice more adhesive than wild-type cells (Stepp et al., 2010). The syndecan-1-*null* corneal epithelial cells assemble an abnormal ECM which can affect their interaction with intraepithelial nerves, resulting in altered morphology and regeneration after injury (Pal-Ghosh et al., 2017). Syndecan-1 deficient mice also present increased corneal neovascularization and adhesion of leukocytes to endothelial cells after alkali burn injury, indicating that syndecan-1 negatively regulates leukocyte-mediated angiogenesis (Götte et al., 2002). Interestingly, the overexpression of syndecan-1 in transgenic mice also delays wound closure and re-epithelialization due to shedding of soluble syndecan-1 ectodomains and inhibition of cell proliferation at wound edges (Elenius et al., 2004). Syndecan-4 is ubiquitous and necessary for focal adhesion formation by the interaction of fibronectin, integrin and intracellular components (Echtermeyer et al., 2001). After skin injury, syndecan-4 is upregulated in fibroblasts and endothelial cells within granulation tissue, and syndecan-4-deficient mice present delayed wound healing and reduced vessel size within granulation tissue of the wound bed (Echtermeyer et al., 2001), indicating that syndecan-4 regulates fibroblast migration, wound contraction and angiogenesis. However, a similar role for syndecan-4 in corneal wound healing has not been demonstrated.

Glypicans are a family of HS PGs linked to the cell surface by GPI-anchors. Studies have shown that GPCs influence growth factor activity in signaling pathways associated with developmental morphogenesis and disease processes in *Drosophila*, zebrafish, *Xenopus*, and mammals. The location of the HS chain insertion site in the C-terminus is conserved in all GPCs (Veugelers et al., 1999). In *Drosophila*, the GPC genes are called *division abnormally delayed* (*dally*) and *dally-like protein* (*dlp*). Mutation studies in the *dally* gene indicate that it is necessary for G2-M progression in the cell cycle during eye development (Nakato et al., 1995; Jackson et al., 1997). Ten GPC genes have been identified in zebrafish (Gupta and Brand, 2013) and six (GPC1-6) in mammals, which have all been shown to be important in embryonic development (Brown and Waneck, 1992). The expression and function of GPCs in the ocular surface remains to be established, and further research in this area is needed.

Perlecan is a major basement membrane-specific HS PG 2 (HSPG2) with four potential sites for HS/CS side chain attachment (Iozzo, 2005). Constitutive loss of perlecan is embryonic lethal due to heart and brain defects with a few animals developing chondrodysplasia after birth (Arikawa-Hirasawa et al., 1999; Costell et al., 1999). In order to study the role of perlecan in adult mice, researchers have used mutant mice lacking exon 3 of the perlecan gene, which have smaller eyes (microphthalmia) and develop lens degeneration (congenital cataract) (Rossi et al., 2003). In the human cornea, perlecan was detected by immunofluorescence in the entire corneal and conjunctival epithelial basement membrane (**Figure 4**), and also between the endothelium and Descemet's membrane (Ljubimov et al., 1995; Torricelli et al., 2015). *Hspg2*$^{-/-}$-Tg are perinatal lethality rescued mice produced in a perlecan-*null* (Hspg2$^{-/-}$) genetic background that express recombinant perlecan specifically in the cartilage and not in other tissues (Ishijima et al., 2012). *Hspg2*$^{-/-}$-Tg mice have small eyes with thinner corneal epithelial wing cell layers and significantly reduced expression of corneal epithelial differentiation markers (Inomata et al., 2012). Similarly, thin and poorly organized epidermis was formed in engineered human skin when perlecan expression was disrupted in keratinocytes (Sher et al., 2006). The HS side chains of perlecan have also been suggested to play a role in corneal epithelial homeostasis and wound healing since transgenic mice lacking the *Ext1* gene in epithelial cells have an increased rate of epithelial cells sloughing off

due to disrupted tight junctions and a reduced number of cell-basement membrane adhesion complexes (Coulson-Thomas et al., 2015). If the basement membrane of the mouse cornea is exposed, perlecan can act as a binding site for *Pseudomonas aeruginosa*; however, when the HS side chains are removed by heparanase, bacterial binding decreases (Chen and Hazlett, 2000). The regeneration of normal basement membrane relies on the production of perlecan during corneal wound healing, which is modulated by IL-1 and TGF-β (Saikia et al., 2018). Perlecan has also been shown to be expressed by stromal keratocytes and is upregulated after epithelial injury (Torricelli et al., 2015).

Agrin is a multidomain HSPG expressed as an alternatively spliced protein, with the different isoforms playing important roles during embryonic development, especially of the nervous system (Stetefeld et al., 2004). In zebrafish, agrin morphants that were generated using antisense morpholino oligonucleotides show that agrin is important for neurite outgrowth during retina development (Kim et al., 2007; Liu et al., 2008). Since the disruption of this neuromuscular development process causes perinatal mortality in agrin-deficient mice, the role of agrin has been studied in transgenic mice by tissue-specific inactivation of agrin (Gautam et al., 1996) and overexpression of agrin (Fuerst et al., 2007). Alteration of agrin expression presents highly variable developmental defects in the eye including anophthalmia, microphthalmia, optic nerve hypoplasia, optic stalk coloboma, vitreous vessel persistence, and adhesion of iris and lens to the cornea (Fuerst et al., 2007). In the ocular surface, agrin is highly expressed in the limbal regions partially colocalized with limbal stem cells (ABCG2 and p63-positive cells), and the expression of agrin decreases toward the conjunctiva (weakly expressed) and central cornea (absent or weakly expressed) (**Figure 4**) (Schlötzer-Schrehardt et al., 2007). A recent report has shown that agrin promotes limbal stem cell proliferation and corneal wound healing via the Hippo-Yap signaling pathway (Hou et al., 2020). Conditional knockout of agrin in the cornea could potentially help further our understanding of the role of agrin in supporting limbal stem cells.

Collagen XVIII is a basement membrane collagen/PG with HS side chains that is abundant in the eye, skin, muscles, kidney, lungs and blood vessels (Halfter et al., 1998). In the posterior segment of the eye, collagen XVIII immunolabeling is present in the retinal inner limiting membrane, retinal pigmented epithelium and Bruch's membrane (Halfter et al., 1998; Zatterstrom et al., 2000; Fukai et al., 2002). Collagen XVIII anchors collagen fibrils to the inner limiting membrane, and the inactivation of collagen XVIII in mice causes vitreous separation from the retina. In humans, a collagen XVIII loss-of-function mutation causes Knobloch syndrome, characterized by high myopia, vitreoretinal degeneration and retinal detachment in humans (Fukai et al., 2002). When cleaved, the C-terminal fragment of collagen XVIII generates endostatin, an angiogenesis inhibitor (O'Reilly et al., 1997). Mice lacking collagen XVIII and endostatin show abnormal retinal vessel outgrowth and delayed hyaloid vessel regression after birth (Zatterstrom et al., 2000; Lin et al., 2001). These findings indicate that collagen XVIII can be targeted for the regulation of angiogenesis in the eye. In the anterior segment of the eye, collagen XVIII has been immunolocalized in the corneal epithelium, conjunctival epithelial basement membrane, corneal nerve basement membrane, Descemet's membrane, limbal and conjunctival capillaries, ciliary epithelium and lens capsule (Zatterstrom et al., 2000; Fukai et al., 2002; Sakimoto et al., 2008). The expression of collagen XVIII and endostatin is altered in different types of corneal injuries and pathologies. The immunolabeling of collagen XVIII and endostatin is irregular in the epithelial basement membrane of keratoconic corneas and highly increased in the stroma of scarred corneas (Määttä et al., 2006). Similarly, collagen XVIII expression increases in the stroma and epithelial basement membrane after linear corneal incision (Kato et al., 2003). Following excimer laser keratectomy, collagen XVIII immunoreactivity is absent in the epithelial basement membrane in wild-type mice (Kato et al., 2003), and corneal reinnervation is impaired in collagen XVIII knockout mice (*col18a1*$^{-/-}$) with decreased corneal neurite extension (Sakimoto et al., 2008).

HEPARIN

Heparin is a heavily sulfated GAG synthesized upon a serglycin core protein found only in mast cells and some hematopoietic cells (Kolset and Gallagher, 1990). It has the highest negative charge density among all biological macromolecules due to the fact that it contains trisulfated disaccharides (**Figure 1**) (Capila and Linhardt, 2002). During biosynthesis, heparin is released from serglycin by tissue proteases followed by endoglucuronidase (Kolset and Gallagher, 1990; Capila and Linhardt, 2002). Although HS and HEP have the same core structure and most HS-binding proteins can also bind to heparin, they have different levels of sulfation and epimerization (Kolset and Gallagher, 1990). Heparin is widely used for its anticoagulant effects but recent experimental and clinical evidence shows that it also has anti-viral, anti-inflammatory and wound healing properties (Galvan, 1996; Olczyk et al., 2015; He et al., 2019; Çevirme et al., 2020; Gavioli et al., 2020; Magro, 2020; Zheng et al., 2020). Heparin exhibits anti-inflammatory activities and has an effect on the hemostatic phase of wound healing by various mechanisms such as inhibition of leukocyte recruitment, reduced vascular permeability, neutralization of cationic mediators, and inhibition of heparanase (Olczyk et al., 2015). The wound healing effect of heparin is mostly through binding and regulating the activity of enzymes and growth factors such as heparin-binding EGF-like growth factor (HB-EGF), which is known to promote re-epithelialization of murine partial-thickness burns, increase keratinocyte proliferation and heal intestinal anastomotic wounds (Cribbs et al., 1998; Radulescu et al., 2011). Topical application of heparin in rabbit tracheal autografts has also shown effective tissue repair after surgery (Sen et al., 2009). In eyes, polymer pellets impregnated with heparin and cortisone inhibit corneal vascularization in rabbit models of corneal injury and transplantation (Nikolic et al., 1986). Heparin eye drops have also been shown to reduce the occurrence of conjunctival pseudomembrane in the ocular surface after a chemical injury with paraquat (Jian-Wei et al., 2017).

HYALURONAN

Hyaluronan is composed of alternating residues of β-D-(1 → 3)GlcA and β-D-(1 → 4)-GlcNAc and is neither sulfated nor covalently attached to a protein core. It is synthesized by HAS enzymes, namely HAS1, HAS2, and HAS3, and is directly extruded into the ECM without epimerization or sulfation (Itano et al., 1999; Hascall and Esko, 2015). It has a very high negative charge that can attract sodium and retain water. HA is ubiquitous and serves a variety of functions in vertebrate tissues such as providing cushioning and lubrication in synovial joints (Balazs et al., 1967), forming hydrated complexes in skin and cartilage (Hardingham and Fosang, 1992), binding proteins and growth factors involved in cell signaling important in regulating homeostasis, tissue repair, inflammation, and cancer (Fraser et al., 1997; Schwertfeger et al., 2015).

Studies have used biotinylated-HA binding protein to detect HA in various tissues of the eye. In the posterior segment of the eye, HA has been detected in the vitreous humor, neurosensory retina, retinal pigmented epithelium, Bruch's membrane and choroid (Clark et al., 2011). In the anterior segment of normal eyes, HA has been detected in the aqueous humor, trabecular meshwork, iris stroma, lens capsule, corneal endothelium, conjunctival epithelium and limbal epithelium (**Figure 4**) (Härfstrand et al., 1992; Gong et al., 1994; Lerner et al., 1998; Gartaganis et al., 2001; Gesteira et al., 2017). Although studies have shown that the biological function of HA is dictated by its molecular weight, the molecular size of HA in these tissues have not been determined.

The spatial and temporal expression pattern of HA has been shown to play important roles in development, homeostasis, and diseases of the ocular surface. During development, HA is present throughout the cornea and facilitates the movement of mesenchymal cells and lymphatic vessel growth into the cornea (Toole and Trelstad, 1971; Hart, 1978; Sun et al., 2019). HA is cleared from the central cornea by hyaluronidase enzyme digestion during later stages of development accompanied by regression of lymphatic vessels (Toole and Trelstad, 1971; Sun et al., 2019). To date, HA is the only GAG that has been identified to be decreased in aged human corneas when compared to corneas from younger individuals (Pacella et al., 2015). In adult eyes, HA is highly expressed in the limbal epithelium, especially in the basal layer (Gesteira et al., 2017). HA is also expressed in the conjunctival epithelium and very low expression levels are detected in the corneal epithelium of murine (Gesteira et al., 2017; Sun et al., 2019), bovine (Gong et al., 1994), and human (Lerner et al., 1998) corneas. This HA specific matrix in the limbus is important for the limbal stem cell niche and the disruption of this HA matrix leads to altered LSC phenotype (Gesteira et al., 2017). HA is significantly increased in the cornea after corneal injuries like penetrating wounds, excimer laser surgeries and alkali burns (Hassell et al., 1983; Fagerholm et al., 1992; Fitzsimmons et al., 1997; Gesteira et al., 2017; Sun et al., 2019). This increase in HA is believed to be necessary for binding provisional fibronectin and stimulating corneal epithelial migration for corneal wound healing (Nakamura et al., 1992; Camillieri et al., 2004). HA expression in the cornea after alkali burn also regulates corneal lymphangiogenesis by acting as a substrate for lymphatic vessel growth (Sun et al., 2019). The precise mechanism of action of HA and involvement in cell signaling pathways in the ocular surface remain elusive. Although HA is currently widely used in ophthalmic products, the actual mechanism of action and long-term effects of HA in the eye are not clearly understood.

INVOLVEMENT OF PROTEOGLYCANS AND GLYCOSAMINOGLYCANS IN CORNEAL PATHOLOGY

Glycosaminoglycans and PGs have been associated with numerous diseases of the ocular surface. Changes in the levels of GAGs and PGs can be the primary cause of a disease, such as in mucopolysaccharidosis (MPS), cornea plana and macular corneal dystrophy, or secondary to the disease, such as in corneal scarring and keratoconus. MPS is a family of lysosomal disorders caused by a mutation in a gene encoding enzymes involved in the sequential degradation of GAGs, which leads to their gradual build-up in cells and tissues (Cantz and Gehler, 1976; Freeze et al., 2015). MPS patients suffer from numerous ocular manifestations, such as corneal clouding, retinal dystrophy and retinal degeneration (Javed et al., 2017). In more severe cases flat and thickened corneas have been noted using anterior segment optical coherence tomography (Matoba et al., 2020). The current treatment modalities for MPS include enzyme replacement therapy and bone marrow transplantation, which significantly delay progression of the disease but are not effective in preventing corneal clouding (Vogler et al., 1996; Rohrbach and Clarke, 2007; Clarke, 2008; Papadia et al., 2011; Beck, 2018). Ultimately, patients with severe corneal clouding require corneal transplantation in order to regain vision, thus, there is an unmet need to develop treatment options to prevent the build-up of GAG products within the cornea. Importantly, research is also warranted to explore ocular manifestations early in the disease since ophthalmologists and optometrists are often the first to suspect a MPS diagnosis (Del Longo et al., 2018). In the cornea, the accumulation of GAGs is primarily evident in keratocytes, which over time causes them to swell and lose their fibroblast-like shape (Young et al., 2007; Quantock and Young, 2008; Coulson-Thomas et al., 2014). Granules, containing primarily partially degraded GAGs, are gradually deposited throughout all corneal layers disrupting the orthogonal arrangement of the collagen fibrils as the disease progresses (Fahnehjelm et al., 2012). The use of gene therapy for treating MPS has been tested in the corneas of human cadavers, mice, rabbits and dogs (Thomas et al., 2012; Vance et al., 2016; Miyadera et al., 2020). Strikingly, AAV-opt-IDUA administered via a single intrastromal injection in a spontaneous MPS I canine model significantly cleared the accumulated GAGs within the corneal tissue and prevented further accumulation (Miyadera et al., 2020). Cell therapy has also been explored for treating the corneal defects associated with MPS. Umbilical cord mesenchymal stem cells have been shown to significantly decrease the accumulation of GAGs throughout the corneal tissue and within keratocytes (Coulson-Thomas et al., 2013).

Macular corneal dystrophy is a rare condition characterized by the build-up of poorly sulfated or non-sulfated KS chains (poly-lactosamine chains) within keratocytes and the corneal endothelium (Funderburgh et al., 1990; Lewis et al., 2000). Clinical manifestations can resemble certain MPS subtypes, and include corneal clouding (Funderburgh et al., 1990; Lewis et al., 2000). Macular corneal dystrophy has mostly been correlated with mutations in the carbohydrate sulfotransferase 6 (CHST6) gene, which encodes the enzyme carbohydrate sulfotransferase 6, which catalyzes the transfer of a sulfate group to the GlcNAc residue of KS (Hasegawa et al., 2000). To date, over 130 mutations have been reported in the CHST6 gene and linked to macular corneal dystrophy (Hasegawa et al., 2000; El-Ashry et al., 2002; Sultana et al., 2005; Patel et al., 2011; Nejat et al., 2018).

Cornea plana is a rare disorder that is characterized by small flat corneas, hypermetropia, haze in the corneal limbal region and corneal clouding (Ebenezer et al., 2005; Khan et al., 2006a,b). To date 15 different mutations in the keratocan (KERA) gene have been reported in families with cornea plana (Khan et al., 2004, 2005, 2006a,b; Liskova et al., 2007; Huang et al., 2019). In fact, mutations in the KERA gene have been associated with the more severe forms of cornea plana (Pellegata et al., 2000). Interestingly, keratocan knock-out mice present narrow anterior chamber angles and thin corneal stroma, clinical features that resemble cornea plana (Huang et al., 2019). Changes in GAG and PG levels, and also changes in GAG processing enzymes, have also been reported in other ocular pathologies, such as reduced levels of sulfated KS in pellucid marginal degeneration and ocular autoimmune diseases (Funderburgh et al., 1990; Woodward et al., 2019).

As mentioned, changes in the expression of GAGs and PGs can also occur secondary to many diseases. These changes can often play a role in the pathogenesis of the disease and, therefore, can often serve as a pharmaceutical target. Keratoconus is a common progressive corneal ectasia that drastically impairs vision due to the bulging, thinning and scarring of the cornea (Rabinowitz, 1998). Although the etiology of keratoconus is poorly understood and research indicates it is a multifactorial degenerative disease, changes to the ECM are believed to play a key role in its pathogenesis. There are limited treatments available for keratoconus, primarily due to the fact that so little is known about the disease itself; however, collagen cross-linking has emerged as a ground breaking treatment option to slow the progression of corneal distortions (Kobashi and Rong, 2017). Studies have indicated that the expression of GAGs and PGs, such as sulfated KS, decorin, lumican, and fibromodulin, are down-regulated in keratoconus corneas compared to healthy controls (Funderburgh et al., 1990; García et al., 2016; Foster et al., 2018). Further research is needed to understand the role GAGs and PGs play in keratoconus and also to understand their involvement in collagen cross-linking therapy. Importantly, riboflavin and ultraviolet-A collagen cross-linking has been shown to cross-link certain PG core proteins culminating in the formation of higher molecular weight macromolecules (Zhang et al., 2011). Specifically, mimecan and decorin form cross-links with collagen both *in vitro* and *ex vivo*, and keratocan and lumican core proteins strongly inhibit collagen cross-linking *in vitro*, while glycosylated keratocan and lumican form cross-links with collagen *ex vivo* (Zhang et al., 2011).

Another disease that has been shown to cause secondary changes to GAG and PG expression is Marfan syndrome. Marfan syndrome is a disease that affects the ECM of connective tissues due to mutations in the gene that encodes fibrillin-1, necessary for the formation of elastic fibers (Feneck et al., 2020). Patients suffer many ocular manifestations, including thinned and flattened corneas. Decorin expression has been shown to be significantly decreased in the corneas of a mouse model of Marfan syndrome and fibroblasts from a patient with Marfan syndrome (Superti-Furga et al., 1992; Feneck et al., 2020). The Meek group speculate the decrease in decorin expression could be a consequence of the increased levels of TGF-β expression found in the corneas of individuals with Marfan disease (Feneck et al., 2020). However, whether the loss of decorin could further contribute to the pathogenesis of Marfan syndrome remains to be established.

Pterygium is a benign fibrovascular hyperplasia of the conjunctiva that gradually grows into the cornea. Although the cause of pterygium remains unknown, studies have suggested UV exposure as a major cause. KS (stroma), HS (epithelial layer of blood vessels) and DS (stroma) have been shown to be increased in pterygium tissue when compared to normal conjunctiva and have been speculated to potentially be involved in the hyperplastic process of pterygium (Georgakopoulos et al., 2019).

Dry eye is a common condition that is caused by an insufficient and/or unstable tear film that leads to an itchy feeling in the eye, foreign object sensation, stinging and/or burning sensation, red eyes, sensitivity to light, blurry vision, fatigue, and, ultimately, inflammation, corneal erosions and compromised vision (Craig et al., 2017). Dry eye can be caused by reduced or altered secretion from lacrimal glands, which produce the aqueous layer of the tear film, Meibomian glands, which produce the lipid layer of the tear film, or conjunctival cells, which produce the mucin layer (Bron et al., 2017). Unfortunately, the etiology of dry eye remains unknown and treatment options are limited to palliative care (Bron et al., 2017; Jones et al., 2017). Given the basic characteristics of GAGs, which are highly hydrophilic, and have high viscosity and low compressibility, they have emerged as powerful lubricating agents in artificial tears. The anti-inflammatory characteristics that have been attributed to GAGs and PGs, such as high molecular weight HA (HMWHA), makes them even more attractive candidates for use in treating dry eye. The number of studies using HA, chemically modified HA and HA analogs has increased exponentially over the past few years (Salwowska et al., 2016; Ang et al., 2017; Pinto-Fraga et al., 2017). Lubricin is also emerging as a powerful agent in treating dry eye (Lambiase et al., 2017; Regmi et al., 2017). Despite the countless studies dedicated toward establishing the therapeutic benefits of using HA and lubricin for treating ocular conditions, such as dry eye, and also the fact that eye drops containing HA are widely sold around the world, limited studies have investigated the long-term effects of continuous exposure of the ocular surface to HA and lubricin. We have recently shown that alterations in HA expression in keratin 14 positive cells leads to Meibomian gland and conjunctival hyperplasia (Sun et al., 2018). Also, increased expression of HA throughout the

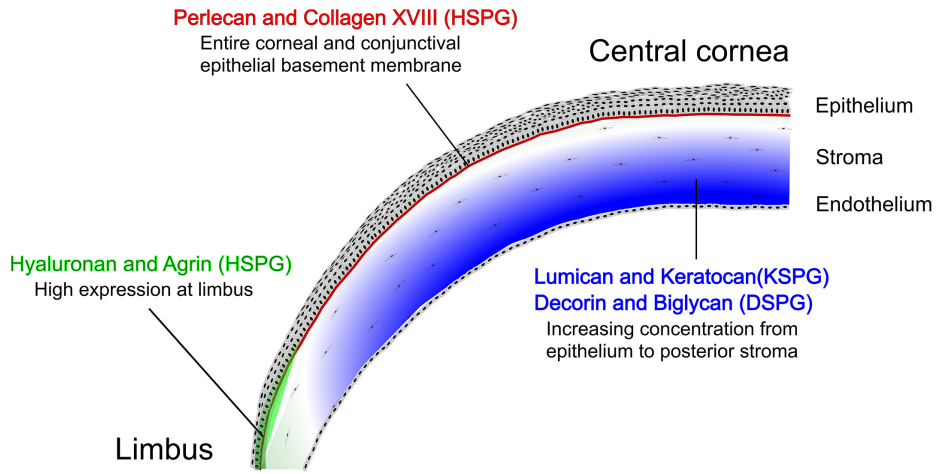

FIGURE 7 | Representation of the major GAGs and PGs in the cornea and limbal region. Diagram of a cross-sectional view of the cornea and limbal region showing the distribution of major GAGs and PGs in the cornea. The different layers of the cornea and limbus are represented, specifically the epithelium (stratified squamous epithelium), stroma (ECM with sparse keratocytes) and endothelium. The basement membrane can be seen as a line (represented in green in the limbal region and red in the cornea) between the epithelium and the stroma.

cornea leads to lymphangiogenesis (Sun et al., 2019). This work supports the need for more research focused on understanding the long-term effects of the topical administration of GAGs/PGs to the ocular surface. Some interesting studies have suggested that changes in HS and HA expression can lead to changes within lacrimal glands and Meibomian glands, and the expression of HS glycosyltransferases, such as HS2ST, HS3ST, and EXTL2, have been shown to be significantly downregulated in dry eye (Pan et al., 2008; Mantelli et al., 2009; Qu et al., 2011; Patel et al., 2017; Sun et al., 2018).

For many years the cornea has been a valuable tool for studying the processes of wound healing and scarring due to the fact it is transparent, easily accessible and has an anatomy that is highly conserved inter- and intraspecies. Corneal injury leads to a cascade of events that are aimed at rapidly repairing the damaged tissue and preventing infection. Although a similar cascade of events is triggered upon corneal injury, the wound healing response varies significantly based on the insult, specifically, damage and/or perforation of the basement membrane, damage to the stroma, delayed epithelial wound closure and infection can all lead to an exacerbated inflammatory response (Ishizaki et al., 1993; Wilson et al., 2001; Torricelli and Wilson, 2014). Upon injury, corneal epithelial cells migrate toward the injured area to rapidly resurface the wound, there is increased proliferation of peripheral epithelial cells and limbal stem cells to enable wound closure and stratification, and a subset of keratocytes differentiate into myofibroblasts (Wilson, 2020). These myofibroblasts play a pivotal role in corneal wound healing and scarring since they deposit a significant amount of ECM components that form a "provisional matrix," which is needed during the wound healing process (Xue and Jackson, 2015). Excessive deposition of ECM components and/or failure to replace this "provisional matrix" and regenerate the stromal matrix leads to fibrosis/scarring and loss of vision (Jester et al., 1999; Hassell and Birk, 2010). Essentially, corneal scarring is caused by excessive disorganized stromal matrix remodeling that occurs after injury. These fibrotic changes have been shown to primarily take place following damage to the corneal epithelial basement membrane (Torricelli et al., 2016). Epithelium-derived growth factors such as TGF-β and platelet-derived growth factor (PDGF) along with inflammatory cytokines like interleukin-1 released from epithelial cells trigger apoptosis or transdifferentiation of keratocytes to myofibroblasts (Wilson et al., 2001; Torricelli et al., 2016). These myofibroblasts express CS/DS with longer chains and increased sulfation and KS with shorter chains and decreased sulfation when compared to normal keratocytes (Funderburgh et al., 2003). The change in structure of these GAG chains leads to modification of the PG profile in the stroma during stromal scar formation (Funderburgh et al., 2003; Saikia et al., 2018). During corneal epithelial wound healing, the loss of HA was shown to delay wound healing (Gesteira et al., 2017), while an increase in HA leads to corneal lymphangiogenesis and corneal scarring (Sun et al., 2019). The intensity of the inflammatory response and transdifferentiation of keratocytes into myofibroblasts, which together up-regulate the expression GAGs and PGs during the wound healing process, ultimately determine whether the corneal injury will result in restoration of transparency or fibrosis/scarring. Further studies are warranted to elucidate the role of these ECM components in corneal regeneration and to determine methods of intervention that could limit excessive ECM deposition and scarring.

SUMMARY

Significant progress has been made in understanding the distribution and function of different types of GAGs and PGs in the development, homeostasis and pathology of the ocular surface. A schematic of the cornea and limbal region with the distribution of the major corneal PGs and GAGs is shown in

TABLE 1 | Summary of studies characterizing the expression profiles of the different GAGs and PGs in the cornea.

GAGs	Gene	Expression in ocular surface	Function/deficiency	References
Keratan sulfate	Lumican	Primarily expressed in the stroma. Expressed by stromal keratocytes and corneal epithelial cells (during wound healing).	Deficiency causes corneal opacity and thinning due to abnormal collagen fibril structure, and delayed corneal wound healing.	Chakravarti et al., 1998, 2000; Saika et al., 2000
	Keratocan	Expressed throughout the corneal stroma by keratocytes only.	Deficiency causes corneal thinning and abnormal collagen fibril spacing. Mutation causes cornea plana congenital.	Pellegata et al., 2000; Kao and Liu, 2002; Carlson et al., 2005
	Fibromodulin	Expressed in the stroma of the peripheral cornea, limbus and sclera.	Deficiency causes a change in corneal curvature and the axial length of the eye.	Chen et al., 2010
	Mimecan	Expressed in the corneal stroma.	Deficiency causes an increase in collagen fiber diameter in the cornea.	Beecher et al., 2005
Heparan sulfate	Syndecan-1	Expressed in the corneal epithelium.	Deficiency causes delayed wound healing and abnormal intraepithelial nerve terminals in the cornea, as well as increased corneal neovascularization after alkali burn. Overexpression inhibits cell proliferation at the wound edge.	Götte et al., 2002; Stepp et al., 2002, 2010; Elenius et al., 2004; Pal-Ghosh et al., 2017
	Perlecan	Expressed in the entire corneal and conjunctival epithelial basement membrane and also between the endothelium and Descemet's membrane. Expressed by corneal epithelial cells and keratocytes.	Deficiency causes a thinner corneal epithelium with decreased expression of epithelial differentiation markers.	Ljubimov et al., 1995; Inomata et al., 2012; Torricelli et al., 2015
	Agrin	High expression at the limbus decreasing toward the central cornea and conjunctiva.	Deficiency can cause anophthalmia, microphthalmia, or iris adhesion to the cornea.	Fuerst et al., 2007; Schlötzer-Schrehardt et al., 2007
	Collagen XVIII	Expressed in the corneal epithelium, corneal and conjunctival epithelial basement membrane, corneal nerve, Descemet's membrane, and limbal and conjunctival capillaries. Increased expression in the stroma after injury.	Deficiency causes impaired corneal reinnervation after injury.	Zatterstrom et al., 2000; Fukai et al., 2002; Kato et al., 2003; Määttä et al., 2006; Sakimoto et al., 2008
	Exostosin glycosyltransferase 1 (*Ext1*) enzymes	Primarily expressed in the corneal epithelium.	Deletion of *Ext1* in the corneal epithelium causes defective corneal stratification and delayed wound healing due to loss of tight junctions.	Coulson-Thomas et al., 2015
Chondroitin sulfate	Lubricin	Expressed in corneal and conjunctival epithelia.	Functions as a boundary lubricant. Deficiency causes the dry eye phenotype.	Cheriyan et al., 2011; Schmidt et al., 2013
	Aggrecan	Expressed in corneal and conjunctival epithelia, low expression in the anterior corneal stroma and moderate expression in the scleral stroma.	Increased expression in the stroma of sclerocornea.	Bouhenni et al., 2013
	Versican	Expressed in the subepithelial region of the anterior limbus.		Schlötzer-Schrehardt et al., 2007
Dermatan sulfate	Decorin	Expressed throughout the corneal stroma.	Plays a role in corneal fibrillogenesis. Mutation causes congenital stromal dystrophy of the cornea.	Danielson et al., 1997; Bredrup et al., 2005; Rødahl et al., 2006; Zhang et al., 2009
	Biglycan	Expressed throughout the corneal stroma.	Plays a role in corneal fibrillogenesis.	Zhang et al., 2009
Hyaluronan	Hyaluronan synthases 1, 2, and 3	Highly expressed in the limbus and to some point in the conjunctiva.	Regulates limbal stem cell differentiation. Facilitates corneal epithelial wound healing. Regulates corneal lymphangiogenesis.	Gong et al., 1994; Lerner et al., 1998; Gesteira et al., 2017; Sun et al., 2019

Figure 7. A summary of the studies characterizing the expression profiles of the different GAGs and PGs has been provided in **Table 1**. Even though significant progress has been made in characterizing the distribution of GAGs and PGs throughout the ocular surface, the potential therapeutic uses of these molecules in ocular health and diseases are still largely unexplored and/or poorly understood.

AUTHOR CONTRIBUTIONS

SP and VC-T wrote the manuscript. SP, TG, and VC-T made the figures. TG and YC-T contributed toward parts of the manuscript and read and approved the final version. All authors contributed to the article and approved the submitted version.

FUNDING

This work was supported by a grant from The Mizutani Foundation to VC-T, a SeFAC grant awarded to VC-T and the National Institutes of Health/National Eye Institute, Grant R01 EY029289 to VC-T and the Core Grant P30 EY07551.

ACKNOWLEDGMENTS

The authors acknowledge the use of the Opuntia Cluster and the advanced support from the Center of Advanced Computing and Data Science at the University of Houston.

REFERENCES

Afratis, N., Gialeli, C., Nikitovic, D., Tsegenidis, T., Karousou, E., Theocharis, A. D., et al. (2013). Glycosaminoglycans: key players in cancer cell biology and treatment. *FEBS J.* 1177–1197. doi: 10.1111/j.1742-4658.2012.08529.x

Ang, B. C. H., Sng, J. J., Wang, P. X. H., Htoon, H. M., and Tong, L. H. T. (2017). Sodium hyaluronate in the treatment of dry eye syndrome: a systematic review and meta-analysis. *Sci. Rep.* 7:5. doi: 10.1038/s41598-017-08534-5

Anseth, A. (1969). Studies on corneal polysaccharides: VIII. Changes in the glycosaminoglycans in some human corneal disorders. *Exp. Eye Res.* 8, 438–441. doi: 10.1016/S0014-4835(69)80010-2

Arikawa-Hirasawa, E., Watanabe, H., Takami, H., Hassell, J. R., and Yamada, Y. (1999). Perlecan is essential for cartilage and cephalic development. *Nat. Genet.* 23, 354–358. doi: 10.1038/15537

Badylak, S. F., Freytes, D. O., and Gilbert, T. W. (2009). Extracellular matrix as a biological scaffold material: Structure and function. *Acta Biomater.* 5, 1–13. doi: 10.1016/j.actbio.2008.09.013

Baier, G., Wollensak, G., Mur, E., Redl, B., Stöffler, G., and Göttinger, W. (1990). Analysis of human tear proteins by different high-performance liquid chromatographic techniques. *J. Chromatogr. B. Biomed. Sci. App.* 525, 319–328. doi: 10.1016/S0378-4347(00)83408-8

Balazs, E. A., Watson, D., Duff, I. F., and Roseman, S. (1967). Hyaluronic acid in synovial fluid. I. Molecular parameters of hyaluronic acid in normal and arthritic human fluids. *Arthritis Rheum.* 10, 357–376. doi: 10.1002/art.1780100407

Bao, J., Chen, W., and Wu, L. (2011). Lubricin: a novel potential biotherapeutic approaches for the treatment of osteoarthritis. *Mol. Biol. Rep. Dordr.* 38, 2879–2885. doi: 10.1007/s11033-010-9949-9

Beck, M. (2018). Treatment strategies for lysosomal storage disorders. *Dev. Med. Child Neurol.* 60, 13–18. doi: 10.1111/dmcn.13600

Beecher, N., Carlson, C., Allen, B. R., Kipchumba, R., Conrad, G. W., Meek, K. M., et al. (2005). An X-ray diffraction study of corneal structure in mimecan-deficient mice. *Invest. Ophthalmol. Vis. Sci.* 46, 4046–4049. doi: 10.1167/iovs.05-0325

Bernfield, M., Götte, M., Park, P. W., Reizes, O., Fitzgerald, M. L., Lincecum, J., et al. (1999). Functions of cell surface heparan sulfate proteoglycans. *Annu. Rev. Biochem.* 68, 729–777. doi: 10.1146/annurev.biochem.68.1.729

Bhowmick, N. A., Zent, R., Ghiassi, M., McDonnell, M., and Moses, H. L. (2001). Integrin β1 signaling is necessary for transforming growth factor-β activation of p38MAPK and epithelial plasticity. *J. Biol. Chem.* 276, 46707–46713. doi: 10.1074/jbc.M106176200

Bi, Y., Stuelten, C. H., Kilts, T., Wadhwa, S., Iozzo, R. V., Robey, P. G., et al. (2005). Extracellular matrix proteoglycans control the fate of bone marrow stromal cells. *J. Biol. Chem.* 280, 30481–30489. doi: 10.1074/jbc.M500573200

Borcherding, M. S., Blacik, L. J., Sittig, R. A., Bizzell, J. W., Breen, M., and Weinstein, H. G. (1975). Proteoglycans and collagen fibre organization in human corneoscleral tissue. *Exp. Eye Res.* 21, 59–70. doi: 10.1016/0014-4835(75)90057-3

Bouhenni, R., Hart, M., Al-Jastaneiah, S., AlKatan, H., and Edward, D. P. (2013). Immunohistochemical expression and distribution of proteoglycans and collagens in sclerocornea. *Int. Ophthalmol.* 33, 691–700. doi: 10.1007/s10792-012-9710-6

Bredrup, C., Knappskog, P. M., Majewski, J., Rødahl, E., and Boman, H. (2005). Congenital stromal dystrophy of the cornea caused by a mutation in the decorin gene. *Invest. Ophthalmol. Vis. Sci.* 46, 420–426. doi: 10.1167/iovs.04-0804

Bredrup, C., Stang, E., Bruland, O., Palka, B. P., Young, R. D., Haavik, J., et al. (2010). Decorin accumulation contributes to the stromal opacities found in congenital stromal corneal dystrophy. *Invest. Ophthalmol. Vis. Sci.* 51, 5578–5582. doi: 10.1167/iovs.09-4933

Brockhausen, I., Elimova, E., Woodward, A. M., and Argüeso, P. (2018). Glycosylation pathways of human corneal and conjunctival epithelial cell mucins. *Carbohydr. Res.* 470, 50–56. doi: 10.1016/j.carres.2018.10.004

Bron, A. J., de Paiva, C. S., Chauhan, S. K., Bonini, S., Gabison, E. E., Jain, S., et al. (2017). TFOS DEWS II pathophysiology report. *Ocul. Surf.* 15, 438–510. doi: 10.1016/j.jtos.2017.05.011

Brown, D., and Waneck, G. L. (1992). Glycosyl-phosphatidylinositol-anchored membrane proteins. *J. Am. Soc. Nephrol.* 3, 895–906.

Camillieri, G., Bucolo, C., Rossi, S., and Drago, F. (2004). Hyaluronan-induced stimulation of corneal wound healing is a pure pharmacological effect. *J. Ocul. Pharmacol. Ther.* 20, 548–553. doi: 10.1089/jop.2004.20.548

Cantz, M., and Gehler, J. (1976). The mucopolysaccharidoses: inborn errors of glycosaminoglycan catabolism. *Hum. Genet.* 32, 233–255. doi: 10.1007/BF00295816

Capila, I., and Linhardt, R. J. (2002). Heparin–protein interactions. *Angew. Chem. Int. Ed.* 41, 390–412. doi: 10.1002/1521-3773(20020201)41:3<390::AID-ANIE390>3.0.CO;2-B

Carlson, E. C., Liu, C.-Y., Chikama, T., Hayashi, Y., Kao, C. W.-C., Birk, D. E., et al. (2005). Keratocan, a cornea-specific keratan sulfate proteoglycan, is regulated by lumican. *J. Biol. Chem.* 280, 25541–25547. doi: 10.1074/jbc.M500249200

Çevirme, D., Savluk, ÖF., Başaran, E. K., Aksoy, R., Elibol, A., Baş, T., et al. (2020). Effects of anticoagulant drugs on wound healing process in a rat model: a comparative study. *J. Wound Care* 29, 44–50. doi: 10.12968/jowc.2020.29.1.44

Chakravarti, S., Magnuson, T., Lass, J. H., Jepsen, K. J., LaMantia, C., and Carroll, H. (1998). Lumican regulates collagen fibril assembly: skin fragility and corneal opacity in the absence of lumican. *J. Cell Biol.* 141, 1277–1286. doi: 10.1083/jcb.141.5.1277

Chakravarti, S., Paul, J., Roberts, L., Chervoneva, I., Oldberg, A., and Birk, D. E. (2003). Ocular and scleral alterations in gene-targeted lumican-fibromodulin double-null mice. *Invest. Ophthalmol. Vis. Sci.* 44, 2422–2432. doi: 10.1167/iovs.02-0783

Chakravarti, S., Petroll, W. M., Hassell, J. R., Jester, J. V., Lass, J. H., Paul, J., et al. (2000). Corneal opacity in lumican-null mice: defects in collagen fibril structure and packing in the posterior stroma. *Invest. Ophthalmol. Vis. Sci.* 41, 3365–3373.

Chakravarti, S., Stallings, R. L., SundarRaj, N., Cornuet, P. K., and Hassell, J. R. (1995). Primary structure of human lumican (Keratan Sulfate Proteoglycan)

and localization of the gene (LUM) to chromosome 12q21.3-q22. *Genomics* 27, 481–488. doi: 10.1006/geno.1995.1080

Chandran, P. L., and Horkay, F. (2012). Aggrecan, an unusual polyelectrolyte: review of solution behavior and physiological implications. *Acta Biomater.* 8, 3–12. doi: 10.1016/j.actbio.2011.08.011

Cheifetz, S., Andres, J. L., and Massagué, J. (1988). The transforming growth factor-beta receptor type III is a membrane proteoglycan. Domain structure of the receptor. *J. Biol. Chem.* 263, 16984–16991.

Chen, C.-L., Huang, S. S., and Huang, J. S. (2006). Cellular Heparan sulfate negatively modulates transforming growth factor-β1 (TGF-β1) responsiveness in epithelial cells. *J. Biol. Chem.* 281, 11506–11514. doi: 10.1074/jbc.M512821200

Chen, J., Wong-Chong, J., and SundarRaj, N. (2011). FGF-2– and TGF-β1–induced downregulation of lumican and keratocan in activated corneal keratocytes by JNK signaling pathway. *Invest. Ophthalmol. Vis. Sci.* 52, 8957–8964. doi: 10.1167/iovs.11-8078

Chen, L. D., and Hazlett, L. D. (2000). Perlecan in the basement membrane of corneal epithelium serves as a site for *P. aeruginosa* binding. *Curr. Eye Res.* 20, 260–267. doi: 10.1076/0271-3683(200004)2041-5ft260

Chen, S., Oldberg, A., Chakravarti, S., and Birk, D. E. (2010). Fibromodulin regulates collagen fibrillogenesis during peripheral corneal development. *Dev. Dyn. Off. Publ. Am. Assoc. Anat.* 239, 844–854. doi: 10.1002/dvdy.22216

Cheriyan, T., Schmid, T. M., and Spector, M. (2011). Presence and distribution of the lubricating protein, lubricin, in the meibomian gland in rabbits. *Mol. Vis.* 17, 3055–3061.

Clark, S. J., Keenan, T. D. L., Fielder, H. L., Collinson, L. J., Holley, R. J., Merry, C. L. R., et al. (2011). Mapping the differential distribution of glycosaminoglycans in the adult human retina, choroid, and sclera. *Invest. Ophthalmol. Vis. Sci.* 52, 6511–6521. doi: 10.1167/iovs.11-7909

Clarke, L. A. (2008). The mucopolysaccharidoses: a success of molecular medicine. *Expert Rev. Mol. Med.* 10:E1. doi: 10.1017/S1462399408000550

Clause, K. C., and Barker, T. H. (2013). Extracellular matrix signaling in morphogenesis and repair. *Curr. Opin. Biotechnol.* 24, 830–833. doi: 10.1016/j.copbio.2013.04.011

Cornuet, P. K., Blochberger, T. C., and Hassell, J. R. (1994). Molecular polymorphism of lumican during corneal development. *Invest. Ophthalmol. Vis. Sci.* 35, 870–877.

Costell, M., Gustafsson, E., Aszódi, A., Mörgelin, M., Bloch, W., Hunziker, E., et al. (1999). Perlecan maintains the integrity of cartilage and some basement membranes. *J. Cell Biol.* 147, 1109–1122. doi: 10.1083/jcb.147.5.1109

Coulson-Thomas, V. J., Chang, S.-H., Yeh, L.-K., Coulson-Thomas, Y. M., Yamaguchi, Y., Esko, J., et al. (2015). Loss of corneal epithelial heparan sulfate leads to corneal degeneration and impaired wound healing. *Invest. Ophthalmol. Vis. Sci.* 56, 3004–3014. doi: 10.1167/iovs.14-15341

Coulson-Thomas, V. J., Coulson-Thomas, Y. M., Gesteira, T. F., de Paula, C. A. A., Carneiro, C. R. W., Ortiz, V., et al. (2013). Lumican expression, localization and antitumor activity in prostate cancer. *Exp. Cell Res.* 319, 967–981. doi: 10.1016/j.yexcr.2013.01.023

Coulson-Thomas, V. J., Gesteira, T. F., Hascall, V., and Kao, W. (2014). Umbilical cord mesenchymal stem cells suppress host rejection. *J. Biol. Chem.* 289, 23465–23481. doi: 10.1074/jbc.M114.557447

Coulson-Thomas, V. J., Lauer, M. E., Soleman, S., Zhao, C., Hascall, V. C., Day, A. J., et al. (2016). TSG-6 is constitutively expressed in adult CNS and associated with astrocyte-mediated glial scar formation following spinal cord injury. *J. Biol. Chem.* 16, 710673. doi: 10.1074/jbc.M115.710673

Coulson-Thomas, Y. M., Coulson-Thomas, V. J., Filippo, T. R., Mortara, R. A., da Silveira, R. B., Nader, H. B., et al. (2008). Adult bone marrow-derived mononuclear cells expressing chondroitinase AC transplanted into CNS injury sites promote local brain chondroitin sulphate degradation. *J. Neurosci. Methods* 171, 19–29. doi: 10.1016/j.jneumeth.2008.01.030

Craig, J. P., Nichols, K. K., Akpek, E. K., Caffery, B., Dua, H. S., Joo, C.-K., et al. (2017). TFOS DEWS II definition and classification report. *Ocul. Surf.* 15, 276–283. doi: 10.1016/j.jtos.2017.05.008

Cribbs, R. K., Luquette, M. H., and Besner, G. E. (1998). Acceleration of partial-thickness burn wound healing with topical application of heparin-binding EGF-like growth factor (HB-EGF). *J. Burn Care Rehabil.* 19, 95–101. doi: 10.1097/00004630-199803000-00002

Cui, D., Zhang, B. W., Matubayasi, N., and Levy, R. M. (2018). The role of interfacial water in protein-ligand binding: insights from the indirect solvent mediated PMF. *J. Chem. Theory Comput.* 14, 512–526. doi: 10.1021/acs.jctc.7b01076

Cursiefen, C., Cao, J., Chen, L., Liu, Y., Maruyama, K., Jackson, D., et al. (2004). Inhibition of hemangiogenesis and lymphangiogenesis after normal-risk corneal transplantation by neutralizing VEGF promotes graft survival. *Invest. Ophthalmol. Vis. Sci.* 45, 2666–2673. doi: 10.1167/iovs.03-1380

Danielson, K. G., Baribault, H., Holmes, D. F., Graham, H., Kadler, K. E., and Iozzo, R. V. (1997). Targeted disruption of decorin leads to abnormal collagen fibril morphology and skin fragility. *J. Cell Biol.* 136, 729–743. doi: 10.1083/jcb.136.3.729

De Souza, G. A., Godoy, L. M. F., and Mann, M. (2006). Identification of 491 proteins in the tear fluid proteome reveals a large number of proteases and protease inhibitors. *Genome Biol.* 7:R72. doi: 10.1186/gb-2006-7-8-R72

Del Longo, A., Piozzi, E., and Schweizer, F. (2018). Ocular features in mucopolysaccharidosis: diagnosis and treatment. *Ital. J. Pediatr.* 44:9. doi: 10.1186/s13052-018-0559-9

Dunlevy, J. R., Beales, M. P., Berryhill, B. L., Cornuet, P. K., and Hassell, J. R. (2000). Expression of the keratan sulfate proteoglycans lumican, keratocan and osteoglycin/mimecan during chick corneal development. *Exp. Eye Res.* 70, 349–362. doi: 10.1006/exer.1999.0789

Dunlevy, J. R., Neame, P. J., Vergnes, J.-P., and Hassell, J. R. (1998). Identification of the N-linked oligosaccharide sites in chick corneal lumican and keratocan that receive keratan sulfate. *J. Biol. Chem.* 273, 9615–9621. doi: 10.1074/jbc.273.16.9615

Ebenezer, N. D., Patel, C. B., Hariprasad, S. M., Chen, L. L., Patel, R. J., Hardcastle, A. J., et al. (2005). Clinical and molecular characterization of a family with autosomal recessive cornea plana. *Arch. Ophthalmol.* 123, 1248–1253. doi: 10.1001/archopht.123.9.1248

Echtermeyer, F., Streit, M., Wilcox-Adelman, S., Saoncella, S., Denhez, F., Detmar, M., et al. (2001). Delayed wound repair and impaired angiogenesis in mice lacking syndecan-4. *J. Clin. Invest.* 107, R9–R14.

El-Ashry, M. F., El-Aziz, M. M. A., Wilkins, S., Cheetham, M. E., Wilkie, S. E., Hardcastle, A. J., et al. (2002). Identification of Novel mutations in the carbohydrate sulfotransferase gene (CHST6) causing macular corneal dystrophy. *Invest. Ophthalmol. Vis. Sci.* 43, 377–382.

Elenius, K., and Jalkanen, M. (1994). Function of the syndecans–a family of cell surface proteoglycans. *J. Cell Sci.* 107, 2975–2982.

Elenius, V., Götte, M., Reizes, O., Elenius, K., and Bernfield, M. (2004). Inhibition by the soluble syndecan-1 ectodomains delays wound repair in mice overexpressing syndecan-1. *J. Biol. Chem.* 279, 41928–41935. doi: 10.1074/jbc.M404506200

Esko, J. D., and Lindahl, U. (2001). Molecular diversity of heparan sulfate. *J. Clin. Invest.* 108, 169–173. doi: 10.1172/jci200113530

Fagerholm, P., Fitzsimmons, T., Härfstrand, A., and Schenholm, M. (1992). Reactive formation of hyaluronic acid in the rabbit corneal alkali burn. *Acta Ophthalmol. Suppl.* 92, 67–72. doi: 10.1111/j.1755-3768.1992.tb02171.x

Fahnehjelm, K. T., Ashworth, J. L., Pitz, S., Olsson, M., Törnquist, A. L., Lindahl, P., et al. (2012). Clinical guidelines for diagnosing and managing ocular manifestations in children with mucopolysaccharidosis. *Acta Ophthalmol. (Copenh.)* 90, 595–602. doi: 10.1111/j.1755-3768.2011.02280.x

Feneck, E. M., Souza, R. B., Lewis, P. N., Hayes, S., Pereira, L. V., and Meek, K. M. (2020). Developmental abnormalities in the cornea of a mouse model for Marfan syndrome. *Exp. Eye Res.* 194:108001. doi: 10.1016/j.exer.2020.108001

Fisher, L. W., Termine, J. D., and Young, M. F. (1989). Deduced protein sequence of bone small proteoglycan I (biglycan) shows homology with proteoglycan II (decorin) and several nonconnective tissue proteins in a variety of species. *J. Biol. Chem.* 264, 4571–4576.

Fitzsimmons, T. D., Fagerholm, P., and Wallin, Ö (1997). Hyaluronan in the exfoliation syndrome. *Acta Ophthalmol. Scand.* 75, 257–260. doi: 10.1111/j.1600-0420.1997.tb00768.x

Foster, J. W., Shinde, V., Soiberman, U. S., Sathe, G., Liu, S., Wan, J., et al. (2018). Integrated stress response and decreased ECM in cultured stromal cells from keratoconus corneas. *Invest. Ophthalmol. Vis. Sci.* 59, 2977–2986. doi: 10.1167/iovs.18-24367

Frantz, C., Stewart, K. M., and Weaver, V. M. (2010). The extracellular matrix at a glance. *J. Cell Sci.* 123, 4195–4200. doi: 10.1242/jcs.023820

Fraser, J. R. E., Laurent, T. C., and Laurent, U. B. G. (1997). Hyaluronan: its nature, distribution, functions and turnover. *J. Intern. Med.* 242, 27–33. doi: 10.1046/j.1365-2796.1997.00170.x

Freeze, H. H., Kinoshita, T., and Schnaar, R. L. (2015). "Genetic disorders of glycan degradation," in *Essentials of Glycobiology*, eds A. Varki, R. D. Cummings, J. D. Esko, P. Stanley, G. W. Hart, M. Aebi, et al. (Cold Spring Harbor,NY: Cold Spring Harbor Laboratory Press).

Fuerst, P. G., Rauch, S. M., and Burgess, R. W. (2007). Defects in eye development in transgenic mice overexpressing the heparan sulfate proteoglycan agrin. *Dev. Biol.* 303, 165–180. doi: 10.1016/j.ydbio.2006.11.033

Fukai, N., Eklund, L., Marneros, A. G., Oh, S. P., Keene, D. R., Tamarkin, L., et al. (2002). Lack of collagen XVIII/endostatin results in eye abnormalities. *EMBO J.* 21, 1535–1544. doi: 10.1093/emboj/21.7.1535

Funderburgh, J. L. (2000). MINI REVIEW Keratan sulfate: structure, biosynthesis, and function. *Glycobiology* 10, 951–958. doi: 10.1093/glycob/10.10.951

Funderburgh, J. L., Corpuz, L. M., Roth, M. R., Funderburgh, M. L., Tasheva, E. S., and Conrad, G. W. (1997). Mimecan, the 25-kDa corneal keratan sulfate proteoglycan, is a product of the gene producing osteoglycin. *J. Biol. Chem.* 272, 28089–28095. doi: 10.1074/jbc.272.44.28089

Funderburgh, J. L., Funderburgh, M. L., Rodrigues, M. M., Krachmer, J. H., and Conrad, G. W. (1990). Altered antigenicity of keratan sulfate proteoglycan in selected corneal diseases. *Invest. Ophthalmol. Vis. Sci.* 31, 419–428.

Funderburgh, J. L., Mann, M. M., and Funderburgh, M. L. (2003). Keratocyte phenotype mediates proteoglycan structure a role for fibroblasts in corneal fibrosis. *J. Biol. Chem.* 278, 45629–45637. doi: 10.1074/jbc.M303292200

Galvan, L. (1996). Effects of heparin on wound healing. *J. Wound Ostomy Cont. Nurs. Off. Publ. Wound Ostomy Cont. Nurses Soc.* 23, 224–226. doi: 10.1016/s1071-5754(96)90095-9

García, B., García-Suárez, O., Merayo-Lloves, J., Alcalde, I., Alfonso, J. F., Cueto, L. F.-V., et al. (2016). Differential expression of proteoglycans by corneal stromal cells in keratoconus. *Invest. Ophthalmol. Vis. Sci.* 57, 2618–2628. doi: 10.1167/iovs.15-16692

Gartaganis, S. P., Georgakopoulos, C. D., Exarchou, A. M., Mela, E. K., Lamari, F., and Karamanos, N. K. (2001). Increased aqueous humor basic fibroblast growth factor and hyaluronan levels in relation to the exfoliation syndrome and exfoliative glaucoma. *Acta Ophthalmol. Scand.* 79, 572–575. doi: 10.1034/j.1600-0420.2001.790605.x

Gassner, H. L., Esco, M., Smithson, M. W., and Kurpakus, M. A. (1997). Differential effects of transforming growth factors on localization of adhesion complex proteins following corneal epithelial cell wounding. *Curr. Eye Res.* 16, 387–395. doi: 10.1076/ceyr.16.4.387.10692

Gautam, M., Noakes, P. G., Moscoso, L., Rupp, F., Scheller, R. H., Merlie, J. P., et al. (1996). Defective neuromuscular synaptogenesis in agrin-deficient mutant mice. *Cell* 85, 525–535. doi: 10.1016/S0092-8674(00)81253-2

Gavioli, E. M., Sikorska, G., Man, A., Rana, J., and Vider, E. (2020). Current Perspectives of Anticoagulation in Patients with COVID-19. *J. Cardiovasc. Pharmacol*. doi: 10.1097/FJC.0000000000000861 [Epub ahead of print].

Georgakopoulos, C. D., Makri, O. E., Pagoulatos, D., and Karamanos, N. K. (2019). Expression and localization of glycosaminoglycans/proteoglycan in pterygium: an immunohistochemical study. *Med. Hypothesis Discov. Innov. Ophthalmol.* 8, 39–43.

Gesteira, T. F., Coulson-Thomas, Y. M., and Coulson-Thomas, V. J. (2016). Anti-inflammatory properties of the glial scar. *Neural Regen. Res.* 11, 1742–1743. doi: 10.4103/1673-5374.194710

Gesteira, T. F., Sun, M., Coulson-Thomas, Y. M., Yamaguchi, Y., Yeh, L.-K., Hascall, V., et al. (2017). Hyaluronan rich microenvironment in the limbal stem cell niche regulates limbal stem cell differentiation. *Invest. Ophthalmol. Vis. Sci.* 58, 4407–4421. doi: 10.1167/iovs.17-22326

Gong, H., Underhill, C. B., and Freddo, T. F. (1994). Hyaluronan in the bovine ocular anterior segment, with emphasis on the outflow pathways. *Invest. Ophthalmol. Vis. Sci.* 35, 4328–4332.

Götte, M., Joussen, A. M., Klein, C., Andre, P., Wagner, D. D., Hinkes, M. T., et al. (2002). Role of syndecan-1 in leukocyte–endothelial interactions in the ocular vasculature. *Invest. Ophthalmol. Vis. Sci.* 43, 1135–1141.

Gubbiotti, M. A., Vallet, S. D., Ricard-Blum, S., and Iozzo, R. V. (2016). Decorin interacting network: a comprehensive analysis of decorin-binding partners and their versatile functions. *Matrix Biol. J. Int. Soc. Matrix Biol.* 55, 7–21. doi: 10.1016/j.matbio.2016.09.009

Gupta, M., and Brand, M. (2013). Identification and expression analysis of zebrafish glypicans during embryonic development. *PLoS One* 8:824. doi: 10.1371/journal.pone.0080824

Halfter, W., Dong, S., Schurer, B., and Cole, G. J. (1998). Collagen XVIII Is a basement membrane heparan sulfate proteoglycan. *J. Biol. Chem.* 273, 25404–25412. doi: 10.1074/jbc.273.39.25404

Hardingham, T. E., and Fosang, A. J. (1992). Proteoglycans: many forms and many functions. *FASEB J.* 6, 861–870. doi: 10.1096/fasebj.6.3.1740236

Härfstrand, A., Molander, N., Stenevi, U., Apple, D., Schenholm, M., and Madsen, K. (1992). Evidence of hyaluronic acid and hyaluronic acid binding sites on human corneal endothelium. *J. Cataract Refract. Surg.* 18, 265–269. doi: 10.1016/s0886-3350(13)80903-0

Hart, G. W. (1978). Glycosaminoglycan sulfotransferases of the developing chick cornea. *J. Biol. Chem.* 253, 347–353.

Hascall, V., and Esko, J. D. (2015). "Hyaluronan," in *Essentials of Glycobiology*, eds A. Varki, R. D. Cummings, J. D. Esko, P. Stanley, G. W. Hart, M. Aebi, et al. (Cold Spring Harbor, NY: Cold Spring Harbor Laboratory Press)

Hasegawa, N., Torii, T., Kato, T., Miyajima, H., Furuhata, A., Nakayasu, K., et al. (2000). Decreased GlcNAc 6-O-sulfotransferase activity in the cornea with macular corneal dystrophy. *Invest. Ophthalmol. Vis. Sci.* 41, 3670–3677.

Hassell, J. R., and Birk, D. E. (2010). The molecular basis of corneal transparency. *Exp. Eye Res.* 91, 326–335. doi: 10.1016/j.exer.2010.06.021

Hassell, J. R., Cintron, C., Kublin, C., and Newsome, D. A. (1983). Proteoglycan changes during restoration of transparency in corneal scars. *Arch. Biochem. Biophys.* 222, 362–369. doi: 10.1016/0003-9861(83)90532-5

Hattori, N., Carrino, D. A., Lauer, M. E., Vasanji, A., Wylie, J. D., Nelson, C. M., et al. (2011). Pericellular versican regulates the fibroblast-myofibroblast transition. *J. Biol. Chem.* 286, 34298–34310. doi: 10.1074/jbc.M111.254938

Hayashida, Y., Akama, T. O., Beecher, N., Lewis, P., Young, R. D., Meek, K. M., et al. (2006). Matrix morphogenesis in cornea is mediated by the modification of keratan sulfate by GlcNAc 6-O-sulfotransferase. *Proc. Natl. Acad. Sci. U.S.A.* 103, 13333–13338. doi: 10.1073/pnas.0605441103

He, S., Shi, D., Han, Z., Dong, Z., Xie, Y., Zhang, F., et al. (2019). Heparinized silk fibroin hydrogels loading FGF1 promote the wound healing in rats with full-thickness skin excision. *Biomed. Eng. OnLine* 18:4. doi: 10.1186/s12938-019-0716-4

Hienola, A., Tumova, S., Kulesskiy, E., and Rauvala, H. (2006). N-syndecan deficiency impairs neural migration in brain. *J. Cell Biol.* 174, 569–580. doi: 10.1083/jcb.200602043

Hill, L. J., Moakes, R. J. A., Vareechon, C., Butt, G., Ng, A., Brock, K., et al. (2018). Sustained release of decorin to the surface of the eye enables scarless corneal regeneration. *NPJ Regen. Med.* 3:4. doi: 10.1038/s41536-018-0061-4

Hou, L., Fu, W., Liu, Y., Wang, Q., Wang, L., and Huang, Y. (2020). Agrin Promotes limbal stem cell proliferation and corneal wound healing through hippo-yap signaling pathway. *Invest. Ophthalmol. Vis. Sci.* 61:7. doi: 10.1167/iovs.61.5.7

Huang, C., Long, X., Peng, C., Lin, P., Tan, H., Lv, W., et al. (2019). Novel variants in the KERA gene cause autosomal recessive cornea plana in a Chinese family: a case report. *Mol. Med. Rep.* 19, 4711–4718. doi: 10.3892/mmr.2019.10153

Inomata, T., Ebihara, N., Funaki, T., Matsuda, A., Watanabe, Y., Ning, L., et al. (2012). Perlecan-deficient mutation impairs corneal epithelial structure. *Invest. Ophthalmol. Vis. Sci.* 53, 1277–1284. doi: 10.1167/iovs.11-8742

Iozzo, R. V. (1997). The family of the small leucine-rich proteoglycans: key regulators of matrix assembly and cellular growth. *Crit. Rev. Biochem. Mol. Biol.* 32, 141–174. doi: 10.3109/10409239709108551

Iozzo, R. V. (1998). Matrix proteoglycans: from molecular design to cellular function. *Annu. Rev. Biochem.* 67:609. doi: 10.1146/annurev.biochem.67.1.609

Iozzo, R. V. (2005). Basement membrane proteoglycans: from cellar to ceiling. *Nat. Rev. Mol. Cell Biol.* 6, 646–656. doi: 10.1038/nrm1702

Ishijima, M., Suzuki, N., Hozumi, K., Matsunobu, T., Kosaki, K., Kaneko, H., et al. (2012). Perlecan modulates VEGF signaling and is essential for vascularization in endochondral bone formation. *Matrix Biol.* 31, 234–245. doi: 10.1016/j.matbio.2012.02.006

Ishizaki, M., Zhu, G., Haseba, T., Shafer, S. S., and Kao, W. W. (1993). Expression of collagen I, smooth muscle alpha-actin, and vimentin during the healing of alkali-burned and lacerated corneas. *Invest. Ophthalmol. Vis. Sci.* 34, 3320–3328.

Itano, N., Sawai, T., Yoshida, M., Lenas, P., Yamada, Y., Imagawa, M., et al. (1999). Three isoforms of mammalian hyaluronan synthases have distinct enzymatic properties. *J. Biol. Chem.* 274, 25085–25092. doi: 10.1074/jbc.274.35.25085

Ito, K., Shinomura, T., Zako, M., Ujita, M., and Kimata, K. (1995). Multiple forms of mouse PG-M, a large chondroitin sulfate proteoglycan generated by alternative splicing. *J. Biol. Chem.* 270, 958–965. doi: 10.1074/jbc.270.2.958

Jackson, S. M., Nakato, H., Sugiura, M., Jannuzi, A., Oakes, R., Kaluza, V., et al. (1997). dally, a *Drosophila glypican*, controls cellular responses to the TGF-beta-related morphogen. *Dpp. Dev.* 124, 4113–4120.

Javed, A., Aslam, T., Jones, S. A., and Ashworth, J. (2017). Objective quantification of changes in corneal clouding over time in patients with mucopolysaccharidosis. *Invest. Ophthalmol. Vis. Sci.* 58, 954–958. doi: 10.1167/iovs.16-20647

Jester, J. V., Moller-Pedersen, T., Huang, J., Sax, C. M., Kays, W. T., Cavangh, H. D., et al. (1999). The cellular basis of corneal transparency: evidence for 'corneal crystallins.'. *J. Cell Sci.* 112, 613–622.

Jian-Wei, L., Xiu-Yun, L., and Ai-Jun, D. (2017). Effectiveness of heparin eye drops in paraquat-induced ocular injury. *Cutan. Ocul. Toxicol.* 36, 377–380. doi: 10.1080/15569527.2017.1303706

Jones, L., Downie, L. E., Korb, D., Benitez-Del-Castillo, J. M., Dana, R., Deng, S. X., et al. (2017). TFOS DEWS II management and therapy report. *Ocul. Surf.* 15, 575–628. doi: 10.1016/j.jtos.2017.05.006

Kao, W. W.-Y. (2006). Ocular surface tissue morphogenesis in normal and disease states revealed by genetically modified mice. [Miscellaneous Article]. *Cornea* 6:a4. doi: 10.1097/01.ico.0000247207.55520.a4

Kao, W. W. Y., and Liu, C. (2002). Roles of lumican and keratocan on corneal transparency. *Glycoconj. J. N. Y.* 19, 275–285. doi: 10.1023/a:1025396316169

Kato, T., Chang, J.-H., and Azar, D. T. (2003). Expression of type XVIII collagen during healing of corneal incisions and keratectomy wounds. *Invest. Ophthalmol. Vis. Sci.* 44, 78–85. doi: 10.1167/iovs.01-1257

Khan, A., Al-Saif, A., and Kambouris, M. (2004). A novel KERA mutation associated with autosomal recessive cornea plana. *Ophthalmic Genet.* 25, 147–152. doi: 10.1080/13816810490514397

Khan, A. O., Aldahmesh, M., Al-Saif, A., and Meyer, B. (2005). Pellucid marginal degeneration coexistent with cornea plana in one member of a family exhibiting a novel KERA mutation. *Br. J. Ophthalmol.* 89, 1538–1540. doi: 10.1136/bjo.2005.073510

Khan, A. O., Aldahmesh, M., and Meyer, B. (2006a). Corneal ectasia and hydrops in a patient with autosomal recessive cornea plana. *Ophthalmic Genet.* 27, 99–101. doi: 10.1080/13816810600862469

Khan, A. O., Aldahmesh, M., and Meyer, B. (2006b). Recessive cornea plana in the kingdom of saudi arabia. *Ophthalmology* 113, 1773–1778. doi: 10.1016/j.ophtha.2006.04.026

Kiani, C., Chen, L., Wu, Y. J., Yee, A. J., and Yang, B. B. (2002). Structure and function of aggrecan. *Cell Res. Lond.* 12, 19–32. doi: 10.1038/sj.cr.7290106

Kim, M. J., Liu, I.-H., Song, Y., Lee, J.-A., Halfter, W., Balice-Gordon, R. J., et al. (2007). Agrin is required for posterior development and motor axon outgrowth and branching in embryonic zebrafish. *Glycobiology* 17, 231–247. doi: 10.1093/glycob/cwl069

Kobashi, H., and Rong, S. S. (2017). Corneal collagen cross-linking for keratoconus: systematic review. *BioMed Res. Int.* 2017:651. doi: 10.1155/2017/8145651

Koga, T., Inatani, M., Hirata, A., Inomata, Y., Zako, M., Kimata, K., et al. (2005). Expression of a chondroitin sulfate proteoglycan, versican (PG-M), during development of rat cornea. *Curr. Eye Res.* 30, 455–463. doi: 10.1080/02713680590959376

Kolset, S. O., and Gallagher, J. T. (1990). Proteoglycans in haemopoietic cells. *Biochim. Biophys. Acta* 1032, 191–211. doi: 10.1016/0304-419x(90)90004-k

Lambiase, A., Sullivan, B. D., Schmidt, T. A., Sullivan, D. A., Jay, G. D., Truitt, E. R., et al. (2017). A two-week, randomized, double-masked study to evaluate safety and efficacy of lubricin (150 μg/mL) eye drops versus sodium hyaluronate (HA) 0.18% eye drops (Vismed®) in patients with moderate dry eye disease. *Ocul. Surf.* 15, 77–87. doi: 10.1016/j.jtos.2016.08.004

Langford, J. K., Stanley, M. J., Cao, D., and Sanderson, R. D. (1998). Multiple heparan sulfate chains are required for optimal syndecan-1 function. *J. Biol. Chem.* 273, 29965–29971. doi: 10.1074/jbc.273.45.29965

Leask A. (2010). Potential therapeutic targets for cardiac fibrosis. *Circ. Res.* 106, 1675–1680. doi: 10.1161/CIRCRESAHA.110.217737

Ledin, J., Staatz, W., Li, J.-P., Götte, M., Selleck, S., Kjellén, L., et al. (2004). Heparan sulfate structure in mice with genetically modified heparan sulfate production. *J. Biol. Chem.* 279, 42732–42741. doi: 10.1074/jbc.M405382200

Lerner, L. E., Schwartz, D. M., Hwang, D. G., Howes, E. L., and Stern, R. (1998). Hyaluronan and CD44 in the human cornea and limbal conjunctiva. *Exp. Eye Res.* 67, 481–484. doi: 10.1006/exer.1998.0567

Lewis, D., Davies, Y., Nieduszynski, I. A., Lawrence, F., Quantock, A. J., Bonshek, R., et al. (2000). Ultrastructural localization of sulfated and unsulfated keratan sulfate in normal and macular corneal dystrophy type I. *Glycobiology* 10, 305–312. doi: 10.1093/glycob/10.3.305

Lin, H.-C., Chang, J.-H., Jain, S., Gabison, E. E., Kure, T., Kato, T., et al. (2001). Matrilysin cleavage of corneal collagen type XVIII NC1 domain and generation of a 28-kDa fragment. *Invest. Ophthalmol. Vis. Sci.* 42, 2517–2524.

Liskova, P., Hysi, P. G., Williams, D., Ainsworth, J. R., Shah, S., De La Chapelle, A., et al. (2007). Study of p.N247S KERA mutation in a British family with cornea plana. *Mol. Vis.* 13, 1339–1347.

Littlechild, S. L., Young, R. D., Caterson, B., Yoshida, H., Yamazaki, M., Sakimura, K., et al. (2018). Keratan sulfate phenotype in the β-1,3-N-acetylglucosaminyltransferase-7–null mouse cornea. *Invest. Ophthalmol. Vis. Sci.* 59, 1641–1651. doi: 10.1167/iovs.17-22716

Liu, I.-H., Zhang, C., Kim, M. J., and Cole, G. J. (2008). Retina development in zebrafish requires the heparan sulfate proteoglycan agrin. *Dev. Neurobiol.* 68, 877–898. doi: 10.1002/dneu.20625

Liu, S., Shi-wen, X., Kennedy, L., Pala, D., Chen, Y., Eastwood, M., et al. (2007). FAK is required for TGFβ-induced JNK phosphorylation in fibroblasts: implications for acquisition of a matrix-remodeling phenotype. *Mol. Biol. Cell* 18, 2169–2178. doi: 10.1091/mbc.e06-12-1121

Ljubimov, A. V., Burgeson, R. E., Butkowski, R. J., Michael, A. F., Sun, T. T., and Kenney, M. C. (1995). Human corneal basement membrane heterogeneity: topographical differences in the expression of type IV collagen and laminin isoforms. *Lab. Investig. J. Tech. Methods Pathol.* 72, 461–473.

Ljubimov, A. V., and Saghizadeh, M. (2015). Progress in corneal wound healing. *Prog. Retin. Eye Res.* 49, 17–45. doi: 10.1016/j.preteyeres.2015.07.002

Lohr, K., Sardana, H., Lee, S., Wu, F., Huso, D. L., Hamad, A. R., et al. (2012). Extracellular matrix protein lumican regulates inflammation in a mouse model of colitis. *Inflamm. Bowel Dis.* 18, 143–151. doi: 10.1002/ibd.21713

Lord, M. S., Estrella, R. P., Chuang, C. Y., Youssef, P., Karlsson, N. G., Flannery, C. R., et al. (2012). Not all lubricin isoforms are substituted with a glycosaminoglycan chain. *Connect. Tissue Res.* 53, 132–141. doi: 10.3109/03008207.2011.614364

Luchko, T., Gusarov, S., Roe, D. R., Simmerling, C., Case D. A., Tuszynski, J., et al. (2010). Three-dimensional molecular theory of solvation coupled with molecular dynamics in amber. *J. Chem. Theory Comput.* 6, 607–624. doi: 10.1021/ct900460m

Määttä, M., Heljasvaara, R., Sormunen, R., Pihlajaniemi, T., Autio-Harmainen, H., and Tervo, T. (2006). Differential expression of collagen types XVIII/endostatin and XV in normal, keratoconus, and scarred human corneas. *Cornea* 25, 341–349. doi: 10.1097/01.ico.0000178729.57435.96

Maccarana, M., Kalamajski, S., Kongsgaard, M., Magnusson, S. P., Oldberg, Å, and Malmström, A. (2009). Dermatan sulfate epimerase 1-deficient mice have reduced content and changed distribution of iduronic acids in dermatan sulfate and an altered collagen structure in skin. *Mol. Cell. Biol.* 29, 5517–5528. doi: 10.1128/MCB.00430-09

Magro, G. (2020). COVID-19: review on latest available drugs and therapies against SARS-CoV-2. Coagulation and inflammation cross-talking. *Virus Res.* 286:198070. doi: 10.1016/j.virusres.2020.198070

Malmström, A., and Fransson, L. A. (1975). Biosynthesis of dermatan sulfate. I. Formation of L-iduronic acid residues. *J. Biol. Chem.* 250, 3419–3425.

Maltseva, I., Chan, M., Kalus, I., Dierks, T., and Rosen, S. D. (2013). The SULFs, extracellular sulfatases for heparan sulfate, promote the migration of corneal epithelial cells during wound repair. *PLoS One* 8:9642. doi: 10.1371/journal.pone.0069642

Mantelli, F., Schaffer, L., Dana, R., Head, S. R., and Argüeso, P. (2009). Glycogene expression in conjunctiva of patients with dry eye: downregulation of notch signaling. *Invest. Ophthalmol. Vis. Sci.* 50, 2666–2672. doi: 10.1167/iovs.08-2734

Matoba, A., Oie, Y., Tanibuchi, H., Winegarner, A., and Nishida, K. (2020). Anterior segment optical coherence tomography and in vivo confocal microscopy in cases of mucopolysaccharidosis. *Am. J. Ophthalmol. Case Rep.* 19:728. doi: 10.1016/j.ajoc.2020.100728

Mencio, C., Swarup, V. P., Soliai, M., and Kuberan, B. (2015). Synthesis of sulfur isotope-labeled sulfate donor, 3'-phosphoadenosine-5'-phosphosulfate, for studying glycosaminoglycan functions. *Methods Mol. Biol. Clifton N. J.* 1229, 37–42. doi: 10.1007/978-1-4939-1714-3_5

Mertens, G., Van der Schueren, B., van den Berghe, H., and David, G. (1996). Heparan sulfate expression in polarized epithelial cells: the apical sorting of glypican (GPI-anchored proteoglycan) is inversely related to its heparan sulfate content. *J. Cell Biol.* 132, 487–497. doi: 10.1083/jcb.132.3.487

Mikami, T., and Kitagawa, H. (2013). Biosynthesis and function of chondroitin sulfate. *Biochim. Biophys. Acta* 1830, 4719–4733. doi: 10.1016/j.bbagen.2013.06.006

Mikami, T., and Kitagawa, H. (2017). Sulfated glycosaminoglycans: their distinct roles in stem cell biology. *Glycoconj. J. N. Y.* 34, 725–735. doi: 10.1007/s10719-016-9732-9

Miyadera, K., Conatser, L., Llanga, T. A., Carlin, K., O'Donnell, P., Bagel, J., et al. (2020). Intrastromal gene therapy prevents and reverses advanced corneal clouding in a canine model of mucopolysaccharidosis I. *Mol. Ther. J. Am. Soc. Gene Ther.* 28, 1455–1463. doi: 10.1016/j.ymthe.2020.04.004

Moffatt, P., Geng, Y., Lamplugh, L., Nanci, A., and Roughley, P. J. (2017). Absence of the dermatan sulfate chain of decorin does not affect mouse development. *J. Negat. Results Biomed.* 16:3. doi: 10.1186/s12952-017-0074-3

Morgan, M. R., Humphries, M. J., and Bass, M. D. (2007). Synergistic control of cell adhesion by integrins and syndecans. *Nat. Rev. Mol. Cell Biol.* 8, 957–969. doi: 10.1038/nrm2289

Nakamura, M., Hikida, M., and Nakano, T. (1992). Concentration and molecular weight dependency of rabbit corneal epithelial wound healing on hyaluronan. *Curr. Eye Res.* 11, 981–986. doi: 10.3109/02713689209033496

Nakato, H., Futch, T. A., and Selleck, S. B. (1995). The division abnormally delayed (dally) gene: a putative integral membrane proteoglycan required for cell division patterning during postembryonic development of the nervous system in *Drosophila*. *Development* 121, 3687–3702.

Nejat, F., Aghamollaei, H., Pirhadi, S., Jadidi, K., and Nejat, M. A. (2018). Simultaneous presence of macular corneal dystrophy and retinitis pigmentosa in three members of a family. *Iran. J. Med. Sci.* 43, 227–230.

Ng, L., Grodzinsky, A. J., Patwari, P., Sandy, J., Plaas, A., and Ortiz, C. (2003). Individual cartilage aggrecan macromolecules and their constituent glycosaminoglycans visualized via atomic force microscopy. *J. Struct. Biol.* 143, 242–257. doi: 10.1016/j.jsb.2003.08.006

Nguyen, C., Yamazaki, T., Kovalenko, A., Case, D. A., Gilson, M. K., Kurtzman, T., et al. (2019). A molecular reconstruction approach to site-based 3D-RISM and comparison to GIST hydration thermodynamic maps in an enzyme active site. *PLoS One* 14:e0219473. doi: 10.1371/journal.pone.0219473

Nikolic, L., Friend, J., Taylor, S., and Thoft, R. A. (1986). Inhibition of vascularization in rabbit corneas by heparin: cortisone pellets. *Invest. Ophthalmol. Vis. Sci.* 27, 449–456.

Nourian, D. A., Mirahmadi, B. F., Chehelgerdi, M., and Raeisi, D. S. (2019). Skin tissue engineering: wound healing based on stem-cell-based therapeutic strategies. *Stem Cell Res. Ther.* 10:2. doi: 10.1186/s13287-019-1212-2

Ohtsubo, K., and Marth, J. D. (2006). Glycosylation in cellular mechanisms of health and disease. *Cell* 126, 855–867. doi: 10.1016/j.cell.2006.08.019

Olczyk, P., Mencner, Ł, and Komosinska-Vassev, K. (2015). Diverse roles of heparan sulfate and heparin in wound repair. *BioMed Res. Int.* 2015:549417. doi: 10.1155/2015/549417

O'Reilly, M. S., Boehm, T., Shing, Y., Fukai, N., Vasios, G., Lane, W. S., et al. (1997). Endostatin: an endogenous inhibitor of angiogenesis and tumor growth. *Cell* 88, 277–285. doi: 10.1016/s0092-8674(00)81848-6

Pacella, E., Pacella, F., De Paolis, G., Parisella, F. R., Turchetti, P., Anello, G., et al. (2015). Glycosaminoglycans in the human cornea: age-related changes. *Ophthalmol. Eye Dis.* 7, 1–5. doi: 10.4137/OED.S17204

Pai, V. C., Lo, I.-C., Huang, Y., Wun, T. I.-C., Cheng, H.-P., Shi, G.-Y., et al. (2018). The chondroitin sulfate moiety mediates thrombomodulin-enhanced adhesion and migration of vascular smooth muscle cells. *J. Biomed. Sci.* 25:7. doi: 10.1186/s12929-018-0415-7

Pal-Ghosh, S., Tadvalkar, G., and Stepp, M. A. (2017). Alterations in corneal sensory nerves during homeostasis, aging, and after injury in mice lacking the heparan sulfate proteoglycan syndecan-1. *Invest. Ophthalmol. Vis. Sci.* 58, 4959–4975. doi: 10.1167/iovs.17-21531

Pan, Y., Carbe, C., Powers, A., Zhang, E. E., Esko, J. D., Grobe, K., et al. (2008). Bud specific N-sulfation of heparan sulfate regulates Shp2-dependent FGF signaling during lacrimal gland induction. *Development* 135, 301–310. doi: 10.1242/dev.014829

Papadia, F., Lozupone, M. S., Gaeta, A., Capodiferro, D., and Lacalendola, G. (2011). Long-term enzyme replacement therapy in a severe case of mucopolysaccharidosis type II (Hunter syndrome). *Eur. Rev. Med. Pharmacol. Sci.* 15, 253–258.

Patel, D. A., Harocopos, G. J., Chang, S.-H., Vora, S. C., Lubniewski, A. J., and Huang, A. J. W. (2011). Novel CHST6 gene mutations in 2 unrelated cases of macular corneal dystrophy. *Cornea* 30, 664–669. doi: 10.1097/ICO.0b013e3182012888

Patel, V. N., Pineda, D. L., and Hoffman, M. P. (2017). The function of heparan sulfate during branching morphogenesis. *Matrix Biol. J. Int. Soc. Matrix Biol.* 57–58, 311–323. doi: 10.1016/j.matbio.2016.09.004

Pellegata, N. S., Dieguez-Lucena, J. L., Joensuu, T., Lau, S., Montgomery, K. T., Krahe, R., et al. (2000). Mutations in KERA, encoding keratocan, cause cornea plana. *Nat. Genet.* 25, 91–95. doi: 10.1038/75664

Penc, S. F., Pomahac, B., Winkler, T., Dorschner, R. A., Eriksson, E., Herndon, M., et al. (1998). Dermatan sulfate released after injury is a potent promoter of fibroblast growth factor-2 function. *J. Biol. Chem.* 273, 28116–28121. doi: 10.1074/jbc.273.43.28116

Pinto-Fraga, J., López-de la Rosa, A., Blázquez, A. F., Urbano, R. R., and González-García, M. J. (2017). Efficacy and safety of 0.2% hyaluronic Acid in the management of dry eye disease. *Eye Contact Lens* 43, 57–63. doi: 10.1097/ICL.0000000000000236

Plaas, A. H., West, L. A., Thonar, E. J. A., Karcioglu, Z. A., Smith, C. J., Klintworth, G. K., et al. (2001). Altered fine structures of corneal and skeletal keratan sulfate and chondroitin/dermatan sulfate in macular corneal dystrophy. *J. Biol. Chem.* 276, 39788–39796. doi: 10.1074/jbc.M103227200

Poulain, F. E. (2015). Analyzing the role of heparan sulfate proteoglycans in axon guidance in vivo in zebrafish. *Methods Mol. Biol. Clifton N. J.* 1229, 469–482. doi: 10.1007/978-1-4939-1714-3_36

Poulain, F. E., and Yost, H. J. (2015). Heparan sulfate proteoglycans: a sugar code for vertebrate development? *Dev. Camb. Engl.* 142, 3456–3467. doi: 10.1242/dev.098178

Pudełko, A., Wisowski, G., Olczyk, K., and Koźma, E. M. (2019). The dual role of the glycosaminoglycan chondroitin−6−sulfate in the development, progression and metastasis of cancer. *Febs J.* 286, 1815–1837. doi: 10.1111/febs.14748

Qu, X., Carbe, C., Tao, C., Powers, A., Lawrence, R., van Kuppevelt, T. H., et al. (2011). Lacrimal gland development and Fgf10-Fgfr2b signaling are controlled by 2-O- and 6-O-sulfated heparan sulfate. *J. Biol. Chem.* 286, 14435–14444. doi: 10.1074/jbc.M111.225003

Quantock, A. J., and Young, R. D. (2008). Development of the corneal stroma, and the collagen–proteoglycan associations that help define its structure and function. *Dev. Dyn.* 237, 2607–2621. doi: 10.1002/dvdy.21579

Quantock, A. J., Young, R. D., and Akama, T. O. (2010). Structural and biochemical aspects of keratan sulphate in the cornea. *Cell Mol. Life Sci. CMLS* 67, 891–906. doi: 10.1007/s00018-009-0228-7

Rabinowitz, Y. S. (1998). Keratoconus. *Surv. Ophthalmol.* 42, 297–319. doi: 10.1016/S0039-6257(97)00119-7

Radulescu, A., Zhang, H.-Y., Chen, C.-L., Chen, Y., Zhou, Y., Yu, X., et al. (2011). Heparin-binding EGF-like growth factor promotes intestinal anastomotic healing. *J. Surg. Res.* 171, 540–550. doi: 10.1016/j.jss.2010.06.036

Regmi, S. C., Samsom, M. L., Heynen, M. L., Jay, G. D., Sullivan, B. D., Srinivasan, S., et al. (2017). Degradation of proteoglycan 4/lubricin by cathepsin S: potential mechanism for diminished ocular surface lubrication in Sjögren's syndrome. *Exp. Eye Res.* 161, 1–9. doi: 10.1016/j.exer.2017.05.006

Rødahl, E., Van Ginderdeuren, R., Knappskog, P. M., Bredrup, C., and Boman, H. (2006). A second decorin frame shift mutation in a family with congenital

stromal corneal dystrophy. *Am. J. Ophthalmol.* 142, 520–521. doi: 10.1016/j.ajo.2006.03.064

Rohrbach, M., and Clarke, J. T. R. (2007). Treatment of lysosomal storage disorders? progress with enzyme replacement therapy. *Drugs* 67, 2697–2716. doi: 10.2165/00003495-200767180-00005

Rossi, M., Morita, H., Sormunen, R., Airenne, S., Kreivi, M., Wang, L., et al. (2003). Heparan sulfate chains of perlecan are indispensable in the lens capsule but not in the kidney. *EMBO J.* 22, 236–245. doi: 10.1093/emboj/cdg019

Rozario, T., and DeSimone, D. W. (2010). The extracellular matrix in development and morphogenesis: a dynamic view. *Dev. Biol.* 341, 126–140. doi: 10.1016/j.ydbio.2009.10.026

Saika, S., Okada, Y., Miyamoto, T., Yamanaka, O., Ohnishi, Y., Ooshima, A., et al. (2004). Role of p38 MAP kinase in regulation of cell migration and proliferation in healing corneal epithelium. *Invest. Ophthalmol. Vis. Sci.* 45, 100–109. doi: 10.1167/iovs.03-0700

Saika, S., Shiraishi, A., Saika, S., Liu, C.-Y., Funderburgh, J. L., Kao, C. W.-C., et al. (2000). Role of Lumican in the Corneal Epithelium during Wound Healing. *J. Biol. Chem.* 275, 2607–2612. doi: 10.1074/jbc.275.4.2607

Saikia, P., Thangavadivel, S., Medeiros, C. S., Lassance, L., de Oliveira, R. C., and Wilson, S. E. (2018). IL-1 and TGF-β modulation of epithelial basement membrane components perlecan and nidogen production by corneal stromal cells. *Invest. Ophthalmol. Vis. Sci.* 59, 5589–5598. doi: 10.1167/iovs.18-25202

Sakimoto, T., Kim, T., Ellenberg, D., Fukai, N., Jain, S., Azar, D. T., et al. (2008). Collagen XVIII and Corneal Reinnervation Following Keratectomy. *FEBS Lett.* 582, 3674–3680. doi: 10.1016/j.febslet.2008.09.052

Salwowska, N. M., Bebenek, K. A., Żądło, D. A., and Wcisło-Dziadecka, D. L. (2016). Physiochemical properties and application of hyaluronic acid: a systematic review. *J. Cosmet. Dermatol.* 15, 520–526. doi: 10.1111/jocd.12237

Santander, C., and Brandan, E. (2006). Betaglycan induces TGF-β signaling in a ligand-independent manner, through activation of the p38 pathway. *Cell Signal* 18, 1482–1491. doi: 10.1016/j.cellsig.2005.11.011

Sarkar, A., Yu, W., Desai, U. R., MacKerell, A. D., and Mosier, P. D. (2016). Estimating glycosaminoglycan–protein interaction affinity: water dominates the specific antithrombin–heparin interaction. *Glycobiology* 26, 1041–1047. doi: 10.1093/glycob/cww073

Schlötzer-Schrehardt, U., Dietrich, T., Saito, K., Sorokin, L., Sasaki, T., Paulsson, M., et al. (2007). Characterization of extracellular matrix components in the limbal epithelial stem cell compartment. *Exp. Eye Res.* 85, 845–860. doi: 10.1016/j.exer.2007.08.020

Schmidt, T. A., Sullivan, D. A., Knop, E., Richards, S. M., Knop, N., Liu, S., et al. (2013). Transcription, translation, and function of lubricin, a boundary lubricant, at the ocular surface. *JAMA Ophthalmol.* 131:2385. doi: 10.1001/jamaophthalmol.2013.2385

Schwertfeger, K. L., Cowman, M. K., Telmer, P. G., Turley, E. A., and McCarthy, J. B. (2015). Hyaluronan, Inflammation, and Breast Cancer Progression. *Front. Immunol.* 6:236. doi: 10.3389/fimmu.2015.00236

Sen, S., Meteoglu, I., Ogurlu, M., Sen, S., Derincegoz, O. O., Derinceoz, O. O., et al. (2009). Topical heparin: a promising agent for the prevention of tracheal stenosis in airway surgery. *J. Surg. Res.* 157, e23–e29. doi: 10.1016/j.jss.2009.01.028

Sher, I., Zisman-Rozen, S., Eliahu, L., Whitelock, J. M., Maas-Szabowski, N., Yamada, Y., et al. (2006). Targeting perlecan in human keratinocytes reveals novel roles for perlecan in epidermal formation. *J. Biol. Chem.* 281, 5178–5187. doi: 10.1074/jbc.M509500200

Silver, D. J., Siebzehnrubl, F. A., Schildts, M. J., Yachnis, A. T., Smith, G. M., Smith, A. A., et al. (2013). Chondroitin sulfate proteoglycans potently inhibit invasion and serve as a central organizer of the brain tumor microenvironment. *J. Neurosci.* 33, 15603–15617. doi: 10.1523/JNEUROSCI.3004-12.2013

Silver, D. J., and Silver, J. (2014). Contributions of Chondroitin Sulfate Proteoglycans to Neurodevelopment, Injury, and Cancer. *Curr. Opin. Neurobiol.* 0, 171–178. doi: 10.1016/j.conb.2014.03.016

Smith, P. D., Coulson-Thomas, V. J., Foscarin, S., Kwok, J. C. F., and Fawcett, J. W. (2015). "GAG-ing with the neuron": the role of glycosaminoglycan patterning in the central nervous system. *Exp. Neurol.* 274, 100–114. doi: 10.1016/j.expneurol.2015.08.004

Smith, S., and Hassell, J. R. (2006). Focus on molecules: perlecan (HSPG2). *Exp. Eye Res.* 83, 471–472. doi: 10.1016/j.exer.2005.11.015

Ständer, M., Naumann, U., Wick, W., and Weller, M. (1999). Transforming growth factor-β and p-21: multiple molecular targets of decorin-mediated suppression of neoplastic growth. *Cell Tissue Res.* 296, 221–227. doi: 10.1007/s004410051283

Stepp, M. A., Daley, W. P., Bernstein, A. M., Pal-Ghosh, S., Tadvalkar, G., Shashurin, A., et al. (2010). Syndecan-1 regulates cell migration and fibronectin fibril assembly. *Exp. Cell Res.* 316, 2322–2339. doi: 10.1016/j.yexcr.2010.05.020

Stepp, M. A., Gibson, H. E., Gala, P. H., Iglesia, D. D. S., Pajoohesh-Ganji, A., Pal-Ghosh, S., et al. (2002). Defects in keratinocyte activation during wound healing in the syndecan-1-deficient mouse. *J. Cell Sci.* 115, 4517–4531. doi: 10.1242/jcs.00128

Stetefeld, J., Alexandrescu, A. T., Maciejewski, M. W., Jenny, M., Rathgeb-Szabo, K., Schulthess, T., et al. (2004). Modulation of agrin function by alternative splicing and Ca2+ binding. *Structure* 12, 503–515. doi: 10.1016/j.str.2004.02.001

Sugita, M., Hamano, M., Kasahara, K., Kikuchi, T., and Hirata, F. (2020). New protocol for predicting the ligand-binding site and mode based on the 3D-RISM/KH theory. *J. Chem. Theory Comput.* 16, 2864–2876. doi: 10.1021/acs.jctc.9b01069

Sultana, A., Sridhar, M. S., Klintworth, G. K., Balasubramanian, D., and Kannabiran, C. (2005). Allelic heterogeneity of the carbohydrate sulfotransferase-6 gene in patients with macular corneal dystrophy. *Clin. Genet.* 68, 454–460. doi: 10.1111/j.1399-0004.2005.00517.x

Sun, M., Puri, S., Mutoji, K. N., Coulson-Thomas, Y. M., Hascall, V. C., Jackson, D. G., et al. (2019). Hyaluronan derived from the limbus is a key regulator of corneal lymphangiogenesis. *Invest. Ophthalmol. Vis. Sci.* 60, 1050–1062. doi: 10.1167/iovs.18-25920

Sun, M., Puri, S., Parfitt, G. J., Mutoji, N., and Coulson-Thomas, V. J. (2018). Hyaluronan regulates eyelid and meibomian gland morphogenesis. *Invest. Ophthalmol. Vis. Sci.* 59, 3713–3727. doi: 10.1167/iovs.18-24292

Superti-Furga, A., Raghunath, M., and Willems, P. J. (1992). Deficiencies of fibrillin and decorin in fibroblast cultures of a patient with neonatal Marfan syndrome. *J. Med. Genet.* 29, 875–878. doi: 10.1136/jmg.29.12.875

Suzuki, M. (1939). Biochemical studies on carbohydratesl. Prosthetic group of corneamucoid. *J. Biochem. (Tokyo)* 30, 185–191. doi: 10.1093/oxfordjournals.jbchem.a125896

Tandon, A., Tovey, J. C. K., Sharma, A., Gupta, R., and Mohan, R. R. (2010). Role of transforming growth factor beta in corneal function, biology and pathology. *Curr. Mol. Med.* 10, 565–578. doi: 10.2174/1566524011009060565

Tasheva, E. S., Koester, A., Paulsen, A. Q., Garrett, A. S., Boyle, D. L., Davidson, H. J., et al. (2002). Mimecan/osteoglycin-deficient mice have collagen fibril abnormalities. *Mol. Vis.* 8, 407–415.

Thomas, V. J. C., Yamanaka, O., Yuan, Y., Gesteira, T. F., Liu, C.-Y., and Kao, W. (2012). Computational studies of potential binding sites for small leucine rich proteoglycan to growth factor receptors. *Invest. Ophthalmol. Vis. Sci.* 53, 4204–4204.

Toba, Y., Horie, M., Sango, K., Tokashiki, A., Matsui, F., Oohira, A., et al. (2002). Expression and immunohistochemical localization of heparan sulphate proteoglycan N-syndecan in the migratory pathway from the rat olfactory placode. *Eur. J. Neurosci.* 15, 1461–1473. doi: 10.1046/j.1460-9568.2002.01983.x

Toole, B. P., and Trelstad, R. L. (1971). Hyaluronate production and removal during corneal development in the chick. *Dev. Biol.* 26, 28–35. doi: 10.1016/0012-1606(71)90104-7

Torricelli, A. A. M., Marino, G. K., Santhanam, A., Wu, J., Singh, A., and Wilson, S. E. (2015). Epithelial basement membrane proteins perlecan and nidogen-2 are up-regulated in stromal cells after epithelial injury in human corneas. *Exp. Eye Res.* 134, 33–38. doi: 10.1016/j.exer.2015.03.016

Torricelli, A. A. M., Santhanam, A., Wu, J., Singh, V., and Wilson, S. E. (2016). The corneal fibrosis response to epithelial-stromal injury. *Exp. Eye Res.* 142, 110–118. doi: 10.1016/j.exer.2014.09.012

Torricelli, A. A. M., and Wilson, S. E. (2014). Cellular and extracellular matrix modulation of corneal stromal opacity. *Exp. Eye Res.* 0, 151–160. doi: 10.1016/j.exer.2014.09.013

Vance, M., Llanga, T., Bennett, W., Woodard, K., Murlidharan, G., Chungfat, N., et al. (2016). AAV gene therapy for MPS1-associated corneal blindness. *Sci. Rep.* 6:22131. doi: 10.1038/srep22131

Varki, A., Cummings, R., Esko, J., Freeze, H., Hart, G., and Marth, J. (1999). *Proteoglycans and Glycosaminoglycans*. New York, NY: Cold Spring Harbor Laboratory Press.

Veugelers, M., Cat, B. D., Ceulemans, H., Bruystens, A.-M., Coomans, C., Dürr, J., et al. (1999). Glypican-6, a new member of the glypican family of cell surface heparan sulfate proteoglycans. *J. Biol. Chem.* 274, 26968–26977. doi: 10.1074/jbc.274.38.26968

Vij, N., Roberts, L., Joyce, S., and Chakravarti, S. (2004). Lumican suppresses cell proliferation and aids Fas–Fas ligand mediated apoptosis: implications in the cornea. *Exp. Eye Res.* 78, 957–971. doi: 10.1016/j.exer.2003.12.006

Vij, N., Roberts, L., Joyce, S., and Chakravarti, S. (2005). Lumican regulates corneal inflammatory responses by modulating fas-fas ligand signaling. *Invest. Ophthalmol. Vis. Sci.* 46, 88–95. doi: 10.1167/iovs.04-0833

Vogler, C., Sands, M. S., Levy, B., Galvin, N., Birkenmeier, E. H., and Sly, W. S. (1996). Enzyme replacement with recombinant beta-glucuronidase in murine mucopolysaccharidosis type VII: impact of therapy during the first six weeks of life on subsequent lysosomal storage, growth, and survival. *Pediatr. Res.* 39, 1050–1054. doi: 10.1203/00006450-199606000-00019

Warshel, A., Sussman, F., and King, G. (1986). Free energy of charges in solvated proteins: microscopic calculations using a reversible charging process. *Biochemistry* 25, 8368–8372. doi: 10.1021/bi00374a006

Watanabe, H., Gao, L., Sugiyama, S., Doege, K., Kimata, K., and Yamada, Y. (1995). Mouse aggrecan, a large cartilage proteoglycan: protein sequence, gene structure and promoter sequence. *Biochem. J.* 308, 433–440. doi: 10.1042/bj3080433

Watanabe, H., Kimata, K., Line, S., Strong, D., Gao, L., Kozak, C. A., et al. (1994). Mouse cartilage matrix deficiency (cmd) caused by a 7 bp deletion in the aggrecan gene. *Nat. Genet.* 7, 154–157. doi: 10.1038/ng0694-154

Weber, I. T., Harrison, R. W., and Iozzo, R. V. (1996). Model structure of decorin and implications for collagen fibrillogenesis. *J. Biol. Chem.* 271, 31767–31770. doi: 10.1074/jbc.271.50.31767

Wilson, S. E. (2020). Corneal wound healing. *Exp. Eye Res.* 197:108089. doi: 10.1016/j.exer.2020.108089

Wilson, S. E., Mohan, R. R., Mohan, R. R., Ambrósio, R., Hong, J., and Lee, J. (2001). The corneal wound healing response: cytokine-mediated interaction of the epithelium, stroma, and inflammatory cells. *Prog. Retin. Eye Res.* 20, 625–637. doi: 10.1016/s1350-9462(01)00008-8

Woodward, A. M., Lehoux, S., Mantelli, F., Di Zazzo, A., Brockhausen, I., Bonini, S., et al. (2019). Inflammatory stress causes n-glycan processing deficiency in ocular autoimmune disease. *Am. J. Pathol.* 189, 283–294. doi: 10.1016/j.ajpath.2018.10.012

Wu, M., Downie, L. E., Grover, L. M., Moakes, R. J. A., Rauz, S., Logan, A., et al. (2020). The neuroregenerative effects of topical decorin on the injured mouse cornea. *J. Neuroinflammation* 17:1312. doi: 10.1186/s12974-020-01812-6

Xue, M., and Jackson, C. J. (2015). Extracellular matrix reorganization during wound healing and its impact on abnormal scarring. *Adv. Wound Care* 4, 119–136. doi: 10.1089/wound.2013.0485

Yamamoto, T., Otake, H., Hiramatsu, N., Yamamoto, N., Taga, A., and Nagai, N. (2018). A proteomic approach for understanding the mechanisms of delayed corneal wound healing in diabetic keratopathy using diabetic model rat. *Int. J. Mol. Sci.* 19:635. doi: 10.3390/ijms19113635

Yamanaka, O., Yuan, Y., Coulson-Thomas, V. J., Gesteira, T. F., Call, M. K., Zhang, Y., et al. (2013). Lumican binds ALK5 to promote epithelium wound healing. *PLoS One* 8:e82730. doi: 10.1371/journal.pone.0082730

Ying, S., Shiraishi, A., Kao, C. W.-C., Converse, R. L., Funderburgh, J. L., Swiergiel, J., et al. (1997). Characterization and expression of the mouse lumican gene. *J. Biol. Chem.* 272, 30306–30313. doi: 10.1074/jbc.272.48.30306

Young, M. F., Bi, Y., Ameye, L., and Chen, X.-D. (2002). Biglycan knockout mice: new models for musculoskeletal diseases. *Glycoconj. J.* 19, 257–262. doi: 10.1023/A:1025336114352

Young, R. D., Gealy, E. C., Liles, M., Caterson, B., Ralphs, J. R., and Quantock, A. J. (2007). Keratan sulfate glycosaminoglycan and the association with collagen fibrils in rudimentary lamellae in the developing avian cornea. *Invest. Ophthalmol. Vis. Sci.* 48, 3083–3088. doi: 10.1167/iovs.06-1323

Zatterstrom, U. K., Felbor, U., Fukai, N., and Olsen, B. R. (2000). Collagen XVIII/endostatin structure and functional role in angiogenesis. *Cell Struct. Funct.* 25, 97–101. doi: 10.1247/csf.25.97

Zhang, C., Turton, Q. M., Mackinnon, S., Sulik, K. K., and Cole, G. J. (2011). Agrin function associated with ocular development is a target of ethanol exposure in embryonic zebrafish. *Birt. Defects Res. A. Clin. Mol. Teratol.* 91, 129–141. doi: 10.1002/bdra.20766

Zhang, G., Chen, S., Goldoni, S., Calder, B. W., Simpson, H. C., Owens, R. T., et al. (2009). Genetic evidence for the coordinated regulation of collagen fibrillogenesis in the cornea by decorin and biglycan. *J. Biol. Chem.* 284, 8888–8897. doi: 10.1074/jbc.M806590200

Zhang, Y., Kao, W. W.-Y., Hayashi, Y., Zhang, L., Call, M., Dong, F., et al. (2017). Generation and characterization of a novel mouse line, keratocan-rtta (kerart), for corneal stroma and tendon research. *Invest. Ophthalmol. Vis. Sci.* 58, 4800–4808. doi: 10.1167/iovs.17-22661

Zheng, Z., Yu, Y., Wu, Y., Zheng, Z., Lin, Q., Liu, M., et al. (2020). [A real-world study of low molecular weight heparin sodium in the treatment of severe and critical bite by Trimeresurus stejnegeri]. *Zhonghua. Wei. Zhong. Bing Ji. Jiu Yi. Xue.* 32, 601–604. doi: 10.3760/cma.j.cn121430-20200204-00166

Zimmermann, D. R., and Ruoslahti, E. (1989). Multiple domains of the large fibroblast proteoglycan, versican. *EMBO J.* 8, 2975–2981. doi: 10.1002/j.1460-2075.1989.tb08447.x

Conflict of Interest: TG is the co-founder and was employed by Optimvia, LLC.

The remaining authors declare that the research was conducted in the absence of any commercial or financial relationships that could be construed as a potential conflict of interest.

frontiers in Cell and Developmental Biology

REVIEW
published: 26 August 2020
doi: 10.3389/fcell.2020.00749

The Role of Proteoglycans in Cancer Metastasis and Circulating Tumor Cell Analysis

*Theresa D. Ahrens[1], Sara R. Bang-Christensen[1,2], Amalie M. Jørgensen[2], Caroline Løppke[1], Charlotte B. Spliid[1,3], Nicolai T. Sand[1], Thomas M. Clausen[1,3], Ali Salanti[1] and Mette Ø. Agerbæk[1,2]**

[1] Centre for Medical Parasitology at Department of Immunology and Microbiology, Faculty of Health and Medical Sciences, University of Copenhagen and Department of Infectious Diseases, Copenhagen University Hospital, Copenhagen, Denmark, [2] VarCT Diagnostics, Copenhagen, Denmark, [3] Department of Cellular and Molecular Medicine, University of California, San Diego, La Jolla, CA, United States

OPEN ACCESS

Edited by:
Larisa M. Haupt,
Queensland University of Technology, Australia

Reviewed by:
Chiara Nicolazzo,
Sapienza University of Rome, Italy
Wei-Hsiung Yang,
Mercer University, United States
Nikolas Hendrik Stoecklein,
University Hospital Düsseldorf, Germany

***Correspondence:**
Mette Ø. Agerbæk
mettea@sund.ku.dk

Specialty section:
This article was submitted to Signaling, a section of the journal Frontiers in Cell and Developmental Biology

Received: 07 May 2020
Accepted: 17 July 2020
Published: 26 August 2020

Citation:
Ahrens TD, Bang-Christensen SR, Jørgensen AM, Løppke C, Spliid CB, Sand NT, Clausen TM, Salanti A and Agerbæk MØ (2020) The Role of Proteoglycans in Cancer Metastasis and Circulating Tumor Cell Analysis. Front. Cell Dev. Biol. 8:749. doi: 10.3389/fcell.2020.00749

Circulating tumor cells (CTCs) are accessible by liquid biopsies via an easy blood draw. They represent not only the primary tumor site, but also potential metastatic lesions, and could thus be an attractive supplement for cancer diagnostics. However, the analysis of rare CTCs in billions of normal blood cells is still technically challenging and novel specific CTC markers are needed. The formation of metastasis is a complex process supported by numerous molecular alterations, and thus novel CTC markers might be found by focusing on this process. One example of this is specific changes in the cancer cell glycocalyx, which is a network on the cell surface composed of carbohydrate structures. Proteoglycans are important glycocalyx components and consist of a protein core and covalently attached long glycosaminoglycan chains. A few CTC assays have already utilized proteoglycans for both enrichment and analysis of CTCs. Nonetheless, the biological function of proteoglycans on clinical CTCs has not been studied in detail so far. Therefore, the present review describes proteoglycan functions during the metastatic cascade to highlight their importance to CTCs. We also outline current approaches for CTC assays based on targeting proteoglycans by their protein cores or their glycosaminoglycan chains. Lastly, we briefly discuss important technical aspects, which should be considered for studying proteoglycans.

Keywords: cancer, circulating tumor cells, diagnostic, glycosaminoglycan, liquid biopsy, metastasis, proteoglycan, VAR2CSA

INTRODUCTION

During cancer progression, metastatic spread occurs when cancer cells disseminate from the primary tumor and travel to a distant site to form a metastasis (Micalizzi et al., 2017). This can emerge through three major routes: the blood circulation, the lymphatic system, or via serosal or mucosal surfaces (Fidler, 1978). However, cancer cell dissemination through the blood is thought to be the main route of metastasis (Lambert et al., 2017), and the subset of cancer cells that have entered the blood circulation is named circulating tumor cells (CTCs). Intravasation of CTCs into the blood stream is believed to be one of the rate-limiting steps for metastasis formation and can occur through either an active invasion or passive shedding of cells from the tumor

(Cavallaro and Christofori, 2001; Bockhorn et al., 2007; van Zijl et al., 2011). Only a minority of cancer cells reaching the blood circulation manages to survive shear stress, escape immune surveillance, avoid detachment-induced cell death, extravasate at the distant site, and finally establish a metastasis (Massague and Obenauf, 2016). Thus, the process of metastasis is both a complex and inefficient process (van Zijl et al., 2011; Reymond et al., 2013).

In addition to representing the primary tumor, CTCs have also been shown to exit from metastatic lesions (Kim et al., 2009). Such cells have the potential to travel back to the primary tumor site (called tumor self-seeding) or create another metastasis (Mentis et al., 2020). Therefore, CTCs could represent both the primary tumor and potential metastatic lesions (Kim et al., 2009), making CTC analyses highly relevant even years after surgical removal of the primary tumor. Hence, CTC analyses could provide important information about disease progression and relapse. Furthermore, molecular analyses of CTCs including mutational profiling, could provide the basis for personalized therapies in the future (Greene et al., 2012). Thus, CTCs are currently evaluated for clinical diagnostics. However, CTC analysis remains technically challenging, not only due to the rarity of CTCs among billions of normal blood cells, but also due to their inherent high degree of cellular plasticity complicating the choice of detection markers (Alix-Panabieres et al., 2017). Accordingly, CTC enrichment and detection strategies must be based on highly specific biomarkers to achieve the necessary assay specificity and sensitivity. Moreover, targeting a broader CTC population would be beneficial to ensure that the liquid biopsy better reflects the heterogenic cancer cell population.

As a part of discovering novel CTC targets, many strategies focus on proteins known to play an active role in metastatic seeding. Although solid tumors differ in their metastatic patterns, they share certain mechanistic similarities for metastasis formation, which are summarized as the metastatic cascade (**Figure 1**) (de Groot et al., 2017; Lambert et al., 2017; Riggi et al., 2018). Notably, the majority of steps in this process concerns the interaction between the cancer cells and the surrounding extracellular matrix (ECM). Therefore, novel clinically relevant CTC targets may be discovered within the pericellular layer called the glycocalyx.

The glycocalyx is a thick network of carbohydrates bound to glycoproteins, glycolipids, and proteoglycans (**Figure 2A**; reused from Okada et al., 2017). It is present on cell surfaces throughout the entire human body and constitutes a physical barrier between the cell and the surrounding microenvironment (Tarbell and Cancel, 2016). The glycocalyx plays a crucial role for receptor–ligand interactions of cancer cells and their surroundings, enabling migration as well as intra- and extravasation. Furthermore, the composition of the glycocalyx is thought to influence the transportation and survival of CTCs in the bloodstream (Mitchell and King, 2014). However, very few studies have investigated the glycocalyx of CTCs. At present, it is best studied in endothelial cells, where it serves as a physical and electrostatic barrier as well as a mechanotransducer toward other cells, the extracellular matrix (ECM), or shear forces of the blood (Reitsma et al., 2007; Butler and Bhatnagar, 2019). To convey signaling, growth factors, chemokines, and other interaction partners have to navigate through this dense structure. The glycocalyx, which extends beyond the length of most surface receptors, has a dual role in signaling by creating a physical hindrance for ligand receptor interactions or by promoting binding once interaction partners are in close proximity to each other (Kuo et al., 2018). Moreover, certain glycocalyx components are involved in chemokine storage and oligomerization, which strongly modulates their signaling strength (Salanga and Handel, 2011). Therefore, glycocalyx changes can have various effects on cellular behavior and, not surprisingly, cancer cells show specific alterations in their glycocalyx.

The cancer cell glycocalyx is a highly dynamic structure from which most of the components have been linked to the acquisition of oncogenic phenotypes (Daniotti et al., 2015; Buffone and Weaver, 2020). For instance, aberrant glycosylations including hypersialylation support immune evasion mechanisms (Pearce and Läubli, 2016). Moreover, increased expression of bulky glycoproteins like mucin-1 has been linked to aggressive cancers (Paszek et al., 2014; Barnes et al., 2018) and associated with poor survival outcome in patients (Kufe, 2009). This might be explained by the bulkiness of the mucin-1 ectodomain shaped by numerous glycosylations, which facilitates integrin clustering, cell signaling, and cell proliferation (Paszek et al., 2014; Woods et al., 2017; Kuo et al., 2018). Naturally, mucin-1 is of interest as a target for therapy (Pillai et al., 2015), due to its high involvement in cancer. Likewise, CTCs were found to express high mucin-1 levels (Paszek et al., 2014), and mucin-1 has also been explored for CTC capture and detection (Muller et al., 2012; Strati et al., 2013; Schehr et al., 2016).

Another important component of the glycocalyx are proteoglycans (**Figure 2B**) with multiple implications in metastatic dissemination of cancer cells and tumor cell growth (Iozzo and Sanderson, 2011; Vitale et al., 2019). Proteoglycans can be secreted into the ECM or located intracellularly as well as on the cell surface either directly embedded in the plasma membrane or anchored by a glycosylphosphatidylinositol (GPI)-linker (Iozzo and Schaefer, 2015). Proteoglycans consist of two functional units: protein core and glycosaminoglycan (GAG) chains (Walimbe and Panitch, 2019). Most commonly, the assembly of GAG chains occur from a tetrasaccharide linker region covalently attached to serine residues within the protein core (Esko and Zhang, 1996). The GAG family is classified by their chemical composition and includes chondroitin sulfate (CS), dermatan sulfate (DS), keratan sulfate (KS), heparan sulfate (HS), and hyaluronic acid (HA) (**Figures 2C,D**) (Toole, 2004; Bulow and Hobert, 2006). In general, GAGs consist of long linear repeats of disaccharide units consisting of hexuronic acids and hexosamines. The hexuronic acid epimers comprise D-glucuronic acid (GlcA) for CS/HA and L-iduronic acid (IdoA) for DS, whereas the hexosamine units consist of an *N*-acetyl-D-glucosamine (GlcNAc) for HS/KS/HA, and an *N*-acetyl-D-galactosamine (GalNAc) for CS/DS (Schaefer and Schaefer, 2010; Ghiselli and Maccarana, 2016; Pomin and Mulloy, 2018). The structures of GAGs are extremely diverse, as their synthesis in the Golgi apparatus is not based on a precise

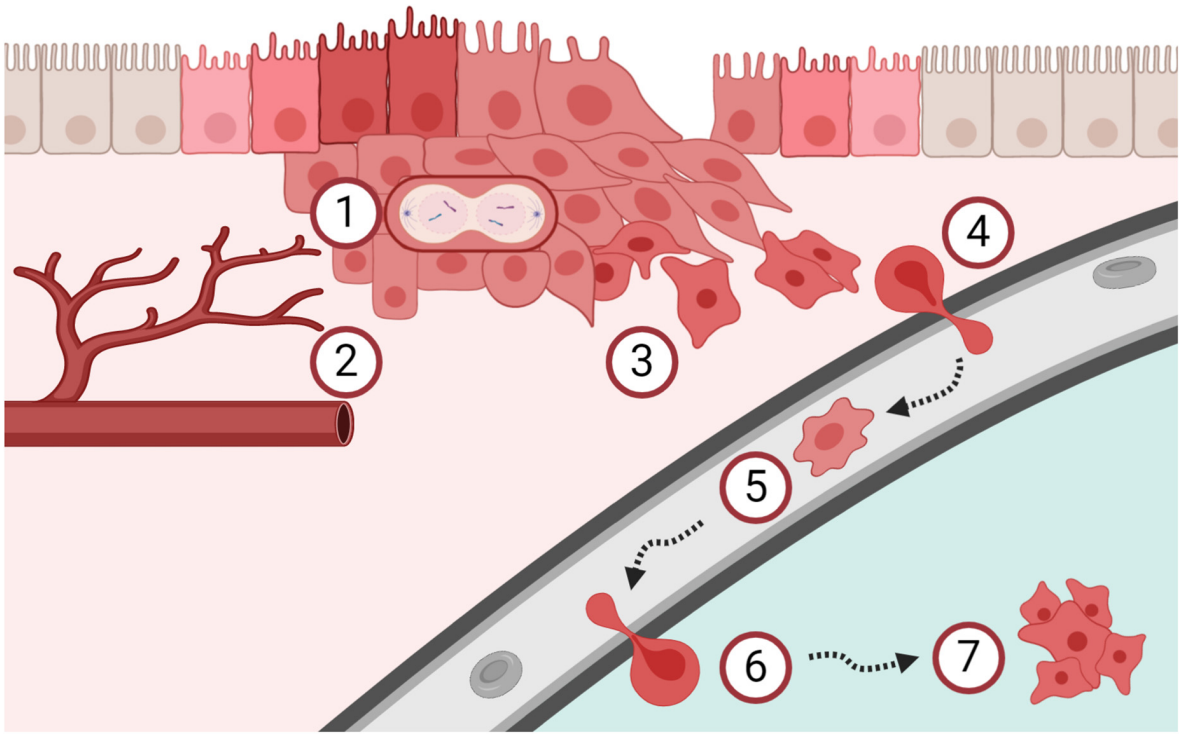

FIGURE 1 | Schematic overview of the metastatic cascade. **(1)** Cancer cells start to proliferate uncontrolled and **(2)** tumor angiogenesis is mandatory to support continued tumor growth, already early during carcinogenesis. **(3)** The process of epithelial-mesenchymal transition increases the migration and invasion capacity of cancer cells. **(4)** Cancer cells intravasate into the blood circulation and **(5)** are then called circulating tumor cells (CTCs). CTCs are easily accessible by liquid biopsies and are currently investigated as tool for cancer diagnostics and surveillance. **(6)** A subpopulation of these CTCs has the potential to extravasate and **(7)** form metastasis in secondary organs. Clearly, the metastatic process is very complex and many of these steps are interconnected. Please refer to the main text for details and references.

template, but on a redundant network of enzymes that seems to be regulated based on tissue and cell types (Dick et al., 2012; Mikami and Kitagawa, 2013; Chen Y. H. et al., 2018).

Besides the variation in the monosaccharide composition, the molecular diversity of GAGs also results from varying polymer lengths and extensive post-translational modifications such as sulfations and epimerizations along the chain (Bulow and Hobert, 2006). GAG sulfation patterns often determine their biological function and serve as specific recognition motifs for a wide variety of growth factors, cytokines, chemokines, and pathogens (Xu and Esko, 2014; Mizumoto et al., 2015; Pinho and Reis, 2015). Therefore, alterations in the GAG composition of proteoglycans in cancers have received a lot of interest (Sweet et al., 1976; Chandrasekaran and Davidson, 1979; De Klerk et al., 1984). A well-studied example is the change in sulfation patterns of GAGs, which likely depends on the specific cancer type. Some studies have reported high expression of CS 4-*O*-sulfotransferases in both ovarian and breast cancers, while a study on cancerous lung tissues found elevated 6-*O*-sulfated CS, compared to nonmalignant tissue (Cooney et al., 2011; Oliveira-Ferrer et al., 2015; Li et al., 2017). Similarly, various HS sulfotransferases have been found upregulated in different cancers. These include 6-*O*-sulfotransferases in ovarian and colorectal cancer; 3-*O*-sulfotransferases in breast and pancreatic cancer; along with *N*-deacetylase and *N*-sulfotransferases in hepatocellular carcinomas (Tatrai et al., 2010; Song et al., 2011; Hatabe et al., 2013; Cole et al., 2014; Vijaya Kumar et al., 2014). Moreover, several studies have reported increases in CS quantity or in expression of CS polymerization genes in malignant tissues, suggesting that CS polymers are pro-tumorigenic (Momose et al., 2016; Li et al., 2017; Hou et al., 2019).

Interestingly, some proteoglycans may be modified with different GAG types simultaneously, as seen for syndecans, which can carry both CS/DS and HS, dependent on the structure of the ectodomain (Kokenyesi and Bernfield, 1994; Iozzo and Schaefer, 2015). Similarly, the HA-binding proteoglycan, versican, undergoes alternative splicing of exons encoding the GAG-attachment region resulting in altered GAG display. Notably, expression of distinct versican isotypes was shown to facilitate cancer progression in multiple cancer types (Dours-Zimmermann and Zimmermann, 1994; Theocharis et al., 2015; Zhangyuan et al., 2020). The protein cores of proteoglycans are, however, not just scaffolds for GAG extension, since they also directly bind ligands and mediate intracellular signaling in GAG-independent manners.

In contrast to the rest of the GAGs, HA stands out by not being covalently attached to a protein core (**Figures 2B,D**). Instead, HA is synthesized as an unmodified polysaccharide

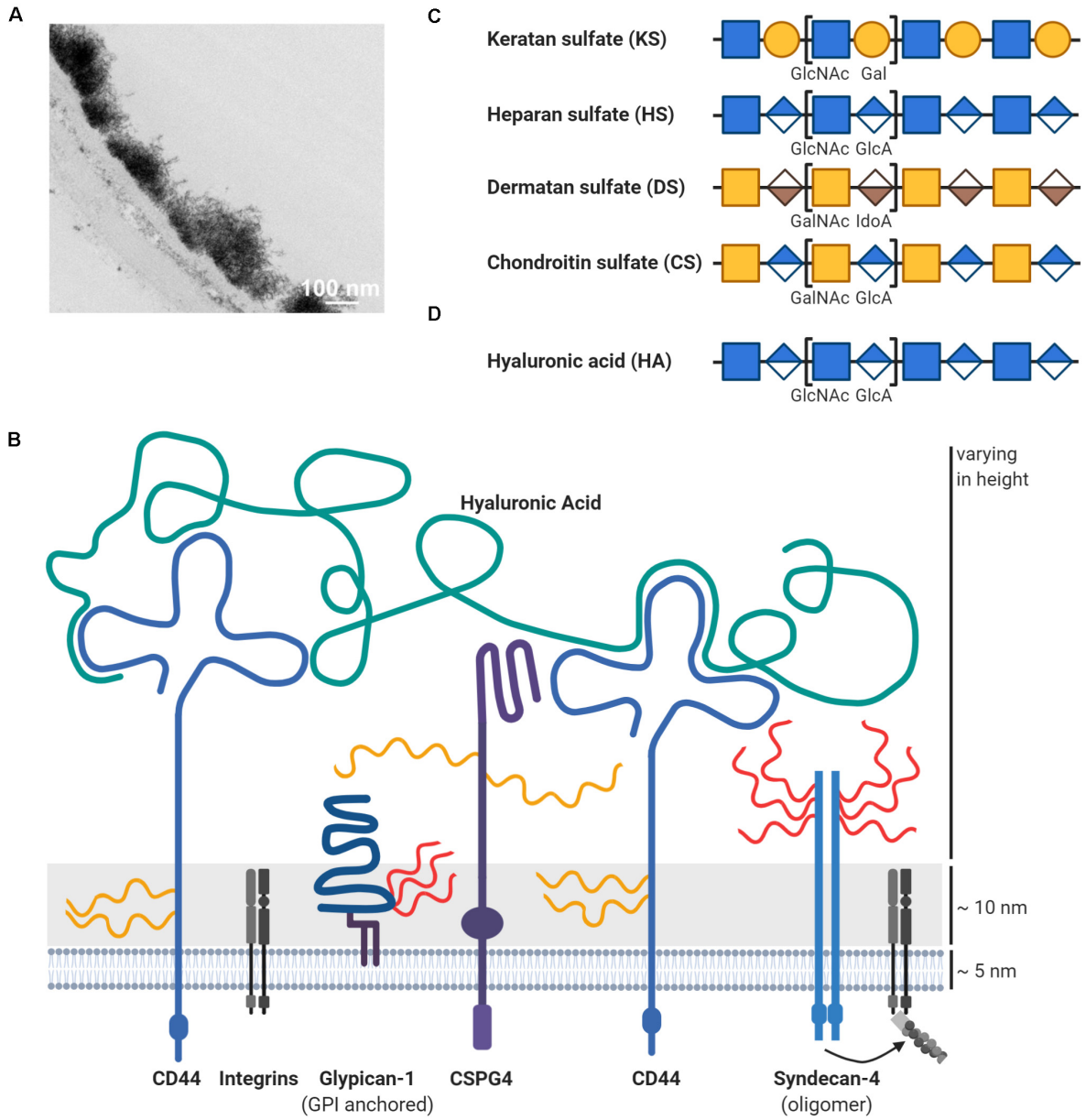

FIGURE 2 | Schematic overview of proteoglycans in the glycocalyx. **(A)** The glycocalyx is a dense network of carbohydrates on the cell surface, here exemplified on top of the endothelium. This transmission electron microscopic image with lanthanum nitrate staining was reused from Okada et al. (2017) under CC BY 4.0 license. **(B)** The thick carbohydrate layer on the cell surface extends beyond the length of membrane proteins like integrins. One important glycocalyx component are proteoglycans, which consist of a protein core (blue) and covalently attached glycosaminoglycans such as heparan sulfate (HS; in red) or chondroitin sulfate (CS; in yellow). Depicted are some proteoglycans, which are mentioned and discussed throughout the review like chondroitin sulfate proteoglycan 4 (CSPG4). Hyaluronic acid (HA; in green) is another important glycosaminoglycan component in the glycocalyx, but is distinct through the lack of a protein core. Hyaluronic acid is attached to the cell surface via interactions with its receptors like CD44, which is itself a proteoglycan. Other glycocalyx components like glycoproteins are not shown due to abstractification. Depiction of the disaccharides units for **(C)** glycosaminoglycans attached to proteoglycans (keratan sulfate/KS, heparan sulfate/HS, dermatan sulfate/DS, and chondroitin sulfate/CS) and **(D)** of hyaluronic acid (HA), which is non-covalently attached to its receptors. Glycosaminoglycans can be subjected to further modifications, such as sulfation or epimerization, which is not shown for simplicity. Please refer to the main text for details and references.

at the plasma membrane, where it is extruded from the cell surface and cleaved off into the ECM (Weigel and DeAngelis, 2007; Itano, 2008). In most cells, HA is an abundant structural component of the glycocalyx, where it interacts with receptors and surface proteoglycans via their hyaluronan-binding motifs and regulates the viscosity of the glycocalyx by its ability to retain water (Toole, 2001, 2004). Upon binding, HA triggers activation of a range of signaling pathways involved in cell proliferation, differentiation, motility, and adhesion, thereby influencing processes such as development, tissue homeostasis,

and carcinogenesis (Turley et al., 2002; Toole, 2004; Liu et al., 2019). Although HA is extensively involved in cancer, it will not be discussed in detail throughout this review, as it is not considered a proteoglycan due to its lack of a protein core.

Altogether, proteoglycans compose a highly heterogeneous group of proteins that diverge by structural alterations of the protein core as well as by differences in their GAGs with regard to chain number, type, length, and post-translational modifications. Notably, proteoglycans are important integrators for cell signaling events with direct implications for carcinogenesis and cancer progression (Iozzo and Sanderson, 2011; Pinho and Reis, 2015; Nikitovic et al., 2018). In spite of this, the functions of proteoglycans and their GAGs in relation to CTCs are currently understudied. Therefore, this review will highlight examples of proteoglycans involved in the metastatic cascade with potential links to CTC biology. More specifically, we will discuss how proteoglycans play active roles in cancer cell proliferation, migration, survival, plasticity, and invasion with a dedicated focus on the function of both the protein core and the GAG chains. Finally, we provide an overview of proteoglycans that are currently evaluated for CTC technologies and briefly highlight some of the technical aspects to consider when studying proteoglycans.

PROTEOGLYCANS IN THE METASTATIC CASCADE

Cancer Cell Proliferation

Cancers show deregulation of their cell proliferation by various mechanisms. Proteoglycans can influence cell growth by interacting with growth factors, either via their core proteins or through their GAG chains, as observed for HS chains of heparan sulfate proteoglycans (HSPGs) (Knelson et al., 2014). Enzymes modifying GAGs may hence influence tumor growth (Morla, 2019) as demonstrated by sulfatases interfering with growth factor signaling through HS desulfation (Ai et al., 2003; Peterson et al., 2010; Vicente et al., 2015).

However, proteoglycans also influence tumor growth by GAG–independent mechanisms. The transmembrane chondroitin sulfate proteoglycan 4 (CSPG4) has been shown to positively regulate cancer cell proliferation in various cancer entities (Wang et al., 2011; Jamil et al., 2016; Hsu et al., 2018) and is currently under investigation for CTC capture and identification, as described in detail later. Studies have found that CSPG4 is involved in growth signaling by interaction through both its cytoplasmic domain and ectodomain (Yang et al., 2009; Stallcup, 2017). Through the extracellular part, CSPG4 potentiates the mitogen-activated protein kinase (MAPK) cascade by high-affinity, largely GAG-independent binding of growth factors, which are thus likely presented to their cognate receptors by CSPG4 (Nishiyama et al., 1996; Goretzki et al., 1999; Stallcup, 2002; Price et al., 2011). In glioma cell models, phosphorylation of the cytoplasmic CSPG4 domain induced proliferation, which was mediated by interaction with integrins (Makagiansar et al., 2007; Stallcup, 2017). Furthermore, CSPG4-mediated activation of one of the same integrins induced chemoresistance and survival in tumor cells (Chekenya et al., 2008). Thus, CSPG4 is an example of a proteoglycan positively regulating growth and survival via its protein domain.

The proteoglycan glypican-3 (GPC3) has also been shown to increase cell proliferation. GPC3 influence several central signaling pathways in hepatocellular carcinoma (Kolluri and Ho, 2019) and is also evaluated for CTC capture as described later. GPC3 and other glypicans are GPI-anchored and known to carry HS chains (Filmus et al., 2008; Yoneda et al., 2012), but were also demonstrated to carry CS chains (Chen and Lander, 2001; Toledo et al., 2020). Their GAG chains are located close to the cell membrane due to their proximity to the C-terminus, which is thought to be critical for their interaction with surface receptors (Filmus et al., 2008). GPC3 overexpression increased cell proliferation *in vitro* and *in vivo* for liver cancer cells by enhancing Wnt signaling (**Figure 3**) (Capurro et al., 2005). Mutagenesis of the GAG attachment site in GPC3 revealed that

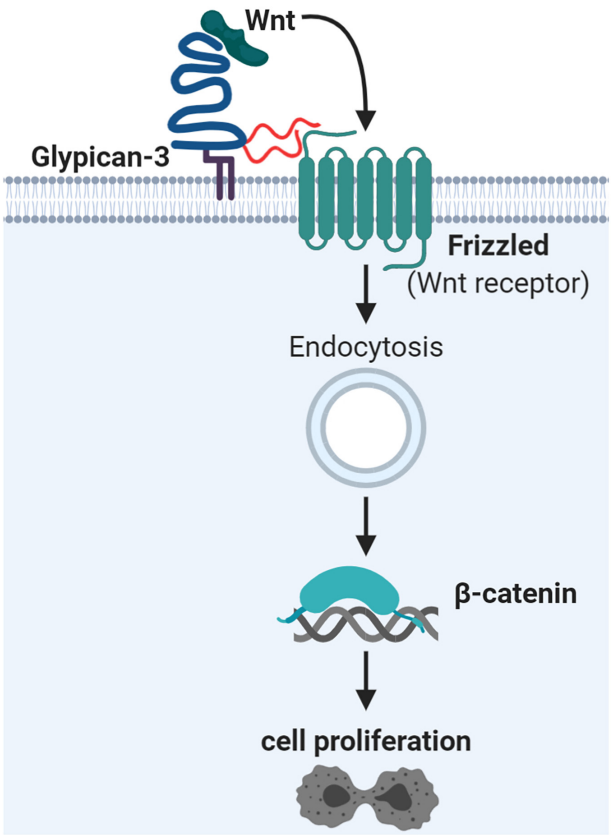

FIGURE 3 | Glypican-3 signaling supports Wnt signaling and hepatocellular proliferation. Glypican-3 (shown in blue) can carry two glycosaminoglycan chains of heparan sulfate (HS; in red) or chondroitin sulfate (CS; not shown). It has been determined that these glycosaminoglycan chains are essential for interaction with Frizzled proteins, the Wnt receptors, but not for Wnt ligand binding. The ternary complex of glypican-3, Frizzled, and Wnt ligand becomes endocytosed as part of canonical Wnt signaling. This leads to nuclear accumulation of β-catenin and subsequent gene expression changes, stimulating cell proliferation. Details and references are given in the main text.

the HS GAGs were not essential for binding of Wnt ligands (Capurro et al., 2005). Supporting this, the Wnt binding site on GPC3 has recently been located to a hydrophobic groove, which works independently of GAG chains (Li et al., 2019). However, the GAG chains of GPC3 are essential for direct interaction with the Wnt receptors, the Frizzled proteins (Capurro et al., 2014). Upon Wnt stimulation a ternary complex is formed and endocytosed (Capurro et al., 2014). Generally, endocytosis of Wnt signaling complexes seems to be important for canonical Wnt signaling with final stabilization and nuclear accumulation of β-catenin and subsequent gene expression changes (Brunt and Scholpp, 2018). In addition, this signaling axis could be a potential therapeutic target for hepatocellular carcinoma based on a monoclonal antibody recognizing the HS chains of GPC3 (Gao et al., 2014). Overall, it was suggested that GPC3 works as a bridging protein between Wnt and its receptor thereby inducing cell proliferation (Li et al., 2019). The exact interaction dependencies could rely on the expression levels of all three partners (Wnt ligands, Wnt receptors, and GPC3) (Li et al., 2019).

However, proteoglycans can also act as negative regulators of cancer biology. One example for this is decorin, which is modified with a single CS or DS side chain. Decorin can act as an inhibitor of cell proliferation by hampering growth signaling. This repression is thought to occur through growth factor sequestering as well as receptor internalization and degradation, mediated by binding to the decorin core protein (Jarvinen and Prince, 2015). For example, *de novo* expression of decorin in breast cancer cell lines suppressed proliferation and anchorage-independent growth (Santra et al., 2000). Consistently, 30% of decorin-knockout mice formed spontaneous intestinal tumors (Bi et al., 2008), highlighting its potential role as tumor suppressor.

To sum up, proteoglycans appear to have a multi-facetted and important role in cancer cell proliferation by diverse mechanisms, which can vary across different cancer types. When CTCs reach the metastatic site, they often go into an inactive dormancy state (Sosa et al., 2014). Reactivation of cell proliferation is therefore an important factor for establishment of clinically relevant metastatic lesions, in which proteoglycans are actively involved (Elgundi et al., 2019) and which will also be discussed later in more detail.

Angiogenesis in Cancer

Oxygen supply is essential for cells and their metabolism. *Ex vivo* measurement on xenografts revealed that oxygen perfuses only to around 100 μm deep into the tumor tissue (Olive et al., 1992). Therefore, cancer cells must secure sustained blood supply at an early stage, which can happen by different mechanisms (Xu et al., 2016; Lugano et al., 2020). Several proteoglycans are involved in the complex process of tumor angiogenesis (Iozzo and Sanderson, 2011; Chiodelli et al., 2015). Interestingly, increased vascularization could be observed already in premalignant lesions (Menakuru et al., 2008), possibly explaining how CTCs can be shed already from early stage cancers (Husemann et al., 2008; Stott et al., 2010; Rhim et al., 2012; Zhang et al., 2014; Tsai et al., 2016; Murlidhar et al., 2017). Studies on early cancer cell dissemination are of high clinical importance as it enables the use of CTCs in screening programs for early cancer detection.

One central molecule for angiogenesis is the vascular endothelial growth factor (VEGF) (Ferrara et al., 2003), which has been linked to different proteoglycans as for example biglycan. Cancer cells have been shown to overexpress biglycan (Zhu et al., 2013; Hu et al., 2014; Andrlova et al., 2017; Jacobsen et al., 2017), which has two potential GAG attachment sites carrying either CS or DS chains (Valiyaveettil et al., 2004). Interestingly, biglycan is a homolog of decorin (Fisher et al., 1989), but seems to have tumor promoting capacities by angiogenesis induction in contrast to decorin (Schaefer et al., 2017). Indeed, elevated biglycan levels induced higher density of blood vessels and increased tumor growth *in vivo* of colorectal cancer xenografts via induction of VEGF expression (Hu et al., 2016). In endothelial cells, biglycan binds to Toll-like receptor 2 (TLR2) and TLR4 with activation of the transcription factor family nuclear factor-κB (NFκB). This subsequently leads to increased levels of hypoxia-inducible factor 1-alpha (HIF1α), which drives VEGF expression (Hu et al., 2016) and could finally lead to tumor angiogenesis. VEGF can potentially regulate expression of another proteoglycan linked to cancer and angiogenesis, namely endocan (Grigoriu et al., 2006; Rennel et al., 2007; Roudnicky et al., 2013). Indeed, endocan was detected in the tumor vasculature (Maurage et al., 2009; Roudnicky et al., 2013) as well as in cancer cells (Rennel et al., 2007; Maurage et al., 2009; Xu et al., 2019). Interestingly, it was suggested by Rocha et al. (2014) that endocan binding replaced VEGF from fibronectin in the ECM, creating a positive feedback loop. In head and neck cancer, endocan was strongly co-expressed with angiopoietin-2 (Xu et al., 2019), which can regulate vascular permeability during intra- and extravasation processes (Garcia-Roman and Zentella-Dehesa, 2013) and potentially affect the dissemination of CTCs during metastasis. Importantly, endocan expression is associated with poor survival rate and might also be used as serum biomarker in cancer patients (Grigoriu et al., 2006; Roudnicky et al., 2013; Kim et al., 2018). Biglycan and endocan are important proteoglycans in angiogenesis and thus tumor progression. However, they might not be ideal candidates for CTC technologies as secreted proteoglycans might not be stable targets for cell analysis.

The neuropilins is another proteoglycan family involved in angiogenesis (Ellis, 2006; Niland and Eble, 2019). Neuropilin-1 helps to bind VEGF to the cell surface and forms a trimeric complex together with VEGF receptor 2 (VEGFR2), which was suggested to act as a potential bridge between cancer cells and endothelial cells (Soker et al., 1998, 2002). Indeed, neuropilin-1 was detected in tumor cells of different cancer entities as well as in endothelial cells of the tumor vasculature (Jubb et al., 2012). Overexpression of neuropilin-1 increased xenograft growth (Miao et al., 2000; Hu et al., 2007). Neuropilin-1 carries a single GAG chain of HS or CS, dependent on the cell type (Shintani et al., 2006; Frankel et al., 2008). However, the exact role of the GAG chain is not fully understood. Mutagenesis of the GAG attachment site in neuropilin-1 increased glioma cell invasion (Frankel et al., 2008). Interestingly, global removal of CS by chondroitinase ABC enzyme treatment led to decreased invasion in the same cells. Neuropilin-1 is also physiologically expressed

as a GAG-deficient splice variant (namely NRP1-Δ7), which attributes to 10–30% of total neuropilin-1 transcripts depending on cell type or tissue (Hendricks et al., 2016). Importantly, NRP1-Δ7 acted anti-tumorigenic and diminished tumor vascularization in prostate cancer xenografts *in vivo* (Hendricks et al., 2016). Moreover, soluble neuropilin-1 isoforms with anti-tumorigenic functions have been described, which block VEGFR signaling (Gagnon et al., 2000; Cackowski et al., 2004). Overexpression of soluble neuropilin-1 in cancer cells led to disturbed tumor vascularization and cancer cell apoptosis in xenografts (Gagnon et al., 2000). Overall, proteoglycans are connected to tumor angiogenesis and to VEGF signaling with various effects.

Epithelial-to-Mesenchymal Transition, Migration, and Intravasation

Another important milestone for cancer cells is to gain migratory capacities to leave the primary tumor and invade the surrounding tissue. During the gastrulation phase of embryogenesis, epithelial-to-mesenchymal transition (EMT) causes stationary epithelial cells to undergo major changes into motile mesenchymal-like cells in order to form new germ layers. Molecular changes in transcription factor networks and gene expression facilitate the loss of cell polarity and cytoskeletal reorganization, resulting in an increased migratory capacity (Lim and Thiery, 2012; Lamouille et al., 2014). Cancer cells imitate this developmental EMT program and several studies suggest that proteoglycans are actively involved in this part of cancer progression, thus supporting the relevance of proteoglycans as targets for CTC capture. Situated in the glycocalyx of cancer cells, proteoglycans provide a contact link between the cell membrane and the surrounding ECM, thereby playing a central role in regulating cancer cell adhesion and migration. Some proteoglycans are downregulated in order to enable detachment from the basement membrane facilitating invasion, others are shed from the surface as a different mode of regulation, and some maintain their function throughout the invasive phase. Importantly, the current standard for CTC isolation is based on antibodies against epithelial cell adhesion molecule (EpCAM), which is often downregulated during EMT (Gorges et al., 2012; Hyun et al., 2016). Thus, understanding the process of EMT in terms of proteoglycan regulation is important for their evaluation as alternative CTC-target candidates.

One important modulator of EMT processes is transforming growth factor β (TGFβ), which is known to drive progression of late state malignancies by promoting invasion (Akhurst and Derynck, 2001; Xu et al., 2009). Indeed, TGFβ regulates a multitude of genes with potential cancer-specific effects (Ranganathan et al., 2007; Kowli et al., 2013). Several proteoglycans are connected to TGFβ-signaling. An example of this is the expression of HS-carrying syndecan-4, which was positively regulated by TGFβ in lung cancer A549 cells (Toba-Ichihashi et al., 2016). Expression of this proteoglycan further induced upregulation of the EMT transcription factor zinc finger protein SNAI1 (sometimes referred to as snail) (Toba-Ichihashi et al., 2016), thereby fueling the migratory behavior. This is somewhat surprising, since syndecan-4 plays a well-established role in focal adhesion sites together with integrins, thereby promoting the adhesive phenotype of cancer cells (Echtermeyer et al., 1999; Saoncella et al., 1999).

Syndecan-1 can also be affected by TGFβ and was suggested as a poor prognostic factor in breast cancer (Hayashida et al., 2006; Nikitovic et al., 2014). Incubation of mouse mammary epithelial cells with TGFβ changed the GAG composition of syndecan-1 from being mainly HS modified to carry nearly equal amounts of HS and CS (Rapraeger, 1989). Notably, increased CS display was not only mediated by attachment of more GAG chains, but also by increased length of individual CS chains (**Figure 4**). This is in line with a later study showing that TGFβ induced expression of CS synthase 1, a key enzyme involved in the elongation of CS and DS GAG chains (Hu et al., 2015). In addition, other GAG polymer-modifying enzymes have been shown to be transcriptionally affected by TGFβ treatment (Tiedemann et al., 2005; Mohamed et al., 2019), suggesting a role of specific GAG modifications on proteoglycans in regulating the cellular response toward this cytokine.

TGFβ signaling is mediated through heteromeric complex formation of type I and type II receptors (Weiss and Attisano, 2013). However, co-receptors like type III TGFβ receptor, also known as betaglycan, can modulate ligand presentation to the type II receptor (**Figure 4**). Betaglycan is a cell membrane proteoglycan which may carry both CS and HS GAG chains (Cheifetz et al., 1988). Sulfated HS-modifications on betaglycan have been proven to sequester the Wnt3a ligand and thereby inhibiting proliferation by dampening Wnt signaling (Jenkins et al., 2016). In contrast, TGFβ binding is mediated by the protein core of the proteoglycan, and is therefore insensitive to point mutations disrupting the GAG-attachment sites (Lopez-Casillas et al., 1994). As any other membrane proteoglycan, betaglycan can undergo ectodomain shedding (Weiss and Attisano, 2013). A soluble form of the receptor was shown to result in reduced ligand availability due to its high-affinity interaction with TGFβ and thus decreased TGFβ signaling (Elderbroom et al., 2014). In line with this, it was shown that increased betaglycan expression decreased the invasive behavior of breast cancer cells *in vitro* in response to TGFβ stimulation and that this effect was abrogated when betaglycan was expressed in a shedding-impaired mutant form (Elderbroom et al., 2014). Importantly, metastatic lesions showed lower betaglycan expression compared to matched primary tumors (Hempel et al., 2007). In ovarian cancer cell lines this seems to be mediated through epigenetic silencing, as expression was restored upon epigenetic-acting drugs (Hempel et al., 2007). This indicates that betaglycan might be involved in the dissemination processes and thus the investigation of its biological function in CTCs and metastasis formation would be interesting.

In addition, proteoglycans might affect cancer cell migration independently of TGFβ signaling. For example, a number of studies have demonstrated a role of serglycin in malignant transformation as described below. Serglycin can carry up to eight CS or HS chains (Kolset and Tveit, 2008) and is widely expressed by hematopoietic cells as well as embryonic stem cells, where it serves functions in storage of intracellular granules and

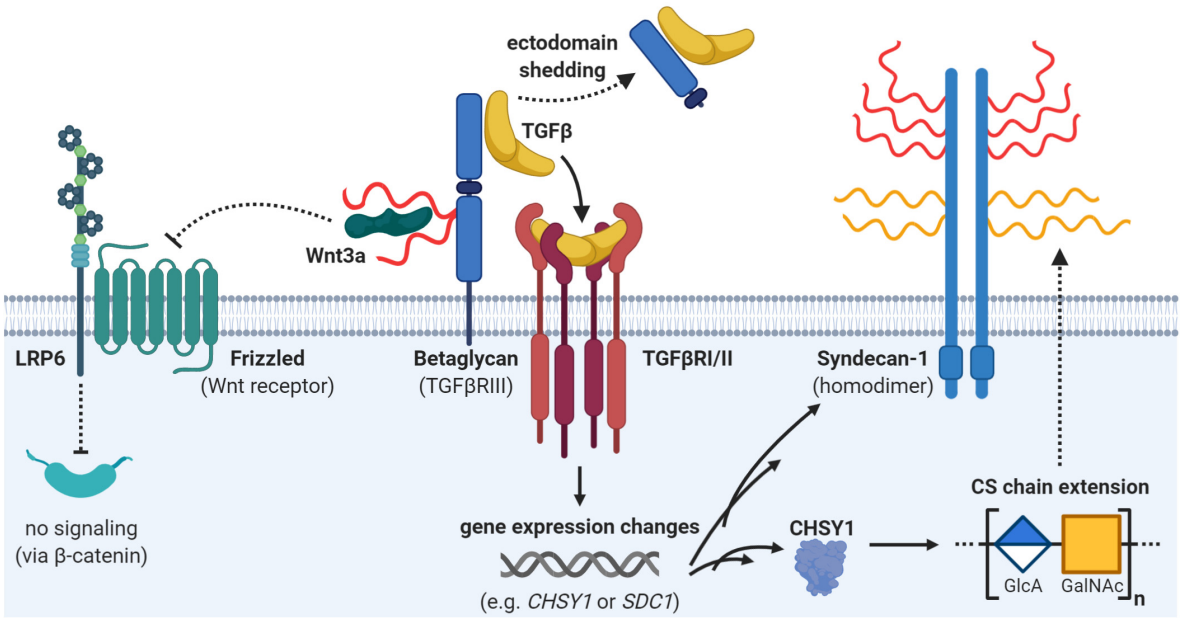

FIGURE 4 | Interplay of proteoglycans and transforming growth factor beta (TGFβ) signaling. The proteoglycan betaglycan is a co-receptor for TGFβ and brings it to the TGFβ receptor (heterodimer of TGFβRI and TGFβRII). However, ectodomain shedding of betaglycan might attenuate TGFβ signaling. Furthermore, betaglycan also dampens Wnt signaling by sequestering Wnt ligands with its heparan sulfate (HS) side chains (in red). Active TGFβ signaling can affect the expression of many different genes such as *SDC1 or CHSY1*. Upregulation of the enzyme chondroitin sulfate synthase 1 (CHSY1) can potentially lead to elongation of chondroitin sulfate (CS) chains on proteoglycans. Indeed, TGFβ can also upregulate one potential CHSY1 targets, namely syndecan-1, which can carry both chondroitin sulfate (CS; in yellow) or heparan sulfate (HS; in red). Details and references are provided in the main text.

secretion of inflammatory mediators (Toyama-Sorimachi et al., 1995; Schick et al., 2001; Abrink et al., 2004). Elevated serglycin expression was reported for cancer cells in patient tissues and has been linked to aggressive cancer cell phenotypes *in vitro* (Korpetinou et al., 2015). Further, serglycin was identified as an unfavorable prognostic factor in patients suffering from a range of cancers, including glioblastoma (Roy et al., 2017), liver (He et al., 2013), lung (Guo et al., 2017), and nasopharynx (Li et al., 2011). Secreted serglycin from cancer cells was shown to be primarily CS-modified, and transgenic expression of serglycin lacking the GAG attachment site led to decreased migratory capacity of breast cancer cells *in vitro* (Korpetinou et al., 2013). This observed GAG-dependency was further supported by another study focused on lung cancer cells (Guo et al., 2017). Here it was demonstrated that serglycin exerts its functional role during migration by binding to the cluster of differentiation 44 antigen (CD44) with downstream activation of EMT (**Figure 5**). Blocking of the post-translational CS modification on serglycin abrogated the effect on motility (Guo et al., 2020). CD44 itself is a transmembrane proteoglycan expressed by various cell types (Goodison et al., 1999; Gronthos et al., 2001; Domev et al., 2012) and is normally involved in hematopoiesis, inflammation, and wound healing (Johnson et al., 2000; Dimitroff et al., 2001b; Cichy and Puré, 2003). CD44 is also involved in several important steps during metastasis formation and has been explored as a CTC target in several studies as described later.

When cells gain migratory and invasive capacity, this is often associated with increased remodeling and breakdown of the ECM, which finally enables breaching of the endothelial basement membrane and intravasation into the blood circulation (Eccles, 1999). One contributing factor is the secretion of different proteases by cancer cells, including for example matrix metalloproteinases (MMPs) (Lynch and Matrisian, 2002). MMPs are produced in a catalytically inactive form, which requires proteolytic cleavage for activation. Interestingly, CSPG4 has been shown to facilitate assembly of a ternary complex consisting of pro-MMP2, MMP-cleaving enzyme (MT3-MMP), and the proteoglycan itself at the cell surface of melanoma cells, leading to cleavage and thus activation of MMP2 (Iida et al., 2007). While the interaction with MT3-MMP was shown to be mediated through the core protein of CSPG4, the association with pro-MMP2 was depending on the CS-modification (Iida et al., 2007).

Another enzyme playing an important role in accessing the blood circulation is heparanase, which cleaves HS polysaccharides located in the basement membrane and on the cancer cell surface, leading to increased invasive behavior of cancers (Sanderson et al., 2017; Masola et al., 2018; Elgundi et al., 2019). Several studies have provided evidence that heparanase plays a major role in progression of a variety of cancers including liver cancer (Koliopanos et al., 2001), sarcomas (Cassinelli and Lanzi, 2020), ovarian cancer (Zhang et al., 2013), breast cancer (Maxhimer et al., 2005), and colon cancer (Nobuhisa et al., 2005). In addition to this, it has recently been shown that overexpression of heparanase promotes the formation of cell clusters in MDA-MB-231 breast cancer cells, most likely by modulating the level of intercellular adhesion molecule 1

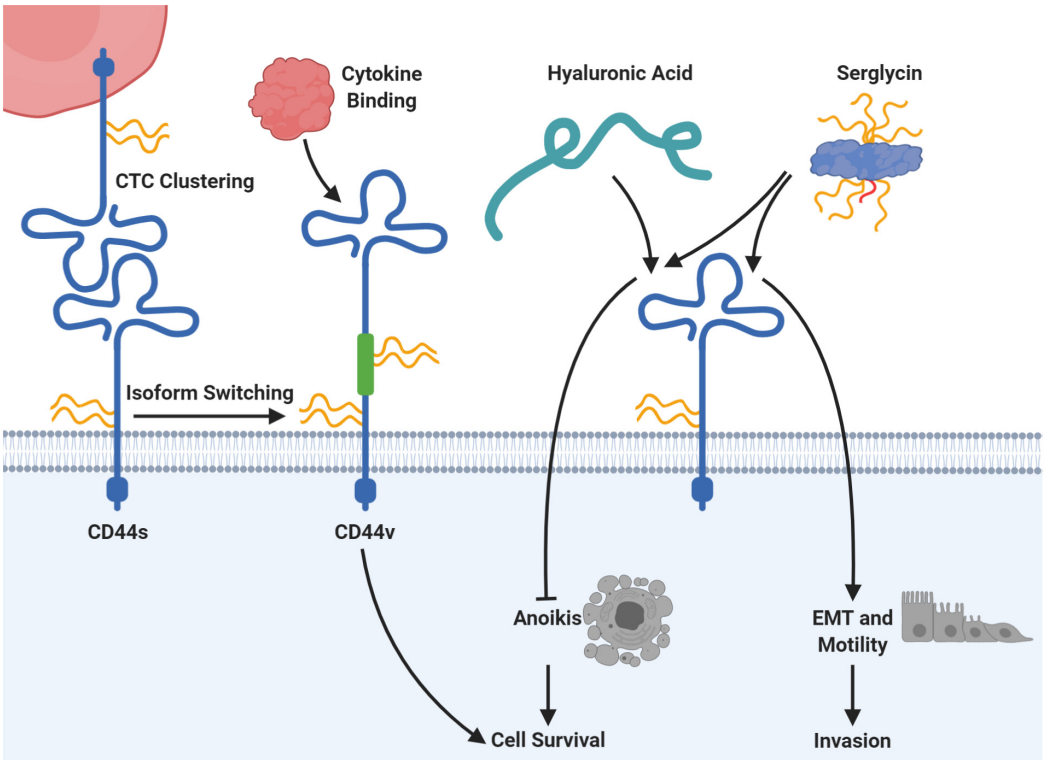

FIGURE 5 | CD44 is connected to several mechanisms of circulating tumor cell (CTC) survival and plasticity. The protein core of CD44 can carry chondroitin sulfate (CS; in yellow), heparan sulfate (HS; in red), or dermatan sulfate (DS; not shown). Homophilic CD44 interactions allow clustering of CTCs, which supports seeding and colonization at the metastatic site in mice. Moreover, expression of the standard CD44 protein form (CD44s) can be switched to expression of CD44 variants (CD44v), which include additional exons via alternative splicing (depicted in green). Those CD44v forms may carry additional glycosaminoglycan chains in dependency of the included exons and promote binding of cancer-related cytokines with downstream signaling for cell survival. The proteoglycan serglycin can carry eight glycosaminoglycan chains of heparan sulfate (HS; in red) or chondroitin sulfate (CS; in yellow) and binds to CD44. Serglycin binding to CD44 induces epithelial-mesenchymal transition (EMT) as well as cell motility and has been proven to be dependent on its CS chains. Moreover, the serglycin-CD44 interaction prevents the induction of anoikis, a specialized form of apoptosis. For this, serglycin competes with hyaluronic acid, which has the same survival promoting effect. Please refer to the specific subsections for details and references.

(ICAM-1) and phosphorylation status of downstream kinases (Wei et al., 2018). Furthermore, the enhanced ability to form clusters correlated with increased number of metastatic foci in the lungs upon tail-vein injection into mice (Wei et al., 2018). Together this data strongly suggests that invasion and intravasation are mediated through HS degradation in the ECM and possibly at the cell surface, leaving behind HS-associated core proteins without this modification.

Surviving the Journey Through Circulation

For normal cells, detachment from the extracellular matrix leads to cell death through a mechanism of detachment-induced apoptosis, called anoikis (Strilic and Offermanns, 2017). Therefore, CTCs must overcome this major challenge in order to survive in circulation. Studies have pointed toward several cellular strategies to circumvent apoptotic signaling, some involving proteoglycans as important players.

Increased syndecan-4 and heparanase expression have been reported in anoikis-resistant rat endothelial cells (Carneiro et al., 2014). Studying these cell lines, Carneiro et al. (2014) also detected increased level of HS in the culture medium, whereas cell lysates contained increased levels of CS. As another example of proteoglycan involvement in anoikis resistance, overexpression of serglycin in a lung cancer cell line led to increased survival in an anchorage-independent growth assay (Guo et al., 2017). This effect was dependent on CD44 expression. In line with this, increased CD44 expression caused by EMT induction also led to anoikis resistance in immortalized human mammary epithelial cells (Cieply et al., 2015). However, in this study the ability of anchorage-independent growth relied on the hyaluronan-binding capacity of CD44. Interestingly, an early study indicated that serglycin and hyaluronan were competing for the binding to CD44 (**Figure 5**) (Toyama-Sorimachi et al., 1995). The prominent role of CD44 in escaping anoikis was further strengthened by a study linking the CD44-expressing subsets of two hepatocellular carcinoma cell lines to anoikis resistance (Okabe et al., 2014). Importantly, this study also observed increased CD44 expression in CTCs compared to patient-matched primary tumor biopsies, again highlighting a potential role of CD44 in CTC analysis.

The ability of the cancer cells to establish an immunosuppressive microenvironment, and thereby escape elimination by the immune system, is considered one of the hallmarks of cancer (Hanahan and Weinberg, 2011). Leaving the primary tumor site and entering the hostile environment of the blood circulation further elevate the requirement for immune cell evasion. One specific strategy for suppressing an immune attack is upregulation of CD47, which constitutes an anti-phagocytotic "do-not-eat-me"-signal on the surface of cancer cells (Jaiswal et al., 2009). CD47 is a proteoglycan carrying both CS and HS, and is widely expressed on white blood cells, where it functions as a receptor for thrombospondin-1 in a GAG-dependent manner (Kaur et al., 2011). Interestingly, CD47 expression was upregulated in colorectal CTCs compared to corresponding primary tumor tissue (Steinert et al., 2014). In addition, Baccelli et al. (2013) characterized the metastasis-initiating subpopulation of breast cancer CTCs as positive for EpCAM, tyrosine-protein kinase Met (cMet), CD44, and CD47 (Baccelli et al., 2013). Another study found that blocking of CD47 on 4T1 mouse breast cancer cells prior to tail vein injection significantly reduced the number of lung metastases in mice (Lian et al., 2019).

Another proteoglycan-based mechanism was shown to provide a strategy to avoid the secretion of lytic granules from NK cells, which would be lethal to the cancer cells. Baccelli et al. (2013) demonstrated that expression of telomeric repeat-binding factor 2 (TRF2) controlled a cell-extrinsic pathway, involving upregulation of HS glucosamine 3-*O*-sulfotransferase 4 (HS3ST4), thereby dampening immune surveillance by NK cells (Biroccio et al., 2013). Further, it was revealed that TRF2 overexpression led to upregulated expression of two HS-carrying proteoglycans, glypican-6 and versican, both of which were shown to decrease NK cell degranulation (Cherfils-Vicini et al., 2019). However, whether TRF2 and associated changes in HSPGs play a role for CTC survival in the circulation still needs to be shown.

Extravasation and Colonization at the Metastatic Site

To form metastatic lesions, CTCs must extravasate and enter the distal tissue. This crucial step in the metastatic cascade is highly inefficient, as the vast majority of CTCs undergo apoptosis, and only a small fraction of the surviving cells succeed in forming metastatic colonies (Massague and Obenauf, 2016; Rejniak, 2016). During extravasation, CTCs adhere to and cross the vascular endothelium in the process of transendothelial migration (TEM) (Reymond et al., 2013). Indeed, multiple factors influence cancer cell extravasation. For instance, capillaries lined with fenestrated endothelial cells and a discontinuous basal membrane in the liver and bone marrow facilitate CTC invasion (Aird, 2007; Strilic and Offermanns, 2017) and contribute to the high incidence of bone and liver metastases (Nguyen et al., 2009; Budczies et al., 2015).

There is ample evidence that CTCs exert what has become known as "leukocyte mimicry," since many of the adhesion and TEM mechanisms are shared with leukocytes (Strell and Entschladen, 2008). Especially, the selectin family of adhesion molecules, important for hematopoietic progenitor cell homing to the bone marrow, have been implicated in cancer cell extravasation (Dimitroff et al., 2001a, 2004). This is mainly mediated by sialofucosylated carbohydrate ligands, particularly the sialyl Lewis (sLe^X) structures, which are primarily found on leukocytes (Fukuda et al., 1999) as well as on various cancer cells (Majuri et al., 1995; Renkonen et al., 1997). A particular sialofucosylated glycoform of the proteoglycan CD44 termed hematopoietic cell E-/L-selectin ligand (HCELL) mediates selectin tethering (Sackstein, 2004). E-selectin is highly expressed on endothelial cells in the bone marrow (Burdick et al., 2012). In cooperation with carcinoembryonic antigen, HCELL facilitates cancer cell rolling through binding to E-selectin (Hanley et al., 2006; Thomas et al., 2008), strongly supporting the hypothesis of HCELL-mediated CTC arrest in the vasculature, a crucial step in CTC extravasation (Lee et al., 2014). Interestingly, studies have investigated the presence of over-sulfated GAGs as alternative ligands for selectins in cancer extravasation mechanisms (Martinez et al., 2013), highlighting the importance of altered display of GAGs.

Besides robust adhesion of CTCs to the endothelial wall, CTC clusters also seem to be important for metastatic seeding and outgrowth. In the circulation, CTCs can exist as single cancer cells or as clusters of cancer cells. The prevalence of polyclonal CTC clusters correlates with poor prognosis in patients, and is believed to be an important component for metastatic success (Aceto et al., 2014; Gundem et al., 2015; Cheung et al., 2016). In a recent study, CD44 was identified as a key component in clustering of cancer cells both in patient-derived xenograft (PDX) models in mice and in metastatic breast cancer patients (Liu et al., 2019). Mechanistically, CD44 formed homophilic interactions independent of HA on the cancer cell surface (**Figure 5**), which in turn triggered activation of a serine/threonine-protein kinase 2 (PAK2) and focal adhesion kinase (FAK) dependent signaling cascade. Knockout of CD44 resulted in loss of CTC cluster formation and reduced lung colonization and metastasis in PDX models.

CD44 is a multi-functional proteoglycan for colonization and priming of the metastatic niche (Zoller, 2011). The standard CD44 (CD44s) comprises exons 1–5 and 16–20, while the splice variants (CD44v) also include various combinations of exons 7–15, whereas exon 6 is missing in humans (Naor et al., 2002). In several cancers isoform switching via alternative splicing of *CD44* is frequently observed (Johnson et al., 2000). For example, CD44v3, CD44v6, and CD44v10 have been implicated in cancer and are the only CD44 isoforms that contain binding sites for cancer-related cytokines and chemokines (Chen C. et al., 2018; Wang Z. et al., 2018). In colorectal cancer, CD44v6 positive cells are able to form metastatic lesions in the liver and lung through interaction with osteopontin (Huang et al., 2012). Importantly, the CD44 protein core can carry HS, CS, KS, or DS, but the GAG content is highly dependent on the isoform and exons involved (Bennett et al., 1995; Greenfield et al., 1999; Clark et al., 2004). Furthermore, cytokines secreted in the tumor microenvironment (e.g., hepatocyte growth factor and stromal-derived factor 1a), increased CD44v6 expression, and assisted colorectal cancer stem cells in colonization and survival through activation of

the phosphatidylinositol 3-kinase-protein kinase B (PI3K-AKT) pathway (Todaro et al., 2014).

Once the CTCs have managed to extravasate into the tissue, the nature of the ECM at the secondary site dictates whether the disseminated cancer cells will proliferate into overt metastases, enter a dormant state, or undergo apoptosis (Ghajar et al., 2013; Sosa et al., 2014; Peinado et al., 2017; Goddard et al., 2018). One way in which cancers prime the pre-metastatic niche is through exosome secretion, which facilitates organ-specific engraftment of cancer cells (Simons and Raposo, 2009; Peinado et al., 2012; Hoshino et al., 2015). Interestingly, HS has been shown to play a role in the syndecan-1 mediated formation of the syntenin-ALG2-interacting protein X (ALIX) complex (Baietti et al., 2012; Thompson et al., 2013; Roucourt et al., 2015). Following vesicular release, HSPGs also take part in exosome docking and delivery of vesicular cargo to the recipient cell. This dual role of HSPGs in exosome-mediated crosstalk between cells is fostered by fibronectin that interacts with HS displayed on the surface of exosomes and functions as a heparan sulfate/HS-binding ligand on target cells (Purushothaman et al., 2016; Colombo et al., 2019). Another study reported a correlation between the expression of glypican-1 on the exosomal surface and the tumor burden in pancreatic cancer patients (Melo et al., 2015), supporting a prognostic value of proteoglycans associated with exosomes in carcinogenesis.

At the metastatic site, proteoglycans also contribute by promoting cancer cell engraftment and colonization (Fares et al., 2020). The potential role of serglycin in metastatic dissemination has been investigated in a mouse model of breast cancer, where knockout of serglycin resulted in CTCs unable to establish metastatic tumors although not affecting primary tumor formation (Roy et al., 2016). Correspondingly, increased serglycin expression was shown to facilitate liver colonization by cancer cells in a patient-derived xenograft model of non-small-cell lung cancer (NSCLC) (Guo et al., 2017) as well as to promote hepatocellular carcinoma metastasis to the bone (He et al., 2014).

In summary, proteoglycans are connected to all steps of the metastatic cascade. Notably, some proteoglycans appear to play active roles in several aspects of cancer progression, highlighting these as potential key players of the cancer cell surface. One such proteoglycan is CD44, which is highly involved in EMT, helps to prevent anoikis due to its HA-receptor function, and furthermore takes actions in generating CTC clusters and extravasation, thereby enabling a successful arrival at the metastatic site (**Figure 5**). Another key proteoglycan seems to be CSPG4, with important roles for the regulation of cancer cell growth and invasion. Furthermore, the studies on CSPG4 presented here demonstrate how transmembrane proteoglycans possess multiple modes of action by engaging with other receptors or signaling molecules through either their cytoplasmic domain, ectodomains, or their GAG chains. With this central role in metastasis and CTC biology, proteoglycans could be an interesting target for CTC technologies. Indeed, proteoglycans are already studied and partly utilized for CTC identification and capture by different technologies. The following section will hence provide a detailed overview on proteoglycans as CTC targets.

PROTEOGLYCANS IN CIRCULATING TUMOR CELL DIAGNOSTICS

Circulating tumor cell detection assays have spurred increasing clinical interest since the prognostic value in progression-free and overall survival was established in patients with metastatic colorectal (Cohen et al., 2009), breast (Cristofanilli et al., 2004), prostate (de Bono et al., 2008), and lung (Krebs et al., 2011) cancer. CTC enumeration from patient blood samples has also demonstrated clinical relevance for several other cancer types such as pancreatic cancer (Kurihara et al., 2008; Bidard et al., 2013; Effenberger et al., 2018) or hepatocellular carcinoma (Schulze et al., 2013; Qi et al., 2018). The presence of detectable levels of CTCs in the peripheral blood is associated with the metastatic capacity of the disease (Allard et al., 2004; Cristofanilli et al., 2004). However, low levels of CTCs have been reported in non-metastatic disease for several cancer indications before and after surgery (Thorsteinsson et al., 2011; Franken et al., 2012; Gazzaniga et al., 2013). Additional studies suggest that CTCs are even shed from premalignant lesions and this opens the possibility for using CTC detection for early diagnosis of cancer (Husemann et al., 2008; Stott et al., 2010; Rhim et al., 2012; Zhang et al., 2014; Tsai et al., 2016; Murlidhar et al., 2017). CTC assays might also have potential as a tool for predicting treatment efficacy and monitoring disease (Schochter et al., 2019; Yang et al., 2019), thereby providing real-time, non-invasive information about the disease by liquid biopsies. Furthermore, many CTC assays do not only enable enumeration but also downstream analyses such as genomic, transcriptomic, proteomic, or phenotypic characterization of cancer cells. Therefore, studying CTCs can also bring novel insight into aspects of metastasis formation, which are still not fully understood (Chaffer and Weinberg, 2011). Despite the interest and potential in analyzing CTCs, the methods are rarely implemented in the clinical setting, as CTC identification requires highly specific markers and an extreme assay sensitivity. Many CTC methods struggle to reach the needed sensitivity, as it is a technical challenge to detect few cancer cells in billions of normal blood cells.

Several CTC enrichment technologies ranging in complexity have been developed (Kowalik et al., 2017; Dianat-Moghadam et al., 2020). From whole blood, CTCs can be enriched along with leukocytes by density fractionation or a simple lysis of the erythrocytes. The crude cell enrichment can be analyzed by direct antibody staining and examined by, e.g., microscopy (Hillig et al., 2015; Werner et al., 2015) or flow cytometry (Hristozova et al., 2012; Watanabe et al., 2014; Lopresti et al., 2019). Because of the rarity of the CTCs, an additional cancer cell-specific enrichment step is, however, often preferred. CTCs can be enriched from the leukocytes based on distinct biophysical properties such as size, density, deformability, or charge (Liu et al., 2015; Mitchell et al., 2015; Shaw Bagnall et al., 2015). Following CTC enrichment, the detection of CTCs will still rely on a staining step, distinguishing for example cytokeratin (CK)-positive CTCs from the remaining CD45-positive leukocytes. Other systems for CTC isolation use cancer- or tissue-specific antibodies to enrich for CTCs (Coumans and Terstappen, 2015)

or even leukocyte cell surface proteins like CD45 to deplete for leukocytes (Ozkumur et al., 2013; Karabacak et al., 2014). The positive selection of CTCs is evidently very dependent on highly specific cancer or tissue markers. In order to demonstrate high potential for clinical application, extensive validation of CTC capture platforms must reveal robust clinical sensitivity and specificity (Parkinson et al., 2012). Most pilot studies do not present large-scale clinical data and should hence be interpreted with caution. Inclusion of healthy controls becomes crucial to demonstrate the specificity of the capture and/or detection strategy. Alternatively, some studies apply downstream molecular analyses to verify the tumor origin of detected CTCs, e.g., by mutation detection, which supports the reliability of the CTC assay (Gasch et al., 2013; Muller et al., 2014). From a more technical perspective, pre-analytical conditions such as blood tubes, storage time, and temperature as well as choice of antibody clones can have a huge effect on assay performance (Qin et al., 2014; Ilie et al., 2018; Wu et al., 2020), making comparisons across studies difficult. Furthermore, in the light of exploring proteoglycans as potential CTC targets, the consideration of technical assay parameters become crucial for, e.g., sustaining the GAG stability.

The current clinical standard for CTC enumeration is the CellSearch® platform, which is approved by the American Food and Drug Administration (FDA) for monitoring patients with metastatic breast, colorectal, and prostate cancer. CellSearch® relies on cell enrichment using anti-EpCAM antibody-coated ferrofluid and CTC detection via fluorescent anti-CK antibody labeling (Liberti et al., 2001; Allard et al., 2004; Coumans and Terstappen, 2015). EpCAM-based capture approaches are, however, rarely efficient for epithelial cancers with downregulated EpCAM expression, likely due to EMT, or cancers of mesenchymal origin. Therefore, several studies have been focusing on finding novel markers, which can distinguish EpCAM-low or -negative CTCs from normal blood cells with high specificity and sensitivity to broaden the spectrum of detectable CTC subpopulations (Lampignano et al., 2017; Nicolazzo et al., 2019). As a part of this, multiple strategies using proteoglycans for CTC enrichment or identification are currently under investigation. See **Table 1** for an overview on the most used proteoglycans and their applications. Some of them are highlighted in the following.

A well-known example is the CellSearch® Circulating Endothelial Cell Kit, which can be used for the enrichment of circulating melanoma cells that are EpCAM-negative by nature (Rao et al., 2011; Khoja et al., 2013). After capture using ferrofluid coupled with antibodies against melanoma cell adhesion molecule (MCAM), circulating melanoma cells are identified by staining with antibodies against high molecular weight melanoma-associated antigen (HMW-MAA), also known as CSPG4.

As described earlier, CSPG4 has been linked to many aspects of the metastatic cascade, including proliferation, migration, as well as ECM-remodeling and is expressed across many cancer types (Ilieva et al., 2018). Moreover, CSPG4 is expressed in a majority of melanoma lesions (Real et al., 1985) and is a well-characterized surface marker for melanoma (Ilieva et al., 2018). Multiple retrospective studies using the MCAM/CSPG4 CellSearch® Kit have found that CTC levels detected at baseline correlates with overall survival in late-stage melanoma (Rao et al., 2011; Khoja et al., 2013; Bidard et al., 2014) (**Table 1**). Recently, two large prospective studies also evaluated the prognostic significance of MCAM/CSPG4-positive CTCs in cutaneous melanoma. In a study of 93 stage IV patients, Hall et al. (2018) found that presence of CTCs at baseline was associated with shorter progression-free survival after 6 months compared to CTC-negative patients. Later, the same research group showed that CTC-positivity at baseline for stage III patients (n = 243) was an independent predictor of relapse-free survival within 6 and 54 months (Lucci et al., 2020). The CTC levels in these studies were not associated with primary tumor characteristics, such as ulcerations, tumor thickness, and mutational status. Therefore, MCAM/CSPG4-positive CTC numbers may add additional information on top of clinicopathological characteristics for clinicians to foresee the disease course in the future.

Interestingly, CTC-negative melanoma patients have been found to have better progression-free or relapse-free survival compared to CTC-positive patients (Hall et al., 2018; Lucci et al., 2020). However, a significant proportion of late-stage melanoma patients still appear to have no CTCs detectable by CellSearch® (Rao et al., 2011; Roland et al., 2015; Hall et al., 2018). This has also been reported for other CSPG4-based methods (Ulmer et al., 2004; Ruiz et al., 2015) as well as for CSPG4-independent isolation methods (Khoja et al., 2014; Aya-Bonilla et al., 2019). This may simply be due to the rare nature of CTCs. However, there could be CSPG4-negative CTC subpopulations, which are not captured by CSPG4-dependent strategies. In fact, one study found that of 31 melanoma patients with CTCs detectable by other markers, only 42% had CSPG4-positive CTCs (Gray et al., 2015), suggesting a need for multi-marker approaches.

During the past decade, multiple other studies investigated the potential of CSPG4 for CTC capture and/or identification in melanoma (**Table 1**). Up to 4 CTCs per mL blood was found using CSPG4 immunomagnetic capture (Sakaizawa et al., 2012), which is similar to the reported CTC numbers using the MCAM/CSPG4 CellSearch® kit (Khoja et al., 2013). However, a study by Ruiz et al. (2015) using a CSPG4-based immunofluorescent microscopy approach without prior enrichment step identified a mean of 14.9 CTCs per 1 mL blood samples from melanoma patients (n = 40), without potential CTC hits in healthy control samples (n = 10). These variations in CSPG4-positive CTCs can be explained to some extent by the use of different CTC enrichment strategies, varying markers for CTC identification or other technical differences in the assays.

Commonly mutated genes in melanoma, such as *BRAF* and *NRAS* (Colombino et al., 2012), are upstream activators of ERK signaling (Savoia et al., 2019). As CSPG4 expression has been connected to ERK signaling (Ampofo et al., 2017), these mutations might be particularly important in CSPG4-positive CTCs. Indeed, a recent study found that CTCs enriched by CSPG4-based method presented more *RAS/RAF* mutated cells compared to CTCs isolated only by physical properties (Gorges et al., 2019). Since some therapeutic approaches target the serine/threonine-protein kinase B-raf

TABLE 1 | Proteoglycans used for isolation or identification of clinical circulating tumor cells.

	Indication	Used for	Finding	References
Carbonic anhydrase 9 (CA9)	RCC	Immunomagnetic capture	Combined approach with CD147, captured CTCs in 94% of patients. CTC amount correlated with disease stage.	Liu et al. (2016)
		CTC detection (On−chip Sort®)	CTCs were detected in 46% of patients (combined CA9 and EpCAM staining).	Naoe et al. (2019)
CD44	BC/TNBC	CTC detection (flow cytometry)	NACT caused significant changes in the quantity of the CTC subsets present in patient blood samples.	Kaigorodova et al. (2018)
		CTC detection (ns)	CTC clusters were associated with poor OS. CTC clusters showed higher CD44 expression.	Liu et al. (2019)
	CRC	CTC detection (flow cytometry	CD133+CD54+CD44+ CTC subset was significantly associated with liver metastasis and had a prognostic value in CRC patients.	Fang et al. (2017)
	Gastric cancer	CTC detection (FACS)	The amount of EpCAM+CD44+ CTCs, but not EpCAM+CD44− CTCs, correlated with disease progression and venous invasion.	Watanabe et al. (2017)
		Negative immunomagnetic enrichment (anti-CD45)	CD44 was a marker for tumorigenic CTCs.	Toyoshima et al. (2015)
	NSCLC	Immunomagnetic capture	CD44+ CTCs were associated with lymphatic invasion and tumor size. CD44+ CTCs were more sensitive to TRAIL-induced apoptosis.	Yan-Bin et al. (2020)
	OSCC	Immunomagnetic capture	CD44+ CTCs showed increased self-renewal capability and chemotherapy-resistance. Clinical correlation between increased CD44v6 and loco-regional aggressiveness and recurrence.	Patel et al. (2016)
Chondroitin sulfate proteoglycan 4 (CSPG4)	Melanoma	Immunomagnetic capture	Analysis of RNA suggested that CSPG4+ CTCs were distinct from CTCs enriched by another melanoma marker, ABCB5.	Aya-Bonilla et al. (2019)
		Immunomagnetic capture	Significant difference between CTC numbers in healthy controls, stage I/II and stage III/IV, using multiple markers. Decrease in CTC numbers during treatments was associated with longer OS and shorter response to treatment.	Freeman et al. (2012), Klinac et al. (2014)
		Immunomagnetic capture (with subsequent depletion of CD45+ cells)	1–20 CTCs found per 5 mL blood and *BRAF* genetic heterogeneity was detected among CTCs.	Sakaizawa et al. (2012)
		Immunomagnetic capture	≥2 CTCs correlated with OS for stage III and IV patients. CTC-positivity correlated with stage.	Ulmer et al. (2004)
		Immunomagnetic capture and IF	MCAM/CSPG4-positive CTCs and *RAS/RAF* mutational status were associated.	Gorges et al. (2019)
		CellSearch® Melanoma Kit	CTC positivity in early-stage disease correlated with OS at 24 months.	Anand et al. (2019)
			Strong correlation between CTC positivity and PFS and OS; and between CTC numbers and ctDNA-levels.	Bidard et al. (2014)
			Prospective study of stage IV patients. Baseline CTC-positivity independently predicted poorer PFS after 180 days.	Hall et al. (2018)
			≥2 CTCs at baseline was an independent prognostic factor for poor OS.	Khoja et al. (2013)

(Continued)

TABLE 1 | Continued

	Indication	Used for	Finding	References
		CellSearch® Melanoma Kit	Prospective study of 243 stage III patients. CTC-positivity at baseline independently predicted poorer relapse-free survival within 6 and 54 months.	Lucci et al. (2020)
			Retrospective study; baseline ≥ 2 CTCs correlated with OS in stage III/IV patients. 95% of healthy subjects had no CTCs.	Rao et al. (2011)
			Difference in CTC positivity for stage I/II vs. IV. Only 2.9% of healthy subject had CTCs.	Roland et al. (2015)
		CTC detection (flow cytometry)	Early-stage CTCs expressed mainly one marker, late-stage CTCs expressed more. 42% of CTCs expressed CSPG4.	Gray et al. (2015)
		CTC detection (flow cytometry)	CTCs were found in 14/22 patients.	Liu et al. (2011)
		CTC detection (IF)	5% of patients had ≥100 CTCs/mL. In these, unique clonal populations were identified.	Ruiz et al. (2015)
		Characterization by Surface-enhanced Raman spectroscopy with αCSPG4	CTC surface marker levels, including CSPG4, were altered during treatment.	Tsao et al. (2018)
C-X-C chemokine receptor type 4 (CXCR4)	HCC	CTC detection (RISH)	CTCs were detected in 89.9% of all patients and CXCR4 expression was associated with different CTC subsets.	Bai et al. (2020)
	NSCLC	CTC detection (flow cytometry)	CXCR4 expression was increased on EpCAM- CTCs.	Yin et al. (2015)
		CTC detection (flow cytometry)	CXCR4+ CTCs showed potential as a predictive marker for OS in NSCLC patients.	Reckamp et al. (2009)
Glypican-3 (GPC3)	HCC	Immunomagnetic capture and CTC detection (flow cytometry)	High GPC3+ CTC amount correlated with shortened disease-free survival in non-metastatic HCC patients.	Hamaoka et al. (2019)
		Immunomagnetic capture	Capture cocktail (together with anti-ASGPR, anti-EpCAM) found higher CTC numbers than each antibody alone.	Court et al. (2018)
		CTC detection (ImageStream®)	12.5% of all found CTCs were GPC3+.	Ogle et al. (2016)
	HCC/CCA	CTC detection (IHC)	1 out of 14 patients with CTCs had GPC3+ CTCs.	Nam et al. (2016)
Syndican-1 (SDC1/CD138)	MM	Immunomagnetic capture	CD138+ CTCs strongly correlated with disease burden and treatment response.	Wang et al. (2019)
	MM	Immunomagnetic capture	20–184 CD138+ CTCs detected in patient blood/mL (2–5/mL healthy blood). Patients in remission had fewer CTCs than other patients.	Qasaimeh et al. (2017)

+, positive; ABCB5, ATP-binding cassette sub-family B member 5; ASGPR, asialoglycoprotein receptor; BC, breast cancer; CA9, carbonic anhydrase 9; CCA, cholangiocarcinoma; CD, cluster of differentiation; CK, cytokeratin; CRC, colorectal cancer; CSPG4, chondroitin sulfate proteoglycan 4; CTC, circulating tumor cell; ctDNA, circulating tumor DNA; CXCR4, C-X-C chemokine receptor type 4; EpCAM, epithelial cell adhesion molecule; FACS, fluorescence-activated cell sorting; GPC3, glypican-3; HCC, hepatocellular carcinoma; IF, immunofluorescence; IHC, immunohistochemistry; ISET, isolation by size of epithelial tumor cells; MCAM, melanoma cell adhesion molecule; MM, multiple myeloma; NACT, neoadjuvant chemotherapy; ns, not specified; OSCC, oral squamous cell carcinoma; OS, overall survival; PFS, progression-free survival; RBC, red blood cell; RCC, renal cell carcinoma; RISH: RNA in situ hybridization; SDC1, syndican-1; TNBC, triple-negative breast cancer; TRAIL, TNF-related apoptosis-inducing ligand.

(BRAF) (Holderfield et al., 2014), it is possible that the CSPG4 expression might also decrease in response to this form of treatment, which could affect the prospect of using CSPG4 alone to monitor CTC numbers. Indeed, initial longitudinal study of CTC heterogeneity in 10 stage IV melanoma patients suggested that expression of CSPG4 on CTCs may be downregulated in response to BRAF and mitogen-activated protein kinase kinase (MEK)-inhibiting therapy (Tsao et al., 2018). However, to our knowledge, none of the major studies on CSPG4-positive CTCs in cutaneous melanoma have yet found any correlation between CTC levels and BRAF-mutational status or adjuvant therapy.

Another recent study revealed that the transcriptomic profile of CSPG4-enriched CTC populations from six patients was dominated by up-regulation of tumor necrosis factor alpha (TNFα)/nuclear factor kappa B (NF-κB) as well as signal transducer and activator of transcription (STAT) pathways

(Aya-Bonilla et al., 2019). Both signaling pathways have central roles for cell proliferation as well as cell survival (Wu and Zhou, 2010; Igelmann et al., 2019). Furthermore, *in silico* analysis found other genes upregulated in the CSPG4-enriched population to be connected to metastasis, tumor growth, and melanoma biology (Aya-Bonilla et al., 2019), which indicates an interesting biological role of CSPG4-positive CTCs for melanoma progression.

Overall, CSPG4 is a relevant surface marker for melanoma CTCs and is hence evaluated in many studies. Although little is still known about the biological role of CSPG4-positive CTCs, they might represent a specific subpopulation. This potential bias should be considered when using only CSPG4 for CTC capture or CTC identification.

CD44 has also been explored for CTC analysis. CD44 is widely expressed (Goodison et al., 1999), and as previously described it acts as a receptor for a variety of ligands. Particularly well-described is the interaction with HA, which constitutes a major part of the glycocalyx and ECM (Banerjee et al., 2016). Upregulation of CD44 confers tumorigenicity, metastatic capacity, and drug resistance to primary tumor cells as well as CTCs (Naor et al., 2002; Fitzgerald and McCubrey, 2014). The abnormal expression of CD44 splice variants is associated with treatment refractoriness, recurrence, and prognosis (Katoh et al., 2015), and overexpression of both CD44s and variants serves a long list of biological functions across many cancer types (Chen C. et al., 2018). Since isoform switching introduces new cancer-related antigens, development of both anti-CD44s and anti-CD44v antibodies has attracted much interest.

As a CTC isolation tool, anti-CD44 antibodies have been used to capture CTCs from cancer patient blood (see **Table 1**). Yan-Bin et al. (2020) investigated the CD44-positive CTC abundance in NSCLC patients by immunomagnetic enrichment and evaluated the correlation to clinical characteristics. None or very few CD44-positive cells were detected in the 30 controls in contrast to frequent CTC observations in the 128 patient samples. Detected CTCs associated negatively with serum TNF-related apoptosis-inducing ligand (TRAIL) levels, suggesting that CD44-positive CTCs could be more vulnerable to TRAIL-induced apoptosis through death receptor 4 and 5 signaling (Yan-Bin et al., 2020). A small study on gastric cancer patients (n = 26) and healthy controls (n = 10) associated increased prevalence of EpCAM- and CD44-positive CTCs in patients with tumor depth, disease progression, and venous invasion (Watanabe et al., 2017). Consequently, CD44-based CTC detection was suggested to reflect the malignant potential of the tumor. The authors, however, disregard EpCAM-positive cells found in all healthy controls and the few double positive cells found in 2 healthy controls as either non-specific immunological reactions or contaminating skin cells. Again, this discrepancy highlights the demand for CTC validation, as for example via genomics. Another study analyzed CD44-positive CTCs isolated by immunomagnetic enrichment from 30 oral squamous cell carcinoma (OSCC) patients and 15 healthy controls (Patel et al., 2016). Self-renewal and proliferation capability of the CD44-positive cells were observed by increased sphere-forming capacity unlike the CD44-negative sorted population. Moreover, cisplatin resistance assays confirmed a drug-resistant phenotype associated with the CD44-positive population. This was specifically associated with high transcript levels of *CD44v6*, as opposed to *CD44s*, as well as elevated levels of the stemness marker *NANOG*. Furthermore, the different expression levels strongly correlated with the primary tumor profile and, importantly, clinicopathological parameters such as late-stage, loco-regional aggressiveness, and relapse. The findings suggest that detection of CD44v6-positive CTCs could be used to predict disease progression, therapy outcome, and recurrence.

In addition, CD44 is being evaluated for novel therapeutic approaches against CTCs. For instance, *in vivo* homophilic CD44-mediated CTC clustering of metastatic breast cancer cells in mice was largely inhibited by the administration of anti-CD44 neutralizing antibody, leading to decreased metastatic capacity (Liu et al., 2019). In summary, numerous studies of applications to target CD44-positive CTCs underline its potential in therapy and as a valuable marker for prognosis and treatment response.

Another interesting proteoglycan for clinical purposes is glypican-3 (GPC3), which is upregulated amongst several cancer entities with highest positive case rates in hepatocellular carcinoma (HCC). Importantly, GPC3 has been reported to discriminate between HCC and non-malignant lesions (Zhu et al., 2001; Wang et al., 2008) or other liver-associated cancers like cholangiocarcinoma (CCA) (Man et al., 2005). Nowadays GPC3 is included in a diagnostic HCC panel together with glutamine synthetase and heat shock protein 70, according to guidelines of the European Society for Medical Oncology (ESMO) (Vogel et al., 2019) and the American Association for the Study of Liver Diseases (AASLD) (Marrero et al., 2018). Furthermore, GPC3 might also be used as a serum biomarker (Capurro et al., 2003; Hippo et al., 2004) and is exploited for different targeted cancer therapy approaches (Sawada et al., 2012; Feng et al., 2013).

Several studies have been utilizing GPC3 for analysis of CTCs in HCC patients (**Table 1**). Anti-GPC3 antibodies have been used for positive immunomagnetic enrichment of CTCs (Court et al., 2018; Hamaoka et al., 2019). Hamaoka et al. (2019) found in a prospective, single-institution study that most of the 85 examined HCC patients had GPC3-positive CTCs with a median of 3 CTCs in 8 mL blood samples, whereas negative controls (in total n = 27) such as healthy individuals (n = 12) or individuals with inflammatory diseases (n = 4), only had a median of 1 GPC3-positive cell in the blood samples (Hamaoka et al., 2019). Moreover, patients with 5 or more CTCs showed shorter disease-free survival compared to patients with fewer GPC3-positive CTCs. Another study by Court et al. (2018) analyzed GPC3 in a capture cocktail together with antibodies against asialoglycoprotein receptor (ASGPR) and EpCAM. Importantly, the combined capture approach with all three targets, isolated higher CTC numbers in patients than each antibody alone. This approach detected CTCs in 96.7% of all HCC patients (n = 61) with a median of 6 CTCs per 4 mL blood. In contrast, in healthy controls (n = 8) maximum one potential CTC hit was found. Moreover, CTC numbers were increased in more advanced stages compared to early stages. This effect was even more pronounced for the

subfraction of vimentin-positive CTCs, which presumably are generated by EMT processes. This highlights the importance of CTC capture strategies independent of potential EMT target proteins like EpCAM, which are often downregulated during EMT. Indeed, varying or low EpCAM expression has already been reported for CTCs originating from other cancer entities (Hyun et al., 2016; de Wit et al., 2018) and should be taken into consideration when designing or interpreting CTC capture assays.

In summary, GPC3 is currently evaluated as a therapeutic target, serum biomarker, and importantly for CTC analyses, where it has been used both for capture (Court et al., 2018; Hamaoka et al., 2019) and identification (Ogle et al., 2016) of CTCs in HCC. Since only few studies have been performed, further studies are needed to prove the feasibility of GPC3 for clinical CTC analyses. Although GPC3 is a well-established diagnostic marker for HCC, further characterization or validation of the potential GPC3-positive CTC hits, for example via molecular analyses, is to our knowledge missing so far.

As described, there is a great diversity among the proteoglycans associated with different cancer types. The different proteoglycans facilitate distinctive processes in the metastatic cascade and their universal expression suggests that proteoglycans are an essential feature for all cancers. The complexity is further expanded when considering the GAG composition. An increasing number of studies indicate that at least some of the functions of proteoglycans are exerted through specific GAG chains. However, only a few studies focused on targeting the GAG part or GAG composition of proteoglycans when isolating CTCs.

A wide variety of qualitative and quantitative methods has been developed for studying glycocalyx components. As the biosynthesis of glycans is non-template driven and complex, their analysis may often be challenging. Several approaches take advantage of the large repertoire of glycan-binding proteins and antibodies to distinguish between different glycan classes. For large screenings, glycan microarrays have been developed that may probe for different glycan classes or subclasses. This approach has been used to screen breast CTCs for glycan markers, which identified a specific *O*-glycan epitope as a potential target (Wang et al., 2015). Microarrays and cell-based libraries have also been developed to screen for GAG-binding proteins (Rogers and Hsieh-Wilson, 2012) and these may be useful for identifying GAG-based CTC targeting reagents. However, microarrays for detection of cell-surface GAGs, which could be useful for identifying GAG biomarkers on CTCs, have not been constructed. CS and HS-specific antibodies, such as CS56 and 10E4, and GAG-binding proteins, like fibroblast growth factor, are also commonly used in flow cytometry and microscopy-based assays (**Figure 6A**). These may assess the relative levels of GAGs, however, they do not convey specific structural information due to their low specificity or affinity toward their targets (Yamagata et al., 1987; Smetsers et al., 2004; ten Dam et al., 2007). For this, GAGs will have to be isolated and analyzed, often by chromatography, mass spectrometry, or nuclear magnetic resonance. The structural characterization of GAGs is challenging due to heterogeneity of the polymers. Hence, analysis is often limited to disaccharide analysis, which does not allow for sequencing of intact GAG chains. This is even more technical challenging for CTCs because of the limited input material due to their low abundance. Similarly, while different proteoglycan core proteins can be probed with antibodies, fine structural analysis of their GAG attachment sites is only achieved by glycoproteomic methods. While these analyses may be laborious, they are highly descriptive and may provide novel insight into structural alterations on cancer cells, both on the protein and GAG level. For example, one study found that several major ECM proteoglycans had elevated levels of N-glycosylation in pancreatic cancer tissues (Pan et al., 2014). In addition, another study identified novel CS linkage region modifications in CS glycopeptides from the inter-α-trypsin inhibitor complex, which is abundant in plasma from cancer patients (Gomez Toledo et al., 2015). To our knowledge, glycoproteomics has not been used for analysis of CTCs, and could potentially help identify novel targets.

If succeeding in finding specific binding moieties, the GAG chains would be an alternative novel approach for CTC enrichment or detection. We have previously shown the use of the recombinant VAR2CSA malaria protein (rVAR2) as a novel CTC-targeting reagent (**Figures 6A**, **7**) (Agerbaek et al., 2018; Bang-Christensen et al., 2019; Sand et al., 2020). rVAR2 binds to a distinct type of CS, termed oncofetal CS, expressed by placental as well as cancer cells (Salanti et al., 2015). The native VAR2CSA binds to a specific CS oligosaccharide motif in the placenta during normal physiological conditions (Gowda, 2006; Ayres Pereira et al., 2016; Toledo et al., 2020). A study using a library of cells with knockouts of GAG biosynthesis genes, indicated that 4-*O*-sulfated CS is essential for rVAR2 binding (Chen Y. H. et al., 2018). The specific oncofetal CS-carrying proteoglycans have been examined by screening of rVAR2 binding to more than 3500 cell surface proteins (Salanti et al., 2015) as well as by rVAR2-affinity chromatography coupled to glycoproteomics, using tumor and placenta samples (Toledo et al., 2020). These studies showed that the distinct oncofetal CS is displayed on multiple proteoglycans such as CSPG4 or CD44 in cancer cells, indicating an important function of oncofetal CS in the disease development. Moreover, rVAR2 binds to cancer cells independently of tumor origin and oncofetal CS is expressed both in primary and metastatic lesions (Salanti et al., 2015). This has also been shown in a metastatic murine model, where rVAR2 binding furthermore inhibited integrin signaling and seeding of CTCs (Clausen et al., 2016). As studies have also indicated that rVAR2 binds to cancer cells independent of EMT processes (Agerbaek et al., 2018; Bang-Christensen et al., 2019), oncofetal CS could be an advantageous target for CTC enrichment. In line with this, rVAR2-coated paramagnetic beads have been used to capture CTCs from blood samples of different carcinoma patients (n = 44) and glioma patients (n = 10) in small proof-of concept studies (Agerbaek et al., 2018; Bang-Christensen et al., 2019). Therefore, the rVAR2-based approach offers an alternative capture approach, demonstrating how GAG-targeting can allow the capture of CTCs independently of single target proteins, like EpCAM.

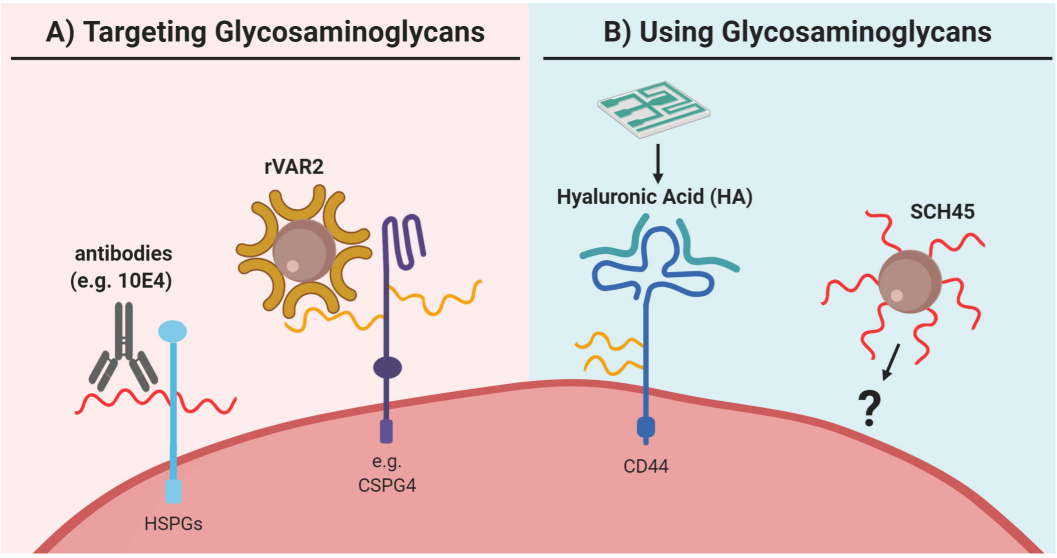

FIGURE 6 | Utilization of glycosaminoglycans for capture of circulating tumor cells (CTCs). **(A)** Glycosaminoglycans can be directly targeted as for example via antibodies like 10E4, which binds to heparan sulfate (HS; in red) of heparan sulfate proteoglycans (HSPGs). However, to our knowledge, this approach has not been explored for CTC capture. Furthermore, for CTC capture the recombinant protein VAR2CSA (rVAR2) can be used, which binds to oncofetal chondroitin sulfate (in yellow) as for example identified on chondroitin sulfate proteoglycan 4 (CSPG4). **(B)** Glycosaminoglycans have been applied in the reversed approach as capture agent for CTC enrichment. Here, glycosaminoglycan-based probes were used to capture CTCs. For example, a microfluidic chip has been coated with hyaluronic acid (HA; in green) to capture CTCs via its interaction with the HA-receptor CD44. Similarly, the heparan sulfate-based probe SCH45 has been coupled to magnetic beads to capture CTCs in hepatocellular carcinoma in a microfluidic setup, but the exact cellular target of SCH45 in these CTCs remains unknown. Generally, both strategies are relatively new for CTC capture and clearly further extensive validation is needed. Please refer to the main text for details and references.

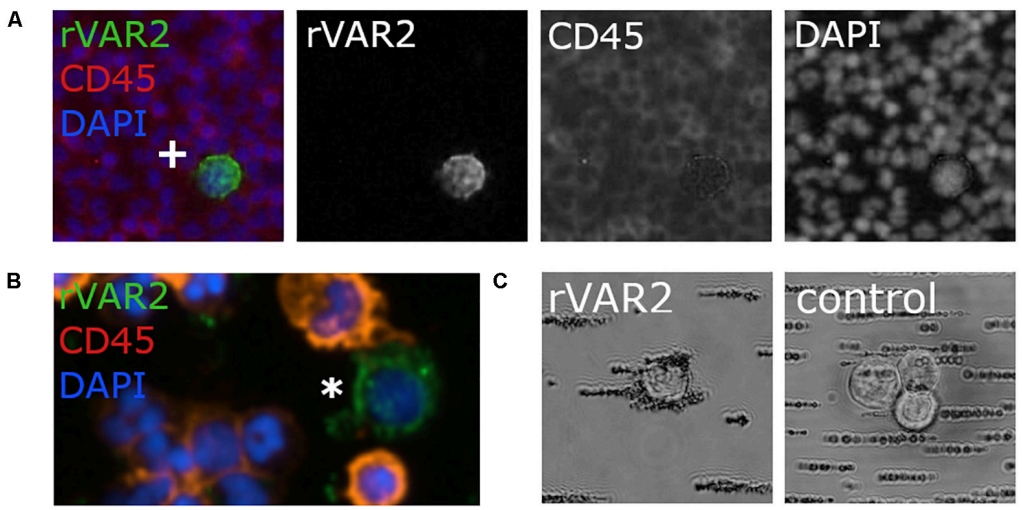

FIGURE 7 | Recombinant VAR2CSA (rVAR2) can be used for staining and capture of potential circulating tumor cells (CTCs). **(A)** Immunofluorescence staining of the colorectal cancer cells COLO205 (marked with cross) with rVAR2 (green), anti-CD45 (in red) to mark normal blood cells, and DAPI (in blue) to mark cell nuclei. **(B)** One potential CTC hit (green by rVAR2 stain; marked with white asterisk) in a blood sample from a colorectal cancer patient with the same staining as described in panel A. **(C)** Magnetic beads coated with rVAR2 bind specifically to COLO205 cells, compared to non-rVAR2 control beads. Pictures were kindly provided by Mette Ø. Agerbæk, Amalie M. Jørgensen, and Nicolai T. Sand.

Actually, the reversed approach can also be utilized for CTC capture (**Figure 6B**). For example, Gopinathan et al. (2020) coated a synthetic HS-based octasaccharide probe (SCH45) onto magnetic beads, that were used in combination with a microfluidic chip to isolate CTCs from 65 advanced or metastatic cholangiocarcinoma patients. Single CTCs or CTC clusters were detected in all samples with $\geq$ 1 CTCs per 1 mL blood, even in patients with no distant metastases. Previous comparable CellSearch®-based studies found only 17% of CCA patients positive for $\geq$2 CTCs per

7.5 mL blood (Yang et al., 2016). However, only three healthy controls were included in the HS-based study. Moreover, the authors reported that studies evaluating whether this approach could be employed to capture EpCAM-negative CTCs are currently ongoing (Gopinathan et al., 2020). In addition it would be interesting to identify the binding target of the SCH45-coated beads in order to characterize the captured CTC population.

Another approach exploited the GAG-receptor function of CD44 in order to capture CTCs (Wang M. et al., 2018). Purified HA, the ligand of CD44, was coated to a microfluidic chip and showed 91% retrieval of CD44-overexpressing A549 cells spiked into blood. Also other cancer cell lines from different cancer entities were captured with comparable efficiencies. Although also lacking healthy controls, the study found between 1–18 putative CTCs per 1 mL blood from 9 of 10 NSCLC and 5 of 5 breast cancer patients as detected through CK- and DAPI-staining.

The utilization of GAGs for CTC technologies is a relatively new approach. Most studies have been limited to smaller pilot studies so far and further molecular characterization of the putative CTC hits is needed to prove their cancer-origin and thus the reliability of the CTC assay. Clearly, the establishment of specific GAGs as biomarkers for clinical CTC diagnostics needs extensive validation in large-scale studies in the future. However, GAGs have the potential to capture or identify broader and more heterogenous CTC populations as they are often independent of a single protein and thus might be less prone to gene expression changes associated with different or transient cancer cell phenotypes.

CONCLUDING REMARKS

Circulating tumor cell analyses have the potential to allow prognostic and predictive insights by convenient liquid biopsies. However, novel biomarkers are needed to enable the necessary assay sensitivity and specificity to detect CTCs. Another unsolved problem is that most CTC assays introduce biases in regards to which CTC subpopulations can be captured as they are often based on single biomarkers. Therefore, a CTC capture approach based on a combination of several biomarkers could be beneficial. Another solution for this problem could be the targeting of cancer-specific changes in the GAGs (the "GAGome"), or other known glycocalyx components, which should in principle, allow the capture of more heterogenous CTC populations. Studies on clinical CTCs and their proteoglycans, GAGs, or general glycocalyx structure are still not strongly represented, probably due to associated technical challenges of glycocalyx characterizations. However, structural insights would be beneficial for improving or defining novel CTC capturing strategies based on proteoglycans or their GAGs and to explore whether these strategies then better reflect the heterogenic cancer cell population.

AUTHOR CONTRIBUTIONS

TA, SB-C, AJ, CL, CS, NS, and MA conceived and drafted the manuscript. TA designed the figures with scientific input from co-authors. All authors critically revised the manuscript.

FUNDING

This research was funded by Independent Research Fund Denmark (Grant Number 8020-00446A), Innovation Fund Denmark (Grant Numbers 7038-00212B and 9090-00024B), HARBOEFONDEN, and Svend Andersen Fonden. TA was supported by the Bridge Translational Excellence Programme, funded by the Novo Nordisk Foundation (Grant Number NNF18SA0034956).

ACKNOWLEDGMENTS

We apologize to anyone whose work was not presented in this review due to space requirements. Schematic figures were created with BioRender.com. **Figure 2A** was reused from Okada et al. (2017), with slight modifications to remove the original panel labeling, under CC BY 4.0 license (https://creativecommons.org/licenses/by/4.0/).

REFERENCES

Abrink, M., Grujic, M., and Pejler, G. (2004). Serglycin is essential for maturation of mast cell secretory granule. *J. Biol. Chem.* 279, 40897–40905. doi: 10.1074/jbc.M405856200

Aceto, N., Bardia, A., Miyamoto, D. T., Donaldson, M. C., Wittner, B. S., Spencer, J. A., et al. (2014). Circulating tumor cell clusters are oligoclonal precursors of breast cancer metastasis. *Cell* 158, 1110–1122. doi: 10.1016/j.cell.2014.07.013

Agerbaek, M. O., Bang-Christensen, S. R., Yang, M. H., Clausen, T. M., Pereira, M. A., Sharma, S., et al. (2018). The VAR2CSA malaria protein efficiently retrieves circulating tumor cells in an EpCAM-independent manner. *Nat. Commun.* 9:3279. doi: 10.1038/s41467-018-05793-2

Ai, X., Do, A. T., Lozynska, O., Kusche-Gullberg, M., Lindahl, U., and Emerson, C. P. (2003). QSulf1 remodels the 6-O sulfation states of cell surface heparan sulfate proteoglycans to promote Wnt signaling. *J. Cell Biol.* 162, 341–351. doi: 10.1083/jcb.200212083

Aird, W. C. (2007). Phenotypic heterogeneity of the endothelium: I. Structure, function, and mechanisms. *Circ. Res.* 100, 158–173. doi: 10.1161/01.RES.0000255691.76142.4a

Akhurst, R. J., and Derynck, R. (2001). TGF-beta signaling in cancer–a double-edged sword. *Trends Cell Biol.* 11, S44–S51. doi: 10.1016/s0962-8924(01)02130-4

Alix-Panabieres, C., Mader, S., and Pantel, K. (2017). Epithelial-mesenchymal plasticity in circulating tumor cells. *J. Mol. Med.* 95, 133–142. doi: 10.1007/978-3-030-35805-1_2

Allard, W. J., Matera, J., Miller, M. C., Repollet, M., Connelly, M. C., Rao, C., et al. (2004). Tumor cells circulate in the peripheral blood of all major carcinomas but not in healthy subjects or patients with nonmalignant diseases. *Clin. Cancer Res.* 10, 6897–6904. doi: 10.1158/1078-0432.CCR-04-0378

Ampofo, E., Schmitt, B. M., Menger, M. D., and Laschke, M. W. (2017). The regulatory mechanisms of NG2/CSPG4 expression. *Cell. Mol. Biol. Lett.* 22:4. doi: 10.1186/s11658-017-0035-3

Anand, K., Roszik, J., Gombos, D., Upshaw, J., Sarli, V., Meas, S., et al. (2019). Pilot study of circulating tumor cells in early-stage and metastatic Uveal Melanoma. *Cancers* 11:856. doi: 10.3390/cancers11060856

Andrlova, H., Mastroianni, J., Madl, J., Kern, J. S., Melchinger, W., Dierbach, H., et al. (2017). Biglycan expression in the melanoma microenvironment promotes invasiveness via increased tissue stiffness inducing integrin-beta1 expression. *Oncotarget* 8, 42901–42916. doi: 10.18632/oncotarget.17160

Aya-Bonilla, C., Gray, E. S., Manikandan, J., Freeman, J. B., Zaenker, P., Reid, A. L., et al. (2019). Immunomagnetic-Enriched Subpopulations of Melanoma Circulating Tumour Cells (CTCs) exhibit distinct transcriptome profiles. *Cancers* 11:157. doi: 10.3390/cancers11020157

Ayres Pereira, M., Mandel Clausen, T., Pehrson, C., Mao, Y., Resende, M., Daugaard, M., et al. (2016). Placental sequestration of plasmodium falciparum malaria parasites is mediated by the interaction between VAR2CSA and chondroitin sulfate A on Syndecan-1. *PLoS Pathog.* 12:e1005831. doi: 10.1371/journal.ppat.1005831

Baccelli, I., Schneeweiss, A., Riethdorf, S., Stenzinger, A., Schillert, A., Vogel, V., et al. (2013). Identification of a population of blood circulating tumor cells from breast cancer patients that initiates metastasis in a xenograft assay. *Nat. Biotechnol.* 31, 539–544. doi: 10.1038/nbt.2576

Bai, T., Mai, R. Y., Ye, J. Z., Chen, J., Qi, L. N., Tang, J., et al. (2020). Circulating tumor cells and CXCR4 in the prognosis of hepatocellular carcinoma. *Transl. Cancer Res.* 9, 1384–1394.

Baietti, M. F., Zhang, Z., Mortier, E., Melchior, A., Degeest, G., Geeraerts, A., et al. (2012). Syndecan-syntenin-ALIX regulates the biogenesis of exosomes. *Nat. Cell Biol.* 14, 677–685. doi: 10.1038/ncb2502

Banerjee, S., Modi, S., Mcginn, O., Zhao, X., Dudeja, V., Ramakrishnan, S., et al. (2016). Impaired synthesis of stromal components in response to minnelide improves vascular function, drug delivery, and survival in pancreatic cancer. *Clin. Cancer Res.* 22, 415–425. doi: 10.1158/1078-0432.CCR-15-1155

Bang-Christensen, S. R., Pedersen, R. S., Pereira, M. A., Clausen, T. M., Loppke, C., Sand, N. T., et al. (2019). Capture and detection of circulating glioma cells using the recombinant VAR2CSA malaria protein. *Cells* 8:998. doi: 10.3390/cells8090998

Barnes, J. M., Kaushik, S., Bainer, R. O., Sa, J. K., Woods, E. C., Kai, F., et al. (2018). A tension-mediated glycocalyx-integrin feedback loop promotes mesenchymal-like glioblastoma. *Nat. Cell Biol.* 20, 1203–1214. doi: 10.1038/s41556-018-0183-3

Bennett, K. L., Jackson, D. G., Simon, J. C., Tanczos, E., Peach, R., Modrell, B., et al. (1995). CD44 isoforms containing exon V3 are responsible for the presentation of heparin-binding growth factor. *J. Cell Biol.* 128, 687–698. doi: 10.1083/jcb.128.4.687

Bi, X., Tong, C., Dockendorff, A., Bancroft, L., Gallagher, L., Guzman, G., et al. (2008). Genetic deficiency of decorin causes intestinal tumor formation through disruption of intestinal cell maturation. *Carcinogenesis* 29, 1435–1440. doi: 10.1093/carcin/bgn141

Bidard, F. C., Huguet, F., Louvet, C., Mineur, L., Bouche, O., Chibaudel, B., et al. (2013). Circulating tumor cells in locally advanced pancreatic adenocarcinoma: the ancillary CirCe 07 study to the LAP 07 trial. *Ann. Oncol.* 24, 2057–2061. doi: 10.1093/annonc/mdt176

Bidard, F. C., Madic, J., Mariani, P., Piperno-Neumann, S., Rampanou, A., Servois, V., et al. (2014). Detection rate and prognostic value of circulating tumor cells and circulating tumor DNA in metastatic uveal melanoma. *Int. J. Cancer* 134, 1207–1213. doi: 10.1002/ijc.28436

Biroccio, A., Cherfils-Vicini, J., Augereau, A., Pinte, S., Bauwens, S., Ye, J., et al. (2013). TRF2 inhibits a cell-extrinsic pathway through which natural killer cells eliminate cancer cells. *Nat. Cell Biol.* 15, 818–828. doi: 10.1038/ncb2774

Bockhorn, M., Jain, R. K., and Munn, L. L. (2007). Active versus passive mechanisms in metastasis: do cancer cells crawl into vessels, or are they pushed? *Lancet Oncol.* 8, 444–448. doi: 10.1016/S1470-2045(07)70140-7

Brunt, L., and Scholpp, S. (2018). The function of endocytosis in Wnt signaling. *Cell. Mol. Life Sci.* 75, 785–795. doi: 10.1007/s00018-017-2654-2

Budczies, J., Von Winterfeld, M., Klauschen, F., Bockmayr, M., Lennerz, J. K., Denkert, C., et al. (2015). The landscape of metastatic progression patterns across major human cancers. *Oncotarget* 6, 570–583. doi: 10.18632/oncotarget.2677

Buffone, A., and Weaver, V. M. (2020). Don't sugarcoat it: how glycocalyx composition influences cancer progression. *J. Cell Biol.* 219:e201910070. doi: 10.1083/jcb.201910070

Bulow, H. E., and Hobert, O. (2006). The molecular diversity of glycosaminoglycans shapes animal development. *Annu. Rev. Cell Dev. Biol.* 22, 375–407. doi: 10.1146/annurev.cellbio.22.010605.093433

Burdick, M. M., Henson, K. A., Delgadillo, L. F., Choi, Y. E., Goetz, D. J., Tees, D. F. J., et al. (2012). Expression of E-selectin ligands on circulating tumor cells: Cross-regulation with cancer stem cell regulatory pathways? *Front. Oncol.* 2:103. doi: 10.3389/fonc.2012.00103

Butler, P. J., and Bhatnagar, A. (2019). Mechanobiology of the abluminal glycocalyx. *Biorheology* 56, 101–112.

Cackowski, F. C., Xu, L., Hu, B., and Cheng, S. Y. (2004). Identification of two novel alternatively spliced Neuropilin-1 isoforms. *Genomics* 84, 82–94. doi: 10.1016/j.ygeno.2004.02.001

Capurro, M., Martin, T., Shi, W., and Filmus, J. (2014). Glypican-3 binds to Frizzled and plays a direct role in the stimulation of canonical Wnt signaling. *J. Cell Sci.* 127, 1565–1575. doi: 10.1242/jcs.140871

Capurro, M., Wanless, I. R., Sherman, M., Deboer, G., Shi, W., Miyoshi, E., et al. (2003). Glypican-3: a novel serum and histochemical marker for hepatocellular carcinoma. *Gastroenterology* 125, 89–97. doi: 10.1016/s0016-5085(03)00689-9

Capurro, M. I., Xiang, Y. Y., Lobe, C., and Filmus, J. (2005). Glypican-3 promotes the growth of hepatocellular carcinoma by stimulating canonical Wnt signaling. *Cancer Res.* 65, 6245–6254. doi: 10.1158/0008-5472.CAN-04-4244

Carneiro, B. R., Pernambuco Filho, P. C., Mesquita, A. P., Da Silva, D. S., Pinhal, M. A., Nader, H. B., et al. (2014). Acquisition of anoikis resistance up-regulates syndecan-4 expression in endothelial cells. *PLoS One* 9:e116001. doi: 10.1371/journal.pone.0116001

Cassinelli, G., and Lanzi, C. (2020). Heparanase: a potential therapeutic target in sarcomas. *Adv. Exp. Med. Biol.* 1221, 405–431. doi: 10.1007/978-3-030-34521-1_15

Cavallaro, U., and Christofori, G. (2001). Cell adhesion in tumor invasion and metastasis: loss of the glue is not enough. *Biochim. Biophys. Acta* 1552, 39–45. doi: 10.1016/s0304-419x(01)00038-5

Chaffer, C. L., and Weinberg, R. A. (2011). A perspective on cancer cell metastasis. *Science* 331, 1559–1564.

Chandrasekaran, E. V., and Davidson, E. A. (1979). Glycosaminoglycans of normal and malignant cultured human mammary cells. *Cancer Res.* 39, 870–880.

Cheifetz, S., Andres, J. L., and Massague, J. (1988). The transforming growth factor-beta receptor type III is a membrane proteoglycan. Domain structure of the receptor. *J. Biol. Chem.* 263, 16984–16991.

Chekenya, M., Krakstad, C., Svendsen, A., Netland, I. A., Staalesen, V., Tysnes, B. B., et al. (2008). The progenitor cell marker NG2/MPG promotes chemoresistance by activation of integrin-dependent PI3K/Akt signaling. *Oncogene* 27, 5182–5194. doi: 10.1038/onc.2008.157

Chen, C., Zhao, S., Karnad, A., and Freeman, J. W. (2018). The biology and role of CD44 in cancer progression: therapeutic implications. *J. Hematol. Oncol.* 11:64. doi: 10.1186/s13045-018-0605-5

Chen, R. L., and Lander, A. D. (2001). Mechanisms underlying preferential assembly of heparan sulfate on glypican-1. *J. Biol. Chem.* 276, 7507–7517. doi: 10.1074/jbc.M008283200

Chen, Y. H., Narimatsu, Y., Clausen, T. M., Gomes, C., Karlsson, R., Steentoft, C., et al. (2018). The GAGOme: a cell-based library of displayed glycosaminoglycans. *Nat. Methods* 15, 881–888. doi: 10.1038/s41592-018-0086-z

Cherfils-Vicini, J., Iltis, C., Cervera, L., Pisano, S., Croce, O., Sadouni, N., et al. (2019). Cancer cells induce immune escape via glycocalyx changes controlled by the telomeric protein TRF2. *EMBO J.* 38:e100012. doi: 10.15252/embj.2018100012

Cheung, K. J., Padmanaban, V., Silvestri, V., Schipper, K., Cohen, J. D., Fairchild, A. N., et al. (2016). Polyclonal breast cancer metastases arise from collective dissemination of keratin 14-expressing tumor cell clusters. *Proc. Natl. Acad. Sci. U.S.A.* 113, E854–E863. doi: 10.1073/pnas.1508541113

Chiodelli, P., Bugatti, A., Urbinati, C., and Rusnati, M. (2015). Heparin/Heparan sulfate proteoglycans glycomic interactome in angiogenesis: biological

implications and therapeutical use. *Molecules* 20, 6342–6388. doi: 10.3390/molecules20046342

Cichy, J., and Puré, E. (2003). The liberation of CD44. *J. Cell Biol.* 161, 839–843.

Cieply, B., Koontz, C., and Frisch, S. M. (2015). CD44S-hyaluronan interactions protect cells resulting from EMT against anoikis. *Matrix Biol.* 48, 55–65. doi: 10.1016/j.matbio.2015.04.010

Clark, R. A. F., Lin, F., Greiling, D., An, J., and Couchman, J. R. (2004). Fibroblast invasive migration into fibronectin/fibrin gels requires a previously uncharacterized dermatan sulfate-CD44 proteoglycan. *J. Invest. Dermatol.* 122, 266–277. doi: 10.1046/j.0022-202X.2004.22205.x

Clausen, T. M., Pereira, M. A., Al Nakouzi, N., Oo, H. Z., Agerbaek, M. O., Lee, S., et al. (2016). Oncofetal chondroitin sulfate glycosaminoglycans are key players in integrin signaling and tumor cell motility. *Mol. Cancer Res.* 14, 1288–1299. doi: 10.1158/1541-7786.MCR-16-0103

Cohen, S. J., Punt, C. J., Iannotti, N., Saidman, B. H., Sabbath, K. D., Gabrail, N. Y., et al. (2009). Prognostic significance of circulating tumor cells in patients with metastatic colorectal cancer. *Ann. Oncol.* 20, 1223–1229. doi: 10.1016/j.yexmp.2018.12.006

Cole, C. L., Rushton, G., Jayson, G. C., and Avizienyte, E. (2014). Ovarian cancer cell heparan sulfate 6-O-sulfotransferases regulate an angiogenic program induced by heparin-binding epidermal growth factor (EGF)-like growth factor/EGF receptor signaling. *J. Biol. Chem.* 289, 10488–10501. doi: 10.1074/jbc.M113.534263

Colombino, M., Capone, M., Lissia, A., Cossu, A., Rubino, C., De Giorgi, V., et al. (2012). BRAF/NRAS mutation frequencies among primary tumors and metastases in patients with melanoma. *J. Clin. Oncol.* 30, 2522–2529. doi: 10.1200/JCO.2011.41.2452

Colombo, M., Giannandrea, D., Lesma, E., Basile, A., and Chiaramonte, R. (2019). Extracellular vesicles enhance multiple myeloma metastatic dissemination. *Int. J. Mol. Sci.* 20:3236. doi: 10.3390/ijms20133236

Cooney, C. A., Jousheghany, F., Yao-Borengasser, A., Phanavanh, B., Gomes, T., Kieber-Emmons, A. M., et al. (2011). Chondroitin sulfates play a major role in breast cancer metastasis: a role for CSPG4 and CHST11 gene expression in forming surface P-selectin ligands in aggressive breast cancer cells. *Breast Cancer Res.* 13:R58.

Coumans, F., and Terstappen, L. (2015). Detection and characterization of circulating tumor cells by the CellSearch approach. *Methods Mol. Biol.* 1347, 263–278. doi: 10.1007/978-1-4939-2990-0_18

Court, C. M., Hou, S., Winograd, P., Segel, N. H., Li, Q. W., Zhu, Y., et al. (2018). A novel multimarker assay for the phenotypic profiling of circulating tumor cells in hepatocellular carcinoma. *Liver Transpl.* 24, 946–960. doi: 10.1002/lt.25062

Cristofanilli, M., Budd, G. T., Ellis, M. J., Stopeck, A., Matera, J., Miller, M. C., et al. (2004). Circulating tumor cells, disease progression, and survival in metastatic breast cancer. *N. Engl. J. Med.* 351, 781–791. doi: 10.1053/j.seminoncol.2006.03.016

Daniotti, J. L., Lardone, R. D., and Vilcaes, A. A. (2015). Dysregulated expression of glycolipids in tumor cells: from negative modulator of anti-tumor immunity to promising targets for developing therapeutic agents. *Front. Oncol.* 5:300. doi: 10.3389/fonc.2015.00300

de Bono, J. S., Scher, H. I., Montgomery, R. B., Parker, C., Miller, M. C., Tissing, H., et al. (2008). Circulating tumor cells predict survival benefit from treatment in metastatic castration-resistant prostate cancer. *Clin. Cancer Res.* 14, 6302–6309. doi: 10.1158/1078-0432.CCR-08-0872

de Groot, A. E., Roy, S., Brown, J. S., Pienta, K. J., and Amend, S. R. (2017). Revisiting seed and soil: examining the primary tumor and cancer cell foraging in metastasis. *Mol. Cancer Res.* 15, 361–370. doi: 10.1158/1541-7786.MCR-16-0436

De Klerk, D. P., Lee, D. V., and Human, H. J. (1984). Glycosaminoglycans of human prostatic cancer. *J. Urol.* 131, 1008–1012.

de Wit, S., Manicone, M., Rossi, E., Lampignano, R., Yang, L., Zill, B., et al. (2018). EpCAM(high) and EpCAM(low) circulating tumor cells in metastatic prostate and breast cancer patients. *Oncotarget* 9, 35705–35716. doi: 10.18632/oncotarget.26298

Dianat-Moghadam, H., Azizi, M., Eslami, S. Z., Cortes-Hernandez, L. E., Heidarifard, M., Nouri, M., et al. (2020). The role of circulating tumor cells in the metastatic cascade: biology, technical challenges, and clinical relevance. *Cancers* 12:867. doi: 10.3390/cancers12040867

Dick, G., Akslen-Hoel, L. K., Grondahl, F., Kjos, I., and Prydz, K. (2012). Proteoglycan synthesis and Golgi organization in polarized epithelial cells. *J. Histochem. Cytochem.* 60, 926–935. doi: 10.1369/0022155412461256

Dimitroff, C. J., Lechpammer, M., Long-Woodward, D., and Kutok, J. L. (2004). Rolling of human bone-metastatic prostate tumor cells on human bone marrow endothelium under shear flow is mediated by E-selectin. *Cancer Res.* 64, 5261–5269.

Dimitroff, C. J., Lee, J. Y., Rafii, S., Fuhlbrigge, R. C., and Sackstein, R. (2001a). Cd44 is a Major E-Selectin Ligand on human hematopoietic progenitor cells. *J. Cell Biol.* 153, 1277–1286. doi: 10.1083/jcb.153.6.1277

Dimitroff, C. J., Lee, J. Y., Schor, K. S., Sandmaier, B. M., and Sackstein, R. (2001b). Differential L-Selectin Binding Activities of Human Hematopoietic Cell L-Selectin Ligands, HCELL and PSGL-1. *J. Biol. Chem.* 276, 47623–47631. doi: 10.1074/jbc.M105997200

Domev, H., Amit, M., Laevsky, I., Dar, A., and Itskovitz-Eldor, J. (2012). Efficient engineering of vascularized ectopic bone from human embryonic stem cell–derived mesenchymal stem cells. *Tissue Eng. Part A* 18, 2290–2302. doi: 10.1089/ten.TEA.2011.0371

Dours-Zimmermann, M. T., and Zimmermann, D. R. (1994). A novel glycosaminoglycan attachment domain identified in two alternative splice variants of human versican. *J. Biol. Chem.* 269, 32992–32998.

Eccles, S. A. (1999). Heparanase: breaking down barriers in tumors. *Nat. Med.* 5, 735–736. doi: 10.1038/10455

Echtermeyer, F., Baciu, P. C., Saoncella, S., Ge, Y., and Goetinck, P. F. (1999). Syndecan-4 core protein is sufficient for the assembly of focal adhesions and actin stress fibers. *J. Cell Sci.* 112(Pt 20), 3433–3441.

Effenberger, K. E., Schroeder, C., Hanssen, A., Wolter, S., Eulenburg, C., Tachezy, M., et al. (2018). Improved risk stratification by circulating tumor cell counts in pancreatic cancer. *Clin. Cancer Res.* 24, 2844–2850. doi: 10.1158/1078-0432.CCR-18-0120

Elderbroom, J. L., Huang, J. J., Gatza, C. E., Chen, J., How, T., Starr, M., et al. (2014). Ectodomain shedding of TbetaRIII is required for TbetaRIII-mediated suppression of TGF-beta signaling and breast cancer migration and invasion. *Mol. Biol. Cell* 25, 2320–2332. doi: 10.1091/mbc.E13-09-0524

Elgundi, Z., Papanicolaou, M., Major, G., Cox, T. R., Melrose, J., Whitelock, J. M., et al. (2019). Cancer metastasis: the role of the extracellular matrix and the heparan sulfate proteoglycan perlecan. *Front. Oncol.* 9:1482. doi: 10.3389/fonc.2019.01482

Ellis, L. M. (2006). The role of neuropilins in cancer. *Mol. Cancer Ther.* 5, 1099–1107.

Esko, J. D., and Zhang, L. (1996). Influence of core protein sequence on glycosaminoglycan assembly. *Curr. Opin. Struct. Biol.* 6, 663–670. doi: 10.1016/s0959-440x(96)80034-0

Fang, C., Fan, C., Wang, C., Huang, Q., Meng, W., Yu, Y., et al. (2017). Prognostic value of CD133(+) CD54(+) CD44(+) circulating tumor cells in colorectal cancer with liver metastasis. *Cancer Med.* 6, 2850–2857. doi: 10.1002/cam4.1241

Fares, J., Fares, M. Y., Khachfe, H. H., Salhab, H. A., and Fares, Y. (2020). Molecular principles of metastasis: a hallmark of cancer revisited. *Signal Transduct. Target. Ther.* 5:28. doi: 10.1038/s41392-020-0134-x

Feng, M., Gao, W., Wang, R., Chen, W., Man, Y. G., Figg, W. D., et al. (2013). Therapeutically targeting glypican-3 via a conformation-specific single-domain antibody in hepatocellular carcinoma. *Proc. Natl. Acad. Sci. U.S.A.* 110, E1083–E1091. doi: 10.1073/pnas.1217868110

Ferrara, N., Gerber, H.-P., and LeCouter, J. (2003). The biology of VEGF and its receptors. 9, 669–676. doi: 10.1038/nm0603-669

Fidler, I. J. (1978). Tumor heterogeneity and the biology of cancer invasion and metastasis. *Cancer Res.* 38, 2651–2660. doi: 10.1158/0008-5472.CAN-16-1330

Filmus, J., Capurro, M., and Rast, J. (2008). Glypicans. *Genome Biol.* 9:224.

Fisher, L. W., Termine, J. D., and Young, M. F. (1989). Deduced protein sequence of bone small proteoglycan I (biglycan) shows homology with proteoglycan II (decorin) and several nonconnective tissue proteins in a variety of species. *J. Biol. Chem.* 264, 4571–4576.

Fitzgerald, T. L., and McCubrey, J. A. (2014). Pancreatic cancer stem cells: association with cell surface markers, prognosis, resistance, metastasis and treatment. *Adv. Biol. Regul.* 56, 45–50. doi: 10.1016/j.jbior.2014.05.001

Frankel, P., Pellet-Many, C., Lehtolainen, P., D'abaco, G. M., Tickner, M. L., Cheng, L., et al. (2008). Chondroitin sulphate-modified neuropilin 1 is expressed

in human tumour cells and modulates 3D invasion in the U87MG human glioblastoma cell line through a p130Cas-mediated pathway. *EMBO Rep.* 9, 983–989. doi: 10.1038/embor.2008.151

Franken, B., De Groot, M. R., Mastboom, W. J., Vermes, I., Van Der Palen, J., Tibbe, A. G., et al. (2012). Circulating tumor cells, disease recurrence and survival in newly diagnosed breast cancer. *Breast Cancer Res.* 14:R133. doi: 10.1186/bcr3333

Freeman, J. B., Gray, E. S., Millward, M., Pearce, R., and Ziman, M. (2012). Evaluation of a multi-marker immunomagnetic enrichment assay for the quantification of circulating melanoma cells. *J. Transl. Med.* 10:192. doi: 10.1186/1479-5876-10-192

Fukuda, M., Hiraoka, N., and Yeh, J.-C. (1999). C-Type Lectins and Sialyl Lewis X oligosaccharides: versatile roles in cell–cell interaction. *J. Cell Biol.* 147, 467–470. doi: 10.1083/jcb.147.3.467

Gagnon, M. L., Bielenberg, D. R., Gechtman, Z., Miao, H. Q., Takashima, S., Soker, S., et al. (2000). Identification of a natural soluble neuropilin-1 that binds vascular endothelial growth factor: *in vivo* expression and antitumor activity. *Proc. Natl. Acad. Sci. U.S.A.* 97, 2573–2578. doi: 10.1073/pnas.040337597

Gao, W., Kim, H., Feng, M., Phung, Y., Xavier, C. P., Rubin, J. S., et al. (2014). Inactivation of Wnt signaling by a human antibody that recognizes the heparan sulfate chains of glypican-3 for liver cancer therapy. *Hepatology* 60, 576–587. doi: 10.1002/hep.26996

Garcia-Roman, J., and Zentella-Dehesa, A. (2013). Vascular permeability changes involved in tumor metastasis. *Cancer Lett.* 335, 259–269. doi: 10.1016/j.canlet.2013.03.005

Gasch, C., Bauernhofer, T., Pichler, M., Langer-Freitag, S., Reeh, M., Seifert, A. M., et al. (2013). Heterogeneity of epidermal growth factor receptor status and mutations of KRAS/PIK3CA in circulating tumor cells of patients with colorectal cancer. *Clin. Chem.* 59, 252–260. doi: 10.1373/clinchem.2012.188557

Gazzaniga, P., Gianni, W., Raimondi, C., Gradilone, A., Lo Russo, G., Longo, F., et al. (2013). Circulating tumor cells in high-risk nonmetastatic colorectal cancer. *Tumour Biol.* 34, 2507–2509. doi: 10.1007/s13277-013-0752-9

Ghajar, C. M., Peinado, H., Mori, H., Matei, I. R., Evason, K. J., Brazier, H., et al. (2013). The perivascular niche regulates breast tumour dormancy. *Nat. Cell Biol.* 15, 807–817. doi: 10.1038/ncb2767

Ghiselli, G., and Maccarana, M. (2016). Drugs affecting glycosaminoglycan metabolism. *Drug Discov. Today* 21, 1162–1169.

Goddard, E. T., Bozic, I., Riddell, S. R., and Ghajar, C. M. (2018). Dormant tumour cells, their niches and the influence of immunity. *Nat. Cell Biol.* 20, 1240–1249. doi: 10.1038/s41556-018-0214-0

Gomez Toledo, A., Nilsson, J., Noborn, F., Sihlbom, C., and Larson, G. (2015). Positive mode LC-MS/MS analysis of chondroitin sulfate modified glycopeptides derived from light and heavy chains of the human Inter-alpha-Trypsin inhibitor complex. *Mol. Cell. Proteomics* 14, 3118–3131. doi: 10.1074/mcp.M115.051136

Goodison, S., Urquidi, V., and Tarin, D. (1999). CD44 cell adhesion molecules. *Mol. Pathol.* 52, 189–196.

Gopinathan, P., Chiang, N.-J., Bandaru, A., Sinha, A., Huang, W.-Y., Hung, S.-C., et al. (2020). Exploring circulating tumor cells in cholangiocarcinoma using a novel glycosaminoglycan probe on a microfluidic platform. *Adv. Healthc. Mater.* 9:1901875. doi: 10.1002/adhm.201901875

Goretzki, L., Burg, M. A., Grako, K. A., and Stallcup, W. B. (1999). High-affinity binding of basic fibroblast growth factor and platelet-derived growth factor-AA to the core protein of the NG2 proteoglycan. *J. Biol. Chem.* 274, 16831–16837. doi: 10.1074/jbc.274.24.16831

Gorges, K., Wiltfang, L., Gorges, T. M., Sartori, A., Hildebrandt, L., Keller, L., et al. (2019). Intra-patient heterogeneity of circulating tumor cells and circulating tumor DNA in blood of melanoma patients. *Cancers* 11:1685. doi: 10.3390/cancers11111685

Gorges, T. M., Tinhofer, I., Drosch, M., Rose, L., Zollner, T. M., Krahn, T., et al. (2012). Circulating tumour cells escape from EpCAM-based detection due to epithelial-to-mesenchymal transition. *BMC Cancer* 12:178. doi: 10.1186/1471-2407-12-178

Gowda, D. C. (2006). Role of chondroitin-4-sulfate in pregnancy-associated malaria. *Adv. Pharmacol.* 53, 375–400. doi: 10.1016/S1054-3589(05)53018-7

Gray, E. S., Reid, A. L., Bowyer, S., Calapre, L., Siew, K., Pearce, R., et al. (2015). Circulating melanoma cell subpopulations: their heterogeneity and differential responses to treatment. *J. Invest. Dermatol.* 135, 2040–2048. doi: 10.1038/jid.2015.127

Greene, B. T., Hughes, A. D., and King, M. R. (2012). Circulating tumor cells: the substrate of personalized medicine? *Front. Oncol.* 2:69. doi: 10.3389/fonc.2012.00069

Greenfield, B., Wang, W.-C., Marquardt, H., Piepkorn, M., Wolff, E. A., Aruffo, A., et al. (1999). Characterization of the heparan sulfate and chondroitin sulfate assembly sites in CD44. *J. Biol. Chem.* 274, 2511–2517. doi: 10.1074/jbc.274.4.2511

Grigoriu, B. D., Depontieu, F., Scherpereel, A., Gourcerol, D., Devos, P., Ouatas, T., et al. (2006). Endocan expression and relationship with survival in human non-small cell lung cancer. *Clin. Cancer Res.* 12, 4575–4582. doi: 10.1158/1078-0432.CCR-06-0185

Gronthos, S., Franklin, D. M., Leddy, H. A., Robey, P. G., Storms, R. W., and Gimble, J. M. (2001). Surface protein characterization of human adipose tissue-derived stromal cells. *J. Cell. Physiol.* 189, 54–63. doi: 10.1002/jcp.1138

Gundem, G., Van Loo, P., Kremeyer, B., Alexandrov, L. B., Tubio, J. M. C., Papaemmanuil, E., et al. (2015). The evolutionary history of lethal metastatic prostate cancer. *Nature* 520, 353–357. doi: 10.1016/j.urolonc.2016.02.004

Guo, J. Y., Chiu, C. H., Wang, M. J., Li, F. A., and Chen, J. Y. (2020). Proteoglycan serglycin promotes non-small cell lung cancer cell migration through the interaction of its glycosaminoglycans with CD44. *J. Biomed. Sci.* 27:2. doi: 10.1186/s12929-019-0600-3

Guo, J. Y., Hsu, H. S., Tyan, S. W., Li, F. Y., Shew, J. Y., Lee, W. H., et al. (2017). Serglycin in tumor microenvironment promotes non-small cell lung cancer aggressiveness in a CD44-dependent manner. *Oncogene* 36, 2457–2471. doi: 10.1038/onc.2016.404

Hall, C. S., Ross, M., Bowman Bauldry, J. B., Upshaw, J., Karhade, M. G., Royal, R., et al. (2018). Circulating tumor cells in stage IV melanoma patients. *J. Am. Coll. Surg.* 227, 116–124. doi: 10.1016/j.jamcollsurg.2018.04.026

Hamaoka, M., Kobayashi, T., Tanaka, Y., Mashima, H., and Ohdan, H. (2019). Clinical significance of glypican-3-positive circulating tumor cells of hepatocellular carcinoma patients: a prospective study. *PLoS One* 14:e0217586. doi: 10.1371/journal.pone.0217586

Hanahan, D., and Weinberg, R. A. (2011). Hallmarks of cancer: the next generation. *Cell* 144, 646–674.

Hanley, W. D., Napier, S. L., Burdick, M. M., Schnaar, R. L., Sackstein, R., and Konstantopoulos, K. (2006). Variant isoforms of CD44 are P- and L-selectin ligands on colon carcinoma cells. *FASEB J.* 20, 337–339.

Hatabe, S., Kimura, H., Arao, T., Kato, H., Hayashi, H., Nagai, T., et al. (2013). Overexpression of heparan sulfate 6-O-sulfotransferase-2 in colorectal cancer. *Mol. Clin. Oncol.* 1, 845–850. doi: 10.3892/mco.2013.151

Hayashida, K., Johnston, D. R., Goldberger, O., and Park, P. W. (2006). Syndecan-1 expression in epithelial cells is induced by transforming growth factor beta through a PKA-dependent pathway. *J. Biol. Chem.* 281, 24365–24374. doi: 10.1074/jbc.M509320200

He, J., Zeng, Z. C., Xiang, Z. L., and Yang, P. (2014). Mass spectrometry-based serum peptide profiling in hepatocellular carcinoma with bone metastasis. *World J. Gastroenterol.* 20, 3025–3032. doi: 10.3748/wjg.v20.i11.3025

He, L., Zhou, X., Qu, C., Tang, Y., Zhang, Q., and Hong, J. (2013). Serglycin (SRGN) overexpression predicts poor prognosis in hepatocellular carcinoma patients. *Med. Oncol.* 30:707. doi: 10.1007/s12032-013-0707-4

Hempel, N., How, T., Dong, M., Murphy, S. K., Fields, T. A., and Blobe, G. C. (2007). Loss of betaglycan expression in ovarian cancer: role in motility and invasion. *Cancer Res.* 67, 5231–5238. doi: 10.1158/0008-5472.CAN-07-0035

Hendricks, C., Dubail, J., Brohee, L., Delforge, Y., Colige, A., and Deroanne, C. (2016). A novel physiological glycosaminoglycan-deficient splice variant of neuropilin-1 is anti-tumorigenic *in vitro* and *in vivo*. *PLoS One* 11:e0165153. doi: 10.1371/journal.pone.0165153

Hillig, T., Horn, P., Nygaard, A. B., Haugaard, A. S., Nejlund, S., Brandslund, I., et al. (2015). *In vitro* detection of circulating tumor cells compared by the CytoTrack and CellSearch methods. *Tumour Biol.* 36, 4597–4601. doi: 10.1007/s13277-015-3105-z

Hippo, Y., Watanabe, K., Watanabe, A., Midorikawa, Y., Yamamoto, S., Ihara, S., et al. (2004). Identification of soluble NH2-terminal fragment of glypican-3 as a serological marker for early-stage hepatocellular carcinoma. *Cancer Res.* 64, 2418–2423. doi: 10.1158/0008-5472.can-03-2191

Holderfield, M., Deuker, M. M., Mccormick, F., and Mcmahon, M. (2014). Targeting RAF kinases for cancer therapy: BRAF-mutated melanoma and beyond. *Nat. Rev. Cancer* 14, 455–467. doi: 10.1038/nrc3760

Hoshino, A., Costa-Silva, B., Shen, T. L., Rodrigues, G., Hashimoto, A., Tesic Mark, M., et al. (2015). Tumour exosome integrins determine organotropic metastasis. *Nature* 527, 329–335. doi: 10.1038/nature15756

Hou, X. M., Zhang, T., Da, Z., and Wu, X. A. (2019). CHPF promotes lung adenocarcinoma proliferation and anti-apoptosis via the MAPK pathway. *Pathol. Res. Pract.* 215, 988–994. doi: 10.1016/j.prp.2019.02.005

Hristozova, T., Konschak, R., Budach, V., and Tinhofer, I. (2012). A simple multicolor flow cytometry protocol for detection and molecular characterization of circulating tumor cells in epithelial cancers. *Cytometry A* 81, 489–495. doi: 10.1002/cyto.a.22041

Hsu, S.-H. C., Nadesan, P., Puviindran, V., Stallcup, W. B., Kirsch, D. G., and Alman, B. A. (2018). Effects of chondroitin sulfate proteoglycan 4 (NG2/CSPG4) on soft-tissue sarcoma growth depend on tumor developmental stage. *J. Biol. Chem.* 293, 2466–2475. doi: 10.1074/jbc.M117.805051

Hu, B., Guo, P., Bar-Joseph, I., Imanishi, Y., Jarzynka, M. J., Bogler, O., et al. (2007). Neuropilin-1 promotes human glioma progression through potentiating the activity of the HGF/SF autocrine pathway. *Oncogene* 26, 5577–5586. doi: 10.1038/sj.onc.1210348

Hu, B., Shi, C., Tian, Y., Zhang, Y., Xu, C., Chen, H., et al. (2015). TGF-beta induces up-regulation of chondroitin sulfate synthase 1 (CHSY1) in nucleus pulposus cells through MAPK signaling. *Cell. Physiol. Biochem.* 37, 793–804. doi: 10.1159/000430396

Hu, L., Duan, Y. T., Li, J. F., Su, L. P., Yan, M., Zhu, Z. G., et al. (2014). Biglycan enhances gastric cancer invasion by activating FAK signaling pathway. *Oncotarget* 5, 1885–1896. doi: 10.18632/oncotarget.1871

Hu, L., Zang, M. D., Wang, H. X., Li, J. F., Su, L. P., Yan, M., et al. (2016). Biglycan stimulates VEGF expression in endothelial cells by activating the TLR signaling pathway. *Mol. Oncol.* 10, 1473–1484. doi: 10.1016/j.molonc.2016.08.002

Huang, J., Pan, C., Hu, H., Zheng, S., and Ding, L. (2012). Osteopontin-enhanced hepatic metastasis of colorectal cancer cells. *PLoS One* 7:e47901. doi: 10.1371/journal.pone.0047901

Husemann, Y., Geigl, J. B., Schubert, F., Musiani, P., Meyer, M., Burghart, E., et al. (2008). Systemic spread is an early step in breast cancer. *Cancer Cell* 13, 58–68. doi: 10.1016/j.ccr.2007.12.003

Hyun, K. A., Koo, G. B., Han, H., Sohn, J., Choi, W., Kim, S. I., et al. (2016). Epithelial-to-mesenchymal transition leads to loss of EpCAM and different physical properties in circulating tumor cells from metastatic breast cancer. *Oncotarget* 7, 24677–24687. doi: 10.18632/oncotarget.8250

Igelmann, S., Neubauer, H. A., and Ferbeyre, G. (2019). STAT3 and STAT5 activation in solid cancers. *Cancers* 11:1428. doi: 10.3390/cancers11101428

Iida, J., Wilhelmson, K. L., Ng, J., Lee, P., Morrison, C., Tam, E., et al. (2007). Cell surface chondroitin sulfate glycosaminoglycan in melanoma: role in the activation of pro-MMP-2 (pro-gelatinase A). *Biochem. J.* 403, 553–563. doi: 10.1042/BJ20061176

Ilie, M., Hofman, V., Leroy, S., Cohen, C., Heeke, S., Cattet, F., et al. (2018). Use of circulating tumor cells in prospective clinical trials for NSCLC patients - standardization of the pre-analytical conditions. *Clin. Chem. Lab. Med.* 56, 980–989. doi: 10.1515/cclm-2017-0764

Ilieva, K. M., Cheung, A., Mele, S., Chiaruttini, G., Crescioli, S., Griffin, M., et al. (2018). Chondroitin sulfate proteoglycan 4 and its potential as an antibody immunotherapy target across different tumor types. *Front. Immunol.* 8:1911. doi: 10.3389/fimmu.2017.01911

Iozzo, R. V., and Sanderson, R. D. (2011). Proteoglycans in cancer biology, tumour microenvironment and angiogenesis. *J. Cell. Mol. Med.* 15, 1013–1031. doi: 10.1111/j.1582-4934.2010.01236.x

Iozzo, R. V., and Schaefer, L. (2015). Proteoglycan form and function: a comprehensive nomenclature of proteoglycans. *Matrix Biol.* 42, 11–55. doi: 10.1016/j.matbio.2015.02.003

Itano, N. (2008). Simple primary structure, complex turnover regulation and multiple roles of hyaluronan. *J. Biochem.* 144, 131–137. doi: 10.1093/jb/mvn046

Jacobsen, F., Kraft, J., Schroeder, C., Hube-Magg, C., Kluth, M., Lang, D. S., et al. (2017). Up-regulation of biglycan is associated with poor prognosis and PTEN deletion in patients with prostate cancer. *Neoplasia* 19, 707–715. doi: 10.1016/j.neo.2017.06.003

Jaiswal, S., Jamieson, C. H., Pang, W. W., Park, C. Y., Chao, M. P., Majeti, R., et al. (2009). CD47 is upregulated on circulating hematopoietic stem cells and leukemia cells to avoid phagocytosis. *Cell* 138, 271–285. doi: 10.1016/j.cell.2009.05.046

Jamil, N. S. M., Azfer, A., Worrell, H., and Salter, D. M. (2016). Functional roles of CSPG4/NG2 in chondrosarcoma. *Int. J. Exp. Pathol.* 97, 178–186. doi: 10.1111/iep.12189

Jarvinen, T. A., and Prince, S. (2015). Decorin: a growth factor antagonist for tumor growth inhibition. *Biomed Res. Int.* 2015:654765. doi: 10.1155/2015/654765

Jenkins, L. M., Singh, P., Varadaraj, A., Lee, N. Y., Shah, S., Flores, H. V., et al. (2016). Altering the proteoglycan state of transforming growth factor beta type III receptor (TbetaRIII)/Betaglycan modulates canonical wnt/beta-catenin signaling. *J. Biol. Chem.* 291, 25716–25728. doi: 10.1074/jbc.M116.748624

Johnson, P., Maiti, A., Brown, K. L., and Li, R. (2000). A role for the cell adhesion molecule CD44 and sulfation in leukocyte–endothelial cell adhesion during an inflammatory response? *Biochem. Pharmacol.* 59, 455–465. doi: 10.1016/s0006-2952(99)00266-x

Jubb, A. M., Strickland, L. A., Liu, S. D., Mak, J., Schmidt, M., and Koeppen, H. (2012). Neuropilin-1 expression in cancer and development. *J. Pathol.* 226, 50–60.

Kaigorodova, E. V., Savelieva, O. E., Tashireva, L. A., Tarabanovskaya, N. A., Simolina, E. I., Denisov, E. V., et al. (2018). Heterogeneity of circulating tumor cells in neoadjuvant chemotherapy of breast cancer. *Molecules* 23:727. doi: 10.3390/molecules23040727

Karabacak, N. M., Spuhler, P. S., Fachin, F., Lim, E. J., Pai, V., Ozkumur, E., et al. (2014). Microfluidic, marker-free isolation of circulating tumor cells from blood samples. *Nat. Protoc.* 9, 694–710. doi: 10.1038/nprot.2014.044

Katoh, S., Goi, T., Naruse, T., Ueda, Y., Kurebayashi, H., Nakazawa, T., et al. (2015). Cancer stem cell marker in circulating tumor cells: expression of CD44 Variant Exon 9 is strongly correlated to treatment refractoriness, recurrence and prognosis of human colorectal cancer. *Anticancer Res.* 35, 239–244.

Kaur, S., Kuznetsova, S. A., Pendrak, M. L., Sipes, J. M., Romeo, M. J., Li, Z., et al. (2011). Heparan sulfate modification of the transmembrane receptor CD47 is necessary for inhibition of T cell receptor signaling by thrombospondin-1. *J. Biol. Chem.* 286, 14991–15002. doi: 10.1074/jbc.M110.179663

Khoja, L., Lorigan, P., Zhou, C., Lancashire, M., Booth, J., Cummings, J., et al. (2013). Biomarker utility of circulating tumor cells in metastatic cutaneous melanoma. *J. Invest. Dermatol.* 133, 1582–1590. doi: 10.1038/jid.2012.468

Khoja, L., Shenjere, P., Hodgson, C., Hodgetts, J., Clack, G., Hughes, A., et al. (2014). Prevalence and heterogeneity of circulating tumour cells in metastatic cutaneous melanoma. *Melanoma Res.* 24, 40–46. doi: 10.1097/CMR.0000000000000025

Kim, K. H., Lee, H. H., Yoon, Y. E., Na, J. C., Kim, S. Y., Cho, Y. I., et al. (2018). Clinical validation of serum endocan (ESM-1) as a potential biomarker in patients with renal cell carcinoma. *Oncotarget* 9, 662–667. doi: 10.18632/oncotarget.23087

Kim, M. Y., Oskarsson, T., Acharyya, S., Nguyen, D. X., Zhang, X. H., Norton, L., et al. (2009). Tumor self-seeding by circulating cancer cells. *Cell* 139, 1315–1326. doi: 10.1016/j.cell.2009.11.025

Klinac, D., Gray, E. S., Freeman, J. B., Reid, A., Bowyer, S., Millward, M., et al. (2014). Monitoring changes in circulating tumour cells as a prognostic indicator of overall survival and treatment response in patients with metastatic melanoma. *BMC Cancer* 14:423. doi: 10.1186/1471-2407-14-423

Knelson, E. H., Nee, J. C., and Blobe, G. C. (2014). Heparan sulfate signaling in cancer. *Trends Biochem. Sci.* 39, 277–288. doi: 10.1016/j.tibs.2014.03.001

Kokenyesi, R., and Bernfield, M. (1994). Core protein structure and sequence determine the site and presence of heparan sulfate and chondroitin sulfate on syndecan-1. *J. Biol. Chem.* 269, 12304–12309.

Koliopanos, A., Friess, H., Kleeff, J., Shi, X., Liao, Q., Pecker, I., et al. (2001). Heparanase expression in primary and metastatic pancreatic cancer. *Cancer Res.* 61, 4655–4659.

Kolluri, A., and Ho, M. (2019). The role of glypican-3 in regulating Wnt, YAP, and hedgehog in liver cancer. *Front. Oncol.* 9:708. doi: 10.3389/fonc.2019.00708

Kolset, S. O., and Tveit, H. (2008). Serglycin–structure and biology. *Cell. Mol. Life Sci.* 65, 1073–1085.

Korpetinou, A., Papachristou, D. J., Lampropoulou, A., Bouris, P., Labropoulou, V. T., Noulas, A., et al. (2015). Increased expression of serglycin in specific

carcinomas and aggressive cancer cell lines. *Biomed Res. Int.* 2015:690721. doi: 10.1155/2015/690721

Korpetinou, A., Skandalis, S. S., Moustakas, A., Happonen, K. E., Tveit, H., Prydz, K., et al. (2013). Serglycin is implicated in the promotion of aggressive phenotype of breast cancer cells. *PLoS One* 8:e78157. doi: 10.1371/journal.pone.0078157

Kowalik, A., Kowalewska, M., and Gozdz, S. (2017). Current approaches for avoiding the limitations of circulating tumor cells detection methods-implications for diagnosis and treatment of patients with solid tumors. *Transl. Res.* 185, 58–84.e15. doi: 10.1016/j.trsl.2017.04.002

Kowli, S., Velidandla, R., Creek, K. E., and Pirisi, L. (2013). TGF-beta regulation of gene expression at early and late stages of HPV16-mediated transformation of human keratinocytes. *Virology* 447, 63–73. doi: 10.1016/j.virol.2013.08.034

Krebs, M. G., Sloane, R., Priest, L., Lancashire, L., Hou, J. M., Greystoke, A., et al. (2011). Evaluation and prognostic significance of circulating tumor cells in patients with non-small-cell lung cancer. *J. Clin. Oncol.* 29, 1556–1563. doi: 10.1200/JCO.2010.28.7045

Kufe, D. W. (2009). Mucins in cancer: function, prognosis and therapy. *Nat. Rev. Cancer* 9, 874–885. doi: 10.1038/nrc2761

Kuo, J. C.-H., Gandhi, J. G., Zia, R. N., and Paszek, M. J. (2018). Physical biology of the cancer cell glycocalyx. *Nat. Phys.* 14, 658–669. doi: 10.1038/s41567-018-0186-9

Kurihara, T., Itoi, T., Sofuni, A., Itokawa, F., Tsuchiya, T., Tsuji, S., et al. (2008). Detection of circulating tumor cells in patients with pancreatic cancer: a preliminary result. *J. Hepatobiliary Pancreat. Surg.* 15, 189–195. doi: 10.1007/s00534-007-1250-5

Lambert, A. W., Pattabiraman, D. R., and Weinberg, R. A. (2017). Emerging biological principles of metastasis. *Cell* 168, 670–691.

Lamouille, S., Xu, J., and Derynck, R. (2014). Molecular mechanisms of epithelial-mesenchymal transition. *Nat. Rev. Mol. Cell Biol.* 15, 178–196.

Lampignano, R., Schneck, H., Neumann, M., Fehm, T., and Neubauer, H. (2017). Enrichment, isolation and molecular characterization of EpCAM-negative circulating tumor cells. *Adv. Exp. Med. Biol.* 994, 181–203. doi: 10.1007/978-3-319-55947-6_10

Lee, N., Barthel, S. R., and Schatton, T. (2014). Melanoma stem cells and metastasis: mimicking hematopoietic cell trafficking? *Lab. Invest.* 94, 13–30. doi: 10.1038/labinvest.2013.116

Li, G., Li, L., Joo, E. J., Son, J. W., Kim, Y. J., Kang, J. K., et al. (2017). Glycosaminoglycans and glycolipids as potential biomarkers in lung cancer. *Glycoconj. J.* 34, 661–669. doi: 10.1007/s10719-017-9790-7

Li, N., Wei, L., Liu, X., Bai, H., Ye, Y., Li, D., et al. (2019). A frizzled-like cysteine-rich domain in glypican-3 mediates Wnt binding and regulates hepatocellular carcinoma tumor growth in mice. *Hepatology* 70, 1231–1245. doi: 10.1002/hep.30646

Li, X.-J., Ong, C. K., Cao, Y., Xiang, Y.-Q., Shao, J.-Y., Ooi, A., et al. (2011). Serglycin is a theranostic target in nasopharyngeal carcinoma that promotes metastasis. *Cancer Res.* 71, 3162–3172. doi: 10.1158/0008-5472.CAN-10-3557

Lian, S., Xie, R., Ye, Y., Lu, Y., Cheng, Y., Xie, X., et al. (2019). Dual blockage of both PD-L1 and CD47 enhances immunotherapy against circulating tumor cells. *Sci. Rep.* 9:4532. doi: 10.1038/s41598-019-40241-1

Liberti, P. A., Rao, C. G., and Terstappen, L. W. M. M. (2001). Optimization of ferrofluids and protocols for the enrichment of breast tumor cells in blood. *J. Magn. Magn. Mater.* 225, 301–307.

Lim, J., and Thiery, J. P. (2012). Epithelial-mesenchymal transitions: insights from development. *Development* 139, 3471–3486. doi: 10.1242/dev.071209

Liu, H. Y., Qian, H. H., Zhang, X. F., Li, J., Yang, X., Sun, B., et al. (2015). Improved method increases sensitivity for circulating hepatocellular carcinoma cells. *World J. Gastroenterol.* 21, 2918–2925. doi: 10.3748/wjg.v21.i10.2918

Liu, S., Tian, Z., Zhang, L., Hou, S., Hu, S., Wu, J., et al. (2016). Combined cell surface carbonic anhydrase 9 and CD147 antigens enable high-efficiency capture of circulating tumor cells in clear cell renal cell carcinoma patients. *Oncotarget* 7, 59877–59891. doi: 10.18632/oncotarget.10979

Liu, X., Taftaf, R., Kawaguchi, M., Chang, Y. F., Chen, W., Entenberg, D., et al. (2019). Homophilic CD44 interactions mediate tumor cell aggregation and polyclonal metastasis in patient-derived breast cancer models. *Cancer Discov.* 9, 96–113. doi: 10.1158/2159-8290.CD-18-0065

Liu, Z., Fusi, A., Klopocki, E., Schmittel, A., Tinhofer, I., Nonnenmacher, A., et al. (2011). Negative enrichment by immunomagnetic nanobeads for unbiased characterization of CTCs from peripheral blood of cancer patients. *J. Transl. Med.* 9:70. doi: 10.1186/1479-5876-9-70

Lopez-Casillas, F., Payne, H. M., Andres, J. L., and Massague, J. (1994). Betaglycan can act as a dual modulator of TGF-beta access to signaling receptors: mapping of ligand binding and GAG attachment sites. *J. Cell Biol.* 124, 557–568. doi: 10.1083/jcb.124.4.557

Lopresti, A., Malergue, F., Bertucci, F., Liberatoscioli, M. L., Garnier, S., Dacosta, Q., et al. (2019). Sensitive and easy screening for circulating tumor cells by flow cytometry. *JCI Insight* 5:e128180. doi: 10.1172/jci.insight.128180

Lucci, A., Hall, C., Patel, S. P., Narendran, B., Bauldry, J. B., Royal, R., et al. (2020). Circulating tumor cells and early relapse in node-positive melanoma. *Clin. Cancer Res.* 26, 1886–1895. doi: 10.1158/1078-0432.CCR-19-2670

Lugano, R., Ramachandran, M., and Dimberg, A. (2020). Tumor angiogenesis: causes, consequences, challenges and opportunities. *Cell. Mol. Life Sci.* 77, 1745–1770.

Lynch, C. C., and Matrisian, L. M. (2002). Matrix metalloproteinases in tumor-host cell communication. *Differentiation* 70, 561–573. doi: 10.1046/j.1432-0436.2002.700909.x

Majuri, M. L., Niemela, R., Tiisala, S., Renkonen, O., and Renkonen, R. (1995). Expression and function of alpha 2,3-sialyl- and alpha 1,3/1,4-fucosyltransferases in colon adenocarcinoma cell lines: role in synthesis of E-selectin counter-receptors. *Int. J. Cancer* 63, 551–559. doi: 10.1002/ijc.2910630416

Makagiansar, I. T., Williams, S., Mustelin, T., and Stallcup, W. B. (2007). Differential phosphorylation of NG2 proteoglycan by ERK and PKCα helps balance cell proliferation and migration. *J. Cell Biol.* 178, 155–165. doi: 10.1083/jcb.200612084

Man, X. B., Tang, L., Zhang, B. H., Li, S. J., Qiu, X. H., Wu, M. C., et al. (2005). Upregulation of Glypican-3 expression in hepatocellular carcinoma but downregulation in cholangiocarcinoma indicates its differential diagnosis value in primary liver cancers. *Liver Int.* 25, 962–966. doi: 10.1111/j.1478-3231.2005.01100.x

Marrero, J. A., Kulik, L. M., Sirlin, C. B., Zhu, A. X., Finn, R. S., Abecassis, M. M., et al. (2018). Diagnosis, staging, and management of hepatocellular carcinoma: 2018 practice guidance by the American association for the study of liver diseases. *Hepatology* 68, 723–750. doi: 10.1002/hep.29913

Martinez, P., Vergoten, G., Colomb, F., Bobowski, M., Steenackers, A., Carpentier, M., et al. (2013). Over-sulfated glycosaminoglycans are alternative selectin ligands: insights into molecular interactions and possible role in breast cancer metastasis. *Clin. Exp. Metastasis* 30, 919–931. doi: 10.1007/s10585-013-9592-7

Masola, V., Bellin, G., Gambaro, G., and Onisto, M. (2018). Heparanase: a multitasking protein involved in extracellular matrix (ECM) remodeling and intracellular events. *Cells* 7:236. doi: 10.3390/cells7120236

Massague, J., and Obenauf, A. C. (2016). Metastatic colonization by circulating tumour cells. *Nature* 529, 298–306. doi: 10.1038/nature17038

Maurage, C. A., Adam, E., Mineo, J. F., Sarrazin, S., Debunne, M., Siminski, R. M., et al. (2009). Endocan expression and localization in human glioblastomas. *J. Neuropathol. Exp. Neurol.* 68, 633–641. doi: 10.1097/NEN.0b013e3181a52a7f

Maxhimer, J. B., Pesce, C. E., Stewart, R. A., Gattuso, P., Prinz, R. A., and Xu, X. (2005). Ductal carcinoma in situ of the breast and heparanase-1 expression: a molecular explanation for more aggressive subtypes. *J. Am. Coll. Surg.* 200, 328–335. doi: 10.1016/j.jamcollsurg.2004.10.034

Melo, S. A., Luecke, L. B., Kahlert, C., Fernandez, A. F., Gammon, S. T., Kaye, J., et al. (2015). Glypican-1 identifies cancer exosomes and detects early pancreatic cancer. 523, 177–182. doi: 10.1038/nature14581

Menakuru, S. R., Brown, N. J., Staton, C. A., and Reed, M. W. (2008). Angiogenesis in pre-malignant conditions. *Br. J. Cancer* 99, 1961–1966.

Mentis, A. A., Grivas, P. D., Dardiotis, E., Romas, N. A., and Papavassiliou, A. G. (2020). Circulating tumor cells as *Trojan Horse* for understanding, preventing, and treating cancer: a critical appraisal. *Cell. Mol. Life Sci.* doi: 10.1007/s00018-020-03529-4 [Epub ahead of print].

Miao, H. Q., Lee, P., Lin, H., Soker, S., and Klagsbrun, M. (2000). Neuropilin-1 expression by tumor cells promotes tumor angiogenesis and progression. *FASEB J.* 14, 2532–2539. doi: 10.1096/fj.00-0250com

Micalizzi, D. S., Maheswaran, S., and Haber, D. A. (2017). A conduit to metastasis: circulating tumor cell biology. *Genes Dev.* 31, 1827–1840. doi: 10.1101/gad.305805.117

Mikami, T., and Kitagawa, H. (2013). Biosynthesis and function of chondroitin sulfate. *Biochim. Biophys. Acta* 1830, 4719–4733.

Mitchell, M. J., Castellanos, C. A., and King, M. R. (2015). Surfactant functionalization induces robust, differential adhesion of tumor cells and blood cells to charged nanotube-coated biomaterials under flow. *Biomaterials* 56, 179–186. doi: 10.1016/j.biomaterials.2015.03.045

Mitchell, M. J., and King, M. R. (2014). Physical biology in cancer. 3. The role of cell glycocalyx in vascular transport of circulating tumor cells. *Am. J. Physiol. Cell Physiol.* 306, C89–C97. doi: 10.1152/ajpcell.00285.2013

Mizumoto, S., Yamada, S., and Sugahara, K. (2015). Molecular interactions between chondroitin-dermatan sulfate and growth factors/receptors/matrix proteins. *Curr. Opin. Struct. Biol.* 34, 35–42. doi: 10.1016/j.sbi.2015.06.004

Mohamed, R., Dayati, P., Mehr, R. N., Kamato, D., Seif, F., Babaahmadi-Rezaei, H., et al. (2019). Transforming growth factor-beta1 mediated CHST11 and CHSY1 mRNA expression is ROS dependent in vascular smooth muscle cells. *J. Cell Commun. Signal.* 13, 225–233. doi: 10.1007/s12079-018-0495-x

Momose, T., Yoshimura, Y., Harumiya, S., Isobe, K., Kito, M., Fukushima, M., et al. (2016). Chondroitin sulfate synthase 1 expression is associated with malignant potential of soft tissue sarcomas with myxoid substance. *Hum. Pathol.* 50, 15–23. doi: 10.1016/j.humpath.2015.11.005

Morla, S. (2019). Glycosaminoglycans and Glycosaminoglycan Mimetics in Cancer and Inflammation. *Int. J. Mol. Sci.* 20:1963. doi: 10.3390/ijms20081963

Muller, C., Holtschmidt, J., Auer, M., Heitzer, E., Lamszus, K., Schulte, A., et al. (2014). Hematogenous dissemination of glioblastoma multiforme. *Sci. Transl. Med.* 6:247ra101.

Muller, V., Riethdorf, S., Rack, B., Janni, W., Fasching, P. A., Solomayer, E., et al. (2012). Prognostic impact of circulating tumor cells assessed with the CellSearch System and AdnaTest Breast in metastatic breast cancer patients: the DETECT study. *Breast Cancer Res.* 14:R118. doi: 10.1186/bcr3243

Murlidhar, V., Reddy, R. M., Fouladdel, S., Zhao, L., Ishikawa, M. K., Grabauskiene, S., et al. (2017). Poor prognosis indicated by venous circulating tumor cell clusters in early-stage lung cancers. *Cancer Res.* 77, 5194–5206. doi: 10.1158/0008-5472.CAN-16-2072

Nam, S. J., Yeo, H. Y., Chang, H. J., Kim, B. H., Hong, E. K., and Park, J. W. (2016). a new cell block method for multiple immunohistochemical analysis of circulating tumor cells in patients with liver cancer. *Cancer Res. Treat.* 48, 1229–1242. doi: 10.4143/crt.2015.500

Naoe, M., Kusaka, C., Ohta, M., Hasebe, Y., Unoki, T., Shimoyama, H., et al. (2019). Development of a highly sensitive technique for capturing renal cell cancer circulating tumor cells. *Diagnostics* 9:96. doi: 10.3390/diagnostics9030096

Naor, D., Nedvetzki, S., Golan, I., Melnik, L., and Faitelson, Y. (2002). CD44 in Cancer. *Crit. Rev. Clin. Lab. Sci.* 39, 527–579.

Nguyen, D. X., Bos, P. D., and Massague, J. (2009). Metastasis: from dissemination to organ-specific colonization. *Nat. Rev. Cancer* 9, 274–284. doi: 10.1038/nrc2622

Nicolazzo, C., Gradilone, A., Loreni, F., Raimondi, C., and Gazzaniga, P. (2019). EpCAM(low) circulating tumor cells: gold in the waste. *Dis. Markers* 2019:1718920. doi: 10.1155/2019/1718920

Nikitovic, D., Berdiaki, A., Spyridaki, I., Krasanakis, T., Tsatsakis, A., and Tzanakakis, G. N. (2018). Proteoglycans-biomarkers and targets in cancer therapy. *Front. Endocrinol.* 9:69.

Nikitovic, D., Kouvidi, K., Voudouri, K., Berdiaki, A., Karousou, E., Passi, A., et al. (2014). The motile breast cancer phenotype roles of proteoglycans/glycosaminoglycans. *Biomed Res. Int.* 2014:124321. doi: 10.1155/2014/124321

Niland, S., and Eble, J. A. (2019). Neuropilins in the context of tumor vasculature. *Int. J. Mol. Sci.* 20:639.

Nishiyama, A., Lin, X. H., Giese, N., Heldin, C. H., and Stallcup, W. B. (1996). Interaction between NG2 proteoglycan and PDGF α-receptor on O2A progenitor cells is required for optimal response to PDGF. *J. Neurosci. Res.* 43, 315–330. doi: 10.1002/(SICI)1097-4547(19960201)43:3\<315::AID-JNR6\>3.0.CO;2-M

Nobuhisa, T., Naomoto, Y., Ohkawa, T., Takaoka, M., Ono, R., Murata, T., et al. (2005). Heparanase expression correlates with malignant potential in human colon cancer. *J. Cancer Res. Clin. Oncol.* 131, 229–237. doi: 10.1007/s00432-004-0644-x

Ogle, L. F., Orr, J. G., Willoughby, C. E., Hutton, C., Mcpherson, S., Plummer, R., et al. (2016). Imagestream detection and characterisation of circulating tumour cells - A liquid biopsy for hepatocellular carcinoma? *J. Hepatol.* 65, 305–313. doi: 10.1016/j.jhep.2016.04.014

Okabe, H., Ishimoto, T., Mima, K., Nakagawa, S., Hayashi, H., Kuroki, H., et al. (2014). CD44s signals the acquisition of the mesenchymal phenotype required for anchorage-independent cell survival in hepatocellular carcinoma. *Br. J. Cancer* 110, 958–966. doi: 10.1038/bjc.2013.759

Okada, H., Takemura, G., Suzuki, K., Oda, K., Takada, C., Hotta, Y., et al. (2017). Three-dimensional ultrastructure of capillary endothelial glycocalyx under normal and experimental endotoxemic conditions. *Crit. Care* 21:261. doi: 10.1186/s13054-017-1841-8

Olive, P. L., Vikse, C., and Trotter, M. J. (1992). Measurement of oxygen diffusion distance in tumor cubes using a fluorescent hypoxia probe. *Int. J. Radiat. Oncol. Biol. Phys.* 22, 397–402. doi: 10.1016/0360-3016(92)90840-e

Oliveira-Ferrer, L., Hessling, A., Trillsch, F., Mahner, S., and Milde-Langosch, K. (2015). Prognostic impact of chondroitin-4-sulfotransferase CHST11 in ovarian cancer. *Tumour Biol.* 36, 9023–9030. doi: 10.1007/s13277-015-3652-3

Ozkumur, E., Shah, A. M., Ciciliano, J. C., Emmink, B. L., Miyamoto, D. T., Brachtel, E., et al. (2013). Inertial focusing for tumor antigen-dependent and -independent sorting of rare circulating tumor cells. *Sci. Transl. Med.* 5:179ra147. doi: 10.1126/scitranslmed.3005616

Pan, S., Chen, R., Tamura, Y., Crispin, D. A., Lai, L. A., May, D. H., et al. (2014). Quantitative glycoproteomics analysis reveals changes in N-glycosylation level associated with pancreatic ductal adenocarcinoma. *J. Proteome Res.* 13, 1293–1306. doi: 10.1021/pr4010184

Parkinson, D. R., Dracopoli, N., Petty, B. G., Compton, C., Cristofanilli, M., Deisseroth, A., et al. (2012). Considerations in the development of circulating tumor cell technology for clinical use. *J. Transl. Med.* 10:138. doi: 10.1186/1479-5876-10-138

Paszek, M. J., Dufort, C. C., Rossier, O., Bainer, R., Mouw, J. K., Godula, K., et al. (2014). The cancer glycocalyx mechanically primes integrin-mediated growth and survival. *Nature* 511, 319–325. doi: 10.1038/nature13535

Patel, S., Shah, K., Mirza, S., Shah, K., and Rawal, R. (2016). Circulating tumor stem like cells in oral squamous cell carcinoma: an unresolved paradox. *Oral Oncol.* 62, 139–146. doi: 10.1016/j.oraloncology.2016.10.019

Pearce, O. M. T., and Läubli, H. (2016). Sialic acids in cancer biology and immunity. *Glycobiology* 26, 111–128. doi: 10.1093/glycob/cwv097

Peinado, H., Aleckovic, M., Lavotshkin, S., Matei, I., Costa-Silva, B., Moreno-Bueno, G., et al. (2012). Melanoma exosomes educate bone marrow progenitor cells toward a pro-metastatic phenotype through MET. *Nat. Med.* 18, 883–891.

Peinado, H., Zhang, H., Matei, I. R., Costa-Silva, B., Hoshino, A., Rodrigues, G., et al. (2017). Pre-metastatic niches: organ-specific homes for metastases. *Nat. Rev. Cancer* 17, 302–317. doi: 10.1038/nrc.2017.6

Peterson, S. M., Iskenderian, A., Cook, L., Romashko, A., Tobin, K., Jones, M., et al. (2010). Human Sulfatase 2 inhibits in vivo tumor growth of MDA-MB-231 human breast cancer xenografts. *BMC Cancer* 10:427. doi: 10.1186/1471-2407-10-427

Pillai, H. K., Pourgholami, C. M., Chua, L. T., and Morris, L. D. (2015). MUC1 as a potential target in anticancer therapies. *Am. J. Clin. Oncol.* 38, 108–118. doi: 10.1097/COC.0b013e31828f5a07

Pinho, S. S., and Reis, C. A. (2015). Glycosylation in cancer: mechanisms and clinical implications. *Nat. Rev. Cancer* 15, 540–555. doi: 10.1038/nrc3982

Pomin, V. H., and Mulloy, B. (2018). Glycosaminoglycans and proteoglycans. *Pharmaceuticals* 11:27.

Price, M. A., Colvin Wanshura, L. E., Yang, J., Carlson, J., Xiang, B., Li, G., et al. (2011). CSPG4, a potential therapeutic target, facilitates malignant progression of melanoma. *Pigment Cell Melanoma Res.* 24, 1148–1157. doi: 10.1111/j.1755-148X.2011.00929.x

Purushothaman, A., Bandari, S. K., Liu, J., Mobley, J. A., Brown, E. E., and Sanderson, R. D. (2016). Fibronectin on the surface of myeloma cell-derived exosomes mediates exosome-cell interactions. *J. Biol. Chem.* 291, 1652–1663. doi: 10.1074/jbc.M115.686295

Qasaimeh, M., Wu, Y., Bose, S., Menachery, A., Talluri, S., Gonzalez, G., et al. (2017). Isolation of circulating plasma cells in multiple myeloma using CD138 antibody-based capture in a microfluidic device. *Sci. Rep.* 7:45681. doi: 10.1038/srep45681

Qi, L. N., Xiang, B. D., Wu, F. X., Ye, J. Z., Zhong, J. H., Wang, Y. Y., et al. (2018). Circulating tumor cells undergoing EMT provide a metric for diagnosis and prognosis of patients with hepatocellular carcinoma. *Cancer Res.* 78, 4731–4744. doi: 10.1158/0008-5472.CAN-17-2459

Qin, J., Alt, J. R., Hunsley, B. A., Williams, T. L., and Fernando, M. R. (2014). Stabilization of circulating tumor cells in blood using a collection device with a preservative reagent. *Cancer Cell Int.* 14:23. doi: 10.1186/1475-2867-14-23

Ranganathan, P., Agrawal, A., Bhushan, R., Chavalmane, A. K., Kalathur, R. K., Takahashi, T., et al. (2007). Expression profiling of genes regulated by TGF-beta: differential regulation in normal and tumour cells. *BMC Genomics* 8:98. doi: 10.1186/1471-2164-8-98

Rao, C., Bui, T., Connelly, M., Doyle, G., Karydis, I., Middleton, M. R., et al. (2011). Circulating melanoma cells and survival in metastatic melanoma. *Int. J. Oncol.* 38, 755–760. doi: 10.3892/ijo.2011.896

Rapraeger, A. (1989). Transforming growth factor (type beta) promotes the addition of chondroitin sulfate chains to the cell surface proteoglycan (syndecan) of mouse mammary epithelia. *J. Cell Biol.* 109, 2509–2518. doi: 10.1083/jcb.109.5.2509

Real, F. X., Houghton, A. N., Albino, A. P., Cordon-Cardo, C., Melamed, M. R., Oettgen, H. F., et al. (1985). Surface antigens of melanomas and melanocytes defined by mouse monoclonal antibodies: specificity analysis and comparison of antigen expression in cultured cells and tissues. *Cancer Res.* 45, 4401–4411.

Reckamp, K., Figlin, R., Burdick, M., Dubinett, S., Elashoff, R., and Strieter, R. (2009). CXCR4 expression on circulating pan-cytokeratin positive cells is associated with survival in patients with advanced non-small cell lung cancer. *BMC Cancer* 9:213. doi: 10.1186/1471-2407-9-213

Reitsma, S., Slaaf, D. W., Vink, H., Van Zandvoort, M. A. M. J., and Oude Egbrink, M. G. A. (2007). The endothelial glycocalyx: composition, functions, and visualization. *Pflugers Arch.* 454, 345–359. doi: 10.1007/s00424-007-0212-8

Rejniak, K. A. (2016). Circulating tumor cells: when a solid tumor meets a fluid microenvironment. *Adv. Exp. Med. Biol.* 936, 93–106. doi: 10.1007/978-3-319-42023-3_5

Renkonen, J., Paavonen, T., and Renkonen, R. (1997). Endothelial and epithelial expression of sialyl Lewis(x) and sialyl Lewis(a) in lesions of breast carcinoma. *Int. J. Cancer* 74, 296–300. doi: 10.1002/(sici)1097-0215(19970620)74:3\<296::aid-ijc11\>3.0.co;2-a

Rennel, E., Mellberg, S., Dimberg, A., Petersson, L., Botling, J., Ameur, A., et al. (2007). Endocan is a VEGF-A and PI3K regulated gene with increased expression in human renal cancer. *Exp. Cell Res.* 313, 1285–1294. doi: 10.1016/j.yexcr.2007.01.021

Reymond, N., D'agua, B. B., and Ridley, A. J. (2013). Crossing the endothelial barrier during metastasis. *Nat. Rev. Cancer* 13, 858–870.

Rhim, A. D., Mirek, E. T., Aiello, N. M., Maitra, A., Bailey, J. M., Mcallister, F., et al. (2012). EMT and dissemination precede pancreatic tumor formation. *Cell* 148, 349–361. doi: 10.1016/j.cell.2011.11.025

Riggi, N., Aguet, M., and Stamenkovic, I. (2018). Cancer metastasis: a reappraisal of its underlying mechanisms and their relevance to treatment. *Annu. Rev. Pathol. Mech. Dis.* 13, 117–140. doi: 10.1146/annurev-pathol-020117-044127

Rocha, S. F., Schiller, M., Jing, D., Li, H., Butz, S., Vestweber, D., et al. (2014). Esm1 modulates endothelial tip cell behavior and vascular permeability by enhancing VEGF bioavailability. *Circ. Res.* 115, 581–590. doi: 10.1161/CIRCRESAHA.115.304718

Rogers, C. J., and Hsieh-Wilson, L. C. (2012). Microarray method for the rapid detection of glycosaminoglycan-protein interactions. *Methods Mol. Biol.* 808, 321–336. doi: 10.1007/978-1-61779-373-8_22

Roland, C. L., Ross, M. I., Hall, C. S., Laubacher, B., Upshaw, J., Anderson, A. E., et al. (2015). Detection of circulating melanoma cells in the blood of melanoma patients: a preliminary study. *Melanoma Res.* 25, 335–341. doi: 10.1097/CMR.0000000000000168

Roucourt, B., Meeussen, S., Bao, J., Zimmermann, P., and David, G. (2015). Heparanase activates the syndecan-syntenin-ALIX exosome pathway. *Cell Res.* 25, 412–428. doi: 10.1038/cr.2015.29

Roudnicky, F., Poyet, C., Wild, P., Krampitz, S., Negrini, F., Huggenberger, R., et al. (2013). Endocan is upregulated on tumor vessels in invasive bladder cancer where it mediates VEGF-A-induced angiogenesis. *Cancer Res.* 73, 1097–1106. doi: 10.1158/0008-5472.CAN-12-1855

Roy, A., Attarha, S., Weishaupt, H., Edqvist, P. H., Swartling, F. J., Bergqvist, M., et al. (2017). Serglycin as a potential biomarker for glioma: association of serglycin expression, extent of mast cell recruitment and glioblastoma progression. *Oncotarget* 8, 24815–24827. doi: 10.18632/oncotarget.15820

Roy, A., Femel, J., Huijbers, E. J., Spillmann, D., Larsson, E., Ringvall, M., et al. (2016). Targeting serglycin prevents metastasis in murine mammary carcinoma. *PLoS One* 11:e0156151. doi: 10.1371/journal.pone.0156151

Ruiz, C., Li, J., Luttgen, M. S., Kolatkar, A., Kendall, J. T., Flores, E., et al. (2015). Limited genomic heterogeneity of circulating melanoma cells in advanced stage patients. *Phys. Biol.* 12:016008. doi: 10.1088/1478-3975/12/1/016008

Sackstein, R. (2004). The bone marrow is akin to skin: HCELL and the biology of hematopoietic stem cell homing. *J. Invest. Dermatol.* 122, 1061–1069. doi: 10.1111/j.0022-202X.2004.09301.x

Sakaizawa, K., Goto, Y., Kiniwa, Y., Uchiyama, A., Harada, K., Shimada, S., et al. (2012). Mutation analysis of BRAF and KIT in circulating melanoma cells at the single cell level. *Br. J. Cancer* 106, 939–946. doi: 10.1038/bjc.2012.12

Salanga, C. L., and Handel, T. M. (2011). Chemokine oligomerization and interactions with receptors and glycosaminoglycans: the role of structural dynamics in function. *Exp. Cell Res.* 317, 590–601. doi: 10.1016/j.yexcr.2011.01.004

Salanti, A., Clausen, T. M., Agerbaek, M. O., Al Nakouzi, N., Dahlback, M., Oo, H. Z., et al. (2015). Targeting human cancer by a glycosaminoglycan binding malaria protein. *Cancer Cell* 28, 500–514. doi: 10.1016/j.ccell.2015.09.003

Sand, N. T., Petersen, T. B., Bang-Christensen, S. R., Ahrens, T. D., Loppke, C., Jorgensen, A. M., et al. (2020). Optimization of rVAR2-based isolation of cancer cells in blood for building a robust assay for clinical detection of circulating tumor cells. *Int. J. Mol. Sci.* 21:2401. doi: 10.3390/ijms21072401

Sanderson, R. D., Elkin, M., Rapraeger, A. C., Ilan, N., and Vlodavsky, I. (2017). Heparanase regulation of cancer, autophagy and inflammation: new mechanisms and targets for therapy. *FEBS J.* 284, 42–55. doi: 10.1111/febs.13932

Santra, M., Eichstetter, I., and Iozzo, R. V. (2000). An anti-oncogenic role for decorin: down-regulation of ErbB2 leads to growth suppression and cytodifferentiation of mammary carcinoma cells. *J. Biol. Chem.* 275, 35153–35161. doi: 10.1074/jbc.M006821200

Saoncella, S., Echtermeyer, F., Denhez, F., Nowlen, J. K., Mosher, D. F., Robinson, S. D., et al. (1999). Syndecan-4 signals cooperatively with integrins in a Rho-dependent manner in the assembly of focal adhesions and actin stress fibers. *Proc. Natl. Acad. Sci. U.S.A.* 96, 2805–2810. doi: 10.1073/pnas.96.6.2805

Savoia, P., Fava, P., Casoni, F., and Cremona, O. (2019). Targeting the ERK signaling pathway in melanoma. *Int. J. Mol. Sci.* 20:1483. doi: 10.3390/ijms20061483

Sawada, Y., Yoshikawa, T., Nobuoka, D., Shirakawa, H., Kuronuma, T., Motomura, Y., et al. (2012). Phase I trial of a glypican-3-derived peptide vaccine for advanced hepatocellular carcinoma: immunologic evidence and potential for improving overall survival. *Clin. Cancer Res.* 18, 3686–3696. doi: 10.1158/1078-0432.CCR-11-3044

Schaefer, L., and Schaefer, R. M. (2010). Proteoglycans: from structural compounds to signaling molecules. *Cell Tissue Res.* 339, 237–246. doi: 10.1007/s00441-009-0821-y

Schaefer, L., Tredup, C., Gubbiotti, M. A., and Iozzo, R. V. (2017). Proteoglycan neofunctions: regulation of inflammation and autophagy in cancer biology. *FEBS J.* 284, 10–26. doi: 10.1111/febs.13963

Schehr, J. L., Schultz, Z. D., Warrick, J. W., Guckenberger, D. J., Pezzi, H. M., Sperger, J. M., et al. (2016). High specificity in circulating tumor cell identification is required for accurate evaluation of programmed death-ligand 1. *PLoS One* 11:e0159397. doi: 10.1371/journal.pone.0159397

Schick, B. P., Gradowski, J. F., and San Antonio, J. D. (2001). Synthesis, secretion, and subcellular localization of serglycin proteoglycan in human endothelial cells. *Blood* 97, 449–458. doi: 10.1182/blood.v97.2.449

Schochter, F., Friedl, T. W. P., Degregorio, A., Krause, S., Huober, J., Rack, B., et al. (2019). Are Circulating Tumor Cells (CTCs) ready for clinical use in breast cancer? An overview of completed and ongoing trials using CTCs for clinical treatment decisions. *Cells* 8:1412. doi: 10.3390/cells8111412

Schulze, K., Gasch, C., Staufer, K., Nashan, B., Lohse, A. W., Pantel, K., et al. (2013). Presence of EpCAM-positive circulating tumor cells as biomarker for systemic disease strongly correlates to survival in patients with hepatocellular carcinoma. *Int. J. Cancer* 133, 2165–2171. doi: 10.1002/ijc.28230

Shaw Bagnall, J., Byun, S., Begum, S., Miyamoto, D. T., Hecht, V. C., Maheswaran, S., et al. (2015). Deformability of tumor cells versus blood cells. *Sci. Rep.* 5:18542. doi: 10.1038/srep18542

Shintani, Y., Takashima, S., Asano, Y., Kato, H., Liao, Y., Yamazaki, S., et al. (2006). Glycosaminoglycan modification of neuropilin-1 modulates VEGFR2 signaling. *EMBO J.* 25, 3045–3055. doi: 10.1038/sj.emboj.7601188

Simons, M., and Raposo, G. (2009). Exosomes–vesicular carriers for intercellular communication. *Curr. Opin. Cell Biol.* 21, 575–581. doi: 10.1016/j.ceb.2009.03.007

Smetsers, T. F., Van De Westerlo, E. M., Ten Dam, G. B., Overes, I. M., Schalkwijk, J., Van Muijen, G. N., et al. (2004). Human single-chain antibodies reactive with native chondroitin sulfate detect chondroitin sulfate alterations in melanoma and psoriasis. *J. Invest. Dermatol.* 122, 707–716. doi: 10.1111/j.0022-202X.2004.22316.x

Soker, S., Miao, H. Q., Nomi, M., Takashima, S., and Klagsbrun, M. (2002). VEGF165 mediates formation of complexes containing VEGFR-2 and neuropilin-1 that enhance VEGF165-receptor binding. *J. Cell. Biochem.* 85, 357–368. doi: 10.1002/jcb.10140

Soker, S., Takashima, S., Miao, H. Q., Neufeld, G., and Klagsbrun, M. (1998). Neuropilin-1 is expressed by endothelial and tumor cells as an isoform-specific receptor for vascular endothelial growth factor. *Cell* 92, 735–745. doi: 10.1016/s0092-8674(00)81402-6

Song, K., Li, Q., Jiang, Z. Z., Guo, C. W., and Li, P. (2011). Heparan sulfate D-glucosaminyl 3-O-sulfotransferase-3B1, a novel epithelial-mesenchymal transition inducer in pancreatic cancer. *Cancer Biol. Ther.* 12, 388–398. doi: 10.4161/cbt.12.5.15957

Sosa, M. S., Bragado, P., and Aguirre-Ghiso, J. A. (2014). Mechanisms of disseminated cancer cell dormancy: an awakening field. *Nat. Rev. Cancer* 14, 611–622. doi: 10.1038/nrc3793

Stallcup, W. B. (2002). The NG2 proteoglycan: past insights and future prospects. *J. Neurocytol.* 31, 423–435. doi: 10.1023/a:1025731428581

Stallcup, W. B. (2017). NG2 proteoglycan enhances brain tumor progression by promoting beta-1 integrin activation in both Cis and trans orientations. *Cancers* 9:31. doi: 10.3390/cancers9040031

Steinert, G., Scholch, S., Niemietz, T., Iwata, N., Garcia, S. A., Behrens, B., et al. (2014). Immune escape and survival mechanisms in circulating tumor cells of colorectal cancer. *Cancer Res.* 74, 1694–1704. doi: 10.1158/0008-5472.CAN-13-1885

Stott, S. L., Lee, R. J., Nagrath, S., Yu, M., Miyamoto, D. T., Ulkus, L., et al. (2010). Isolation and characterization of circulating tumor cells from patients with localized and metastatic prostate cancer. *Sci. Transl. Med.* 2:25ra23. doi: 10.1126/scitranslmed.3000403

Strati, A., Kasimir-Bauer, S., Markou, A., Parisi, C., and Lianidou, E. S. (2013). Comparison of three molecular assays for the detection and molecular characterization of circulating tumor cells in breast cancer. *Breast Cancer Res.* 15:R20. doi: 10.1186/bcr3395

Strell, C., and Entschladen, F. (2008). Extravasation of leukocytes in comparison to tumor cells. *Cell Commun. Signal.* 6:10. doi: 10.1186/1478-811X-6-10

Strilic, B., and Offermanns, S. (2017). Intravascular survival and extravasation of tumor cells. *Cancer Cell* 32, 282–293. doi: 10.1016/j.ccell.2017.07.001

Sweet, M. B., Thonar, E. M., and Immelman, A. R. (1976). Glycosaminoglycans and proteoglycans of human chondrosarcoma. *Biochim. Biophys. Acta* 437, 71–86. doi: 10.1016/0304-4165(76)90348-2

Tarbell, J. M., and Cancel, L. M. (2016). The glycocalyx and its significance in human medicine. *J. Intern. Med.* 280, 97–113.

Tatrai, P., Egedi, K., Somoracz, A., Van Kuppevelt, T. H., Ten Dam, G., Lyon, M., et al. (2010). Quantitative and qualitative alterations of heparan sulfate in fibrogenic liver diseases and hepatocellular cancer. *J. Histochem. Cytochem.* 58, 429–441. doi: 10.1369/jhc.2010.955161

ten Dam, G. B., Van De Westerlo, E. M., Purushothaman, A., Stan, R. V., Bulten, J., Sweep, F. C., et al. (2007). Antibody GD3G7 selected against embryonic glycosaminoglycans defines chondroitin sulfate-E domains highly up-regulated in ovarian cancer and involved in vascular endothelial growth factor binding. *Am. J. Pathol.* 171, 1324–1333. doi: 10.2353/ajpath.2007.070111

Theocharis, A. D., Skandalis, S. S., Neill, T., Multhaupt, H. A. B., Hubo, M., Frey, H., et al. (2015). Insights into the key roles of proteoglycans in breast cancer biology and translational medicine. *Biochim. Biophys. Acta* 1855, 276–300. doi: 10.1016/j.bbcan.2015.03.006

Thomas, S. N., Zhu, F., Schnaar, R. L., Alves, C. S., and Konstantopoulos, K. (2008). Carcinoembryonic antigen and CD44 variant isoforms cooperate to mediate colon carcinoma cell adhesion to E- and L-selectin in shear flow. *J. Biol. Chem.* 283, 15647–15655.

Thompson, C. A., Purushothaman, A., Ramani, V. C., Vlodavsky, I., and Sanderson, R. D. (2013). Heparanase regulates secretion, composition, and function of tumor cell-derived exosomes. *J. Biol. Chem.* 288, 10093–10099. doi: 10.1074/jbc.C112.444562

Thorsteinsson, M., Soletormos, G., and Jess, P. (2011). Low number of detectable circulating tumor cells in non-metastatic colon cancer. *Anticancer Res.* 31, 613–617.

Tiedemann, K., Olander, B., Eklund, E., Todorova, L., Bengtsson, M., Maccarana, M., et al. (2005). Regulation of the chondroitin/dermatan fine structure by transforming growth factor-beta1 through effects on polymer-modifying enzymes. *Glycobiology* 15, 1277–1285. doi: 10.1093/glycob/cwj027

Toba-Ichihashi, Y., Yamaoka, T., Ohmori, T., and Ohba, M. (2016). Up-regulation of Syndecan-4 contributes to TGF-beta1-induced epithelial to mesenchymal transition in lung adenocarcinoma A549 cells. *Biochem. Biophys. Rep.* 5, 1–7. doi: 10.1016/j.bbrep.2015.11.021

Todaro, M., Gaggianesi, M., Catalano, V., Benfante, A., Iovino, F., Biffoni, M., et al. (2014). CD44v6 is a marker of constitutive and reprogrammed cancer stem cells driving colon cancer metastasis. *Cell Stem Cell* 14, 342–356. doi: 10.1016/j.stem.2014.01.009

Toledo, A. G., Pihl, J., Spliid, C. B., Persson, A., Nilsson, J., Pereira, M. A., et al. (2020). An Affinity-Chromatography and Glycoproteomics Workflow to Profile the Chondroitin Sulfate Proteoglycans that interact with malarial VAR2CSA in the Placenta and in Cancer. *Glycobiology*. doi: 10.1093/glycob/cwaa039 [Epub ahead of print].

Toole, B. P. (2001). Hyaluronan in morphogenesis. *Semin. Cell Dev. Biol.* 12, 79–87.

Toole, B. P. (2004). Hyaluronan: from extracellular glue to pericellular cue. *Nat. Rev. Cancer* 4, 528–539. doi: 10.1038/nrc1391

Toyama-Sorimachi, N., Sorimachi, H., Tobita, Y., Kitamura, F., Yagita, H., Suzuki, K., et al. (1995). A novel ligand for CD44 is serglycin, a hematopoietic cell lineage-specific proteoglycan. Possible involvement in lymphoid cell adherence and activation. *J. Biol. Chem.* 270, 7437–7444. doi: 10.1074/jbc.270.13.7437

Toyoshima, K., Hayashi, A., Kashiwagi, M., Hayashi, N., Iwatsuki, M., Ishimoto, T., et al. (2015). Analysis of circulating tumor cells derived from advanced gastric cancer. *Int. J. Cancer* 137, 991–998. doi: 10.1002/ijc.29455

Tsai, W. S., Chen, J. S., Shao, H. J., Wu, J. C., Lai, J. M., Lu, S. H., et al. (2016). Circulating tumor cell count correlates with colorectal neoplasm progression and is a prognostic marker for distant metastasis in non-metastatic patients. *Sci. Rep.* 6:24517. doi: 10.1038/srep24517

Tsao, S. C.-H., Wang, J., Wang, Y., Behren, A., Cebon, J., and Trau, M. (2018). Characterising the phenotypic evolution of circulating tumour cells during treatment. *Nat. Commun.* 9:1482. doi: 10.1038/s41467-018-03725-8

Turley, E. A., Noble, P. W., and Bourguignon, L. Y. (2002). Signaling properties of hyaluronan receptors. *J. Biol. Chem.* 277, 4589–4592.

Ulmer, A., Schmidt-Kittler, O., Fischer, J., Ellwanger, U., Rassner, G., Riethmüller, G., et al. (2004). Immunomagnetic enrichment, genomic characterization, and prognostic impact of circulating melanoma cells. *Clin. Cancer Res.* 10, 531–537. doi: 10.1158/1078-0432.ccr-0424-03

Valiyaveettil, M., Achur, R. N., Muthusamy, A., and Gowda, D. C. (2004). Characterization of chondroitin sulfate and dermatan sulfate proteoglycans of extracellular matrices of human umbilical cord blood vessels and Wharton's jelly. *Glycoconj. J.* 21, 361–375. doi: 10.1023/B:GLYC.0000046276.77147.b2

van Zijl, F., Krupitza, G., and Mikulits, W. (2011). Initial steps of metastasis: cell invasion and endothelial transmigration. *Mutat. Res.* 728, 23–34. doi: 10.1016/j.mrrev.2011.05.002

Vicente, C. M., Lima, M. A., Yates, E. A., Yates, H. B., and Toma, L. (2015). Enhanced tumorigenic potential of colorectal cancer cells by extracellular sulfatases. *Mol. Cancer Res.* 13, 510–523. doi: 10.1158/1541-7786.MCR-14-0372

Vijaya Kumar, A., Salem Gassar, E., Spillmann, D., Stock, C., Sen, Y. P., Zhang, T., et al. (2014). HS3ST2 modulates breast cancer cell invasiveness via MAP kinase- and Tcf4 (Tcf7l2)-dependent regulation of protease and cadherin expression. *Int. J. Cancer* 135, 2579–2592. doi: 10.1002/ijc.28921

Vitale, D., Kumar Katakam, S., Greve, B., Jang, B., Oh, E. S., Alaniz, L., et al. (2019). Proteoglycans and glycosaminoglycans as regulators of cancer stem cell function and therapeutic resistance. *FEBS J.* 286, 2870–2882. doi: 10.1111/febs.14967

Vogel, A., Cervantes, A., Chau, I., Daniele, B., Llovet, J. M., Meyer, T., et al. (2019). Hepatocellular carcinoma: ESMO Clinical Practice Guidelines for diagnosis, treatment and follow-up. *Ann. Oncol.* 30, 871–873.

Walimbe, T., and Panitch, A. (2019). Proteoglycans in biomedicine: resurgence of an underexploited class of ECM molecules. *Front. Pharmacol.* 10:1661. doi: 10.3389/fphar.2019.01661

Wang, D., Liu, X., Hsieh, B., Bruce, R., Somlo, G., Huang, J., et al. (2015). Exploring glycan markers for immunotyping and precision-targeting of breast circulating tumor cells. *Arch. Med. Res.* 46, 642–650. doi: 10.1016/j.arcmed.2015.11.007

Wang, H. L., Anatelli, F., Zhai, Q. J., Adley, B., Chuang, S. T., and Yang, X. J. (2008). Glypican-3 as a useful diagnostic marker that distinguishes hepatocellular carcinoma from benign hepatocellular mass lesions. *Arch. Pathol. Lab. Med.* 132, 1723–1728. doi: 10.1043/1543-2165-132.11.1723

Wang, J., Svendsen, A., Kmiecik, J., Immervoll, H., Skaftnesmo, K. O., Planagumà, J., et al. (2011). Targeting the NG2/CSPG4 proteoglycan retards tumour growth and angiogenesis in preclinical models of GBM and melanoma. *PLoS One* 6:e23062. doi: 10.1371/journal.pone.0023062

Wang, M., Xiao, Y., Lin, L., Zhu, X., Du, L., and Shi, X. (2018). A microfluidic chip integrated with hyaluronic acid-functionalized electrospun chitosan nanofibers for specific capture and nondestructive release of CD44-overexpressing circulating tumor cells. *Bioconj. Chem.* 29, 1081–1090. doi: 10.1021/acs.bioconjchem.7b00747

Wang, N., Tesfaluul, N., Li, J., Gao, X., Liu, S., and Yue, B. (2019). Enrichment of circulating myeloma cells by immunomagnetic beads combined with flow cytometry for monitoring minimal residual disease and relapse in patients with multiple myeloma. *Ann. Hematol.* 98, 2769–2780. doi: 10.1007/s00277-019-03833-5

Wang, Z., Zhao, K., Hackert, T., and Zoller, M. (2018). CD44/CD44v6 a reliable companion in cancer-initiating cell maintenance and tumor progression. *Front. Cell Dev. Biol.* 6:97. doi: 10.3389/fcell.2018.00097

Watanabe, M., Uehara, Y., Yamashita, N., Fujimura, Y., Nishio, K., Sawada, T., et al. (2014). Multicolor detection of rare tumor cells in blood using a novel flow cytometry-based system. *Cytometry A* 85, 206–213. doi: 10.1002/cyto.a.22422

Watanabe, T., Okumura, T., Hirano, K., Yamaguchi, T., Sekine, S., Nagata, T., et al. (2017). Circulating tumor cells expressing cancer stem cell marker CD44 as a diagnostic biomarker in patients with gastric cancer. *Oncol. Lett.* 13, 281–288. doi: 10.3892/ol.2016.5432

Wei, R. R., Sun, D. N., Yang, H., Yan, J., Zhang, X., Zheng, X. L., et al. (2018). CTC clusters induced by heparanase enhance breast cancer metastasis. *Acta Pharmacol. Sin.* 39, 1326–1337. doi: 10.1038/aps.2017.189

Weigel, P. H., and DeAngelis, P. L. (2007). Hyaluronan synthases: a decade-plus of novel glycosyltransferases. *J. Biol. Chem.* 282, 36777–36781. doi: 10.1074/jbc.R700036200

Weiss, A., and Attisano, L. (2013). The TGFbeta superfamily signaling pathway. *Wiley Interdiscip. Rev. Dev. Biol.* 2, 47–63.

Werner, S. L., Graf, R. P., Landers, M., Valenta, D. T., Schroeder, M., Greene, S. B., et al. (2015). Analytical validation and capabilities of the epic CTC platform: enrichment-free circulating tumour cell detection and characterization. *J. Circ. Biomark.* 4:3. doi: 10.5772/60725

Woods, E. C., Kai, F., Barnes, J. M., Pedram, K., Pickup, M. W., Hollander, M. J., et al. (2017). A bulky glycocalyx fosters metastasis formation by promoting G1 cell cycle progression. *eLife* 6:e25752. doi: 10.7554/eLife.25752

Wu, J., Raba, K., Guglielmi, R., Behrens, B., Van Dalum, G., Flugen, G., et al. (2020). Magnetic-based enrichment of rare cells from high concentrated blood samples. *Cancers* 12:E933. doi: 10.3390/cancers12040933

Wu, Y., and Zhou, B. P. (2010). TNF-α/NF-κB/Snail pathway in cancer cell migration and invasion. *Br. J. Cancer* 102, 639–644. doi: 10.1038/sj.bjc.6605530

Xu, D., and Esko, J. D. (2014). Demystifying heparan sulfate-protein interactions. *Annu. Rev. Biochem.* 83, 129–157.

Xu, H., Chen, X., and Huang, Z. (2019). Identification of ESM1 overexpressed in head and neck squamous cell carcinoma. *Cancer Cell Int.* 19:118. doi: 10.1186/s12935-019-0833-y

Xu, J., Lamouille, S., and Derynck, R. (2009). TGF-beta-induced epithelial to mesenchymal transition. *Cell Res.* 19, 156–172.

Xu, J., Vilanova, G., and Gomez, H. (2016). A mathematical model coupling tumor growth and angiogenesis. *PLoS One* 11:e0149422. doi: 10.1371/journal.pone.0149422

Yamagata, M., Kimata, K., Oike, Y., Tani, K., Maeda, N., Yoshida, K., et al. (1987). A monoclonal antibody that specifically recognizes a glucuronic acid 2-sulfate-containing determinant in intact chondroitin sulfate chain. *J. Biol. Chem.* 262, 4146–4152.

Yan-Bin, S., Guang-Hao, S., Shun, X., and Jing-Jing, X. (2020). Tumor-suppressive activity of sTRAIL on circulating CD44+ cells in patients with non-small cell lung cancer. *Biol. Chem.* 401, 417–422. doi: 10.1515/hsz-2019-0339

Yang, C., Xia, B. R., Jin, W. L., and Lou, G. (2019). Circulating tumor cells in precision oncology: clinical applications in liquid biopsy and 3D organoid model. *Cancer Cell Int.* 19:341. doi: 10.1186/s12935-019-1067-8

Yang, J., Price, M. A., Li, G. Y., Bar-Eli, M., Salgia, R., Jagedeeswaran, R., et al. (2009). Melanoma proteoglycan modifies gene expression to stimulate tumor cell motility, growth, and epithelial-to-mesenchymal transition. *Cancer Res.* 69, 7538–7547. doi: 10.1158/0008-5472.CAN-08-4626

Yang, J. D., Campion, M. B., Liu, M. C., Chaiteerakij, R., Giama, N. H., Ahmed Mohammed, H., et al. (2016). Circulating tumor cells are associated with poor overall survival in patients with cholangiocarcinoma. *Hepatology* 63, 148–158. doi: 10.1002/hep.27944

Yin, J., Wang, Y., Yin, H., Chen, W., Jin, G., Ma, H., et al. (2015). Circulating tumor cells enriched by the depletion of leukocytes with Bi-antibodies in non-small cell lung cancer: potential clinical application. *PLoS One* 10:e0137076. doi: 10.1371/journal.pone.0137076

Yoneda, A., Lendorf, M. E., Couchman, J. R., and Multhaupt, H. A. (2012). Breast and ovarian cancers: a survey and possible roles for the cell surface heparan sulfate proteoglycans. *J. Histochem. Cytochem.* 60, 9–21. doi: 10.1369/0022155411428469

Zhang, W., Chan, H., Wei, L., Pan, Z., Zhang, J., and Li, L. (2013). Overexpression of heparanase in ovarian cancer and its clinical significance. *Oncol. Rep.* 30, 2279–2287. doi: 10.3892/or.2013.2701

Zhang, Z., Shiratsuchi, H., Lin, J., Chen, G., Reddy, R. M., Azizi, E., et al. (2014). Expansion of CTCs from early stage lung cancer patients using a microfluidic co-culture model. *Oncotarget* 5, 12383–12397. doi: 10.18632/oncotarget.2592

Zhangyuan, G., Wang, F., Zhang, H., Jiang, R., Tao, X., Yu, D., et al. (2020). VersicanV1 promotes proliferation and metastasis of hepatocellular carcinoma through the activation of EGFR–PI3K–AKT pathway. *Oncogene* 39, 1213–1230. doi: 10.1038/s41388-019-1095-9

Zhu, Y. H., Yang, F., Zhang, S. S., Zeng, T. T., Xie, X., and Guan, X. Y. (2013). High expression of biglycan is associated with poor prognosis in patients with esophageal squamous cell carcinoma. *Int. J. Clin. Exp. Pathol.* 6, 2497–2505.

Zhu, Z. W., Friess, H., Wang, L., Abou-Shady, M., Zimmermann, A., Lander, A. D., et al. (2001). Enhanced glypican-3 expression differentiates the majority of hepatocellular carcinomas from benign hepatic disorders. *Gut* 48, 558–564. doi: 10.1136/gut.48.4.558

Zoller, M. (2011). CD44: Can a cancer-initiating cell profit from an abundantly expressed molecule? *Nat. Rev. Cancer* 11, 254–267. doi: 10.1038/nrc3023

Conflict of Interest: TC, AS, and MA are shareholders in VAR2 Pharmaceuticals holding the intellectual property rights to use rVAR2 for binding oncofetal chondroitin sulfate and to capture circulating tumor cells. VarCT Diagnostics is a subsidiary to VAR2 Pharmaceuticals.

The remaining authors declare that the research was conducted in the absence of any other commercial or financial relationships that could be construed as a potential conflict of interest.

frontiers in Cell and Developmental Biology

ORIGINAL RESEARCH
published: 28 August 2020
doi: 10.3389/fcell.2020.00792

The Cardiac Syndecan-2 Interactome

*Sabrina Bech Mathiesen[1], Marianne Lunde[1], Maria Stensland[2], Marita Martinsen[1], Tuula A. Nyman[2], Geir Christensen[1,3] and Cathrine Rein Carlson[1]**

[1] Institute for Experimental Medical Research and Oslo University Hospital, University of Oslo, Oslo, Norway, [2] Department of Immunology, Institute of Clinical Medicine, University of Oslo, Oslo, Norway, [3] K.G. Jebsen Center for Cardiac Research, University of Oslo, Oslo, Norway

The extracellular matrix (ECM) is important in cardiac remodeling and syndecans have gained increased interest in this process due to their ability to convert changes in the ECM to cell signaling. In particular, syndecan-4 has been shown to be important for cardiac remodeling, whereas the role of its close relative syndecan-2 is largely unknown in the heart. To get more insight into the role of syndecan-2, we here sought to identify interaction partners of syndecan-2 in rat left ventricle. By using three different affinity purification methods combined with mass spectrometry (MS) analysis, we identified 30 novel partners and 9 partners previously described in the literature, which together make up the first cardiac syndecan-2 interactome. Eleven of the novel partners were also verified in HEK293 cells (i.e., AP2A2, CAVIN2, DDX19A, EIF4E, JPH2, MYL12A, NSF, PFDN2, PSMC5, PSMD11, and RRAD). The cardiac syndecan-2 interactome partners formed connections to each other and grouped into clusters mainly involved in cytoskeletal remodeling and protein metabolism, but also into a cluster consisting of a family of novel syndecan-2 interaction partners, the CAVINs. MS analyses revealed that although syndecan-2 was significantly enriched in fibroblast fractions, most of its partners were present in both cardiomyocytes and fibroblasts. Finally, a comparison of the cardiac syndecan-2 and -4 interactomes revealed surprisingly few protein partners in common.

Keywords: syndecan-2, syndecan, proteoglycans, interactome, cardiac, heart, CAVIN, junctophilin

OPEN ACCESS

Edited by:
Jeremy Turnbull, University of Liverpool, United Kingdom

Reviewed by:
Jun Zhou, German Cancer Research Center (DKFZ), Germany
Sandeep Gopal, Monash University, Australia
James R. Whiteford, Queen Mary University of London, United Kingdom

****Correspondence:***
Cathrine Rein Carlson
c.r.carlson@medisin.uio.no

Specialty section:
This article was submitted to Signaling, a section of the journal Frontiers in Cell and Developmental Biology

Received: *08 May 2020*
Accepted: *28 July 2020*
Published: *28 August 2020*

Citation:
Mathiesen SB, Lunde M, Stensland M, Martinsen M, Nyman TA, Christensen G and Carlson CR (2020) The Cardiac Syndecan-2 Interactome. Front. Cell Dev. Biol. 8:792. doi: 10.3389/fcell.2020.00792

INTRODUCTION

To cope with injury and mechanical stress, the heart can change its shape and function, a process associated with alterations of the extracellular matrix (ECM) and progression toward heart failure (Cohn et al., 2000). At the cellular level, this includes hypertrophy or death of cardiomyocytes and activation of fibroblasts to ECM producing myofibroblasts, which manifests itself as hypertrophy of the myocardium and stiffening through fibrosis (Cohn et al., 2000). Proteoglycans are emerging as important players in ECM remodeling in the heart, including members of the syndecan family (Christensen et al., 2019). Syndecan-4 has been shown to be a pro-remodeling molecule, acting in both cardiomyocytes and fibroblasts (Finsen et al., 2011;

Abbreviations: AP, affinity purification; AP-MS, affinity purification coupled to mass spectrometry; ECM, extra cellular matrix; GST, glutathione *S*-transferase; HRP, horseradish peroxidase; IP, immunoprecipitation; literature partner, syndecan-2 interaction partner previously described in the literature; LV, left ventricle; MS partner, syndecan-2 interaction partner identified in AP-MS in this study; MS, mass spectrometry; Scram, scrambled peptide; SDC2, syndecan-2; $SDC2_{cyt}$, cytoplasmic domain of syndecan-2.

Herum et al., 2015). Knock-out of syndecan-4 in mice has been shown to hinder development of pressure overload induced hypertrophy and stiffening of the myocardium through the calcineurin-NFAT pathway and collagen crosslinking (Finsen et al., 2011; Herum et al., 2013; Herum et al., 2015). Although syndecan-4 has been identified as an important signaling mediator, little is known about its close relative, syndecan-2 in the heart. Both syndecan-2 and -4 are expressed in the heart and upregulated following aortic banding (Strand et al., 2013).

The vertebrate syndecan family arose as a result of two rounds of gene duplication, resulting in four family members where syndecan-2 and -4 form one subfamily (Chakravarti and Adams, 2006). While syndecan-4 is ubiquitously expressed, syndecan-2 is primarily expressed in cells from mesenchymal origin, including fibroblasts, endothelial and neuronal cells and is upregulated during development (David et al., 1993; Kim et al., 1994; Ethell and Yamaguchi, 1999; Chen E. et al., 2004). However, syndecan-2 expression has also been observed in cardiomyocytes (Balza and Misra, 2006). Syndecan-2 has been implicated in diverse cellular events, including highly dynamic processes such as angiogenesis and cancer metastasis, but also in formation of mature structures like dendritic spines and control of ECM assembly, all of which appear to require the intact cytoplasmic domain (Ethell and Yamaguchi, 1999; Klass et al., 2000; Chen E. et al., 2004; Essner et al., 2006; Lee et al., 2011; Lim and Couchman, 2014). Its cytoplasmic tail is short, can be subdivided into three regions and has no known intrinsic enzymatic activity, but can connect to multiple proteins (Couchman, 2010). The membrane proximal C1 region can connect to ezrin, which associates with the actin cytoskeleton (Granes et al., 2000). The membrane distal C2 region binds PDZ domain proteins and is mainly involved in intracellular trafficking (Ethell et al., 2000; Zimmermann et al., 2005). The C1 and C2 regions are in common, whereas the middle V (variable) region is unique to each of the syndecans and is probably responsible for syndecan specific signaling (Couchman et al., 2015).

To better understand the role of syndecan-2 in the heart, we here aimed to identify cytoplasmic interaction partners of syndecan-2 in rat left ventricle (LV) and to construct the cardiac syndecan-2 interactome.

RESULTS

Combining Three Affinity Purification Approaches to Capture Syndecan-2 Interaction Partners

We identified putative syndecan-2 interaction partners from rat LV lysates by combining three AP approaches with MS. **Figure 1A** depicts the experimental design, emphasizing the three different baits and respective controls (bottom of the boxes). The left panel (i) shows biotinylated peptides of the syndecan-2 cytoplasmic domain ($SDC2_{cyt}$) used as bait to pull down interaction partners by streptavidin coated beads. An ahx linker was inserted in between the biotin-tag and the syndecan-2 cytoplasmic sequence to avoid steric hindrance (**Figure 1B**, upper sequence). A scrambled syndecan-2 peptide (scram) (**Figure 1B**, lower sequence) and beads without peptides (beads only) were used as negative controls. The middle panel of **Figure 1A**, (ii), illustrates IP with anti-syndecan-2 (anti-SDC2) where endogenous syndecan-2 was used as bait. Specificity of the antibody was demonstrated by overlaying anti-SDC2 onto membranes with spot-synthesized 20-mer overlapping peptides, which covered the protein sequence of either mouse, rat or human syndecan-2 or rat syndecan-4. This revealed an ectodomain epitope in syndecan-2 across species, which left the cytoplasmic tail free to interact with protein partners (**Figure 1C**). Importantly, the antibody only recognized syndecan-2 and showed no cross reactivity toward rat syndecan-4 (**Figure 1C**, lower panel). Anti-SDC2 was also demonstrated to be able to precipitate endogenous syndecan-2 from rat LV lysates (**Figure 1D**). The right panel of **Figure 1A**, (iii), illustrates IP-GST where a recombinant N-terminal GST-tagged full-length syndecan-2 protein (GST-SDC2) was used as bait to capture interaction partners. Recombinant GST without syndecan-2 and beads were used as negative controls. The GST antibody was demonstrated to precipitate GST-SDC2 in rat LV lysates prior to the large AP-MS analysis (**Figure 1E**). Following the three different APs, the precipitated interaction partners were subjected to trypsin digestion and subsequent MS analysis (**Figure 1A**, bottom part).

Identification of 30 Novel Syndecan-2 Interaction Partners

All APs were done in biological triplicates. To be considered as a syndecan-2 interaction partner, proteins had to be identified in IP-SDC2 (**Figure 2** peach colored circle) and additionally in either IP-GST (**Figure 2** dark green circle) or pull down with $SDC2_{cyt}$ (**Figure 2** light green circle). Proteins known to be confined in the nucleus, ribosome and mitochondria were excluded since they were regarded as contaminants. Overall, 30 novel syndecan-2 interaction partners were identified by AP-MS with these criteria (hereafter referred to as MS partners) and are listed in **Table 1** (detailed overview in **Supplementary Table S1**). **Table 2** summarizes syndecan-2 protein interaction partners described in the literature across tissues and species (hereafter referred to as literature partners). Importantly, both the literature partners cortactin (CTTN) and syntenin-1 (SDCBP) were identified in either two or three of the AP-MS approaches (underlined in **Figure 2** and in **Tables 1**, **2**). In addition, seven literature partners were identified by fishing with the $SDC2_{cyt}$ peptide or GST-SDC2 in the LV lysate. These were the cell division control protein 42 homolog (CDC42), band 4.1-like protein 1 (EPB41L1), ezrin (EZR), β1 integrin (ITGB1), matrix metalloproteinase-2 (MMP2), matrix metalloproteinase-9 (MMP9) and ras-related C3 botulinum toxin substrate 1 (RAC1) (underlined in **Figure 2** and **Table 2**, $n = 3$).

Verification of 11 Syndecan-2 Interaction Partners in HEK293 Cells

We decided to verify selected MS partners in additional binding studies using HEK293 cells and chose a set-up that reversed the

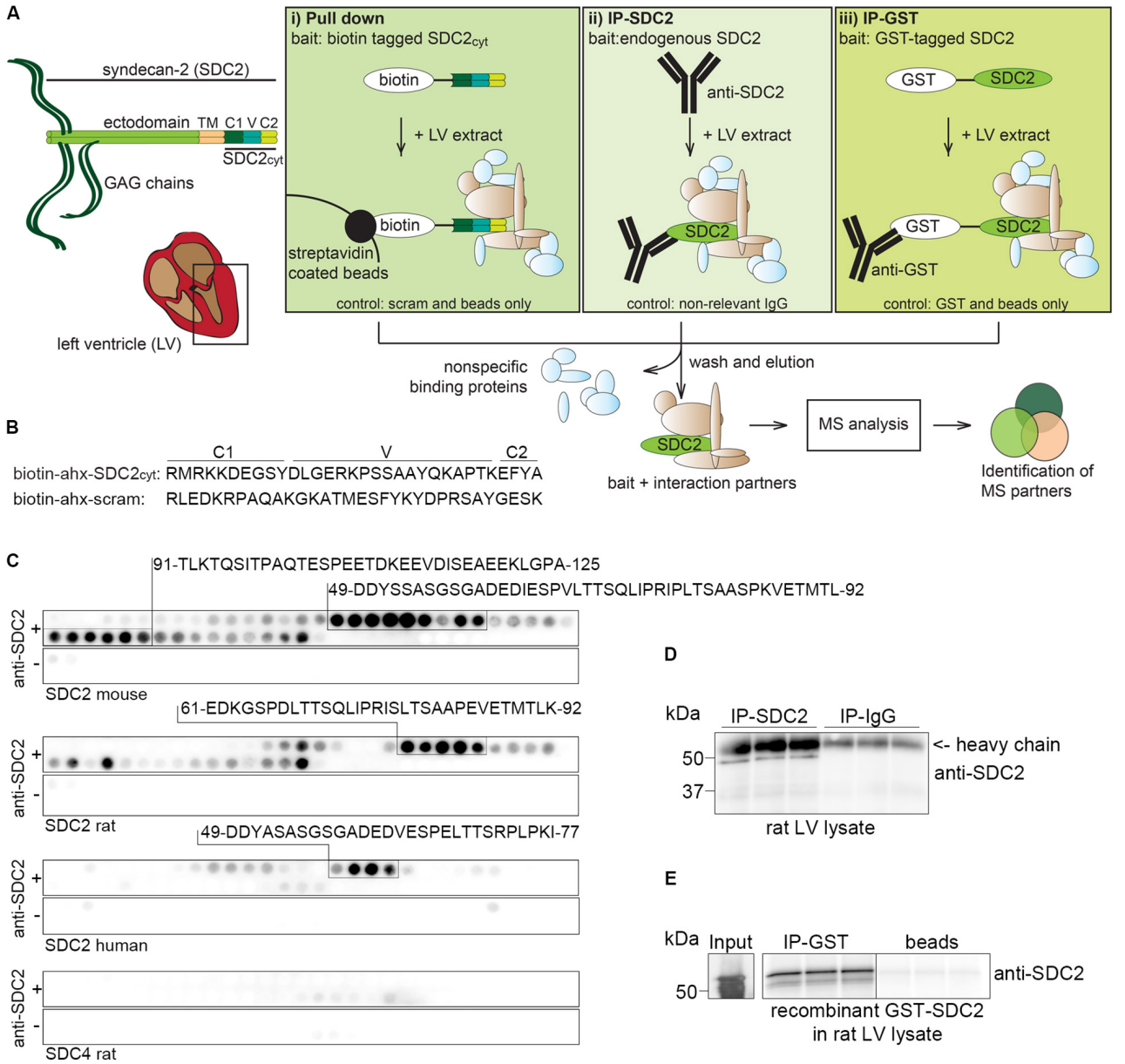

FIGURE 1 | Experimental design to identify syndecan-2 interaction partners in LV lysate. **(A)** Schematic illustration of the three different AP-MS experiments used to capture syndecan-2 interaction partners: (i) pull down with biotinylated peptides covering the cytoplasmic tail of syndecan-2 ($SDC2_{cyt}$, left panel), (ii) precipitation of endogenous cardiac syndecan-2 using anti-SDC2 (middle panel) and (iii) fishing with recombinant GST-tagged syndecan-2 and precipitation by GST antibodies (right panel). After washing away non-specific proteins, putative interaction partners were eluted, trypsin digested and analyzed by mass spectrometry. **(B)** Protein sequences of the $SDC2_{cyt}$ and a scrambled (scram) control peptide used for the pull down approach described in **(Ai)**. An ahx linker was inserted between the biotin-tag and the sequence to avoid steric hindrance. **(C)** Epitope mapping of the syndecan-2 antibody (anti-SDC2) used in **(Aii)**, using peptide array membranes containing 20-mer overlapping syndecan-2 (mouse, rat, and human) and syndecan-4 (rat) peptides. **(D)** Validation of anti-SDC2 in immunoprecipitation experiments of endogenous syndecan-2 in rat LV lysates. **(E)** Validation of the GST antibody in immunoprecipitation experiments of recombinant GST-syndecan-2 in rat LV lysates.

strategy used for MS. Two syndecan-2 bands of approximately 30 (doublet) and 45 kDa were detected when HA-tagged syndecan-2 (HA-SDC2) was analyzed by immunoblotting (**Figure 3A**). The core domain of human syndecan-2 is predicted to approximately 23 kDa and is known to form SDS resistant dimers through the transmembrane domain. Eleven of the 30 MS partners were expressed with a FLAG-tag together with HA-SDC2 in HEK293 cells and subjected to IP-FLAG. Cortactin (CTTN) was included as a positive control and heat shock protein beta-6 (HSPB6) and serine/threonine-protein phosphatase PP1-alpha catalytic subunit (PPP1CA) were included as negative controls. The latter controls were included to ensure that protein precipitation was not due to simple overexpression. As expected, CTTN precipitated HA-SDC2 (**Figure 3B**), whereas the

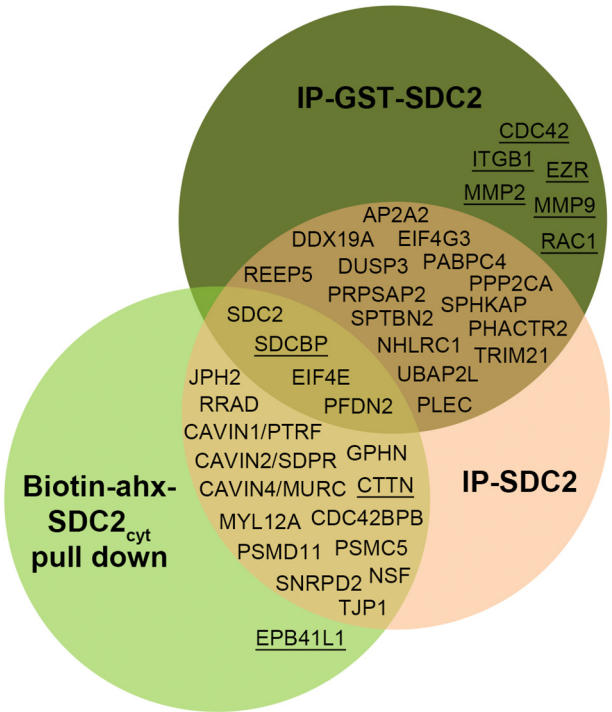

FIGURE 2 | Venn diagram depicting the distribution of syndecan-2 interaction partners in the three AP-MS approaches. Overall, 30 novel putative syndecan-2 partners were identified and they are given in the circles representing the AP-MS methods where they were identified. Syndecan-2 interaction partners previously described in the literature are underlined. The literature partner SDCBP was found in all three AP-MS approaches and the literature partner CTTN was found in two.

negative controls did not show specific binding (**Figures 3C,D**). The 11 MS partners that precipitated HA-SDC2 were AP-2 complex subunit alpha-2 (AP2A2), caveolae-associated protein 2 (CAVIN2), ATP-dependent RNA helicase DDX19A (DDX19A), eukaryotic translation initiation factor 4E (EIF4E), junctophilin-2 (JPH2), myosin regulatory light chain 12A (MYL12A), vesicle-fusing ATPase (NSF), prefoldin subunit 2 (PFDN2), 26S protease regulatory subunit 8 (PSMC5), 26S proteasome non-ATPase regulatory subunit 11 (PSMD11) and GTP-binding protein RAD (RRAD) (**Figures 3E–O**, respectively).

Overview of the Syndecan-2 Interactome

To get a more comprehensive overview of the syndecan-2 interactome, we combined the 30 novel MS partners (**Table 1**) together with the 41 literature partners identified in different tissues and species (**Table 2**) and grouped them according to the GO annotation biological process (**Figure 4A**). The MS partners (in green) distributed into several groups together with literature partners (**Figure 4A**), where the three largest were; cell communication, protein metabolism and cell growth and/or maintenance (**Figure 4A**). Within the three largest groups we also found the nine literature partners identified in our MS approach (**Figure 4A** underlined). We further performed a STRING database network analysis to predict connections among the 30 novel MS partners and the nine literature partners (**Figure 4B**). This revealed that the cardiac syndecan-2 interactome contained more connections than expected from a random set of proteins (PPI enrichment p-value: <0.000117, a list of all connections is given in **Supplementary Table S2**). Importantly, several of the novel MS partners connected with the literature partners and formed clusters (**Figure 4B**).

Functional Annotation of the Syndecan-2 Interactome

The syndecan-2 interactome was also subjected to a functional annotation analysis through the DAVID Bioinformatics Resources[1]. The disease-class enrichment database revealed "cancer" and "cardiovascular" to be the top most prevalent enriched disease classes (**Table 3**). In line with this, the Kyoto Encyclopedia of Genes and Genome (KEGG) enrichment analysis predicted "proteoglycans in cancer," "focal adhesion," "leukocyte transendothelial migration," "regulation of actin cytoskeleton," and "pathways in cancer" as the top five pathways, but also "VEGF signaling" and different "cardiomyopathies" were predicted (**Table 4**). The DAVID tool was also used to search for enriched protein domains in the syndecan-2 interactome through the PFAM database (**Table 5**). The two most significant enriched protein domains were "integrin alpha" and" FG-GAP repeat," which is part of the propeller structure of integrin alpha subunits. The third most enriched protein domain group was the "putative peptidoglycan binding domain," which included several metalloproteinases. Interestingly, the fourth most enriched protein domain group was the CAVIN family, which contained the three novel MS partners caveolae-associated protein 1 (CAVIN1/PTRF), caveolae-associated protein 2 (CAVIN2/SDPR) and caveolae-associated protein 4 (CAVIN4/MURC).

Relative Levels of the Syndecan-2 Interactome Partners in Cardiac Fibroblasts and Cardiomyocytes

We decided to test whether the interactome proteins were mostly expressed in primary rat neonatal fibroblast or cardiomyocytes by MS analysis (**Figure 5**). Troponin-3 (TNNI3) was included as a marker for cardiomyocytes and vimentin (VIM) as a marker for fibroblasts (**Figure 5** in bold). Purity of the cell fractions was based on the enrichment of TNN13 in the cardiomyocyte fraction and the lack thereof in the fibroblast fraction. Both endothelial cells and fibroblasts express vimentin [reviewed in Ivey and Tallquist (2016)] and some contamination of endothelial cells might have occurred. Except for NHLRC1, PHACTR2, RRAD, and TRIM21 (**Table 1**, marked[b)]), all novel MS partners and several of the syndecan-2 literature partners were identified in both cell types and most were enriched in one of the cell fractions (**Figure 5**). Syndecan-2 was enriched in the fibroblast fraction. The reason that not all interactome partners were detected might be because they are expressed at a more mature stage or expressed in other cell types.

[1]https://david.ncifcrf.gov/

TABLE 1 | Thirty novel syndecan-2 interaction partners identified by AP-MS.

Gene	Protein (Uniprot)	AP-MS (n = 3)	Molecular function (HPRD)
AP2A2[(a)FB]	AP-2 complex subunit alpha-2	IP-SDC2, GST-SDC2	Transporter activity
CAVIN1/PTRF[CM]	Caveolae-associated protein 1	IP-SDC2, $SDC2_{cyt}$	Transcription regulator activity
CAVIN2/SDPR[(a)FB]	Caveolae-associated protein 2	IP-SDC2, $SDC2_{cyt}$	Serine-type peptidase activity
CAVIN4/MURC[CM]	Caveolae-associated protein 4	IP-SDC2, $SDC2_{cyt}$	Unknown
*CDC42BPB/MRCK*β	Serine/threonine-protein kinase MRCK beta	IP-SDC2, $SDC2_{cyt}$	Protein serine/threonine kinase activity
CTTN[(a)FB]	Src substrate cortactin	IP-SDC2, $SDC2_{cyt}$	Cytoskeletal protein binding
DDX19A[(a)]	ATP-dependent RNA helicase DDX19A	IP-SDC2, GST-SDC2	Unknown
DUSP3	Dual-specificity phosphatase 3	IP-SDC2, GST-SDC2	Protein tyrosine/serine/threonine phosphatase activity
EIF4E[(a)]	Eukaryotic translation initiation factor 4E	IP-SDC2, GST-SDC2, $SDC2_{cyt}$	Translation regulator activity
EIF4G3	Eukaryotic translation initiation factor 4 gamma, 3	IP-SDC2, GST-SDC2	Translation regulator activity
GPHN[CM]	Gephyrin	IP-SDC2, $SDC2_{cyt}$	Unknown
JPH2[(a)CM]	Junctophilin-2	IP-SDC2, $SDC2_{cyt}$	Cell adhesion molecule activity
NHLRC1[(b)]	E3 ubiquitin-protein ligase NHLRC1	IP-SDC2, GST-SDC2	Ubiquitin-specific protease activity
MYL12A[(a)CM]	Myosin regulatory light chain 12A	IP-SDC2, $SDC2_{cyt}$	Calcium ion binding
NSF[(a)]	Vesicle-fusing ATPase	IP-SDC2, $SDC2_{cyt}$	ATPase activity
PABPC4[CM]	Polyadenylate-binding protein 4	IP-SDC2, GST-SDC2	RNA binding
PFDN2[(a)]	Prefoldin subunit 2	IP-SDC2, GST-SDC2, $SDC2_{cyt}$	Chaperone activity
PHACTR2[(b)]	Phosphatase and actin regulator 2	IP-SDC2, GST-SDC2	Phosphatase regulator activity
PLEC[CM]	Plectin	IP-SDC2, GST-SDC2	Cytoskeletal anchoring activity
PPP2CA[CM]	Serine/threonine-protein phosphatase 2A catalytic subunit alpha isoform	IP-SDC2, GST-SDC2	Protein serine/threonine phosphatase activity
PRPSAP2[CM]	Phosphoribosyl pyrophosphate synthase-associated protein 2	IP-SDC2, GST-SDC2	Unknown
PSMC5[(a)CM]	26S protease regulatory subunit 8	IP-SDC2, $SDC2_{cyt}$	Ubiquitin-specific protease activity
PSMD11[(a)]	26S proteasome non-ATPase regulatory subunit 11	IP-SDC2, $SDC2_{cyt}$	Ubiquitin-specific protease activity
REEP5	Receptor expression-enhancing protein 5	IP-SDC2, GST-SDC2	Unknown
RRAD[(a,b)]	GTP-binding protein RAD	IP-SDC2, $SDC2_{cyt}$	GTPase activity
SDCBP[(a)CM]	Syntenin-1	IP-SDC2, GST-SDC2, $SDC2_{cyt}$	Receptor signaling complex scaffold activity
SNRPD2	Small nuclear ribonucleoprotein Sm D2	IP-SDC2, $SDC2_{cyt}$	RNA binding
SPHKAP	A-kinase anchor protein SPHKAP	IP-SDC2, GST-SDC2	Unknown
SPTBN2	Spectrin beta chain, non-erythrocytic 2	IP-SDC2, GST-SDC2	Cytoskeletal protein binding
TJP1/ZO-1[CM]	Tight junction protein ZO-1	IP-SDC2, $SDC2_{cyt}$	Cell adhesion molecule activity
TRIM21[(b)]	E3 ubiquitin-protein ligase TRIM21	IP-SDC2, GST-SDC2	Ribonucleoprotein
UBAP2l	Ubiquitin-associated protein 2-like	IP-SDC2, GST-SDC2	Unknown

[(a)]*Precipitated also HA-SDC2 in HEK293 cells.* [(b)]*Not found in rat neonatal cardiomyocytes or fibroblasts by MS analyses.* [CM]*Enriched in rat neonatal cardiomyocytes.* [FB]*Enriched in rat neonatal fibroblasts. Underlined proteins have previously been described in the literature.*

DISCUSSION

In order to understand the mechanisms of cardiac disease, it is important to know the underlying players. Here we used three different AP-MS approaches to identify protein partners of the poorly described cardiac proteoglycan syndecan-2. In total, we identified 30 novel syndecan-2 partners and 9 out of 41 literature partners in rat LV lysates, which together constitute the first cardiac syndecan-2 interactome. Importantly, several of the interactome partners formed connections to each other, suggesting that these proteins are important for the role of syndecan-2 in the heart (**Figure 4B**).

Unlike a genome, a proteome is highly dynamic (Bonetta, 2010) and an interactome analysis like ours only provide a snapshot view of interaction partners in the given tissue. To include all potential syndecan-2 interaction partners, we used a membrane dissolving lysis buffer containing 1% triton to extract the LVs. We chose a relatively stringent set-up, where novel MS partners had to be detected in at least two of three AP-MS approaches. Although this strategy probably left out more transient binders, it increased the confidence in the novel syndecan-2 partners we identified in this study. Accordingly, all the novel partners tested in HEK293 cells showed binding to syndecan-2. Peptides of the syndecan-4 cytoplasmic domain have been shown to form dimers (Shin et al., 2001), but it is unsure if the syndecan-2 cytoplasmic tail without the transmembrane domain also form proper dimers (Choi et al., 2005). However, we identified both the C1 binder

TABLE 2 | Protein interaction partners previously reported for syndecan-2 or a conserved syndecan motif across species and tissue[a].

Gene	Protein	Where in SDC2	Evidence[c]	Biological role	Reference	AP-MS[b]
ARHGAP35[CM]	Rho GTPase-activating protein 35/p190ARhoGAP		Functional interaction	Actin cytoskeletal organization (SDC2 might control localization of p190RhoGAP)	Lim and Couchman, 2014	
CASK	Peripheral plasma membrane protein CASK	C2 (motif: EFYA) Direct	Peptide binding assays, Y2H and co-localization	Link to actin cytoskeleton and protein 4.1	Cohen et al., 1998; Hsueh et al., 1998	
CAV2	Caveolin-2		Co-IP	Regulation of adhesion. SDC2 might also be in complex with CAV1 (Shi et al., 2013)	Huang and Chuang, 2006; Lim et al., 2015	
CDC42[CM]	Cell division control protein 42 homolog		Cooperative interaction Cell adhesion studies	Filopodia formation in fibroblasts	Granes et al., 1999	IP-GST
CDH1	Cadherin-1/E-cadherin		Functional interaction	SDC2 promote E-cadherin shedding probably by MMP7	Jang et al., 2016	
CTTN	Cortactin	C1 (Motif: RMKKKDEGSY) Indirect	Affinity chromatography	Cortical actin organization	Kinnunen et al., 1998; Halden et al., 2004	IP-SDC2, $SDC2_{cyt}$
IL8/CXCL8	Interleukin-8	HS chains and possibly ectodomain	Co-IP, isothermal titration	Inflammation signaling	Halden et al., 2004	
CXCR2	C-X-C chemokine receptor type 2		Co-IP, co-localization	After stimulation CXCR2 and SDC2 co-localize	Renga et al., 2012	
DNM2	Dynamin-2	C1 Indirect	Co-IP, Y2H, pull down		Yoo et al., 2005	
EPB41L1	Band 4.1-like protein 1/Protein 4.1N	Cytoplasmic domain	Pull down	Formation of quaternary complex InsP3R1–4.1N–CASK–SDC2 in brain	Maximov et al., 2003	$SDC2_{cyt}$
EPHB2	EphB2 receptor tyrosine kinase/Ephrin type-B receptor 2	C1 + V region Direct	Co-IP, phosphorylation assay, co-localization	Phosphorylation on Y179 and Y191 (human numbering) Phosphorylation causes SDC2 clustering and is important for dendritic spine maturation	Ethell et al., 2001	
EZR[CM]	Ezrin	C1 (motif: DEGSYD) Direct	Co-IP, pull-down with peptides, co-localization, triton resistant complex	Link to actin cytoskeleton Interaction enhanced by RhoA	Granes et al., 2000; Granés et al., 2003	IP-GST
FYN	Fyn	C1	Affinity chromatography	Protein complex in brain	Kinnunen et al., 1998	
GIPC1	Synectin/PDZ domain-containing protein GIPC	C2	Y2H, Co-IP	Migration	Gao et al., 2000	
ITGA2	Integrin α2		Cooperative interaction, cell adhesion experiments	Cancer migration	Choi et al., 2009	
ITGA5	Integrin α5		Cooperative interaction, cell adhesion experiments	Stress fiber formation in lung carcinoma cell line	Kusano et al., 2000	
ITGAL	Integrin alpha-L (LFA-1)	Cytoplasmic domain	Cooperative interaction	SDC2 regulates the activity conformation of ITGAL	Rovira-Clave et al., 2014	
ITGAV[CM]	Integrin alpha-V		Cooperative interaction	Localization and virus entry	Cheshenko et al., 2007	
ITGB1	Integrin β1	Indirect ectodomain	Cooperative interaction, cell adhesion experiments	Adhesion	Kusano et al., 2000; Whiteford et al., 2007	IP-GST
ITGB4	Integrin β4	C2	Y2H	Cell spreading	Wang et al., 2010	
ITPR1[FB]	Inositol 1,4,5-trisphosphate receptor type 1/InsP3R1	Cyt domain Indirect	Pull down with SDC2 cytoplasmic peptides	Quaternary complex with SDC2-CASK-EPB41L1 in brain	Maximov et al., 2003	
MMP2[FB]	Matrix metalloproteinase-2/72 kDa type IV collagenase	Direct?	Ability to shed from cell surface (MMP added to cells, cell lysate dot blotted)	Shedding	Fears et al., 2006	IP-GST
MMP7	Matrix metalloproteinase-7	Direct, ectodomain	Co-IP, overlay assay	SDC2 might regulate processing of pro-MMP7	Ryu et al., 2009	

(Continued)

TABLE 2 | Continued

Gene	Protein	Where in SDC2	Evidence	Biological role	Reference	AP-MS[b]
MMP9	Matrix metalloproteinase-9	Direct?	Ability to shed from cell surface	Shedding	Fears et al., 2006	IP-GST
MMP14[FB]	Matrix metalloproteinase-14	Direct	Cleavage analysis	Shedding of SDC2 by membrane anchored MMP14	Lee et al., 2017	
NF1	Neurofibromin	Membrane proximal region of cytoplasmic domain Direct	Y2H, pull down, co-localization	Syndecans might localize neurofibromin to the membrane	Hsueh et al., 2001	
NOTCH3	Neurogenic locus notch homolog protein 3		Co-IP	SDC2 might amplify notch signaling	Zhao et al., 2012	
PRKC *–PRKCA* *–PRKCB* *–PRKCG*	Protein kinase C	V region Direct	*In vitro* peptide phosphorylation studies, PKC inhibitor blocks phosphorylation	Phosphorylation on S187 and S188 (human numbering)	Prasthofer et al., 1995; Oh et al., 1997	
PTPRJ	Protein tyrosine phosphatase receptor CD148/Receptor-type tyrosine-protein phosphatase eta	Membrane proximal region of shed SDC2 Direct	Solid-phase binding assay	Adhesion	Whiteford et al., 2011	
RAC1	Ras-related C3 botulinum toxin substrate 1		Functional interaction, overexpression of SDC2 increase Rac1 activity in cancer cells	Cancer migration	Choi et al., 2010	IP-GST
RACK1/NB2L1	Receptor of activated protein C kinase 1	FL	Co-IP, affinity chromatography	Scaffolding and downstream signaling	Huang et al., 2005a,b; Renga et al., 2012	
RASA1	Ras GTPase-activating protein 1/P120-GAP	FL	Co-IP	Downstream signaling	Huang et al., 2005a	
SARM1	Sarm1/Sterile alpha and TIR motif-containing protein 1	Cytoplasmic domain Direct	Pull down, co-IP	Regulation of dendritic outgrowth	Chen et al., 2011	
SDC2[FB]	Syndecan-2	TM: GXXXG	Mutation studies	Oligomerization	Choi et al., 2005; Dews and Mackenzie, 2007	IP-SDC2, IP-GST, $SDC2_{cyt}$
SDC4	Syndecan-4	TM: GXXXG		Hetero-oligomerization	Choi et al., 2015	
SDCBP	Syntenin/syntenin-1	C2 (motif: EFYA) Direct	Y2H, surface plasmon resonance, peptide binding assays and co-localization	Adaptor and intracellular trafficking	Grootjans et al., 1997	IP-SDC2, IP-GST, $SDC2_{cyt}$
SRC	Proto-oncogene tyrosine-protein kinase Src	C1	Affinity purification	Protein complex in brain	Kinnunen et al., 1998	
TGFBR1	TGF-beta receptor type-1 (TβRI)		Co-IP, functional studies	SDC2 may attenuate TGF-β1 signaling by internalizing	Shi et al., 2013	
TGFBR3	Transforming growth factor beta receptor type 3 (Betaglycan)	Cytoplasmic domain is needed	Co-IP	May be involved in fibrosis	Chen L. et al., 2004	
TIAM1	Tiam1	C2 (EFYA)	Co-IP, fluorescence- and NMR-based binding assays	Cell migration	Shepherd et al., 2010	
TRAPPC4/SBDN	Trafficking protein particle complex subunit 4/Synbindin	C2 (motif: EFYA) Direct	Co-IP, pull-down, ligand overlay, Y2H and co-localization	Vesicle trafficking (neurons, spine maturation)	Ethell et al., 2000	

[a]Core-protein binders only, partners who bind exclusively to glycosaminoglycan (GAG) chains were excluded. [b]This includes all three affinity purification methods (each in triplicates, $p < 0.05$). Pull down with SDC2 peptides is given as "$SDC2_{cyt}$". Expanded information is given in ***Supplementary Table S1****. [c]Functional and cooperative interactions refer to partners where there is no evidence of direct binding, but good evidence that the two molecules collaborate together. Previously scientists have referred to the syndecan-integrin interactions as cooperation and we have kept that nomenclature here. ns, not significant. [CM]Enriched in rat neonatal cardiomyocytes. [FB]Enriched in rat neonatal fibroblasts.*

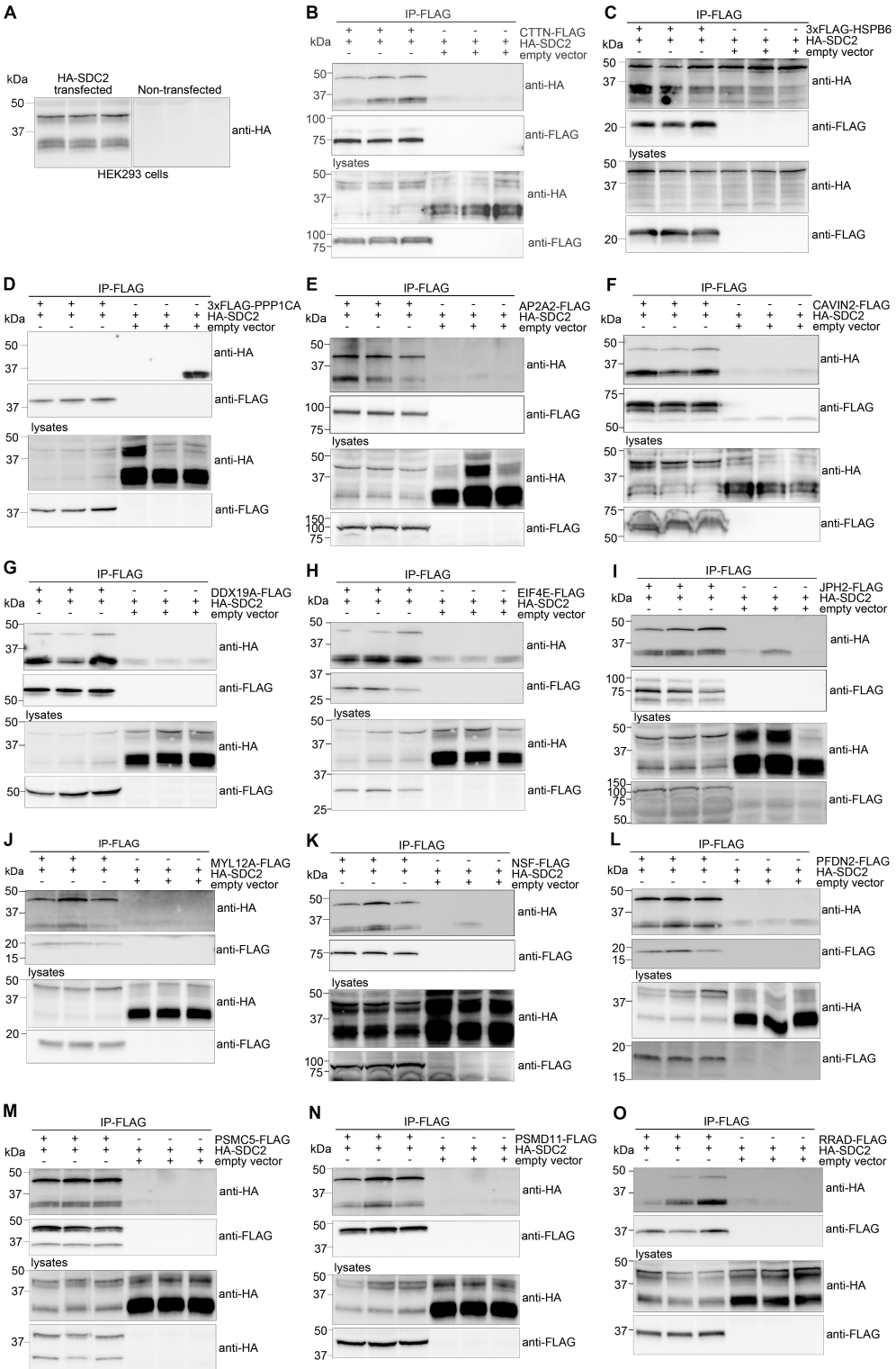

FIGURE 3 | Experimental design for validation of MS partners in HEK293 cells. The MS partner was FLAG-tagged and expressed together with HA-tagged syndecan-2 (HA-SDC2) in HEK293 cells and subjected to IP-FLAG (reversed set-up of **Figure 1A**). **(A)** Lysates from non-transfected or HA-SDC2 transfected HEK293 cells were developed with anti-HA. IP-FLAG in lysate from HEK293 cells co-transfected with HA-SDC2 and **(B)** CTTN-FLAG (pos. ctrl), **(C)** 3xFLAG-HSPB6 (neg. ctrl.), **(D)** 3xFLAG-PPP1CA (neg. ctrl.), **(E)** AP2A2-FLAG, **(F)** CAVIN2-FLAG, **(G)** DDX19A-FLAG, **(H)** EIF4E-FLAG, **(I)** JPH2-FLAG, **(J)** MYL12A-FLAG, **(K)** NSF-FLAG, **(L)** PFDN2-FLAG, **(M)** PSMC5-FLAG, **(N)** PSMD11-FLAG and **(O)** RRAD-FLAG or an empty vector (neg. ctrl.). The IPs (two upper membranes) and lysates (two lower membranes) were analyzed with anti-HA and anti-FLAG. The HA-SDC2 blots are cropped to show the core protein.

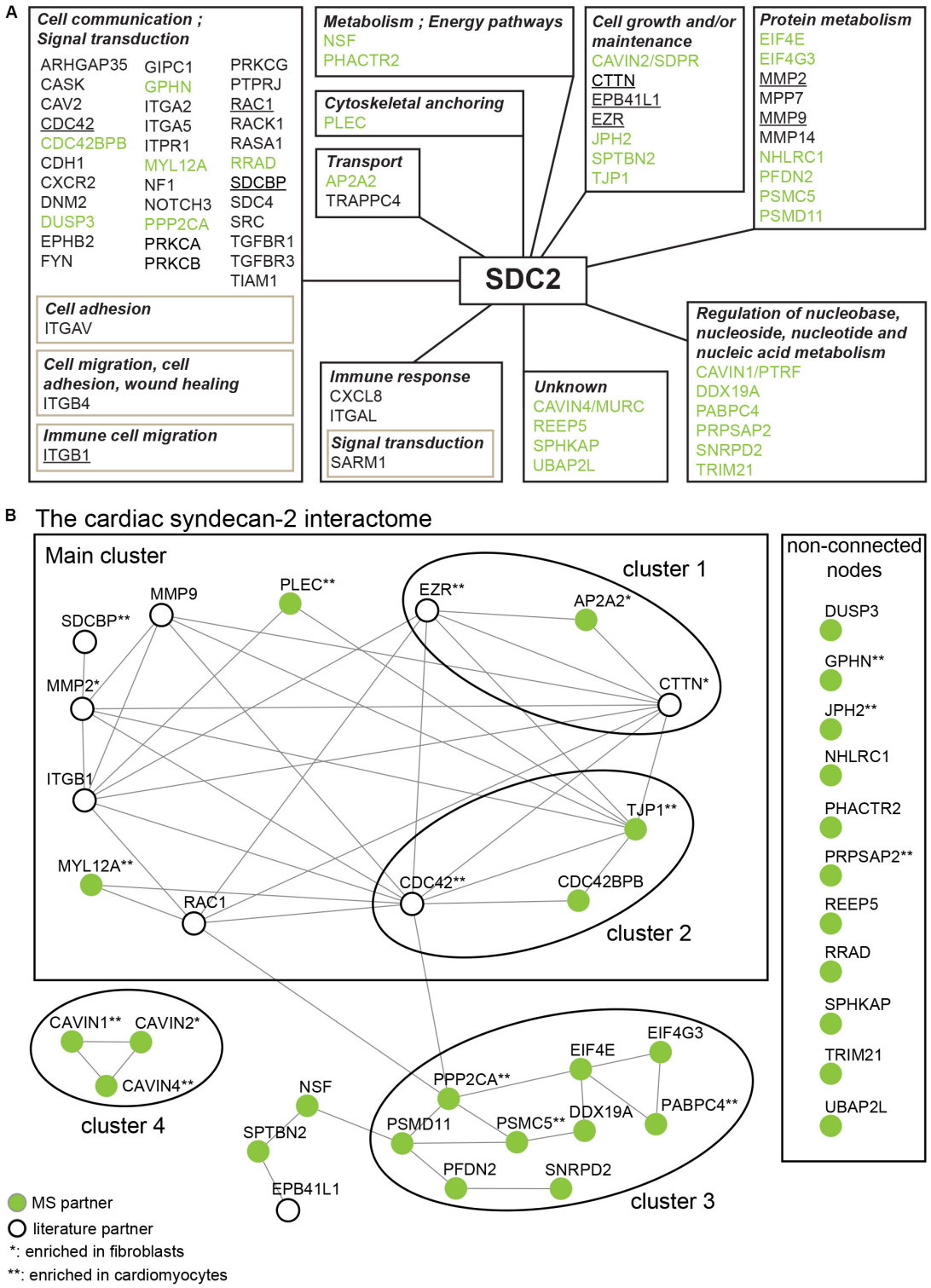

FIGURE 4 | The syndecan-2 interactome. **(A)** The 30 novel syndecan-2 interaction partners identified in this study (green), together with the 41 syndecan-2 partners previously described in the literature (**Table 2**), were grouped according to the GO annotation biological process (hprd.org). Partners in brown boxes represent subcategories. Syndecan-2 literature partners also found in this study are underlined. **(B)** The 30 novel syndecan-2 partners (green circles) and the 9 literature partners that were also found in this study (white circles) constitute the cardiac syndecan-2 interactome. The proteins were assessed for interconnectivity via STRING database network analysis (Szklarczyk et al., 2017). The literature partners CDC42, ITGB1, EZR, MMP2, MMP9, RAC1, and EPB41L1 were identified in only one of our AP-MS approaches (**Figure 2**), but were included since they connected well to the novel MS partners and might thus play a role with syndecan-2 in heart. The literature partners CTTN and SDCBP were identified in at least two MS approaches (**Figure 2**).

TABLE 3 | The genetic disease-class database analysis of the syndecan-2 interactome, 81.7% annotated.

Term	Gene name	Count	*p*-value
CANCER	*CXCL8, CXCR2, CDC42BPB, EPHB2, GIPC1, RASA1, SPHKAP, SRC, TIAM1, CDH1, CAV2, EZR, ITPR1, ITGA2, ITGAV, ITGB1, ITGB4, MMP14, MMP2, MMP7, MMP9, NF1, NOTCH3, PRKCA, PTPRJ, RAC1, RACK1, TGFBR1, TGFBR3, TRIM21*	30	1.7×10^{-5}
CARDIOVASCULAR	*CAVIN4/MURC, CXCL8, CXCR2, FYN, RASA1, ARHGAP35, SPHKAP, TIAM1, CAV2, GPHN, ITPR1, ITGA2, ITGAV, ITGB1, JPH2, MMP14, MMP2, MMP7, MMP9, NF1, NOTCH3, PHACTR2, PRKCB, RAC1, REEP5, SDC2, SDC4, TGFBR1, TGFBR3*	29	2.0×10^{-2}

TABLE 4 | Enriched KEGG pathways in the syndecan-2 interactome, 70.4% annotated.

Term	Gene name	Count	*p*-value
Proteoglycans in cancer	*CAV2, CDC42, CTTN, EZR, ITPR1, ITGA2, ITGA5, ITGAV, ITGB1, MMP2, MMP9, PRKCA, PRKCB, PRKCG, RAC1, SDC2, SDC4, SRC, TIAM1*	19	5.1×10^{-16}
Focal adhesion	*ARHGAP35, CAV2, CDC42, FYN, ITGA2, ITGA5, ITGAV, ITGB1, ITGB4, MYL12A, PRKCA, PRKCB, PRKCG, RAC1, SRC*	15	8.0×10^{-11}
Leukocyte transendothelial migration	*ARHGAP35, CDC42, EZR, ITGAL, ITGB1, MMP2, MMP9, MYL12A, PRKCA, PRKCB, PRKCG, RAC1*	12	3.0×10^{-11}
Regulation of actin cytoskeleton	*ARHGAP35, CDC42, EZR, ITGA2, ITGA5, ITGAL, ITGAV, ITGB1, ITGB4, MYL12A, RAC1, SRC, TIAM1*	13	1.6×10^{-8}
Pathways in cancer	*CXCL8, CDH1, CDC42, ITGA2, ITGAV, ITGB1, MMP2, MMP9, PRKCA, PRKCB, PRKCG, RAC1, TGFBR1*	13	1.4×10^{-5}
VEGF signaling pathway	*CDC42, PRKCA, PRKCB, PRKCG, RAC1, SRC*	6	6.6×10^{-5}
Arrhythmogenic right ventricular cardiomyopathy (ARVC)	*ITGA2, ITGA5, ITGAV, ITGB1, ITGB4*	5	1.3×10^{-3}
Hypertrophic cardiomyopathy (HCM)	*ITGA2, ITGA5, ITGAV, ITGB1, ITGB4*	5	2.2×10^{-3}
Dilated cardiomyopathy	*ITGA2, ITGA5, ITGAV, ITGB1, ITGB4*	5	2.9×10^{-3}
Vascular smooth muscle contraction	*ITPR1, PRKCA, PRKCB, PRKCG*	4	5.0×10^{-2}
Viral myocarditis	*EIF4G3, FYN, ITGAL, RAC1*	4	7.6×10^{-3}

TABLE 5 | PFAM protein domains enriched in the syndecan-2 interactome, annotated 100%.

Term	Gene name	Count	*p*-value
Integrin alpha	*ITGA2, ITGA5, ITGAL, ITGAV,*	4	4.8×10^{-5}
FG-GAP repeat	*ITGA2, ITGA5, ITGAL, ITGAV*	4	5.7×10^{-5}
Putative peptidoglycan binding domain	*MMP2, MMP7, MMP9, MMP14*	4	6.7×10^{-5}
PTRF/SDPR family	*CAVIN1/PTRF, CAVIN2/SDPR, CAVIN4/MURC*	3	9.4×10^{-5}

cortactin (CTTN) (Kinnunen et al., 1998) as well as the C2 binder syntenin-1 (SDCBP) (Grootjans et al., 1997) with the $SDC2_{cyt}$ peptide, suggesting that the peptide did retain some functionality. However, to increase confidence in our results, we included a third AP approach using GST-SDC2, which successfully precipitated the C1 binder EZR (Granés et al., 2003). We detected more proteins in either pull down with biotin-ahx-$SDC2_{cyt}$ or IP-GST-SDC2 than in both, which is probably due to the different nature of the baits.

Syndecans have generally been regarded as regulators of cell-matrix and cell-cell communication, and in particular, syndecan-2 has been coupled to dynamic processes and motile events (Oh and Couchman, 2004; Couchman et al., 2015). This was reflected in the syndecan-2 interactome where the largest group was "cell communication" (**Figure 4A**), the top disease enrichment was "cancer" and "cardiovascular" (**Table 3**), and the top KEGG pathway was "proteoglycans in cancer" (**Table 4**). In line with this, the largest cluster of connected proteins was involved in cytoskeletal remodeling and migration (**Figure 4B**, main cluster). One of these novel partners was the AP-2 complex subunit α-2 (AP2A2), which connected with the two literature partners CTTN and EZR (**Figure 4B**, cluster 1). AP2A2 is an adaptor molecule involved in endocytosis of cargo and has been shown to mediate endocytosis of the syndecan-2 co-receptor CXCR2 (Renga et al., 2012; Raman et al., 2014). It also coordinates intracellular trafficking together with ARF6, a GTP binding protein found to regulate intracellular traffic of the syndecans, along with the literature partner SDCBP (Zimmermann et al., 2005; Lau and Chou, 2008). EZR links the plasma membrane to the actin cytoskeleton and has been found to regulate podosomal rosette formation together with CTTN in pancreatic cancer cells (Kocher et al., 2009). The rosette structures have been associated with invasive properties and reported to require adhesion to fibronectin (FN) and subsequent digestion of the ECM (Kocher et al., 2009). CTTN has been shown to regulate the secretion of FN, which is necessary for cell motility (Sung et al., 2011; Schnoor et al., 2018) and is also reported to regulate secretion of ECM digesting matrix metalloproteinases (MMPs) (Clark et al., 2007), which were also present in the syndecan-2 interactome (**Figure 4B**, main cluster). Interestingly, knockdown of syndecan-2 in fibroblasts has been shown to block FN matrix assembly (Galante and Schwarzbauer, 2007) and cells expressing syndecan-2 without the cytoplasmic tail have been found unable to assemble matrix at the cell surface (Klass et al., 2000) and to form proper FN fibrils in *Xenopus* (Kramer and Yost, 2002). Because of the involvement of CTTN in FN secretion, it is tempting to speculate that CTTN might act prior to the FN assembly role of syndecan-2. Overall, this points to a role for syndecan-2 in regulating cortical actin dynamics, possibly mediated through trafficking of co-receptors, cargo or syndecan-2 itself. AP2A2, CTTN and syndecan-2 were all found enriched in fibroblast

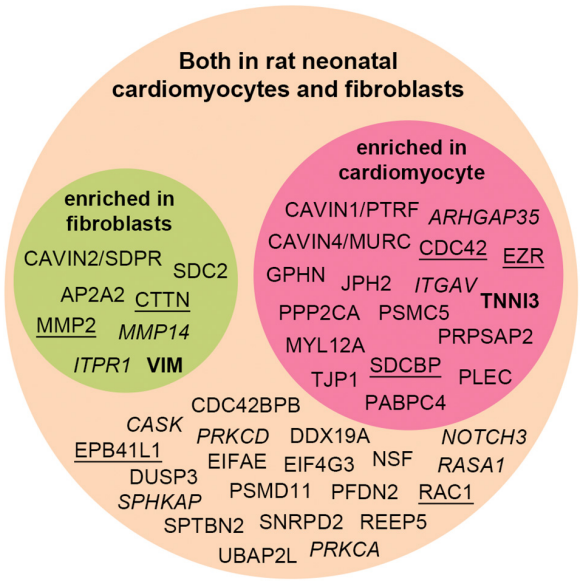

FIGURE 5 | Distribution of the syndecan-2 interaction partners (novel and literature) in rat neonatal fibroblasts and cardiomyocytes identified by MS analyses. Literature partners also found in the AP-MS approach in this study are underlined, whereas literature partners we did not detect are in italic. Several proteins were significantly enriched in either fibroblast (green circle) or cardiomyocytes (red circle) and identified in both cell types (orange circle). VIM and TNNI3 are markers of fibroblasts and cardiomyocytes.

fractions (**Figure 5**). Since ECM secretion is a characteristic feature of myofibroblasts [reviewed in Frangogiannis (2019)] and syndecan-2 has been shown to cooperate with integrin β1 (ITGB1) (**Figure 4B**, main cluster) in stress fiber formation (Kusano et al., 2000), another myofibroblast feature, we speculate whether this cluster of proteins might play a role in cardiac fibroblast activation.

The two novel MS partners serine/threonine-protein kinase MRCKβ (CDC42BPB) and tight junction protein ZO-1 (TJP1) connected to the syndecan-2 literature partner cell division control protein 42 homolog (CDC42) (**Figure 4B**, cluster 2). CDC42 is a plasma membrane associated small GTPase involved in syndecan-2 mediated filopodia extensions (Granes et al., 1999), and CDC42BPB is a CDC42 effector kinase (Huo et al., 2011). After binding of CDC42, CDC42BPB has been shown to form a complex with TJP1, which targets the CDC42BPB-TJP1 complex to the leading edge of migrating cells (Huo et al., 2011). TJP1 is a scaffolding protein that has been found to bind to cell surface transmembrane receptors through its N-terminal PDZ domain and further couples them to the actin cytoskeleton through its C-terminal proline rich region (Fanning et al., 1998; González-Mariscal et al., 2000). Although initially identified in tight junctions, TJP1 has also been found to regulate dynamic processes like angiogenesis and migration (Mattagajasingh et al., 2000; Tornavaca et al., 2015). Since syndecan-2 spans the plasma membrane, we speculate whether syndecan-2 is involved in the membrane localization of the CDC42BPB-TJP1 complex, and perhaps these proteins work together in cytoskeletal rearrangements and/or angiogenesis. TJP1 also connects to the MS partner plectin (PLEC) (**Figure 4B**, main cluster), which has been shown to be important in vascular integrity and to dysregulate tight junctions when absent (Osmanagic-Myers et al., 2015). Less is known about the novel MS partner myosin regulatory light chain 12A (MYL12A) (**Figure 4B**, main cluster), but it has been suggested to be involved in fibroblast contractility (Park et al., 2011).

Protein metabolism is important during cardiac remodeling (Chorghade et al., 2017). Interestingly, several MS partners were involved in protein metabolism, including the eukaryotic initiation factor 4E (EIF4E) and prefoldin subunit 2 (PFDN2) (**Figure 4B**, cluster 3). EIF4E is involved in regulation of translation initiation [reviewed in Shahbazian et al. (2006) and Siddiqui and Sonenberg (2015)] and PFDN2 is a co-chaperone involved in folding of cytosolic protein [reviewed in Sahlan et al. (2018)]. Like the well-known syndecan partner SDCBP (Grootjans et al., 1997), both EIF4E and PFDN2 precipitated in all three AP-MS approaches (**Figure 2**), which suggested that these bind syndecan-2 quite robustly. The third cluster was connected to the main cluster through the novel partner serine/threonine-protein phosphatase 2A catalytic subunit α (PPP2CA), which is known to regulate multiple cardiac signaling pathways [reviewed in Lubbers and Mohler (2016)] and to have a vast amount of targets, including EIF4E (Li et al., 2010). We cannot exclude that PPP2CA might also dephosphorylate syndecan-2. Although dephosphorylation of syndecans is less well understood, we have previously found that dephosphorylation of syndecan-4 might work as a molecular switch in the progression toward heart failure (Finsen et al., 2011). Future studies are needed to investigate the role of syndecan-2 in protein metabolism.

The last cluster consisted of three novel syndecan-2 partners, all from one of the most abundant families in the interactome, the CAVIN family (**Table 5** and **Figure 4B**, cluster 4). Members of the CAVIN family have been reported to form homo- and heterologous complexes at caveolae sites, where CAVIN1 and CAVIN2 are involved in caveolae formation and curvature (Hill et al., 2008; Hansen et al., 2009; Nassar and Parat, 2015). In addition, individual signaling roles have been reported for all members. In response to insulin like growth factor 1 (IGF-1) and in consort with caveolin-1 (CAV1), CAVIN1 has been reported to regulate endocytosis and thereby signaling of the IGF-1 receptor (Aboulaich et al., 2006; Salani et al., 2010). IGF-1 has also been proposed to regulate syndecan-2-mediated actin polymerization and migration of a fibroblast cell line (Mytilinaiou et al., 2017). Moreover, in lungs, syndecan-2 has been reported to be involved in the sequestering of pro-fibrotic TGF-β1 receptors into intracellular vesicles together with CAV1 (Shi et al., 2013; Tsoyi et al., 2018). Taken together this could suggest that syndecan-2 might mediate the binding of growth factors, like IGF-1, to co-receptors at caveolae sites, leading to internalization in cooperation with the CAVINs and CAV1. Since, e.g., insulin has been suggested to mediate translocation of CAVIN1 (Liu and Pilch, 2016), it is also possible that syndecan-2 in response to growth factor stimulation, regulates the release of CAVINs from the membrane. Less is known about CAVIN2, but like syndecan-2, CAVIN2 has been found to be upregulated after

aortic banding (Ogata et al., 2008), able to regulate angiogenesis in zebrafish (Chen E. et al., 2004; Ogata et al., 2008; Boopathy et al., 2017) and enriched in cardiac fibroblasts (**Figure 5**). Future studies will reveal the role of their interaction in cardiac fibroblasts and if CAVIN2 has a role in the syndecan-2 mediated angiogenesis. The CAVIN1 knock-out mouse shows cardiac dysfunction including fibrosis (Taniguchi et al., 2016), whereas CAVIN2 has not yet been coupled to fibrosis. CAVIN4 is restricted to muscle cells and involved in cardiac dysfunction (Ogata et al., 2008; Ogata et al., 2014). Overall, this could point to a role for syndecan-2 and the CAVINs in heart disease.

In two recent studies, syndecan-2 interaction partners were extracted from various interactome databases and previous high-throughput AP-MS experiments (Huttlin et al., 2015; Gondelaud and Ricard-Blum, 2019; Zandonadi et al., 2019). These did not overlap with the novel MS partners identified in our study and is probably a consequence of the different AP methods, tissues and cell models used. Recently we also identified the cardiac syndecan-4 interactome using similar strategy as described here (Mathiesen et al., 2019). Despite the close relationship between syndecan-2 and syndecan-4, their cardiac interactomes were surprisingly different, suggesting different functions. Except for the literature partners CTTN, ITGB1, MMP2, MMP9, RAC1, and SDCBP, we only found the novel MS partner CAVIN1 to be a common partner (**Figure 6**). The two syndecans also connected to some proteins within the same family, including the adaptor protein complexes (AP2A2 and AP3D1), tight junction proteins (TJP1 and TJP2) and the protein 4.1 proteins (EPB41L1 and EPB41) (**Figure 6**). Notably, proteins that bind to the common C1 or C2 region are often listed to bind all four syndecans (Gondelaud and Ricard-Blum, 2019; Mathiesen et al., 2019) (**Table 2**). However, the relatively low overlap of the C1 and C2 binding partners in the cardiac syndecan-2 and syndecan-4 interactomes suggests that this might not always be the case. On the other hand, CTTN has previously only been described as a syndecan-3 partner, but its presence in both the syndecan-2 and syndecan-4 interactomes suggests that it can indeed bind multiple syndecans.

All four syndecans are expressed in the heart (Strand et al., 2013), however, previous studies have focused on syndecan-1 and -4. Syndecan-1 is mainly known as a pro-fibrotic player and regulator of immune cell infiltration after a myocardial infarct (Vanhoutte et al., 2007; Frangogiannis Nikolaos, 2010; Schellings Mark et al., 2010). Syndecan-4 has been shown to act as a pro-remodeling molecule in both cardiomyocytes and fibroblasts in addition to recruiting immune cells (Finsen et al., 2011; Herum et al., 2013, 2015; Strand et al., 2013). Based on our data, the notion that the expression of syndecan-2 increases after aortic banding (Strand et al., 2013) and that syndecan-2 has been correlated with fibrosis in other tissues (Chen L. et al., 2004; Renga et al., 2012; Ruiz et al., 2012) it is tempting to speculate that syndecan-2 might be involved in cardiac fibrosis, perhaps together with CTTN and the CAVINs. Another important observation is that the interactome partners are not necessarily involved in cell adhesion, which is a primary feature associated with syndecans, thus the main role of syndecan-2 in the heart might be found outside the major adhesion sites.

Future studies are needed to verify the syndecan-2 interactions identified in this study and to determine their biological significance. Altogether, we hope that the interactome will spur future hypotheses and direct future studies on syndecan-2 in the heart.

MATERIALS AND METHODS

Antibodies

Immunoprecipitations and immunoblotting were carried out using anti-SDC2 (LS-C150258, Nordic Biosite, Sweden), normal

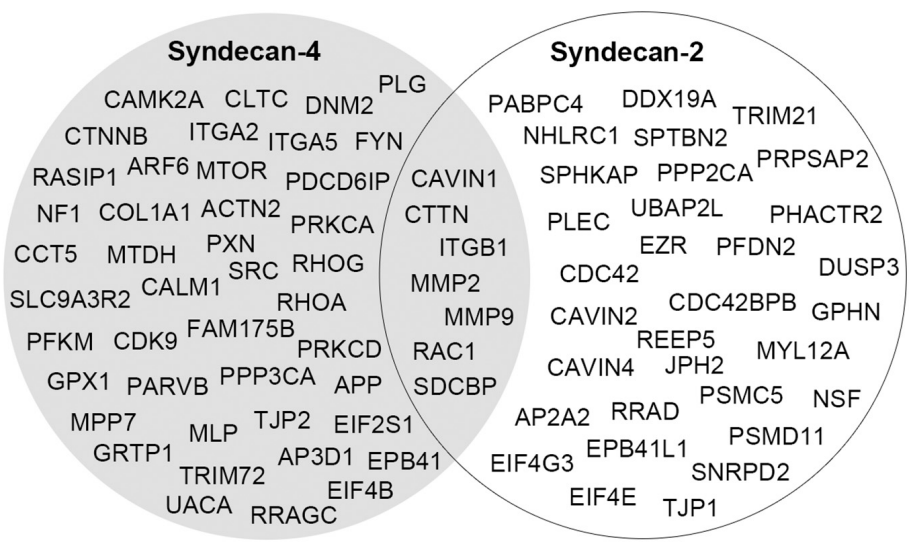

FIGURE 6 | A comparison of the cardiac interactomes of syndecan-2 (white circle) and the syndecan-4 (Mathiesen et al., 2019) (gray circle).

sheep IgG (6C0333, Merck KGaA, Germany), anti-GST (sc-80998, Santa Cruz Biotechnology, Inc., United States), anti-FLAG (F1804, Sigma-Aldrich, United States), anti-HA (#3724, clone C29F4, Cell Signaling, Netherlands) and anti-biotin-HRP (A0185, Sigma-Aldrich, United States). HRP conjugated anti-sheep (6150-05, SouthernBiotech, United States), anti-mouse (NA931V, GE Healthcare, United States) and anti-rabbit (NA934V, GE Healthcare) were used as secondary antibodies.

Peptides and Recombinant Proteins

Customized peptides were synthesized to >80% purity by Genscript Corp. (United States): Biotin-ahx-$SDC2_{cyt}$: RMRKKDEGSYDLGERKPSSAAYQKAPTKEFYA and biotin-ahx-scrambled (scram): RLEDKRPAQAKGKATMESFYKYDPRSAYGESK. Recombinant GST and N-terminal GST-tagged SDC2 (mouse) proteins were also made by Genscript Corp.

Transfection of HEK293 Cells

Human Embryonic Kidney 293 (HEK) cells (ATCC CRL-1573™, United States) were kept in Dulbecco's modified Eagles's medium (DMEM) (41965-039, Gibco, Life Technologies, Inc., United States) supplemented with 10% fetal bovine serum (FBS) and 1% penicillin/streptomycin (PS) (P0781, Sigma-Aldrich) humidified at 37°C in 5% CO_2. HEK293 cells were transfected with the $CaCl_2$ method as previously described (Jordan et al., 1996; Mathiesen et al., 2019). Briefly, cells were cultured without PS 24 h before transfection. Plasmid DNA (8 μg) in 500 μL $CaCl_2$ solution (248 mM) was mixed with 500 μL 2x HEPES buffer (50 mM HEPES, 280 mM NaCl, 1.5 mM Na_2HPO4, pH 7.0), incubated at room temperature (RT) for 20–30 min (min) before drippled onto the cells. After 24 h cells were harvested in IP buffer [150 mM NaCl, 20 mM HEPES (pH 7.5), 1 mM EDTA, 1%Triton X-100] with cOmplete protease inhibitor cocktail (#05050489001, Roche, Switzerland). All genes were cloned with either a FLAG or HA tag in the pcDNA3.1 vector unless otherwise stated (Genscript Corp., United States). The DNA constructs were: DDX19A-FLAG human (NM_018332), NSF-FLAG human (NM_006178), PFDN2-FLAG human (NM_012394), PSMC5-FLAG human (NM_001199163), PSMD11-FLAG mouse (NM_178616), MYL12A/RLC-A-FLAG rat (NM_001135017), CAVIN2/SDPR-FLAG human (NM_004657), CTTN-FLAG human (NM_138565), EIF4E-FLAG human (NM_001968), JPH2-FLAG human (NM_020433.4), RRAD-FLAG human (NM_001128850), 3x FLAG-HSPB6 rat (NM_138887.1), FLAG-His6-PPP1CA rat (P62138) and HA-SDC2 human (NM_002998) (pCEP4 vector). AP2A2-FLAG human (NM_001242837.1) was cloned by Cyagen US Inc. (United States). The 11 interactors were selected based on a combination of their distribution in the pull down, IP-GST and IP-SDC2 AP-MS groups, distribution in the cardiac syndecan-2 interactome (**Figure 4B**) as well as availability from the Genscript clone collection.

Immunoprecipitation (IP) in Cell Lysates

Lysates were mixed with 2 μg anti-FLAG, anti-SDC2 or anti-GST (with recombinant GST-SDC2) and protein A/G-agarose beads (sc-2003, Santa Cruz Biotechnology) and rotating overnight (ON) at 4°C. After three times wash in IP buffer (150 mM NaCl, 20 mM HEPES, pH 7.5, 1 mM EDTA, 1%Triton X-100) with cOmplete protease inhibitor cocktail (#5050489001, Roche), samples were eluted by boiling in 2 × SDS loading buffer and analyzed by immunoblotting.

Immunoblotting

Samples were analyzed on 4–15% or 15% Criterion™ Tris-HCl precast gel (#3450028 and #3450021, Bio-Rad, United States) and blotted onto a PVDF membrane (#1704157, Bio-Rad). After blocking in either 5% non-fat dried milk or 1% casein in TBS-T [Tris-buffered saline with 1% Tween-20 (#1610781, Bio-Rad)] for 1 h at RT, membranes were incubated with primary antibodies for 1 h at RT or ON at 4°C. Following three times 5 min wash in TBS-T, membranes were incubated with HRP-conjugated secondary antibody for 1 h at RT, washed three times 5 min in TBS-T and signal developed using ECL Prime (RPN 2232, GE Healthcare). Reprobing was performed after stripping with Restore™ Western Blot Stripping Buffer (#21059, Thermo Scientific, United States).

Peptide Overlay

Syndecan-2 (rat, mouse, and human) and syndecan-4 (rat) were spot-synthesized as 20-mer peptides with 3 amino acids offset on a cellulose membrane by a Multiprep automated peptide synthesizer (INTAVIS Bioanalytical Instruments AG, Germany) (Frank and Overwin, 1996). The peptide array membranes were blocked for minimum 1 h in 1% casein in TBS-T at RT before incubation with anti-syndecan-2 ON at 4°C. Binding was detected by immunoblotting with anti-sheep-HRP and signal detected by ECL Prime.

Rat Neonatal FB and CM

The study conforms to the "Guide for the Care and Use of Laboratory Animals" (NIH publication No. 85-23, revised 2011, United States) and was preapproved by the Norwegian National Animal Research Committee (Permit of approval number IV1-17U). Lysates from primary cardiomyocytes and fibroblasts were prepared as previously described (Mathiesen et al., 2019) and thereafter analyzed by MS.

LV Lysate and Affinity Purification for MS

Frozen LV's from Wistar 230-250 g male rats (Janvier Labs, France) were pulverized in liquid nitrogen in a mortar, transferred to lysis buffer [150 mM NaCl, 20 mM Hepes, pH 7.5, 1 mM EDTA, 0.5% Triton supplemented with complete protease inhibitor cocktail (Roche)] on ice and homogenized with a Polytron 1200 homogenizer in three series of 1 min. The suspensions were centrifuged at 100,000 × *g* for 60 min at 4°C and supernatants were stored at −80°C.

In pull down experiments with peptides, pooled LV lysates were mixed with 0.01 mM of the biotinylated $SDC2_{cyt}$ peptide or 0.02 mM of the biotinylated scrambled control peptide (to secure excess of negative control) and rotated ON at 4°C. LV lysates without any peptides was included as a second negative control (beads only). Streptavidin coated dynabeads (Dynabeads™ M-270 Streptavidin, #65305, Life Technologies, United States) were

washed three times in PBS before they were added to the LV lysate with or without peptides and rotated for 40 min at RT. The beads were washed five times in PBS and captured proteins were eluted in 250 μL 25 mM biotin for 3 h at 60°C. Proteins were precipitated in 1 ml of 4 × ice-cold acetone added glycoblue at −20°C ON. The tubes were centrifuged and the pellets were air-dried before MS analysis.

For large scale IP, 10 μg/mg of anti-syndecan-2, anti-sheep IgG or anti-GST were coupled to magnetic dynabeads (Dynabeads^{TM} Antibody Coupling Kit, #14311D, Thermo Fisher, United States) according to manufacturer's protocol. The antibody coupled beads were incubated with the LV lysates with or without supplementation of GST or GST-SDC2 recombinant protein and rotated ON at 4°C. After three times wash in cold PBS and two times wash in cold water to remove salts (Mlynarcik et al., 2012), captured protein complexes were eluted in 0.1% TFA in freshly made 50% acetonitrile for 30 min while rotating at RT. The elution step was repeated once with fresh TFA before precipitation in 1 ml 4 × ice-cold acetone added glycoblue at −20°C. Samples were spun at max speed for 15 min and the pellets were air-dried before MS analysis.

Protein Identification and Label-Free Quantification by LC-MS/MS

The 2-D Clean Up-Kit (80-6484-51, GE healthcare) was used to precipitate proteins from the fibroblast and cardiomyocyte fractions. The precipitate was then dissolved in 40 μL 0.2% ProteaseMAX^{TM} Surfactant, Trypsin Enhancer (Promega) in 50 mM NH_4HCO_3 before protein reduction, alkylation and in-solution trypsin digestion (Promega) ON at 37°C. Following digestion, centrifugation at 14,000 × *g* for 10 min, trypsin inactivation by adding 100 μl 1% TFA and another round of centrifugation at 14,000 × *g* for 10 min followed.

The air dired IP samples were resuspended in 20 μl 6 M Urea in 10 mM HEPES, pH 8 before reduction, alkylation and 4 h in-solution lysyl endopeptidase digestion (Wako) in room temperature. Samples were diluted four times before over night trypsin (Promega) digestion at room temperature. Following digestion, centrifugation at 14,000 × *g* for 10 min, trypsin inactivation by adding 100 μl 1% TFA and another round of centrifugation at 14,000 × *g* for 10 min followed.

Desalting and upconcentration of peptides was performed before MS by the STAGE-TIP method using a C18 resin disk (3M Empore). The peptides were eluted with 80 μl 80% ACN/0.1% FA, dried, and solubilized in 7 μL 0.1% FA for MS analysis. Each peptide mixture was analyzed by a nEASY-LC coupled to QExactive Plus (Thermo Electron, Bremen, Germany) as previously described (Mathiesen et al., 2019), except that a 50 cm column was used. Gradients of 60 and 120 min were used for the IPs and fractions, respectively. The resulting MS raw files were submitted to the MaxQuant software for protein identification and label-free quantification and Perseus software was used for the statistical analysis as described in detail previously (Mathiesen et al., 2019).

To allow quantitative comparisons and determine the significance between MS samples, LFQ intensities were loaded into Perseus (Version 1.4.0.20), log2 transformed and a *t*-test was performed ($p < 0.05$ was accepted as statistically significant). To be considered a MS partner, proteins had to be identified in IP-SDC2 and at least one of the other APs. Non-specific binders to the $SDC2_{cyt}$ peptide were sorted away through the two negative controls; scramble or beads only. Non-specific binders to GST-SDC2 were sorted away through the two negative controls; GST or beads only. Then the pools of proteins identified in the pull down and IP-GST were compared with the pool of proteins obtained from IP-SDC2 corrected against IP-IgG.

Generating the Cardiac Interactome Map

The 30 MS partners and 41 literature partners were grouped according to the GO annotation biological process extracted from hprd.org (Keshava Prasad et al., 2009) (**Figure 4A**). The MS partners and literature partners found in our AP-MS screens (this study) (**Figure 2**) made up the cardiac interactome and STRING database version 10.5 (Szklarczyk et al., 2017) was used to predict connections (**Figure 4B**). Data was extracted with the following setting: species: *Homo sapiens* (created more connections than *Rattus norvegicus*), confidence: medium, active interaction sources: Experiments, databases, and co-expression. The network stats were: number of nodes: 39, number of edges: 48, average node degree: 2.46, avg. local clustering coefficient: 0.395, expected number of edges: 27. PPI enrichment *p*-value: <0.000117. CAVIN4 has been shown to interact with CAVIN1 and -2 in the literature (Ogata et al., 2008, 2014) and was therefore added to the interactome. The literature partners CDC42, ITGB1, EZR, MMP2, MMP9, RAC1, and EPB41L1 were detected in only one AP-MS approach. However, since they were identified both in this and in another study (**Table 2**), their potential for being important for syndecan-2 in the heart was heightened, and they were therefore included in the STRING analysis.

Functional Annotation

The DAVID bioinformatics tool (Huang da et al., 2009a,b), version 6.8, was used for functional annotation. Through the DAVID tool enrichment in genetic disease-class database annotation, KEGG pathways, and PFAM (Finn et al., 2016) domains were analyzed. The SDC2 interactome gene list was imported as official gene names and *Homo sapiens* was used as both species and background and the following settings were used count (2) and EASE score (0.1) (Modified Fisher Exact *p*-value).

DATA AVAILABILITY STATEMENT

The datasets generated in this study can be found in online repositories. The names of the repository/repositories and accession number(s) can be found below: http://www.proteomexchange.org/, PXD018942.

ETHICS STATEMENT

The animal study was reviewed and approved by Norwegian National Animal Research Committee.

AUTHOR CONTRIBUTIONS

SM and CC designed and conceived the experiments. SM wrote the manuscript under the guidance of CC and GC. SM performed the largescale AP. MS and TN performed the mass spectrometry analysis. MM performed the transfections. SM and ML performed the small scale IPs and epitope mapping. All authors read and approved the manuscript.

FUNDING

This study was supported by Nasjonalforeningen for folkehelsen, Stiftelsen Kristian Gerhard Jebsen, The Research Council of Norway, Olav Raagholt og Gerd Meidel Raagholts stiftelse for forskning (http://www.raagholtstiftelsen.no/), Anders Jahre's Fund for the Promotion of Science and the South-Eastern Regional Health Authority, Fondsstiftelsen from Oslo University Hospital, Norway. Proteomics Core Facility was supported by the Core Facilities Program of the South-Eastern Norway Regional Health Authority.

ACKNOWLEDGMENTS

We are grateful to Tone Asknes Lian and Anita Kaupang for technical assistance.

SUPPLEMENTARY MATERIAL

The Supplementary Material for this article can be found online at: https://www.frontiersin.org/articles/10.3389/fcell.2020.00792/full#supplementary-material

REFERENCES

Aboulaich, N., Ortegren, U., Vener, A. V., and Stralfors, P. (2006). Association and insulin regulated translocation of hormone-sensitive lipase with PTRF. *Biochem. Biophys. Res. Commun.* 350, 657–661. doi: 10.1016/j.bbrc.2006.09.094

Balza, R. O. Jr., and Misra, R. P. (2006). Role of the serum response factor in regulating contractile apparatus gene expression and sarcomeric integrity in cardiomyocytes. *J. Biol. Chem.* 281, 6498–6510. doi: 10.1074/jbc.M509487200

Bonetta, L. (2010). Interactome under construction. *Nature* 468:851. doi: 10.1038/468851a

Boopathy, G. T. K., Kulkarni, M., Ho, S. Y., Boey, A., Chua, E. W. M., Barathi, V. A., et al. (2017). Cavin-2 regulates the activity and stability of endothelial nitric-oxide synthase (eNOS) in angiogenesis. *J. Biol. Chem.* 292, 17760–17776. doi: 10.1074/jbc.M117.794743

Chakravarti, R., and Adams, J. C. (2006). Comparative genomics of the syndecans defines an ancestral genomic context associated with matrilins in vertebrates. *BMC Genomics* 7:83. doi: 10.1186/1471-2164-7-83

Chen, C. Y., Lin, C. W., Chang, C. Y., Jiang, S. T., and Hsueh, Y. P. (2011). Sarm1, a negative regulator of innate immunity, interacts with syndecan-2 and regulates neuronal morphology. *J. Cell Biol.* 193, 769–784. doi: 10.1083/jcb.201008050

Chen, E., Hermanson, S., and Ekker, S. C. (2004). Syndecan-2 is essential for angiogenic sprouting during zebrafish development. *Blood* 103, 1710–1719. doi: 10.1182/blood-2003-06-1783

Chen, L., Klass, C., and Woods, A. (2004). Syndecan-2 regulates transforming growth factor-beta signaling. *J. Biol. Chem.* 279, 15715–15718. doi: 10.1074/jbc.C300430200

Cheshenko, N., Liu, W., Satlin, L. M., and Herold, B. C. (2007). Multiple receptor interactions trigger release of membrane and intracellular calcium stores critical for herpes simplex virus entry. *Mol. Biol. Cell* 18, 3119–3130. doi: 10.1091/mbc.e07-01-0062

Choi, S., Kim, Y., Park, H., Han, I. O., Chung, E., Lee, S. Y., et al. (2009). Syndecan-2 overexpression regulates adhesion and migration through cooperation with integrin alpha2. *Biochem. Biophys. Res. Commun.* 384, 231–235. doi: 10.1016/j.bbrc.2009.04.093

Choi, S., Lee, E., Kwon, S., Park, H., Yi, J. Y., Kim, S., et al. (2005). Transmembrane domain-induced oligomerization is crucial for the functions of syndecan-2 and syndecan-4. *J. Biol. Chem.* 280, 42573–42579. doi: 10.1074/jbc.M509238200

Choi, Y., Kim, H., Chung, H., Hwang, J. S., Shin, J. A., Han, I. O., et al. (2010). Syndecan-2 regulates cell migration in colon cancer cells through Tiam1-mediated Rac activation. *Biochem. Biophys. Res. Commun.* 391, 921–925. doi: 10.1016/j.bbrc.2009.11.165

Choi, Y., Kwon, M. J., Lim, Y., Yun, J. H., Lee, W., and Oh, E. S. (2015). Trans-regulation of Syndecan Functions by Hetero-oligomerization. *J. Biol. Chem.* 290, 16943–16953. doi: 10.1074/jbc.M114.611798

Chorghade, S., Seimetz, J., Emmons, R., Yang, J., Bresson, S. M., Lisio, M. D., et al. (2017). Poly(A) tail length regulates PABPC1 expression to tune translation in the heart. *eLife* 6:e24139. doi: 10.7554/eLife.24139

Christensen, G., Herum, K. M., and Lunde, I. G. (2019). Sweet, yet underappreciated: proteoglycans and extracellular matrix remodeling in heart disease. *Matrix Biol.* 75-76, 286–299. doi: 10.1016/j.matbio.2018.01.001

Clark, E. S., Whigham, A. S., Yarbrough, W. G., and Weaver, A. M. (2007). Cortactin is an essential regulator of matrix metalloproteinase secretion and extracellular matrix degradation in invadopodia. *Cancer Res.* 67, 4227–4235. doi: 10.1158/0008-5472.can-06-3928

Cohen, A. R., Woods, D. F., Marfatia, S. M., Walther, Z., Chishti, A. H., and Anderson, J. M. (1998). Human CASK/LIN-2 binds syndecan-2 and protein 4.1 and localizes to the basolateral membrane of epithelial cells. *J. Cell Biol.* 142, 129–138. doi: 10.1083/jcb.142.1.129

Cohn, J. N., Ferrari, R., and Sharpe, N. (2000). Cardiac remodeling–concepts and clinical implications: a consensus paper from an international forum on cardiac remodeling. Behalf of an International forum on cardiac remodeling. *J. Am. Coll. Cardiol.* 35, 569–582. doi: 10.1016/s0735-1097(99)00630-0

Couchman, J. R. (2010). Transmembrane signaling proteoglycans. *Annu. Rev. Cell Dev. Biol.* 26, 89–114. doi: 10.1146/annurev-cellbio-100109-104126

Couchman, J. R., Gopal, S., Lim, H. C., Norgaard, S., and Multhaupt, H. A. (2015). Fell-muir lecture: syndecans: from peripheral coreceptors to mainstream regulators of cell behaviour. *Int. J. Exp. Pathol.* 96, 1–10. doi: 10.1111/iep.12112

David, G., Bai, X. M., Van der Schueren, B., Marynen, P., Cassiman, J. J., and Van den Berghe, H. (1993). Spatial and temporal changes in the expression of fibroglycan (syndecan-2) during mouse embryonic development. *Development* 119, 841–854.

Dews, I. C., and Mackenzie, K. R. (2007). Transmembrane domains of the syndecan family of growth factor coreceptors display a hierarchy of homotypic and heterotypic interactions. *Proc. Natl. Acad. Sci. U.S.A.* 104, 20782–20787. doi: 10.1073/pnas.0708909105

Essner, J. J., Chen, E., and Ekker, S. C. (2006). Syndecan-2. *Int. J. Biochem. Cell Biol.* 38, 152–156. doi: 10.1016/j.biocel.2005.08.012

Ethell, I. M., Hagihara, K., Miura, Y., Irie, F., and Yamaguchi, Y. (2000). Synbindin, a novel syndecan-2-binding protein in neuronal dendritic spines. *J. Cell Biol.* 151, 53–68. doi: 10.1083/jcb.151.1.53

Ethell, I. M., Irie, F., Kalo, M. S., Couchman, J. R., Pasquale, E. B., and Yamaguchi, Y. (2001). EphB/syndecan-2 signaling in dendritic spine morphogenesis. *Neuron* 31, 1001–1013. doi: 10.1016/s0896-6273(01)00440-8

Ethell, I. M., and Yamaguchi, Y. (1999). Cell surface heparan sulfate proteoglycan syndecan-2 induces the maturation of dendritic spines in rat hippocampal neurons. *J. Cell Biol.* 144, 575–586. doi: 10.1083/jcb.144.3.575

Fanning, A. S., Jameson, B. J., Jesaitis, L. A., and Anderson, J. M. (1998). The tight junction protein ZO-1 establishes a link between the transmembrane protein occludin and the actin cytoskeleton. *J. Biol. Chem.* 273, 29745–29753. doi: 10.1074/jbc.273.45.29745

Fears, C. Y., Gladson, C. L., and Woods, A. (2006). Syndecan-2 is expressed in the microvasculature of gliomas and regulates angiogenic processes in microvascular endothelial cells. *J. Biol. Chem.* 281, 14533–14536. doi: 10.1074/jbc.C600075200

Finn, R. D., Coggill, P., Eberhardt, R. Y., Eddy, S. R., Mistry, J., Mitchell, A. L., et al. (2016). The Pfam protein families database: towards a more sustainable future. *Nucleic Acids Res.* 44, D279–D285. doi: 10.1093/nar/gkv1344

Finsen, A. V., Lunde, I. G., Sjaastad, I., Ostli, E. K., Lyngra, M., Jarstadmarken, H. O., et al. (2011). Syndecan-4 is essential for development of concentric myocardial hypertrophy via stretch-induced activation of the calcineurin-NFAT pathway. *PLoS One* 6:e28302. doi: 10.1371/journal.pone.0028302

Frangogiannis, N. G. (2019). Cardiac fibrosis: cell biological mechanisms, molecular pathways and therapeutic opportunities. *Mol. Aspects Med.* 65, 70–99. doi: 10.1016/j.mam.2018.07.001

Frangogiannis Nikolaos, G. (2010). Syndecan-1. *Hypertension* 55, 233–235. doi: 10.1161/HYPERTENSIONAHA.109.147256

Frank, R., and Overwin, H. (1996). "SPOT synthesis," in *Epitope Mapping Protocols*, ed. G. E. Morris (Totowa, NJ: Humana Press), 149–169.

Galante, L. L., and Schwarzbauer, J. E. (2007). Requirements for sulfate transport and the diastrophic dysplasia sulfate transporter in fibronectin matrix assembly. *J. Cell Biol.* 179, 999–1009. doi: 10.1083/jcb.200707150

Gao, Y., Li, M., Chen, W., and Simons, M. (2000). Synectin, syndecan-4 cytoplasmic domain binding PDZ protein, inhibits cell migration. *J. Cell Physiol.* 184, 373–379. doi: 10.1002/1097-4652(200009)184:3<373::aid-jcp12>3.0.co;2-i

Gondelaud, F., and Ricard-Blum, S. (2019). Structures and interactions of syndecans. *FEBS J.* 286, 2994–3007. doi: 10.1111/febs.14828

González-Mariscal, L., Betanzos, A., and Ávila-Flores, A. (2000). MAGUK proteins: structure and role in the tight junction. *Semin. Cell Dev. Biol.* 11, 315–324. doi: 10.1006/scdb.2000.0178

Granés, F., Berndt, C., Roy, C., Mangeat, P., Reina, M., and Vilaró, S. (2003). Identification of a novel Ezrin-binding site in syndecan-2 cytoplasmic domain. *FEBS Lett.* 547, 212–216. doi: 10.1016/s0014-5793(03)00712-9

Granes, F., Garcia, R., Casaroli-Marano, R. P., Castel, S., Rocamora, N., Reina, M., et al. (1999). Syndecan-2 induces filopodia by active cdc42Hs. *Exp. Cell Res.* 248, 439–456. doi: 10.1006/excr.1999.4437

Granes, F., Urena, J. M., Rocamora, N., and Vilaro, S. (2000). Ezrin links syndecan-2 to the cytoskeleton. *J. Cell Sci.* 113(Pt 7), 1267–1276.

Grootjans, J. J., Zimmermann, P., Reekmans, G., Smets, A., Degeest, G., Durr, J., et al. (1997). Syntenin, a PDZ protein that binds syndecan cytoplasmic domains. *Proc. Natl. Acad. Sci. U.S.A.* 94, 13683–13688. doi: 10.1073/pnas.94.25.13683

Halden, Y., Rek, A., Atzenhofer, W., Szilak, L., Wabnig, A., and Kungl, A. J. (2004). Interleukin-8 binds to syndecan-2 on human endothelial cells. *Biochem. J.* 377(Pt 2), 533–538. doi: 10.1042/bj20030729

Hansen, C. G., Bright, N. A., Howard, G., and Nichols, B. J. (2009). SDPR induces membrane curvature and functions in the formation of caveolae. *Nat. Cell Biol.* 11, 807–814. doi: 10.1038/ncb1887

Herum, K. M., Lunde, I. G., Skrbic, B., Florholmen, G., Behmen, D., Sjaastad, I., et al. (2013). Syndecan-4 signaling via NFAT regulates extracellular matrix production and cardiac myofibroblast differentiation in response to mechanical stress. *J. Mol. Cell Cardiol.* 54, 73–81. doi: 10.1016/j.yjmcc.2012.11.006

Herum, K. M., Lunde, I. G., Skrbic, B., Louch, W. E., Hasic, A., Boye, S., et al. (2015). Syndecan-4 is a key determinant of collagen cross-linking and passive myocardial stiffness in the pressure-overloaded heart. *Cardiovasc. Res.* 106, 217–226. doi: 10.1093/cvr/cvv002

Hill, M. M., Bastiani, M., Luetterforst, R., Kirkham, M., Kirkham, A., Nixon, S. J., et al. (2008). PTRF-Cavin, a conserved cytoplasmic protein required for caveola formation and function. *Cell* 132, 113–124. doi: 10.1016/j.cell.2007.11.042

Hsueh, Y. P., Roberts, A. M., Volta, M., Sheng, M., and Roberts, R. G. (2001). Bipartite interaction between neurofibromatosis type I protein (neurofibromin) and syndecan transmembrane heparan sulfate proteoglycans. *J. Neurosci.* 21, 3764–3770. doi: 10.1523/jneurosci.21-11-03764.2001

Hsueh, Y. P., Yang, F. C., Kharazia, V., Naisbitt, S., Cohen, A. R., Weinberg, R. J., et al. (1998). Direct interaction of CASK/LIN-2 and syndecan heparan sulfate proteoglycan and their overlapping distribution in neuronal synapses. *J. Cell Biol.* 142, 139–151. doi: 10.1083/jcb.142.1.139

Huang, J. W., Chen, C. L., and Chuang, N. N. (2005a). P120-GAP associated with syndecan-2 to function as an active switch signal for Src upon transformation with oncogenic ras. *Biochem. Biophys. Res. Commun.* 329, 855–862. doi: 10.1016/j.bbrc.2005.02.045

Huang, J. W., Chen, C. L., and Chuang, N. N. (2005b). Trap RACK1 with Ras to mobilize Src signaling at syndecan-2/p120-GAP upon transformation with oncogenic ras. *Biochem. Biophys. Res. Commun.* 330, 1087–1094. doi: 10.1016/j.bbrc.2005.02.189

Huang, J. W., and Chuang, N. N. (2006). Shift syndecan-2 from RACK1 to caveolin-2 upon transformation with oncogenic ras. *Biochem. Biophys. Res. Commun.* 350, 227–232. doi: 10.1016/j.bbrc.2006.09.035

Huang da, W., Sherman, B. T., and Lempicki, R. A. (2009a). Systematic and integrative analysis of large gene lists using DAVID bioinformatics resources. *Nat. Protoc.* 4, 44–57. doi: 10.1038/nprot.2008.211

Huang da, W., Sherman, B. T., Zheng, X., Yang, J., Imamichi, T., Stephens, R., et al. (2009b). Extracting biological meaning from large gene lists with DAVID. *Curr. Protoc. Bioinform.* Chapter 13, Unit13.11. doi: 10.1002/0471250953.bi1311s27

Huo, L., Wen, W., Wang, R., Kam, C., Xia, J., Feng, W., et al. (2011). Cdc42-dependent formation of the ZO-1/MRCKbeta complex at the leading edge controls cell migration. *EMBO J.* 30, 665–678. doi: 10.1038/emboj.2010.353

Huttlin, E. L., Ting, L., Bruckner, R. J., Gebreab, F., Gygi, M. P., Szpyt, J., et al. (2015). The BioPlex network: a systematic exploration of the human interactome. *Cell* 162, 425–440. doi: 10.1016/j.cell.2015.06.043

Ivey, M. J., and Tallquist, M. D. (2016). Defining the cardiac fibroblast. *Circ. J.* 80, 2269–2276. doi: 10.1253/circj.CJ-16-1003

Jang, B., Jung, H., Chung, H., Moon, B. I., and Oh, E. S. (2016). Syndecan-2 enhances E-cadherin shedding and fibroblast-like morphological changes by inducing MMP-7 expression in colon cancer cells. *Biochem. Biophys. Res. Commun.* 477, 47–53. doi: 10.1016/j.bbrc.2016.06.019

Jordan, M., Schallhorn, A., and Wurm, F. M. (1996). Transfecting mammalian cells: optimization of critical parameters affecting calcium-phosphate precipitate formation. *Nucleic Acids Res.* 24, 596–601. doi: 10.1093/nar/24.4.596

Keshava Prasad, T. S., Goel, R., Kandasamy, K., Keerthikumar, S., Kumar, S., Mathivanan, S., et al. (2009). Human protein reference database—2009 update. *Nucleic Acids Res.* 37(suppl. 1), D767–D772. doi: 10.1093/nar/gkn892

Kim, C. W., Goldberger, O. A., Gallo, R. L., and Bernfield, M. (1994). Members of the syndecan family of heparan sulfate proteoglycans are expressed in distinct cell-, tissue-, and development-specific patterns. *Mol. Biol. Cell* 5, 797–805. doi: 10.1091/mbc.5.7.797

Kinnunen, T., Kaksonen, M., Saarinen, J., Kalkkinen, N., Peng, H. B., and Rauvala, H. (1998). Cortactin-Src kinase signaling pathway is involved in N-syndecan-dependent neurite outgrowth. *J. Biol. Chem.* 273, 10702–10708. doi: 10.1074/jbc.273.17.10702

Klass, C. M., Couchman, J. R., and Woods, A. (2000). Control of extracellular matrix assembly by syndecan-2 proteoglycan. *J. Cell Sci.* 113(Pt 3), 493–506.

Kocher, H. M., Sandle, J., Mirza, T. A., Li, N. F., and Hart, I. R. (2009). Ezrin interacts with cortactin to form podosomal rosettes in pancreatic cancer cells. *Gut* 58, 271–284. doi: 10.1136/gut.2008.159871

Kramer, K. L., and Yost, H. J. (2002). Ectodermal syndecan-2 mediates left-right axis formation in migrating mesoderm as a cell-nonautonomous Vg1 cofactor. *Dev. Cell* 2, 115–124. doi: 10.1016/s1534-5807(01)00107-1

Kusano, Y., Oguri, K., Nagayasu, Y., Munesue, S., Ishihara, M., Saiki, I., et al. (2000). Participation of Syndecan 2 in the induction of stress fiber formation in cooperation with integrin α5β1: structural characteristics of heparan sulfate chains with avidity to COOH-terminal heparin-binding domain of fibronectin. *Exp. Cell Res.* 256, 434–444. doi: 10.1006/excr.2000.4802

Lau, A. W., and Chou, M. M. (2008). The adaptor complex AP-2 regulates post-endocytic trafficking through the non-clathrin Arf6-dependent endocytic pathway. *J. Cell Sci.* 121:4008. doi: 10.1242/jcs.033522

Lee, H., Kim, Y., Choi, Y., Choi, S., Hong, E., and Oh, E. S. (2011). Syndecan-2 cytoplasmic domain regulates colon cancer cell migration via interaction with syntenin-1. *Biochem. Biophys. Res. Commun.* 409, 148–153. doi: 10.1016/j.bbrc.2011.04.135

Lee, Y. H., Park, J. H., Cheon, D. H., Kim, T., Park, Y. E., Oh, E. S., et al. (2017). Processing of syndecan-2 by matrix metalloproteinase-14 and effect of its cleavage on VEGF-induced tube formation of HUVECs. *Biochem. J.* 474, 3719–3732. doi: 10.1042/bcj20170340

Li, Y., Yue, P., Deng, X., Ueda, T., Fukunaga, R., Khuri, F. R., et al. (2010). Protein phosphatase 2A negatively regulates eukaryotic initiation factor 4E

phosphorylation and eIF4F assembly through direct dephosphorylation of Mnk and eIF4E. *Neoplasia* 12, 848–855. doi: 10.1593/neo.10704

Lim, H. C., and Couchman, J. R. (2014). Syndecan-2 regulation of morphology in breast carcinoma cells is dependent on RhoGTPases. *Biochim. Biophys. Acta* 1840, 2482–2490. doi: 10.1016/j.bbagen.2014.01.018

Lim, H. C., Multhaupt, H. A., and Couchman, J. R. (2015). Cell surface heparan sulfate proteoglycans control adhesion and invasion of breast carcinoma cells. *Mol. Cancer* 14:15. doi: 10.1186/s12943-014-0279-8

Liu, L., and Pilch, P. F. (2016). PTRF/Cavin-1 promotes efficient ribosomal RNA transcription in response to metabolic challenges. *eLife* 5:e17508. doi: 10.7554/eLife.17508

Lubbers, E. R., and Mohler, P. J. (2016). Roles and regulation of protein phosphatase 2A (PP2A) in the heart. *J. Mol. Cell Cardiol.* 101, 127–133. doi: 10.1016/j.yjmcc.2016.11.003

Mathiesen, S. B., Lunde, M., Aronsen, J. M., Romaine, A., Kaupang, A., Martinsen, M., et al. (2019). The cardiac syndecan-4 interactome reveals a role for syndecan-4 in nuclear translocation of muscle LIM protein (MLP). *J. Biol. Chem.* 294, 8717–8731. doi: 10.1074/jbc.RA118.006423

Mattagajasingh, S. N., Huang, S.-C., Hartenstein, J. S., and Benz, E. J. (2000). Characterization of the interaction between protein 4.1R and ZO-2: a possible link between the tight junction and the actin cytoskeleton. *J. Biol. Chem.* 275, 30573–30585. doi: 10.1074/jbc.M004578200

Maximov, A., Tang, T. S., and Bezprozvanny, I. (2003). Association of the type 1 inositol (1,4,5)-trisphosphate receptor with 4.1N protein in neurons. *Mol. Cell Neurosci.* 22, 271–283. doi: 10.1016/s1044-7431(02)00027-1

Mlynarcik, P., Bencurova, E., Madar, M., Mucha, R., Pulzova, L., Hresko, S., et al. (2012). Development of simple and rapid elution methods for proteins from various affinity beads for their direct MALDI-TOF downstream application. *J. Proteomics* 75, 4529–4535. doi: 10.1016/j.jprot.2012.03.001

Mytilinaiou, M., Nikitovic, D., Berdiaki, A., Papoutsidakis, A., Papachristou, D. J., Tsatsakis, A., et al. (2017). IGF-I regulates HT1080 fibrosarcoma cell migration through a syndecan-2/Erk/ezrin signaling axis. *Exp. Cell Res.* 361, 9–18. doi: 10.1016/j.yexcr.2017.09.035

Nassar, Z. D., and Parat, M. O. (2015). Cavin family: new players in the biology of caveolae. *Int. Rev. Cell Mol. Biol.* 320, 235–305. doi: 10.1016/bs.ircmb.2015.07.009

Ogata, T., Naito, D., Nakanishi, N., Hayashi, Y. K., Taniguchi, T., Miyagawa, K., et al. (2014). MURC/Cavin-4 facilitates recruitment of ERK to caveolae and concentric cardiac hypertrophy induced by α1-adrenergic receptors. *Proc. Natl. Acad. Sci. U.S.A.* 111, 3811–3816. doi: 10.1073/pnas.1315359111

Ogata, T., Ueyama, T., Isodono, K., Tagawa, M., Takehara, N., Kawashima, T., et al. (2008). MURC, a muscle-restricted coiled-coil protein that modulates the Rho/ROCK pathway, induces cardiac dysfunction and conduction disturbance. *Mol. Cell Biol.* 28, 3424–3436. doi: 10.1128/mcb.02186-07

Oh, E. S., and Couchman, J. R. (2004). Syndecans-2 and -4; close cousins, but not identical twins. *Mol. Cells* 17, 181–187.

Oh, E. S., Couchman, J. R., and Woods, A. (1997). Serine phosphorylation of syndecan-2 proteoglycan cytoplasmic domain. *Arch. Biochem. Biophys.* 344, 67–74. doi: 10.1006/abbi.1997.0180

Osmanagic-Myers, S., Rus, S., Wolfram, M., Brunner, D., Goldmann, W. H., Bonakdar, N., et al. (2015). Plectin reinforces vascular integrity by mediating crosstalk between the vimentin and the actin networks. *J. Cell Sci.* 128:4138. doi: 10.1242/jcs.172056

Park, I., Han, C., Jin, S., Lee, B., Choi, H., Kwon, J. T., et al. (2011). Myosin regulatory light chains are required to maintain the stability of myosin II and cellular integrity. *Biochem. J.* 434:171. doi: 10.1042/BJ20101473

Prasthofer, T., Ek, B., Ekman, P., Owens, R., Hook, M., and Johansson, S. (1995). Protein kinase C phosphorylates two of the four known syndecan cytoplasmic domains in vitro. *Biochem. Mol. Biol. Int.* 36, 793–802.

Raman, D., Sai, J., Hawkins, O., and Richmond, A. (2014). Adaptor protein2 (AP2) orchestrates CXCR2-mediated cell migration. *Traffic* 15, 451–469. doi: 10.1111/tra.12154

Renga, B., Francisci, D., D'Amore, C., Schiaroli, E., Mencarelli, A., Cipriani, S., et al. (2012). The HIV matrix protein p17 subverts nuclear receptors expression and induces a STAT1-dependent proinflammatory phenotype in monocytes. *PLoS One* 7:e35924. doi: 10.1371/journal.pone.0035924

Rovira-Clave, X., Angulo-Ibanez, M., Reina, M., and Espel, E. (2014). The PDZ-binding domain of syndecan-2 inhibits LFA-1 high-affinity conformation. *Cell Signal.* 26, 1489–1499. doi: 10.1016/j.cellsig.2014.03.012

Ruiz, X. D., Mlakar, L. R., Yamaguchi, Y., Su, Y., Larregina, A. T., Pilewski, J. M., et al. (2012). Syndecan-2 is a novel target of insulin-like growth factor binding protein-3 and is over-expressed in fibrosis. *PLoS One* 7:e43049. doi: 10.1371/journal.pone.0043049

Ryu, H. Y., Lee, J., Yang, S., Park, H., Choi, S., Jung, K. C., et al. (2009). Syndecan-2 functions as a docking receptor for pro-matrix metalloproteinase-7 in human colon cancer cells. *J. Biol. Chem.* 284, 35692–35701. doi: 10.1074/jbc.M109.054254

Sahlan, M., Zako, T., and Yohda, M. (2018). Prefoldin, a jellyfish-like molecular chaperone: functional cooperation with a group II chaperonin and beyond. *Biophys. Rev.* 10, 339–345. doi: 10.1007/s12551-018-0400-0

Salani, B., Passalacqua, M., Maffioli, S., Briatore, L., Hamoudane, M., Contini, P., et al. (2010). IGF-IR internalizes with Caveolin-1 and PTRF/Cavin in HaCat cells. *PLoS One* 5:e14157. doi: 10.1371/journal.pone.0014157

Schellings Mark, W. M., Vanhoutte, D., van Almen Geert, C., Swinnen, M., Leenders Joost, J. G., Kubben, N., et al. (2010). Syndecan-1 amplifies Angiotensin II–induced cardiac fibrosis. *Hypertension* 55, 249–256. doi: 10.1161/HYPERTENSIONAHA.109.137885

Schnoor, M., Stradal, T. E., and Rottner, K. (2018). Cortactin: cell functions of a multifaceted actin-binding protein. *Trends Cell Biol.* 28, 79–98. doi: 10.1016/j.tcb.2017.10.009

Shahbazian, D., Roux, P. P., Mieulet, V., Cohen, M. S., Raught, B., Taunton, J., et al. (2006). The mTOR/PI3K and MAPK pathways converge on eIF4B to control its phosphorylation and activity. *EMBO J.* 25, 2781–2791. doi: 10.1038/sj.emboj.7601166

Shepherd, T. R., Klaus, S. M., Liu, X., Ramaswamy, S., DeMali, K. A., and Fuentes, E. J. (2010). The Tiam1 PDZ domain couples to Syndecan1 and promotes cell-matrix adhesion. *J. Mol. Biol.* 398, 730–746. doi: 10.1016/j.jmb.2010.03.047

Shi, Y., Gochuico, B. R., Yu, G., Tang, X., Osorio, J. C., Fernandez, I. E., et al. (2013). Syndecan-2 exerts antifibrotic effects by promoting caveolin-1-mediated transforming growth factor-beta receptor I internalization and inhibiting transforming growth factor-beta1 signaling. *Am. J. Respir. Crit. Care Med.* 188, 831–841. doi: 10.1164/rccm.201303-0434OC

Shin, J., Lee, W., Lee, D., Koo, B.-K., Han, I., Lim, Y., et al. (2001). Solution structure of the dimeric cytoplasmic domain of Syndecan-4. *Biochemistry* 40, 8471–8478. doi: 10.1021/bi002750r

Siddiqui, N., and Sonenberg, N. (2015). Signalling to eIF4E in cancer. *Biochem. Soc. Trans.* 43, 763–772. doi: 10.1042/bst20150126

Strand, M. E., Herum, K. M., Rana, Z. A., Skrbic, B., Askevold, E. T., Dahl, C. P., et al. (2013). Innate immune signaling induces expression and shedding of the heparan sulfate proteoglycan syndecan-4 in cardiac fibroblasts and myocytes, affecting inflammation in the pressure-overloaded heart. *FEBS J.* 280, 2228–2247. doi: 10.1111/febs.12161

Sung, B. H., Zhu, X., Kaverina, I., and Weaver, A. M. (2011). Cortactin controls cell motility and lamellipodial dynamics by regulating ECM secretion. *Curr. Biol.* 21, 1460–1469. doi: 10.1016/j.cub.2011.06.065

Szklarczyk, D., Morris, J. H., Cook, H., Kuhn, M., Wyder, S., Simonovic, M., et al. (2017). The STRING database in 2017: quality-controlled protein-protein association networks, made broadly accessible. *Nucleic Acids Res.* 45, D362–D368. doi: 10.1093/nar/gkw937

Taniguchi, T., Maruyama, N., Ogata, T., Kasahara, T., Nakanishi, N., Miyagawa, K., et al. (2016). PTRF/Cavin-1 deficiency causes cardiac dysfunction accompanied by cardiomyocyte hypertrophy and cardiac fibrosis. *PLoS One* 11:e0162513. doi: 10.1371/journal.pone.0162513

Tornavaca, O., Chia, M., Dufton, N., Almagro, L. O., Conway, D. E., Randi, A. M., et al. (2015). ZO-1 controls endothelial adherens junctions, cell–cell tension, angiogenesis, and barrier formation. *J. Cell Biol.* 208, 821–838. doi: 10.1083/jcb.201404140

Tsoyi, K., Chu, S. G., Patino-Jaramillo, N. G., Wilder, J., Villalba, J., Doyle-Eisele, M., et al. (2018). Syndecan-2 attenuates radiation-induced pulmonary fibrosis and inhibits fibroblast activation by regulating PI3K/Akt/ROCK pathway via CD148. *Am. J. Respir. Cell Mol. Biol.* 58, 208–215. doi: 10.1165/rcmb.2017-0088OC

Vanhoutte, D., Schellings Mark, W. M., Götte, M., Swinnen, M., Herias, V., Wild Martin, K., et al. (2007). Increased expression of Syndecan-1 protects against

cardiac dilatation and dysfunction after myocardial infarction. *Circulation* 115, 475–482. doi: 10.1161/CIRCULATIONAHA.106.644609

Wang, H., Leavitt, L., Ramaswamy, R., and Rapraeger, A. C. (2010). Interaction of syndecan and α6β4 integrin cytoplasmic domains: regulation of ErbB2-mediated integrin activation. *J. Biol. Chem.* 285, 13569–13579. doi: 10.1074/jbc.M110.102137

Whiteford, J. R., Behrends, V., Kirby, H., Kusche-Gullberg, M., Muramatsu, T., and Couchman, J. R. (2007). Syndecans promote integrin-mediated adhesion of mesenchymal cells in two distinct pathways. *Exp. Cell Res.* 313, 3902–3913. doi: 10.1016/j.yexcr.2007.08.002

Whiteford, J. R., Xian, X., Chaussade, C., Vanhaesebroeck, B., Nourshargh, S., and Couchman, J. R. (2011). Syndecan-2 is a novel ligand for the protein tyrosine phosphatase receptor CD148. *Mol. Biol. Cell* 22, 3609–3624. doi: 10.1091/mbc.E11-02-0099

Yoo, J., Jeong, M. J., Cho, H. J., Oh, E. S., and Han, M. Y. (2005). Dynamin II interacts with syndecan-4, a regulator of focal adhesion and stress-fiber formation. *Biochem. Biophys. Res. Commun.* 328, 424–431. doi: 10.1016/j.bbrc.2004.12.179

Zandonadi, F. S., Castaneda Santa Cruz, E., and Korvala, J. (2019). New SDC function prediction based on protein-protein interaction using bioinformatics tools. *Comput. Biol. Chem.* 83:107087. doi: 10.1016/j.compbiolchem.2019.107087

Zhao, N., Liu, H., and Lilly, B. (2012). Reciprocal regulation of syndecan-2 and Notch signaling in vascular smooth muscle cells. *J. Biol. Chem.* 287, 16111–16120. doi: 10.1074/jbc.M111.322107

Zimmermann, P., Zhang, Z., Degeest, G., Mortier, E., Leenaerts, I., Coomans, C., et al. (2005). Syndecan recycling is controlled by syntenin-PIP2 interaction and Arf6. *Dev. Cell* 9, 377–388. doi: 10.1016/j.devcel.2005.07.011

Conflict of Interest: The authors declare that the research was conducted in the absence of any commercial or financial relationships that could be construed as a potential conflict of interest.

frontiers in Cell and Developmental Biology

BRIEF RESEARCH REPORT
published: 25 September 2020
doi: 10.3389/fcell.2020.559554

The Heparan Sulfate Sulfotransferases HS2ST1 and HS3ST2 Are Novel Regulators of Breast Cancer Stem-Cell Properties

Felipe C. O. B. Teixeira[1,2†], Archana Vijaya Kumar[2†], Sampath Kumar Katakam[2], Cinzia Cocola[3], Paride Pelucchi[3], Monika Graf[2‡], Ludwig Kiesel[2], Rolland Reinbold[3], Mauro S. G. Pavão[1], Burkhard Greve[4] and Martin Götte[2]**

[1] Instituto de Bioquímica Médica Leopoldo de Meis, Hospital Universitário Clementino Fraga Filho, Universidade Federal do Rio de Janeiro, Rio de Janeiro, Brazil, [2] Department of Gynecology and Obstetrics, Münster University Hospital, Münster, Germany, [3] Istituto di Tecnologie Biomediche, Consiglio Nazionale delle Ricerche, Segrate, Italy, [4] Department of Radiotherapy and Radiooncology, University Hospital of Münster, Münster, Germany

Heparan sulfate (HS) is a glycosaminoglycan found mainly in its protein-conjugated form at the cell surface and the extracellular matrix. Its high sulfation degree mediates functional interactions with positively charged amino acids in proteins. 2-O sulfation of iduronic acid and 3-O sulfation of glucosamine in HS are mediated by the sulfotransferases HS2ST and HS3ST, respectively, which are dysregulated in several cancers. Both sulfotransferases regulate breast cancer cell viability and invasion, but their role in cancer stem cells (CSCs) is unknown. Breast CSCs express characteristic markers such as $CD44^{+}/CD24^{-/low}$, CD133 and ALDH1 and are involved in tumor initiation, formation, and recurrence. We studied the influence of HS2ST1 and HS3ST2 overexpression on the CSC phenotype in breast cancer cell lines representative of the triple-negative (MDA-MB-231) and hormone-receptor positive subtype (MCF-7). The $CD44^{+}/CD24^{-/low}$ phenotype was significantly reduced in MDA-MB-231 cells after overexpression of both enzymes, remaining unaltered in MCF-7 cells. ALDH1 activity was increased after HS2ST1 and HS3ST2 overexpression in MDA-MB-231 cells and reduced after HS2ST1 overexpression in MCF-7 cells. Colony and spheroid formation were increased after HS2ST1 and HS3ST2 overexpression in MCF-7 cells. Moreover, MDA-MB-231 cells overexpressing HS2ST1 formed more colonies and could not generate spheres. The phenotypic changes were associated with complex changes in the expression of the stemness-associated notch and Wnt-signaling pathways constituents, syndecans, heparanase and Sulf1. The results improve our understanding of breast CSC function and mark a subtype-specific impact of HS modifications on the CSC phenotype of triple-negative and hormone receptor positive breast cancer model cell lines.

Keywords: breast cancer, sulfotransferase, heparan sulfate, epithelial-to-mesenchymal transition, cancer stem cell (CSC), syndecan, notch, Sulf1

OPEN ACCESS

Edited by:
Jeremy Turnbull, University of Liverpool, United Kingdom

Reviewed by:
Maria Aparecida Silva Pinhal, Federal University of São Paulo, Brazil
Fabrice Allain, Université de Lille, France

***Correspondence:**
Burkhard Greve
greveb@uni-muenster.de
Martin Götte
mgotte@uni-muenster.de

† These authors have contributed equally to this work

‡ Present address:
Monika Graf, Department of Pediatric Hematology and Oncology, University Children's Hospital Münster, Münster, Germany

Specialty section:
This article was submitted to Signaling, a section of the journal Frontiers in Cell and Developmental Biology

Received: *06 May 2020*
Accepted: *02 September 2020*
Published: *25 September 2020*

Citation:
Teixeira FCOB, Vijaya Kumar A, Kumar Katakam S, Cocola C, Pelucchi P, Graf M, Kiesel L, Reinbold R, Pavão MSG, Greve B and Götte M (2020) The Heparan Sulfate Sulfotransferases HS2ST1 and HS3ST2 Are Novel Regulators of Breast Cancer Stem-Cell Properties. Front. Cell Dev. Biol. 8:559554. doi: 10.3389/fcell.2020.559554

INTRODUCTION

Heparan sulfate (HS) is a highly sulfated glycosaminoglycan (GAG) found on the cell surface and in the extracellular matrix (ECM) (Zhang, 2010; Karamanos et al., 2018). Its localization is determined by the core protein, while the HS chains determine the affinity to numerous ligands such as growth factors, cytokines, proteases, lipoproteins and ECM components (Denys and Allain, 2019). HS mediates cell-cell and cell-ECM communication, leading to different pathological and physiological effects, including embryonic development, cell growth and differentiation, homeostasis, inflammatory responses, tumor growth and microbial infection (Li and Kusche-Gullberg, 2016). These interactions are driven by the high degree of sulfation of this molecule, which interacts with positively charged amino acid residues in the protein ligands (Morla, 2019). The spatial arrangement of sulfate groups in different HS domains is equally crucial to ensure optimal binding to different ligands (Esko and Selleck, 2002). The high structural variability of HS stems from enzymatic modifications of its glycan backbone of repeated disaccharide units of D-glucuronic acid (GlcA) and *N*-acetyl-D-glucosamine (GlcNAc) synthesized in the Golgi apparatus. Sequential modification steps include deacetylation, epimerization and, finally, sulfation catalyzed by the enzymes *N*-deacetylases/*N*-sulfotransferases (NDSTs) and 2-O, 6-O and 3-O sulfotransferases (HS2ST, HS6ST, and HS3ST, respectively) (Li and Kusche-Gullberg, 2016). While 2-O sulfation occurs at the uronic acids (mainly IdoA), 6-O and 3-O sulfation occur at the GlcN residues (Zhang, 2010). Aberrant regulation of sulfotransferase expression affects several processes regulated by HS, ranging from organ development to inflammation (Merry and Wilson, 2002; Denys and Allain, 2019).

The 2-O sulfated iduronic acid (IdoA2S) is a widely common HS motif and mediates the binding and signaling of several growth factors, whereas 3-O-sulfation of glucosamine is the rarest HS modification step, yet strongly mediating selective cellular processes (Kreuger et al., 2001; Witt et al., 2013). In humans, seven HS3STs and one HS2ST have been characterized, and its expression depends on the cell type and tissue environment (Gulberti et al., 2020). Notably, HS3ST is misexpressed in different types of cancers. However, its effect on cancer is still not clear, as some reports show antitumoral effects and others describe tumor-promoting activities (Vijaya Kumar et al., 2014; Denys and Allain, 2019).

Cancer stem cells (CSC), represent a population of cancer cells within a tumor responsible for tumor initiation, formation, and recurrence (Eun et al., 2017; Vitale et al., 2019). Breast cancer stem cells (BCSC) have a number of markers, such as CD44, CD24, aldehyde dehydrogenase 1 (ALDH1), among others.

CD44 is a transmembrane glycoprotein that acts as a receptor for hyaluronic acid and its expression in CSCs is associated with a mesenchymal phenotype, associated with increased adhesion, invasion and cell migration (Jaggupilli and Elkord, 2012; Li et al., 2017; Vitale et al., 2019). On the other hand, CD24 is associated with carbohydrate metabolism and a more epithelial phenotype in breast cancer (Park et al., 2010). CSCs that have the $CD44^{+}/CD24^{-}$ phenotype, therefore, are associated with a more mesenchymal and highly metastatic/invasive phenotype with greater tumorigenic potential (Li et al., 2017). Expression of ALDH1, an intracellular enzyme that oxidizes aldehydes and retinol in CSCs, is associated with an epithelial phenotype and has been shown to lead to treatment resistance, a more aggressive phenotype, and a worse prognosis on patients (Liu et al., 2014; Saeg and Anbalagan, 2018).

HS2ST1 expression is dysregulated in several tumor entities, suggesting a role in tumor progression (Bonuccelli et al., 2009; Zhao and Wang, 2020). Dysregulated expression of HS2ST1 is associated with a CSC and metastasis-associated signature in breast cancer cells carrying a mutation in caveolin (Bonuccelli et al., 2009), and upregulation of HS2ST1 is associated with reduced invasive behavior and senescence in breast cancer cells (Kang et al., 2020; Vijaya Kumar et al., 2020). HS3ST2 overexpression, on the other hand, has breast cancer cell-type-dependent effects on invasion and proliferation, affects stemness-associated signaling pathways and protects breast cancer cells against apoptosis and natural killer cell-mediated cell death (Vijaya Kumar et al., 2014; Hellec et al., 2018). In this scenario, we aimed to elucidate the influence of HS2ST1 and HS3ST2 HS sulfotransferases on the acquisition of a CSC phenotype and the expression of BCSC markers in two distinct breast cancer cell lines, MDA-MB-231 (triple negative, mesenchymal phenotype) and MCF-7 (ER+/ PR+/HER2−, epitheloid morphology).

MATERIALS AND METHODS

Cell Lines and Reagents

MDA-MB-231 and MCF-7 cells were from ATCC/LGC Promochem (Wesel, Germany) and stably transfected with a pcDNA3.1 control plasmid (Invitrogen, Karlsruhe, Germany) or a plasmid allowing for expression of the open reading frame (1104 bp) of human HS2ST1 (NCBI Reference Sequence: NM_012262) or human HS3ST2 (NCBI Reference Sequence: NM_006043.1) in the vector pReceiver-M02 under control of the cytomegalovirus promoter (RZPD/ImaGenes, Berlin, Germany) as previously described (Nikolova et al., 2009; Vijaya Kumar et al., 2014, 2020). Stable clones were selected using 1 mg/ml G418. MDA-MB-231 cells were maintained in Dulbecco's Modified Eagle Medium – High Glucose (DMEM-HG) containing 10% fetal calf serum (FCS), 1% penicillin/streptomycin and 600 mg/ml G418 in a humidified atmosphere of 7% CO_2 at 37°C. Successful transfection was confirmed by qPCR (Vijaya Kumar et al., 2014, 2020). MCF-7 cells were cultured in RPMI-1640 medium containing 10% FCS, 1% penicillin/streptomycin and 600 mg/ml G418 in a humidified atmosphere of 5% CO_2 at 37°C. Media, FCS and tissue culture supplies were from Gibco BRL (Karlsruhe, Germany). siRNA knockdown of Syndecan-1 and Syndecan-4 in some experiments was done as previously described (Ibrahim et al., 2012) using siRNAs #s12634 (Sdc1), # s12638 (Sdc4) and a

Abbreviations: ALDH, aldehyde dehydrogenase; BCSC, breast cancer stem cell; CSC, cancer stem cell; ECM, extracellular matrix; ER, estrogen receptor; GAG, glycosaminoglycan; HS, heparan sulfate; MFI, mean fluorescence intensity; NDST, *N*-deacetylase/*N*-sulfotransferase; PBS, phosphate-buffered saline; PR, progesterone receptor.

negative control siRNA (negative control #1; all from Ambion, Cambridgeshire, United Kingdom). Unless stated otherwise, all chemicals were from Sigma (Deisenhofen, Germany). In some experiments, cells were treated with 1 μM gamma secretase inhibitor (GSI, Calbiochem, Darmstadt, Germany) for 24 h as previously described (Ramirez Williams et al., 2019).

CD24 and CD44 Identification With Flow Cytometry

To detect CD24 and CD44, cells were incubated with 10 μl of anti-human-CD44-FITC and anti-human-CD24-PE or the IgG2b-FITC and IgG1-PE isotype control antibodies (Immunotools, Friesoythe, Germany) for 30 min at room temperature in the dark. Stained cells were analyzed by a Cyflow Space flow cytometer (Sysmex/Partec, Münster, Germany).

Identification of ALDH-1 Positive Cells

For ALDH1 activity assessment, we used the ALDEFLUOR™ kit (StemCell Technologies, Köln, Germany) as previously described (Ibrahim et al., 2013). Briefly, 2×10^5 MDA-MB-231 and MCF-7 control cells or overexpressing HS2ST1 and HS3ST2 were resuspended in assay buffer containing ALDH1 substrate (1 μmol/L). Another pool of control cells were incubated with 50 mM ALDH1 inhibitor diethylaminobenzaldehyde (DEAB) as negative control. These solutions of cells were incubated for 1 h at 37°C in a water bath in the dark with agitation at 10 min interval. After 1 h, the cells were centrifuged at 400G for 5 min and resuspended in 1 mL assay buffer and stored on ice prior to acquisition with a Cyflow Space cytometer.

Colony Formation Assay

To examine the effect of the overexpression of HS2ST1 and HS3ST2 on colony formation, 800 control and transfected cells were seeded in 35 mm gridded dishes and maintained in their respective media with 10% FCS for 10–14 days. The total number of colonies was counted using a microscope and the percentage of altered colony numbers was accessed as a ratio between sulfotransferase overexpressing cells and vector control cells.

Analysis of Spheroid Size by the Hanging Drop Method

To access the spheroid formation ability and compare the spheroid size of the cells, we first prepared a solution of 10^6 cells/mL in complete medium and placed several 20 μl drops into the lid of a Petri dish, after which we added 7 mL sterile PBS to the bottom of the dish and left it in the cell incubator for 1 week. Pictures of the spheroids inside the drop were taken using a Zeiss Axiophot camera and their comparative size was obtained measuring the area occupied by the spheres using the software NIH ImageJ (NIH, Bethesda, United States).

Mammosphere Assay

For the mammosphere formation assay, a culture medium containing DMEM/F12 supplemented with 2 mM L-glutamine and 100 U/mL penicillin/streptomycin was prepared. Immediately before use, 20 ng/ml of recombinant human epidermal growth factor (EGF) and 10 ng/ml of basic human fibroblast growth factor (bFGF) were added. Cells were detached from the flasks and resuspended in complete mammosphere medium. 2×10^3 cells of each condition were added to the wells of an ultra-low adhesion 6-well plate (Cornind Costar, Darmstadt, Germany) and placed in a cell incubator at 37°C and 5% CO_2 for 9 or 15 days. Subsequently, spheres were counted and the number of spheres per number of cells initially plated was calculated.

Quantitative Real-Time PCR

The total RNA isolated from cultured cells using a kit (Analytik Jena, Jena, Germany) was reverse transcribed into cDNA using the high capacity cDNA kit (Applied Biosystems, Foster City, CA, United States). Quantitative real-time PCR was conducted in duplicate for each gene of interest using TaqMan probes or SYBR Green dye and gene expression levels were measured in a steponeplus detection system (Applied Biosystems). Relative gene expression was evaluated using the $2^{-\Delta\Delta Ct}$ method after normalization to 18S rRNA or beta-actin as previously described (Ibrahim et al., 2012). Primer information is provided in **Supplementary Table I**.

Western Blotting

Western blotting was performed using 30 μg of cell extract/lane exactly as previously described (Ibrahim et al., 2012). Membranes were stripped and reprobed with tubulin antibodies as loading control. Antibodies are listed in **Supplementary Table II**.

Statistical Analysis

All Data are presented as mean ± SEM or SD as indicated in the figure legends and mean ± SEM in the text. Biological replicates per independent experiments were as follows: Flow cytometry and colony formation (3 × 3), Mammosphere and hanging drop assay (3 × 10), qPCR (1–3 × 3–5). Western blot (2–4 × 2). Comparisons among two distinct groups were evaluated using Student's *t*-test (for normally distributed data) or Mann–Whitney *U*-test (for non-normally distributed data). The statistical difference between more than two groups was evaluated by one-way ANOVA followed by Tukey's multiple comparison test. The level of significance was set at $p < 0.05$. Graphs were plotted and analyses were performed by GraphPad Prism 7 software (San Diego, CA, United States).

RESULTS

HS2ST1 and HS3ST2 Overexpression in MDA-MB-231 and MCF-7 Cells Alter the Expression of the CSC Markers CD24 and CD44, and ALDH1 Enzymatic Activity

First, we analyzed by flow cytometry whether the percentage of MDA-MB-231 and MCF-7 breast cancer cells displaying the $CD44^+/CD24^-$ phenotype was changed by HS2ST1 and HS3ST2 overexpression. The clones were already stablished and characterized by our group (Vijaya Kumar et al., 2014, 2020).

qPCR revealed that HS2ST1 overexpression led to an 25-37-fold increase in HS2ST1 mRNA expression (**Table 1**), while we could only detect HS3ST2 mRNA in cells transfected with a HS3ST2 expression plasmid (Vijaya Kumar et al., 2014). In triple-negative MDA-MB-231 cells, upregulation of both sulfotransferases led to a significant decrease in the percentage of cells with the $CD44^+/CD24^-$ phenotype in comparison to the vector control cells (**Figure 1A**, highlighted in the box). HS2ST1 overexpression reduced this phenotype from 94.05% (±0.24%) in control cells to 52.83% (±1.06%) in the transfected cells, whilst cells overexpressing the HS3ST2 sulfotransferase presented 90.2% (±1.16%) of cells with the $CD44^+/CD24^-$ phenotype. In contrast, hormone-receptor positive MCF-7 cells did not undergo a significant change in this $CD44^+/CD24^-$ phenotype after HS2ST1 or HS3ST2 overexpression (**Figure 1A**). The number of $CD44^+/CD24^+$ cells significantly increased in the MDA-MB-231 cells after overexpression of HS2ST1 and HS3ST2, respectively, from 5.82% (±0.24%) in the vector control cells to 47.07% (±1.06%) in the HS2ST1 overexpressing cells and 9.72% (±1.17%) in the cells overexpressing HS3ST2 (data not shown). In MCF-7 cells, the overexpression of HS3ST2 significantly decreased the double-positive phenotype from 37.91% (±1.06%) in the vector control cells to 12.71% (±0.98%) in the transfected cells. Compared to the vector control cells (MDA-MB-231: 0.88 ± 0.02; MCF-7: 17.1 ± 1.03), overexpression of the HS2ST1 enzyme led to a significant increase in CD24 expression on the membrane of MDA-MB-231 cells (3.28 ± 0.09) and a significant reduction of this marker in MCF-7 cells (14.12 ± 0.32), as determined by measuring the mean fluorescence intensity (MFI) (**Figure 1A**). Compared to the vector control cells (MDA-MB-231: 264.93 ± 17.91; MCF-7: 5.58 ± 0.59), HS3ST2 overexpression led to a significant increase of CD44 in MDA-MB-231 cells (333.61 ± 11.07) and a reduction of its expression in MCF-7 cells (1.91 ± 0.39) (**Figure 1A**).

Next, we analyzed the activity of the enzyme ALDH1, another BCSC marker, by flow cytometry (ALDEFLUOR^{TM} assay). In MDA-MB-231 cells, ALDH1 activity increased from 2.88% (±0.66%) in the control transfected cells to 9.99% (±0.76%) after overexpression of HS2ST1, and 5.36% (±0.33%) in the HS3ST2 overexpressing cells (**Figure 1B**). HS2ST1 overexpression in the MCF-7 cells had the inverse effect, decreasing the activity of ALDH from 4.42% (±0.34%) in the control transfected cells to 0.91% (±0.10%) after its overexpression (**Figure 1B**).

HS2ST1 and HS3ST2 Overexpression Modifies Colony Formation, and Number and Size of MDA-MB-231 and MCF-7 Tumor Spheres

One of the main features related to the high tumorigenicity and self-renewal capacity of CSCs is the ability to form colonies *in vitro* after being seeded in low concentrations on cell culture plates (Yang et al., 2017). Overexpression of HS2ST1 significantly increased the number of colonies per dish by 101.86% in MDA-MB-231 (**Figure 2A**) and 61.93% in MCF-7 cells. HS3ST2 overexpression strongly increased the number of colonies per dish by 245.6% only in the MCF-7 cells (**Figure 2A**).

Three-dimensional cell culture models mimic important features of the tumor, such as spatial organization, cell–cell interaction, differentiation, tumor growth and hypoxia (Djomehri et al., 2019). One important scaffold-free liquid-based system to form such spheroids is the hanging drop technique. In this assay, MDA-MB-231 cells could not form compact spheres but formed compact aggregates of cells (**Figure 2B**). The overexpression of HS2ST1 decreased the average size of the aggregates by 14.71% (±3.2%) and the overexpression of HS3ST2 decreased its size by 37.93% (±3.34%), compared to control. MCF-7 cells, on the other hand, generated larger spheres after overexpression of HS3ST2, an increase of 40.48% (±2.85%) on the average size compared to control (**Figure 2B**).

Since the MCF-7 cells seemed to form more compact and bigger spheres by the hanging drop method, we further analyzed the sphere formation capacity in non-adherent culture conditions, which promotes sphere formation from single cells and allows us to quantify the number of generated spheres. After 9 and 15 days of non-adherent culture, sphere formation was around 75% more efficient on both transfected cells. This result corroborates the hypothesis that HS2ST1 and HS3ST2 overexpression modifies and possibly enhances the stem-cell phenotype of these cells (**Figure 2C**).

The Overexpression of HS2ST1 and HS3ST2 Regulates the Expression of Factors Related to EMT and Stem Cell Function

Recent developments in the field demonstrate that many tumor cells undergo epithelial-to-mesenchymal transition (EMT) and the reverse process (MET) in order to acquire the CSC phenotype (Zhang and Weinberg, 2018). This prompted us to analyze the expression of EMT markers in HS2ST1 and HS3ST2 overexpressing MDA-MB-231 and MCF-7 cells (**Table 1**). Moreover, as a link between HS2ST1 and the expression of PGs of the syndecan-family has recently been demonstrated (Kang et al., 2020), we investigated the expression of all family members, of the functionally linked HS degrading enzyme heparanase (HPSE) and of the HS sulfate editing enzymes SULF1 and SULF2 by qPCR. HS2ST1 overexpression levels were comparable in transfected MCF-7 and MDA-MB-231 cells (**Figure 3A**). Regarding further HS-related gene expression, we noted a significant upregulation of SULF1 in all sulfotransferase-expressing cells, whereas SULF2 was downregulated in HS3ST2 overexpressing MCF-7 cells (**Table 1** and **Figure 3B**). HPSE and SDC4 were significantly upregulated in MCF-7 cells overexpressing HS2ST1 and HS3ST2. In contrast, HPSE was significantly downregulated, and SDC2 upregulated in HS2ST1-transfected MDA-MB-231 cell, indicating context-dependent effects (**Figure 3** and **Table 1**). Regarding EMT-related factors, in MCF-7 cells, overexpression of HS2ST1 and HS3ST2 reduced the gene expression of Vimentin, a marker of mesenchymal cells, and of the EMT-inducing transcription factors Snail1, Twist and Snail 2 (only HS2ST1), compared to the vector control cells. *E*-cadherin gene expression was reduced, while β-catenin was upregulated (**Table 1** and **Figures 3C,D**). In MDA-MB-231

TABLE 1 | pPCR analysis of breast cancer cell lines overexpressing HS sulfotransferases.

Genes	MCF-7					MDA-MB-231				
	Control	HS2ST1	*P*	HS3ST2	*P*	Control	HS2ST1	*P*	HS3ST2	*P*
HS related										
HS2ST1 (*n* ≥ 10)	1.00 ± 0.07	**24.89 ± 16.56**	**<0.001**	1.06 ± 0.23	0.51	1.01 ± 0.11	**37.42 ± 18.47**	**<0.0001**	1.10 ± 0.18	0.15
HS3ST2 (*n* ≥ 6)*	–	–	n.a.	+++	n.a.	–	–	n.a.	+++	n.a.
Sulf1 (*n* ≥ 8)	1.00 ± 0.20	**15.46 ± 12.02**	**<0.05**	**7.52 ± 4.53**	**<0.01**	1.02 ± 0.23	**3.88 ± 1.59**	**<0.01**	**1.65 ± 0.51**	**<0.01**
Sulf2 (*n* ≥ 8)	1.01 ± 0.12	0.84 ± 0.19	0.06	**0.72 ± 0.24**	**<0.05**	1.08 ± 0.42	2.62 ± 2.66	0.15	1.87 ± 1.42	0.17
HPSE (*n* ≥ 10)	1.03 ± 0.28	**1.97 ± 0.91**	**<0.001**	**1.50 ± 0.92**	**<0.05**	1.02 ± 0.20	**0.57 ± 0.31**	**<0.0001**	1.02 ± 0.31	0.97
Syndecans										
Sdc-1 (*n* ≥ 6)	1.02 ± 0.21	1.03 ± 0.18	0.93	1.03 ± 0.24	0.91	1.03 ± 0.27	0.75 ± 0.54	0.28	0.75 ± 0.60	0.33
Sdc-2 (*n* ≥ 6)	1.03 ± 0.28	1.04 ± 0.19	0.92	0.84 ± 0.26	0.31	1.01 ± 0.10	**2.04 ± 0.67**	**<0.04**	1.19 ± 0.31	0.86
Sdc-3 (*n* ≥ 3)	1.00 ± 0.09	1.09 ± 0.18	0.53	0.84 ± 0.07	0.07	1.01 ± 0.13	1.14 ± 0.58	0.74	0.79 ± 0.05	0.09
Sdc-4 (*n* ≥ 8)	1.02 ± 0.23	**1.80 ± 0.66**	**<0.001**	**2.06 ± 0.68**	**<0.01**	1.01 ± 0.16	1.54 ± 0.72	0.07	1.25 ± 0.70	0.37
EMT										
***E*-Cadherin (*n* ≥ 9)**	1.01 ± 0.06	**0.79 ± 0.20**	**<0.01**	0.88 ± 0.37	0.28	1.00 ± 0.04	1.24 ± 0.85	0.38	1.43 ± 0.67	0.09
***N*-Cadherin (*n* ≥ 7)**	1.15 ± 0.60	1.00 ± 0.50	0.60	0.96 ± 0.41	0.48	1.01 ± 0.12	**1.23 ± 0.19**	**<0.05**	0.82 ± 0.25	0.09
β-catenin (*n* ≥ 7)	1.01 ± 0.18	**1.42 ± 0.33**	**<0.05**	1.21 ± 0.29	0.13	1.01 ± 0.12	0.81 ± 0.32	0.14	1.15 ± 0.46	0.42
ZEB1 (*n* ≥ 8)	1.08 ± 0.46	1.34 ± 0.77	0.39	1.42 ± 0.63	0.23	1.00 ± 0.07	1.12 ± 0.29	0.27	**0.80 ± 0.22**	**<0.05**
ZEB2 (*n* ≥ 7)	0.93 ± 0.36	2.74 ± 4.02	0.28	2.38 ± 2.21	0.17	1.01 ± 0.17	1.51 ± 0.77	0.11	1.23 ± 0.34	0.14
Vimentin (*n* ≥ 9)	1.01 ± 0.05	**0.62 ± 0.34**	**<0.01**	0.79 ± 0.45	0.13	1.00 ± 0.01	1.02 ± 0.08	0.42	**0.87 ± 0.06**	**<0.0001**
Snail1 (*n* ≥ 9)	1.02 ± 0.24	**0.58 ± 0.46**	**<0.001**	**0.90 ± 0.19**	**<0.001**	1.00 ± 0.08	**0.67 ± 0.21**	**<0.01**	**1.41 ± 0.41**	**<0.05**
Snail2 (*n* ≥ 16)	1.08 ± 0.33	**0.64 ± 0.32**	**<0.05**	0.87 ± 0.50	0.54	1.01 ± 0.13	**0.68 ± 0.22**	**<0.01**	**1.32 ± 0.34**	**<0.05**
Twist (*n* ≥ 9)	1.00 ± 0.06	**0.08 ± 0.19**	**<0.0001**	**0.11 ± 0.25**	**<0.0001**	1.03 ± 0.27	3.05 ± 3.81	0.15	2.56 ± 3.70	0.25
Notch signaling										
Notch-1 (*n* ≥ 5)	1.03 ± 0.27	1.09 ± 0.17	0.67	0.92 ± 0.29	0.57	1.06 ± 0.41	1.33 ± 1.18	0.51	0.98 ± 0.27	0.58
Notch-2 (*n* ≥ 3)	1.00 ± 0.01	5.78 ± 6.25	0.32	4.62 ± 4.44	0.29	1.09 ± 0.50	**3.19 ± 1.57**	**<0.001**	**6.81 ± 5.72**	**<0.05**
Notch-3 (*n* ≥ 5)	1.02 ± 0.23	**1.69 ± 0.10**	**<0.01**	**1.54 ± 0.27**	**<0.05**	1.13 ± 0.62	1.59 ± 1.17	0.31	2.56 ± 2.52	0.11
Notch-4** (*n* ≥ 5)	1.35 ± 1.19	0.39 ± 0.39	0.08	1.21 ± 1.40	0.84	0.98 ± 0.34	0.65 ± 0.44	0.09	0.86 ± 0.52	0.59
Numb (*n* ≥ 12)	1.00 ± 0.11	1.20 ± 0.33	0.06	**1.16 ± 0.18**	**<0.01**	1.02 ± 0.21	**1.74 ± 1.07**	**<0.05**	1.04 ± 0,41	0.87
DLL1 (*n* ≥ 3)	1.00 ± 0.09	0.93 ± 0.33	0.75	**1.27 ± 0.28**	**<0.05**	1.01 ± 0.08	**1.23 ± 0.14**	**<0.0001**	n.d.	n.d.
DLL3 (*n* ≥ 8)	1.07 ± 0.42	1.43 ± 2.21	0.66	0.88 ± 0.96	0.52	1.04 ± 0.32	0.94 ± 0.48	0.61	0.82 ± 0.45	0.25
DLL4 (*n* ≥ 8)	1.03 ± 0.28	0.83 ± 0.40	0.26	**0.70 ± 0.32**	**<0.05**	1.03 ± 0.28	**1.77 ± 0.72**	**<0.05**	0.93 ± 0.18	0.43
Hes1 (*n* ≥ 9)	1.04 ± 0.29	1.05 ± 0.41	0.69	**0.80 ± 0.31**	**0.05**	1.02 ± 0.24	**2.04 ± 1.18**	**<0.05**	**1.73 ± 0.73**	**<0.05**
Hes2 (*n* ≥ 16)	1.03 ± 0.25	**0.72 ± 0.18**	**<0.0001**	0.87 ± 0.40	0.18	1.03 ± 0.18	**1.88 ± 0.80**	**<0.0001**	1.01 ± 0.47	0.91
Hey1 (*n* ≥ 11)	1.02 ± 0.10	**1.30 ± 0.29**	**<0.001**	1.01 ± 0.38	0.94	1.00 ± 0.07	0.87 ± 0.30	0.17	1.01 ± 0.13	0.88
Hey2 (*n* ≥ 17)	1.15 ± 0.69	**5.58 ± 7.96**	**<0.05**	**3.77 ± 4.18**	***p* < 0.05**	1.07 ± 0.44	1.10 ± 0.71	0.86	**1.66 ± 1.08**	***p* < 0.05**
Jag1 (*n* ≥ 15)	1.10 ± 0.50	**2.60 ± 1.28**	**<0.001**	**2.41 ± 0.94**	**<0.001**	1.02 ± 0.23	**1.45 ± 0.57**	**<0.05**	1.18 ± 0.78	0.46
Wnt signaling										
Wnt1 (*n* ≥ 8)	–	–	n.a.	–	n.a.	1.01 ± 0.46	1.07 ± 0.65	0.82	**2.48 ± 1.11**	**<0.01**
Wnt3a (*n* ≥ 8)	1.01 ± 0.18	1.61 ± 1.42	0.20	1.83 ± 1.62	0.13	1.07 ± 0.42	1.18 ± 0.77	0.71	1.32 ± 0.90	0.48
Wnt5a (*n* ≥ 8)	1.38 ± 1.15	1.39 ± 0.68	0.99	1.58 ± 0.92	0.72	1.00 ± 0.04	**0.49 ± 0.11**	**<0.0001**	**0.29 ± 0.11**	**<0.0001**
FZD7 (*n* ≥ 8)	1.02 ± 0.24	1.12 ± 0.40	0.57	1.13 ± 0.58	0.66	1.00 ± 0.08	**1.19 ± 0.14**	**<0.01**	**1.73 ± 0.60**	**<0.05**
SFRP1 (*n* ≥ 8)	1.20 ± 0.74	1.40 ± 1.69	0.73	1.16 ± 0.81	0.90	1.03 ± 0.27	1.58 ± 0.66	0.06	0.89 ± 0.54	0.52
TCF7L1 (*n* ≥ 8)	1.09 ± 0.31	**0.65 ± 0.40**	**<0.001**	**0.58 ± 0.24**	**<0.001**	1.02 ± 0.23	**4.23 ± 3.10**	**<0.05**	**1.63 ± 0.40**	**<0.01**
Others										
CD133 (*n* ≥ 7)	0.95 ± 0.36	1.16 ± 0.95	0.58	**1.43 ± 0.39**	**<0.05**	1.02 ± 0.22	**1.46 ± 0.41**	**<0.05**	**0.67 ± 0.14**	**<0.01**
Myc (*n* ≥ 9)	1.01 ± 0.18	**0.49 ± 0.21**	**<0.0001**	**0.56 ± 0.20**	**<0.01**	1.01 ± 0.18	1.46 ± 0.43	0.06	**0.71 ± 0.30**	**<0.01**
CyclinD1 (*n* ≥ 8)	1.02 ± 0.19	**0.62 ± 0.18**	**<0.001**	**0.50 ± 0.22**	**<0.001**	1.00 ± 0.06	**1.23 ± 0.26**	**<0.05**	1.00 ± 0.29	0.96

*Gene expression data are displayed as fold-change value ($2^{-\Delta\Delta Ct}$) relative to vector control cells (mean ± SD). Statistically significant data are displayed in bold typing. *HS2ST3 is not expressed in MCF-7 and MDA-MB-231 cells. – denotes absence of expression. +++, denotes high expression due to stable transfection. **, Notch4 expression data were at the limit of detection (Ct values > 32). n.d., not determined. n.a., not applicable.*

cells, we observed a significant reduction of Vimentin and ZEB1 mRNA expression after HS3ST2 overexpression, and of Snail1 and Snail2 after HS2ST1 overexpression. In contrast, these two factors were significantly upregulated in HS3ST2-overexpressing MDA-MB-231 cells. While the expression of *E*-cadherin was not significantly affected, *N*-cadherin was moderately upregulated

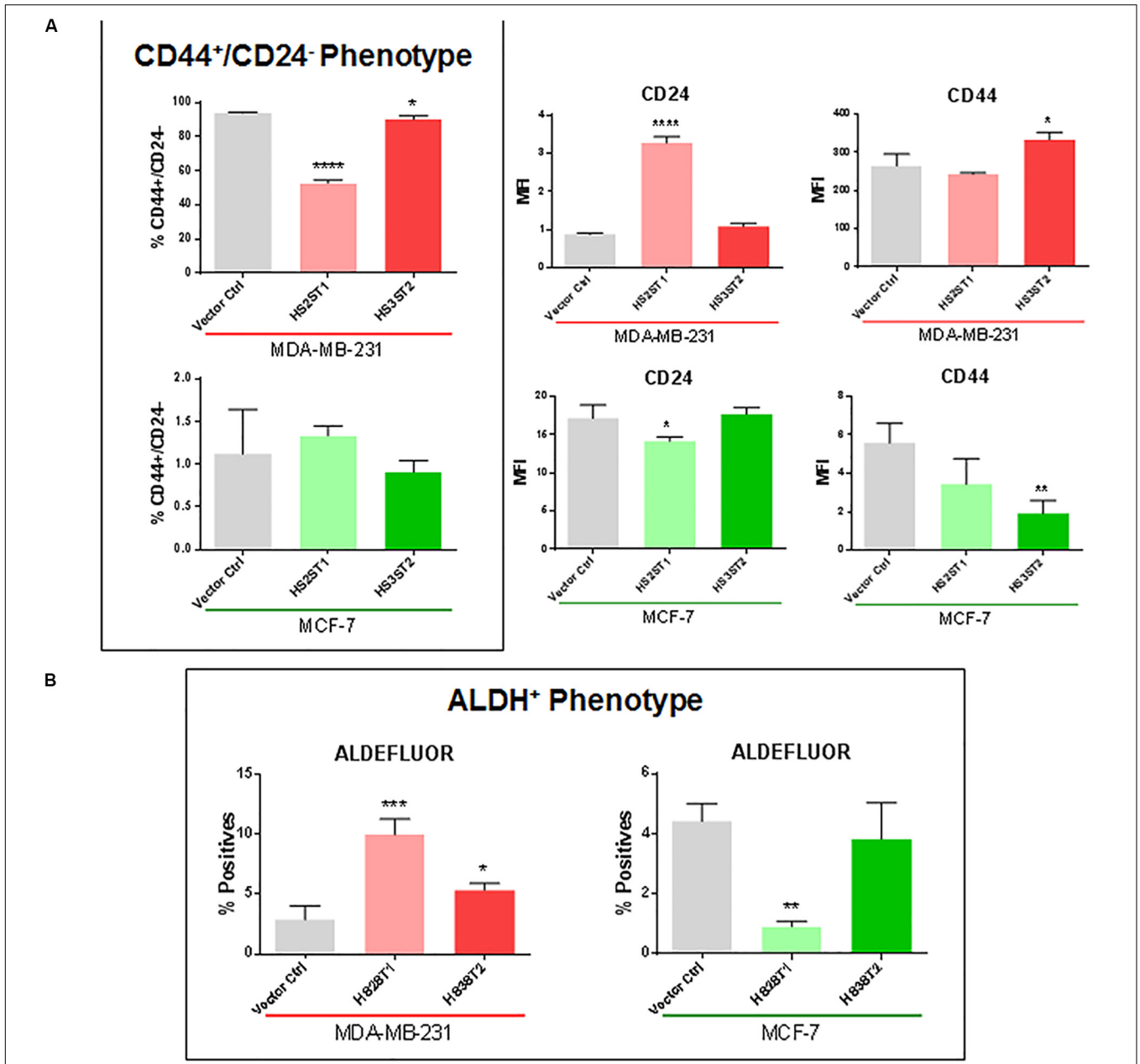

FIGURE 1 | Expression of cancer stem cell markers CD24 and CD44 and ALDH1 enzyme activity. MDA-MB-231 and MCF-7 cells modified to overexpress HS2ST1 and HS3ST2 were labeled with anti-CD24 and anti-CD44 antibodies or incubated with the ALDEFLUOR™ kit reagent and analyzed by flow cytometry. **(A, inside the box)** percentage of cells having the $CD44^+/CD24^-$ phenotype in the MDA-MB-231 and MCF-7 cells. **(A, outside the box)** Mean fluorescence intensity (MFI) of CD24 and CD44 in the MDA-MB-231 cells (top), or MCF-7 cells (bottom). **(B)** percentage of $ALDH^+$ phenotype in the MDA-MB-231 and in the MCF-7 cells. Data represent mean ± SD, $n = 3$. $^*P < 0.05$, $^{**}P < 0.01$, $^{***}P < 0.001$, $^{****}P < 0.0001$.

upon HS2ST1 upregulation in this cell line (**Table 1**). Overall, our data indicate a general trend for downregulation of mesenchymal markers upon sulfotransferase overexpression, with context-dependent cell-type and sulfotransferase-specific effects, as also noted for the transcription factor Myc, the stem cell marker CD133 and the proliferation marker CyclinD1 (**Table 1**).

The Notch pathway plays an important role in the activation and maintenance of CSCs (Hovinga et al., 2010; Chen et al., 2014; Takebe et al., 2015). Notably, Syndecan HSPGs modulate notch signaling, suggesting an impact of HS on this pathway (Ibrahim et al., 2017; Vitale et al., 2019). In line with this hypothesis, the MDA-MB-231 cell line showed an apparent increase in the activation of the Notch pathway after HS sulfotransferase

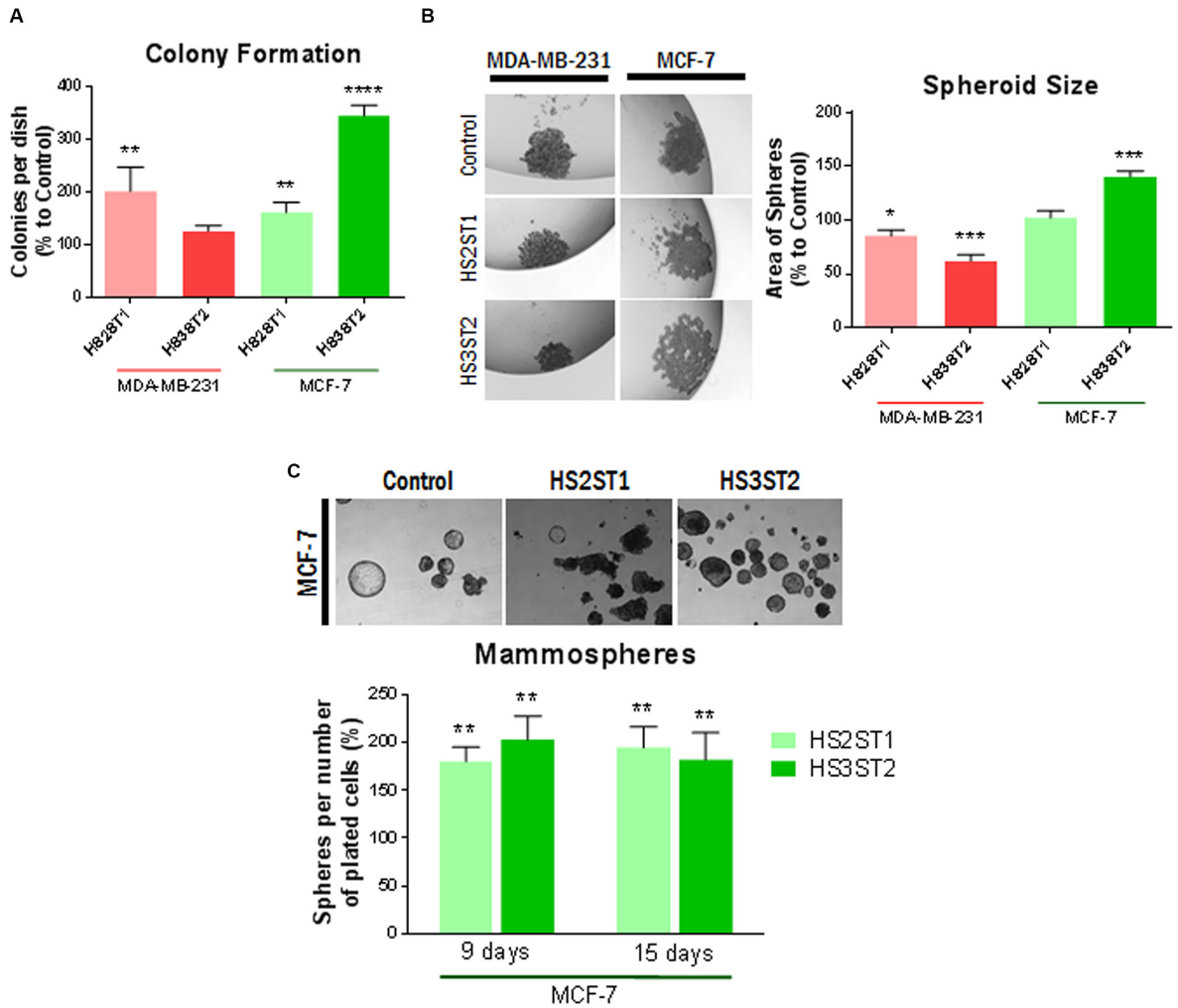

FIGURE 2 | Functional assays for the CSC-phenotype. MDA-MB-231 and MCF-7 cell lines modified to overexpress HS2ST1 and HS3ST2 and control cells were submitted to a series of functional assays to investigate the acquisition of a CSC-phenotype. From top to bottom: **(A, Colony Formation)** Percentage of colonies relative to control (100%) present in each well after 14 days. **(B, Spheroid formation)** Examples of spheres found in the drops (left). Area of the spheres relative to the vector controls (100%) present in each drop after 1 week (right). **(C, Mammosphere assay)** Examples of mammospheres generated after 15 days (top). Percentage of mammospheres formed per number of plated cells relative to control (100%) in the MCF-7 cell line after 9 or 15 days. Data represent mean ± SD, $n = 3$. $^{*}P < 0.05$, $^{**}P < 0.01$, $^{***}P < 0.001$, $^{****}P < 0.0001$.

upregulation (**Figure 3**). In HS2ST1 overexpressing MDA-MB-231 cells, an increase in the expression of Notch2, of the transcriptional regulators HES1 and HES2, markers of activation of this pathway, and of the notch ligands DLL1 and JAG1 was observed, whereas the notch modulator NUMB was also upregulated. Overexpression of HS3ST2 was associated with significant upregulation of Notch2, Hes1, and Hey1, another notch activation marker (**Table 1** and **Figures 3E–J**). HS2ST1 overexpressing MCF-7 cells showed upregulation of Notch-3, Hey1, Hey2, and Jag1 and downregulation of Hes2, whereas HS3ST2 overexpression resulted in upregulation of Notch-3, NUMB, DLL1, Hey2 and JAG1, and downregulation of DLL4 and Hes1 (**Figures 3E–J** and **Table 1**). qPCR analysis of Wnt pathway-related genes revealed a downregulation of the transcription factor TCF7L1 in HS –sulfotransferase overexpressing MCF-7 cells, whereas the Wnt receptor FZD7 was upregulated, and Wnt5a was downregulated in HS sulfotransferase overexpressing MDA-MB-231 cells (**Table 1** and **Figure 3K**). Wnt1 was upregulated in HS3St1 overexpressing MDA-MB-231 only (**Table 1**). We next confirmed selected results at the protein level (**Figure 3L**). Western blot analysis revealed upregulation of Notch3 in Sulfotransferase overexpressing MCF-7 cells, and in HS2ST1 overexpressing MDA-MB-231 cells. Results for Hes1 were ambiguous, indicating a slight upregulation in HS3ST2 expressing MDA-MB-231 cells. Hes2 was downregulated in HS2ST1 overexpressing MDA-MB-231 cells, whereas Vimentin protein expression (undetectable in epithelial MCF-7 cells) was largely unaltered. In MCF-7 cells, HS3ST2 overexpression resulted in an upregulation of Snail1 protein (**Figure 3L**).

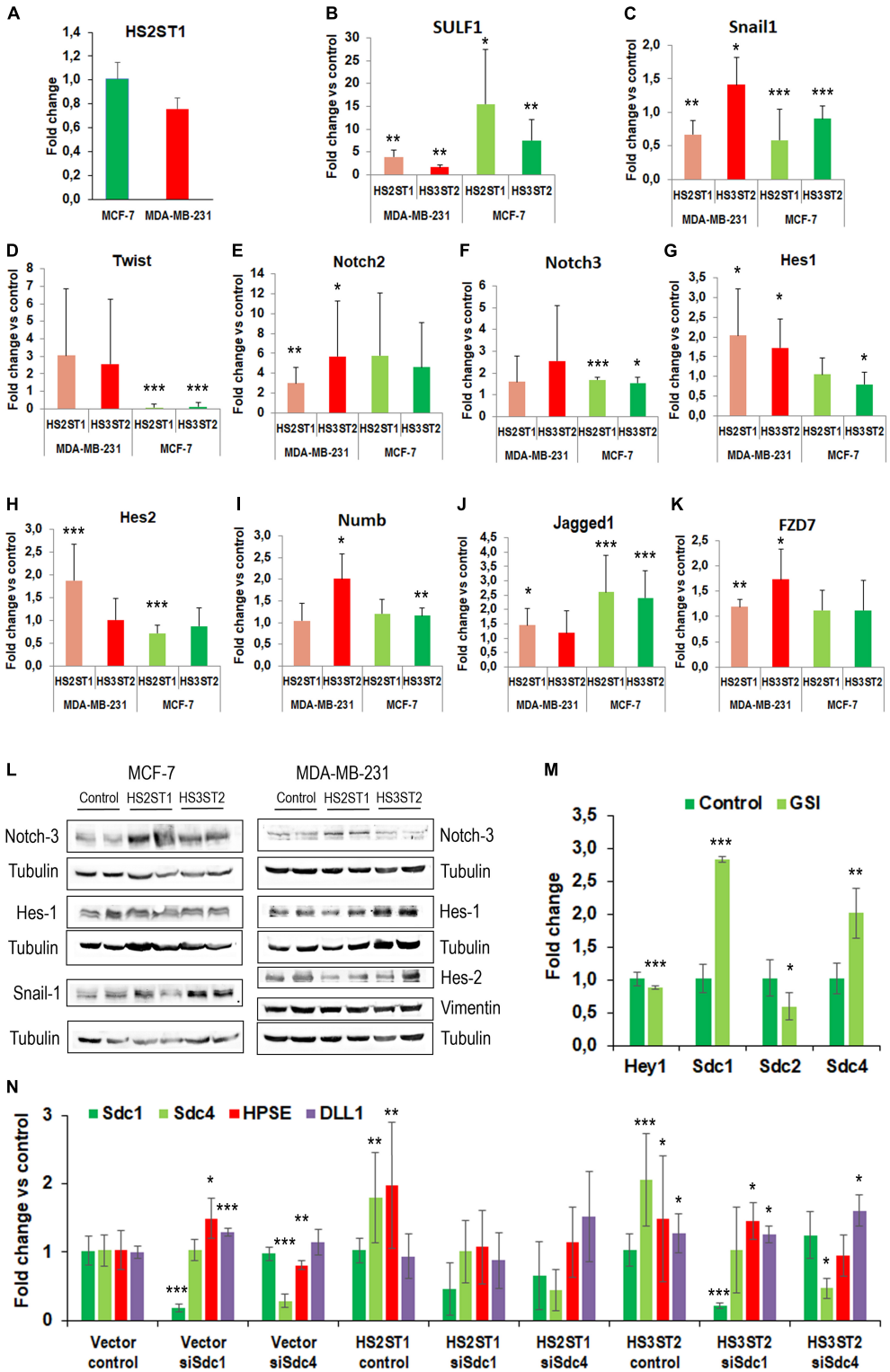

FIGURE 3 | Impact of HS sulfotransferases on HS- and stemness-associated gene expression. **(A–K)** Total RNA was isolated from the cells, reverse transcribed into cDNA and subjected into quantitative real-time PCR for analysis of Notch pathway related genes. Data represent mean ± SD from at least three independent experiments (see **Table 1** for **N**). $^{*}P < 0.05$, $^{**}P < 0.001$, $^{***}P < 0.0001$, **L**) Western blot analysis of stemness-associated factors in HS2ST1- and HS3ST2 overexpressing cells compared to controls. Loading control = tubulin. Representative data from at least 4 biological replicates. **(M)** Impact of notch pathway inhibition with gamma-secretase inhibitor (GSI) on Hey1 and Sdc-family members in MCF-7 cells. qPCR analysis as described in **(A–K)**. $N \geq 3$. **(F)** Impact of Sdc-1 and Sdc-4 knockdown on altered gene expression in HS-sulfotransferase overexpressing MCF-7 cells. Data are shown relative to vector control cells as described in **(A–K)**. $N \geq 3$.

The Syndecan Family of HSPGs and the Notch Pathway Are Part of the Regulatory Circuit of HS Sulfotransferases

As our gene expression analysis had indicated a complex impact of altered HS sulfotransferase expression on stemness-related signaling pathways and on members of the syndecan family, we further explored the interdependence of these pathways in inhibitor studies. Application of gamma secretase inhibitor (GSI), which inhibits both activation of the notch pathway and shedding of Sdc-1 (Pasqualon et al., 2015; Ramirez Williams et al., 2019) resulted in a modest, but significant inhibition of Hey1 and Sdc-2 expression, whereas Sdc-1 and Sdc-4 were strongly upregulated in MCF-7 cells (**Figure 3M**). As HS2ST1-dependent modification of Sdc-1 has recently been linked to breast cancer pathogenetic properties (Kang et al., 2020), we employed an siRNA depletion approach to downregulate the expression of Sdc-1 and Sdc-4 in sulfotransferase overexpressing MCF-7 cells, followed by qPCR analysis of HSPE, Sdc-1, Sdc4 and the notch ligand DLL1. Sdc-1 knockdown resulted in upregulation of HPSE and DLL1 in control cells, and abolished HS2ST1-dependent upregulation of Sdc-4 and HPSE, and HS3ST2 dependent upregulation of Sdc-4 (**Figure 3N**). Sdc-4 siRNA knockdown was associated with HSPE downregulation in control cells, and abolished HS2ST1 and HS3ST2-dependent HPSE upregulation in MCF-7 cells. Overall, these data provide evidence for a complex regulatory interplay of HS sulfotransferases, syndecans and the notch signaling pathway.

DISCUSSION

Studying HS sulfotransferases is a promising tool for understanding the biological functions of these enzymes on the tumor cell phenotype. Previous studies demonstrated an important role of HS3ST2 and HS2ST1 and the associated changes in HS structure in modulating receptor tyrosine kinase dependent signaling and breast cancer cell invasion, proliferation and senescence (Vijaya Kumar et al., 2014, 2020; Kang et al., 2020). However, the functional impact on CSCs was unknown. Here, we demonstrate an impact of altered HS2ST1 and HS3ST2 expression on the CSC phenotype, which is associated with complex expression changes in the stemness-associated Notch and Wnt signaling pathways, and with altered expression of proteoglycans of the syndecan family. Similar to our previous work on HS3ST2 (Vijaya Kumar et al., 2014), we observed both common and context-dependent effects of altered HS sulfotransferase expression. In the present study, colony and mammosphere formation – two important functional readouts of CSCs - were consistently upregulated in both model cell lines upon overexpression of both sulfotransferases, indicating a stemness-promoting function of these enzymes. At the molecular level, our data point at an upregulation of several components of the notch signaling pathway, which we previously linked to Sdc-1 function in breast and colon cancer (Ibrahim et al., 2017; Katakam et al., 2020a). For example, Sdc-1 expression in inflammatory breast cancer is correlated with CD44, Notch-1, and Notch-3 expression, and siRNA knockdown of Sdc-1 results in a weaker CSC phenotype and reduced expression of Notch-1-4 and Hey1 in inflammatory breast cancer cells (Ibrahim et al., 2017). Our data are in line with these findings, demonstrating that altered HS structure is linked to the CSC phenotype as well as altered expression of syndecans and notch constituents. While our GSI inhibitor studies demonstrate that the notch pathway has a regulatory impact on syndecan expression, our Sdc siRNA data reveal context-dependent effects. Knockdown of Sdc-4 largely affected basal and HS-sulfotransferase dependent HPSE expression, whereas Sdc-1 knockdown affected HPSE, Sdc-4 and DLL1. The underlying mechanisms are apparently complex and require further study. Obvious mechanisms include altered receptor tyrosine kinase signaling conform with the coreceptor concept of HSPGs, as demonstrated for the MAPK pathway in HS2ST1 and HS3ST2 overexpressing cells (Vijaya Kumar et al., 2014, 2020), and altered signaling via the Wnt pathway, as exemplified by altered expression of the Wnt-dependent transcription factor TCF4 for both sulfotransferases, and by the Sdc-1 and Wnt-dependent modulation of a colon cancer stem cell phenotype (Katakam et al., 2020b). Our finding of a upregulated expression of the Wnt receptor FZD7 in HS sulfotransferase overexpressing MDA-MB-231 cells may be mechanistically relevant, as this receptor acts along with Sdc-4 during foregut progenitor development (Zhang et al., 2016). Moreover, altered HS sulfation patterns, including upregulation of 2-O- and 6-O-sulfation, are linked to myoblast cell fate and FGF2 signaling (Ghadiali et al., 2017). However, more complex regulatory mechanisms may occur at the level of cell surface availability of signaling receptors and co-receptors. For example, both the shedding of Sdc-1 and activation of notch can be mediated by gamma-secretase (Pasqualon et al., 2015), and Sdc-1 shedding is regulated by HPSE (Rangarajan et al., 2020), which is expressed in a HS-sulfotransferase-dependent manner according to our study. Finally, HS2ST1-modified Sdc-1 was shown to prevent cellular senescence through the regulation of FGFR1 endocytosis (Kang et al., 2020), and similar mechanisms could play a role in the HS2ST1-dependent CSC phenotype. With respect to HS3ST2, our observation of an impact on the CSC phenotype are in line with studies that showed an important function of HS 3-O-sulfation in the differentiation of murine embryonic stem cells, as demonstrated by upregulation of 3-O-sulfated HS structures during critical stages of differentiation, and by functional knockdown studies on another 3-O-Sulfotransferase, 3OST-5 (Hirano et al., 2013). Along with previous reports on a potential role of 3-O-Sulfation in notch signaling in the fruit fly (Kamimura et al., 2004), our data extend this concept to the field of CSC research. As an interesting finding, we have observed upregulation of the HS editing enzyme SULF1 in both HS3ST2 and HS2ST1 overexpressing MDA-MB-231 cells. While this observation (along with upregulation of HPSE) may be a cellular attempt to compensate for the alterations in HS structure exerted by sulfotransferase dysregulation, it may be relevant in the context of stem cell function as well: For example, Sulf1 is

required for the termination of Drosophila intestinal stem cell division during regeneration (Takemura and Nakato, 2017), and regulates Wnt signaling in the context of myoblast fusion (Tran et al., 2012).

Apart from notch and Wnt signaling, our study has revealed an impact on the expression of EMT markers. While we previously demonstrated upregulation of *E*-cadherin protein in HS2ST1 and HS3ST2 overexpressing MDA-MB-231 and MCF-7 cells (Vijaya Kumar et al., 2014, 2020), the demonstration of downregulated mesenchymal factors is a new finding of this study. Snail1 and Snail2 are implicated in EMT via the upregulation of mesenchymal markers such as vimentin and suppression of epithelial markers such as *E*-cadherin. The link between EMT and the CSC phenotype may serve to explain differences in the impact of HS2ST1 and HS3ST2 on the different model cell lines of this study, as MCF-7 cells show an epithelial phenotype, whereas MDA-MB-231 cells have mesenchymal properties. Notably, mesenchymal ($CD44^+/CD24^-$) and epithelial ($ALDH^+$) CSCs are two distinct populations with different functionalities (Liu et al., 2014). Overexpression of HS2ST1 and HS3ST2 decreased the stemness-associated $CD44^+/CD24^-$ phenotype only in the MDA-MB-231 cell line. CD44 is associated with a mesenchymal phenotype, while CD24 is associated with an epithelial phenotype in breast cancer (Jaggupilli and Elkord, 2012). From a phenotypic point of view, these changes may mean a change in the epithelial or mesenchymal phenotype of these cells, possibly leading to the acquisition of a CSC phenotype as well. In MDA-MB-231 cells a decrease in the $CD44^+/CD24^-$ phenotype could be transitioning to an epithelial-like state, which is corroborated by a greater ALDH1 activity. In MCF-7 cells, there is less activity of ALDH1 upon HS2ST1 overexpression, which could possibly lead to a mesenchymal-like phenotype (see Ibrahim et al., 2013, for discussion). Considering the analysis of CD44, CD24, and ALDH, it seems that overexpression of HS3ST2 triggered antagonistic results compared to those obtained by HS2ST1 overexpression in both MDA-MB-231 and MCF-7 cells. We can only speculate that the HS pattern generated by HS3ST2 overexpression may be capable of activating or inactivating ligands that are not affected in the same manner by HS2ST1-modified HS, and vice versa. Famous examples are specific structural requirements for HS interactions, such as the antithrombin binding motif of the FGF2 binding sequence (Karamanos et al., 2018). For example, we have demonstrated that HS2ST1 upregulation in our cell lines results in reduced surface binding of FGF2 (Vijaya Kumar et al., 2020). The differential regulation of distinct components of the Wnt and notch signaling pathway in our cells supports this view (**Table 1**). Furthermore, context-dependent effects of HS in different cell types can be explained by the fact that not all ligands and receptors that are influenced by HS are expressed by all cells. For example, Wnt1 was upregulated in HS3ST2 overexpressing MDA-MB-231 cells, while this factor was not expressed in MCF-7 cells and could therefore not be affected by this HS modification.

Regarding our functional readouts, the origin of our cells (epithelial vs. mesenchymal) may have influenced the impact of HS-dependent changes in EMT markers, resulting in the formation of smaller and more compact aggregates in the case of sulfotransferase overexpressing MDA-MB-231 cells, which may have shifted toward a more epithelial-like phenotype, as discussed previously (**Figure 2B**). Some caveats are associated with our research communication. Several findings of our study rely on mRNA expression data and require further validation at the protein and functional level. While we could, e.g., confirm HS-sulfotransferase-dependent upregulation of Notch-3 in both cell lines, and of Hes-1 in HS3ST2-expressing MDA-MB-231 cells, other factors were either less consistently regulated at the mRNA and protein level, or have not been confirmed, yet. In addition, not all factors within a given pathway were consistently regulated in the same direction, and some factors were only moderately altered, requiring more study. Our GSI inhibitor and siRNA studies demonstrate that the signaling pathways and compounds involved are highly interdependent and subject to potential compensatory mechanisms. While this observation impedes a straightforward and simple mechanistic explanation, it reflects the complexity of HS-dependent processes, which affect signaling via numerous pathways, and additional cellular functions beyond classical signaling, such as endocytosis (affecting receptor downregulation), proteolysis and cell-matrix interactions (Karamanos et al., 2018). Finally, while sulfotransferase overexpression promoted functional stem cell properties, it is likely that not only the CSC population, but also the overall tumor cell population was affected by alterations in HS. Possibly a selected analysis of sorted CSCs could lead to an enhancement of the observed changes, as previously demonstrated for the impact of Sdc-1 knockdown on the colon CSC phenotype (Katakam et al., 2020b).

Taken together, HS2ST1 and HS3ST2 partially had a differential impact on the CSC phenotype of representative triple-negative and hormone-receptor positive breast cancer cell lines. This finding may reflect differences in HS-dependent signaling pathways, as previously shown for the invasion phenotype of HS3ST2 overexpressing cells (Vijaya Kumar et al., 2014). Our results furthermore show that the overexpression of HS2ST1 and HS3ST2 significantly alters several CSC-related characteristics in breast cancer cells in general, which is worthy of future evaluation in more complex *in vivo* systems. Finally, our data open a perspective for manipulating the CSC phenotype with drugs modulating HS either in a general way, or in a sequence-specific manner (Zubkova et al., 2018; Vitale et al., 2019; Espinoza-Sánchez and Götte, 2020).

DATA AVAILABILITY STATEMENT

All datasets generated for this study are included in the article/**Supplementary Material**.

AUTHOR CONTRIBUTIONS

FT, AV, and SK performed the major part of the experiments and analyzed the data. CC, PP, and RR performed the mammosphere assays, analyzed the data, and provided the expertise on CSC

analysis. MoG performed the siRNA experiments and qPCRs. FT drafted the figures and wrote the draft of the manuscript. MaG, MP, and BG supervised the data. LK provided the general support, co-supervised the MoG, and was involved in the data interpretation. MaG conceived and coordinated the study and generated the figures and tables of the revised manuscript. All authors revised and approved the final draft.

FUNDING

This work was supported by Open Access Publishing Fonds of the Westfälische Wilhelms-Universität Münster (WWU), Deutsche Forschungsgemeinschaft DFG IRTG "Molecular and Cellular GlycoSciences": Grant number: GRK 1549 (to MaG, SK, and AV), EU-H2020-MSCA-RISE grant GLYCANC #645756 (to MaG and MP), Conselho Nacional de Desenvolvimento Científico e Tecnológico (Grants 290231/2017-5–SWE to FT and 302171/2018-8-PQ to MP), Fundação de Amparo à Pesquisa do Estado do Rio de Janeiro (FAPERJ) to MP, CNR-MIUR Flagship Epigen and Interomics, the Fondo per gli Investimenti della Ricerca di Base of the Italian Ministry of Education, and the University and Research FIRB MIUR project Newton RBAP11BYNP_003 (to RR). Funding for the CC fellowship was endowed by Tiziano Oggionni, Walkyria Ferri and by the Academia Servorum Scientiae.

ACKNOWLEDGMENTS

The authors would like to thank Birgit Pers and Annette van Dülmen for technical assistance, and Ileana Zucchi for expertise and critical discussions.

SUPPLEMENTARY MATERIAL

The Supplementary Material for this article can be found online at: https://www.frontiersin.org/articles/10.3389/fcell.2020.559554/full#supplementary-material

REFERENCES

Bonuccelli, G., Casimiro, M. C., Sotgia, F., Wang, C., Liu, M., Katiyar, S., et al. (2009).). Caveolin-1 (P132L), a Common Breast Cancer Mutation, Confers Mammary Cell Invasiveness and Defines a Novel Stem Cell/Metastasis-Associated Gene Signature. *Am. J. Pathol.* 174, 1650–1662. doi: 10.2353/ajpath.2009.080648

Chen, H.-F., Huang, C.-H., Liu, C.-J., Hung, J.-J., Hsu, C.-C., Teng, S.-C., et al. (2014). Twist1 induces endothelial differentiation of tumour cells through the Jagged1-KLF4 axis. *Nat. Commun.* 5, 1–13. doi: 10.1038/ncomms5697

Denys, A., and Allain, F. (2019)). *The Emerging Roles of Heparan Sulfate 3-O-Sulfotransferases in Cancer*. Available online at: https://www.frontiersin.org/articles/10.3389/fonc.2019.00507/full. (accessed July 11, 2019)

Djomehri, S. I., Burman, B., Gonzalez, M. E., Takayama, S., and Kleer, C. G. (2019). A reproducible scaffold-free 3D organoid model to study neoplastic progression in breast cancer. *J. Cell Commun. Signal.* 13, 129–143. doi: 10.1007/s12079-018-0498-7

Esko, J. D., and Selleck, S. B. (2002). Order Out of Chaos: Assembly of Ligand Binding Sites in Heparan Sulfate. *Annu. Rev. Biochem.* 71, 435–471. doi: 10.1146/annurev.biochem.71.110601.135458

Espinoza-Sánchez, N. A., and Götte, M. (2020). Role of cell surface proteoglycans in cancer immunotherapy. *Semin. Cancer Biol.* 62, 48–67. doi: 10.1016/j.semcancer.2019.07.012

Eun, K., Ham, S. W., and Kim, H. (2017). Cancer stem cell heterogeneity: origin and new perspectives on CSC targeting. *BMB Rep.* 50, 117–125. doi: 10.5483/BMBRep.2017.50.3.222

Ghadiali, R. S., Guimond, S. E., Turnbull, J. E., and Pisconti, A. (2017). Dynamic changes in heparan sulfate during muscle differentiation and ageing regulate myoblast cell fate and FGF2 signalling. *Matrix Biol.* 59, 54–68. doi: 10.1016/j.matbio.2016.07.007

Gulberti, S., Mao, X., Bui, C., and Fournel-Gigleux, S. (2020). The role of heparan sulfate maturation in cancer: A focus on the 3O-sulfation and the enigmatic 3O-sulfotransferases (HS3STs). *Semin Cancer Biol.* 62, 68–85. doi: 10.1016/j.semcancer.2019.10.009

Hellec, C., Delos, M., Carpentier, M., Denys, A., and Allain, F. (2018). The heparan sulfate 3-O-sulfotransferases (HS3ST) 2, 3B and 4 enhance proliferation and survival in breast cancer MDA-MB-231 cells. *PLoS One* 13:e0194676. doi: 10.1371/journal.pone.0194676

Hirano, K., Van Kuppevelt, T. H., and Nishihara, S. (2013). The transition of mouse pluripotent stem cells from the naïve to the primed state requires Fas signaling through 3-O sulfated heparan sulfate structures recognized by the HS4C3 antibody. *Biochem. Biophys. Res. Commun.* 430, 1175–1181. doi: 10.1016/j.bbrc.2012.12.005

Hovinga, K. E., Shimizu, F., Wang, R., Panagiotakos, G., Heijden, M. V. D., Moayedpardazi, H., et al. (2010). Inhibition of Notch Signaling in Glioblastoma Targets Cancer Stem Cells via an Endothelial Cell Intermediate. *Stem Cells* 28, 1019–1029. doi: 10.1002/stem.429

Ibrahim, S. A., Gadalla, R., El-Ghonaimy, E. A., Samir, O., Mohamed, H. T., Hassan, H., et al. (2017). Syndecan-1 is a novel molecular marker for triple negative inflammatory breast cancer and modulates the cancer stem cell phenotype via the IL-6/STAT3, Notch and EGFR signaling pathways. *Mol. Cancer* 16:57. doi: 10.1186/s12943-017-0621-z

Ibrahim, S. A., Hassan, H., Vilardo, L., Kumar, S. K., Kumar, A. V., Kelsch, R., et al. (2013). Syndecan-1 (CD138) modulates triple-negative breast cancer stem cell properties via regulation of LRP-6 and IL-6-mediated STAT3 signaling. *PLoS One* 8:e85737. doi: 10.1371/journal.pone.0085737

Ibrahim, S. A., Yip, G. W., Stock, C., Pan, J.-W., Neubauer, C., Poeter, M., et al. (2012). Targeting of syndecan-1 by microRNA miR-10b promotes breast cancer cell motility and invasiveness via a Rho-GTPase- and E-cadherin-dependent mechanism. *Int. J. Cancer* 131, E884–E896. doi: 10.1002/ijc.27629

Jaggupilli, A., and Elkord, E. (2012). Significance of CD44 and CD24 as cancer stem cell markers: an enduring ambiguity. *Clin. Dev. Immunol.* 2012:708036. doi: 10.1155/2012/708036

Kamimura, K., Rhodes, J. M., Ueda, R., McNeely, M., Shukla, D., Kimata, K., et al. (2004). Regulation of Notch signaling by Drosophila heparan sulfate 3-O sulfotransferase. *J. Cell Biol.* 166, 1069–1079. doi: 10.1083/jcb.200403077

Kang, D., Jung, S. H., Lee, G. H., Lee, S., Park, H. J., Ko, Y. G., et al. (2020). Sulfated syndecan 1 is critical to preventing cellular senescence by modulating fibroblast growth factor receptor endocytosis. *FASEB J.* 2020:32530114. doi: 10.1096/fj.201902714R

Karamanos, N. K., Piperigkou, Z., Theocharis, A. D., Watanabe, H., Franchi, M., Baud, S., et al. (2018). Proteoglycan Chemical Diversity Drives Multifunctional Cell Regulation and Therapeutics. *Chem. Rev.* 118, 9152–9232. doi: 10.1021/acs.chemrev.8b00354

Katakam, S. K., Pelucchi, P., Cocola, C., Reinbold, R., Vlodavsky, I., Greve, B., et al. (2020a). Syndecan-1-Dependent Regulation of Heparanase Affects Invasiveness, Stem Cell Properties, and Therapeutic Resistance of Caco2 Colon Cancer Cells. *Front. Oncol.* 10:774. doi: 10.3389/fonc.2020.00774

Katakam, S. K., Tria, V., Sim, W. C., Yip, G. W., Molgora, S., Karnavas, T., et al. (2020b). The heparan sulfate proteoglycan syndecan-1 regulates colon cancer stem cell function via a focal adhesion kinase-Wnt signaling axis. *FEBS J.* 2020:32367652. doi: 10.1111/febs.15356

Kreuger, J., Salmivirta, M., Sturiale, L., Giménez-Gallego, G., and Lindahl, U. (2001). Sequence Analysis of Heparan Sulfate Epitopes with Graded Affinities for Fibroblast Growth Factors 1 and 2. *J. Biol. Chem.* 276, 30744–30752. doi: 10.1074/jbc.M102628200

Li, J.-P., and Kusche-Gullberg, M. (2016). Heparan Sulfate: Biosynthesis, Structure, and Function. *Int. Rev. Cell Mol. Biol.* 325, 215–273. doi: 10.1016/bs.ircmb.2016.02.009

Li, W., Ma, H., Zhang, J., Zhu, L., Wang, C., and Yang, Y. (2017). Unraveling the roles of CD44/CD24 and ALDH1 as cancer stem cell markers in tumorigenesis and metastasis. *Sci. Rep.* 7:13856. doi: 10.1038/s41598-017-1436414362

Liu, S., Cong, Y., Wang, D., Sun, Y., Deng, L., Liu, Y., et al. (2014). Breast cancer stem cells transition between epithelial and mesenchymal states reflective of their normal counterparts. *Stem Cell Rep.* 2, 78–91. doi: 10.1016/j.stemcr.2013.11.009

Merry, C. L. R., and Wilson, V. A. (2002). Role of heparan sulfate-2-O-sulfotransferase in the mouse. *Biochim. Biophys. Acta* 1573, 319–327. doi: 10.1016/s0304-4165(02)00399-9

Morla, S. (2019). Glycosaminoglycans and Glycosaminoglycan Mimetics in Cancer and Inflammation. *Int. J. Mol. Sci.* 20:1963. doi: 10.3390/ijms20081963

Nikolova, V., Koo, C.-Y., Ibrahim, S. A., Wang, Z., Spillmann, D., Dreier, R., et al. (2009). Differential roles for membrane-bound and soluble syndecan-1 (CD138) in breast cancer progression. *Carcinogenesis* 30, 397–407. doi: 10.1093/carcin/bgp001

Park, S. Y., Lee, H. E., Li, H., Shipitsin, M., Gelman, R., and Polyak, K. (2010). Heterogeneity for stem cell-related markers according to tumor subtype and histologic stage in breast cancer. *Clin. Cancer Res. Off. J. Am. Assoc. Cancer Res.* 16, 876–887. doi: 10.1158/1078-0432.CCR-091532

Pasqualon, T., Pruessmeyer, J., Jankowski, V., Babendreyer, A., Groth, E., Schumacher, J., et al. (2015). A cytoplasmic C-terminal fragment of Syndecan-1 is generated by sequential proteolysis and antagonizes Syndecan-1 dependent lung tumor cell migration. *Oncotarget* 6, 31295–31312. doi: 10.18632/oncotarget.5174

Ramirez Williams, L., Brüggemann, K., Hubert, M., Achmad, N., Kiesel, L., Schäfer, S. D., et al. (2019). γ-Secretase inhibition affects viability, apoptosis, and the stem cell phenotype of endometriotic cells. *Acta Obstet. Gynecol. Scand.* 98, 1565–1574. doi: 10.1111/aogs.13707

Rangarajan, S., Richter, J. R., Richter, R. P., Bandari, S. K., Tripathi, K., Vlodavsky, I., et al. (2020). Heparanase-enhanced Shedding of Syndecan-1 and Its Role in Driving Disease Pathogenesis and Progression. *J. Histochem. Cytochem.* 6:22155420937087. doi: 10.1369/0022155420937087

Saeg, F., and Anbalagan, M. (2018). Breast cancer stem cells and the challenges of eradication: a review of novel therapies. *Stem Cell Investig.* 5:39. doi: 10.21037/sci.2018.10.05

Takebe, N., Miele, L., Harris, P. J., Jeong, W., Bando, H., Kahn, M., et al. (2015). Targeting Notch, Hedgehog, and Wnt pathways in cancer stem cells: clinical update. *Nat. Rev. Clin. Oncol.* 12, 445–464. doi: 10.1038/nrclinonc.2015.61

Takemura, M., and Nakato, H. (2017). Drosophila Sulf1 is required for the termination of intestinal stem cell division during regeneration. *J. Cell Sci.* 130, 332–343. doi: 10.1242/jcs.195305

Tran, T. H., Shi, X., Zaia, J., and Ai, X. (2012). Heparan sulfate 6-O-endosulfatases (Sulfs) coordinate the Wnt signaling pathways to regulate myoblast fusion during skeletal muscle regeneration. *J. Biol. Chem.* 287, 32651–32664. doi: 10.1074/jbc.m112.353243

Vijaya Kumar, A., Brézillon, S., Untereiner, V., Sockalingum, G. D., Kumar Katakam, S., Mohamed, H. T., et al. (2020). HS2ST1-dependent signaling pathways determine breast cancer cell viability, matrix interactions, and invasive behavior. *Cancer Sci.* 2020:32573871. doi: 10.1111/cas.14539

Vijaya Kumar, A., Salem Gassar, E., Spillmann, D., Stock, C., Sen, Y.-P., Zhang, T., et al. (2014). HS3ST2 modulates breast cancer cell invasiveness via MAP kinase- and Tcf4 (Tcf7l2)-dependent regulation of protease and cadherin expression. *Int. J. Cancer* 135, 2579–2592. doi: 10.1002/ijc.28921

Vitale, D., Katakam, S. K., Greve, B., Jang, B., Oh, E.-S., Alaniz, L., et al. (2019). Proteoglycans and glycosaminoglycans as regulators of cancer stem cell function and therapeutic resistance. *FEBS J.* 286, 2870–2882. doi: 10.1111/febs.14967

Witt, R. M., Hecht, M.-L., Pazyra-Murphy, M. F., Cohen, S. M., Noti, C., Kuppevelt, T. H., et al. (2013). Heparan Sulfate Proteoglycans Containing a Glypican 5 Core and 2-O-Sulfo-iduronic Acid Function as Sonic Hedgehog Co-receptors to Promote Proliferation. *J. Biol. Chem.* 288, 26275–26288. doi: 10.1074/jbc.M112.438937

Yang, F., Xu, J., Tang, L., and Guan, X. (2017). Breast cancer stem cell: the roles and therapeutic implications. *Cell Mol. Life. Sci.* 74, 951–966. doi: 10.1007/s00018-016-2334-7

Zhang, L. (2010). Glycosaminoglycan (GAG) biosynthesis and GAG-binding proteins. *Prog. Mol. Biol. Transl. Sci.* 93, 1–17. doi: 10.1016/S1877-1173(10)9300193009

Zhang, Y., and Weinberg, R. A. (2018). Epithelial-to-mesenchymal transition in cancer: complexity and opportunities. *Front. Med.* 12:361–373. doi: 10.1007/s11684-018-0656-6

Zhang, Z., Rankin, S. A., and Zorn, A. M. (2016). Syndecan4 coordinates Wnt/JNK and BMP signaling to regulate foregut progenitor development. *Dev. Biol.* 416, 187–199. doi: 10.1016/j.ydbio.2016.05.025

Zhao, S., and Wang, Z. (2020). Changes in heparan sulfate sulfotransferases and cell-surface heparan sulfate during SKM-1 cells granulocytic differentiation and A549 cells epithelial-mesenchymal transition. *Glycoconj. J.* 37, 151–164. doi: 10.1007/s10719-019-099039900

Zubkova, O. V., Ahmed, Y. A., Guimond, S. E., Noble, S. L., Miller, J. H., Alfred Smith, R. A., et al. (2018). Dendrimer Heparan Sulfate Glycomimetics: Potent Heparanase Inhibitors for Anticancer Therapy. *ACS Chem. Biol.* 13, 3236–3242. doi: 10.1021/acschembio.8b00909

Conflict of Interest: The authors declare that the research was conducted in the absence of any commercial or financial relationships that could be construed as a potential conflict of interest.

frontiers in Cell and Developmental Biology

MINI REVIEW
published: 09 October 2020
doi: 10.3389/fcell.2020.569454

Three-Dimensional Models as a New Frontier for Studying the Role of Proteoglycans in the Normal and Malignant Breast Microenvironment

Julien Clegg[1], Maria K. Koch[1], Erik W. Thompson[1,2,3], Larisa M. Haupt[1,2,4], Priyakshi Kalita-de Croft[5†] and Laura J. Bray[1,3,6†]*

[1] Institute of Health and Biomedical Innovation, Queensland University of Technology, Kelvin Grove, QLD, Australia, [2] School of Biomedical Sciences, Faculty of Health, Queensland University of Technology, Brisbane, QLD, Australia, [3] Translational Research Institute, Woolloongabba, QLD, Australia, [4] Centre for Genomics and Personalized Health, Genomics Research Centre, School of Biomedical Sciences, Institute of Health and Biomedical Innovation, Queensland University of Technology, Kelvin Grove, QLD, Australia, [5] UQ Centre for Clinical Research, Faculty of Medicine, University of Queensland, Herston, QLD, Australia, [6] Faculty of Science and Engineering, School of Mechanical, Medical and Process Engineering, Queensland University of Technology, Brisbane, QLD, Australia

OPEN ACCESS

Edited by:
José Lozano, University of Malaga, Spain

Reviewed by:
Achilleas D. Theocharis, University of Patras, Greece
Qi Cao, University of Maryland, United States

***Correspondence:**
Laura J. Bray
laura.bray@qut.edu.au

[†] These authors share senior authorship

Specialty section:
This article was submitted to Signaling, a section of the journal Frontiers in Cell and Developmental Biology

Received: *04 June 2020*
Accepted: *15 September 2020*
Published: *09 October 2020*

Citation:
Clegg J, Koch MK, Thompson EW, Haupt LM, Kalita-de Croft P and Bray LJ (2020) Three-Dimensional Models as a New Frontier for Studying the Role of Proteoglycans in the Normal and Malignant Breast Microenvironment. Front. Cell Dev. Biol. 8:569454. doi: 10.3389/fcell.2020.569454

The extracellular matrix (ECM) provides cues to direct mammogenesis, tumourigenesis and metastatic processes. Over the past several decades, two-dimensional (2D) culture models have been invaluable in furthering our understanding of the tumor microenvironment (TME), however, they still do not accurately emulate the associated biological complexities. In contrast, three-dimensional (3D) culture models provide a more physiologically relevant platform to study relevant physicochemical signals, stromal-epithelial cell interactions, vascular and immune components, and cell-ECM interactions in the human breast microenvironment. A common thread that may weave these multiple interactions are the proteoglycans (PGs), a prominent family of molecules in breast tissue. This review will discuss how these PGs contribute to the breast cancer TME and provide a summary of the traditional and emerging technologies that have been utilized to better understand the role of PGs during malignant transformation. Furthermore, this review will emphasize the differences that PGs exhibit between normal tissues and tumor ECM, providing a rationale for the investigation of underexplored roles of PGs in breast cancer progression using state-of-the-art 3D culture models.

Keywords: breast cancer, proteoglycans (PGs), extracellular matrix (ECM), 3D models, tumor microenvironment (TME)

INTRODUCTION

Proteoglycans (PGs) are functional proteins that constitute major signaling and structural components of the breast microenvironment, playing a role in morphogenesis, vascularisation, tumor progression and metastasis. During breast cancer development and growth, PG expression undergoes substantial changes within both the tumor cells and the tumor microenvironment (TME). These changes result in the alteration of cell proliferation, survival adhesion and migration, making PGs a potential target for breast cancer treatments. While PGs have been studied for some decades, the models of choice to study their function and contributions toward drug development

has varied. In this review, we present an overview of PGs in the human breast microenvironment along with state-of-the-art PG-focussed investigations in mammary development and breast cancer, and the emerging role of three-dimensional (3D) culture methods in modeling PGs, followed by a discussion on novel bioengineered scaffold-based approaches for future studies. We critically discuss the benefits and limitations of current models and present emerging concepts of novel cancer model systems that can mimic the role of PGs in human breast biology and its malignant transformation.

BREAST CANCER

Globally, breast cancer is the most frequent cancer in women after nonmelanoma skin cancer. The worldwide incidence of newly diagnosed breast cancer in 2018 was estimated to be 2.1 million women, which approximates to one new case diagnosed every 18 s, and 626,679 women with breast cancer succumbing to the disease in 2018 (Bray et al., 2018). As a disease, breast cancer is molecularly heterogeneous. The seminal study by Perou and Sorlie defined an intrinsic classification of four subtypes of breast cancer (Perou et al., 2000): luminal A, luminal B, basal-like and human epidermal growth factor receptor 2 (HER2). This study initiated a shift toward more biology-based approaches in the clinical management of breast cancer. This also led to further molecular subtyping in numerous studies to provide clinically relevant subgroups (Lehmann et al., 2011; Cancer Genome Atlas Network, 2012; Nik-Zainal et al., 2016; Jackson et al., 2020).

Due to this heterogeneity, breast cancer treatment paradigms have evolved over the last decade. Despite this progress, some characteristics such as the impact of the regional tumor burden or size and patterns of metastases are shared amongst breast cancers and influence therapy. Treatment decisions are generally impacted by the clinical features (stage and grade), histological biomarkers and molecular features of the cancer. In the case of non-metastatic tumors, the main goal is to eradicate the tumor from the breast and regional lymph nodes, thus preventing metastatic spread. This includes surgical resection and sampling and/or removal of axillary lymph nodes. Furthermore, postoperative radiation is also commonly used. Systemic therapy may be performed preoperatively (neoadjuvant), postoperatively (adjuvant), or both, and it is mainly guided by breast cancer subtype, stage and grade. In clinical practice, three biomarkers are used to distinguish the subtypes and guide targeted therapies; estrogen receptor (ER), progesterone receptor (PR), and HER2. Tumors expressing ER and PR are called hormone receptor-positive, whereas tumors that do not express ER, PR, and HER2 are termed triple-negative breast cancers (TNBCs). Hormone-receptor positive breast cancers usually receive endocrine therapy such as tamoxifen or aromatase inhibitors, while patients with more advanced disease or those refractory to endocrine therapy also receive chemotherapy (Burstein et al., 2010). Tumors expressing HER2 receptor receive anti-HER2 monoclonal antibodies and/or HER2-targeted agents, along with chemotherapy (Lehmann et al., 2011). Chemotherapy remains the mainstay treatment for TNBCs, however, poly ADP-ribose polymerase inhibitors (PARPi) have emerged as a promising therapy that exploit synthetic lethality associated with defective DNA damage repair mechanisms in cancer (Dulaney et al., 2017).

PROTEOGLYCANS AND THEIR ROLE IN HUMAN MAMMARY TISSUE

In breast tissue, normal and malignant epithelial cells interact with their surrounding microenvironment, determining both cell fate and disease progression. The microenvironment contains various cell types, including endothelial cells, endothelial precursors, pericytes, adipocytes, fibroblasts, and immune cell populations. These distinct cell types are embedded in a biofunctional extracellular matrix (ECM), which is composed of numerous molecules including PGs, collagen, laminin, fibronectin, and their associated proteases (Naba et al., 2012). PGs, which contain a core protein to which different numbers and types of glycosaminoglycan (GAG) side chains are attached, are a major ECM component and are additionally expressed on cell surfaces. The cellular location and types of GAG side chains built upon a core protein are used to classify PGs into different groups (Ruoslahti, 1988). They vary extensively in structure, localisation and functionality (Pearson et al., 1983). Based upon their localization, PGs fall into four families (Iozzo and Schaefer, 2015) (intracellular, cell-surface, pericellular, and extracellular), with the functionality of PGs occurring mainly through their GAG content. Serglycin is the sole PG characterized to be intracellular in breast tissue (Scully et al., 2012) and is widely investigated in cancer (Korpetinou et al., 2014). Pericellular and cell surface PGs include decorin, versican, glypican, and perlecan as well as collagens XVIII and XV. The extracellular PGs comprise hyaluronan-binding hyalectans, small-leucine rich PGs (SLRPs) and calcium-binding heparan sulfate PGs (HSPGs) (Nikitovic et al., 2018). This stratification is extremely useful for discussing the function of these PGs from the cellular biology perspective and it has been reviewed extensively by Nikitovic and colleagues (Nikitovic et al., 2018). From a translational and clinical perspective, PGs localized to different compartments may contribute to the same function therefore, this review will mostly focus on the subgroups defined by GAG type; the implicated functionally interacting parts of PGs. We will describe how uniquely each of these contribute to normal function and pathophysiological features at different stages of the development of the mammary gland as well its malignant transformation. These GAGs include; heparan sulfate (HS), chondroitin sulfate (CS), dermatan sulfate (DS), keratan sulfate (KS), and hyaluronic acid (HA).

MODELING THE FUNCTION OF PGS IN HEALTHY MAMMARY TISSUE

Attaining an understanding of the role of PGs in mammary development and homeostatic processes is central to

understanding their significance in the pathology of breast cancer. Tissue development and remodeling are seen throughout life, where the fetus undergoes initial development to hormonal directed tissue remodeling through adolescence, adulthood and the periods prior, during and following pregnancy, enabled by PGs found within the mammary ECM and cell surfaces (Baker et al., 2017; **Figure 1**). During fetal development, transmembrane matrix members of the syndecan PG family (syndecans 1–4), synergistically interact with integrins to aid in embryonic angiogenesis (Morgan et al., 2007). Syndecans, along with integrins, work with the glycoprotein dystroglycan to adhere to the cytoskeleton and can influence cell fate and behavior, along with other cell-ECM and cell-cell interactions (Barresi and Campbell, 2006; Morgan et al., 2007; Garner et al., 2011). Moreover, a study by Liu et al. (2003) found that syndecan-1 greatly influences tertiary ductal branching in mice, further highlighting the importance of the syndecan PG family in mammary development (Liu et al., 2003).

There is a dynamic and ever-evolving microenvironmental remodeling that occurs throughout adolescence and pregnancy, such as ductal morphogenesis driven by cell-ECM interactions with the basement membrane (Hinck and Silberstein, 2005). Epithelial proliferation and migration contribute to the development of the internal ductal system, facilitated by estrogen and local growth factors that interact with epithelial and stromal cells (Lu et al., 2008). Perlecan, a HSPG found largely in the basement membrane, captures anionic growth factors such as stromal fibroblast-growth factor 10 (FGF10), delivering it to the epithelium for growth (Patel et al., 2007). The complex interplay between such HSPG-bound growth factors is modulated by the enzyme heparanase, which cleaves HS side chains and liberates the free growth factors (Chhabra and Ferro, 2018).

Another feature during breast development is the migration and maturation of adipocytes, which comprise a large part of the mammary stroma and are involved in energy delivery for lactation (Gouon-Evans and Pollard, 2002; Alvarenga et al., 2019). Fat deposits in the mammary microenvironment, and further, their maturation and adipocyte growth play an important role in supporting homeostasis and later remodeling and milk production during and following pregnancy (Muschler and Streuli, 2010). It has been reported by Wilsie et al. (2005) that adipocyte growth is heavily dependent upon cell membrane HSPGs, along with the onset of estrogen production by pre-adipocytes (Wilsie et al., 2005). During pregnancy, hormone-driven changes are characterized by an increase in epithelial density, ductal growth and a complexifying of the regional vascularization (Macias and Hinck, 2012). This is facilitated by PGs that bind with growth factors, activating cellular pathways to upregulate cell growth and proliferation (**Figure 1**). As an example, the HSPG syndecan-4 has been postulated to have a functional role in lactogenesis, including lobuloalveolar development as seen by its involvement in proliferation, migration and angiogenesis (Moon et al., 2005; Bishop et al., 2007; Morrison and Cutler, 2010). The HS GAGs bind with many pro-angiogenic factors that include; transforming growth factor-beta (TGF-β), hepatocyte growth factor, heparin-binding EGF, and FGFs-1, 2, 4, 7, and 10. This coordinated network directly facilitates the controlled proliferation of the endothelium and migration of cells for angiogenesis. A lack of HS GAGs leads to a failure of lobuloalveolar development, resulting in a lack of milk production (Segev et al., 2004; Crawford et al., 2010).

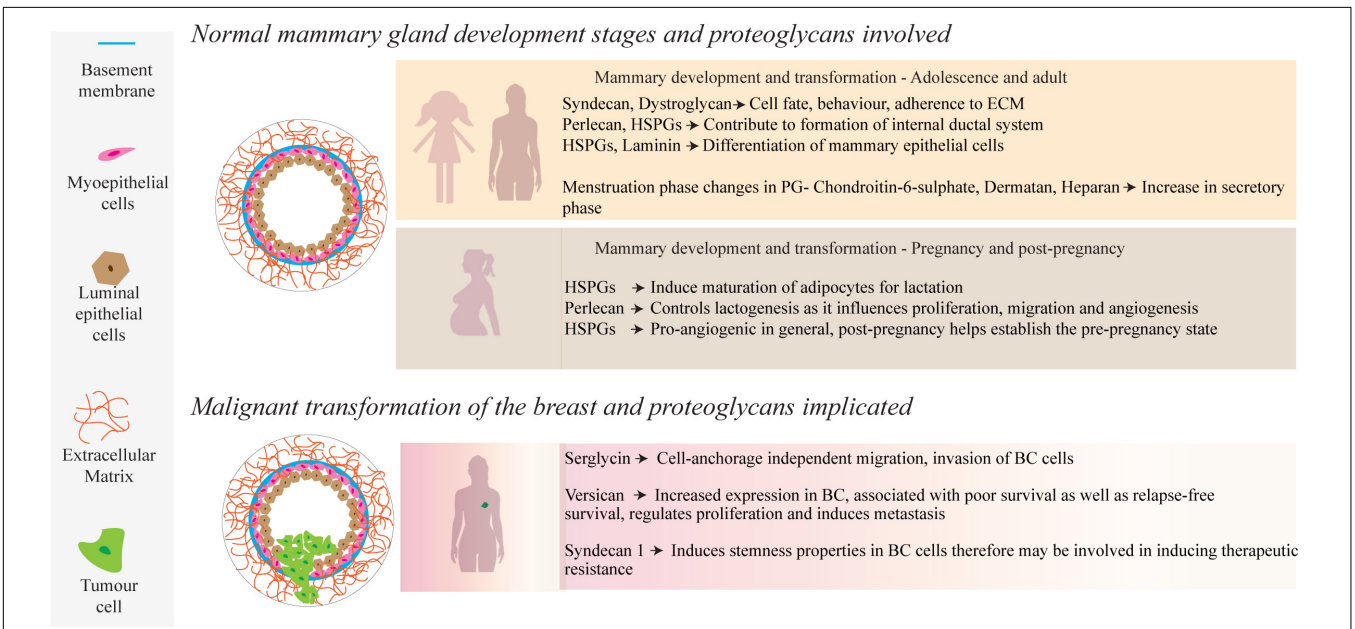

FIGURE 1 | During normal mammary development, a number of PGs, such as those containing HS side-chains, interact with growth factors, ECM molecules and cell receptors to mediate physiological and cellular remodeling. Several of these PGs also play a role in mammary tumor progression through up or down regulation of their local concentrations.

Apoptotic events to re-establish the pre-pregnancy adult state of the mammary microenvironment are also directly regulated by HSPGs through interactions with Fas ligand and tumor necrosis factor-related apoptosis-inducing ligand (TRAIL), among others (Liu et al., 2004; Wu et al., 2012).

Ensuring that the right model is used for the research question is imperative in all investigations (**Figure 2**). 2D systems, in conjunction with animal studies (Pumphrey et al., 2002; Liu et al., 2003; Kelly et al., 2005; Bischof et al., 2013) and biopsy material, have facilitated our current understanding of the biosynthesis of PGs, their biochemistry including interactions with other biological substances and their functions within the development of normal and pathological mammary microenvironments, as extensively reviewed by Theocharis (Theocharis et al., 2015). In this review, we chose to focus on the details of studies using patient biopsies or cell suspensions in a 3D context. Histological studies of human specimens have played a pivotal role in the elucidation of healthy mammary development, and the life-long remodeling that occurs. The study conducted by Ferguson et al. (1992) investigated the changes of ECM molecules during the menstrual cycle in human females (Ferguson et al., 1992). It was discovered that over the 4-week menstrual cycle, ECM molecules such as heparan and chondroitin sulfate PGs, changed in their concentration and localization. Understanding the anatomical and molecular changes of the healthy mammary microenvironment also allows for a better understanding of the contribution of PGs to the development of breast TMEs. For example, biopsy studies by De Lima et al. (2012) and Ricciardelli et al. (2002) compared normal and cancerous mammary tissue and discovered independently, that the levels of PGs in the healthy tissue were widely different when compared with pathological tissue (Ricciardelli et al., 2002; De Lima et al., 2012), including an upregulation of heparan and dermatan sulfate PGs. Moreover, a recent study using breast tissue explants cultured on a gelatin sponge investigated the role of PGs in mammographic density (Huang et al., 2020). Application of a syndecan-1 inhibitory peptide, synstatin, to denser breast tissue reduced the amount of fibrillar collagen and overall mammographic density. However, histological studies and 2D models/cultures present a number of issues, predominantly in their inability to directly observe the mechanistic pathways that ultimately drive normal development and homeostatic processes (**Figure 2**). Future studies could take advantage of more sophisticated 3D platforms, explored in the following sections.

MODELING THE FUNCTION OF PROTEOGLYCANS IN THE BREAST TME

Breast cancer is a dynamic heterogeneous pathophysiological disease and while we have formulated comprehensive mechanisms of development underlining the disease, we lack an equally comprehensive understanding of how the ECM contributes to the known cancer hallmarks and how we can leverage this understanding into developing novel treatments. The TME remodels the associated stroma, resulting in an increased content of various PGs (**Figure 1**). Serglycin promotes anchorage-independent cell migration, growth and invasion of breast cancer cells and is associated with aggressive properties of cancer (Korpetinou et al., 2013). In contrast, lumican possesses anti-migratory and anti-invasive properties as demonstrated in aggressive breast cancer cell lines (Karamanou et al., 2017). Studies by Dawoody Nejad et al. (2017) and Recktenwald et al. (2012) have investigated decorin and biglycan, respectively, using cell culture dishes (Recktenwald et al., 2012; Dawoody Nejad et al., 2017). Dawoody found that decorin and fibromodulin overexpression downregulated NF-kB and TGF-β1, vital signaling complexes during epithelial-mesenchymal transitioning, in the metastatic 4T1 breast cancer cell line, which

	Pros	Cons
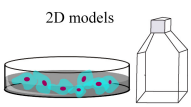 2D models	♦ Quick and simple model for experimentation ♦ Relatively cost-effective ♦ Allows studying fundamental interactions between PGs and tumours cells	♦ Unable to recapitulate complex TME interactions- »Tumour cell -ECM » Tumour cell-PG »Angiogenesis
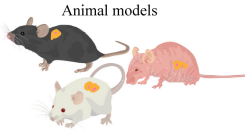 Animal models	♦ Physiologically intact model system »Intact immune system » Similar mammary microenvironment » Realistic nutrient delivery and waste removal systems »Potential PG-drug testing system	♦ High financial and ethical costs ♦ Low biochemical control ♦ Does not always mimic the human system accurately
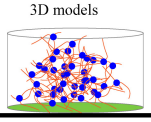 3D models	♦ Physiologically intact model system ♦ Cost-effective compared to animal models ♦ Easily and highly customisable ♦ More accurate nutrient and drug penetration	♦ No standardised established methods ♦ Lower reproducibility ♦ Slower throughput

FIGURE 2 | Culture models ultimately have an innate advantage over histological samples taken from breast cancer patients, as they provide a controlled but dynamic environment for experimentation over longer periods. However, each culture model system presents their own unique limitations, leading researchers to choose which system is best for their research or needing to use multiple culture systems.

may lead to an opportunity to prevent metastatic phenotype conversion in cancer cells. Recktenwald demonstrated that downregulation of biglycan led to the promotion of cell proliferation and migration in $HER2^+$ cell lines, suggesting that biglycan also has an inhibitory effect on tumor cells.

Overall, growing evidence indicates the importance of versican as a potential PG involved in mammary carcinogenesis. Versican is a large PG that is localized to the ECM and can be found in many tissue regions (Wight, 2002). It is one of the most widely researched PGs in cancer. and has been implicated within cancerous samples but not within their healthy control samples (Ricciardelli et al., 2002). Ricciardelli et al. (2002) investigated versican, using biopsy material from 58 node-negative patients and found that versican was detected in all samples from confirmed breast cancer patients. Additionally, the study showed that the relapse rate was lower in patients with lower versican levels in their biopsy specimens and increased in samples with higher versican levels.

These studies by Dawoody Nejad et al. (2017); Recktenwald et al. (2012), and Ricciardelli et al. (2002) provide examples of specific PGs but did not explore their mechanisms of action, nor their explicit interactions with cancerous cells. Histology-based assessments such as these could be considered as static assessments, while dynamic assessments using culture models allow for more extensive investigations and facilitate examination of a changing microenvironment. Versican also plays an essential role in the structural architecture of vascular walls, and is upregulated in breast cancer (Du et al., 2010), regulating tumor growth by promoting angiogenesis (Asano et al., 2017). Furthermore, it assists in regulating proliferation and inducing metastasis through its interaction with various ECM components and tumor cells (Laoui et al., 2011; Du et al., 2013). Interestingly, dos Reis and co-workers recently demonstrated the correlation of versican expression with tumor associated macrophage (TAM) accumulation and progression using two *in vivo* models of mammary carcinomas (Dos Reis et al., 2019). The evidence from various studies highlights the unique roles that each PG plays in mammary tumourgenesis and progression. Uniform upregulation or downregulation is clearly not what propagates this progression, but rather a complex interplay of up and downregulation leading to a variety of signaling interactions, ultimately resulting in increased proliferation, invasion and poor survival outcomes (Troup et al., 2003; Prinz et al., 2011).

In *in vitro* studies, a potential role for syndecan-1 in modulating breast cancer brain metastasis has been identified (Sayyad et al., 2019). On the other hand, *in vivo* studies such as by Pumphrey et al. (2002), explored the interactions of syndecan-1 HSPG analogs that were synthetically produced by carbodiimide conjugation of GAG chains. Their anticancer properties were evaluated by injection into breast tumors that were grown in nude mice in which they observed a significant reduction in growth without cytotoxicity to neighboring healthy tissue. However, animal models do come with their limitations and have led researchers to look for alternatives. They are financially and ethically expensive and although *in vivo* models encapsulate a physiologically robust and similar microenvironment to that found in humans, they do not fully represent human biology nor are a platform for customisability of microenvironmental parameters. This is where 3D models aim to exploit the best qualities of both 2D and *in vivo* models and combine them in a cost-effective, reproducible and most importantly, physiologically relevant, yet highly customisable, human model (**Figure 2**). In an attempt to combat the difficulties presented by previous models, 3D culture models such as organ-on-a-chip, hydrogels, scaffolds, and spheroid formation provide viable *in vitro* alternatives that extend throughout many cell-based medical research fields. These customisable models predominantly aim to recreate a physiologically relevant ECM to better mimic biologically relevant cell-cell and cell-ECM interactions.

Naturally derived hydrogels such as Matrigel and collagen provide a growth factor rich 3D environment for cancer cells to grow in. Matrigel, a reconstituted basement membrane extract from the Engelbreth-Holm-Swarm (EHS) sarcoma (Vukicevic et al., 1992), is rich in basement membrane components, including the HSPG perlecan and has been used to study the invasion of breast cancer cells in response to syndecan-1 knockdown (Nikolova et al., 2009; Ibrahim et al., 2013). The authors found that proteolytic conversion of syndecan-1 from being membrane-bound to a soluble form switched breast cancer cells from a proliferative to an invasive phenotype (Nikolova et al., 2009). Consistent with this, the overexpression of miR-10b resulted in downregulated syndecan-1 and increased invasiveness into a Matrigel matrix (Ibrahim et al., 2013). Moreover, syndecan-1 has further been found to modulate the phenotype of cancer stem cells in triple negative breast cancer types, and when silenced, reduced 3D spheroid formation *in vitro* (Ibrahim et al., 2017). Collagen-derived hydrogels have also been used to study PGs. In a recent study by Singh et al. (2019), MCF-7 and MDA-MB-231 cells were cultured in 3D collagen hydrogels to explore the role of dermatan sulfate PGs in breast cancer invasion (Singh et al., 2019). The authors artificially decreased the expression of iduronate-2-sulphatase (IDS) in the cell lines, increasing the levels of dermatan sulfate, which led to a more mesenchymal morphology and increased breast cancer cell invasion into a collagen matrix. A recent study from Karamanou et al. (2020) also utilized collagen-derived hydrogels to explore the effects of lumican on cell adhesion, including the molecular mechanisms behind its anti-cancer activities, demonstrating its potential as a target for anti-cancer therapies (Karamanou et al., 2020).

HA-based hydrogels have also been employed to investigate GAG/PG relationships, consisting of a scaffold architecture aimed to provide a biomimetic ECM for PG signaling. Bonnesœur et al. (2020) demonstrated that HA-hydrogels were capable of supporting both mammary and brain-derived cancer cell lines while showing the tunability and biomimetic capabilities of PG-based hydrogels (Bonnesœur et al., 2020). Moreover, a study by Fisher et al. (2015) utilized HA and matrix-metalloproteinase (MMP) cleavable peptides to investigate MDA-MB-231 invasion capabilities (Fisher et al., 2015). In this case, HA was furan-modified and combined with a bismaleimide peptide crosslinker resulting in a Diels-Alder click reaction. The

researchers created several hydrogels with and without MMP-cleavable peptides. Increased crosslinking density resulted in decreased invasion, while hydrogels incorporated with MMPs and low crosslinking density, showed higher levels of invasion. This was corroborated by Hubka et al. (2019), who also utilized thiolated HA with a poly(ethylene glycol)diacrylate (PEGDA) crosslinker to form hydrogels in order to investigate the role of perlecan domain 1 (Hubka et al., 2019). Using FGF-2 along with the perlecan domain 1, they demonstrated higher migratory and invasive behaviors in sections of the hydrogels with higher concentrations of perlecan domain 1 and thereby FGF-2. Baker and colleagues developed this further (formed by a Diels-Alder reaction) when they assessed drug infiltration into spheroid colonies within their HA-hydrogels in MCF-7 and T47D cells (Baker et al., 2017). They saw that not only was there reduced penetration into inner cells by the drugs, but drug and multi-drug resistance occurred, and more accurately represented the phenomenon of drug resistance that occurs in the clinic.

An example of a non-hydrogel 3D *in vitro* system was formulated by Hinderer et al. (2018), where electrospun scaffolds were functionalised to assess decorin interaction with endothelial cells (Hinderer et al., 2018). Decorin and stromal cell-derived factor-1 (SDF-1) coated scaffolds showed high levels of adhesion, migration and interaction with human endothelial progenitor cells (hEPCs) when compared to non-functionalized scaffold controls. Further, they found that decorin had higher levels of interaction and influence over the migration of the hEPCs compared to SDF-1. Le Borgne-Rochet et al. (2019), also using a scaffold system, studied the role of decorin in cell migration, illustrating the interactions decorin has with the adhesion molecule P-cadherin (Le Borgne-Rochet et al., 2019). This further supported Hindere's work regarding the many interactions of decorin and showed that P-cadherin mediated the directional cell migration and collagen fiber orientation required the presence of decorin. They also discovered that decorin activation resulted in upregulation of β1 integrin and the β-Pix/CDC42 axis promoting directional cell migration.

CONCLUSION AND PERSPECTIVES

These studies implicate a multifaceted role for PGs in breast cancer. It is tempting to suggest that the stromal-breast tumor PG microenvironment may shape the fate of these programmable ever adapting tumor cells. However, it is a balancing act where subtle changes in the content of PGs and associated ECM may be utilized by the tumor cells to overcome the intrinsic resistances and hostilities presented to them. Current findings from the literature warrant undertaking comprehensive mechanistic studies where this balance could be exploited to favor a healthy microenvironment. To date, the study of breast PGs in a 3D *in vitro* context has been limited. While 2D cultures have been utilized for their ease-of-use, there is a substantial difference in cellular behavior and morphology when the context of the cellular microenvironment is changed (Weigelt et al., 2014). Advances in 3D cell culture have led to novel findings, including biological events that transpire during cancer development that were previously not known. The establishment of these relatively new systems as dominant platforms for medical research, will enable further novel findings, including further study of the complex interactions of PGs. In particular, 3D model systems provide the ideal platform to assess PGs with a significant lack of studies leveraging these physiological relevant systems currently employed in breast cancer and other cancer research.

State-of-the-art biomaterials and tissue engineering strategies enable the reconstruction of different microenvironments by providing biomechanical and biochemical compositions specific to various tissues. In previous work, we have shown how semi-synthetic hydrogels prepared from PEG and heparin GAGs represent a platform for TME modeling (Bray et al., 2015). Likewise, hydrogels formed from gelatin-methacryloyl (GelMA) have been used to successfully recapitulate breast cancer invasion and chemoresponses *in vitro* (Yue et al., 2015; Loessner et al., 2016; Donaldson et al., 2018; Meinert et al., 2018). Exploiting such biohybrid 3D matrices allows for the control of batch-to-batch physicochemical properties, which are known to affect cellular behavior in the TME. The implementation of 3D systems further allows for the extensive analysis of ECM and basement membrane deposition by the cells in their surrounding microenvironment. In order to study the role of PGs in breast cancer *in vitro*, attention should be paid to give microenvironmental and PG context, and to allow for the heterogeneous culture of various supporting cell types resulting from patient tissues (Foley, 2017). Finally, dynamic culture conditions, such as bioreactors (Selden and Fuller, 2018), microfluidics (Shang et al., 2019), and tumor-on-chip (Rothbauer et al., 2019; Sun et al., 2019) technologies, exemplify options to raise the physiological relevance of PG studies specific to the breast tissue microenvironment. Taken together, we anticipate that the development of novel and sophisticated 3D models in which to study the role of PGs in the breast microenvironment will allow for the identification of novel therapeutic targets for preventing and treating malignant transformation in breast cancer patients, such as in the case of the syndecan-1 inhibitor, synstatin (Beauvais et al., 2009; Jung et al., 2016).

AUTHOR CONTRIBUTIONS

LB and PK-dC delineated the topic and outline. JC, PK-dC, and LB reviewed and evaluated the literature, designed, and wrote the manuscript. MK, LH, and ET provided feedback and edited the final manuscript.

FUNDING

LB was supported by a grant from the National Breast Cancer Foundation (PF-16-004). ET received support from the Princess Alexandra Research Foundation for PG research in mammographic density. The Translational Research Institute received support from the Australian government. All authors contributed to the article and approved the submitted version.

REFERENCES

Alvarenga, E., Vasconcellos, R., and Medrado, N. (2019). Behavior of adipocytes in the mammary niche during pregnancy and lactation. *J. Stem Cell Res. Ther.* 5, 1–6.

Asano, K., Nelson, C. M., Nandadasa, S., Aramaki-Hattori, N., Lindner, D. J., Alban, T., et al. (2017). Stromal versican regulates tumor growth by promoting angiogenesis. *Sci. Rep.* 7:17225. doi: 10.1038/s41598-017-17613-6

Baker, A. E., Tam, R. Y., and Shoichet, M. S. (2017). Independently tuning the biochemical and mechanical properties of 3D hyaluronan-based hydrogels with oxime and Diels–Alder chemistry to culture breast cancer spheroids. *Biomacromolecules* 18, 4373–4384. doi: 10.1021/acs.biomac.7b01422

Barresi, R., and Campbell, K. P. (2006). Dystroglycan: from biosynthesis to pathogenesis of human disease. *J Cell Sci.* 119, 199–207. doi: 10.1242/jcs.02814

Beauvais, D. M., Ell, B. J., McWhorter, A. R., and Rapraeger, A. C. (2009). Syndecan-1 regulates αvβ3 and αvβ5 integrin activation during angiogenesis and is blocked by synstatin, a novel peptide inhibitor. *J. Exp. Med.* 206, 691–705. doi: 10.1084/jem.20081278

Bischof, A. G., Yüksel, D., Mammoto, T., Mammoto, A., Krause, S., and Ingber, D. E. (2013). Breast cancer normalization induced by embryonic mesenchyme is mediated by extracellular matrix biglycan. *Integrative Biol.* 5, 1045–1056. doi: 10.1039/c3ib40103k

Bishop, J. R., Schuksz, M., and Esko, J. D. (2007). Heparan sulphate proteoglycans fine-tune mammalian physiology. *Nature* 446, 1030–1037. doi: 10.1038/nature05817

Bonnesœur, S., Morin−Grognet, S., Thoumire, O., Le Cerf, D., Boyer, O., Vannier, J. P., et al. (2020). Hyaluronan−based hydrogels as versatile tumor−like models: tunable ECM and stiffness with genipin−crosslinking. *J. Biomed. Mater. Res. Part A* 108, 1256–1268. doi: 10.1002/jbm.a.36899

Bray, F., Ferlay, J., Soerjomataram, I., Siegel, R. L., Torre, L. A., and Jemal, A. (2018). Global cancer statistics 2018: GLOBOCAN estimates of incidence and mortality worldwide for 36 cancers in 185 countries. *CA Cancer J. Clin.* 68, 394–424. doi: 10.3322/caac.21492

Bray, L. J., Binner, M., Holzheu, A., Friedrichs, J., Freudenberg, U., Hutmacher, D. W., et al. (2015). Multi-parametric hydrogels support 3D in vitro bioengineered microenvironment models of tumour angiogenesis. *Biomaterials* 53, 609–620. doi: 10.1016/j.biomaterials.2015.02.124

Burstein, H. J., Griggs, J. J., Prestrud, A. A., and Temin, S. (2010). American society of clinical oncology clinical practice guideline update on adjuvant endocrine therapy for women with hormone receptor-positive breast cancer. *J. Oncol. Pract.* 6, 243–246. doi: 10.1200/jop.000082

Cancer Genome Atlas Network (2012). Comprehensive molecular portraits of human breast tumours. *Nature* 490, 61–70. doi: 10.1038/nature11412

Chhabra, M., and Ferro, V. (2018). The development of assays for heparanase enzymatic activity: towards a gold standard. *Molecules* 23:2971. doi: 10.3390/molecules23112971

Crawford, B. E., Garner, O. B., Bishop, J. R., Zhang, D. Y., Bush, K. T., Nigam, S. K., et al. (2010). Loss of the heparan sulfate sulfotransferase, Ndst1, in mammary epithelial cells selectively blocks lobuloalveolar development in mice. *PLoS One* 5:e10691. doi: 10.1371/journal.pone.0010691

Dawoody Nejad, L., Biglari, A., Annese, T., and Ribatti, D. (2017). Recombinant fibromodulin and decorin effects on NF-κB and TGFβ1 in the 4T1 breast cancer cell line. *Oncol. Lett.* 13, 4475–4480. doi: 10.3892/ol.2017.5960

De Lima, C. R., Dos Santos Junior, J. D. A., Nazário, A. C. P., and Michelacci, Y. M. (2012). Changes in glycosaminoglycans and proteoglycans of normal breast and fibroadenoma during the menstrual cycle. *Biochim. Biophys. Acta* 1820, 1009–1019. doi: 10.1016/j.bbagen.2012.04.010

Donaldson, A. R., Tanase, C. E., Awuah, D., Vasanthi Bathrinarayanan, P., Hall, L., Nikkhah, M., et al. (2018). Photocrosslinkable gelatin hydrogels modulate the production of the major pro-inflammatory cytokine, TNF-α, by human mononuclear cells. *Front. Bioeng. Biotech.* 6:116. doi: 10.3389/fbioe.2018.00116

Dos Reis, D. C., Damasceno, K. A., De Campos, C. B., Veloso, E. S., Pegas, G. R. A., Kraemer, L. R., et al. (2019). Versican and tumor-associated macrophages promotes tumor progression and metastasis in canine and murine models of breast carcinoma. *Front. Oncol.* 9:577. doi: 10.3389/fonc.2019.00577

Du, W. W., Fang, L., Yang, X., Sheng, W., Yang, B. L., Seth, A., et al. (2013). The role of versican in modulating breast cancer cell self-renewal. *Mol. Cancer Res.* 11, 443–455. doi: 10.1158/1541-7786.mcr-12-0461

Du, W. W., Yang, B. B., Shatseva, T. A., Yang, B. L., Deng, Z., Shan, S. W., et al. (2010). Versican G3 promotes mouse mammary tumor cell growth, migration, and metastasis by influencing EGF receptor signalling. *PLoS One* 5:e13828. doi: 10.1371/journal.pone.0013828

Dulaney, C., Marcrom, S., Stanley, J., and Yang, E. S. (2017). Poly(ADP-ribose) polymerase activity and inhibition in cancer. *Semin. Cell Dev. Biol.* 63, 144–153. doi: 10.1016/j.semcdb.2017.01.007

Ferguson, J. E., Schor, A. M., Howell, A., and Ferguson, M. (1992). Changes in the extracellular matrix of the normal human breast during the menstrual cycle. *Cell Tissue Res.* 268, 167–177. doi: 10.1007/bf00338066

Fisher, S. A., Anandakumaran, P. N., Owen, S. C., and Shoichet, M. S. (2015). Tuning the microenvironment: click−crosslinked hyaluronic acid−based hydrogels provide a platform for studying breast cancer cell invasion. *Adv. Funct. Mater.* 25, 7163–7172. doi: 10.1002/adfm.201502778

Foley, K. E. (2017). Organoids: a better in vitro model. *Nat. Methods* 14, 559–562. doi: 10.1038/nmeth.4307

Garner, O. B., Bush, K. T., Nigam, K. B., Yamaguchi, Y., Xu, D., Esko, J. D., et al. (2011). Stage-dependent regulation of mammary ductal branching by heparan sulfate and HGF-cMet signaling. *Dev. Biol.* 355, 394–403. doi: 10.1016/j.ydbio.2011.04.035

Gouon-Evans, V. R., and Pollard, J. W. (2002). Unexpected deposition of brown fat in mammary gland during postnatal development. *Mol. Endocrinol.* 16, 2618–2627. doi: 10.1210/me.2001-0337

Hinck, L., and Silberstein, G. B. (2005). Key stages in mammary gland development: the mammary end bud as a motile organ. *Breast Cancer Res.* 7:245. doi: 10.1186/bcr1331

Hinderer, S., Sudrow, K., Schneider, M., Holeiter, M., Layland, S. L., Seifert, M., et al. (2018). Surface functionalization of electrospun scaffolds using recombinant human decorin attracts circulating endothelial progenitor cells. *Sci. Rep.* 8:110. doi: 10.1038/s41598-017-18382-y

Huang, X., Reye, G., Momot, K. I., Blick, T., Lloyd, T., Tilley, W. D., et al. (2020). Heparanase promotes Syndecan-1 expression to mediate fibrillar collagen and mammographic density in human breast tissue cultured ex vivo. *Front. Cell Dev. Biol.* 8:599. doi: 10.3389/fcell.2020.00599

Hubka, K. M., Carson, D. D., Harrington, D. A., and Farach-Carson, M. C. (2019). Perlecan domain I gradients establish stable biomimetic heparin binding growth factor gradients for cell migration in hydrogels. *Acta Biomater.* 97, 385–398. doi: 10.1016/j.actbio.2019.07.040

Ibrahim, S. A., Gadalla, R., El-Ghonaimy, E. A., Samir, O., Mohamed, H. T., Hassan, H., et al. (2017). Syndecan-1 is a novel molecular marker for triple negative inflammatory breast cancer and modulates the cancer stem cell phenotype via the IL-6/STAT3, Notch and EGFR signaling pathways. *Mol. Cancer* 16:57. doi: 10.1186/s12943-017-0621-z

Ibrahim, S. A., Hassan, H., Vilardo, L., Kumar, S. K., Kumar, A. V., Kelsch, R., et al. (2013). Syndecan-1 (CD138) modulates triple-negative breast cancer stem cell properties via regulation of LRP-6 and IL-6-mediated STAT3 signaling. *PLoS One* 8:e85737. doi: 10.1371/journal.pone.0085737

Iozzo, R. V., and Schaefer, L. (2015). Proteoglycan form and function: a comprehensive nomenclature of proteoglycans. *Matrix Biol.* 42, 11–55. doi: 10.1016/j.matbio.2015.02.003

Jackson, H. W., Fischer, J. R., Zanotelli, V. R. T., Ali, H. R., Mechera, R., Soysal, S. D., et al. (2020). The single-cell pathology landscape of breast cancer. *Nature* 578, 615–620. doi: 10.1038/s41586-019-1876-x

Jung, O., Trapp-Stamborski, V., Purushothaman, A., Jin, H., Wang, H., Sanderson, R. D., et al. (2016). Heparanase-induced shedding of syndecan-1/CD138 in myeloma and endothelial cells activates VEGFR2 and an invasive phenotype: prevention by novel synstatins. *Oncogenesis* 5:e202. doi: 10.1038/oncsis.2016.5

Karamanou, K., Franchi, M., Onisto, M., Passi, A., Vynios, D. H., and Brézillon, S. (2020). Evaluation of lumican effects on morphology of invading breast cancer cells, expression of integrins and downstream signaling. *FEBS J.* doi: 10.1111/febs.15289 [Epub ahead of print].

Karamanou, K., Franchi, M., Piperigkou, Z., Perreau, C., Maquart, F. X., Vynios, D. H., et al. (2017). Lumican effectively regulates the estrogen receptors-associated functional properties of breast cancer cells, expression of matrix effectors and epithelial-to-mesenchymal transition. *Sci. Rep.* 7:45138. doi: 10.1038/srep45138

Kelly, T., Suva, L. J., Huang, Y., Macleod, V., Miao, H. Q., Walker, R. C., et al. (2005). Expression of heparanase by primary breast tumors promotes bone

resorption in the absence of detectable bone metastases. *Cancer Res.* 65, 5778–5784. doi: 10.1158/0008-5472.can-05-0749

Korpetinou, A., Skandalis, S. S., Labropoulou, V. T., Smirlaki, G., Noulas, A., Karamanos, N. K., et al. (2014). Serglycin: at the crossroad of inflammation and malignancy. *Front. Oncol.* 3:327. doi: 10.3389/fonc.2013.00327

Korpetinou, A., Skandalis, S. S., Moustakas, A., Happonen, K. E., Tveit, H., Prydz, K., et al. (2013). Serglycin is implicated in the promotion of aggressive phenotype of breast cancer cells. *PLoS One* 8:e78157. doi: 10.1371/journal.pone.0078157

Laoui, D., Movahedi, K., Van Overmeire, E., Van Den Bossche, J., Schouppe, E., Mommer, C., et al. (2011). Tumor-associated macrophages in breast cancer: distinct subsets, distinct functions. *Int. J. Dev. Biol.* 55, 861–867. doi: 10.1387/ijdb.113371dl

Le Borgne-Rochet, M., Angevin, L., Bazellières, E., Ordas, L., Comunale, F., Denisov, E. V., et al. (2019). P-cadherin-induced decorin secretion is required for collagen fiber alignment and directional collective cell migration. *J. Cell Sci.* 132:jcs233189. doi: 10.1242/jcs.233189

Lehmann, B. D., Bauer, J. A., Chen, X., Sanders, M. E., Chakravarthy, A. B., Shyr, Y., et al. (2011). Identification of human triple-negative breast cancer subtypes and preclinical models for selection of targeted therapies. *J. Clin. Invest.* 121, 2750–2767. doi: 10.1172/jci45014

Liu, B. Y., Kim, Y. C., Leatherberry, V., Cowin, P., and Alexander, C. M. (2003). Mammary gland development requires syndecan-1 to create a β-catenin/TCF-responsive mammary epithelial subpopulation. *Oncogene* 22, 9243–9253. doi: 10.1038/sj.onc.1207217

Liu, J. J., Zhang, J., Ramanan, S., Julian, J., Carson, D. D., and Hooi, S. C. (2004). Heparin/heparan sulfate interacting protein plays a role in apoptosis induced by anticancer drugs. *Carcinogenesis* 25, 873–879. doi: 10.1093/carcin/bgh081

Loessner, D., Meinert, C., Kaemmerer, E., Martine, L. C., Yue, K., Levett, P. A., et al. (2016). Functionalization, preparation and use of cell-laden gelatin methacryloyl–based hydrogels as modular tissue culture platforms. *Nat. Protoc.* 11:727. doi: 10.1038/nprot.2016.037

Lu, P., Ewald, A. J., Martin, G. R., and Werb, Z. (2008). Genetic mosaic analysis reveals FGF receptor 2 function in terminal end buds during mammary gland branching morphogenesis. *Dev. Biol.* 321, 77–87. doi: 10.1016/j.ydbio.2008.06.005

Macias, H., and Hinck, L. (2012). Mammary gland development. *Wiley Interdiscip. Rev. Dev. Biol.* 1, 533–557. doi: 10.1002/wdev.35

Meinert, C., Theodoropoulos, C., Klein, T. J., Hutmacher, D. W., and Loessner, D. (2018). A method for prostate and breast cancer cell spheroid cultures using gelatin methacryloyl-based hydrogels. *Methods Mol. Biol.* 1786, 175–194. doi: 10.1007/978-1-4939-7845-8_10

Moon, J. J., Matsumoto, M., Patel, S., Lee, L., Guan, J. L., and Li, S. (2005). Role of cell surface heparan sulfate proteoglycans in endothelial cell migration and mechanotransduction. *J. Cell Phys.* 203, 166–176. doi: 10.1002/jcp.20220

Morgan, M. R., Humphries, M. J., and Bass, M. D. (2007). Syngeristic control of cell adhesion by integrins and syndecans. *Nat. Rev. Mol. Cell Biol.* 8, 957–969. doi: 10.1038/nrm2289

Morrison, B., and Cutler, M. L. (2010). The contribution of adhesion signaling to lactogenesis. *J. Cell Commun. Signal.* 4, 131–139. doi: 10.1007/s12079-010-0099-6

Muschler, J., and Streuli, C. H. (2010). Cell-matrix interactions in mammary gland development and breast cancer. *Cold Spring Harb. Perspect. Biol.* 2:a003202. doi: 10.1101/cshperspect.a003202

Naba, A., Clauser, K. R., Hoersch, S., Liu, H., Carr, S. A., and Hynes, R. O. (2012). The matrisome: in silico definition and in vivo characterization by proteomics of normal and tumor extracellular matrices. *Mol. Cell Proteomics* 11:M111.014647. doi: 10.1074/mcp.M111.014647

Nikitovic, D., Berdiaki, A., Spyridaki, I., Krasanakis, T., Tsatsakis, A., and Tzanakakis, G. N. (2018). Proteoglycans–biomarkers and targets in cancer therapy. *Front. Endocrinol.* 9:69. doi: 10.3389/fendo.2018.00069

Nikolova, V., Koo, C.-Y., Ibrahim, S. A., Wang, Z., Spillmann, D., Dreier, R., et al. (2009). Differential roles for membrane-bound and soluble syndecan-1 (CD138) in breast cancer progression. *Carcinogenesis* 30, 397–407. doi: 10.1093/carcin/bgp001

Nik-Zainal, S., Davies, H., Staaf, J., Ramakrishna, M., Glodzik, D., Zou, X., et al. (2016). Landscape of somatic mutations in 560 breast cancer whole-genome sequences. *Nature* 534, 47–54.

Patel, V. N., Knox, S. M., Likar, K. M., Lathrop, C. A., Hossain, R., Eftekhari, S., et al. (2007). Heparanse cleavage of perlecan heparan sulfate modulates FGF10 activity during ex vivo submandibular gland branching morphogenesis. *Dev. Biol.* 134, 4177–4186. doi: 10.1242/dev.011171

Pearson, C. H., Winterbottom, N., Fackre, D. S., Scott, P. G., and Capenter, M. R. (1983). The NH2-terminal amino acid sequence of bovine skin proteodermatan sulfate. *J. Biol. Chem.* 258, 15101–15104.

Perou, C. M., Sorlie, T., Eisen, M. B., Van De Rijn, M., Jeffrey, S. S., Rees, C. A., et al. (2000). Molecular portraits of human breast tumours. *Nature* 406, 747–752. doi: 10.1038/35021093

Prinz, R. D., Willis, C. M., Viloria-Petit, A., and Kluppel, M. (2011). Elimination of breast tumor-associated chondroitin sulfate promotes metastasis. *Genet. Mol. Res.* 10, 3901–3913. doi: 10.4238/2011.december.8.9

Pumphrey, C. Y., Theus, A. M., Li, S., Parrish, R. S., and Sanderson, R. D. (2002). Neoglycans, carbodiimide-modified glycosaminoglycans: a new class of anticancer agents that inhibit cancer cell proliferation and induce apoptosis. *Cancer Res.* 62, 3722–3728.

Recktenwald, C. V., Leisz, S., Steven, A., Mimura, K., Müller, A., Wulfänger, J., et al. (2012). HER-2/neu-mediated down-regulation of biglycan associated with altered growth properties. *J. Biol. Chem.* 287, 24320–24329. doi: 10.1074/jbc.m111.334425

Ricciardelli, C., Brooks, J. H., Suwiwat, S., Sakko, A. J., Mayne, K., Raymond, W. A., et al. (2002). Regulation of stromal versican expression by breast cancer cells and importance to relapse-free survival in patients with node-negative primary breast cancer. *Clin. Cancer Res.* 8, 1054–1060.

Rothbauer, M., Rosser, J. M., Zirath, H., and Ertl, P. (2019). Tomorrow today: organ-on-a-chip advances towards clinically relevant pharmaceutical and medical in vitro models. *Curr. Opin. Biotech.* 55, 81–86. doi: 10.1016/j.copbio.2018.08.009

Ruoslahti, E. (1988). Structure and biology of proteoglycans. *Ann. Rev. Cell Biol.* 4, 229–255. doi: 10.1146/annurev.cb.04.110188.001305

Sayyad, M. R., Puchalapalli, M., Vergara, N. G., Wangensteen, S. M., Moore, M., Mu, L., et al. (2019). Syndecan-1 facilitates breast cancer metastasis to the brain. *Breast Cancer Res. Treat.* 178, 35–49. doi: 10.1007/s10549-019-05347-0

Scully, O. J., Chua, P. J., Harve, K. S., Bay, B. H., and Yip, G. W. (2012). Serglycin in health and diseases. *Anat. Rec.* 295, 1415–1420. doi: 10.1002/ar.22536

Segev, A., Nili, N., and Strauss, B. H. (2004). The role of perlecan in arterial injury and angiogenesis. *Cardiovasc. Res.* 63, 603–610. doi: 10.1016/j.cardiores.2004.03.028

Selden, C., and Fuller, B. (2018). Role of bioreactor technology in tissue engineering for clinical use and therapeutic target design. *Bioengineering (Basel)* 5:32. doi: 10.3390/bioengineering5020032

Shang, M., Soon, R. H., Lim, C. T., Khoo, B. L., and Han, J. (2019). Microfluidic modelling of the tumor microenvironment for anti-cancer drug development. *Lab Chip* 19, 369–386. doi: 10.1039/c8lc00970h

Singh, V., Jha, K. K., Kumar, R. V., Raghunathan, V., and Bhat, R. (2019). Iduronate-2-sulfatase-regulated dermatan sulfate levels potentiate the invasion of breast cancer epithelia through collagen matrix. *J. Clin. Med.* 8:1562. doi: 10.3390/jcm8101562

Sun, W., Luo, Z., Lee, J., Kim, H. J., Lee, K., Tebon, P., et al. (2019). Organ−on−a−chip for cancer and immune organs modeling. *Adv. Healthcare Mater.* 8:1801363. doi: 10.1002/adhm.201801363

Theocharis, A. D., Skandalis, S. S., Neill, T., Multhaupt, H. A., Hubo, M., Frey, H., et al. (2015). Insights into the key roles of proteoglycans in breast cancer biology and translational medicine. *Biochem. Biophys. Acta* 1855, 276–300. doi: 10.1016/j.bbcan.2015.03.006

Troup, S., Njue, C., Kliewer, E. V., Parisien, M., Roskelley, C., Chakravarti, S., et al. (2003). Reduced expression of the small leucine-rich proteoglycans, lumican, and decorin is associated with poor outcome in node-negative invasive breast cancer. *Clin. Cancer Res.* 9, 207–214.

Vukicevic, S., Kleinman, H. K., Luyten, F. P., Roberts, A. B., Roche, N. S., and Reddi, A. H. (1992). Identification of multiple active growth factors in basement membrane Matrigel suggests caution in interpretation of cellular activity related to extracellular matrix components. *Exp. Cell Res.* 202, 1–8. doi: 10.1016/0014-4827(92)90397-q

Weigelt, B., Ghajar, C. M., and Bissell, M. J. (2014). The need for complex 3D culture models to unravel novel pathways and identify accurate biomarkers in breast cancer. *Adv. Drug Deliv. Rev.* 69, 42–51. doi: 10.1016/j.addr.2014.01.001

Wight, T. N. (2002). Versican: a versatile extracellular matrix proteoglycan in cell biology. *Curr. Opin. Cell Biol.* 14, 617–623. doi: 10.1016/s0955-0674(02)00375-7

Wilsie, L. C., Chanchani, S., Navaratna, D., and Orlando, R. A. (2005). Cell surface heparan sulfate proteoglycans contribute to intracellular lipid accumulation in adipocytes. *Lipids Health Dis.* 4:2. doi: 10.1186/1476-511X-4-2

Wu, Y. H., Yang, C. Y., Chien, W. L., Lin, K. I., and Lai, M. Z. (2012). Removal of syndecan-1 promotes TRAIL-induced apoptosis in myeloma cells. *J. Immunol.* 188, 2914–2921. doi: 10.4049/jimmunol.1102065

Yue, K., Trujillo-De Santiago, G., Alvarez, M. M., Tamayol, A., Annabi, N., and Khademhosseini, A. (2015). Synthesis, properties, and biomedical applications of gelatin methacryloyl (GelMA) hydrogels. *Biomaterials* 73, 254–271. doi: 10.1016/j.biomaterials.2015.08.045

Conflict of Interest: The authors declare that the research was conducted in the absence of any commercial or financial relationships that could be construed as a potential conflict of interest.

frontiers in Cell and Developmental Biology

REVIEW
published: 19 November 2020
doi: 10.3389/fcell.2020.581213

Heparan Sulfate Proteoglycans: Key Mediators of Stem Cell Function

*Maanasa Ravikumar[1,2], Raymond Alexander Alfred Smith[1], Victor Nurcombe[1,3] and Simon M. Cool[1,2]**

[1] Glycotherapeutics Group, Institute of Medical Biology, Agency for Science, Technology and Research (A*STAR), Singapore, Singapore, [2] Department of Orthopaedic Surgery, Yong Loo Lin School of Medicine, National University of Singapore, Singapore, Singapore, [3] Lee Kong Chian School of Medicine, Nanyang Technological University–Imperial College London, Singapore, Singapore

Heparan sulfate proteoglycans (HSPGs) are an evolutionarily ancient subclass of glycoproteins with exquisite structural complexity. They are ubiquitously expressed across tissues and have been found to exert a multitude of effects on cell behavior and the surrounding microenvironment. Evidence has shown that heterogeneity in HSPG composition is crucial to its functions as an essential scaffolding component in the extracellular matrix as well as a vital cell surface signaling co-receptor. Here, we provide an overview of the significance of HSPGs as essential regulators of stem cell function. We discuss the various roles of HSPGs in distinct stem cell types during key physiological events, from development through to tissue homeostasis and regeneration. The contribution of aberrant HSPG production to altered stem cell properties and dysregulated cellular homeostasis characteristic of cancer is also reviewed. Finally, we consider approaches to better understand and exploit the multifaceted functions of HSPGs in influencing stem cell characteristics for cell therapy and associated culture expansion strategies.

Keywords: proteoglycans, GAGs, stem cells, embryonic stem cells, adult stem cells, extracellular matrix, glycosaminoglycan, heparan sulfate

OPEN ACCESS

Edited by:
Jeremy Turnbull, University of Liverpool, United Kingdom

Reviewed by:
Martin Götte, University of Münster, Germany
Deirdre R. Coombe, Curtin University, Australia

***Correspondence:**
Simon M. Cool
Simon.COOL@imb.a-star.edu.sg

Specialty section:
This article was submitted to Signaling, a section of the journal Frontiers in Cell and Developmental Biology

Received: *08 July 2020*
Accepted: *29 October 2020*
Published: *19 November 2020*

Citation:
Ravikumar M, Smith RAA, Nurcombe V and Cool SM (2020) Heparan Sulfate Proteoglycans: Key Mediators of Stem Cell Function. Front. Cell Dev. Biol. 8:581213. doi: 10.3389/fcell.2020.581213

INTRODUCTION

The glycocalyx is a dense layer of glycoproteins and glycolipids that coats the exterior of the cell membrane. It is comprised of a variety of polysaccharides covalently attached to lipids or proteins, and functions as an essential interface between external and internal cellular environments. Heparan sulfate (HS) is one of the many constituent polysaccharides, and is long (40–300 residues), linear and highly charged (Sarrazin et al., 2011). HS belongs to the glycosaminoglycan (GAG) family of carbohydrates, which also includes the closely related heparin, hyaluronan (HA), chondroitin and dermatan sulfate (CS/DS), and keratan sulfate (KS) (Esko and Lindahl, 2001; Gallagher, 2001). The base structure of HS is highly conserved throughout multicellular organisms, including mammals, fruit flies (*Drosophila melanogaster*) (Nakato et al., 1995), nematodes (*Caenorhabditis elegans*) (Townley and Bülow, 2011) and hydra (*Hydra Magnipapillata* and *Hydra vulgaris*) (Sarras et al., 1991; Yamada et al., 2007), indicating an ancient evolutionary origin.

HS is present in the extracellular matrix (ECM) of every tissue and on the surface of virtually every cell within an organism. HS chains are covalently attached to core proteins belonging

to multiple families, and are collectively known as heparan sulfate proteoglycans (HSPGs). Mammalian HSPGs may be present as transmembrane proteins (syndecan 1–4, CD44, neuropilin-1, betaglycan) (Rapraeger et al., 1985; Sanderson and Bernfield, 1988; Andres et al., 1989; Brown et al., 1991; Kojima et al., 1992; Shintani et al., 2006; Multhaupt et al., 2009; Couchman, 2010; Gopal et al., 2010), GPI-anchored membrane proteins (glypican 1–6) (David et al., 1990; Filmus and Selleck, 2001; Filmus et al., 2008; Feil et al., 2009), secreted proteins retained within the ECM (perlecan, agrin, and collagen XVIII) (Noonan et al., 1991; Tsen et al., 1995; Halfter et al., 1998; Knox et al., 2002; Knox and Whitelock, 2006) or in secretory granules (serglycin) (Tantravahi et al., 1986; Stevens et al., 1988; Kolset and Tveit, 2008).

The ubiquitous presence of HSPGs is indicative of the multitude of important biological roles they play within an organism. For example, HS-rich perlecan is an integral basement membrane constituent, along with agrin and collagen XVIII, and a critical scaffolding component of the ECM (Hassell et al., 1980; Costell et al., 1999; Farach-Carson and Carson, 2007). In this regard, HSPGs provide biomechanical support and help maintain integrity of the extracellular microenvironment. Apart from their structural functions, HS chains can bind to a large number of proteins, of which at least 437 have been identified, and serve as low-affinity co-receptors during signaling events (Xu and Esko, 2014; Rudd et al., 2017; Dubey et al., 2020). Additionally, the protein-binding properties of HS afford it the ability to arrange morphogens into spatial and temporal gradients, which is vital for orderly development and tissue repair (Bernfield et al., 1999). HS can also bind and sequester various proteins, protecting them from thermal or proteolytic degradation (Sadir et al., 2004; Makarenkova et al., 2009; Xu and Esko, 2014; Kjellén and Lindahl, 2018; Poon et al., 2018; Sun C. et al., 2019). The distinct combinations of functional groups and chain modifications laid down during biosynthesis confer unique structural conformations and binding properties to an HS chain, underpinning its propensity to interact with a wide array of ligands and cognate receptors (Kreuger et al., 2006; Lindahl and Li, 2009).

HSPGs may also interact with proteins via the cytoplasmic domains of their core proteins. The syndecans are especially known to engage components of the cytoskeleton and focal adhesions, such as α-actinin and integrins, despite an absence of inherent kinase activity (Rapraeger et al., 1986; Saoncella et al., 1999; Greene et al., 2003). Such interactions implicate HSPGs as crucial components of protein binding events not only at the cell surface, but also those within adjacent intracellular regions that may influence cytoskeletal organization and downstream signaling cascades. All of these functional features confer an indispensability of HSPGs in cellular responses that influence cell morphology, adhesion, migration, and fate decisions (Longley et al., 1999; Cool and Nurcombe, 2006; Gopal et al., 2010; Bass et al., 2011; Okina et al., 2012; Vuong et al., 2015; Mitsou et al., 2017). In this review, we highlight some of the intricate structural features of HS and their proteoglycans (PGs) that underpin such functionality, and discuss the importance of specific HSPG signatures in mediating the behavior of different stem cell types.

HS STRUCTURE AND BIOSYNTHESIS

The basic structural unit of the HS polysaccharide is that of a repeating disaccharide composed of uronic acid (either glucuronic acid or its C5-epimer, iduronic acid) β1,4 linked to *N*-glucosamine, which may be *N*-acetylated, *N*-sulfated or in rare circumstances, *N*-unsubstituted (free amine) (**Figure 1**; Esko and Lindahl, 2001). A wide range of structural diversity and functional complexity is conferred upon modification of the constituent monosaccharides—the uronic acid may be sulfated at the C2 position and the glucosamine at the *N*, C6 and rarely, C3 positions. The synthesis of HS is carried out within the Golgi apparatus by a series of biosynthetic enzymes (**Figure 2**), through the catalysis of nucleotide sugars (such as UDP-glucosamine) and the nucleotide sulfate donor 3′-phosphoadenosine-5′-phosphosulfate (PAPS) (Esko and Lindahl, 2001). The majority of HS biosynthetic enzymes are type II integral Golgi membrane proteins except for 3-*O*-sulphotransferase 1 (3OST1), which possesses an intraluminal resident form (Shworak et al., 1997).

HS chains are attached to PG core proteins as post-translational modifications via a linkage tetrasaccharide. This "linker" sequence is composed of a glucuronic acid residue, two galactose residues and a xylose residue covalently bound to a serine hydroxyl group through a xylosidic bond (Lindahl and Rodén, 1965; Lindahl, 1966). A heterodimeric complex of the HS co-polymerases exostosin 1 and 2 (EXT1 and EXT2) alternatively adds *N*-glucosamine and glucuronic acid residues, resulting in the basic structure and length of the chain. Following this, *N*-deacetylase/*N*-sulphotransferase (NDST; 4 isoforms) removes acetyl groups and adds a sulfate moiety to the *N* position of select glucosamine residues. This process yields short *N*-sulfated domains that serve as substrates for further modification. On rare occasion, deacetylated glucosamine residues may be left as free amine groups (Sheng et al., 2011; Dou et al., 2015). Next, glucuronyl C5-epimerase (GLCE) selectively converts glucuronic acid residues into iduronic acid, a process that requires an adjacent *N*-sulphoglucosamine at the non-reducing end (Hagner-McWhirter et al., 2004). This is followed by 2-*O*-sulfation at the C2 position of the uronic acid, brought about by 2-*O*-sulphotransferase (2OST); this modification occurs predominantly in iduronic acid residues rather than glucuronic acid (Smeds et al., 2010). Subsequently, the C6 positions of select glucosamine residues are sulfated by 6-*O*-sulphotransferase (6OST; 3 isoforms) (Xu et al., 2017). In rare cases, the C3 position may also be sulfated by 3-*O*-sulphotransferase (3OST; 7 isoforms) (Shworak et al., 1999). At this stage, HS is transported to the cell surface where a final modification involving the selective removal of 6-*O*-sulfate groups from glucosamine residues may occur, through the action of extracellular 6-*O*-endosulphatase (SULF; 2 isoforms collectively referred to as "sulfatases") (Ai et al., 2003).

THE INTRICATE STRUCTURE OF HS IMPARTS ESSENTIAL FUNCTIONS

A complete HS chain possesses complex structural heterogeneity seldom observed in most biomolecules. Short, highly sulfated,

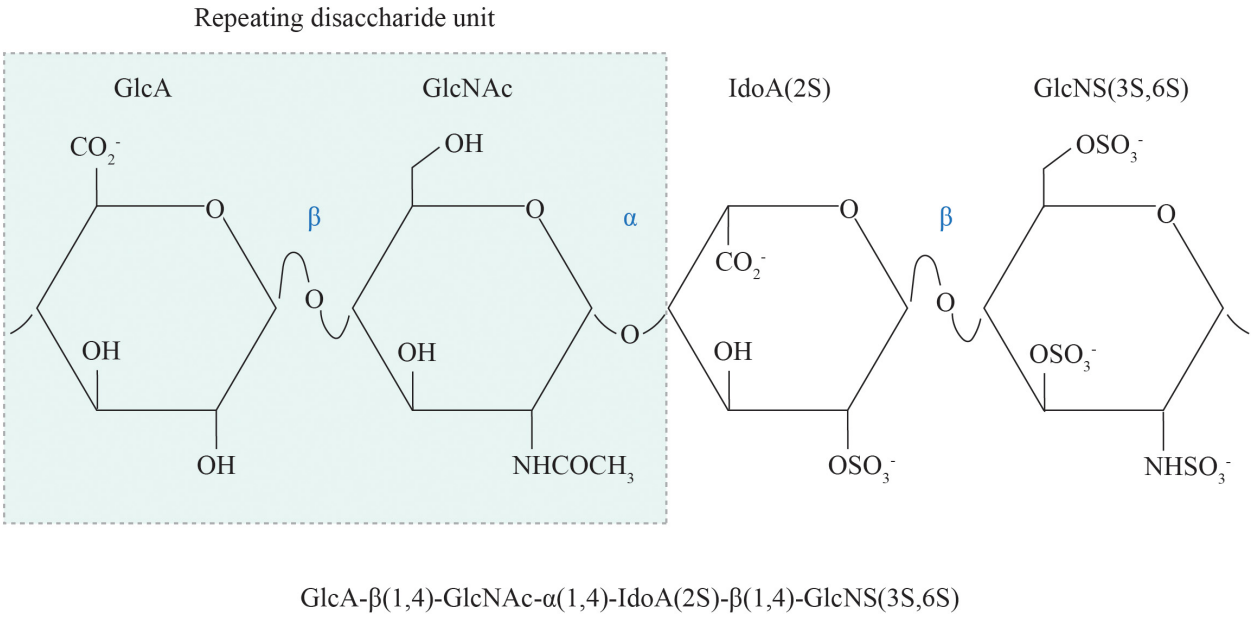

FIGURE 1 | The chemical structure of HS. The repeating disaccharide unit of HS comprises a GlcA residue linked to GlcNAc residue via a β1,4 glycosidic bond. Selective GlcA monosaccharides undergo epimerization to IdoA, which is particularly susceptible to sulfation at the C2 position. Sulfate moieties may also be added to the *N*, C6 and rarely, C3 positions of the glucosamine residue. GlcA, glucuronic acid; GlcNAc, *N*-acetyl glucosamine; IdoA, iduronic acid; GlcNS, *N*-sulfated glucosamine; 2S, 2-*O*-sulfation; 6S, 6-*O*-sulfation; 3S, 3-*O*-sulfation.

and heterogeneous regions (NS domains) are flanked by short transition domains of variable sulfation (NA/NS domains) (**Figure 2**). The NA/NS domains are interconnected by long, flexible regions of little to no modification (NA domains) (Turnbull and Gallagher, 1990, 1991; Maccarana et al., 1996; Gallagher, 2001). HS functionality is imparted predominantly by the highly negatively charged NS domains. The disaccharide residues in these regions are capable of interacting with small hydrophilic clusters of positively charged amino acid residues, such as lysine and arginine, common characteristics observed within the three-dimensional structure of HS-binding proteins (Cardin and Weintraub, 1989; Faham et al., 1996; Rudd et al., 2017). Interactions of HS with the fibroblast growth factor (FGF) family and their cognate receptors (FGFRs) serve as quintessential examples of this feature, which underpins the role of HSPGs as low-affinity co-receptors (Rapraeger et al., 1991; Yayon et al., 1991; Nurcombe et al., 1993).

A high affinity binding site for FGF2 in fibroblast-derived HS was discovered to be an oligosaccharide that is 7 disaccharides in length or has a degree of polymerization of 7 (dp7) (Turnbull et al., 1992). This dp7 fragment and other longer heparin/HS-derived oligosaccharides containing the dp7 sequence were characterized by an enrichment of 2-*O*-sulfated iduronic acid (IdoA2S) and *N*-sulfated glucosamine (GlcNS) residues (Turnbull et al., 1992; Ishihara et al., 1994; Kreuger et al., 1999). The necessity of these IdoA2S and GlcNS residues for FGF2 binding was evidenced when treatment of the dp7 fragment with heparinase led to an abolishment of FGF2 binding. Moreover, other similarly sized oligosaccharides with reduced 2-*O*-sulfation exhibited lower affinities for FGF2, highlighting the requirement of contiguous stretches of highly sulfated disaccharides for strong FGF2 binding (Turnbull et al., 1992). Further enquiry into the compositional features of HS and heparin oligosaccharides that are required for FGF interactions has shown that the FGFs bind to certain shared HS epitopes with low affinity and selectivity (Kreuger et al., 2005). However, distinct sulfation patterns and chain lengths allow for the formation of specialized NS domains in the GAG chain, which preferentially bind specific FGFs with a higher affinity than others (Guimond and Turnbull, 1999; Schultz et al., 2017). For example, while IdoA2S and GlcNS residues are essential for FGF2 binding, additional 6-*O*-sulfation of GlcNS residues (GlcNS6S) is required for high affinity binding to FGF1 and FGF4 (Ishihara, 1994; Kreuger et al., 1999; Ashikari-Hada et al., 2004). The binding affinity of HS/heparin oligosaccharides to FGF1 and FGF4 is also reported to correlate with chain length. Kreuger et al. (1999) have shown that the minimum length required for a heparin oligosaccharide to exhibit binding affinity to FGF1 is dp6. However, dp10 fragments and larger are needed for tight binding with both FGF1 and FGF4 (Ishihara, 1994; Kreuger et al., 1999).

In addition to FGF binding, HS chains bind to corresponding FGFRs to enhance ligand–receptor interactions and promote receptor dimerization for ternary complex formation (Ornitz et al., 1992; Spivak-Kroizman et al., 1994; Pellegrini et al., 2000; Schlessinger et al., 2000). While 6-*O*-sulfate moieties on glucosamine residues of HS/heparin are dispensable for FGF2 binding (Guimond et al., 1993; Maccarana et al., 1993; Ishihara et al., 1994), they are required for engaging FGFR, facilitating ternary complex formation and subsequently,

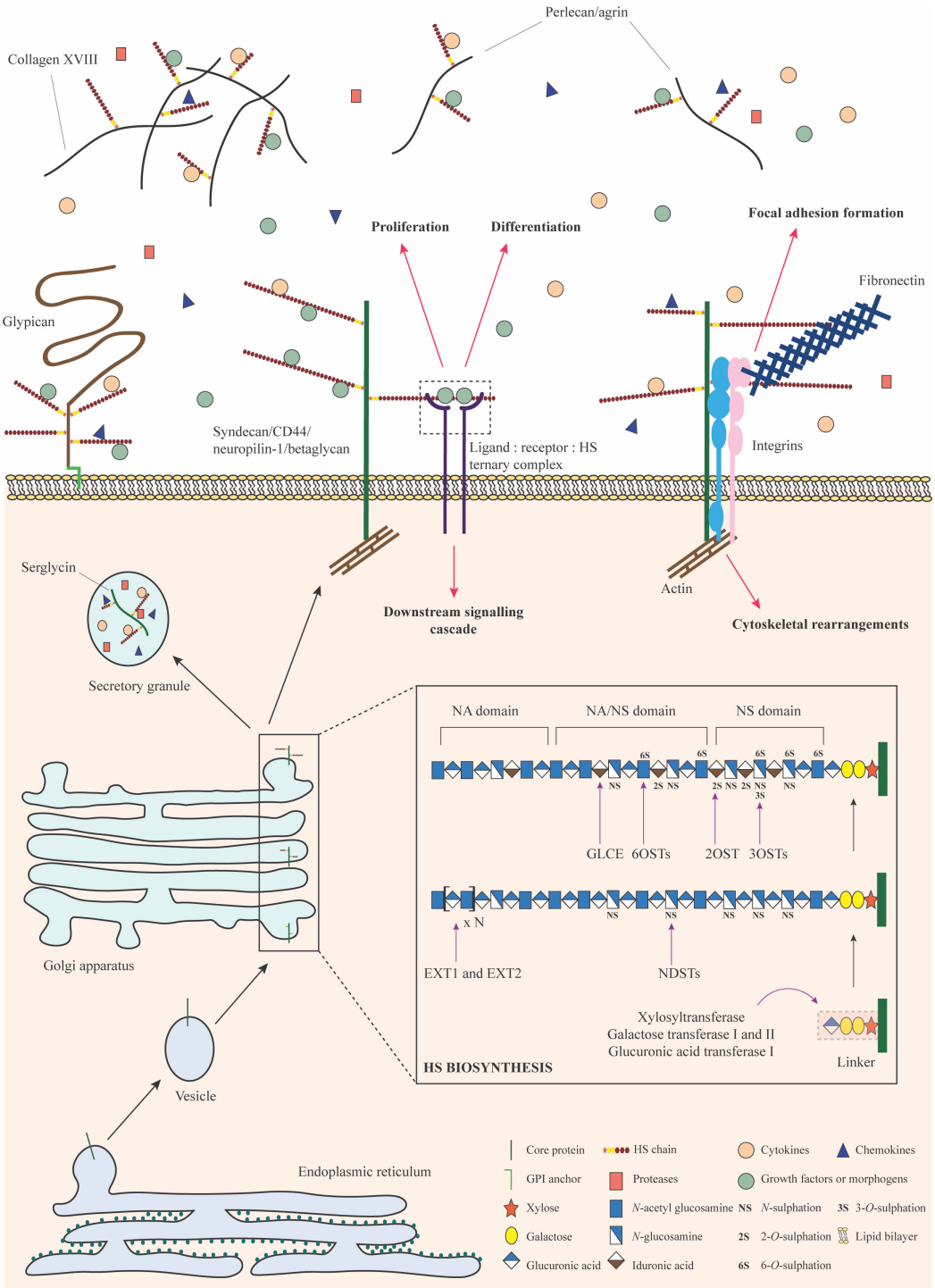

FIGURE 2 | HSPG biosynthesis and functions. HS biosynthesis is a sequential process that occurs in the Golgi apparatus. It is initiated by the formation and attachment of a tetrasaccharide linker to a serine residue on the core protein. Subsequently, chain polymerization is carried out by EXT1 and EXT2, where *N*-acetylglucosamine and glucuronic acid residues are added in succession. The HS chain is then modified by a collection of enzymes including the NDSTs, GLCE, 2OST, 6OSTs, and 3OSTs. Selective sulfation and epimerization confer intricate structural nuances to the HS chain, underpinning the formation of domains with distinct functional features. Upon exit from the Golgi apparatus, HSPGs may be stored in secretory granules, transported to the plasma membrane or secreted into the ECM. They bind to a variety of signaling factors and function as co-receptors to mediate signaling cascades important for stem cell proliferation and differentiation. HSPGs may engage with integrins, fibronectin, and actin filaments to bring about cytoskeletal reorganization for focal adhesion formation or migration. HSPGs can also sequester signaling molecules in the ECM and regulate their bioavailability. Monosaccharides in this figure have been represented in accordance with the symbol nomenclature for glycans (SNFG) (Varki et al., 2015).

activating the mitogenic effect of FGF2–FGFR interactions (Ostrovsky et al., 2002). In a study by Guimond and colleagues, exogenous full-length heparin was capable of rescuing the mitogenic effect of FGF2 in fibroblasts devoid of HS. However, selective 6-*O*-desulfation of heparin inactivated FGF2-induced mitogenesis, even though the oligosaccharide was able to bind FGF2 and compete with endogenous heparin for FGF2 binding (Guimond et al., 1993). The requirement of 6-*O*-sulfate moieties for activating FGF2-dependent mitogenesis upon HS/heparin binding was further established when disaccharide analysis of a range of different HS oligosaccharides clearly showed that the major distinguishing factor between activating and inhibitory fragments was the extent of 6-*O*-sulfation (Pye et al., 1998). Apart from appropriately 6-*O*-sulfated residues, chain length was also found to be an important factor for determining the ability of a HS/heparin oligosaccharide to support FGF2 mitogenic activity. An exogenous heparin-derived dodecasaccharide (dp12) was comparable to full-length heparin in rescuing the mitogenic effect of FGF2 in fibroblasts devoid of HS, whereas HS/heparin fragments lower than dp10 lacked the ability to support this activity (Guimond et al., 1993; Ishihara, 1994; Pye et al., 1998). Therefore, the structural and compositional features of HS heavily influence the functional properties of the chain, and consequently, the ability of HSPGs to operate effectively as signaling co-receptors (Goodger et al., 2008; Jastrebova et al., 2010).

HETEROGENEITY IN HSPG COMPOSITION AND LOCALIZATION CAN INFLUENCE STEM CELL FATE

Structural and functional heterogeneity in HSPGs has been observed between different cell types and within particular cell populations over time (Turnbull and Gallagher, 1988; Allen et al., 2001). The HSPGs produced by a cell (heparanome) can be rapidly altered with changes in cell state. Such alterations can influence cell activity in distinct ways depending on the compositional complexity of the heparanome (Turnbull et al., 2001).

HSPG heterogeneity can be seen at both the GAG chain and core protein levels. Heterogeneity at the HS chain level has largely been attributed to the non-template and incomplete nature of the HS biosynthetic process, as well as the activity of multiple biosynthetic enzyme isoforms that may differ in their substrate specificities and the products they generate (Aikawa and Esko, 1999; Liu et al., 1999; Habuchi et al., 2000; Turnbull et al., 2001). Post-biosynthetic alterations to sulfation and chain length are also known to contribute to the structural diversity and associated functional variability in HS. For example, selective removal of 6-*O*-sulfate groups by the SULF enzymes, SULF2 in particular, may lead to domain reorganization within the HS chain, prevent the binding of HS to signaling factors and consequently, alter ligand–receptor interactions that influence stem cell or progenitor cell fate decisions (Ai et al., 2003; Lai et al., 2003; Hammond et al., 2014). The drastic effects that a lack of appropriate HS moieties can have on signaling and progenitor cell function was examined in MM14 myoblast cultures *in vitro*—desulfation of cell surface HS by heparinase or chlorate treatment prevented FGF2 binding to cognate cell surface receptors and removed the suppressive effect of FGF2 on myoblast differentiation (Rapraeger et al., 1991). A similar trend was observed with the addition of selectively 6-*O*-desulfated heparin to MM14 cultures. The heparin oligosaccharides competed with endogenous HS for FGF2 binding and precluded FGF2–FGFR interactions that normally suppress cell cycle exit and myogenic activation (Guimond et al., 1993). The cleavage of 6-*O*-sulfates from cell surface and secreted HSPGs can also lead to the release of previously bound signaling factors and an increase in the bioavailability of these factors within the ECM (Uchimura et al., 2006; Rosen and Lemjabbar-Alaoui, 2010). Alternatively, the biodistribution of signaling molecules in the ECM may be altered as a result of HS chain cleavage by the single copy heparanase enzyme (HPSE), since cleavage releases biologically active HS fragments that are capable of binding and sequestering signaling factors within the extracellular space (Kussie et al., 1999; Hulett et al., 2000; Vlodavsky et al., 2002).

In the case of core proteins, heterogeneity can result from the differential expression of encoding genes. Spatiotemporal variability in the expression of core proteins, especially during development and wound healing, can influence signaling events at the cell surface and affect a stem cell's responsiveness to its surroundings (Bernfield et al., 1993; Olczyk et al., 2015). The collection of core proteins present at the cell surface and their localization may also be altered upon cleavage of PG ectodomains in a process known as "shedding" (Nam and Park, 2012). Studies have shown that shedding is mediated by a variety of proteases and phospholipases, collectively known as "sheddases," which can exhibit specificity toward particular core proteins. For example, the syndecans are known targets of a number of matrix metalloproteinases (MMPs), such as MMP7, MMP9, and ADAM17 (Ding et al., 2005; Brule et al., 2006; Pruessmeyer et al., 2010). Recently, ADAM17 has also been reported as a glypican sheddase, in addition to conventional phospholipases, such as Notum, that cleave at the GPI anchor (Traister et al., 2008; Kawahara et al., 2017). The shedding process yields bioactive soluble forms of HSPGs in the ECM that act as paracrine or autocrine effectors, and compete against cell-surface/matrix-bound HS (Nam and Park, 2012). The intact HS chains attached to the cleaved PG ectodomains can also operate as reservoirs that bind signaling molecules and regulate their diffusion, aiding in the maintenance of morphogen gradients that direct stem cell responses (Yan and Lin, 2009).

Heterogeneity in chain composition, core protein expression and PG localization underpin a highly diverse heparanome, which may directly influence the repertoire of molecular cues within a cell's microenvironment as well as the cell's ability to respond to them. However, there are several important questions yet to be answered regarding this diversity, especially pertaining to potential differences in functionality between cell surface HSPGs, cleaved or shed HSPGs, and secreted HSPGs. It remains to be understood whether HSPGs vary in the HS chains they carry depending on the core protein type and positional status. Current experimental methods to examine HSPG composition

and function involve the extraction of PG pools from cell cultures or tissues and therefore, lack the resolution to interrogate distinct HSPG fractions or individual HSPGs. Such an inability to probe potentially unique compositional characteristics and mechanisms of action of specific HSPGs presents a major challenge in the field, and has hindered an understanding of fine functional nuances that may exist between HSPGs.

HSPGS AS ORCHESTRATORS OF DEVELOPMENT AND DIFFERENTIATION

Lessons From Knockout Mouse Models

Over the past two decades, genetic modification has been one of the primary methods used for investigating the functions of HS modifications in mediating stem cell fate during development and differentiation. The knockout (KO) of individual genes from the HS biosynthetic pathway has revealed essential roles played by distinct modifications in tuning cellular responses to GFs, cytokines, chemokines, and morphogens.

Ext1 Knockout

In 2000, Lin and colleagues first developed the *Ext1*$^{-/-}$ mouse, which was devoid of HS due to the loss of the HS co-polymerase EXT1 (Lin et al., 2000). *Ext1*$^{-/-}$ embryos failed to develop beyond the blastocyst stage, clearly indicating that HS is an essential regulator of gastrulation and embryogenesis. Analysis of *Ext1*$^{-/-}$ embryonic stem cell (ESC) behavior *in vitro* has been carried out extensively by the Merry lab, specifically with regards to the development of the neurectoderm and mesoderm (Johnson et al., 2007; Baldwin et al., 2008; Holley et al., 2011; Pickford et al., 2011; Meade et al., 2013). Over the course of several studies, the essential regulatory role of HS in the exit of murine ESCs (mESCs) from pluripotency was discovered; *Ext1*$^{-/-}$ ESCs were incapable of exiting the pluripotent state under neural (Johnson et al., 2007; Pickford et al., 2011; Meade et al., 2013) or mesodermal (Holley et al., 2011) differentiation conditions, instead retaining characteristics of pluripotent cells, such as high levels of OCT4 expression. Interestingly, the addition of exogenous heparin or HS was able to rescue differentiation in these studies, further indicating that HS is a crucial regulator of stem cell function.

These findings were further validated in two studies by Kraushaar et al. (2010, 2012), who revealed that *Ext1*$^{-/-}$ mESCs were capable of maintaining pluripotency despite the removal of leukemia inhibitory factor. The absence of HS resulted in defective FGF and BMP signaling, such that the KO mESCs were unable to respond to pro-differentiation factors. Additional studies have revealed potential compensatory mechanisms by which the levels of other sulfated GAGs (such as CS and DS) appear to be upregulated in *Ext1*- null cells. This idea was initially proposed in a study by Le Jan and colleagues, wherein *Ext1*$^{-/-}$ embryoid bodies (EBs; spheroid cell aggregates capable of crudely recapitulating early embryonic development) displayed increased levels of CS/DS, and were able to respond to VEGF as well as undergo sprouting angiogenesis despite the loss of HS (Le Jan et al., 2012). The existence of putative compensatory mechanisms between different GAG species and consequent effects on signaling cascades suggests yet another layer of complexity in the GAG-dependent modulation of stem cell behavior, which is yet to be fully explored.

Ndst1/2 Knockout

Whilst the loss of *Ext1*$^{-/-}$ highlights the absolute requirement of HS in development and differentiation, it does little to reveal how changes in specific modifications within the HS chain, such as *N*-sulfation, within the HS chain could affect the behavior of cells. As described previously, NDST1 and 2 are primarily responsible for laying down *N*-sulfate modifications and forming NS domains within HS (NDST1) and heparin (NDST2) (Forsberg and Kjellén, 2001). In 2004, Holmborn and colleagues derived *Ndst1/2*$^{-/-}$ mESCs; analysis of the HS produced in these cells indicated a total loss of *N*- and 2-*O*-sulfation. Interestingly, 6-*O*-sulfation was still present and transcripts for all three 6OSTs were expressed, with 6OST1 displaying the greatest transcript abundance (Holmborn et al., 2004). Although functional assays were not performed, it was revealed that the presence of NS domains was not a pre-requisite for 6-*O*-sulfation. This important observation may be attributed to the unique orientation in which the 6OSTs engage with the HS chain, which is markedly different to that adopted by other sulphotransferases (Xu et al., 2017).

A number of other studies have sought to better elucidate the role of HS *N*-sulfation in early differentiation events and maintenance of pluripotency through use of the *Ndst1/2*$^{-/-}$ mESC line. The loss of *N*-sulfation results in perturbed FGF4 signaling, which in turn manifests as a similar phenotype to *Ext1*$^{-/-}$ mESCs: an inability to exit the pluripotent state (Lanner et al., 2010). Subsequent investigation indicated that despite the loss of *N*-sulfation, *Ndst1/2*$^{-/-}$ mESCs were still able to respond to stimulation by BMP4 (Forsberg et al., 2012). This finding clearly reflected the differential nature and context-dependent role of HS in FGF and BMP signaling. HS is not essential for BMP:BMPRI complex formation, as is the case for FGF:FGFR. Instead, HS binds to BMPRII and enhances its recruitment to BMP:BMPRI complexes, facilitating receptor hetero-oligomerisation for signaling (Kuo et al., 2010). Recent studies have suggested that HS is also able to antagonize BMP signaling (Mundy et al., 2018), offering an insight into why *Ndst1/2*$^{-/-}$ mESCs are still capable of responding to BMP4 and differentiating down an osteoblastic lineage.

Further studies have revealed an essential requirement for *N*-sulfation in angiogenic sprouting and the response to VEGF (Jakobsson et al., 2006). Lack of *N*-sulfation prevented *Ndst1/2*$^{-/-}$ EBs from undergoing angiogenesis. However, chimeric EBs formed with *Vegfr2*$^{-/-}$ mESCs were able to effectively respond to VEGF. This indicated that HS in *trans* was capable of potentiating VEGF signaling and was sufficient to rescue the differentiation capacity of cells devoid of *N*-sulfated residues.

Embryonic Stem Cells

Preliminary studies on HS expression and function in ESCs focused on mESCs. Immortal, easy to culture and rapidly

proliferating, these cells were ideal for obtaining sufficient quantities of biological material to conduct detailed analyses of HS and its biosynthetic pathway. Nairn et al. (2007) used mESCs to study changes in GAG content and composition during differentiation to EBs and extra embryonic endoderm. Findings indicated that HS synthesis was upregulated, together with that of HA and CS/DS, during differentiation. Overall GAG sulfation increased as cells differentiated, with particularly high levels of *N*-sulfated HS disaccharides and di-sulfated CS type E disaccharides (Nairn et al., 2007).

Further studies from the Merry lab focused on early lineage commitment through the use of well-defined differentiation protocols aimed at recapitulating early germ layer specification (Smith et al., 2011). In 2007, an mESC Sox1-green fluorescence protein (GFP) reporter line, 46C, was used to analyze changes in HS sulfation through the course of differentiation to neural progenitor cells (NPCs) (Johnson et al., 2007). The study reported a clear rise in HS sulfation as cells exited a pluripotent state and differentiated into NPCs. Increases in HS biosynthetic enzyme transcripts, FGF2 cell surface binding and *N*, 6- and 2-*O*-sulfated disaccharides were also observed. A similar study in 2008 assessed the changes in HS expression through the course of early mesoderm commitment in mESCs by using an epitope-specific single chain fragment-variable antibody (HS4C3) (Baldwin et al., 2008). During mesodermal differentiation toward the haemangioblast lineage, cells upregulated the HS4C3 epitope [previously identified as containing 3-*O*-sulfation (ten Dam et al., 2006)], coinciding with an upregulation in the transcription factor brachyury. Isolation and reaggregation of cells with high expression of the HS4C3 epitope and brachyury yielded a higher efficiency of differentiation into haemangioblasts, indicating that specific changes in HS fine structure are correlated with enhanced commitment to a particular mature lineage (Baldwin et al., 2008). This was further confirmed via immunocytochemical staining of sectioned primitive streak stage mouse embryos, which displayed high expression of the HS4C3 epitope in the developing mesoderm during gastrulation (Baldwin et al., 2008).

Hirano et al. (2012) proposed that the HS4C3 epitope influenced Fas signaling during mESC differentiation, with overexpression of 3-*O*-sulfation leading to enhanced Fas signaling and differentiation. Conversely, removal of 3-*O*-sulfation reduced Fas signaling and the differentiation potential of mESCs. A follow-up study showed that Fas signaling via the 3-*O*-sulfated epitope recognized by HS4C3 was indeed required for the transition between naïve and primed states, as mESCs differentiated into murine epiblast-like cells (Hirano et al., 2013). Such observations confirmed the importance of understanding rapid and subtle changes in HS fine structure during early differentiation events and tissue specification. Temporal and lineage-specific alterations in mESC HS structure can influence signaling pathways that mediate exit from pluripotency, highlighting HS as a key orchestrator of early developmental events.

Whilst many studies investigating the role of HS in pluripotent stem cell function have utilized mESCs due to their relative ease of culture and ability to readily produce genetic mutants, focus has begun to shift onto more relevant human ESCs (hESCs) and induced pluripotent stem cells (iPSCs). Gasimli and colleagues investigated changes in the structure of various GAGs, including HS, during the differentiation of hESCs toward mesodermal and endodermal lineages (Gasimli et al., 2014). Upon differentiation toward splanchnic mesoderm, several PG transcripts were markedly upregulated and an increase in HS sulfation was observed (predominantly *N*-sulfation). Differentiation toward an immature hepatocyte lineage yielded similar increases in HS sulfation, with an accentuation of *N*-sulfated, 6-*O*-sulfated HS (Gasimli et al., 2014). Such evidence highlights the potential importance of regulated variation in HSPG expression and HS fine structure during specification toward different germ layers and cell lineages. It also suggests a possibility that particular HSPG signatures, which predominate over others at distinct stages of lineage commitment, may be used to develop potential markers of differentiation. However, more evidence detailing chronological changes in HSPG composition and associated sequence motifs during lineage commitment is needed to improve an understanding of the relationship between the heparanome and differentiation status.

The use of hESCs has also expanded knowledge regarding the requirement of HS within the extracellular environment for guiding stem cell fate. A 2012 study indicated that matrix-bound HS is essential for the effective culture expansion and maintenance of pluripotency of hESCs (Stelling et al., 2012). Cells were cultured on a variety of substrates, including mouse embryonic fibroblasts (MEFs), ethanol-fixed MEFs, and MEFs devoid of HS. It was observed that hESCs maintained pluripotency marker gene expression when cultured on feeder layers presenting HS (both live and fixed). In contrast, HS-deficient layers were unable to support hESC attachment and growth (Stelling et al., 2012). Another group demonstrated that decellularized organ matrices were capable of influencing differentiation and lineage commitment of pluripotent stem cell-derived mesoderm progenitors through HSPG-bound tissue-specific factors (Ullah et al., 2020). Together, these data highlight that HS in *trans* within the surrounding matrix or culture substrata is crucial for the maintenance of homeostasis, as well as the regulation of ESC function.

Neuroepithelial Cells

The significance of HSPGs in early central nervous system (CNS) development was established from studies where the absence of key biosynthetic enzymes resulted in pronounced developmental abnormalities (Poulain and Yost, 2015). Conditional knockout of *Ext1* in the nervous system of murine embryos gave rise to severe midbrain and cerebellar deformities, underdeveloped cerebral cortices and a lack of key neuronal tracts, leading to postnatal lethality (Inatani et al., 2003). Defects in forebrain development, cerebral hypoplasia as well as craniofacial malformations, such as hydrocephalus, have also been described with deficiencies in *Ndst1, Hs2st1,* and *Sulf2*, respectively (McLaughlin et al., 2003; Grobe et al., 2005; Kalus et al., 2009). Notably, these developmental phenotypes were observed to overlap extensively with those obtained by knocking out genes encoding key morphogens, such as *Fgf8*, *Wnt1,* and *Shh*, during embryogenesis (Thomas et al., 1991; Chiang et al., 1996; Meyers et al., 1998).

This suggested an HS-dependency of these signaling factors in directing stem cell function for neural tube patterning.

Further inquiry revealed that HSPGs are essential prior to and during neurogenesis (Yamaguchi, 2001). Distinct spatiotemporal expression patterns of HS-binding FGFs have been observed to mediate the proliferation, survival and differentiation of neuroepithelial cells (NECs) as well as their radial glial cell (RGC) progeny (Murphy et al., 1990; Guillemot and Zimmer, 2011). For example, FGF2 and FGF8 support the expansion of NECs soon after specification in the neural tube, while the onset of FGF10 expression promotes the asymmetric division of mature NECs to form RGCs (Raballo et al., 2000; Storm et al., 2006; Sahara and O'Leary, 2009). Such nuanced FGF expression, FGF2 in particular, is accompanied by the presence of HSPGs as early as embryonic day 9 (E9) in murine neuroepithelial tissue (Nurcombe et al., 1993). Importantly, the functional properties of neuroepithelial HS were observed to change as embryogenesis progressed, in synchrony with changes in FGF expression. While HS derived from E9 tissue was able to bind FGF2 effectively in comparison to FGF1, a shift in binding affinity toward FGF1, rather than FGF2, was found in HS from E11. Such an alteration in binding affinity at E11 was attributed to compositional variations of HS, including longer chain length, greater number of sulfated domains and increased 6-*O*-sulfation in comparison to E9 chains (Brickman et al., 1998). Furthermore, a single core protein species was detected in both E9 and E11 neuroepithelial cultures, suggesting that HS chains on an individual PG may be rapidly modulated to complement, or even augment, the action of signaling molecules that regulate distinct NEC phenotypes (Nurcombe et al., 1993).

Several aspects of NEC behavior, including quiescence, responses to morphogen gradients, migration, self-renewal, and the generation of RGCs capable of differentiating, are regulated by HS-binding signaling factors. Moreover, distinct HSPGs appear to mediate such cellular events within the developing CNS. Perlecan has been identified to promote NSC proliferation by providing HS chains that function as co-receptors for FGF2 signaling, and also operate as an important component of the neural tube basement membrane (Joseph et al., 1996; Haubst et al., 2006; Girós et al., 2007). The presence of several membrane-bound syndecans has also been determined as important for neurogenesis. At E10, all 4 syndecans were found on the surface of NECs, with syndecan-1 mRNA expressed at the highest level (Ford-Perriss et al., 2003). Knockdown of syndecan-1 has been observed to attenuate canonical WNT signaling in NECs and RGCs, and severely diminish the proliferative capacity of these cells (Wang et al., 2012). This suggests that syndecan-1 normally functions to modulate proliferation-associated signaling cascades in early CNS development, much like syndecan-4, which has also been described to regulate proliferation during zebrafish neurogenesis (Luo et al., 2016). Additionally, syndecan-3 has been reported to facilitate neuroblast migration by triggering actin cytoskeletal changes. HS-dependent interactions with pleiotrophin and GDNF activate key intracellular signaling proteins, such as SRC kinase, and induce morphological changes required for cell motility (Raulo et al., 1994; Bespalov et al., 2011).

In addition to the syndecans, Ford-Perriss and colleagues also reported mRNA expression of most of the glypicans in E10 murine neuroepithelial tissue, with the exception of glypican-5 (Ford-Perriss et al., 2003). While knowledge regarding the exact functions of glypicans during neurogenesis remains limited, some studies have suggested roles in regulating stem cell proliferation, presumably via associations with FGFs. A loss of glypican-1 and corresponding FGF17 interactions in homozygous-null murine mutant embryos has been observed to hamper the proliferation of neuronal precursors and induce premature differentiation around E9, leading to a reduction in brain size (Jen et al., 2009). Maintenance of a proliferative stem cell phenotype has also been shown to depend on appropriate glypican-4 expression and putative FGF-binding. Glypican-4 has been observed to be persistently present in NECs within the ventricular zone but downregulated in their post-mitotic progeny (Hagihara et al., 2000). Although the mechanisms regulating such spatiotemporal variations in HSPG expression are yet to be elucidated, dynamic PG patterns seem to be hallmarks of neurogenesis, where distinct PG combinations function to fine-tune NEC responses at each stage of the developmental process. Such findings have led to the identification of particular HSPGs as potential biomarkers for neural lineage commitment, and have also suggested therapeutic targeting of these HSPGs for regulating neural stem cell function (Oikari et al., 2016; Yu et al., 2017).

HSPGS AS REGULATORS OF ADULT STEM CELL AND PROGENITOR FUNCTIONS

The role of HSPGs in adult stem cell (AdSC) populations is less well understood compared to ESCs and their progeny, primarily because such analysis is dependent on the ability to identify and purify tissue-specific stem cells. While some AdSC populations have been relatively easy to access for cell isolation, others remain elusive.

Haematopoietic Stem Cells and Progenitors

Studies investigating the presence and role of polysaccharides in the bone marrow stroma gained momentum during the 1970s; a 1978 study demonstrated that GAGs or mucopolysaccharides could influence *in vitro* erythrocytic proliferation and differentiation (Ploemacher et al., 1978). Other investigations detected the presence of sulfated GAGs in the bone marrow stroma and suggested a role for stromal cells in producing them to support haematopoiesis (McCuskey and Meineke, 1973; Del Rosso et al., 1981). Simultaneous inquiry into the conditions required for long-term culture of HSCs and their progenitors (HPCs) revealed the dependence of these cells on adhesion with mesenchymal stromal cell feeder layers (Dexter et al., 1977; Reimann and Burger, 1979; Gartner and Kaplan, 1980; Bentley and Tralka, 1983), further endorsing the idea of stroma-derived HS as a putative mediator of cell–cell and cell–matrix interactions required for HSC survival and function.

The significance of stromal cell HS for *in vitro* haematopoiesis was confirmed when HS was found to be enriched in extracts of stromal feeder cells of long-term haematopoietic cultures and haematopoiesis-supportive bone marrow stromal cell lines (Gallagher et al., 1983; Wight et al., 1986; Kirby and Bentley, 1987). In a study by Gallagher et al. (1983), high proportions of disaccharide and tetrasaccharide species obtained by nitrous acid digestion of stromal HS demonstrated the presence of *N*-sulfate rich domains. Oligosaccharide mapping revealed that HS produced by cultured bone marrow stromal cells is enriched in highly sulfated disaccharides, indicating extensive protein-binding properties (Turnbull and Gallagher, 1988). Furthermore, work from our group has shown that in the presence of pro-haematopoietic cytokines, an exogenous 6-*O*-sulfate-rich bone marrow stromal cell-derived HS variant is capable of maintaining a subset of primitive HSCs during *ex vivo* expansion. These cells exhibit improved clonogenicity and an increased propensity to form erythroid and granulocyte progenitors, highlighting the capacity of 6-*O*-sulfate-rich HS fragments to enhance HSC properties (Bramono et al., 2011). Other studies have detailed the role of extracellular HS in inducing differentiation of naïve HPC-like cells. For example, HL-60 promyelocytic leukemia cells were observed to acquire a mature phenotype when grown on marrow stroma-derived matrix, which was abrogated upon heparinase treatment (Luikart et al., 1990). Moreover, the pro-differentiation effect was recapitulated when exogenous heparin was added to the cultures. The ability of HS/heparin in *trans* to guide HPC fate was similarly exhibited, when addition of HS to megakaryocyte progenitor cultures augmented megakaryocytopoiesis (Han et al., 1996).

To better understand the function of stromal HS during haematopoiesis, several studies investigated HS binding to bone marrow-relevant signaling molecules. Gordon and colleagues found that stroma-derived GAGs, of which HS was a major constituent, were capable of binding to granulocyte-macrophage colony stimulating factor (GM-CSF), while negligible binding was observed between liver-derived GAGs and GM-CSF (Gordon et al., 1987). They posited that this selective binding was due to stroma-specific structural features of GAGs that enabled compartmentalization and appropriate presentation of signaling molecules important for HPC function. In addition to GM-CSF, stroma-derived HS was also capable of binding interleukin (IL)-3, a key multilineage haematopoietic signaling factor (Roberts et al., 1988). Subsequently, various heparin/HS-binding proteins were found in the bone marrow stroma including GFs, chemokines as well as morphogenetic proteins such as BMPs, WNT, and SHH (reviewed in Papy-Garcia and Albanese, 2017).

In addition to its involvement in signaling events, HS produced by the bone marrow stroma was also found to be involved in the adhesion of HPCs and HSCs to stromal cells. Treating HPC-stromal cell cultures with sodium borohydride was observed to strip HS from cell-surface protein cores and destroy cell–cell binding activity (Siczkowski et al., 1992). De-sulfation of HSPGs as a result of sodium chlorate treatment was also found to decrease HPC adhesion to stromal feeder cells (Zweegman et al., 2004). Apart from adhesion, HSPGs in the marrow stroma are important participants in CXCL12/CXCR4-dependent cascades that orchestrate HPC migration, homing and retention, especially after transplantation. Netelenbos and colleagues conducted a study where subendothelial matrices produced by bone marrow endothelial cells were used to coat filters in a transwell migration assay using HPCs (Netelenbos et al., 2002). Cells were observed to migrate through the filters toward CXCL12 (stromal cell-derived factor-1; SDF-1)-enriched media, which did not occur in the absence of CXCL12. Importantly, HPC migration was significantly reduced when the matrix filter was treated with heparinases. This indicated that subendothelial ECM-associated HS was essential for trans-matrix migration in response to CXCL12 and is likely involved in CXCL12 presentation. A follow-up paper by the same group demonstrated that HS produced by bone marrow endothelial cells binds to cell surface CXCL12 in an autocrine manner, and assists in its interactions with CXCR4 on migrating HPCs (Netelenbos et al., 2003).

While the requirement of stromal HS in mediating HSC and HPC function has been well established, the significance of specific sequence motifs and particular PG core proteins remains to be understood. In-depth compositional analysis of stroma-derived HS coupled with gene expression profiling of HSPG core proteins in stromal cells may provide preliminary insights. Nonetheless, studies exploring the significance of HS in HSC and HPC function has progressed at a rapid pace, whereas evidence of the roles of HS in other marrow resident progenitor functions has unfolded more slowly. An important factor that has facilitated thorough investigations of HSC properties is a well-defined, robust *in vitro* culture system. This highlights the need for similar approaches to be adopted to further our understanding of other tissue-specific stem cell types that may be less amenable to *ex vivo* expansion.

Mesenchymal Stem Cells

Mesenchymal stem cells (MSCs) were initially described as marrow-derived proliferative, colony-forming and plastic adherent cells (Friedenstein et al., 1974). Subsequent studies led by Caplan's group to better characterize these cells led to the discovery of their multilineage potency: they were able to form osteoblasts, chondrocytes and adipocytes *in vitro* and when transplanted *in vivo* (Osdoby and Caplan, 1976; Caplan, 1991). Although the *in situ* identity and function of MSCs has remained controversial, these cells continue to be widely studied and are valuable tools for use in cell therapy applications, especially by virtue of their immunomodulatory secretome (Weiss and Dahlke, 2019).

An important challenge for the successful clinical use of MSCs is their inherent heterogeneity, particularly after culture expansion. MSCs have been reported to show variability in both surface marker expression and function, including biased differentiation potential and clonogenic capacity, depending on their tissue of origin and/or culture conditions (da Silva Meirelles et al., 2006; Traktuev et al., 2008; Hagmann et al., 2013; Holley et al., 2015; Elabd et al., 2018). While transcriptomic approaches have dominated the toolkit for MSC analysis, glycomic analysis and GAG profiling of MSCs are yet to be adopted for more comprehensive characterization. As discussed earlier (see section "Heterogeneity in HSPG Composition and

Localization Can Influence Stem Cell Fate"), heterogeneity in HS composition can influence stem cell fate decisions. Owing to the significant tissue-dependent differences observed in MSC functional properties, it is highly likely that these are accompanied by distinct tissue-specific HS signatures. Therefore, we deem it prudent to investigate the status of HSPGs, as well as other GAGs/PGs, in MSCs.

Together with transcriptomic analysis, glycomic data will allow for a better understanding of the mechanisms related to the functional heterogeneity of these cells. Furthermore, knowledge regarding the roles of particular HS signatures in mediating MSC properties will allow for the synthesis of desirable HS adjuvants to culture media (see section "Exploiting the HSPG-Stem Cell Relationship for Therapeutic Use: HS as an Adjuvant for the Expansion of Potent MSCs"). This approach may permit the development of improved expansion regimens, wherein tailored HS oligosaccharides are capable of maintaining reservoirs of appropriate GFs and other signaling molecules in the ECM for better control of MSC fate *in vitro*.

Osteogenic and Chondrogenic Progenitors

Osteogenic and chondrogenic differentiation have been widely studied *in vitro*. Both trajectories involve drastic changes in the composition of the ECM, with the laying down of a mineralized matrix being a hallmark of osteogenesis (Assis-Ribas et al., 2018). Importantly, alterations in the expression of genes encoding PG core proteins and HS biosynthetic machinery have been reported during osteogenesis (Haupt et al., 2009). Pre-osteoblasts cultured in osteogenic media were observed to increase the mRNA and protein levels of several PG core proteins as they matured. While glypican-3 displayed the most significant increase, followed by all 4 syndecans, glypican-2 and glypican-4 showed moderate increases. There were also variations in gene expression levels of some biosynthetic enzymes: a decrease in *Ext1/2* gene expression was noted, with contrasting increases in *Ndst1/2*, *Hs2st1,* and *Hs6st1* as differentiation progressed.

A study from Zhao and colleagues also reported an upregulation of 6OST3 at the mRNA and protein levels as MSCs underwent calcification (Zhao et al., 2015). Collectively, data from these studies indicate that as pre-osteoblasts or MSCs progress through osteogenesis, HS chain initiation may decrease while overall chain sulfation may be increased. Moreover, siRNA knockdown of glypican-3 or 6OST3 was found to decrease differentiation down the osteogenic lineage (Haupt et al., 2009; Zhao et al., 2015), suggesting the necessity of unique HSPG motifs for progression through the lineage commitment process. Further investigations into the functional features of unique HS/heparin signatures in osteogenesis have demonstrated distinct binding properties for proteins that mediate important pro-differentiation signaling cascades. For example, bone marrow-derived HS is able to bind with high affinity to, and enhance the osteoinductivity of BMP2 (Bramono et al., 2012). In another study, highly sulfated heparin was found to bind WNT3A with high affinity and promote the osteogenic activity of pre-osteoblasts (Ling et al., 2010). To improve our understanding of how the heparanome may be altered during osteogenesis and the resulting functional effects this may have on stem cell differentiation, additional studies may be undertaken where HS pools are extracted from cultures at various stages of the osteogenic process. Subsequent HS disaccharide isolation and characterization would provide information regarding the compositional features of HS during differentiation, and also offer evidence to complement existing gene expression data for biosynthetic enzymes.

The role of HS as an important regulator of chondrogenesis was first demonstrated in 1987 using micromass cultures of chick limb bud mesenchyme (San Antonio et al., 1987). Addition of either exogenous HS or heparin was found to enhance chondrogenesis and cartilage nodule formation in a dose-dependent manner. The involvement of HSPG core proteins in chondrogenesis has also been demonstrated *in vitro* (Gomes et al., 2004). The ability of perlecan to induce chondrogenesis was tested by plating MSCs on surfaces coated with intact perlecan or recombinant perlecan domain 1. Plated cells were found to attach and aggregate into dense cell condensations, and proceed to express chondrogenic differentiation markers such as collagen type II and aggrecan. This phenotype was not obtained with cells plated with other PGs or perlecan domains, suggesting that only certain HSPGs possess structural features that support chondrogenesis. Other groups have further explored the role of HS in chondrogenesis primarily by assessing the effects of exogenous HS on chick limb mesenchymal cells (LMCs) or MSC cultures. Addition of HS or BMP2 alone to LMC cultures led to only a moderate improvement of Alcian blue staining (Fisher et al., 2006). However, the addition of HS and BMP2 together significantly accentuated staining compared to individual treatments. The presence of HS was able to potentiate the activity of BMP2, as indicated by increased phosphorylation of SMAD proteins, and lowered the concentration required to stimulate chondrogenesis to an equal or even greater extent as compared to high concentrations of BMP2 alone. Similarly, combined exposure of HS and TGF-β3 resulted in higher cartilage-specific gene expression levels and even induced remodeling of the surrounding microenvironment by increasing cartilage matrix protein production compared to TGF-β3-only or HS-only treatments (Chen et al., 2016).

While the significance of HSPGs in mediating chondrogenesis has been documented mainly through examining the effects of exogenous HSPGs on differentiation, the heparanome status of the stem cells themselves during chondrogenic lineage commitment is unknown. Gene expression analysis of biosynthetic enzymes coupled with glycomic profiling of cultures undergoing chondrogenesis would strengthen our knowledge of how HSPGs may influence this differentiation process. Furthermore, such data would provide a basis for subsequent mechanistic studies that probe into the functional attributes of the heparanome as chondrogenesis ensues.

Muscle Satellite Cells and Myoblasts

Satellite cells (MuSCs) are stem cells within skeletal muscle that are normally quiescent within a specialized niche located between the plasma membrane and basement membrane of myofibres

(Mauro, 1961). They exit quiescence, resume cell cycle activity and acquire a myoblast identity for muscle regeneration, in response to triggers such as exercise or injury. A fine balance of signaling events is essential for an appropriate MuSC response. Of the many families of signaling factors, FGFs emerged as key participants in mediating MuSC activity (Pawlikowski et al., 2017). Studies in the 1980s showed that exposure of muscle progenitors to FGF1 or FGF2 resulted in strong mitogenic effects and concomitant repression of terminal differentiation (Lathrop et al., 1985; Clegg et al., 1987). FGF deprivation of cells that were initially exposed resulted in withdrawal from the cell cycle and simultaneous expression of myosin heavy chain. The indication of FGFs as inhibitors of myogenic differentiation was further corroborated when it was shown that exposure of myoblasts to FGF also inhibited myogenin expression (Brunetti and Goldfine, 1990). Not long after, the integral role of HS, and their 6-*O*-sulfated residues in particular, in facilitating FGF signaling in MuSCs became evident. Rapraeger and colleagues demonstrated that treatment of MM14 cultures with either sodium chlorate or heparinase abolished FGF signaling (Rapraeger et al., 1991). Cells ceased proliferation and stained positive for myosin heavy chain, recapitulating results obtained upon FGF deprivation (Lathrop et al., 1985; Clegg et al., 1987). In a follow up study, the group reported that the addition of heparin to chlorate-treated cultures rescued FGF signaling, further highlighting the role of HS in mediating FGF-dependent repression of myogenic differentiation (Olwin and Rapraeger, 1992).

The use of the MM14 culture system has provided information on another key feature of myogenesis, which is a change in the expression of myoblast HSPG core proteins. Analysis of MM14 PGs showed a decrease in syndecan expression in differentiated cells compared to proliferative counterparts (Olwin and Rapraeger, 1992). A decrease in syndecan-3 expression along with perlecan, at both protein and mRNA levels, was also observed as C2C12 myoblasts differentiated into myotubes (Larraín et al., 1997; Fuentealba et al., 1999). Inhibition or genetic ablation of syndecan-3 expression in myoblasts or MuSCs drastically decreases sensitivity to FGF2-dependent inhibition of myogenesis, and also precludes signaling via the Notch pathway (Fuentealba et al., 1999; Pisconti et al., 2010). As a result, cells undergo reduced self-renewal and precocious acquisition of a differentiated phenotype, which can be reversed by exogenous heparin. In contrast to syndecan and perlecan, glypican-1 expression has been observed to be maintained both on the cell surface and as a secreted form in the ECM throughout the myogenic process (Campos et al., 1993; Brandan et al., 1996). Localization of glypican-1 in lipid rafts at the cell membrane was found to be an important mechanism that sequesters FGF2, prevents interactions with FGFRs and inhibits myoblast differentiation. A deficiency in glypican-1 was unable to restrict FGF:FGFR interactions and led to defective differentiation of C2C12 cells (Gutierrez and Brandan, 2010). Collectively, these results indicate that intricate spatiotemporal variation and control of HSPG expression *in vitro* is pivotal in modulating FGF signaling for myogenic activity.

Further investigations of the roles of HSPGs in myogenesis have extended such *in vitro* findings and shown that heterogeneity in core protein expression *in vivo* is crucial during muscle development and in adult skeletal muscle. While syndecans-1, -3, and -4 were found to be enriched in developing mouse skeletal muscle tissue, only syndecan-3 and syndecan-4 expression persisted in adult muscle, colocalized with FGFR1 (Cornelison et al., 2001; Olguin and Brandan, 2001). Cornelison and colleagues observed that the expression of both these FGFR-associated syndecans overlapped with c-MET, a key MuSC marker, suggesting a role for HSPG-mediated signaling in MuSC function *in vivo*. Moreover, treatment of adult myofibre explant cultures with sodium chlorate led to a significant decrease in MuSC numbers, and an associated increase in the percentage of cells expressing MyoD (Cornelison et al., 2001). Thus, a switch from MuSC proliferation to differentiation could be triggered in response to disruption of HS-dependent FGF signaling in MuSCs. The significance of specific patterns of HSPG expression in adult skeletal muscle was further supported by a study conducted by Casar and colleagues. They detected widespread HSPG expression by immunostaining [using the 3G10 monoclonal antibody (David et al., 1992)] in the myofibres of healthy mouse muscle (Casar et al., 2004). Following injury, an increased 3G10 signal was detected in the regenerating myotubes. Subsequent analysis of upregulated HSPGs identified syndecan-3, syndecan-4, glypican, and perlecan, with syndecan-3 upregulated the earliest in regenerating structures. In comparison, dysregulated HSPG expression, as in the case of syndecan-$3^{-/-}$ and syndecan-$4^{-/-}$ mice, severely impacted the ability to maintain homeostasis in the myogenic tissue and activate regenerative programs upon injury (Cornelison et al., 2004).

Apart from dynamic PG core protein expression patterns, variability in HS biosynthetic enzyme expression has also been identified in MuSCs. Langsdorf and colleagues found that only SULF1 was expressed, both at protein and mRNA levels, in quiescent mouse MuSCs. However, following muscle injury, a shift in *Sulf* expression was observed such that both SULF1 and SULF2 were detected in *Pax7*-positive MuSCs. To investigate the role of the SULF enzymes in myofibre regeneration, the group went on to characterize *Sulf* double mutant mice (Langsdorf et al., 2007; Tran et al., 2012). In the absence of *Sulf1* and *Sulf2*, the animals displayed an acutely delayed and compromised ability to regenerate muscle. GAG disaccharide analysis revealed that the lack of SULF enzymes led to a significant increase in 6-*O*-sulfation, with a notable rise in trisulfated disaccharide levels. Such an overtly sulfated HS signature was associated with an overactivation of the FGF pathway as well as an elevation in non-canonical WNT signaling, leading to an inhibition of differentiation and myoblast fusion (Langsdorf et al., 2007; Tran et al., 2012). These results identified SULF proteins as repressors of inhibitory FGF signaling in activated MuSCs and important gatekeepers of HS composition.

Although specific patterns of PG and biosynthetic enzyme expression seem to be important for myogenic activity during development and regeneration, the significance of specific HS domain structures and sulfation patterns in mediating these processes is largely unknown. Future studies focused on glycomic characterization are required for a better

mechanistic understanding of the functions of HS in regulating myoblast or MuSC fate.

Skin Stem Cells and Progenitors

Homeostasis within the skin layers and its appendages is maintained by several distinct stem cell and progenitor populations. The epidermal basal layer consists of rapidly diving stem cell progenitors (transit-amplifying cells) that work to continually replenish the epidermal layers (Potten and Morris, 1988; Fuchs and Raghavan, 2002). In response to appropriate triggers, these cells lose their attachment, both to one another as well as the underlying basement membrane (BM), and differentiate into keratinocytes (KCs) destined for stratification (Barrandon and Green, 1987; Blanpain and Fuchs, 2009). The involvement of HS and its PGs in the functional fidelity of KCs and the structural integrity of the skin BM has been an important area of research.

The role of HSPGs as key regulators of signaling is conserved in epidermal progenitors, as in the case of other previously discussed AdSC types. Several studies have highlighted the necessity of HS-binding GFs, including FGFs, GM-CSF and TGF-β, for the control of basal layer progenitor proliferation as well as differentiation (Mansbridge and Hanawalt, 1988; Finch et al., 1989; Szabowski et al., 2000; Zhu et al., 2014). The expression of HSPG core proteins has also been well established within the epidermis as well as along the entire length of the dermo-epidermal junction in the BM (Hassell et al., 1980; Caughman et al., 1987; Horiguchi et al., 1989). Importantly, the patterns of core protein expression within the epidermis are dynamic and have been found to change as KCs progress through terminal differentiation. Syndecan-1 expression was reported as modest in the basal layer, enriched in the suprabasal layer, and absent in superficial layers (Sanderson et al., 1992). This trend in syndecan-1 expression was recapitulated when stratification of KC monolayers was induced *in vitro*. The purified syndecan-1 from stratified samples was found to be more abundant than in monolayer controls and also had a lower molecular mass, which was attributed to differences in the composition of HS chains (Sanderson et al., 1992).

Unlike the syndecans, the expression patterns of glypicans are less well known in the epidermis. A study from 2006 utilized an immunohistochemical staining approach and detected diffused glypican-1 expression throughout the epidermis, while glypican-3 appeared restricted to the basal layer (Patterson et al., 2008). These results collectively indicate that unique profiles of HSPGs at different stages of KC differentiation serve specific functions in mediating cell fate decisions. In this regard, Sanderson et al. (1992) suggested that changes in HSPG composition are essential to facilitate the drastic alterations in KC adhesive properties required for detachment from the basal layer and subsequent migration. Likewise, the presence of HSPGs, such as perlecan, within the ECM has been found to heavily influence KC migration and organization. In a study by Sher et al. (2006), perlecan was detected in all epidermal layers apart from the stratum corneum when KCs were seeded on dermal equivalents. However, upon transfecting a perlecan antisense construct into KCs, differentiation was significantly altered. The cells formed an aberrantly organized epidermis that was only 1–2 layers thick. Notably, exogenous perlecan addition rescued the ability of KCs to form a well-differentiation, stratified epidermis.

Apart from the epidermis, HSPGs, syndecans in particular, have been identified in stem cell-rich hair follicles (HFs) (Couchman, 1993). To elucidate the role of HS in the HF, Coulson-Thomas et al. (2014) characterized a transgenic mouse model that was devoid of *Ext1* only in the outer root sheath (ORS), inner root sheath (IRS) and hair shaft. They observed a significantly increased number of HFs in transgenic mice compared to littermate controls. These HFs were observed to be arrested at anagen, unable to transition into catagen and telogen. Subsequent analysis revealed that cells within these HFs had impaired differentiation potential, due to uncontrolled signaling involving SHH. Thus, in the absence of HS, control of the intricate molecular networks that preside over stem cell fate decisions during HF cycling and homeostasis is severely perturbed. Widespread HSPG expression has also been observed in dermal papillae (DP), important stem cell-containing signaling centers at the base of HFs that regulate epithelial stem cells and keratinocytes for HF cycling (Driskell et al., 2011; Morgan, 2014). Notably, HSPG expression patterns have been found to be spatiotemporally variable in the DP matrix and the adjacent ORS (contiguous with the epidermal BM) throughout HF cycle stages, except for telogen (Couchman, 1986; Westgate et al., 1991; Couchman, 1993). While perlecan expression persisted in both the BM and DP, syndecans localized at different positions during the HF cycle (Kaplan and Holbrook, 1994). During anagen, syndecan-1 is strongly detected in the ORS of the HF and to a lesser extent in DP (Malgouries et al., 2008). As follicles proceed through catagen, syndecan-1 levels diminish in the ORS, below that within the DP (Bayer-Garner et al., 2002).

Stem cell populations within the epidermis, HF and DP appear to share a commonality in that distinct PG core protein expression patterns appear to correlate with specific stem cell responses and fate decisions. However, the role of HS chains attached to these proteins and their functional significance is currently unknown. The extraction of HS from epidermal tissue and subsequent structural analysis may provide preliminary insights into the overall status of the epidermal heparanome, and may also help identify sequence motifs that impart protein-binding properties.

Cancer Stem Cells

Dysregulated HSPG biosynthesis and aberrant chain modifications have been documented in several solid tumors and hematological malignancies. Changes in HS sulfation patterns due to alterations in expression of the sulphotransferases and SULF enzymes, coupled with increased cleavage by HPSE, have long been implicated in key tumorigenic events (Vlodavsky et al., 2007; Rosen and Lemjabbar-Alaoui, 2010; Hammond et al., 2014; Nagarajan et al., 2018). Increased localization of HS binding signaling factors and ECM remodeling events (such as breakdown of HSPGs in the basement membrane) are known to underpin tumor proliferation, angiogenesis and metastasis (Knelson et al., 2014). Research over the last decade has also

uncovered vital roles for HSPGs in mediating cancer stem cell (CSC) function.

CSCs have been described to fuel tumor growth and heterogeneity due to their highly proliferative, phenotypically plastic, and treatment-resistant nature (Plaks et al., 2015; Batlle and Clevers, 2017). Several HSPG signatures have been identified to promote CSC survival and oncogenic properties. For example, upon profiling triple negative inflammatory breast CSCs, Ibrahim, and colleagues found significantly high levels of syndecan-1 mRNA and protein levels (Ibrahim et al., 2017). Notably, siRNA knockdown of syndecan-1 was observed to directly affect CSC survival and decrease the pool of available cells. These knockdown cells were unable to efficiently form colonies and spheroids, highlighting a perturbation in their self-renewal capacity. Such a dependency on syndecan-1 for maintaining oncogenic CSC activity was also observed in murine mammary glands (Liu et al., 2004). Overexpression of *Wnt1* failed to trigger the accumulation of mammary CSCs and progenitors for oncogenic transformation in syndecan-1-null mice, whereas an enrichment in the progenitor population and tumor initiation were induced in syndecan-1 expressing counterparts. A follow up study showed that the tumor resistance conferred by the absence of syndecan-1 extended beyond the mammary glands in null mice and was a multi-organ effect (McDermott et al., 2007). While this evidence clearly indicates an involvement of syndecan-1 in augmenting the tumorigenic properties of CSCs, it is unclear whether this phenomenon relates to the properties of the HS chains they carry. Further investigation is required to establish if syndecan-1-dependent enhancement of CSC activity is an HS-independent feature or not.

Although syndecan-1 may be important for tumorigenesis in certain tumor types, patterns of HSPG expression in CSC populations appear to be contextual and tissue-specific. For example, decreases in syndecan-1 expression have been observed to correlate with epithelial-mesenchymal transitions (EMT) and poorly differentiated phenotypes in colon cancer (Hashimoto et al., 2008). To understand the significance of syndecan-1 in colon CSCs, Kumar Katakam et al. (2020) performed an siRNA knockdown study. Silenced cells showed enhanced expression of stemness markers, such as *SOX2* and *NANOG*, an accentuated ability to self-renew and a greater tendency to undergo EMT compared to control cells. Furthermore, it was observed that dampened syndecan-1 levels in the knockdown cells were accompanied by a concomitant rise in WNT signaling and expression of downstream transcription factors of the TCF/LEF family, boosting the CSC phenotype. Attenuated HSPG expression in colon CSCs was thus sufficient to induce pro-oncogenic features and trigger associated signaling events. In a follow-up study, the group also found that HPSE expression was elevated in syndecan-1 depleted colon cancer cells (Katakam et al., 2020). These cells exhibited enhanced stem cell properties including sphere formation capacity and strong expression of stemness markers. While such observations suggest the involvement of HS remodeling mechanisms in tumor progression, accompanying analyses at the level of HS compositional characterization and associated bioactivity will be essential to confirm this, and to discern whether particular glycan signatures are associated with enhanced CSC function. Apart from the syndecans, variations in CSC glypican expression have also been reported. Enriched glypican-4 expression has been identified in chemotherapy-resistant pancreatic CSCs (Cao et al., 2018). Knockdown of glypican-4 resulted in a dramatic decrease in stemness marker expression (such as *OCT4*, *SOX2,* and *NANOG*) in these cells and increased their vulnerability to 5-fluorouracil, a chemotherapeutic agent. Moreover, glypican-4 knockdown cells exhibited suppressed WNT signaling and a decreased level of nuclear β-catenin. This highlights a dependence on the expression of particular HSPGs for the progression of important signaling cascades that accentuate stemness features in CSCs.

In addition to the HSPG core proteins, the significance of unique HS fragments in mediating CSC responses has also emerged as an important area of research, mainly through investigating the effects of exogenous HS on CSC properties. Patel et al. (2016) adopted a screening strategy to test the effects of treating CSCs with a library of heparin/HS oligosaccharides of varying chain lengths. These oligosaccharides shared a common repeating disaccharide structure comprising a 2-*O*-sulfated iduronic acid residue linked to a glucosamine residue with sulfate moieties at the C6 and *N* positions (i.e., IdoA2S-GlcNS6S). The group discovered a chain length-dependent inhibition of self-renewal in CSCs across a variety of tumor cell lines. Spheroid growth was inhibited upon exposure to HS chains from dp6 to dp12, while longer and shorter chains were ineffective. Importantly, the dp6 oligosaccharide was the most potent and treatment was found to induce a decrease in the expression of CSC markers *CD44* and *LGRF5*. The group found that these effects on CSCs were brought about by a dp6-dependent activation of a specific isoform of p38, a stress-activated mitogen activated protein kinase (MAPK) with tumor suppressive functions. Although the mechanistic details of this interaction are yet to be fully elucidated and the functional properties of the HS fragments require validation, the results from this study offer important insights into the roles of HS oligosaccharides as anti-cancer therapy agents, depending on their compositional signatures.

Examining how chain attributes, such as length, domain organization, sulfate modifications and protein binding sites, may be tailored for the synthesis of HS oligosaccharides with desirable therapeutic properties holds immense promise in expanding the scope of glycotherapeutics. Moreover, modulating the expression levels and localization of HSPG core proteins, and utilizing methods to enhance or inhibit HS function may be adopted as potential approaches to regulate the heparanome of CSCs and consequently, ameliorate their aberrant behavior.

EXPERIMENTAL METHODS TO STRENGTHEN OUR UNDERSTANDING OF THE HSPG-STEM CELL RELATIONSHIP

Current knowledge regarding the specific compositional and associated functional features of HSPGs in mediating AdSC fate is limited, with unaddressed gaps in mechanistic understanding and

restricted clinical relevance. To acquire a holistic appreciation of the HSPG-stem cell relationship, future studies may adopt a multi-omics approach that examines the heparanome of different stem cell types using a combination of glycomic, genomic, chemical, and proteomic methods. Thorough HS compositional profiling would be useful for uncovering distinct glycomic signatures that may predominate during differentiation down a particular lineage. Employing liquid chromatography-tandem mass spectrometry (LC-MS/MS) would allow for the necessary identification of fine structural features of HS and associated temporal changes, with a high level of sensitivity and accuracy (Zaia, 2013). Additionally, perturbation of HS structure and subsequent loss-of-function effects in differentiating stem cells may be investigated to identify the required structural nuances and roles of HSPGs at distinct time-points during lineage commitment.

Apart from traditional genetic manipulation approaches, gene editing through drug-inducible CRISPR/Cas9 systems may be utilized to knockout key HS biosynthetic and regulatory enzymes or PG core proteins (Cao et al., 2016; Sun N. et al., 2019). The loss of such key HSPG-related proteins at specific stages of differentiation will provide insights into the relationship between the HSPG profiles of progenitors or stem cells and their differentiation status. A range of chemical methods have also been developed to inhibit HS function *in vitro*, including the use of sodium chlorate, xylosides, and surfen (Humphries and Silbert, 1988; Garud et al., 2008; Weiss et al., 2015). Xylosides serve as primers for HS chain synthesis, while fluoroxylosides prevent chain elongation and effectively inhibit HS and CS/DS biosynthesis (Garud et al., 2008). In a 2018 study, Huang and colleagues investigated effects of the heparin/heparan sulfate antagonist surfen (bis-2-methyl-4-amino-quinolyl-6-carbamide) (Weiss et al., 2015) on HS function in *Oct4*-GFP and *Sox1*-GFP mESC reporter lines (Huang et al., 2018). Treated cells showed persistent pluripotency and an inability to differentiate, iterating a requirement of HS in mediating lineage commitment decisions. Moreover, this effect was reversible through the removal of surfen, suggesting that this molecule could prove useful for the temporal inhibition of HS activity throughout various stages of differentiation *in vitro* (Huang et al., 2018).

Other than chemical inhibition, the most widespread method to perturb HS function is the use of heparinases isolated from bacteria (*Flavobacterium heparinum*). When all three enzymes are used together, HS chains are cleaved into constituent disaccharides. Whilst this approach is simple to execute in cell culture models, the rapid turnover of cell surface HS allows only for a limited period to conduct subsequent live cell experiments. Alternatively, heparinase digestion may be carried out prior to fixation of cells, followed by immunostaining and flow cytometry analysis (Ayerst et al., 2017). HS participation as a signaling co-receptor can also be inhibited through a variety of peptide or protein-based methods. The HS/heparin-binding domain of HS binding proteins may be engineered, such that GAG-protein interactions are precluded. A non-HS binding variant of BMP2 has been generated in this manner, through the replacement of the first 12 of the 17 N-terminal amino acids which constitute the heparin-binding domain (Ruppert et al., 1996; Kuo et al., 2010). Alternatively, HS-protein interactions can be hindered by ligand binding competition. For example, synthetic heparin-binding peptides competed with and prevented the attachment of cytomegalovirus envelop proteins to cell surface HS in fibroblasts (Dogra et al., 2015). Another approach involves the use of soluble decoy FGFR fusion proteins, which compete with cell surface FGFR for FGF binding and affect ternary complex formation with HS (Harding et al., 2013; Li et al., 2014). HS/heparin binding to protein partners and signaling complex formation may also be intercepted by the use of custom designed antibodies that mask the GAG binding site on the protein. Our lab has previously developed an antibody (IMB-R1) that was able to bind to FGFR1 and prevent FGFR1-heparin interactions (Ling et al., 2015).

EXPLOITING THE HSPG-STEM CELL RELATIONSHIP FOR THERAPEUTIC USE: HS AS AN ADJUVANT FOR THE EXPANSION OF POTENT MSCS

The critical roles HS plays in mediating stem cell function *in vitro* and *in vivo* makes it an ideal candidate for use as an adjuvant in cell therapy and associated culture expansion strategies. Our own work has focused on enhancing the expansion of potent human MSCs (hMSCs) by using exogenous HS as a supplement to culture media throughout expansion. Initial studies using rat MSCs revealed that the addition of exogenous HS resulted in enhanced proliferation and enhanced osteogenic differentiation (Dombrowski et al., 2009). Importantly, this effect was potentiated through FGFR1, a mechanism that has since become an extensive focus in our studies. In 2012, we sought to understand the effects of adding exogenous HS (HS2, a murine embryonic forebrain-derived variant that displays enhanced binding affinity toward FGF2) to hMSCs during *in vitro* culture (Helledie et al., 2012). As with rat MSCs, addition of exogenous HS augmented hMSC proliferation, especially of subpopulations with long telomeres and high expression of multipotency markers as well as the cell surface marker STRO-1. When HS2-treated hMSCs were assessed in an animal model of a critical-sized bone defect, bone regeneration was enhanced over hMSCs which were not pre-cultured with HS2. This gave us some indication that HS, specifically the HS2 variant, could contribute to the selection and expansion of a more potent sub-population of hMSCs.

Due to the difficulties of isolating sufficient HS2 from developing mouse brains for extensive analyses, we went on to develop an affinity isolation platform that utilizes the heparin-binding domain (HBD) of proteins. HBDs were peptide synthesized and bound to streptavidin-functionalised resin through a terminal biotin molecule (Murali et al., 2013; Wang et al., 2014; Wijesinghe et al., 2017). Using such methods, we developed a peptide modeled on an HBD from within FGF2. We then fractionated commercial porcine intestinal mucosal HS over the column. The retained material, termed "HS8," was subjected to comprehensive testing against hMSCs

(Wijesinghe et al., 2017). Addition of HS8 to culture media enhanced the proliferation and colony-forming efficiency of hMSCs, much like the effects observed after the addition of HS2. HS8 enhanced the stability of FGF2 in media and led to an accumulation over time, resulting in prolonged FGFR1 and ERK1/2 phosphorylation in hMSCs treated with sub-optimal concentrations of FGF2. The affinity isolation methodology demonstrated our ability to effectively scale production of a desired HS variant, yielding larger quantities suitable for more extensive biochemical and cellular analysis, including larger animal studies. HS variants isolated in this manner proved to be amiable to gamma irradiation, without a loss of structure or function (Smith et al., 2018). This technique could be used to sterilize potential HS-based cell media supplements prior to use in stem cell expansion. We next employed a microbioreactor array to further elucidate the mechanism by which HS8 functions in the *in vitro* hMSC microenvironment (Titmarsh et al., 2017). Using microfluidics, various concentrations of HS8 and FGF2 were mixed and applied to hMSCs under constant flow across sequential flow cells. The addition of HS8 not only increased production of endogenous FGF2, but also facilitated release of FGF2 from the cell surface (and likely ECM), resulting in perfusion of released FGF2 into downstream flow cells. HS8 also sustained FGF2 availability over time, an effect we have observed in previous studies.

Our most recent work explored the therapeutic potential of clinically sourced hMSCs isolated from fresh bone marrow aspirates (Ling et al., 2020). Extensive analysis revealed that HS supplementation of culture media increased hMSC proliferation, telomere length, expression of desirable cell surface markers and multipotency. We hypothesize that this is a result of the expansion of a sub-population of MSCs that display a more "naïve" phenotype. MSCs were subsequently expanded in media with or without HS8 and used in two animal models of a knee osteochondral defect (rat and pig). In the rat model, MSCs cultured with HS8 demonstrated enhanced defect healing over the control groups (empty, carrier, MSCs cultured without HS8), including increased type II collagen and GAG deposition within the wound site. Using a large animal model of an osteochondral defect, the micro pig, we found that animals treated with cells cultured in HS8 showed a marked improvement in wound healing, increased collagen II and GAG deposition, and improved mechanical properties at 4 and 8 months post-surgery. Throughout these studies, there was clear indication that supplementation of HS to the *in vitro* MSC microenvironment leads to an expansion of an MSC subpopulation with increased potency. HS supports this potent MSC cell type at least in part through its influence as a co-receptor in the FGF2:FGFR1 signaling cascade. Indeed, the rapid expansion of MSCs to desirable quantities for cell therapies often utilizes large quantities of FGF2 and other recombinant factors, many of which are heparin-binding. For this reason, the development of HS variants for the purpose of stem cell expansion could yield greater numbers of more potent cells by promoting the secretion of autocrine factors, or by increasing the stability of decreased concentrations of the exogenous factors ordinarily supplemented into the culture media.

Apart from media supplementation, HS may be introduced into cell cultures in other formats. In a 2019 study, Treiger and colleagues developed a novel heparinoid-bovine serum albumin (BSA) bioconjugate, wherein a copper-free click reaction was used to conjugate various heparin derivatives to cyclooctyne-functionalized BSA (Trieger et al., 2019). These constructs were passively adsorbed onto tissue culture plastic surfaces and served as ECM PGs. They were found to variably sequester FGF2 based on their sulfation patterns, resulting in increased proliferation of cultured hMSCs. One benefit of such reactions and methodologies is the ability to use a generic anchoring molecule (in this case, BSA) for surface coating, whilst a library of different functional moieties may be generated and employed depending upon the required use. Surface coatings offer potential advantages over traditional supplementation in solution: firstly, a much lower quantity of HS is required to achieve a maximum surface coating. Secondly, surface coatings more effectively recapitulate the extracellular environment of a typical stem cell, as HSPGs are either found contained within the ECM, on the cell surface or immediately adjacent to it, not as free-floating HS chains in solution. Finally, the large-scale culture of hMSCs requires the use of large bioreactors, utilizing microcarriers to which hMSCs may bind and proliferate in suspension. The use of HS-coated microcarriers should greatly reduce the amounts of HS required for such culture systems over HS supplementation into the bulk media. The last of these points is yet to be investigated but could provide useful insights into the importance of HS localization during stem cell expansion in artificial environments.

CONCLUDING REMARKS

HSPGs have emerged as key mediators of stem cell function, essential for the regulation of development, homeostasis and regeneration. Early evidence from ESC studies highlighted the significance of HSPGs and their biosynthetic machinery in mediating key lineage commitment and cell fate decisions. Recent observations have indicated conservation in HSPG function and compositional regulation across AdSC types, as well as perturbation in analogous mechanisms in CSC populations. The use of HS variants as media adjuvants offers an encouraging avenue for the development of customized media formulations for bioprocessing cells suitable for clinical application. However, further investigations are required to unravel the importance of particular HSPG compositional characteristics and associated functional features in guiding the behavior of various stem cell types, especially prior to clinical adoption.

It is worth noting that in our own experience, the structure and composition of HS varies widely depending upon the source, with highly sulfated HS variants more akin to heparin. We and others have previously discussed the negative impact of long-term culture supplementation with heparin has on the molecular phenotype of MSCs (Hemeda et al., 2013; Ling et al., 2016), in addition to the negative impact heparin has on GDF5 signaling (Ayerst et al., 2017). Yet, we do not observe such phenomena with HS, a molecule which relies on smaller but distinctly

heparin-like NS domains to facilitate interactions with ligands and receptors. These subtle distinctions in structure, which yield significant differences in subsequent biological events, require more exhaustive examination. Rigorous inquiry into the biochemistry of HSPGs will accelerate their development as tools and pharmacological agents to modulate stem cell responses *in vitro* or *in vivo*, and is a necessary step to be undertaken if HS is to see widespread therapeutic application. Despite this, the amalgamation of glycotherapeutics and stem cell therapy holds considerable promise in bringing forth novel strategies for regenerative medicine.

AUTHOR CONTRIBUTIONS

MR and RS conceptualized, drafted and edited the manuscript. VN contributed to editing the manuscript. SC was invited by the journal to provide the review, revised the manuscript and approved the final version for submission. All authors contributed to the article and approved the submitted version.

FUNDING

This work was supported by the Industry Alignment Fund Pre-Positioning (IAF-PP) funding (H18/01/a0/021) from the Agency for Science, Technology and Research (A*STAR), Singapore.

ACKNOWLEDGMENTS

We also thank A*STAR for providing MR with support for her graduate studies through a Singapore International Graduate Award (SINGA). The authors further acknowledge support from the Institute of Medical Biology (IMB) and the Biomedical Research Council (BMRC), A*STAR.

REFERENCES

Ai, X., Do, A.-T., Lozynska, O., Kusche-Gullberg, M., Lindahl, U., and Emerson, C. P. Jr. (2003). QSulf1 remodels the 6-O sulfation states of cell surface heparan sulfate proteoglycans to promote Wnt signaling. *J. Cell Biol.* 162, 341–351. doi: 10.1083/jcb.200212083

Aikawa, J., and Esko, J. D. (1999). Molecular cloning and expression of a third member of the heparan sulfate/heparin GlcNAc N-deacetylase/N-sulfotransferase family. *J. Biol. Chem.* 274, 2690–2695. doi: 10.1074/jbc.274.5.2690

Allen, B. L., Filla, M. S., and Rapraeger, A. C. (2001). Role of heparan sulfate as a tissue-specific regulator of FGF-4 and FGF receptor recognition. *J. Cell Biol.* 155, 845–858. doi: 10.1083/jcb.200106075

Andres, J. L., Stanley, K., Cheifetz, S., and Massagué, J. (1989). Membrane-anchored and soluble forms of betaglycan, a polymorphic proteoglycan that binds transforming growth factor-beta. *J. Cell Biol.* 109, 3137–3145. doi: 10.1083/jcb.109.6.3137

Ashikari-Hada, S., Habuchi, H., Kariya, Y., Itoh, N., Reddi, A. H., and Kimata, K. (2004). Characterization of growth factor-binding structures in heparin/heparan sulfate using an octasaccharide library. *J. Biol. Chem.* 279, 12346–12354. doi: 10.1074/jbc.M313523200

Assis-Ribas, T., Forni, M. F., Winnischofer, S. M. B., Sogayar, M. C., and Trombetta-Lima, M. (2018). Extracellular matrix dynamics during mesenchymal stem cells differentiation. *Dev. Biol.* 437, 63–74. doi: 10.1016/j.ydbio.2018.03.002

Ayerst, B. I., Smith, R. A., Nurcombe, V., Day, A. J., Merry, C. L., and Cool, S. M. (2017). Growth differentiation factor 5-mediated enhancement of chondrocyte phenotype is inhibited by heparin: implications for the use of heparin in the clinic and in tissue engineering applications. *Tissue Eng. Part A* 23, 275–292. doi: 10.1089/ten.TEA.2016.0364

Baldwin, R. J., ten Dam, G. B., van Kuppevelt, T. H., Lacaud, G., Gallagher, J. T., Kouskoff, V., et al. (2008). A developmentally regulated heparan sulfate epitope defines a subpopulation with increased blood potential during mesodermal differentiation. *Stem Cells* 26, 3108–3118. doi: 10.1634/stemcells.2008-0311

Barrandon, Y., and Green, H. (1987). Three clonal types of keratinocyte with different capacities for multiplication. *Proc. Natl. Acad. Sci. U.S.A.* 84, 2302–2306. doi: 10.1073/pnas.84.8.2302

Bass, M. D., Williamson, Rosalind, C., Nunan, Robert, D., Humphries, et al. (2011). A Syndecan-4 hair trigger initiates wound healing through caveolin- and RhoG-regulated integrin endocytosis. *Dev. Cell* 21, 681–693. doi: 10.1016/j.devcel.2011.08.007

Batlle, E., and Clevers, H. (2017). Cancer stem cells revisited. *Nat. Med.* 23, 1124–1134. doi: 10.1038/nm.4409

Bayer-Garner, I. B., Sanderson, R. D., and Smoller, B. R. (2002). Syndecan-1 is strongly expressed in the anagen hair follicle outer root sheath and in the dermal papilla but expression diminishes with involution of the hair follicle. *Am. J. Dermatopathol.* 24, 484–489. doi: 10.1097/00000372-200212000-00005

Bentley, S. A., and Tralka, T. S. (1983). Fibronectin-mediated attachment of hematopoietic cells to stromal elements in continuous bone marrow culture. *Exp. Hematol.* 11, 129–138.

Bernfield, M., Götte, M., Park, P. W., Reizes, O., Fitzgerald, M. L., Lincecum, J., et al. (1999). Functions of cell surface heparan sulfate proteoglycans. *Annu. Rev. Biochem.* 68, 729–777. doi: 10.1146/annurev.biochem.68.1.729

Bernfield, M., Hinkes, M. T., and Gallo, R. L. (1993). Developmental expression of the syndecans: possible function and regulation. *Development* 119, 205–212. doi: 10.1006/dbio.1997.8824

Bespalov, M. M., Sidorova, Y. A., Tumova, S., Ahonen-Bishopp, A., Magalhães, A. C., Kulesskiy, E., et al. (2011). Heparan sulfate proteoglycan syndecan-3 is a novel receptor for GDNF, neurturin, and artemin. *J. Cell Biol.* 192, 153–169. doi: 10.1083/jcb.201009136

Blanpain, C., and Fuchs, E. (2009). Epidermal homeostasis: a balancing act of stem cells in the skin. *Nat. Rev. Mol. Cell Biol.* 10, 207–217. doi: 10.1038/nrm2636

Bramono, D. S., Murali, S., Rai, B., Ling, L., Poh, W. T., Lim, Z. X., et al. (2012). Bone marrow-derived heparan sulfate potentiates the osteogenic activity of bone morphogenetic protein-2 (BMP-2). *Bone* 50, 954–964. doi: 10.1016/j.bone.2011.12.013

Bramono, D. S., Rider, D. A., Murali, S., Nurcombe, V., and Cool, S. M. (2011). The effect of human bone marrow stroma-derived heparan sulfate on the ex vivo expansion of human cord blood hematopoietic stem cells. *Pharm. Res.* 28, 1385–1394. doi: 10.1007/s11095-010-0352-y

Brandan, E., Carey, D. J., Larrain, J., Melo, F., and Campos, A. (1996). Synthesis and processing of glypican during differentiation of skeletal muscle cells. *Eur. J. Cell Biol.* 71, 170–176.

Brickman, Y. G., Ford, M. D., Gallagher, J. T., Nurcombe, V., Bartlett, P. F., and Turnbull, J. E. (1998). Structural modification of fibroblast growth factor-binding heparan sulfate at a determinative stage of neural development. *J. Biol. Chem.* 273, 4350–4359. doi: 10.1074/jbc.273.8.4350

Brown, T. A., Bouchard, T., St John, T., Wayner, E., and Carter, W. G. (1991). Human keratinocytes express a new CD44 core protein (CD44E) as a heparan-sulfate intrinsic membrane proteoglycan with additional exons. *J. Cell Biol.* 113, 207–221. doi: 10.1083/jcb.113.1.207

Brule, S., Charnaux, N., Sutton, A., Ledoux, D., Chaigneau, T., Saffar, L., et al. (2006). The shedding of syndecan-4 and syndecan-1 from HeLa cells and human primary macrophages is accelerated by SDF-1/CXCL12 and mediated by the matrix metalloproteinase-9. *Glycobiology* 16, 488–501. doi: 10.1093/glycob/cwj098

Brunetti, A., and Goldfine, I. D. (1990). Role of myogenin in myoblast differentiation and its regulation by fibroblast growth factor. *J. Biol. Chem.* 265, 5960–5963.

Campos, A., Nùñez, R., Koenig, C. S., Carey, D. J., and Brandan, E. (1993). A lipid-anchored heparan sulfate proteoglycan is present in the surface of differentiated skeletal muscle cells. *Eur. J. Biochem.* 216, 587–595. doi: 10.1111/j.1432-1033.1993.tb18178.x

Cao, J., Ma, J., Sun, L., Li, J., Qin, T., Zhou, C., et al. (2018). Targeting glypican-4 overcomes 5-FU resistance and attenuates stem cell-like properties via suppression of Wnt/beta-catenin pathway in pancreatic cancer cells. *J. Cell. Biochem.* 119, 9498–9512. doi: 10.1002/jcb.27266

Cao, J., Wu, L., Zhang, S. M., Lu, M., Cheung, W. K., Cai, W., et al. (2016). An easy and efficient inducible CRISPR/Cas9 platform with improved specificity for multiple gene targeting. *Nucleic Acids Res.* 44, e149. doi: 10.1093/nar/gkw660

Caplan, A. I. (1991). Mesenchymal stem cells. *J. Orthop. Res.* 9, 641–650. doi: 10.1002/jor.1100090504

Cardin, A. D., and Weintraub, H. J. (1989). Molecular modeling of protein-glycosaminoglycan interactions. *Arteriosclerosis* 9, 21–32. doi: 10.1161/01.ATV.9.1.21

Casar, J. C., Cabello-Verrugio, C., Olguin, H., Aldunate, R., Inestrosa, N. C., and Brandan, E. (2004). Heparan sulfate proteoglycans are increased during skeletal muscle regeneration: requirement of syndecan-3 for successful fiber formation. *J. Cell Sci.* 117(Pt 1), 73–84. doi: 10.1242/jcs.00828

Caughman, S. W., Krieg, T., Timpl, R., Hintner, H., and Katz, S. I. (1987). Nidogen and heparan sulfate proteoglycan: detection of newly isolated basement membrane components in normal and epidermolysis bullosa skin. *J. Invest. Dermatol.* 89, 547–550. doi: 10.1111/1523-1747.ep12461192

Chen, J., Wang, Y., Chen, C., Lian, C., Zhou, T., Gao, B., et al. (2016). Exogenous heparan sulfate enhances the TGF-beta3-induced chondrogenesis in human mesenchymal stem cells by activating TGF-beta/Smad signaling. *Stem Cells Int.* 2016:1520136. doi: 10.1155/2016/1520136

Chiang, C., Litingtung, Y., Lee, E., Young, K. E., Corden, J. L., Westphal, H., et al. (1996). Cyclopia and defective axial patterning in mice lacking Sonic hedgehog gene function. *Nature* 383, 407–413. doi: 10.1038/383407a0

Clegg, C. H., Linkhart, T. A., Olwin, B. B., and Hauschka, S. D. (1987). Growth factor control of skeletal muscle differentiation: commitment to terminal differentiation occurs in G1 phase and is repressed by fibroblast growth factor. *J. Cell Biol.* 105, 949–956. doi: 10.1083/jcb.105.2.949

Cool, S. M., and Nurcombe, V. (2006). Heparan sulfate regulation of progenitor cell fate. *J. Cell. Biochem.* 99, 1040–1051. doi: 10.1002/jcb.20936

Cornelison, D. D., Filla, M. S., Stanley, H. M., Rapraeger, A. C., and Olwin, B. B. (2001). Syndecan-3 and syndecan-4 specifically mark skeletal muscle satellite cells and are implicated in satellite cell maintenance and muscle regeneration. *Dev. Biol.* 239, 79–94. doi: 10.1006/dbio.2001.0416

Cornelison, D. D., Wilcox-Adelman, S. A., Goetinck, P. F., Rauvala, H., Rapraeger, A. C., and Olwin, B. B. (2004). Essential and separable roles for Syndecan-3 and Syndecan-4 in skeletal muscle development and regeneration. *Genes Dev.* 18, 2231–2236. doi: 10.1101/gad.1214204

Costell, M., Gustafsson, E., Aszódi, A., Mörgelin, M., Bloch, W., Hunziker, E., et al. (1999). Perlecan maintains the integrity of cartilage and some basement membranes. *J. Cell Biol.* 147, 1109–1122. doi: 10.1083/jcb.147.5.1109

Couchman, J. R. (1986). Rat hair follicle dermal papillae have an extracellular matrix containing basement membrane components. *J. Invest. Dermatol.* 87, 762–767. doi: 10.1111/1523-1747.ep12456955

Couchman, J. R. (1993). Hair follicle proteoglycans. *J. Invest. Dermatol.* 101, S60–S64. doi: 10.1016/0022-202X(93)90502-9

Couchman, J. R. (2010). Transmembrane signaling proteoglycans. *Annu. Rev. Cell Dev. Biol.* 26, 89–114. doi: 10.1146/annurev-cellbio-100109-104126

Coulson-Thomas, V. J., Gesteira, T. F., Esko, J., and Kao, W. (2014). Heparan sulfate regulates hair follicle and sebaceous gland morphogenesis and homeostasis. *J. Biol. Chem.* 289, 25211–25226. doi: 10.1074/jbc.M114.572511

da Silva, Meirelles, L., Chagastelles, P. C., and Nardi, N. B. (2006). Mesenchymal stem cells reside in virtually all post-natal organs and tissues. *J. Cell Sci.* 119(Pt 11), 2204–2213. doi: 10.1242/jcs.02932

David, G., Bai, X. M., Van der Schueren, B., Cassiman, J. J., and Van den Berghe, H. (1992). Developmental changes in heparan sulfate expression: in situ detection with mAbs. *J. Cell Biol.* 119, 961–975. doi: 10.1083/jcb.119.4.961

David, G., Lories, V., Decock, B., Marynen, P., Cassiman, J. J., and Van den Berghe, H. (1990). Molecular cloning of a phosphatidylinositol-anchored membrane heparan sulfate proteoglycan from human lung fibroblasts. *J. Cell Biol.* 111, 3165–3176. doi: 10.1083/jcb.111.6.3165

Del Rosso, M., Cappelletti, R., Dini, G., Fibbi, G., Vannucchi, S., Chiarugi, V., et al. (1981). Involvement of glycosaminoglycans in detachment of early myeloid precursors from bone-marrow stromal cells. *Biochim. Biophys. Acta* 676, 129–136. doi: 10.1016/0304-4165(81)90180-x

Dexter, T. M., Allen, T. D., and Lajtha, L. G. (1977). Conditions controlling the proliferation of haemopoietic stem cells in vitro. *J. Cell. Physiol.* 91, 335–344. doi: 10.1002/jcp.1040910303

Ding, K., Lopez-Burks, M., Sanchez-Duran, J. A., Korc, M., and Lander, A. D. (2005). Growth factor-induced shedding of syndecan-1 confers glypican-1 dependence on mitogenic responses of cancer cells. *J. Cell Biol.* 171, 729–738. doi: 10.1083/jcb.200508010

Dogra, P., Martin, E. B., Williams, A., Richardson, R. L., Foster, J. S., Hackenback, N., et al. (2015). Novel heparan sulfate-binding peptides for blocking herpesvirus entry. *PLoS One* 10:e0126239. doi: 10.1371/journal.pone.0126239

Dombrowski, C., Song, S. J., Chuan, P., Lim, X., Susanto, E., Sawyer, A. A., et al. (2009). Heparan sulfate mediates the proliferation and differentiation of rat mesenchymal stem cells. *Stem Cells Dev.* 18, 661–670. doi: 10.1089/scd.2008.0157

Dou, W., Xu, Y., Pagadala, V., Pedersen, L. C., and Liu, J. (2015). Role of deacetylase activity of N-Deacetylase/N-Sulfotransferase 1 in forming n-sulfated domain in heparan sulfate. *J. Biol. Chem.* 290, 20427–20437. doi: 10.1074/jbc.m115.664409

Driskell, R. R., Clavel, C., Rendl, M., and Watt, F. M. (2011). Hair follicle dermal papilla cells at a glance. *J. Cell Sci.* 124(Pt 8), 1179–1182. doi: 10.1242/jcs.082446

Dubey, R., van Kerkhof, P., Jordens, I., Malinauskas, T., Pusapati, G. V., McKenna, J. K., et al. (2020). R-spondins engage heparan sulfate proteoglycans to potentiate WNT signaling. *eLife* 9:e54469. doi: 10.7554/eLife.54469

Elabd, C., Ichim, T. E., Miller, K., Anneling, A., Grinstein, V., Vargas, V., et al. (2018). Comparing atmospheric and hypoxic cultured mesenchymal stem cell transcriptome: implication for stem cell therapies targeting intervertebral discs. *J. Transl. Med.* 16:222. doi: 10.1186/s12967-018-1601-9

Esko, J. D., and Lindahl, U. (2001). Molecular diversity of heparan sulfate. *J. Clin. Invest.* 108, 169–173. doi: 10.1172/jci200113530

Faham, S., Hileman, R. E., Fromm, J. R., Linhardt, R. J., and Rees, D. C. (1996). Heparin structure and interactions with basic fibroblast growth factor. *Science* 271, 1116–1120. doi: 10.1126/science.271.5252.1116

Farach-Carson, M. C., and Carson, D. D. (2007). Perlecan–a multifunctional extracellular proteoglycan scaffold. *Glycobiology* 17, 897–905. doi: 10.1093/glycob/cwm043

Feil, S., Valtcheva, N., and Feil, R. (2009). Inducible cre mice. *Methods Mol. Biol.* 530, 343–363. doi: 10.1007/978-1-59745-471-1_18

Filmus, J., Capurro, M., and Rast, J. (2008). Glypicans. *Genome Biol.* 9:224.

Filmus, J., and Selleck, S. B. (2001). Glypican: proteoglycans with a suprise. *J. Clin. Invest.* 108, 497–501.

Finch, P. W., Rubin, J. S., Miki, T., Ron, D., and Aaronson, S. A. (1989). Human KGF is FGF-related with properties of a paracrine effector of epithelial cell growth. *Science* 245, 752–755. doi: 10.1126/science.2475908

Fisher, M. C., Li, Y., Seghatoleslami, M. R., Dealy, C. N., and Kosher, R. A. (2006). Heparan sulfate proteoglycans including syndecan-3 modulate BMP activity during limb cartilage differentiation. *Matrix Biol.* 25, 27–39. doi: 10.1016/j.matbio.2005.07.008

Ford-Perriss, M., Turner, K., Guimond, S., Apedaile, A., Haubeck, H. D., Turnbull, J., et al. (2003). Localisation of specific heparan sulfate proteoglycans during the proliferative phase of brain development. *Dev. Dyn.* 227, 170–184. doi: 10.1002/dvdy.10298

Forsberg, E., and Kjellén, L. (2001). Heparan sulfate: lessons from knockout mice. *J. Clin. Invest.* 108, 175–180. doi: 10.1172/JCI13561

Forsberg, M., Holmborn, K., Kundu, S., Dagalv, A., Kjellen, L., and Forsberg-Nilsson, K. (2012). Undersulfation of heparan sulfate restricts differentiation potential of mouse embryonic stem cells. *J. Biol. Chem.* 287, 10853–10862. doi: 10.1074/jbc.M111.337030

Friedenstein, A. J., Chailakhyan, R. K., Latsinik, N. V., Panasyuk, A. F., and Keiliss-Borok, I. V. (1974). Stromal cells responsible for transferring the microenvironment of the hemopoietic tissues. Cloning in vitro and retransplantation in vivo. *Transplantation* 17, 331–340. doi: 10.1097/00007890-197404000-00001

Fuchs, E., and Raghavan, S. (2002). Getting under the skin of epidermal morphogenesis. *Nat. Rev. Genet.* 3, 199–209. doi: 10.1038/nrg758

Fuentealba, L., Carey, D. J., and Brandan, E. (1999). Antisense inhibition of syndecan-3 expression during skeletal muscle differentiation accelerates myogenesis through a basic fibroblast growth factor-dependent mechanism. *J. Biol. Chem.* 274, 37876–37884. doi: 10.1074/jbc.274.53.37876

Gallagher, J. T. (2001). Heparan sulfate: growth control with a restricted sequence menu. *J. Clin. Invest.* 108, 357–361. doi: 10.1172/jci13713

Gallagher, J. T., Spooncer, E., and Dexter, T. M. (1983). Role of the cellular matrix in haemopoiesis. I. Synthesis of glycosaminoglycans by mouse bone marrow cell cultures. *J. Cell Sci.* 63, 155–171.

Gartner, S., and Kaplan, H. S. (1980). Long-term culture of human bone marrow cells. *Proc. Natl. Acad. Sci. U.S.A.* 77, 4756–4759. doi: 10.1073/pnas.77.8.4756

Garud, D. R., Tran, V. M., Victor, X. V., Koketsu, M., and Kuberan, B. (2008). Inhibition of heparan sulfate and chondroitin sulfate proteoglycan biosynthesis. *J. Biol. Chem.* 283, 28881–28887. doi: 10.1074/jbc.m805939200

Gasimli, L., Hickey, A. M., Yang, B., Li, G., dela Rosa, M., Nairn, A. V., et al. (2014). Changes in glycosaminoglycan structure on differentiation of human embryonic stem cells towards mesoderm and endoderm lineages. *Biochim. Biophys. Acta* 1840, 1993–2003. doi: 10.1016/j.bbagen.2014.01.007

Girós, A., Morante, J., Gil-Sanz, C., Fairén, A., and Costell, M. (2007). Perlecan controls neurogenesis in the developing telencephalon. *BMC Dev. Biol.* 7:29. doi: 10.1186/1471-213x-7-29

Gomes, R. R. Jr., Farach-Carson, M. C., and Carson, D. D. (2004). Perlecan functions in chondrogenesis: insights from in vitro and in vivo models. *Cells Tissues Organs* 176, 79–86. doi: 10.1159/000075029

Goodger, S. J., Robinson, C. J., Murphy, K. J., Gasiunas, N., Harmer, N. J., Blundell, T. L., et al. (2008). Evidence that heparin saccharides promote FGF2 mitogenesis through two distinct mechanisms. *J. Biol. Chem.* 283, 13001–13008. doi: 10.1074/jbc.M704531200

Gopal, S., Bober, A., Whiteford, J. R., Multhaupt, H. A. B., Yoneda, A., and Couchman, J. R. (2010). Heparan sulfate chain valency controls syndecan-4 function in cell adhesion. *J. Biol. Chem.* 285, 14247–14258. doi: 10.1074/jbc.m109.056945

Gordon, M. Y., Riley, G. P., Watt, S. M., and Greaves, M. F. (1987). Compartmentalization of a haematopoietic growth factor (GM-CSF) by glycosaminoglycans in the bone marrow microenvironment. *Nature* 326, 403–405. doi: 10.1038/326403a0

Greene, D. K., Tumova, S., Couchman, J. R., and Woods, A. (2003). Syndecan-4 associates with alpha-actinin. *J. Biol. Chem.* 278, 7617–7623. doi: 10.1074/jbc.M207123200

Grobe, K., Inatani, M., Pallerla, S. R., Castagnola, J., Yamaguchi, Y., and Esko, J. D. (2005). Cerebral hypoplasia and craniofacial defects in mice lacking heparan sulfate Ndst1 gene function. *Development* 132, 3777–3786. doi: 10.1242/dev.01935

Guillemot, F., and Zimmer, C. (2011). From cradle to grave: the multiple roles of fibroblast growth factors in neural development. *Neuron* 71, 574–588. doi: 10.1016/j.neuron.2011.08.002

Guimond, S., Maccarana, M., Olwin, B. B., Lindahl, U., and Rapraeger, A. C. (1993). Activating and inhibitory heparin sequences for FGF-2 (basic FGF). Distinct requirements for FGF-1, FGF-2, and FGF-4. *J. Biol. Chem.* 268, 23906–23914.

Guimond, S. E., and Turnbull, J. E. (1999). Fibroblast growth factor receptor signalling is dictated by specific heparan sulphate saccharides. *Curr. Biol.* 9, 1343–1346. doi: 10.1016/s0960-9822(00)80060-3

Gutierrez, J., and Brandan, E. (2010). A novel mechanism of sequestering fibroblast growth factor 2 by glypican in lipid rafts, allowing skeletal muscle differentiation. *Mol. Cell. Biol.* 30, 1634–1649. doi: 10.1128/MCB.01164-09

Habuchi, H., Tanaka, M., Habuchi, O., Yoshida, K., Suzuki, H., Ban, K., et al. (2000). The occurrence of three isoforms of heparan sulfate 6-O-sulfotransferase having different specificities for hexuronic acid adjacent to the targeted N-sulfoglucosamine. *J. Biol. Chem.* 275, 2859–2868. doi: 10.1074/jbc.275.4.2859

Hagihara, K., Watanabe, K., Chun, J., and Yamaguchi, Y. (2000). Glypican-4 is an FGF2-binding heparan sulfate proteoglycan expressed in neural precursor cells. *Dev. Dyn.* 219, 353–367. doi: 10.1002/1097-017720009999:9999<::AID-DVDY1059<3.0.CO;2-\#

Hagmann, S., Moradi, B., Frank, S., Dreher, T., Kämmerer, P. W., Richter, W., et al. (2013). Different culture media affect growth characteristics, surface marker distribution and chondrogenic differentiation of human bone marrow-derived mesenchymal stromal cells. *BMC Musculoskelet. Disord.* 14:223. doi: 10.1186/1471-2474-14-223

Hagner-McWhirter, Å, Li, J.-P., Oscarson, S., and Lindahl, U. (2004). Irreversible Glucuronyl C5-epimerization in the biosynthesis of heparan sulfate. *J. Biol. Chem.* 279, 14631–14638. doi: 10.1074/jbc.m313760200

Halfter, W., Dong, S., Schurer, B., and Cole, G. J. (1998). Collagen XVIII is a basement membrane heparan sulfate proteoglycan. *J. Biol. Chem.* 273, 25404–25412. doi: 10.1074/jbc.273.39.25404

Hammond, E., Khurana, A., Shridhar, V., and Dredge, K. (2014). The role of heparanase and sulfatases in the modification of heparan sulfate proteoglycans within the tumor microenvironment and opportunities for novel cancer therapeutics. *Front. Oncol.* 4:195. doi: 10.3389/fonc.2014.00195

Han, Z. C., Bellucci, S., Shen, Z. X., Maffrand, J. P., Pascal, M., Petitou, M., et al. (1996). Glycosaminoglycans enhance megakaryocytopoiesis by modifying the activities of hematopoietic growth regulators. *J. Cell. Physiol.* 168, 97–104. doi: 10.1002/(sici)1097-4652(199607)168:1<97::Aid-jcp12<3.0.Co;2-m

Harding, T. C., Long, L., Palencia, S., Zhang, H., Sadra, A., Hestir, K., et al. (2013). Blockade of nonhormonal fibroblast growth factors by FP-1039 inhibits growth of multiple types of cancer. *Sci. Transl. Med.* 5:178ra139. doi: 10.1126/scitranslmed.3005414

Hashimoto, Y., Skacel, M., and Adams, J. C. (2008). Association of loss of epithelial syndecan-1 with stage and local metastasis of colorectal adenocarcinomas: an immunohistochemical study of clinically annotated tumors. *BMC Cancer* 8:185. doi: 10.1186/1471-2407-8-185

Hassell, J. R., Robey, P. G., Barrach, H. J., Wilczek, J., Rennard, S. I., and Martin, G. R. (1980). Isolation of a heparan sulfate-containing proteoglycan from basement membrane. *Proc. Natl. Acad. Sci. U.S.A.* 77, 4494–4498. doi: 10.1073/pnas.77.8.4494

Haubst, N., Georges-Labouesse, E., De Arcangelis, A., Mayer, U., and Götz, M. (2006). Basement membrane attachment is dispensable for radial glial cell fate and for proliferation, but affects positioning of neuronal subtypes. *Development* 133, 3245–3254. doi: 10.1242/dev.02486

Haupt, L. M., Murali, S., Mun, F. K., Teplyuk, N., Mei, L. F., Stein, G. S., et al. (2009). The heparan sulfate proteoglycan (HSPG) glypican-3 mediates commitment of MC3T3-E1 cells toward osteogenesis. *J. Cell. Physiol.* 220, 780–791. doi: 10.1002/jcp.21825

Helledie, T., Dombrowski, C., Rai, B., Lim, Z. X., Hin, I. L., Rider, D. A., et al. (2012). Heparan sulfate enhances the self-renewal and therapeutic potential of mesenchymal stem cells from human adult bone marrow. *Stem Cells Dev.* 21, 1897–1910. doi: 10.1089/scd.2011.0367

Hemeda, H., Kalz, J., Walenda, G., Lohmann, M., and Wagner, W. (2013). Heparin concentration is critical for cell culture with human platelet lysate. *Cytotherapy* 15, 1174–1181. doi: 10.1016/j.jcyt.2013.05.006

Hirano, K., Sasaki, N., Ichimiya, T., Miura, T., Van Kuppevelt, T. H., and Nishihara, S. (2012). 3-O-Sulfated heparan sulfate recognized by the antibody HS4C3 contribute to the differentiation of mouse embryonic stem cells via fas signaling. *PLoS One* 7:e43440. doi: 10.1371/journal.pone.0043440

Hirano, K., Van Kuppevelt, T. H., and Nishihara, S. (2013). The transition of mouse pluripotent stem cells from the naïve to the primed state requires Fas signaling through 3-O sulfated heparan sulfate structures recognized by the HS4C3 antibody. *Biochem. Biophys. Res. Commun.* 430, 1175–1181. doi: 10.1016/j.bbrc.2012.12.005

Holley, R. J., Pickford, C. E., Rushton, G., Lacaud, G., Gallagher, J. T., Kouskoff, V., et al. (2011). Influencing hematopoietic differentiation of mouse embryonic stem cells using soluble heparin and heparan sulfate saccharides. *J. Biol. Chem.* 286, 6241–6252. doi: 10.1074/jbc.m110.178483

Holley, R. J., Tai, G., Williamson, A. J., Taylor, S., Cain, S. A., Richardson, S. M., et al. (2015). Comparative quantification of the surfaceome of human multipotent mesenchymal progenitor cells. *Stem Cell Rep.* 4, 473–488. doi: 10.1016/j.stemcr.2015.01.007

Holmborn, K., Ledin, J., Smeds, E., Eriksson, I., Kusche-Gullberg, M., and Kjellen, L. (2004). Heparan sulfate synthesized by mouse embryonic stem cells deficient in NDST1 and NDST2 is 6-O-sulfated but contains no N-sulfate groups. *J. Biol. Chem.* 279, 42355–42358. doi: 10.1074/jbc.C400373200

Horiguchi, Y., Couchman, J. R., Ljubimov, A. V., Yamasaki, H., and Fine, J. D. (1989). Distribution, ultrastructural localization, and ontogeny of the core protein of a heparan sulfate proteoglycan in human skin and other basement membranes. *J. Histochem. Cytochem.* 37, 961–970. doi: 10.1177/37.7.2659664

Huang, M. L., Michalak, A. L., Fisher, C. J., Christy, M., Smith, R. A. A., and Godula, K. (2018). Small molecule antagonist of cell surface glycosaminoglycans

restricts mouse embryonic stem cells in a pluripotent state. *Stem Cells* 36, 45–54. doi: 10.1002/stem.2714

Hulett, M. D., Hornby, J. R., Ohms, S. J., Zuegg, J., Freeman, C., Gready, J. E., et al. (2000). Identification of active-site residues of the pro-metastatic endoglycosidase heparanase. *Biochemistry* 39, 15659–15667. doi: 10.1021/bi002080p

Humphries, D. E., and Silbert, J. E. (1988). Chlorate: a reversible inhibitor of proteoglycan sulfation. *Biochem. Biophys. Res. Commun.* 154, 365–371. doi: 10.1016/0006-291X(88)90694-8

Ibrahim, S. A., Gadalla, R., El-Ghonaimy, E. A., Samir, O., Mohamed, H. T., Hassan, H., et al. (2017). Syndecan-1 is a novel molecular marker for triple negative inflammatory breast cancer and modulates the cancer stem cell phenotype via the IL-6/STAT3, Notch and EGFR signaling pathways. *Mol. Cancer* 16:57. doi: 10.1186/s12943-017-0621-z

Inatani, M., Irie, F., Plump, A. S., Tessier-Lavigne, M., and Yamaguchi, Y. (2003). Mammalian brain morphogenesis and midline axon guidance require heparan sulfate. *Science* 302, 1044–1046. doi: 10.1126/science.1090497

Ishihara, M. (1994). Structural requirements in heparin for binding and activation of FGF-1 and FGF-4 are different from that for FGF-2. *Glycobiology* 4, 817–824. doi: 10.1093/glycob/4.6.817

Ishihara, M., Shaklee, P. N., Yang, Z., Liang, W., Wei, Z., Stack, R. J., et al. (1994). Structural features in heparin which modulate specific biological activities mediated by basic fibroblast growth factor. *Glycobiology* 4, 451–458. doi: 10.1093/glycob/4.4.451

Jakobsson, L., Kreuger, J., Holmborn, K., Lundin, L., Eriksson, I., Kjellen, L., et al. (2006). Heparan sulfate in trans potentiates VEGFR-mediated angiogenesis. *Dev. Cell* 10, 625–634. doi: 10.1016/j.devcel.2006.03.009

Jastrebova, N., Vanwildemeersch, M., Lindahl, U., and Spillmann, D. (2010). Heparan sulfate domain organization and sulfation modulate FGF-induced cell signaling. *J. Biol. Chem.* 285, 26842–26851. doi: 10.1074/jbc.M109.093542

Jen, Y. H., Musacchio, M., and Lander, A. D. (2009). Glypican-1 controls brain size through regulation of fibroblast growth factor signaling in early neurogenesis. *Neural Dev.* 4:33. doi: 10.1186/1749-8104-4-33

Johnson, C. E., Ward, C. M., Wilson, V., van Kuppevelt, T. H., Esko, J. D., Smith, A., et al. (2007). Essential alterations of heparan sulfate during the differentiation of embryonic stem cells to Sox1-enhanced green fluorescent protein-expressing neural progenitor cells. *Stem Cells* 25, 1913–1923. doi: 10.1634/stemcells.2006-0445

Joseph, S. J., Ford, M. D., Barth, C., Portbury, S., Bartlett, P. F., Nurcombe, V., et al. (1996). A proteoglycan that activates fibroblast growth factors during early neuronal development is a perlecan variant. *Development* 122, 3443–3452.

Kalus, I., Salmen, B., Viebahn, C., Figura, K. V., Schmitz, D., D'Hooge, R., et al. (2009). Differential involvement of the extracellular 6-O-endosulfatases Sulf1 and Sulf2 in brain development and neuronal and behavioural plasticity. *J. Cell Mol. Med.* 13, 4505–4521. doi: 10.1111/j.1582-4934.2008.00558.x

Kaplan, E. D., and Holbrook, K. A. (1994). Dynamic expression patterns of tenascin, proteoglycans, and cell adhesion molecules during human hair follicle morphogenesis. *Dev. Dyn.* 199, 141–155. doi: 10.1002/aja.1001990207

Katakam, S. K., Pelucchi, P., Cocola, C., Reinbold, R., Vlodavsky, I., Greve, B., et al. (2020). Syndecan-1-dependent regulation of heparanase affects invasiveness, stem cell properties, and therapeutic resistance of Caco2 colon cancer cells. *Front. Oncol.* 10:774. doi: 10.3389/fonc.2020.00774

Kawahara, R., Granato, D. C., Yokoo, S., Domingues, R. R., Trindade, D. M., and Paes Leme, A. F. (2017). Mass spectrometry-based proteomics revealed Glypican-1 as a novel ADAM17 substrate. *J. Proteomics* 151, 53–65. doi: 10.1016/j.jprot.2016.08.017

Kirby, S. L., and Bentley, S. A. (1987). Proteoglycan synthesis in two murine bone marrow stromal cell lines. *Blood* 70, 1777–1783. doi: 10.1182/blood.v70.6.1777.bloodjournal7061777

Kjellén, L., and Lindahl, U. (2018). Specificity of glycosaminoglycan–protein interactions. *Curr. Opin. Struct. Biol.* 50, 101–108. doi: 10.1016/j.sbi.2017.12.011

Knelson, E. H., Nee, J. C., and Blobe, G. C. (2014). Heparan sulfate signaling in cancer. *Trends Biochem. Sci.* 39, 277–288. doi: 10.1016/j.tibs.2014.03.001

Knox, S., Merry, C., Stringer, S., Melrose, J., and Whitelock, J. (2002). Not all perlecans are created equal: interactions with fibroblast growth factor (FGF) 2 and FGF receptors. *J. Biol. Chem.* 277, 14657–14665. doi: 10.1074/jbc.M111826200

Knox, S. M., and Whitelock, J. M. (2006). Perlecan: how does one molecule do so many things? *Cell. Mol. Life Sci.* 63, 2435–2445. doi: 10.1007/s00018-006-6162-z

Kojima, T., Shworak, N. W., and Rosenberg, R. D. (1992). Molecular cloning and expression of two distinct cDNA-encoding heparan sulfate proteoglycan core proteins from a rat endothelial cell line. *J. Biol. Chem.* 267, 4870–4877.

Kolset, S. O., and Tveit, H. (2008). Serglycin–structure and biology. *Cell Mol. Life. Sci.* 65, 1073–1085. doi: 10.1007/s00018-007-7455-6

Kraushaar, D. C., Rai, S., Condac, E., Nairn, A., Zhang, S., Yamaguchi, Y., et al. (2012). Heparan sulfare facilitates FGF and BMP signaling to drive mesoderm differentiation of mouse embryonic stem cells. *J. Biol. Chem.* 287, 22691–22700. doi: 10.1074/jbc.m112.368241

Kraushaar, D. C., Yamaguchi, Y., and Wang, L. (2010). Heparan sulfate is required for embryonic stem cells to exit from self-renewal. *J. Biol. Chem.* 285, 5907–5916. doi: 10.1074/jbc.m109.066837

Kreuger, J., Jemth, P., Sanders-Lindberg, E., Eliahu, L., Ron, D., Basilico, C., et al. (2005). Fibroblast growth factors share binding sites in heparan sulphate. *Biochem. J.* 389(Pt 1), 145–150. doi: 10.1042/bj20042129

Kreuger, J., Prydz, K., Pettersson, R. F., Lindahl, U., and Salmivirta, M. (1999). Characterization of fibroblast growth factor 1 binding heparan sulfate domain. *Glycobiology* 9, 723–729. doi: 10.1093/glycob/9.7.723

Kreuger, J., Spillmann, D., Li, J. P., and Lindahl, U. (2006). Interactions between heparan sulfate and proteins: the concept of specificity. *J. Cell Biol.* 174, 323–327. doi: 10.1083/jcb.200604035

Kumar Katakam, S., Tria, V., Sim, W. C., Yip, G. W., Molgora, S., Karnavas, T., et al. (2020). The heparan sulfate proteoglycan Syndecan-1 regulates colon cancer stem cell function via a focal adhesion kinase - Wnt signaling axis. *FEBS J.* [Epub ahead of print]. doi: 10.1111/febs.15356

Kuo, W. J., Digman, M. A., and Lander, A. D. (2010). Heparan sulfate acts as a bone morphogenetic protein coreceptor by facilitating ligand-induced receptor hetero-oligomerization. *Mol. Biol. Cell* 21, 4028–4041. doi: 10.1091/mbc.E10-04-0348

Kussie, P. H., Hulmes, J. D., Ludwig, D. L., Patel, S., Navarro, E. C., Seddon, A. P., et al. (1999). Cloning and functional expression of a human heparanase gene. *Biochem. Biophys. Res. Commun.* 261, 183–187. doi: 10.1006/bbrc.1999.0962

Lai, J., Chien, J., Staub, J., Avula, R., Greene, E. L., Matthews, T. A., et al. (2003). Loss of HSulf-1 up-regulates heparin-binding growth factor signaling in cancer. *J. Biol. Chem.* 278, 23107–23117. doi: 10.1074/jbc.M302203200

Langsdorf, A., Do, A. T., Kusche-Gullberg, M., Emerson, C. P. Jr., and Ai, X. (2007). Sulfs are regulators of growth factor signaling for satellite cell differentiation and muscle regeneration. *Dev. Biol.* 311, 464–477. doi: 10.1016/j.ydbio.2007.08.053

Lanner, F., Lee, K. L., Sohl, M., Holmborn, K., Yang, H., Wilbertz, J., et al. (2010). Heparan sulfation–dependent fibroblast growth factor signaling maintains embryonic stem cells primed for differentiation in a heterogeneous state. *Stem Cells* 28, 191–200. doi: 10.1002/stem.265

Larraín, J., Alvarez, J., Hassell, J. R., and Brandan, E. (1997). Expression of perlecan, a proteoglycan that binds myogenic inhibitory basic fibroblast growth factor, is down regulated during skeletal muscle differentiation. *Exp. Cell Res.* 234, 405–412. doi: 10.1006/excr.1997.3648

Lathrop, B., Olson, E., and Glaser, L. (1985). Control by fibroblast growth factor of differentiation in the BC3H1 muscle cell line. *J. Cell Biol.* 100, 1540–1547. doi: 10.1083/jcb.100.5.1540

Le Jan, S., Hayashi, M., Kasza, Z., Eriksson, I., Bishop, J. R., Weibrecht, I., et al. (2012). Functional overlap between chondroitin and heparan sulfate proteoglycans during VEGF-induced sprouting angiogenesis. *Arterioscler. Thromb. Vasc. Biol.* 32, 1255–1263. doi: 10.1161/atvbaha.111.240622

Li, D., Wei, X., Xie, K., Chen, K., Li, J., and Fang, J. (2014). A novel decoy receptor fusion protein for FGF-2 potently inhibits tumour growth. *Br. J. Cancer* 111, 68–77. doi: 10.1038/bjc.2014.282

Lin, X., Wei, G., Shi, Z., Dryer, L., Esko, J. D., Wells, D. E., et al. (2000). Disruption of gastrulation and heparan sulfate biosynthesis in EXT1-deficient mice. *Dev. Biol.* 224, 299–311. doi: 10.1006/dbio.2000.9798

Lindahl, U. (1966). The structures of xylosylserine and galactosylxylosylserine from heparin. *Biochim. Biophys. Acta* 130, 361–367. doi: 10.1016/0304-4165(66)90232-7

Lindahl, U., and Li, J. P. (2009). Interactions between heparan sulfate and proteins - design and functional implications. *Int. Rev. Cell Mol. Biol.* 276, 105–159. doi: 10.1016/s1937-6448(09)76003-4

Lindahl, U., and Rodén, L. (1965). The role of galactose and xylose in the linkage of heparin to protein. *J. Biol. Chem.* 240, 2821–2826.

Ling, L., Camilleri, E. T., Helledie, T., Samsonraj, R. M., Titmarsh, D. M., Chua, R. J., et al. (2016). Effect of heparin on the biological properties and molecular signature of human mesenchymal stem cells. *Gene* 576(1 Pt 2), 292–303. doi: 10.1016/j.gene.2015.10.039

Ling, L., Dombrowski, C., Foong, K. M., Haupt, L. M., Stein, G. S., Nurcombe, V., et al. (2010). Synergism between Wnt3a and heparin enhances osteogenesis via a phosphoinositide 3-kinase/Akt/RUNX2 pathway. *J. Biol. Chem.* 285, 26233–26244. doi: 10.1074/jbc.M110.122069

Ling, L., Ren, X., Cao, X., Hassan, A. B. M., Mah, S., Sathiyanathan, P., et al. (2020). Enhancing the efficacy of stem cell therapy with glycosaminoglycans. *Stem Cell Rep.* 14, 105–121. doi: 10.1016/j.stemcr.2019.12.003

Ling, L., Tan, S. K., Goh, T. H., Cheung, E., Nurcombe, V., van Wijnen, A. J., et al. (2015). Targeting the heparin-binding domain of fibroblast growth factor receptor 1 as a potential cancer therapy. *Mol. Cancer* 14:136. doi: 10.1186/s12943-015-0391-4

Liu, B. Y., McDermott, S. P., Khwaja, S. S., and Alexander, C. M. (2004). The transforming activity of Wnt effectors correlates with their ability to induce the accumulation of mammary progenitor cells. *Proc. Natl. Acad. Sci. U.S.A.* 101, 4158–4163. doi: 10.1073/pnas.0400699101

Liu, J., Shworak, N. W., Sinay, P., Schwartz, J. J., Zhang, L., Fritze, L. M. S., et al. (1999). Expression of heparan Sulfate d-Glucosaminyl 3-O-Sulfotransferase isoforms reveals novel substrate specificities. *J. Biol. Chem.* 274, 5185–5192. doi: 10.1074/jbc.274.8.5185

Longley, R. L., Woods, A., Fleetwood, A., Cowling, G. J., Gallagher, J. T., and Couchman, J. R. (1999). Control of morphology, cytoskeleton and migration by syndecan-4. *J. Cell Sci.* 112, 3421.

Luikart, S. D., Maniglia, C. A., Furcht, L. T., McCarthy, J. B., et al. (1990). A heparan sulfate-containing fraction of bone marrow stroma induces maturation of HL-60 cells in vitro. *Cancer Res.* 50, 3781–3785.

Luo, N., Li, H., Xiang, B., Qiao, L., He, J., Ji, Y., et al. (2016). Syndecan-4 modulates the proliferation of neural cells and the formation of CaP axons during zebrafish embryonic neurogenesis. *Sci. Rep.* 6, 25300–25300. doi: 10.1038/srep25300

Maccarana, M., Casu, B., and Lindahl, U. (1993). Minimal sequence in heparin/heparan sulfate required for binding of basic fibroblast growth factor. *J. Biol. Chem.* 268, 23898–23905.

Maccarana, M., Sakura, Y., Tawada, A., Yoshida, K., and Lindahl, U. (1996). Domain structure of heparan sulfates from bovine organs. *J. Biol. Chem.* 271, 17804–17810. doi: 10.1074/jbc.271.30.17804

Makarenkova, H. P., Hoffman, M. P., Beenken, A., Eliseenkova, A. V., Meech, R., Tsau, C., et al. (2009). Differential interactions of FGFs with heparan sulfate control gradient formation and branching morphogenesis. *Sci. Signal.* 2:ra55. doi: 10.1126/scisignal.2000304

Malgouries, S., Thibaut, S., and Bernard, B. A. (2008). Proteoglycan expression patterns in human hair follicle. *Br. J. Dermatol.* 158, 234–242. doi: 10.1111/j.1365-2133.2007.08339.x

Mansbridge, J. N., and Hanawalt, P. C. (1988). Role of transforming growth factor beta in the maturation of human epidermal keratinocytes. *J. Invest. Dermatol.* 90, 336–341. doi: 10.1111/1523-1747.ep12456286

Mauro, A. (1961). Satellite cell of skeletal muscle fibers. *J. Biophys. Biochem. Cytol.* 9, 493–495. doi: 10.1083/jcb.9.2.493

McCuskey, R. S., and Meineke, H. A. (1973). Studies of the hemopoietic microenvironment. 3. Differences in the splenic microvascular system and stroma between SL-SL d and W-W v anemic mice. *Am. J. Anat.* 137, 187–197. doi: 10.1002/aja.1001370205

McDermott, S. P., Ranheim, E. A., Leatherberry, V. S., Khwaja, S. S., Klos, K. S., and Alexander, C. M. (2007). Juvenile syndecan-1 null mice are protected from carcinogen-induced tumor development. *Oncogene* 26, 1407–1416. doi: 10.1038/sj.onc.1209930

McLaughlin, D., Karlsson, F., Tian, N., Pratt, T., Bullock, S. L., Wilson, V. A., et al. (2003). Specific modification of heparan sulphate is required for normal cerebral cortical development. *Mech. Dev.* 120, 1481–1488. doi: 10.1016/j.mod.2003.08.008

Meade, K. A., White, K. J., Pickford, C. E., Holley, R. J., Marson, A., Tillotson, D., et al. (2013). Immobilization of heparan sulfate on electrospun meshes to support embryonic stem cell culture and differentiation. *J. Biol. Chem.* 288, 5530–5538. doi: 10.1074/jbc.M112.423012

Meyers, E. N., Lewandoski, M., and Martin, G. R. (1998). An Fgf8 mutant allelic series generated by Cre- and Flp-mediated recombination. *Nat. Genet.* 18, 136–141. doi: 10.1038/ng0298-136

Mitsou, I., Multhaupt, H. A. B., and Couchman, J. R. (2017). Proteoglycans, ion channels and cell-matrix adhesion. *Biochem. J.* 474, 1965–1979. doi: 10.1042/BCJ20160747

Morgan, B. A. (2014). The dermal papilla: an instructive niche for epithelial stem and progenitor cells in development and regeneration of the hair follicle. *Cold Spring Harb. Perspect. Med.* 4:a015180. doi: 10.1101/cshperspect.a015180

Multhaupt, H. A. B., Yoneda, A., Whiteford, J. R., Oh, E. S., Lee, W., and Couchman, J. R. (2009). Syndecan signalling: when, where and why? *J. Physiol. Pharmacol.* 60(Suppl. 4), 31–38.

Mundy, C., Yang, E., Takano, H., Billings, P. C., and Pacifici, M. (2018). Heparan sulfate antagonism alters bone morphogenetic protein signaling and receptor dynamics, suggesting a mechanism in hereditary multiple exostoses. *J. Biol. Chem.* 293, 7703–7716. doi: 10.1074/jbc.ra117.000264

Murali, S., Rai, B., Dombrowski, C., Lee, J. L., Lim, Z. X., Bramono, D. S., et al. (2013). Affinity-selected heparan sulfate for bone repair. *Biomaterials* 34, 5594–5605. doi: 10.1016/j.biomaterials.2013.04.017

Murphy, M., Drago, J., and Bartlett, P. F. (1990). Fibroblast growth factor stimulates the proliferation and differentiation of neural precursor cells in vitro. *J. Neurosci. Res.* 25, 463–475. doi: 10.1002/jnr.490250404

Nagarajan, A., Malvi, P., and Wajapeyee, N. (2018). Heparan sulfate and heparan sulfate proteoglycans in cancer initiation and progression. *Front. Endocrinol.* 9:483. doi: 10.3389/fendo.2018.00483

Nairn, A. V., Kinoshita-Toyoda, A., Toyoda, H., Xie, J., Harris, K., Dalton, S., et al. (2007). Glycomics of proteoglycan biosynthesis in murine embryonic stem cell differentiation. *J. Proteome Res.* 6, 4374–4387. doi: 10.1021/pr070446f

Nakato, H., Futch, T. A., and Selleck, S. B. (1995). The division abnormally delayed (dally) gene: a putative integral membrane proteoglycan required for cell division patterning during postembryonic development of the nervous system in Drosophila. *Development* 121:3687.

Nam, E. J., and Park, P. W. (2012). Shedding of cell membrane-bound proteoglycans. *Methods Mol. Biol.* 836, 291–305. doi: 10.1007/978-1-61779-498-8_19

Netelenbos, T., van den Born, J., Kessler, F. L., Zweegman, S., Merle, P. A., van Oostveen, J. W., et al. (2003). Proteoglycans on bone marrow endothelial cells bind and present SDF-1 towards hematopoietic progenitor cells. *Leukemia* 17, 175–184. doi: 10.1038/sj.leu.2402738

Netelenbos, T., Zuijderduijn, S., Van Den Born, J., Kessler, F. L., Zweegman, S., Huijgens, P. C., et al. (2002). Proteoglycans guide SDF-1-induced migration of hematopoietic progenitor cells. *J. Leukoc. Biol.* 72, 353–362.

Noonan, D. M., Fulle, A., Valente, P., Cai, S., Horigan, E., Sasaki, M., et al. (1991). The complete sequence of perlecan, a basement membrane heparan sulfate proteoglycan, reveals extensive similarity with laminin A chain, low density lipoprotein-receptor, and the neural cell adhesion molecule. *J. Biol. Chem.* 266, 22939–22947.

Nurcombe, V., Ford, M. D., Wildschut, J. A., and Bartlett, P. F. (1993). Developmental regulation of neural response to FGF-1 and FGF-2 by heparan sulfate proteoglycan. *Science* 260:103. doi: 10.1126/science.7682010

Oikari, L. E., Okolicsanyi, R. K., Qin, A., Yu, C., Griffiths, L. R., and Haupt, L. M. (2016). Cell surface heparan sulfate proteoglycans as novel markers of human neural stem cell fate determination. *Stem Cell Res.* 16, 92–104. doi: 10.1016/j.scr.2015.12.011

Okina, E., Grossi, A., Gopal, S., Multhaupt, H. A. B., and Couchman, J. R. (2012). Alpha-actinin interactions with syndecan-4 are integral to fibroblast–matrix adhesion and regulate cytoskeletal architecture. *Int. J. Biochem. Cell Biol.* 44, 2161–2174. doi: 10.1016/j.biocel.2012.08.017

Olczyk, P., Mencner, Ł, and Komosinska-Vassev, K. (2015). Diverse roles of heparan sulfate and heparin in wound repair. *BioMed Res. Int.* 2015, 549417. doi: 10.1155/2015/549417

Olguin, H., and Brandan, E. (2001). Expression and localization of proteoglycans during limb myogenic activation. *Dev. Dyn.* 221, 106–115. doi: 10.1002/dvdy.1129

Olwin, B. B., and Rapraeger, A. (1992). Repression of myogenic differentiation by aFGF, bFGF, and K-FGF is dependent on cellular heparan sulfate. *J. Cell Biol.* 118, 631–639. doi: 10.1083/jcb.118.3.631

Ornitz, D. M., Yayon, A., Flanagan, J. G., Svahn, C. M., Levi, E., and Leder, P. (1992). Heparin is required for cell-free binding of basic fibroblast growth factor to a soluble receptor and for mitogenesis in whole cells. *Mol. Cell. Biol.* 12, 240–247. doi: 10.1128/mcb.12.1.240

Osdoby, P., and Caplan, A. I. (1976). The possible differentiation of osteogenic elements in vitro from chick limb mesodermal cells. I. Morphological evidence. *Dev. Biol.* 52, 283–299. doi: 10.1016/0012-1606(76)90246-3

Ostrovsky, O., Berman, B., Gallagher, J., Mulloy, B., Fernig, D. G., Delehedde, M., et al. (2002). Differential effects of heparin saccharides on the formation of specific fibroblast growth factor (FGF) and FGF receptor complexes. *J. Biol. Chem.* 277, 2444–2453. doi: 10.1074/jbc.M108540200

Papy-Garcia, D., and Albanese, P. (2017). Heparan sulfate proteoglycans as key regulators of the mesenchymal niche of hematopoietic stem cells. *Glycoconj. J.* 34, 377–391. doi: 10.1007/s10719-017-9773-8

Patel, N. J., Sharon, C., Baranwal, S., Boothello, R. S., Desai, U. R., and Patel, B. B. (2016). Heparan sulfate hexasaccharide selectively inhibits cancer stem cells self-renewal by activating p38 MAP kinase. *Oncotarget* 7, 84608–84622. doi: 10.18632/oncotarget.12358

Patterson, A. M., Cartwright, A., David, G., Fitzgerald, O., Bresnihan, B., Ashton, B. A., et al. (2008). Differential expression of syndecans and glypicans in chronically inflamed synovium. *Ann. Rheum. Dis.* 67, 592–601. doi: 10.1136/ard.2006.063875

Pawlikowski, B., Vogler, T. O., Gadek, K., and Olwin, B. B. (2017). Regulation of skeletal muscle stem cells by fibroblast growth factors. *Dev. Dyn.* 246, 359–367. doi: 10.1002/dvdy.24495

Pellegrini, L., Burke, D. F., von Delft, F., Mulloy, B., and Blundell, T. L. (2000). Crystal structure of fibroblast growth factor receptor ectodomain bound to ligand and heparin. *Nature* 407, 1029–1034. doi: 10.1038/35039551

Pickford, C. E., Holley, R. J., Rushton, G., Stavridis, M., Ward, C. M., and Merry, C. L. R. (2011). Specific glycosaminoglycans modulate neural specification of mouse embryonic stem cells. *Stem Cells* 29, 629–640. doi: 10.1002/stem.610

Pisconti, A., Cornelison, D. D., Olguin, H. C., Antwine, T. L., and Olwin, B. B. (2010). Syndecan-3 and Notch cooperate in regulating adult myogenesis. *J. Cell Biol.* 190, 427–441. doi: 10.1083/jcb.201003081

Plaks, V., Kong, N., and Werb, Z. (2015). The cancer stem cell niche: how essential is the niche in regulating stemness of tumor cells? *Cell Stem Cell* 16, 225–238. doi: 10.1016/j.stem.2015.02.015

Ploemacher, R. E., van't Hull, E., and van Soest, P. L. (1978). Studies of the hemopoietic microenvironments: effects of acid mucopolysaccharides and dextran sulphate on erythroid and granuloid differentiation in vitro. *Exp. Hematol.* 6, 311–320.

Poon, S., Lu, X., Smith, R. A. A., Ho, P., Bhakoo, K., Nurcombe, V., et al. (2018). Improved recovery from limb ischaemia by delivery of an affinity-isolated heparan sulphate. *Angiogenesis* 21, 777–791. doi: 10.1007/s10456-018-9622-9

Potten, C. S., and Morris, R. J. (1988). Epithelial stem cells in vivo. *J. Cell Sci. Suppl.* 10, 45–62. doi: 10.1242/jcs.1988.supplement_10.4

Poulain, F. E., and Yost, H. J. (2015). Heparan sulfate proteoglycans: a sugar code for vertebrate development? *Development* 142, 3456–3467. doi: 10.1242/dev.098178

Pruessmeyer, J., Martin, C., Hess, F. M., Schwarz, N., Schmidt, S., Kogel, T., et al. (2010). A disintegrin and metalloproteinase 17 (ADAM17) mediates inflammation-induced shedding of syndecan-1 and -4 by lung epithelial cells. *J. Biol. Chem.* 285, 555–564. doi: 10.1074/jbc.M109.059394

Pye, D. A., Vives, R. R., Turnbull, J. E., Hyde, P., and Gallagher, J. T. (1998). Heparan sulfate oligosaccharides require 6-O-sulfation for promotion of basic fibroblast growth factor mitogenic activity. *J. Biol. Chem.* 273, 22936–22942. doi: 10.1074/jbc.273.36.22936

Raballo, R., Rhee, J., Lyn-Cook, R., Leckman, J. F., Schwartz, M. L., and Vaccarino, F. M. (2000). Basic fibroblast growth factor (Fgf2) is necessary for cell proliferation and neurogenesis in the developing cerebral cortex. *J. Neurosci.* 20:5012. doi: 10.1523/JNEUROSCI.20-13-05012.2000

Rapraeger, A., Jalkanen, M., and Bernfield, M. (1986). Cell surface proteoglycan associates with the cytoskeleton at the basolateral cell surface of mouse mammary epithelial cells. *J. Cell Biol.* 103, 2683–2696. doi: 10.1083/jcb.103.6.2683

Rapraeger, A., Jalkanen, M., Endo, E., Koda, J., and Bernfield, M. (1985). The cell surface proteoglycan from mouse mammary epithelial cells bears chondroitin sulfate and heparan sulfate glycosaminoglycans. *J. Biol. Chem.* 260, 11046–11052.

Rapraeger, A. C., Krufka, A., and Olwin, B. B. (1991). Requirement of heparan sulfate for bFGF-mediated fibroblast growth and myoblast differentiation. *Science* 252:1705. doi: 10.1126/science.1646484

Raulo, E., Chernousov, M. A., Carey, D. J., Nolo, R., and Rauvala, H. (1994). Isolation of a neuronal cell surface receptor of heparin binding growth-associated molecule (HB-GAM). Identification as N-syndecan (syndecan-3). *J. Biol. Chem.* 269, 12999–13004.

Reimann, J., and Burger, H. (1979). In vitro proliferation of haemopoietic cells in the presence of adherent cell layers. II. Differential effect of adherent cell layers derived from various organs. *Exp. Hematol.* 7, 52–58.

Roberts, R., Gallagher, J., Spooncer, E., Alien, T. D., Bloomfield, F., and Dexter, T. M. (1988). Heparan sulphate bound growth factors: a mechanism for stromal cell mediated haemopoiesis. *Nature* 332, 376–378. doi: 10.1038/332376a0

Rosen, S. D., and Lemjabbar-Alaoui, H. (2010). Sulf-2: an extracellular modulator of cell signaling and a cancer target candidate. *Expert Opin. Ther. Targets* 14, 935–949. doi: 10.1517/14728222.2010.504718

Rudd, T. R., Preston, M. D., and Yates, E. A. (2017). The nature of the conserved basic amino acid sequences found among 437 heparin binding proteins determined by network analysis. *Mol. BioSyst.* 13, 852–865. doi: 10.1039/c6mb00857g

Ruppert, R., Hoffmann, E., and Sebald, W. (1996). Human bone morphogenetic protein 2 contains a heparin-binding site which modifies its biological activity. *Eur. J. Biochem.* 237, 295–302. doi: 10.1111/j.1432-1033.1996.0295n.x

Sadir, R., Imberty, A., Baleux, F., and Lortat-Jacob, H. (2004). Heparan sulfate/heparin oligosaccharides protect stromal cell-derived Factor-1 (SDF-1)/CXCL12 against proteolysis induced by CD26/Dipeptidyl Peptidase IV. *J. Biol. Chem.* 279, 43854–43860. doi: 10.1074/jbc.m405392200

Sahara, S., and O'Leary, D. D. M. (2009). Fgf10 regulates transition period of cortical stem cell differentiation to radial glia controlling generation of neurons and basal progenitors. *Neuron* 63, 48–62. doi: 10.1016/j.neuron.2009.06.006

San Antonio, J. D., Winston, B. M., and Tuan, R. S. (1987). Regulation of chondrogenesis by heparan sulfate and structurally related glycosaminoglycans. *Dev. Biol.* 123, 17–24. doi: 10.1016/0012-1606(87)90422-2

Sanderson, R. D., and Bernfield, M. (1988). Molecular polymorphism of a cell surface proteoglycan: distinct structures on simple and stratified epithelia. *Proc. Natl. Acad. Sci. U.S.A.* 85:9562. doi: 10.1073/pnas.85.24.9562

Sanderson, R. D., Hinkes, M. T., and Bernfield, M. (1992). Syndecan-1, a cell-surface proteoglycan, changes in size and abundance when keratinocytes stratify. *J. Invest. Dermatol.* 99, 390–396. doi: 10.1111/1523-1747.ep12616103

Saoncella, S., Echtermeyer, F., Denhez, F., Nowlen, J. K., Mosher, D. F., Robinson, S. D., et al. (1999). Syndecan-4 signals cooperatively with integrins in a Rho-dependent manner in the assembly of focal adhesions and actin stress fibers. *Proc. Natl. Acad. Sci. U.S.A.* 96, 2805–2810. doi: 10.1073/pnas.96.6.2805

Sarras, M. P., Madden, M. E., Zhang, X., Gunwar, S., Huff, J. K., and Hudson, B. G. (1991). Extracellular matrix (mesoglea) of Hydra vulgaris: I. Isolation and characterization. *Dev. Biol.* 148, 481–494. doi: 10.1016/0012-1606(91)90266-6

Sarrazin, S., Lamanna, W. C., and Esko, J. D. (2011). Heparan sulfate proteoglycans. *Cold Spring Harb. Perspect. Biol.* 3:a004952. doi: 10.1101/cshperspect.a004952

Schlessinger, J., Plotnikov, A. N., Ibrahimi, O. A., Eliseenkova, A. V., Yeh, B. K., Yayon, A., et al. (2000). Crystal structure of a ternary FGF-FGFR-Heparin complex reveals a dual role for heparin in FGFR binding and dimerization. *Mol. Cell.* 6, 743–750. doi: 10.1016/S1097-2765(00)00073-3

Schultz, V., Suflita, M., Liu, X., Zhang, X., Yu, Y., Li, L., et al. (2017). Heparan sulfate domains required for fibroblast growth factor 1 and 2 signaling through fibroblast growth factor receptor 1c. *J. Biol. Chem.* 292, 2495–2509. doi: 10.1074/jbc.M116.761585

Sheng, J., Liu, R., Xu, Y., and Liu, J. (2011). The dominating role of N-Deacetylase/N-Sulfotransferase 1 in forming domain structures in heparan sulfate. *J. Biol. Chem.* 286, 19768–19776. doi: 10.1074/jbc.m111.224311

Sher, I., Zisman-Rozen, S., Eliahu, L., Whitelock, J. M., Maas-Szabowski, N., Yamada, Y., et al. (2006). Targeting perlecan in human keratinocytes reveals novel roles for perlecan in epidermal formation. *J. Biol. Chem.* 281, 5178–5187. doi: 10.1074/jbc.M509500200

Shintani, Y., Takashima, S., Asano, Y., Kato, H., Liao, Y., Yamazaki, S., et al. (2006). Glycosaminoglycan modification of neuropilin-1 modulates VEGFR2 signaling. *Embo J.* 25, 3045–3055. doi: 10.1038/sj.emboj.7601188

Shworak, N. W., Liu, J., Fritze, L. M. S., Schwartz, J. J., Zhang, L., Logeart, D., et al. (1997). Molecular cloning and expression of mouse and human cDNAs encoding heparan sulfate d-Glucosaminyl 3-O-Sulfotransferase. *J. Biol. Chem.* 272, 28008–28019. doi: 10.1074/jbc.272.44.28008

Shworak, N. W., Liu, J., Petros, L. M., Zhang, L., Kobayashi, M., Copeland, N. G., et al. (1999). Multiple isoforms of heparan Sulfate d-Glucosaminyl 3-O-Sulfotransferase: isolation, characterization, and expression of human cdnas and identification of distinct genomic loci. *J. Biol. Chem.* 274, 5170–5184. doi: 10.1074/jbc.274.8.5170

Siczkowski, M., Clarke, D., and Gordon, M. Y. (1992). Binding of primitive hematopoietic progenitor cells to marrow stromal cells involves heparan sulfate. *Blood* 80, 912–919. doi: 10.1182/blood.v80.4.912.912

Smeds, E., Feta, A., and Kusche-Gullberg, M. (2010). Target selection of heparan sulfate hexuronic acid 2-O-sulfotransferase. *Glycobiology* 20, 1274–1282. doi: 10.1093/glycob/cwq089

Smith, R. A. A., Chua, R. J. E., Carnachan, S. M., Tan, C. L. L., Sims, I. M., Hinkley, S. F. R., et al. (2018). Retention of the structure and function of heparan sulfate biomaterials after gamma irradiation. *Tissue Eng. Part A* 24, 729–739. doi: 10.1089/ten.TEA.2017.0263

Smith, R. A. A., Meade, K., Pickford, C. E., Holley, R. J., and Merry, C. L. (2011). Glycosaminoglycans as regulators of stem cell differentiation. *Biochem. Soc. Trans.* 39, 383–387. doi: 10.1042/BST0390383

Spivak-Kroizman, T., Lemmon, M. A., Dikic, I., Ladbury, J. E., Pinchasi, D., Huang, J., et al. (1994). Heparin-induced oligomerization of FGF molecules is responsible for FGF receptor dimerization, activation, and cell proliferation. *Cell* 79, 1015–1024. doi: 10.1016/0092-8674(94)90032-9

Stelling, M. P., Lages, Y. M. V., Tovar, A. M. F., Mourão, P. A. S., and Rehen, S. K. (2012). Matrix-bound heparan sulfate is essential for the growth and pluripotency of human embryonic stem cells. *Glycobiology* 23, 337–345. doi: 10.1093/glycob/cws133

Stevens, R. L., Fox, C. C., Lichtenstein, L. M., and Austen, K. F. (1988). Identification of chondroitin sulfate E proteoglycans and heparin proteoglycans in the secretory granules of human lung mast cells. *Proc. Natl. Acad. Sci. U.S.A.* 85, 2284. doi: 10.1073/pnas.85.7.2284

Storm, E. E., Garel, S., Borello, U., Hebert, J. M., Martinez, S., McConnell, S. K., et al. (2006). Dose-dependent functions of Fgf8 in regulating telencephalic patterning centers. *Development* 133, 1831–1844. doi: 10.1242/dev.02324

Sun, C., Liu, M., Sun, P., Yang, M., Yates, E. A., Guo, Z., et al. (2019). Sulfated polysaccharides interact with fibroblast growth factors and protect from denaturation. *FEBS Open Biol.* 9, 1477–1487. doi: 10.1002/2211-5463.12696

Sun, N., Petiwala, S., Wang, R., Lu, C., Hu, M., Ghosh, S., et al. (2019). Development of drug-inducible CRISPR-Cas9 systems for large-scale functional screening. *BMC Genomics* 20:225. doi: 10.1186/s12864-019-5601-9

Szabowski, A., Maas-Szabowski, N., Andrecht, S., Kolbus, A., Schorpp-Kistner, M., Fusenig, N. E., et al. (2000). c-Jun and JunB antagonistically control cytokine-regulated mesenchymal-epidermal interaction in skin. *Cell* 103, 745–755. doi: 10.1016/s0092-8674(00)00178-1

Tantravahi, R. V., Stevens, R. L., Austen, K. F., and Weis, J. H. (1986). A single gene in mast cells encodes the core peptides of heparin and chondroitin sulfate proteoglycans. *Proc. Natl. Acad. Sci. U.S.A.* 83, 9207–9210. doi: 10.1073/pnas.83.23.9207

ten Dam, G. B., Kurup, S., van de Westerlo, E. M. A., Versteeg, E. M. M., Lindahl, U., Spillmann, D., et al. (2006). 3-O-Sulfated Oligosaccharide Structures Are Recgonized by Anti-heparan Sulfate Antibody HS4C3. *J. Biol. Chem.* 281, 4654–4662. doi: 10.1074/jbc.m506357200

Thomas, K. R., Musci, T. S., Neumann, P. E., and Capecchi, M. R. (1991). Swaying is a mutant allele of the proto-oncogene Wnt-1. *Cell* 67, 969–976. doi: 10.1016/0092-8674(91)90369-a

Titmarsh, D. M., Tan, C. L. L., Glass, N. R., Nurcombe, V., Cooper-White, J. J., and Cool, S. M. (2017). Microfluidic screening reveals heparan sulfate enhances human mesenchymal stem cell growth by modulating fibroblast growth factor-2 transport. *Stem Cells Transl. Med.* 6, 1178–1190. doi: 10.1002/sctm.16-0343

Townley, R. A., and Bülow, H. E. (2011). Genetic analysis of the heparan modification network in *Caenorhabditis elegans*. *J. Biol. Chem.* 286, 16824–16831. doi: 10.1074/jbc.m111.227926

Traister, A., Shi, W., and Filmus, J. (2008). Mammalian Notum induces the release of glypicans and other GPI-anchored proteins from the cell surface. *Biochem. J.* 410, 503–511. doi: 10.1042/BJ20070511

Traktuev, D. O., Merfeld-Clauss, S., Li, J., Kolonin, M., Arap, W., Pasqualini, R., et al. (2008). A population of multipotent CD34-positive adipose stromal cells share pericyte and mesenchymal surface markers, reside in a periendothelial location, and stabilize endothelial networks. *Circ. Res.* 102, 77–85. doi: 10.1161/CIRCRESAHA.107.159475

Tran, T. H., Shi, X., Zaia, J., and Ai, X. (2012). Heparan sulfate 6-O-endosulfatases (Sulfs) coordinate the Wnt signaling pathways to regulate myoblast fusion during skeletal muscle regeneration. *J. Biol. Chem.* 287, 32651–32664. doi: 10.1074/jbc.M112.353243

Trieger, G. W., Verespy, S. III, Gordts, P., and Godula, K. (2019). Efficient synthesis of heparinoid bioconjugates for tailoring FGF2 activity at the stem cell-matrix interface. *Bioconjug. Chem.* 30, 833–840. doi: 10.1021/acs.bioconjchem.8b00921

Tsen, G., Halfer, W., Kroger, S., and Cole, G. J. (1995). Agrin is a heparan sulfate proteoglycan. *J. Biol. Chem.* 270, 3392–3399. doi: 10.1074/jbc.270.7.3392

Turnbull, J., Powell, A., and Guimond, S. (2001). Heparan sulfate: decoding a dynamic multifunctional cell regulator. *Trends Cell Biol.* 11, 75–82. doi: 10.1016/S0962-8924(00)01897-3

Turnbull, J. E., Fernig, D. G., Ke, Y., Wilkinson, M. C., and Gallagher, J. T. (1992). Identification of the basic fibroblast growth factor binding sequence in fibroblast heparan sulfate. *J. Biol. Chem.* 267, 10337–10341.

Turnbull, J. E., and Gallagher, J. T. (1988). Oligosaccharide mapping of heparan sulphate by polyacrylamide-gradient-gel electrophoresis and electrotransfer to nylon membrane. *Biochem. J.* 251, 597–608. doi: 10.1042/bj2510597

Turnbull, J. E., and Gallagher, J. T. (1990). Molecular organization of heparan sulphate from human skin fibroblasts. *Biochem. J.* 265, 715–724. doi: 10.1042/bj2650715

Turnbull, J. E., and Gallagher, J. T. (1991). Distribution of iduronate 2-sulphate residues in heparan sulphate. Evidence for an ordered polymeric structure. *Biochem. J.* 273, 553–559. doi: 10.1042/bj2730553

Uchimura, K., Morimoto-Tomita, M., Bistrup, A., Li, J., Lyon, M., Gallagher, J., et al. (2006). HSulf-2, an extracellular endoglucosamine-6-sulfatase, selectively mobilizes heparin-bound growth factors and chemokines: effects on VEGF, FGF-1, and SDF-1. *BMC Biochem.* 7:2. doi: 10.1186/1471-2091-7-2

Ullah, I., Busch, J. F., Rabien, A., Ergün, B., Stamm, C., Knosalla, C., et al. (2020). Adult tissue extracellular matrix determines tissue specification of human iPSC-derived embryonic stage mesodermal precursor cells. *Adv. Sci.* 7:1901198. doi: 10.1002/advs.201901198

Varki, A., Cummings, R. D., Aebi, M., Packer, N. H., Seeberger, P. H., Esko, J. D., et al. (2015). Symbol nomenclature for graphical representations of glycans. *Glycobiology* 25, 1323–1324. doi: 10.1093/glycob/cwv091

Vlodavsky, I., Goldshmidt, O., Zcharia, E., Atzmon, R., Rangini-Guatta, Z., Elkin, M., et al. (2002). Mammalian heparanase: involvement in cancer metastasis, angiogenesis and normal development. *Semin Cancer Biol.* 12, 121–129. doi: 10.1006/scbi.2001.0420

Vlodavsky, I., Ilan, N., Naggi, A., and Casu, B. (2007). Heparanase: structure, biological functions, and inhibition by heparin-derived mimetics of heparan sulfate. *Curr. Pharm. Des.* 13, 2057–2073. doi: 10.2174/138161207780319742

Vuong, T. T., Reine, T. M., Sudworth, A., Jenssen, T. G., and Kolset, S. O. (2015). Syndecan-4 is a major syndecan in primary human endothelial cells in vitro, modulated by inflammatory stimuli and involved in wound healing. *J. Histochem. Cytochem.* 63, 280–292. doi: 10.1369/0022155415568995

Wang, C., Poon, S., Murali, S., Koo, C. Y., Bell, T. J., Hinkley, S. F., et al. (2014). Engineering a vascular endothelial growth factor 165-binding heparan sulfate for vascular therapy. *Biomaterials* 35, 6776–6786. doi: 10.1016/j.biomaterials.2014.04.084

Wang, Q., Yang, L., Alexander, C., and Temple, S. (2012). The niche factor syndecan-1 regulates the maintenance and proliferation of neural progenitor cells during mammalian cortical development. *PLoS One* 7:e42883. doi: 10.1371/journal.pone.0042883

Weiss, A. R. R., and Dahlke, M. H. (2019). Immunomodulation by mesenchymal stem cells (MSCs): mechanisms of action of living, apoptotic, and dead MSCs. *Front. Immunol.* 10:1191. doi: 10.3389/fimmu.2019.01191

Weiss, R. J., Gordts, P. L. S. M., Le, D., Xu, D., Esko, J. D., and Tor, Y. (2015). Small molecule antagonists of cell-surface heparan sulfate and heparin–protein interactions. *Chem. Sci.* 6, 5984–5993. doi: 10.1039/C5SC01208B

Westgate, G. E., Messenger, A. G., Watson, L. P., and Gibson, W. T. (1991). Distribution of proteoglycans during the hair growth cycle in human skin. *J. Invest. Dermatol.* 96, 191–195. doi: 10.1111/1523-1747.ep12461019

Wight, T. N., Kinsella, M. G., Keating, A., and Singer, J. W. (1986). Proteoglycans in human long-term bone marrow cultures: biochemical and ultrastructural analyses. *Blood* 67, 1333–1343. doi: 10.1182/blood.v67.5.1333.bloodjournal6751333

Wijesinghe, S. J., Ling, L., Murali, S., Qing, Y. H., Hinkley, S. F., Carnachan, S. M., et al. (2017). Affinity selection of FGF2-binding heparan sulfates for ex vivo expansion of human mesenchymal stem cells. *J. Cell. Physiol.* 232, 566–575. doi: 10.1002/jcp.25454

Xu, D., and Esko, J. D. (2014). Demystifying heparan sulfate-protein interactions. *Annu. Rev. Biochem*. 83, 129–157. doi: 10.1146/annurev-biochem-060713-035314

Xu, Y., Moon, A. F., Xu, S., Krahn, J. M., Liu, J., and Pedersen, L. C. (2017). Structure based substrate specificity analysis of heparan sulfate 6-O-Sulfotransferases. *ACS Chem. Biol.* 12, 73–82. doi: 10.1021/acschembio.6b00841

Yamada, S., Morimoto, H., Fujisawa, T., and Sugahara, K. (2007). Glycosaminoglycans in Hydra magnipapillata (Hydrozoa, Cnidaria): demonstration of chondroitin in the developing nematocyst, the sting organelle, and structural characterization of glycosaminoglycans. *Glycobiology* 17, 886–894. doi: 10.1093/glycob/cwm051

Yamaguchi, Y. (2001). Heparan sulfate proteoglycans in the nervous system: their diverse roles in neurogenesis, axon guidance, and synaptogenesis. *Semin. Cell Dev. Biol.* 12, 99–106. doi: 10.1006/scdb.2000.0238

Yan, D., and Lin, X. (2009). Shaping morphogen gradients by proteoglycans. *Cold Spring Harb. Perspect. Biol.* 1:a002493. doi: 10.1101/cshperspect.a002493

Yayon, A., Klagsbrun, M., Esko, J. D., Leder, P., and Ornitz, D. M. (1991). Cell surface, heparin-like molecules are required for binding of basic fibroblast growth factor to its high affinity receptor. *Cell* 64, 841–848. doi: 10.1016/0092-8674(91)90512-W

Yu, C., Griffiths, L. R., and Haupt, L. M. (2017). Exploiting heparan sulfate proteoglycans in human neurogenesis-controlling lineage specification and fate. *Front. Integr. Neurosci.* 11:28. doi: 10.3389/fnint.2017.00028

Zaia, J. (2013). Glycosaminoglycan glycomics using mass spectrometry. *Mol. Cell. Proteomics* 12, 885–892. doi: 10.1074/mcp.R112.026294

Zhao, S., Deng, C., Wang, Z., Teng, L., and Chen, J. (2015). Heparan sulfate 6-O-sulfotransferase 3 is involved in bone marrow mesenchymal stromal cell osteogenic differentiation. *Biochemistry* 80, 379–389. doi: 10.1134/s000629791503013x

Zhu, X. J., Liu, Y., Dai, Z. M., Zhang, X., Yang, X., Li, Y., et al. (2014). BMP-FGF signaling axis mediates Wnt-induced epidermal stratification in developing mammalian skin. *PLoS Genet.* 10:e1004687. doi: 10.1371/journal.pgen.1004687

Zweegman, S., Van Den Born, J., Mus, A. M., Kessler, F. L., Janssen, J. J., Netelenbos, T., et al. (2004). Bone marrow stromal proteoglycans regulate megakaryocytic differentiation of human progenitor cells. *Exp. Cell Res.* 299, 383–392. doi: 10.1016/j.yexcr.2004.06.018

Conflict of Interest: The authors declare that the research was conducted in the absence of any commercial or financial relationships that could be construed as a potential conflict of interest.

frontiers in Cell and Developmental Biology

REVIEW
published: 30 November 2020
doi: 10.3389/fcell.2020.569377

Proteoglycans as Mediators of Cancer Tissue Mechanics

*Anna Barkovskaya[1], Alexander Buffone Jr.[1,2], Martin Žídek[1] and Valerie M. Weaver[1,3,4,5,6]**

[1] Center for Bioengineering & Tissue Regeneration, Department of Surgery, University of California, San Francisco, San Francisco, CA, United States, [2] Department of Bioengineering, University of Pennsylvania, Philadelphia, PA, United States, [3] Department of Radiation Oncology, Eli and Edythe Broad Center of Regeneration Medicine and Stem Cell Research, University of California, San Francisco, San Francisco, CA, United States, [4] Department of Bioengineering, Eli and Edythe Broad Center of Regeneration Medicine and Stem Cell Research, University of California, San Francisco, San Francisco, CA, United States, [5] Department of Therapeutic Sciences, Eli and Edythe Broad Center of Regeneration Medicine and Stem Cell Research, University of California, San Francisco, San Francisco, CA, United States, [6] UCSF Helen Diller Family Comprehensive Cancer Center, University of California, San Francisco, San Francisco, CA, United States

Proteoglycans are a diverse group of molecules which are characterized by a central protein backbone that is decorated with a variety of linear sulfated glycosaminoglycan side chains. Proteoglycans contribute significantly to the biochemical and mechanical properties of the interstitial extracellular matrix where they modulate cellular behavior by engaging transmembrane receptors. Proteoglycans also comprise a major component of the cellular glycocalyx to influence transmembrane receptor structure/function and mechanosignaling. Through their ability to initiate biochemical and mechanosignaling in cells, proteoglycans elicit profound effects on proliferation, adhesion and migration. Pathologies including cancer and cardiovascular disease are characterized by perturbed expression of proteoglycans where they compromise cell and tissue behavior by stiffening the extracellular matrix and increasing the bulkiness of the glycocalyx. Increasing evidence indicates that a bulky glycocalyx and proteoglycan-enriched extracellular matrix promote malignant transformation, increase cancer aggression and alter anti-tumor therapy response. In this review, we focus on the contribution of proteoglycans to mechanobiology in the context of normal and transformed tissues. We discuss the significance of proteoglycans for therapy response, and the current experimental strategies that target proteoglycans to sensitize cancer cells to treatment.

Keywords: proteoglycans, GAG, cancer, mechanosignaling, glycocalyx

OPEN ACCESS

Edited by:
Rachel K. Okolicsanyi, Queensland University of Technology, Australia

Reviewed by:
Rizaldy Paz Scott, Northwestern University, United States
Martin Götte, University of Münster, Germany

***Correspondence:**
Valerie M. Weaver
valerie.weaver@ucsf.edu

Specialty section:
This article was submitted to Signaling, a section of the journal Frontiers in Cell and Developmental Biology

Received: *03 June 2020*
Accepted: *04 November 2020*
Published: *30 November 2020*

Citation:
Barkovskaya A, Buffone A Jr, Žídek M and Weaver VM (2020) Proteoglycans as Mediators of Cancer Tissue Mechanics. Front. Cell Dev. Biol. 8:569377. doi: 10.3389/fcell.2020.569377

Abbreviations: bFGF, basic fibroblast growth factor; CSC, cancer stem cell; CAFs, cancer-associated fibroblasts; CNS, central nervous system; CS, chondroitin sulfate; JNK, c-Jun N-terminal kinase; DS, dermatan sulfate; EGFR, epidermal growth factor receptor; EMT, epithelial to mesenchymal transition; ER, estrogen receptor; ECM, extracellular matrix; FGF, fibroblast growth factor; FAK, focal adhesion kinase; FA, focal adhesion; GlcA, glucuronic acid; GPI, glycosyl-phosphatidyl-inositol; GPC3, GPC4, glypican-3, 4; GAG, glycosaminoglycan; HS, heparan sulfate; HSPG, heparan sulphate proteoglycans; HIF1α, hypoxia-inducible factor 1α; IdoA, iduronic acid; IGFR1; insulin-like growth factor receptor 1; KS, keratan sulfate; Lrp4, lipoprotein-related receptor-4; MAPK, MAP kinase; MMPs, matrix metalloproteinases; MUSK, MMP domain-containing muscle-specific kinase; GalNAc, *N*-acetylgalactosamine; GlcNAc, *N*-acetylglucosamine; NCAMs, neural cell adhesion molecules; NG2, Neural/glial antigen 2; NRP1, Neuropilin-1; PDAC, pancreatic ductal adenocarcinoma; TAZ, PDZ-binding motif; ROCKI and ROCKII, Rho-associated protein kinase 1 and 2; SLRPs, small leucine-rich proteoglycans; Sdc-1, 2, Syndecan 1 and 2; TGFβR3, transforming growth factor β-receptor 3; VEGFR, vascular endothelial growth factor receptor; VASP, vasodilator-stimulated phosphoprotein; YAP, yes-associated protein; ADAM 12, protein 12.

INTRODUCTION

Proteoglycans are proteins with covalently attached GAG chains, which regulate tissue development and have been implicated in pathologies such as cancer. Proteoglycans engage cell surface receptors to induce biochemical signaling, and help modulate the mechanical properties of the ECM including its stiffness. Alongside glycoproteins and glycolipids, proteoglycans act as structural components of the cellular glycocalyx, where they influence cell signaling by regulating the structure function of transmembrane receptors. Here we focus on the role of proteoglycans in tumor mechanics including their impact on extracellular matrix stiffness and the tumor glycocalyx.

MECHANO-SENSING IN CANCER

In cancer development, oncogenic mutations and the loss of tumor suppressors have long been viewed as the critical initiating events. Nevertheless, there is a growing consensus that even the cells carrying the most powerful oncogenic mutations require an intricate set of microenvironmental conditions to foster their malignant transformation and cancer progression. Among these microenvironmental factors, tissue stiffening which accompanies the fibrotic response that characterizes all solid tumors, has emerged as a key factor that can foster malignancy and collaborate with oncogenes to disrupt tissue organization and promote the growth, survival, invasion and ultimately the metastatic dissemination of the cancer cells (Northey et al., 2017). Maintaining tissue organization requires retention of a state of tensional homeostasis that is mediated by a balance between the stiffness of the tissue stroma and the actomyosin contractility of the cells within the tissue. An abnormal and sustained increase in the stiffness of the stroma such as occurs with fibrosis will increase the contractility of the cells in the tissue to destabilize cell-cell junctions, compromise polarity and destroy tissue architecture. Similarly, an increase in cellular contractility, that is induced following oncogene activation (e.g., Ras or Her2), disrupts tissue architecture as well. It destabilizes cell-cell adhesions, and stimulates the remodeling and stiffening of the ECM until such time as the cell reaches a state of tensional equilibrium with its mechanical microenvironment (Paszek et al., 2005). Thus, chronically elevated tension will compromise tissue architecture and this in turn can foster malignant transformation and promote tumor progression (DuFort et al., 2011; Samuel et al., 2011).

A stiffened tissue is frequently accompanied by chronic inflammation which, in turn, increases stiffness even further (Maller et al., 2020). Consistently, pathologies such as kidney, lung and liver fibrosis are characterized by inflammation as well as increased levels of ECM proteins including interstitial collagen, that stiffen the stroma of the tissue. Tissue fibrosis is accompanied by increased risk of cancer development (Adler et al., 2016; Noguchi et al., 2018). Moreover, tissue stiffening correlates clinically with tumor progression and aggression in malignant gliomas (Miroshnikova et al., 2016; Barnes et al., 2018), as well as adenocarcinoma of the breast (Acerbi et al., 2015), and pancreas (Laklai et al., 2016).

MECHANICAL STRESS AND MECHANO-TRANSDUCTION

There are three types of mechanical stress that tumor cells experience: tensile, compressive and shear pressure, reviewed in (Butcher et al., 2009; Northey et al., 2017) (**Figure 1**).

Tensile Stress

Tensile stress, or tension, arises from an increase in the local tissue stiffness caused by a rigid ECM and its ability to stimulate actomyosin contractility in the cells within the tissue. This is associated with ECM remodeling, accumulation of proteins such as fibronectin and increased abundance and cross-linking of collagen fibers (Levental et al., 2009; Schedin and Keely, 2011). While type I collagen is critical for increasing the tensile strength of most peripheral tissues, hyaluronic acid, tenascin and small proteoglycans including biglycan and lumican, contribute substantially to the stiffness of the brain parenchyma (Kim and Kumar, 2014; Miroshnikova et al., 2016).

Cellular tension can also arise through the increased activity of GTPases such as Rho that are stimulated by elevated cytokine activation of G protein coupled receptors or by activated oncogenes such as Ras (Samuel et al., 2011; Sanz-Moreno et al., 2011; Laklai et al., 2016). High mechanical tension is sensed by cellular transmembrane receptors such as integrins. Integrins are hetero-dimeric transmembrane proteins that serve as primary receptors of ECM components. Integrins consist of dimeric α and β chains that each have multiple isoforms, creating 24 known unique combinations that are expressed in a tissue-specific way and selectively bind to the ECM proteins (Humphries et al., 2006). Integrin activation can be induced either outside – in via ligand binding or inside - out via intracellular signaling. In either instance, integrin activation induces a conformational change in the heterodimer that unfolds the integrin to potentiate its ligand binding and facilitate recruitment of cytoplasmic proteins that initiate integrin clustering to form nascent adhesions.

Focal adhesion formation, however, requires cellular actomyosin contractility to reach a sufficient level that is proportional to the stiffness of the ECM. At a critical threshold talin-vinculin binding is favored as is the recruitment and activation of focal adhesion kinase (FAK), ROCKI and ROCKII, Src, as well as several adaptor proteins, including paxillin that foster the assembly of focal adhesions. Within these adhesion complexes vinculin and talin function as "molecular clutches" linking the integrin directly to the network of actin filaments underneath the cell membrane. When cellular tension is sufficiently high and prolonged, these molecular clutches will promote the formation of stress fibers which will then be further strengthened and stabilized with participation of the final components of the focal adhesion complex – zyxin and VASP (Kanchanawong et al., 2010) (**Figure 2**).

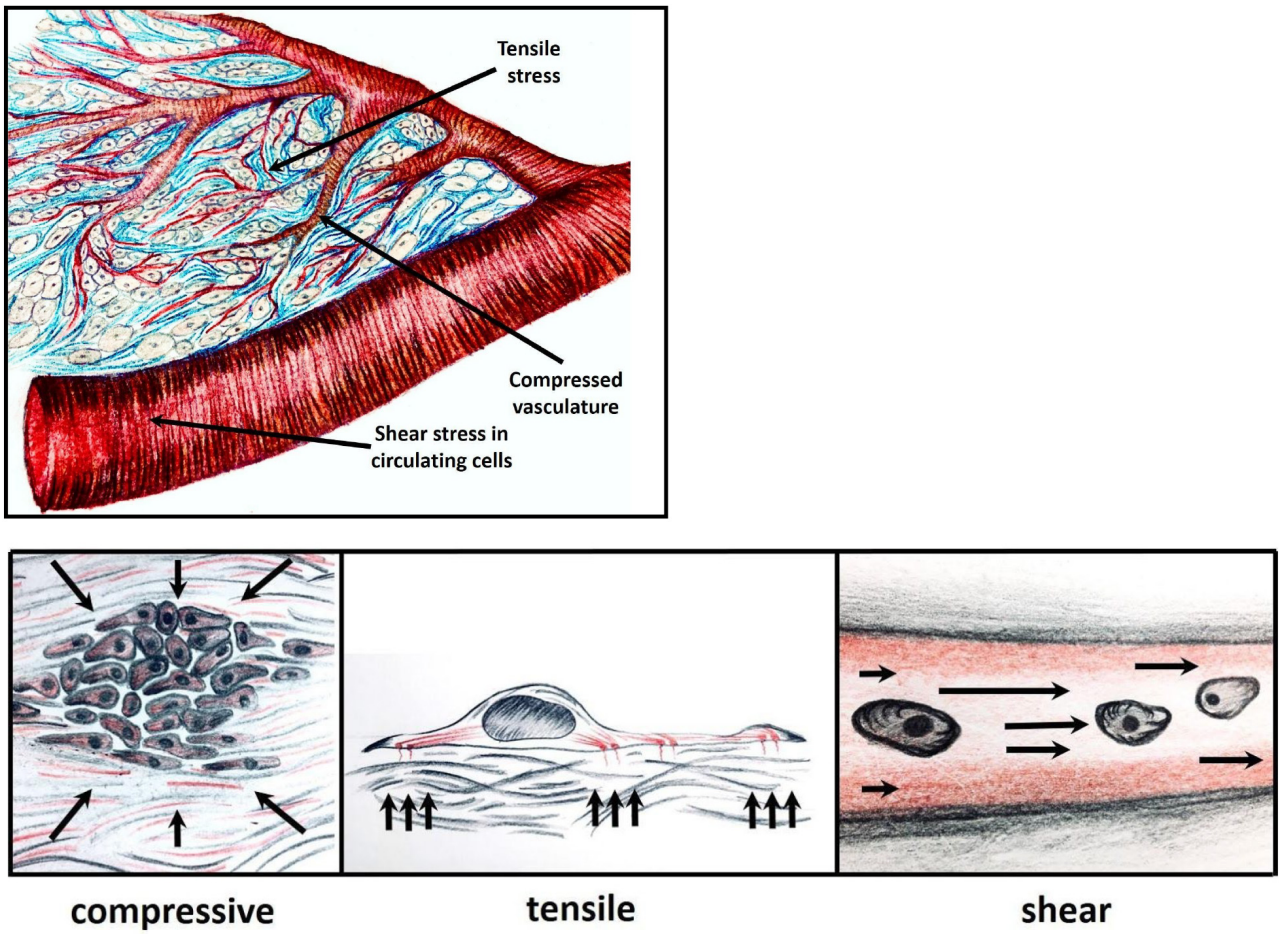

FIGURE 1 | Within a growing tumor, cells are subjected to mechanical forces, in response to which the cells exert tensile, compressive or shear stress. Tensile pressure (tissue tension), stems from ECM stiffening and remodeling; compressive pressure applied occurs when tumor cells proliferate in a confined space leading to vascular compression and damage; and shear force that is experienced by the cancer cells in the circulation.

In response to focal adhesion assembly, FAK and Src kinases, phosphorylate a large scaffolding protein p130Cas. p130Cas acts as a docking block for multiple signaling proteins that can activate each other in close proximity, therefore amplifying their down-stream signaling cascades. These include ILK – CDC42 and ILK – Rac pathways, which regulate filopodia and invadopodia formation and cell polarization and contractility (Alexander et al., 2008). These functions allow the cells to initiate movement in response to mechano-stimulation, or, in the case of cancer cells, to move toward and invade the neighboring tissues after being exposed to a stiff environment.

In addition, cell survival and proliferative pathways are also induced via interaction with p130Cas. Erk and PI3K signaling is up-regulated upon integrin activation in a p130Cas-dependent manner (Cabodi et al., 2010; Janoštiak et al., 2014). Further evidence of p130Cas involvement in mechanosignaling comes from a study which determined that physical stretching of the cells on elastic substrates induced p130Cas to assume an unfolded conformation, open to phosphorylation by Src. This, in turn, promoted down-stream signaling. Notably, p130Cas unfolding and phosphorylation is significantly higher among the cells on the edges of the 3D *in vitro* colonies, compared to the bulk of the cells inside. This suggests that mechanical stretching directly activates pro-survival signaling in invading cells enabling them to migrate and disseminate (Sawada et al., 2006).

Elevated cellular contractility is also characteristic of the cells that carry a bulky glycocalyx. Glycocalyx is a dense cell surface coating composed of glycoproteins and proteoglycans, which reinforce the external barrier of a cell, and actively regulate mechano-transduction and growth factor signaling. In aggressive metastatic cancer cells, glycocalyx is frequently enhanced (Paszek et al., 2014; Barnes et al., 2018). Bulky glycocalyx was shown to facilitate adhesion assembly and augment integrin-mediated signaling (Paszek et al., 2014).

Finally, stiff microenvironment activates a critical mechanosignaling pathway –YAP and transcriptional coactivator with a PDZ-binding motif (TAZ) (Dupont et al., 2011). YAP/TAZ are transcriptional co-activators that shuttle between cytoplasm and the nucleus, where they bind to DNA transcription factor TEAD and activate expression of its target genes, supporting

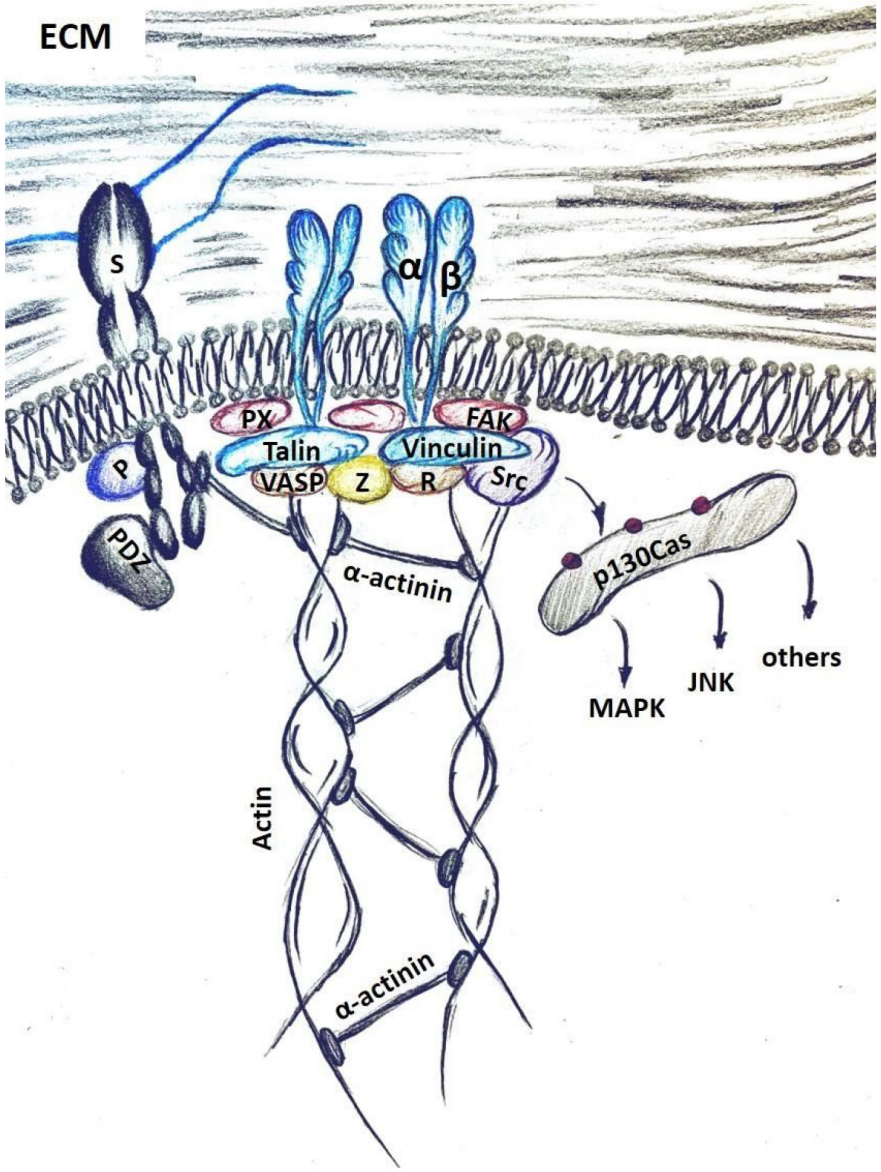

FIGURE 2 | Mechano-transduction in cells is mediated through integrin activation upon binding to the ECM components, such as fibronectin. Syndecans (S) facilitate this interaction by binding the ECM with HS chains. Intracellular syndecan domains activate signaling with PKCα (P) and via binding to PDZ-motif proteins. Integrin activation recruits a host of focal adhesion components, including integrin-binding adaptor proteins – talin and paxillin (PX); actin binding cytoskeletal proteins VASP and vinculin (V); and focal-adhesion associated kinases Src, FAK and ROCK. VASP and zyxin (Z) facilitate actin polymerization and connect it to the focal adhesion complex. Phosphorylation of p130Cas by Src allows docking and activation of several signaling pathways, such as the MAPK, the c-Jun N-terminal kinase (JNK) pathway and others.

cell survival and decreasing apoptosis. This signaling pathway is mechano-responsive, and several mechanisms for mechano-regulation of YAP/TAZ have been proposed. First, inhibition of ROCK kinase prevents YAP/TAZ nuclear localization (Dupont et al., 2011), which suggests that focal adhesion assembly is required for YAP/TAZ signaling. In addition, inhibitors of actomyosin and actin polymerization, as well as integrins, also inhibit YAP/TAZ (Dupont, 2016). Finally, it has also been shown that in cells stretched out on a stiff substrate, the nucleus is compressed. This causes YAP/TAZ to translocate directly inside via nuclear import channels, bypassing up-stream regulation, and to induce expression of its target genes (Elosegui-Artola et al., 2017). These results point to YAP/TAZ activation as a sensor of mechanosignaling.

Several approaches have been developed to explore the causal relationship between tissue tension and disease development including malignant transformation and tumor progression. Cellular mechanosignaling and actomyosin actomyosin tension reduction can be achieved by inhibiting integrin focal adhesion signaling or integrin focal adhesion assembly via knockdown

or inhibition of key adhesion components including talin, vinculin, focal adhesion kinase and ROCK. Mechanosignaling and actomyosin tension can be enhanced through expression of a β1-integrin engineered to promote inter-molecular associations that foster clustering of the molecules by introducing a mutant β1-integrin with a single amino acid substitution: V737N. This single substitution of hydrophobic valine residue with a hydrophilic asparagine promotes integrin clustering by reducing repulsive forces in the transmembrane domain of the integrin. Expression of the V737N β1-integrin enhances the assembly of focal adhesions accompanied by elevated p397FAK and increased ROCK activity that translate into higher actomyosin contractility and potentiate growth factor receptor dependent activation of MAPK, PI3K and Stat3 signaling (Paszek et al., 2005; Levental et al., 2009; Laklai et al., 2016). Conversely, reducing tenascin C expression in aggressive glioblastoma cells significantly decreases the stiffness of the brain tumor ECM leading to significantly lower tumor aggression (Miroshnikova et al., 2016).

In matrix collagen-rich tissues, higher stiffness coupled with the reorganization of the collagen into thickened, oriented fibers facilitates the directed invasion of the cancer cells to promote their migration through the interstitial stroma that ultimately favors their dissemination and metastasis (Ahmadzadeh et al., 2017). Cells exposed to a chronically stiffened ECM with sustained myc, catenin, YAP/TAZ and TGFβ activity often undergo an EMT that promotes their phenotypic switch to a motile state that is highly resistant to anti-cancer treatments (Barnes et al., 2018). Epithelial tumor cells that have undergone an EMT down-regulate cell-cell adhesion receptors such as E-cadherin that compromise their potential to maintain polarized tissue structures. In addition to the loss of E-cadherin, polarization is also accompanied by a decrease in syndecan-1 proteoglycan on the cell surface (Sun et al., 1998). Syndecan-1 loss was later found to independently induce the EMT in several cancers, leading to increased migration and invasion (Wang et al., 2018). Cells that have undergone EMT are also more contractile and exert higher forces at their integrin adhesions (Mekhdjian et al., 2017), decrease cytokeratin expression and upregulate the intermediate filament protein vimentin and exhibit a softening of their nuclei (Liu et al., 2015; Northey et al., 2017). Intriguingly, EMT substantially increases expression of glycoproteins that contribute to the cellular glycocalyx. Cells with a bulky glycocalyx can relax the bulk of their cortical tension and this allows them to squeeze through the confined spaces often encountered within a rigid, dense tumor microenvironment (Shurer et al., 2019). Consistently, tumors that express a bulkier glycocalyx are often more aggressive and metastatic and circulating tumor cells frequently express high levels of glycoproteins that contribute to a bulky glycocalyx (Paszek et al., 2014).

Not surprisingly, the stiffened, high-tension tumor environment stimulates growth factor and cytokine dependent cancer cell growth and survival, and promotes invasion, migration and dissemination of the tumor cells. Consistently, breast and pancreatic tumor cells and glioblastoma cells in which integrin-dependent mechanosignaling was potentiated through expression of the V737N mutant β1-integrin, undergo an EMT that fosters their motility and invasion in culture and *in vivo*, and reduces the survival of experimentally manipulated mice (Laklai et al., 2016; Mekhdjian et al., 2017; Barnes et al., 2018).

Compression Stress

The rapid proliferation of tumor cells within a confined area can increase compression stress. Compression stress in tumors can also arise through elevated water retention mediated by increased concentration of proteoglycans and hyaluronic acid (DuFort et al., 2016). Compression stress within a confined tumor can create a mechanical stress gradient with the forces declining at the tumor periphery. High compression stress within the tumor can occlude blood and lymphatic vessel integrity that induces tumor hypoxia and increases interstitial fluid pressure (Sarntinoranont et al., 2003). High tumor compression stress contributes to cancer aggression either by directly activating signaling pathways or by indirectly inducing hypoxia to stimulate HIF1a-dependent gene expression that each can increase tumor cell growth, survival and invasion, and promote EMT to drive cancer aggression and metastasis (Tse et al., 2012).

Shear Stress

Shear stress is yet another type of mechanical stress cancer cells experience in the tumor tissue. The shear stress is created by the blood and interstitial fluid flow the cancer cells encounter once they extravasate into the vasculature or lymphatics during their metastatic dissemination. These shear stresses can stimulate signaling pathways that enhance tumor cell aggression and influence vessel patency. For instance, Polacheck et al. (2017) show how vascular flow can induce cleavage of the transmembrane Notch 1 receptor that permits the resulting Notch transmembrane domain to form a complex with adherens junctions that enhanced cell-cell adhesion stability. In cancer cells, continuous exposure to fluid flow promotes migration and invasion capacity. Some reports suggest that proteoglycan-rich glycocalyx acts as a mechano-sensor of the interstitial flow and enables mechanosignaling activation, while enzymatic reduction of glycocalyx bulk inhibits flow-induced signaling (Shi et al., 2011; Qazi et al., 2013).

In summary, as structural components of the glycocalyx and the ECM, proteoglycans function as integral regulators of bio-mechanics in both normal and malignant tissues. The following sections provide an overview of the proteoglycan diversity, describe their known function in cancer development, and summarize the reports of proteoglycans' involvement in the regulation of mechanosignaling.

GLYCOSAMINOGLYCAN (GAG) ATTACHMENTS TO PROTEOGLYCANS

Proteoglycans are a class of glycosylated proteins widely expressed in various tissues, which play an important role in a variety of cellular interactions and signaling events (Couchman and Pataki, 2012). Proteoglycans are one of the principal components of the mammalian glycocalyx, which along with glycoproteins and glycolipids form the sponge-like mix of proteins and lipids which acts as a barrier between the cell

surface and the extracellular matrix (ECM), and regulates the inter actions between the two (Monne et al., 2013; Buffone and Weaver, 2020). In addition, proteoglycans are a major component of the ECM and are also present intracellularly and pericellularly. Proteoglycans are characterized by at least one covalently bound GAG chain, although they can also contain other N-, and O-linked glycans found in glycoproteins or glycolipids (Mulloy and Rider, 2006; Nikitovic et al., 2018). These GAG chains have very distinct glycosylation patterns which consist of repeating disaccharide units, are long (∼80 monosaccharides for GAGs while ∼10–15 for *N*-glycans), are sulfated at various different points of the GAG chain and of each monosaccharide, and have a much more linear structure as compared to *N*- or *O*-glycans (Iozzo and Schaefer, 2015; Lindahl et al., 2015). Furthermore, GAG chains are characterized by the Galactose–Galactose–Xylose motif (Gal–Gal–Xyl), which initiates the chains and can contain either IdoA or GlcA, monosaccharides unique to GAG (Gandhi and Mancera, 2008; Pomin and Mulloy, 2018). Furthermore, GAGs differ from glycoproteins and glycolipids in that the GlcA/IdoA and hexosamine sugars form repeating disaccharides which compose the long GAG chains.

There are five main GAG chains: heparin, CS, DS, KS, and HS, all of which are sulfated (Soares da Costa et al., 2017). Each GAG consists of unique monosaccharide building blocks as: heparin contains GlcNAc, GalNAc, IdoA, and GlcA (Shriver et al., 2012), CS contains GalNAc and GlcA, DS contains IdoA and GalNAc, KS contains galactose (Gal) and GlcNAc (Funderburgh, 2002), and HS contains GlcNAc, GalNAc, IdoA, and GlcA (Lindahl et al., 2015). The differences in composition of each of the GAGs, which have been determined by sequencing for most of the GAGs except for KS, expressed on proteoglycans have profound effects on their function both inside and outside of the cell.

CELLULAR LOCALIZATION OF PROTEOGLYCANS

An important distinction between proteoglycans and other glycosylated molecules such as mucins, glycoproteins, and glycolipids, which are primarily present on the cell surface (Buffone et al., 2013, 2017; Mondal et al., 2016), is that proteoglycans can be localized either intracellularly, pericellularly, on the cell surface, or be shed into the extracellular matrix (**Figure 3**) (Vogel and Peterson, 1981; Yanagishita, 1993; Lin, 2004; Iozzo et al., 2009). The different members of the

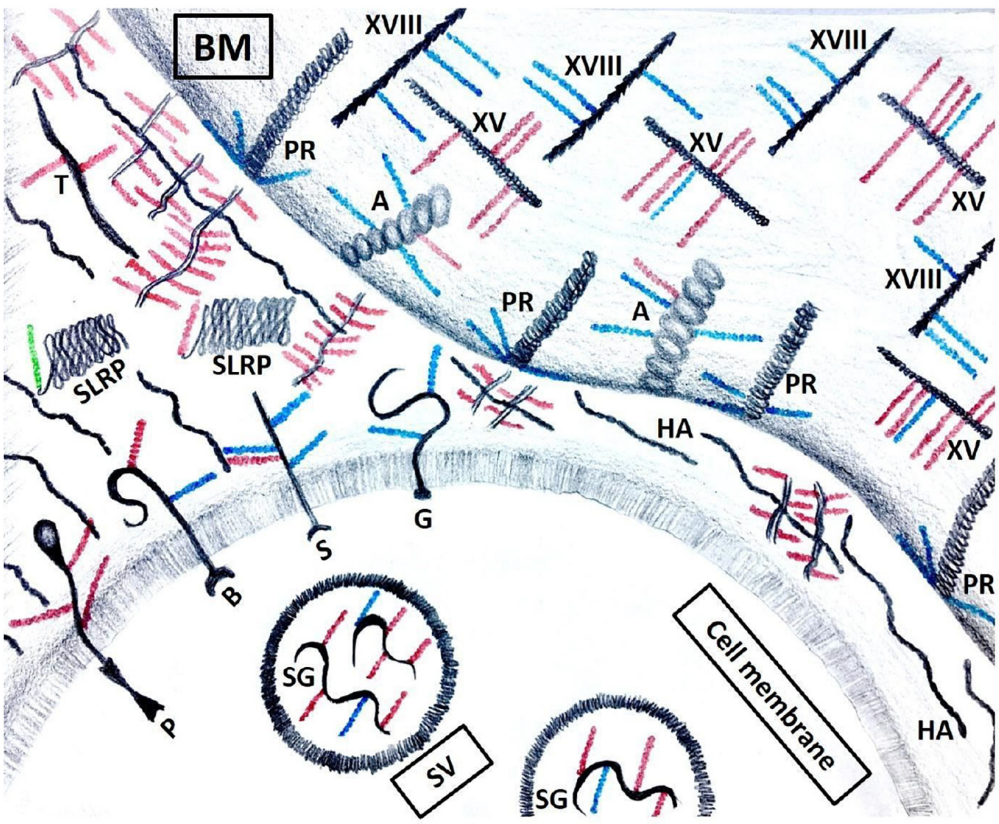

FIGURE 3 | Proteoglycans' localization. Serglycin (SG) is the only intracellular proteoglycan, found in secretory vesicles (SV). It carries both HS (blue) and CS (red) GAG chains. Transmembrane proteoglycans include, but are not limited to phosphacan (P), betaglycan (B), syndecans (S) and glypicans (G). In the ECM, SLRPs are short proteoglycans that carry either a CS or a DS (green) GAG chain. Other proteoglycans include testican (T) and hyalectins that aggregate with hyaluronic acid (HA). Basement membrane (BM) contains agrin (A), perlecan (PR) and collagens XV (XV) and XVIII (XVIII).

proteoglycan classes and their functions have been beautifully reviewed by others (Iozzo and Schaefer, 2015), but we will briefly cover the pertinent proteoglycans in terms of the topic of this review.

Intracellular Proteoglycans

There is only one proteoglycan in the mammalian genome which resides in the intracellular space and that is serglycin. Serglycin is interesting as it is located in the secretory granules of cells and holds together all of the proteases and other components of the granule (Kolset and Tveit, 2008). Serglycin can carry a variable number of heparin or CS side chains (Nugent, 2000).

Cell-Surface Proteoglycans

There are two major families of cell-surface proteoglycans: syndecans 1–4 (Cheng et al., 2016) which have a transmembrane domain and glypicans 1–6 (Li N. et al., 2018) which are anchored to the cell membrane through a GPI lipid. Syndecans have primarily HS GAGs but can also have CS chains which are implicated in a variety of biological processes, most critically in binding growth factors in tissues (Forsten-Williams et al., 2008). Enzymatic processing of syndecans represents an important regulator of their function. Syndecans can be secreted into the pericellular environment by MMPs (Rossi et al., 2014) and into the extracellular matrix through partial degradation of their domains by proteases to perform other functions (Teng et al., 2012).

Heparanase is an endoglycosidase that can cleave heparan sulfate side chains. This can result in the release of growth factors or chemokines bound by syndecans. In many malignancies, high expression of heparanase has been associated with an aggressive tumor phenotype (Ramani et al., 2013). Furthermore, post-assembly processing by plasma membrane-bound endo-6-*O*-sulfatases (SULF1 and SULF2) changes the sulfation pattern of HS chains, which in turn leads to an altered ligand/receptor interaction (Bishop et al., 2007). In liver cancer, the activation of SULF1/SULF2 promotes the tumor growth (Graham et al., 2016).

Glypicans are HSPGs, that are linked to the cell surface by GPI anchor. Glypicans can modulate a variety of cell signaling pathways including Wnt, frizzled, BMP, hedgehog (Hh), and bFGF (Cassiman et al., 1992; Capurro et al., 2005, 2008; Filmus and Capurro, 2014). Increased expression of glypicans has been found in pediatric cancers and liver cancer (Li N. et al., 2018). Other proteoglycans which reside at the cell surface include betaglycan (Bilandzic and Stenvers, 2012) and phosphacan (Maurel et al., 1994). They are discussed further in other reviews (Iozzo and Schaefer, 2015).

Pericellular Proteoglycans

There are four pericellular proteoglycans that reside predominantly within the basement membrane: perlecan, agrin, and collagens XV and XVIII (Iozzo et al., 2009). Perlecan is a massive proteoglycan (>500 KD) which contains HS GAG chains that cross-link cell surface molecules to ECM components in the basement membrane (Gubbiotti et al., 2017). Perlecan is secreted by smooth muscle and vascular cells and plays a role in a variety of cellular processes including cell adhesion, inflammation, wound healing, endocytosis, and cardiovascular development (Whitelock et al., 1999; Sasse et al., 2008; Zoeller et al., 2008; Jung et al., 2013). Agrin is a similar proteoglycan in structure to perlecan that also cross-links the cell surface to the ECM that differs from perlecan by having both HS and CS GAGs and is expressed primarily in the brain where it is known to interact with NCAMs (Tsen et al., 1995; Winzen et al., 2003). Finally, collagen XV, which carries CS GAG chains, and collagen XVIII, with HS chains, are proteoglycans which are present in all human and mouse basement membranes that play distinct roles in the structural support and angiogenesis (Heinämäki et al., 1994; Eklund et al., 2001).

Extracellular Matrix Proteoglycans

The ECM proteoglycans are the largest class of proteoglycans. This group of molecules consists of the calcium binding testican family, the SLRPs and lectin (hyalectin). Hyaluronic acid is also frequently present in the extracellular space. Testican proteoglycans carry HS and CS GAGs (Bonnet et al., 1992), are modular in structure like perlecan, and are found in both the testis and CNS where they play a strong role in neuronal development (Schnepp et al., 2005). Conversely, SLRPs contain over 18 distinct members and are much smaller than other proteoglycans (30–40 kDa). They are defined by a core that consists of leucine-rich repeats (Iozzo et al., 2011). SLRPs are widely present in almost all of the ECM in the meninges, pericardium and peritoneum and are involved in regulating organ shape (Iozzo, 1997, 1999).

The hyalectin class of proteoglycans has four members: aggrecan, versican, neurocan, and brevican, which are characterized by tri-domain structure in which the N-terminus binds hyaluronan, the C-terminus binds lectins, and the central domain contains the GAG (predominantly CS) side chains (Iozzo, 1998). The hyalectins play important roles in maintaining the structure of the brain, cartilage, and vasculature. Aggrecan is known to form large complexes (∼200 MDa) with hyaluronan, collagen, and other proteoglycans and glycoproteins and this hydrated gel-like ECM structure forms the load bearing component of cartilage (Heinegård, 2009; Wight et al., 2011). Versican has four isoforms (V0, V1, V2, and V3) which are differentially expressed in tissues such as the brain, heart, and vascular smooth muscle (Zimmermann and Ruoslahti, 1989; Naso et al., 1994; Zimmermann and Dours-Zimmermann, 2008). Versican's function is to facilitate cell migration and resolution of inflammation as it interacts with cell surface receptors on the leukocyte surface to enhance interactions with the vasculature (Wight et al., 2014). Neurocan is a proteoglycan with CS GAGs expressed in the brain that binds to NCAM, tenascin, and hyaluronan and inhibits neurite outgrowth at the sites of injury (Davies et al., 2004; Liu et al., 2006). Finally, brevican is a critical proteoglycan in brain function as its expression has been linked to glioblastoma, brain tissue injury, and Alzheimer's

disease (Yamada et al., 1994; Frischknecht and Seidenbecher, 2012).

PROTEOGLYCANS IN CANCER

Several distinct functions of proteoglycans define their complex role in biological systems. To begin with, proteoglycans promote cell-to-cell and cell-to-matrix interactions. Proteoglycans also trap and release various growth factors and cytokines. For example, HS GAG chains of transmembrane proteoglycans can bind bFGF (Faham et al., 1996; Li Y. et al., 2016). As bFGF and other growth factors trapped by the GAG chains of proteoglycans are gradually dissolved, they prompt proliferation of the neighboring cells, and induce vascular growth and tissue regeneration (Hao et al., 2018; Li R. et al., 2018). In addition, enzymatic processing of proteoglycans by proteases and heparanases represents another important factor that modifies their biological activity (Cheng et al., 2016).

Proteoglycans, most prominently HSPGs, are often dysregulated during tumor development (Fjeldstad and Kolset, 2005; Varki et al., 2016). However, their role in cancer is highly context dependent. The following section describes the known contribution of intracellular, pericellular and ECM proteoglycans in cancer development and progression.

Intracellular

Heparin- and CS-decorated serglycin is the sole known intracellular proteoglycan, expressed most prominently by the endothelial, hematopoietic and myeloid cells. It can be detected both intracellularly, where it localizes to the secretory vesicles, and is secreted into the extracellular space (Schick et al., 2001; Kolseth et al., 2015). Serglycin secreted by both cancer-associated stroma cells, as well as the cancer cells themselves, binds to the transmembrane glycoprotein CD44 (Guo et al., 2017).

Activation of CD44 in cancer cells promotes stemness, drives sphere formation, and increases invasion and migration (Skandalis et al., 2019). These effects are mediated through a transcription factor, Nanog, which sustains the non-committed state of the cells (Guo et al., 2017). Completing a positive-feedback loop, serglycin itself appears to promote CD44 expression, since a knock-down of serglycin leads to a drop in the cells with high CD44 levels (Zhang et al., 2020). In lung and colorectal cancer, high expression and secretion of serglycin is associated with a poor clinical outlook and treatment resistance (Xu et al., 2018), while the knock-down of serglycin decreases tumor burden *in vivo* (Guo et al., 2017). In line with these findings, serglycin was also found to support stemness in glioblastoma cells, where it prevents astrocytic differentiation and promotes cell proliferation and tumor growth (Manou et al., 2020).

Pericellular

The clinical consequence of high expression of transmembrane proteoglycans is variable among cancer patients. The current consensus emphasizes a highly context- and cancer type-dependent manner in which certain proteoglycans regulate the tumor development and progression.

Syndecan-1 (Sdc-1)

Sdc-1 is found in several normal tissues, as well as in the malignant tumors (Kind et al., 2019). In some cases, high expression of Sdc-1 has been linked to poor prognosis. Notably, high levels of Sdc-1 in breast cancer cells correlated with higher incidence of brain metastasis (Sayyad et al., 2019). Sdc-1 is also more abundant in the ER-negative tumors, suggesting that its expression marks this more aggressive breast cancer phenotype (Barbareschi et al., 2003; Baba et al., 2006; Qiao et al., 2019). This has been corroborated by reports showing that Sdc-1 expression is directly repressed by ER (Fleurot et al., 2019). In agreement with this, recent work described Sdc-1 as an important marker of CSC phenotype in inflammatory breast cancer – a subtype with a notoriously poor prognosis (Ibrahim et al., 2017). In that study, Stat3, NFκB, Notch-1, Notch-2, and EGFR signaling was significantly reduced upon Sdc-1 knock-down. These data suggest that Sdc-1 could serve as a modulator of CSC phenotype and may be a promising therapeutic target. Notch pathway activation may specifically rely on the HS GAG chains of the Sdc-1, as a recent study showed that overexpression of HS-sulfotransferase enzymes regulates Notch signaling in breast cancer cells. However, this effect is specific to the triple-negative breast cancer (TNBC) (Teixeira et al., 2020).

These findings are in contrast with other work, where Sdc-1 depletion led to the increased breast cancer cell motility and invasion facilitated by stronger integrin adhesion to ECM components, such as fibronectin (Ibrahim et al., 2012; Hassan et al., 2013). Some of this discrepancy in the role of Sdc-1 in breast cancer development may also be due to its differential expression between cell types. For example, one study of the normal breast tissue found that Sdc-1 expression was higher in the stromal component compared to lobular epithelium (Lundström et al., 2006). The authors found that in women with high mammographic density (MD), Sdc-1 expression shifted from epithelial to stromal cells. As high MD has been linked to increased breast cancer incidence (Vachon et al., 2007), this suggests that stromal Sdc-1 expression is important for breast cancer development. In support of this, orthotopic injection of aggressive murine mammary tumor cell lines into Sdc-1–/– mice prevented lung metastasis compared to wild-type animals. These findings identify Sdc-1 as a key component of a lung metastatic niche (Chute et al., 2018).

Pro- and anti-tumorigenic role of Sdc-1 may also be context-dependent. In colorectal cancer cells, high expression of Sdc-1 reduced tumor growth and invasion through down-regulation of MAPK and Stat3 signaling (Wang et al., 2019). Additionally, low expression of Sdc-1 corresponded with poor prognosis in colorectal cancer patients (Li K. et al., 2019). In this cancer type, Sdc-1 silencing promoted EMT and a stem-like phenotype and stimulated integrin signaling through FAK kinase phosphorylation. This resulted in accelerated tumor growth and possible resistance to radiation therapy (Katakam et al., 2020). Similarly, in gastric carcinomas, high Sdc-1 expression

correlated with a less aggressive tumor phenotype (Charchanti et al., 2019). Notably, normal tissues of the gastro-intestinal tract have high levels of Sdc-1 (Schick et al., 2001), which suggests that Sdc-1 expression is lost at some point during cancer development and progression in some of the patients, conferring a survival advantage.

This is supported by several studies, which show that Sdc-1 expression is lost during EMT in both cancer (Yang et al., 2011; Farfán et al., 2018; Kalscheuer et al., 2019) and normal tissues (Sun et al., 1998). EMT is an important developmental program of embryogenesis, which can be hijacked by the cancer cells during tumor growth to promote invasion and metastasis. As previously mentioned, increased tissue stiffness promotes EMT and up-regulates mechanosignaling in cancer (Wei et al., 2015; Zhang et al., 2016; Matte et al., 2019). This raises a possibility that high tumor stiffness promotes a mesenchymal-like phenotype in cancer cells, which in turn leads to the loss of Sdc-1, among other consequences.

Syndecan 2, NG2, Betaglycan

Several other transmembrane proteoglycans have also been linked to an aggressive cancer phenotype. Syndecan 2 (Sdc-2) expression is increased in a range of cancers including lung adenocarcinoma and colon cancer, where it promotes expression of matrix metalo-proteinase 9 and 7 (MMP9 and MMP7) respectively (Jang et al., 2016; Tsoyi et al., 2019). MMPs regulate cancer cell invasion by digesting the ECM immediately surrounding the cancer cells, and by inducing shedding of E-cadherin adhesion proteins. Sdc-2 is therefore linked to the EMT and cancer invasion (Mytilinaiou et al., 2017). Similarly, Syndecan 4 (Sdc-4) has been shown to promote EMT in the papillary thyroid carcinoma cells (Chen L.L. et al., 2018). NG2 is another transmembrane proteoglycan, which is often over-expressed in cancer and has been linked to poor prognosis (reviewed in Nicolosi et al., 2015).

In contrast to the transmembrane proteoglycans discussed above, betaglycan, also known as TGFβ-receptor 3 (TGFβR3), has been associated with positive outcome in cancer patients (Nicolosi et al., 2015). Nicolosi et al. found that abundant betaglycan inhibits NF-κB and MAPK signaling and reduces tumor growth and invasion. In line with this, the loss of betaglycan in renal cell carcinoma lifts this inhibition and induces TGF-β signaling. This results in rapid metastasis *in vivo* (Nishida et al., 2018).

Transmembrane Glycosyl-Phosphatidyl-Inositol (GPI) – Anchored Proteoglycans

Glypicans

A recent study described activation of Wnt/β-catenin/c-Myc signaling axis by one of the transmembrane GPI-anchored proteoglycan glypican-4 (GPC4), and the resulting up-regulation of glycolysis in colorectal cancer. Moreover, proteasomal degradation of GPC4 resulted in Wnt/β-catenin/c-Myc signaling attenuation and metabolic reprogramming, which was favorable for the survival of the tumor-bearing mice (Fang et al., 2019). By contrast, glypican-3 (GPC3) has been reported to act as a tumor suppressor. GPC3 silencing promoted breast cancer growth, while ectopic re-expression of GPC3 inhibited growth *in vitro* (Xiang et al., 2001).

Neuropilin-1

The transmembrane proteoglycan Neuropilin-1 (NRP1) is one of the proteoglycans which serves as a co-receptor in several growth-factor signaling pathways, including EGFR-Akt (Rizzolio et al., 2012), fibroblast growth factor 2 (FGF2) (West et al., 2005), PDGF – TGFβ (Cao et al., 2010) and VEGF signaling. Notably, NRP1-mediated activation of the VEGF signaling is dependent on the HS or CS GAG chain attachment to its core protein. In the absence of full glycosylation, stimulation with VEGF no longer promotes growth, invasion and formation of blood vessels (Shintani et al., 2006; Hendricks et al., 2016).

Pericellular and Basement Membrane – Anchored Proteoglycans

Perlecan

Perlecan is a proteoglycan highly expressed in basement membranes, peri-vascular regions and tumor-adjacent stroma regions in most solid cancer types (**Figure 3**) (Cruz et al., 2020). Multiple HS chains attached to perlecan protein core account for its ability to bind a variety of growth factors, cytokines and cell surface receptors (Whitelock et al., 2008). Controlled gradual release of these bound growth factors maintains structured tissue homeostasis, which becomes impaired in malignant tumors (Cruz et al., 2020).

Perlecan has been identified in a recent study, as a mediator of the intricate relationship between cancer cells and CAFs in PDAC (Vennin et al., 2019). The authors found that PDAC cells carrying a p53-gain of function (GOF) mutation, induced a transcriptional change in CAFs, prompting them to support invasion and metastasis. In these tumors, CAFs stimulated cross-linking of collagen fibers, which resulted in higher mechanical stiffness levels compared to the less aggressive counterparts with the loss of p53. Notably, conditioned media, collected from CAFs of p-53-GOF tumors was sufficient to induce collagen remodeling *in vitro*, suggesting that some of the soluble secreted factors are responsible for this change. A mass spectrometry analysis of the CAF-derived secretome revealed a high abundance of perlecan. Further experiments demonstrated that perlecan was necessary and sufficient for induction of collagen remodeling, increase in cancer cell actomyosin contractility and promotion of invasion of the PDAC cells into the matrix (Vennin et al., 2019). Moreover, immune response against the tumor cells was significantly increased following perlecan depletion. In line with this, antibody targeting perlecan inhibited tumor growth in a PDX mouse model of TNBC. Interestingly, a stronger anti-tumor effect was observed in nude mice than in the Nod/scid (NSG) mice, suggesting that perlecan helps create an immunosuppressive tumor microenvironment (Kalscheuer et al., 2019).

It has also been reported that during bone metastasis in prostate cancer, accumulation of perlecan promotes cell-cell adhesion instead of cell-ECM, preventing spreading of the

cancer cells. Perlecan cleavage by matrix metalloproteinase-7 (MMP-7) facilitates cancer cell-ECM adhesion, dispersion and eventually leads to bone metastasis via induction of FAK-dependent invasion (Grindel et al., 2018). These examples underscore the highly context-dependent manner in which various proteoglycans impact tumor progression.

Agrin

In addition to perlecan, other pericellular proteoglycans have also been shown to have pro-metastatic functions. Agrin, another HS-bearing proteoglycan, has a limited expression in the normal tissue, but is progressively up-regulated during malignant transformation in oral cancer (Rivera et al., 2018). A knock-down of agrin reduced cancer cell proliferation, invasion and sphere formation. Similarly to perlecan, agrin from conditioned media was sufficient to rescue proliferation and invasion in the agrin-silenced cells, suggesting that soluble agrin mediates its pro-metastatic function. In addition, it has been shown that agrin facilitates angiogenesis. Agrin produced by cancer cells, binds to and stabilizes its receptors β1-integrin and Lrp4 on the surface of the vascular endothelial cells. Coupled with an increasing stiffness inside a tumor, this interaction promotes formation of focal adhesions and stabilization of VEGFR2. Activation of VEGFR2, in turn, leads to branching and proliferation of the endothelial cells, and formation of new blood vessels (Njah et al., 2019).

Collagen XVIII and Collagen XV

Other pericellular and basal membrane proteoglycans, such as collagen XVIII and collagen XV have also been implicated in cancer progression support, however, limited evidence has been reported on this subject. In metastatic gastric cancer, as well as in non-small cell lung cancer, high expression of collagen XVIII correlated with a poor clinical outcome (Iizasa et al., 2004; Lee et al., 2010). However, both collagen XVIII and XV are integral components of the basal membrane. While their expression in the tumor may be up-regulated, both collagens are often depleted from the basement membrane. This makes it more permeable and thus enables epithelial tumor cells to invade (Amenta et al., 2003).

Extracellular

Abundance of extracellular proteoglycans in the ECM has been linked to a more aggressive phenotype of the tumors and stiffer microenvironment (Varga et al., 2012). Accumulation of ECM proteoglycans is also known to result in higher tissue stiffness. In a normal breast, higher tissue stiffness corresponds to higher mammographic density (MD), a well-established risk-factor for breast cancer development, as mentioned above (Vachon et al., 2007). High MD is characteristic for breast tissue rich in ECM proteoglycans, including hyalectans (aggrecan, versican, neurocan, and brevican), basement membrane proteoglycans (ex. perlecan), and SLRPs such as lumican and decorin (Alowami et al., 2003; Shawky et al., 2015).

It is important to note, however, that while proteoglycan expression level is often associated with cancer, the extent of their modification with GAG chains may be even more important. A recent study examined a pattern of extracellular proteoglycans in the ECM of malignant brain tumors. The authors discovered that CS-modified proteoglycans, such as aggrecan, versican, neurocan, and brevican, concentrated on the edge of the low-grade gliomas. The CS GAGs promoted adhesion between tumor cells and attracted reactive astrocytes, thus helping limit the invasion of the tumor cells into the brain tissue. The more aggressive high-grade tumors, however, had a low abundance of CS GAGs, which the authors connected to the invasive nature of those lesions (Silver et al., 2013). This proposed barrier function is supported by evidence from previous reports, where extracellular proteoglycans were found to direct brain tissue development by imposing spatial limits between distinct regions of the nervous tissue and the outer borders of the brain and spinal cord (Golding et al., 1999).

Testicans

Testican 1, encoded by SPOCK1 gene, has been shown to promote cancer growth. SPOCK1 knock-down strongly reduces tumor growth and metastasis in an *in vivo* model of breast cancer (Perurena et al., 2017). Similarly, in colorectal cancer, SPOCK1 was found to be over-expressed and contributed to the activation of PI3K-Akt signaling (Zhao et al., 2016). This is in agreement with a recent report that demonstrated activation of the same signaling cascade in glioma cells (Yang et al., 2016). In all cases, tumor-supporting role of testican 1 was linked to induction of EMT and activation of Wnt signaling (Miao et al., 2013). A link between testican 1 expression and EMT is further supported by evidence that resistance to a broad range of targeted inhibitors, associated with a mesenchymal-like phenotype, is reversed upon testican 1 knock-down (Kim et al., 2014).

The role of other members of the testican family is less clear, as there are only a handful of published reports on this subject. It appears that testicans have a role in the inhibition of MMPs, a group of enzymes that catalyze matrix digestion and facilitate tumor cell invasion. Testican 3 was found to inhibit certain MMPs, potentially preventing cancer spread. Conversely, testican 2 was found to have an opposite effect, counteracting the inhibition imposed by testican 3 (Kim et al., 2014). In summary, contribution of the broader testican family to cancer progression requires further investigation.

Small Leucine-Rich Proteoglycans (SLRPs)

The role of SLRP family of proteoglycans, which includes decorin, biglycan and lumican, in cancer is different between its members (reviewed in Appunni et al., 2019). SLRPs are abundant in the ECM of most tissues, where they bind to various cell receptors, regulating signaling cascades. For example, one of the SLRPs, decorin, has been shown to bind multiple receptor-tyrosine kinases, inhibiting their activation (Neill et al., 2016). Decorin was shown to have a particularly high affinity for the EGFR. Binding of decorin to EGFR led to ERK-mediated expression of p21 and subsequent cell cycle arrest (Moscatello et al., 1998). In addition, decorin can engage toll-like receptors 2 and 4, inducing inflammatory response. These functions explain the tumor suppressive and anti-metastatic role of decorin,

which has been reported across several cancer types (reviewed in Neill et al., 2016).

Hyalectins

Some of the members of the hyalectin family of proteoglycans have been shown to play a role in cancer. For instance, elevated levels of versican have been reported in gastric (Shen et al., 2015), lung (Asano et al., 2017), and endometrial cancer (Kodama et al., 2007), where its expression correlated with poor clinical prognosis. In breast cancer, expression of versican was only enriched in malignant tumors, but not in the non-malignant lesions (Vachon et al., 2007).

Brevican, has been found to promote motility of astrocytoma cells, supporting progression of this cancer from low- to high-grade glioma (Lu et al., 2012). Neurocan, another hyalectan that is found in the CNS, is increased in neuroblastomas. Several studies found that high neurocan expression has a strong correlation with shortened patient survival (Su et al., 2017; Zhong et al., 2018).

Hyaluronan

Hyaluronan, also referred to as hyaluronic acid, is a unique GAG which is composed entirely of the non-sulfated repeating disaccharides made of *N*-acetyl glucosamine (GlcNAc) and D-GlcA residues. As it does not have a protein core, it cannot be considered a proteoglycan. However, hyaluronan binds to multiple proteins and proteoglycans within the ECM and contributes greatly to structural integrity of different tissues, as well as to cancer development and progression. Its role in cancer is diverse and has been a subject of several comprehensive reviews (Rankin and Frankel, 2016; Liu et al., 2019).

PROTEOGLYCANS ARE INVOLVED IN MECHANOSIGNALING

ECM Proteoglycans

Stiffer tumors are characterized by two important changes involving proteoglycans: a bulkier glycocalyx of the cancer cells, and a stiffer, denser ECM. Both of these changes require abundant proteoglycans with long, bulky GAG chain modifications (**Table 1**). Proteoglycans and hyaluronan, in either unbound or bound form, make up a significant part of cancer ECM and are actively involved in the regulation of its stiffness. One of the starkest pieces of evidence to support this comes from an unusual source – a study of the human tooth. The authors describe the proteoglycans present at the interfaces between different regions of the tooth that come under high levels of mechanical stress. These KS- and CS-decorated SLRPs are essential for the structural integrity of the tooth, as their enzymatic digestion reduces the stiffness of the tissue, making it less resistant to mechanical loads (Kurylo et al., 2016). The implication of this finding is that proteoglycans can markedly contribute to the regulation of tissue mechanics.

In cancer, perhaps the most notable example of this are the tumors of the CNS. Brain ECM contains large quantities of hyaluronan (Wolf et al., 2019), CS-modified proteoglycans, predominantly lecticans, as well as small glycoproteins and adhesive molecules – laminin, tenascin C, and fibronectin. Proteoglycans interact with the adhesive molecules, creating a network of varying density. For example, hyaluronan binding to tenascin C results in a more rigid ECM with higher stiffness. This is coupled with the fact that tenascin C is over-expressed in malignant tumors and is distributed in a gradient manner, with the highest abundance in the central regions, decreasing

TABLE 1 | Proteoglycans control mechanical properties of the tissue and regulate mechanosignaling.

PGs regulate ECM stiffness		
Biglycan and fibromodulin	Maintain structural integrity and load-bearing capacity in the human periodontal complex	Kurylo et al., 2016
Biglycan and decorin	Control collagen fiber assembly	Iozzo et al., 1999; Zhang et al., 2006; Lewis et al., 2010; Robinson et al., 2017
Biglycan	Controls collagen crosslinking and fiber density	Andrlová et al., 2017
Agrin	Stabilizes focal adhesion complexes, promotes ECM stiffness and mechanosignaling	Chakraborty et al., 2015, 2017; Njah et al., 2019
Aggrecan	Prevents ECM stiffening in cartilage tissues	Nia et al., 2015
PGs modulate glycocalyx bulk and tune mechanosignaling		
Sdc-1	Promotes β1-integrin signaling, invasion, cell spreading and re-alignment in response to shear force	Iba et al., 2000; Beauvais and Rapraeger, 2010; Sarrazin et al., 2011; Vuoriluoto et al., 2011; Yang et al., 2011; Ebong et al., 2014
Sdc-4	Conveys direct mechanical cues to β1-integrins, binds ECM protein, supports adhesion complexes and mechanosignaling	Woods and Couchman, 2001; Okina et al., 2012; Cavalheiro et al., 2017; Kennelly et al., 2019; Chronopoulos et al., 2020
Syndecans	Interact with PDZ-domain proteins, control cytoskeletal remodeling, cell spreading and migration	Grootjans et al., 1997; Hsueh et al., 1998; Tkachenko et al., 2006; Sulka et al., 2009; Kashyap et al., 2015; Keller-Pinter et al., 2017
Serglycin		
Serglycin	Promotes FAK signaling and mechanosignaling	Zhang et al., 2020

Notable examples outlined in this review.

toward the periphery. This was shown to be controlled by HIF1α (Miroshnikova et al., 2016; Chen J.E. et al., 2018), which is highly expressed in the poorly vascularized, hypoxic regions in the core parts of the tumors. Both the presence of hypoxic areas and high stiffness have a strong association with poor prognosis in glioblastomas, suggesting that hypoxia-driven production of tenascin C, and its binding to hyaluronan underlie the mechanism of stiffness increase, which fuels glioblastoma progression (Miroshnikova et al., 2016). Other studies have shown that ECM enrichment with hyaluronan independently induces a stretched, contractile phenotype in glioma cells, promoting their invasion (Wang et al., 2014; Pogoda et al., 2017). Notably, hyaluronan abundance does not induce tumor cell proliferation, but instead reduces tumor volume. Despite this, it is associated with poor prognosis, as abundant hyaluronan promotes cancer cell invasion and dissemination, rather than the growth of a single parental tumor.

Outside of the CNS, proteoglycans are involved in mechano-transduction by modulating ECM composition and organization. Two SLRPs – decorin and biglycan are known to be essential for the regulation of collagen fiber assembly in tendons. A knock-down of these proteoglycans results in larger collagen fibers that can tolerate smaller mechanical loads. The overall tendon stiffness is also reduced upon decorin and biglycan knock-down (Zhang et al., 2006; Robinson et al., 2017). In a follow-up study, it was determined that the DS GAG chains attached to decorin were required for binding and remodeling of collagen (Lewis et al., 2010). These and other studies link decorin to mechano-regulation and indicate that the presence of SLRPs is important for the maintenance of soft ECM environments. In support of this, decorin acts as a tumor suppressor in many cancer types, while its loss precipitates cancer progression (Iozzo et al., 1999). Another SLRP, biglycan also contributes to the ECM remodeling. In melanoma models, the loss of biglycan expression in mouse embryonic fibroblasts results in softer ECM with less collagen crosslinking and reduced collagen fiber density. Among patients with melanoma, low expression of biglycan, either by the tumor or the stroma cells, is strongly linked to better clinical prognosis (Andrlová et al., 2017). In summary, the evidence of SLRPs' involvement in regulation of mechanosignaling in cancers is still limited and merits further investigation.

Agrin

Mounting evidence points to another secreted proteoglycan – agrin as a modulator of mechanosignaling in cancer. Agrin was first described as a ligand of Lrp4, which binds to a scaffolding protein MUSK. This complex serves as a platform for multiple signaling pathways, supporting cancer growth and preventing apoptosis (Zong and Jin, 2013). One of the down-stream signaling cascades that is activated by agrin is YAP/TAZ (Chakraborty et al., 2017).

In the same study, the authors uncovered the mechanism of mechano-sensing by agrin. Cells cultured on stiff substrates produce and secrete higher amounts of agrin. In turn, abundant agrin in the ECM potently increases stiffness of the tumors *in vivo*, which is dependent on collagen accumulation. Through its receptors, agrin stimulates YAP signaling, inducing YAP nuclear localization. Conversely, a knock-down of agrin results in YAP translocation back into the cytosol and a decreased expression of YAP target genes. Notably, this effect is exclusively mediated through agrin, while stiffness alone in absence of agrin expression is not sufficient to activate YAP and its target genes (Chakraborty et al., 2017). Corroborating the role of agrin in mechanosignaling, in the subsequent study of hepato-carcinomas, it was determined that agrin stabilizes focal adhesion complexes and facilitates FAK signaling. As a consequence, agrin depletion impedes cell adhesion and invasion and has a dramatic effect on tumor growth, practically eliminating tumors completely (Chakraborty et al., 2015).

In support of these findings, it was shown that agrin, produced both by the cancer cells, as well as the vascular endothelial cells, is required for activation of angiogenesis, blood vessel sprouting and cancer cell adhesion to the endothelial cells (Njah et al., 2019). The authors found that agrin binding to its Lrp4 receptor, induced β1 integrin – FAK signaling, formation of focal adhesion complexes and stabilized protein levels of VEGFR2, which is critical for endothelial cell migration and proliferation. Importantly, these agrin-mediated effects were stiffness-dependent, suggesting that stiff environments in tumors promote angiogenesis via agrin-mediated mechanosignaling (Njah et al., 2019).

Aggrecan

Aggrecan is another proteoglycan of the ECM, whose expression is primarily limited to cartilage. Its abundance and modifications determine cartilage stiffness and elasticity. It has been shown that the length of CS and KS GAG chains attached to aggrecan decreases with age, along with an overall depletion of aggrecan. This results in progressively stiffer tissue (Nia et al., 2015). While this change occurs in normal development, it may become exacerbated with age and lead to development of osteoarthritis – degradation of cartilage (Alberton et al., 2019). It is feasible that aggrecan expression and the length of its GAG chains contribute to the regulation of osteosarcomas, or metastasis of other cancers to the bone. However, to the best of our knowledge, this has not yet been investigated.

Cell Surface Proteoglycans

The role of ECM proteoglycans in mechanosignaling has not been fully investigated. However, more is known about the transmembrane and peri-cellular proteoglycans in the context of mechano-regulation. It has been reported that tumors with up-regulated tissue mechanics have bulkier glycocalyx (Barnes et al., 2018). In addition, bulky glycocalyx further amplifies mechanosignaling through focal adhesions, creating a positive-feedback loop which propagates malignant phenotype (**Figure 4**) (Woods et al., 2017). As key components of glycocalyx, proteoglycans at the interface of the cell-to-matrix interaction, contribute to the regulation of this response.

Syndecans

Some proteoglycans can serve as co-receptors of integrins. One of the best-studied examples of that is syndecans, which facilitate

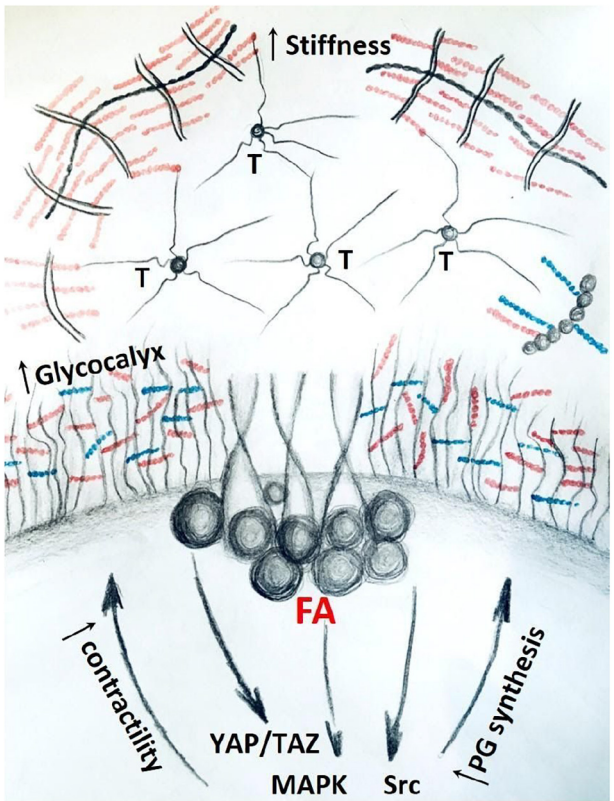

FIGURE 4 | Stiff matrix, rich in tenascin (T) and proteoglycans promote bulkier glycocalyx and up-regulate mechanosignaling through focal adhesions (FA) and down-stream pathways. Activation of mechanosignaling results in production of more proteoglycans that contribute to bulkier glycocalyx and stiffer ECM, thus concluding a positive-feedback loop in tumor tissue.

recognition and binding of external ligands, including growth factors and components of the ECM, through their HS chains within the range of (≈300 nm (Sarrazin et al., 2011). Syndecans interact with different integrins on the cell surface, forming diverse combinations. Their binding can occur both within the cytoplasmic and the extracellular domains, and facilitates formation and maturation of the adhesion complexes. Examples of this include interaction of Sdc-4 and Sdc-1 with α2β1 integrins, which promotes invasion of KRAS-mutant cells into collagen gels (Vuoriluoto et al., 2011). In addition, it was found that Sdc-1 mediates coupling of αvβ3 integrin with IGFR1 (Beauvais and Rapraeger, 2010). Sdc-1 directly binds to the integrins, which prompts formation of an integrin-IGFR1 complex and IGFR1 auto-phosphorylation. Integrin interaction with IGFR1 was found to be necessary for the activation of integrin signaling and cell spreading on substrates (Beauvais and Rapraeger, 2010).

Sdc-1 binding to disintegrin and MMP domain-containing protein 12 (ADAM 12) induces a conformational change that promotes binding of β1 integrins and subsequent cell spreading (Iba et al., 2000). In line with this, Sdc-1 expression in stromal fibroblasts induces rearrangement of the collagen fibers, allowing breast cancer cells to adhere and extravasate more efficiently (Yang et al., 2011). In summary, these studies provide evidence that Sdc-1 is involved in focal adhesion formation and supports activation of the down-stream signaling.

In addition, cell surface proteoglycans have been shown to act as mechano-sensors of shear force in vascular endothelial cells. In normal conditions, the endothelial cells align themselves with the direction of the flow, creating a uniform layer. One study has found that debulking of the endothelial glycocalyx with HS degrading heparinase III prevents such re-alignment of the cells. The authors found that this effect is dependent on Sdc-1, as the Sdc-1 knock-down also abolished cell realignment as well as remodeling of the fibrillar actin network, while a knock-down of glypican-1 did not (Ebong et al., 2014). The distinct roles of these proteoglycans in shear force sensing may be explained by the difference in their membrane tethering. Sdc-1 transverses the plasma membrane with a transmembrane domain that serves as a stable anchor connecting it to the cytoskeleton. In contrast, glypican-1 is more loosely attached with a GPI anchor and is often found within lipid rafts in the membrane. A recent study found that shear stress conditions induce re-distribution and clustering of glypican-1 on the cell surface, while Sdc-1 remains in place (Zeng et al., 2013).

Sdc-4 has also been described as essential for the formation and stabilization of focal adhesions (Woods and Couchman, 2001). Evidence in support of this includes a study, where mechanical force applied directly to the Sdc-4 through magnetic pulling of the conjugated beads, resulted in activation of β1-integrins, activation of down-stream signaling and an increase in cortical stiffness (Chronopoulos et al., 2020). Conversely, cells with a knock-down of Sdc-4 lose FAK and β1 integrins expression at the leading edge and fail to establish stable adhesions. Sdc-4 silencing also results in un-coupling of vinculin from filamentous actin network and its dispersion in the cytosol. As a result of these events, loss of Sdc-4 leads to reduced adhesion and increased proliferation (Cavalheiro et al., 2017). Furthermore, Sdc-4 has been shown to bind to the ECM proteins, such as fibronectin, with the HS chains, forming a stable deformation-resistant bond, adding to the strength of integrin-fibronectin binding (Kennelly et al., 2019).

Sdc-4, has been shown to directly interact with an α-actinin. α-actinin is an actin fiber-remodeling protein, which cooperates with myosin II to facilitate cell contractility and locomotion (**Figure 2**). Sdc-4 therefore serves as an important sensor of mechano-stimulation and regulator of cellular traction force (Okina et al., 2012).

All syndecans have also been shown to interact with a diverse group of PDZ-domain carrying proteins, which are important for tethering receptor proteins to the plasma membrane and serve as scaffolding proteins in signaling cascades (Cheng et al., 2016). Syndecans interact with PDZ-domain proteins through a conserved tetra-peptide region of their intracellular domain (Grootjans et al., 1997; Hsueh et al., 1998). These syndecan-PDZ protein complexes have been shown to be important for the cytoskeletal rearrangement, cell spreading and migration, with implications for cancer dissemination and metastasis (Tkachenko et al., 2006; Kashyap et al., 2015). Since there are four different syndecans and over 250 PDZ-domain proteins, specificity of their

interactions is regulated through post-translational modifications of both the PDZ-domain and the cytoplasmic domain of syndecans, within or next to the PDZ-binding region. For example, phosphorylation of the cytoplasmic region of Sdc-1 prevents its interaction with syntenin-1 (Sulka et al., 2009), but it strengthens its binding with T-lymphoma invasion and metastasis-inducing protein 1 (Tiam1) (Keller-Pinter et al., 2017) – both PDZ-domain proteins, which regulate cytoskeletal organization and cell migration.

Serglycin in Mechanosignaling

Finally, serglycin, as the only known intracellular proteoglycan has not been thoroughly investigated in terms of its contribution to mechanosignaling. One report has linked high abundance of serglycin with up-regulation of both mRNA expression and nuclear localization of YAP/TAZ (Zhang et al., 2020). YAP/TAZ activation is known to occur in response to multiple different inputs, although the mechanism of serglycin-mediated activation of YAP/TAZ is not completely understood. Stimulation of cells with either serglycin over-expression, or treatment with conditioned media collected from serglycin over-expressing cells, induced FAK signaling. This suggests that secreted serglycin promotes focal adhesion signaling, which in turn activates YAP/TAZ. In line with this, serglycin knock-down prevented activation of YAP/TAZ and the down-stream genes in a breast cancer model. This resulted in improved sensitivity to chemotherapeutic treatment (Zhang et al., 2020).

Considering this intriguing observation, further studies are warranted to better understand the regulation of mechanosignaling by serglycin in cancer cells.

PROTEOGLYCANS IN CANCER THERAPY AND DIAGNOSIS

As outlined in chapters above, proteoglycans contribute to cancer progression, which is at least partially mediated through their role in mechanosignaling. From this perspective, proteoglycans represent attractive potential therapeutic targets. The search for clinical applications began in 1983 with the first report of the anti-angiogenic and anti-tumor properties of unfractionated heparin (Folkman et al., 1983). Since then, cancer type- and tumor stage-specific expression of certain proteoglycans have been described, positioning them as useful diagnostic and prognostic markers. For example, high expression of pericellular agrin on the interface between the cancer cells and the surrounding ECM, serves as a strong negative prognostic marker in PDAC. Knock-down of agrin, on the contrary, reduces both the primary and the metastatic tumor load *in vivo* (Tian et al., 2020). The study points to agrin's role in the modulation of mechanosignaling, and support of adhesion and migration as the likely explanation for this effect. Changes in proteoglycan abundance and modifications also contribute to the ECM remodeling during tumor growth and the development of therapeutic resistance (Theocharis and Karamanos, 2019). For example, in melanoma, resistance against BRAF-inhibitor was accompanied by increased ECM levels of versican and biglycan (Girard et al., 2020). There is therefore evidence that inhibition of mechanosignaling, regulated by certain proteoglycans holds substantial therapeutic promise, although it mostly remains to be explored.

Another avenue of modifying proteoglycans for therapeutic gain is through modulation of their enzymatic processing (Shen et al., 2015). GAG chains attached to the protein cores of proteoglycans can be modified by sulfatases, which remove a sulfo group on HS chains, reducing the binding of growth factors. GAG chains can also be shortened or cleaved with a similar effect by appropriate enzymes, depending on the composition of the chain. For instance, in pancreatic cancer, increased levels of heparanase – the enzyme that cleaves HS GAGs, have been implicated in angiogenesis and metastasis, and correlated with poor prognosis (Pirinen et al., 2005).

This prompted investigation of heparanase inhibitors as potential therapeutics. For example, a significant tumor cell growth reduction *in vitro* and prolonged survival *in vivo* were reported upon treatment with a HS-mimetic heparanase inhibitor PG545. In addition to the survival advantage, PGP545 treatment also changed tumor cell phenotype, with the remaining tumor showing reduced levels of VEGF, vimentin, and collagen I. Histological analysis of these tumors showed high level of differentiation, suggesting that PGP545 may reverse tumor EMT (Ostapoff et al., 2013). In agreement with these findings, other studies found that PG545 treatment inhibited angiogenesis and reduced tumor burden in mouse models of breast, lung and prostate cancer (Kodama et al., 2007). Despite these promising preclinical results, as of 2019, no heparanase inhibitor has been tested in patients, as selective targeting of heparanase remains challenging (Shen et al., 2015).

Additionally, expression of specific proteoglycans by the tumor tissues can be exploited in various targeted drug delivery systems (Fuster and Esko, 2005; Misra et al., 2015). Nanocarrier systems such as liposomes or antibody-drug conjugates can improve drug delivery and anti-tumor activity of classical chemotherapeutics, while reducing their toxicity (Peer et al., 2007). Lee et al. developed cisplatin-loaded CS-binding liposomes, that effectively inhibited tumor growth in liver metastasis murine model (Lee et al., 2002). Similarly, antibody-drug conjugate targeting CSPG4 triggered melanoma regression *in vivo* (Hoffmann et al., 2020). Several similar approaches that utilize HSPGs have been proposed for treatment of breast (Khatun et al., 2013) and liver cancers (Longmuir et al., 2009).

Several groups identified cell surface proteoglycan glypican-1 as a specific marker of circulating cancer-cell-derived exosomes in pancreas and breast tumors. Glypican-1-positive exosomes may therefore serve as a tool for early detection of cancer (Melo et al., 2015). Similarly, HS proteoglycan Sdc-1 has been reported as an exosome constituent specific for glioblastoma, but not low-grade glioma (Indira Chandran et al., 2019).

Recently, chimeric antigen receptor (CAR) T-cells have been developed as a therapeutic tool that showed an impressive efficacy in B-cell lymphomas (Jackson et al., 2016). Subsequently, several cell surface proteoglycans have been suggested as CAR T-cell targets in solid tumors. Pellegatta et al. reported CART treatment targeted at CS proteoglycan 4 (CSPG4) was effective in glioblastoma mouse models (Pellegatta et al., 2018). Similarly, Glypican-3 was suggested as CAR-T-cell target for melanoma, lung and

hepatocellular carcinoma, respectively (Shimizu et al., 2019). Despite groundbreaking discovery of CAR T-cell therapy in hematopoietic malignancies, their application in treatment of solid tumors remains challenging, likely due to the characteristic microenvironment of solid tumors (Newick et al., 2017). In summary, application of proteoglycans in cancer therapy holds potential, but requires further studies.

CONCLUSION AND FUTURE PERSPECTIVES

The role of tissue mechanics and mechanosignaling in tumor development and progression is slowly becoming appreciated. Considering that proteoglycans make up a significant part of the ECM and serve as an interface between the cancer cells and their environment, it is safe to assume their involvement in the regulation of mechano-sensing and mechanosignaling. In this review, we summarize published reports that support this assumption. We conclude that the role of proteoglycans in mechanosignaling deserves thorough investigation, as it may uncover novel therapeutic approaches that could potentially curb cancer progression in patients.

AUTHOR CONTRIBUTIONS

AB and VMW both conceived and wrote the review. ABJr and MŽ contributed sections of the review. All authors contributed to the article and approved the submitted version.

FUNDING

This work was supported by NIGMS 1R21GM133060-01 to ABJr, NCI 2R01CA227942-18A1, Cancer Research UK brain tumor award and NCI RO1CA227942, NINDS RO1NS109911-01 NCIRO1CA222508, NINDS 1R01NS109911-01 to VMW. AB and MŽ were supported by a grant from Cancer Research UK - R01CA174929; and an NIH NCI R01CA227942 grant.

REFERENCES

Acerbi, I., Cassereau, L., Dean, I., Shi, Q., Au, A., Park, C., et al. (2015). Human breast cancer invasion and aggression correlates with ECM stiffening and immune cell infiltration. *Integr. Biol.* 7, 1120–1134. doi: 10.1039/c5ib00040h

Adler, M., Larocca, L., Trovato, F. M., Marcinkowski, H., Pasha, Y., and Taylor-Robinson, S. D. (2016). Evaluating the risk of hepatocellular carcinoma in patients with prominently elevated liver stiffness measurements by FibroScan: a multicentre study. *HPB* 18, 678–683. doi: 10.1016/j.hpb.2016.05.005

Ahmadzadeh, H., Webster, M. R., Behera, R., Jimenez Valencia, A. M., Wirtz, D., Weeraratna, A. T., et al. (2017). Modeling the two-way feedback between contractility and matrix realignment reveals a nonlinear mode of cancer cell invasion. *Proc. Natl. Acad. Sci. U. S. A.* 114, E1617–E1626. doi: 10.1073/pnas.1617037114

Alberton, P., Dugonitsch, H. C., Hartmann, B., Li, P., Farkas, Z., Saller, M. M., et al. (2019). Aggrecan hypomorphism compromises articular cartilage biomechanical properties and is associated with increased incidence of spontaneous osteoarthritis. *Int. J. Mol. Sci.* 20:1008. doi: 10.3390/ijms20051008

Alexander, N. R., Branch, K. M., Parekh, A., Clark, E. S., Iwueke, I. C., Guelcher, S. A., et al. (2008). Extracellular matrix rigidity promotes invadopodia activity. *Curr. Biol.* 18, 1295–1299. doi: 10.1016/j.cub.2008.07.090

Alowami, S., Troup, S., Al-Haddad, S., Kirkpatrick, I., and Watson, P. H. (2003). Mammographic density is related to stroma and stromal proteoglycan expression. *Breast Cancer Res.* 5, R129–R135. doi: 10.1186/bcr622

Amenta, P. S., Hadad, S., Lee, M. T., Barnard, N., Li, D., and Myers, J. C. (2003). Loss of types XV and XIX collagen precedes basement membrane invasion in ductal carcinoma of the female breast. *J. Pathol.* 199, 298–308. doi: 10.1002/path.1303

Andrlová, H., Mastroianni, J., Madl, J., Kern, J. S., Melchinger, W., Dierbach, H., et al. (2017). Biglycan expression in the melanoma microenvironment promotes invasiveness via increased tissue stiffness inducing integrin-β1 expression. *Oncotarget* 8, 42901–42916. doi: 10.18632/oncotarget.17160

Appunni, S., Anand, V., Khandelwal, M., Gupta, N., Rubens, M., and Sharma, A. (2019). Small leucine rich proteoglycans (decorin, biglycan and lumican) in cancer. *Clin. Chim. Acta* 491, 1–7. doi: 10.1016/j.cca.2019.01.003

Asano, K., Nelson, C. M., Nandadasa, S., Aramaki-Hattori, N., Lindner, D. J., Alban, T., et al. (2017). Stromal versican regulates tumor growth by promoting angiogenesis. *Sci. Rep.* 7:17225. doi: 10.1038/s41598-017-17613-6

Baba, F., Swartz, K., van Buren, R., Eickhoff, J., Zhang, Y., Wolberg, W., et al. (2006). Syndecan-1 and syndecan-4 are overexpressed in an estrogen receptor-negative, highly proliferative breast carcinoma subtype. *Breast Cancer Res. Treat.* 98, 91–98. doi: 10.1007/s10549-005-9135-2

Barbareschi, M., Maisonneuve, P., Aldovini, D., Cangi, M. G., Pecciarini, L., Mauri, F. A., et al. (2003). High syndecan-1 expression in breast carcinoma is related to an aggressive phenotype and to poorer prognosis. *Cancer* 98, 474–483. doi: 10.1002/cncr.11515

Barnes, J. M., Kaushik, S., Bainer, R. O., Sa, J. K., Woods, E. C., Kai, F., et al. (2018). A tension-mediated glycocalyx-integrin feedback loop promotes mesenchymal-like glioblastoma. *Nat. Cell Biol.* 20, 1203–1214. doi: 10.1038/s41556-018-0183-3

Beauvais, D. M., and Rapraeger, A. C. (2010). Syndecan-1 couples the insulin-like growth factor-1 receptor to inside-out integrin activation. *J. Cell Sci.* 123, 3796–3807. doi: 10.1242/jcs.067645

Bilandzic, M., and Stenvers, K. L. (2012). Reprint of: betaglycan: a multifunctional accessory. *Mol. Cell. Endocrinol.* 359, 13–22. doi: 10.1016/j.mce.2012.03.020

Bishop, J. R., Schuksz, M., and Esko, J. D. (2007). Heparan sulphate proteoglycans fine-tune mammalian physiology. *Nature* 446, 1030–1037. doi: 10.1038/nature05817

Bonnet, F., Perin, J. P., Maillet, P., Jolles, P., and Alliel, P. M. (1992). Characterization of a human seminal plasma glycosaminoglycan-bearing polypeptide. *Biochem. J.* 288, 565–569. doi: 10.1042/bj2880565

Buffone, A., Mondal, N., Gupta, R., McHugh, K. P., Lau, J. T. Y., and Neelamegham, S. (2013). Silencing α1,3-fucosyltransferases in human leukocytes reveals a role for FUT9 enzyme during E-selectin-mediated cell adhesion. *J. Biol. Chem.* 288, 1620–1633. doi: 10.1074/jbc.m112.400929

Buffone, A., Nasirikenari, M., Manhardt, C. T., Lugade, A., Bogner, P. N., Sackstein, R., et al. (2017). Leukocyte-borne α(1,3)-fucose is a negative regulator of β 2 -integrin-dependent recruitment in lung inflammation. *J. Leukoc. Biol.* 101, 459–470. doi: 10.1189/jlb.3a0516-215rr

Buffone, A., and Weaver, V. M. (2020). Don't sugarcoat it: how glycocalyx composition influences cancer progression. *J. Cell Biol.* 219:e201910070. doi: 10.1083/jcb.201910070

Butcher, D. T., Alliston, T., and Weaver, V. M. (2009). A tense situation: forcing tumour progression. *Nat. Rev. Cancer* 9, 108–122. doi: 10.1038/nrc2544

Cabodi, S., del Pilar Camacho-Leal, M., Di Stefano, P., and Defilippi, P. (2010). Integrin signalling adaptors: not only figurants in the cancer story. *Nat. Rev. Cancer* 10, 858–870. doi: 10.1038/nrc2967

Cao, S., Yaqoob, U., Das, A., Shergill, U., Jagavelu, K., Huebert, R. C., et al. (2010). Neuropilin-1 promotes cirrhosis of the rodent and human liver by enhancing PDGF/TGF-beta signaling in hepatic stellate cells. *J. Clin. Invest.* 120, 2379–2394. doi: 10.1172/JCI41203

Capurro, M. I., Xiang, Y.-Y., Lobe, C., and Filmus, J. (2005). Glypican-3 promotes the growth of hepatocellular carcinoma by stimulating canonical Wnt signaling. *Cancer Res.* 65, 6245–6254. doi: 10.1158/0008-5472.CAN-04-4244

Capurro, M. I., Xu, P., Shi, W., Li, F., Jia, A., and Filmus, J. (2008). Glypican-3 inhibits hedgehog signaling during development by competing with patched for Hedgehog binding. *Dev. Cell* 14, 700–711. doi: 10.1016/j.devcel.2008.03.006

Cassiman, J. J., Van den Berghe, H., and David, G. (1992). Differential expression of cell surface heparan sulfate proteoglycans in human mammary epithelial cells and lung fibroblasts. *J. Biol.* 267, 1116–1122.

Cavalheiro, R. P., Lima, M. A., Jarrouge-Bouças, T. R., Viana, G. M., Lopes, C. C., Coulson-Thomas, V. J., et al. (2017). Coupling of vinculin to F-actin demands Syndecan-4 proteoglycan. *Matrix Biol.* 63, 23–37. doi: 10.1016/j.matbio.2016.12.006

Chakraborty, S., Lakshmanan, M., Swa, H. L. F., Chen, J., Zhang, X., Ong, Y. S., et al. (2015). An oncogenic role of Agrin in regulating focal adhesion integrity in hepatocellular carcinoma. *Nat. Commun.* 6:6184. doi: 10.1038/ncomms7184

Chakraborty, S., Njah, K., Pobbati, A. V., Lim, Y. B., Raju, A., Lakshmanan, M., et al. (2017). Agrin as a mechanotransduction signal regulating YAP through the hippo pathway. *Cell Rep.* 18, 2464–2479. doi: 10.1016/j.celrep.2017.02.041

Charchanti, A., Papoudou Bai, A., Samantas, E., Papakostas, P., Skarlos, P., Kanavaros, P., et al. (2019). Association of low Syndecan-1 expression with adverse histopathological parameters in gastric carcinomas. *J. BUON* 24, 1106–1112.

Chen, J. E., Lumibao, J., Blazek, A., Gaskins, H. R., and Harley, B. (2018). Hypoxia activates enhanced invasive potential and endogenous hyaluronic acid production by glioblastoma cells. *Biomater Sci.* 6, 854–862. doi: 10.1039/c7bm01195d

Chen, L. L., Gao, G.-X., Shen, F.-X., Chen, X., Gong, X.-H., and Wu, W.-J. (2018). SDC4 gene silencing favors human papillary thyroid carcinoma cell apoptosis and inhibits epithelial mesenchymal transition via Wnt/β-catenin pathway. *Mol. Cells* 41, 853–867. doi: 10.14348/molcells.2018.0103

Cheng, B., Montmasson, M., Terradot, L., and Rousselle, P. (2016). Syndecans as cell surface receptors in cancer biology. a focus on their interaction with PDZ domain proteins. *Front. Pharmacol.* 7:10. doi: 10.3389/fphar.2016.00010

Chronopoulos, A., Thorpe, S. D., Cortes, E., Lachowski, D., Rice, A. J., Mykuliak, V. V., et al. (2020). Syndecan-4 tunes cell mechanics by activating the kindlin-integrin-RhoA pathway. *Nat. Mater.* 19, 669–678. doi: 10.1038/s41563-019-0567-1

Chute, C., Yang, X., Meyer, K., Yang, N., O'Neil, K., Kasza, I., et al. (2018). Syndecan-1 induction in lung microenvironment supports the establishment of breast tumor metastases. *Breast Cancer Res.* 20:66. doi: 10.1186/s13058-018-0995-x

Couchman, J. R., and Pataki, C. A. (2012). An introduction to proteoglycans and their localization. *J. Histochem. Cytochem.* 60, 885–897. doi: 10.1369/0022155412464638

Cruz, L. A., Tellman, T. V., and Farach-Carson, M. C. (2020). Flipping the molecular switch: influence of perlecan and its modifiers in the tumor microenvironment. *Adv. Exp. Med. Biol.* 1245, 133–146. doi: 10.1007/978-3-030-40146-7_6

Davies, J. E., Tang, X., Denning, J. W., Archibald, S. J., and Davies, S. J. A. (2004). Decorin suppresses neurocan, brevican, phosphacan and NG2 expression and promotes axon growth across adult rat spinal cord injuries. *Eur. J. Neurosci.* 19, 1226–1242. doi: 10.1111/j.1460-9568.2004.03184.x

DuFort, C. C., DelGiorno, K. E., Carlson, M. A., Osgood, R. J., Zhao, C., Huang, Z., et al. (2016). Interstitial pressure in pancreatic ductal adenocarcinoma is dominated by a gel-fluid phase. *Biophys. J.* 110, 2106–2119. doi: 10.1016/j.bpj.2016.03.040

DuFort, C. C., Paszek, M. J., and Weaver, V. M. (2011). Balancing forces: architectural control of mechanotransduction. *Nat. Rev. Mol. Cell Biol.* 12, 308–319. doi: 10.1038/nrm3112

Dupont, S. (2016). Role of YAP/TAZ in cell-matrix adhesion-mediated signalling and mechanotransduction. *Exp. Cell Res.* 343, 42–53. doi: 10.1016/j.yexcr.2015.10.034

Dupont, S., Morsut, L., Aragona, M., Enzo, E., Giulitti, S., Cordenonsi, M., et al. (2011). Role of YAP/TAZ in mechanotransduction. *Nature* 474, 179–183. doi: 10.1038/nature10137

Ebong, E. E., Lopez-Quintero, S. V., Rizzo, V., Spray, D. C., and Tarbell, J. M. (2014). Shear-induced endothelial NOS activation and remodeling via heparan sulfate, glypican-1, and syndecan-1. *Integr. Biol.* 6, 338–347. doi: 10.1039/c3ib40199e

Eklund, L., Piuhola, J., Komulainen, J., Sormunen, R., Ongvarrasopone, C., Fassler, R., et al. (2001). Lack of type XV collagen causes a skeletal myopathy and cardiovascular defects in mice. *Proc. Natl. Acad. Sci. U.S.A.* 98, 1194–1199. doi: 10.1073/pnas.98.3.1194

Elosegui-Artola, A., Andreu, I., Beedle, A. E. M., Lezamiz, A., Uroz, M., Kosmalska, A. J., et al. (2017). Force triggers YAP nuclear entry by regulating transport across nuclear pores. *Cell* 171, 1397.e14–1410.e14. doi: 10.1016/j.cell.2017.10.008

Faham, S., Hileman, R. E., Fromm, J. R., Linhardt, R. J., and Rees, D. C. (1996). Heparin structure and interactions with basic fibroblast growth factor. *Science* 271, 1116–1120. doi: 10.1126/science.271.5252.1116

Fang, Y., Shen, Z.-Y., Zhan, Y.-Z., Feng, X.-C., Chen, K.-L., Li, Y.-S., et al. (2019). CD36 inhibits β-catenin/c-myc-mediated glycolysis through ubiquitination of GPC4 to repress colorectal tumorigenesis. *Nat Commun.* 10:3981. doi: 10.1038/s41467-019-11662-3

Farfán, N., Ocarez, N., Castellón, E. A., Mejía, N., de Herreros, A. G., and Contreras, H. R. (2018). The transcriptional factor ZEB1 represses Syndecan 1 expression in prostate cancer. *Sci. Rep.* 8:11467. doi: 10.1038/s41598-018-29829-1

Filmus, J., and Capurro, M. (2014). The role of glypicans in hedgehog signaling. *Matrix Biol.* 35, 248–252. doi: 10.1016/j.matbio.2013.12.007

Fjeldstad, K., and Kolset, S. O. (2005). Decreasing the metastatic potential in cancers–targeting the heparan sulfate proteoglycans. *Curr. Drug Targets* 6, 665–682. doi: 10.2174/1389450054863662

Fleurot, E., Goudin, C., Hanoux, V., Bonnamy, P.-J., and Levallet, J. (2019). Estrogen receptor α regulates the expression of syndecan-1 in human breast carcinoma cells. *Endocr. Relat. Cancer* 26, 615–628. doi: 10.1530/erc-18-0285

Folkman, J., Langer, R., Linhardt, R. J., Haudenschild, C., and Taylor, S. (1983). Angiogenesis inhibition and tumor regression caused by heparin or a heparin fragment in the presence of cortisone. *Science* 221, 719–725. doi: 10.1126/science.6192498

Forsten-Williams, K., Chu, C. L., Fannon, M., Buczek-Thomas, J. A., and Nugent, M. A. (2008). Control of growth factor networks by heparan sulfate proteoglycans. *Ann. Biomed. Eng.* 36, 2134–2148. doi: 10.1007/s10439-008-9575-z

Frischknecht, R., and Seidenbecher, C. I. (2012). Brevican: a key proteoglycan in the perisynaptic extracellular matrix of the brain. *Int. J. Biochem. Cell Biol.* 44, 1051–1054. doi: 10.1016/j.biocel.2012.03.022

Funderburgh, J. L. (2002). Keratan sulfate biosynthesis. *IUBMB Life* 54, 187–194. doi: 10.1080/15216540214932

Fuster, M. M., and Esko, J. D. (2005). The sweet and sour of cancer: glycans as novel therapeutic targets. *Nat. Rev. Cancer* 5, 526–542. doi: 10.1038/nrc1649

Gandhi, N. S., and Mancera, R. L. (2008). The structure of glycosaminoglycans and their interactions with proteins. *Chem. Biol. Drug Des.* 72, 455–482. doi: 10.1111/j.1747-0285.2008.00741.x

Girard, C. A., Lecacheur, M., Ben Jouira, R., Berestjuk, I., Diazzi, S., Prod'homme, V., et al. (2020). A feed-forward mechanosignaling loop confers resistance to therapies targeting the MAPK pathway in BRAF-mutant melanoma. *Cancer Res.* 80, 1927–1941. doi: 10.1158/0008-5472.CAN-19-2914

Golding, J. P., Tidcombe, H., Tsoni, S., and Gassmann, M. (1999). Chondroitin sulphate-binding molecules may pattern central projections of sensory axons within the cranial mesenchyme of the developing mouse. *Dev. Biol.* 216, 85–97. doi: 10.1006/dbio.1999.9497

Graham, K., Murphy, J. I., and Dhoot, G. K. (2016). SULF1/SULF2 reactivation during liver damage and tumour growth. *Histochem. Cell Biol.* 146, 85–97. doi: 10.1007/s00418-016-1425-8

Grindel, B. J., Martinez, J. R., Tellman, T. V., Harrington, D. A., Zafar, H., Nakhleh, L., et al. (2018). Matrilysin/MMP-7 cleavage of perlecan/HSPG2 complexed with semaphorin 3A supports FAK-mediated stromal invasion by prostate cancer cells. *Sci. Rep.* 8:7262. doi: 10.1038/s41598-018-25435-3

Grootjans, J. J., Zimmermann, P., Reekmans, G., Smets, A., Degeest, G., Dürr, J., et al. (1997). Syntenin, a PDZ protein that binds syndecan cytoplasmic domains. *Proc. Natl. Acad. Sci. U. S. A.* 94, 13683–13688. doi: 10.1073/pnas.94.25.13683

Gubbiotti, M. A., Neill, T., and Iozzo, R. V. (2017). A current view of perlecan in physiology and pathology: a mosaic of functions. *Matrix Biol.* 5, 285–298. doi: 10.1016/j.matbio.2016.09.003

Guo, J.-Y., Hsu, H.-S., Tyan, S.-W., Li, F.-Y., Shew, J.-Y., Lee, W.-H., et al. (2017). Serglycin in tumor microenvironment promotes non-small cell lung cancer aggressiveness in a CD44-dependent manner. *Oncogene* 36, 2457–2471. doi: 10.1038/onc.2016.404

Hao, W., Han, J., Chu, Y., Huang, L., Zhuang, Y., Sun, J., et al. (2018). Collagen/Heparin Bi-affinity multilayer modified collagen scaffolds for controlled bFGF release to improve angiogenesis in vivo. *Macromol. Biosci.* 18:1870028. doi: 10.1002/mabi.201870028

Hassan, H., Greve, B., Pavao, M. S. G., Kiesel, L., Ibrahim, S. A., and Götte, M. (2013). Syndecan-1 modulates β-integrin-dependent and interleukin-6-dependent functions in breast cancer cell adhesion, migration, and resistance to irradiation. *FEBS J.* 280, 2216–2227. doi: 10.1111/febs.12111

Heinämäki, P., Rehn, M., Kivirikko, S., Muona, A., Hintikka, E., and Pihlajaniemi, T. (1994). Exon-intron organization of the human type VI collagen gene and comparison of type XV collagen with its homologue tyep XVIII. *Matrix Biol.* 14, 351–352. doi: 10.1016/0945-053x(94)90035-3

Heinegård, D. (2009). Fell-muir lecture: proteoglycans and more - from molecules to biology. *International J. Exp. Pathol.* 90, 575–586. doi: 10.1111/j.1365-2613.2009.00695.x

Hendricks, C., Dubail, J., Brohee, L., Delforge, Y., Colige, A., and Deroanne, C. (2016). A novel physiological glycosaminoglycan-deficient splice variant of neuropilin-1 is anti-tumorigenic in vitro and in vivo. *PLoS One* 11:e0165153. doi: 10.1371/journal.pone.0165153

Hoffmann, R. M., Crescioli, S., Mele, S., Sachouli, E., Cheung, A., Chui, C. K., et al. (2020). A novel antibody-drug conjugate (ADC) delivering a DNA mono-alkylating payload to chondroitin sulfate proteoglycan (CSPG4)-Expressing Melanoma. *Cancers* 12:1029. doi: 10.3390/cancers12041029

Hsueh, Y. P., Yang, F. C., Kharazia, V., Naisbitt, S., Cohen, A. R., Weinberg, R. J., et al. (1998). Direct interaction of CASK/LIN-2 and syndecan heparan sulfate proteoglycan and their overlapping distribution in neuronal synapses. *J. Cell Biol.* 142, 139–151. doi: 10.1083/jcb.142.1.139

Humphries, J. D., Byron, A., and Humphries, M. J. (2006). Integrin ligands at a glance. *J. Cell Sci.* 119, 3901–3903. doi: 10.1242/jcs.03098

Iba, K., Albrechtsen, R., Gilpin, B., Frohlich, C., Loechel, F., Zolkiewska, A., et al. (2000). The cysteine-rich domain of human ADAM 12 supports cell adhesion through syndecans and triggers signaling events that lead to beta1 integrin-dependent cell spreading. *J. Cell Biol.* 149, 1143–1156. doi: 10.1083/jcb.149.5.1143

Ibrahim, S. A., Gadalla, R., El-Ghonaimy, E. A., Samir, O., Mohamed, H. T., Hassan, H., et al. (2017). Syndecan-1 is a novel molecular marker for triple negative inflammatory breast cancer and modulates the cancer stem cell phenotype via the IL-6/STAT3, Notch and EGFR signaling pathways. *Mol. Cancer* 16:57. doi: 10.1186/s12943-017-0621-z

Ibrahim, S. A., Yip, G. W., Stock, C., Pan, J.-W., Neubauer, C., Poeter, M., et al. (2012). Targeting of syndecan-1 by microRNA miR-10b promotes breast cancer cell motility and invasiveness via a Rho-GTPase- and E-cadherin-dependent mechanism. *Int. J. Cancer* 131, E884–E896. doi: 10.1002/ijc.27629

Iizasa, T., Chang, H., Suzuki, M., Otsuji, M., Yokoi, S., Chiyo, M., et al. (2004). Overexpression of collagen XVIII is associated with poor outcome and elevated levels of circulating serum endostatin in non-small cell lung cancer. *Clin. Cancer Res.* 10, 5361–5366. doi: 10.1158/1078-0432.CCR-04-43

Indira Chandran, V., Welinder, C., Mansson, A.-S., Offer, S., Freyhult, E., Pernemalm, M., et al. (2019). Ultrasensitive immunoprofiling of plasma extracellular vesicles identifies syndecan-1 as a potential tool for minimally invasive diagnosis of glioma. *Clin. Cancer Res.* 25, 3115–3127. doi: 10.1158/1078-0432.CCR-18-2946

Iozzo, R. V. (1997). The family of the small leucine-rich proteoglycans: key regulators of matrix assembly and cellular growth. *Crit. Rev. Biochem. Mol. Biol.* 32, 141–174. doi: 10.3109/10409239709108551

Iozzo, R. V. (1998). Matrix proteoglycans: from molecular design to cellular function. *Annu. Rev. Biochem.* 67, 609–652. doi: 10.1146/annurev.biochem.67.1.609

Iozzo, R. V. (1999). The biology of the small leucine-rich proteoglycans. *J. Biol. Chem.* 274, 18843–18846. doi: 10.1074/jbc.274.27.18843

Iozzo, R. V., Chakrani, F., Perrotti, D., McQuillan, D. J., Skorski, T., Calabretta, B., et al. (1999). Cooperative action of germ-line mutations in decorin and p53 accelerates lymphoma tumorigenesis. *Proc. Natl. Acad. Sci. U. S. A.* 96, 3092–3097. doi: 10.1073/pnas.96.6.3092

Iozzo, R. V., Goldoni, S., Berendsen, A. D., and Young, M. F. (2011). *Small Leucine-Rich Proteoglycans*. Berlin: Springer, doi: 10.1007/978-3-642-16555-9_6

Iozzo, R. V., and Schaefer, L. (2015). Proteoglycan form and function: a comprehensive nomenclature of proteoglycans. *Matrix Biol.* 42, 11–55. doi: 10.1016/j.matbio.2015.02.003

Iozzo, R. V., Zoeller, J. J., and Nyström, A. (2009). Basement membrane proteoglycans: modulators Par Excellence of cancer growth and angiogenesis. *Mol. Cells* 27, 503–513. doi: 10.1007/s10059-009-0069-0

Jackson, H. J., Rafiq, S., and Brentjens, R. J. (2016). Driving CAR T-cells forward. *Nat. Rev. Clin. Oncol.* 13, 370–383. doi: 10.1038/nrclinonc.2016.36

Jang, B., Jung, H., Chung, H., Moon, B.-I., and Oh, E.-S. (2016). Syndecan-2 enhances E-cadherin shedding and fibroblast-like morphological changes by inducing MMP-7 expression in colon cancer cells. *Biochem. Biophys. Res. Commun.* 477, 47–53. doi: 10.1016/j.bbrc.2016.06.019

Janoštiak, R., Pataki, A. C., Brábek, J., and Rösel, D. (2014). Mechanosensors in integrin signaling: the emerging role of p130Cas. *Eur. J. Cell Biol.* 93, 445–454. doi: 10.1016/j.ejcb.2014.07.002

Jung, M., Lord, M. S., Cheng, B., Guy Lyons, J., Alkhouri, H., Margaret Hughes, J., et al. (2013). Mast cells produce novel shorter forms of perlecan that contain functional endorepellin. *J. Biol. Chem.* 288, 3289–3304. doi: 10.1074/jbc.m112.387811

Kalscheuer, S., Khanna, V., Kim, H., Li, S., Sachdev, D., DeCarlo, A., et al. (2019). Discovery of HSPG2 (Perlecan) as a therapeutic target in triple negative breast cancer. *Sci. Rep.* 9:12492. doi: 10.1038/s41598-019-48993-6

Kanchanawong, P., Shtengel, G., Pasapera, A. M., Ramko, E. B., Davidson, M. W., Hess, H. F., et al. (2010). Nanoscale architecture of integrin-based cell adhesions. *Nature* 468, 580–584. doi: 10.1038/nature09621

Kashyap, R., Roucourt, B., Lembo, F., Fares, J., Carcavilla, A. M., Restouin, A., et al. (2015). Syntenin controls migration, growth, proliferation, and cell cycle progression in cancer cells. *Front. Pharmacol.* 6:241. doi: 10.3389/fphar.2015.00241

Katakam, S. K., Tria, V., Sim, W., Yip, G. W., Molgora, S., Karnavas, T., et al. (2020). The heparan sulfate proteoglycan syndecan-1 regulates colon cancer stem cell function via a focal adhesion kinase—Wnt signaling axis. *FEBS J.* Online ahead of print doi: 10.1111/febs.15356

Keller-Pinter, A., Ughy, B., Domoki, M., Pettko-Szandtner, A., Letoha, T., Tovari, J., et al. (2017). The phosphomimetic mutation of syndecan-4 binds and inhibits Tiam1 modulating Rac1 activity in PDZ interaction–dependent manner. *PLoS One* 12:e0187094. doi: 10.1371/journal.pone.0187094

Kennelly, T. M., Li, Y., Cao, Y., Qwarnstrom, E. E., and Geoghegan, M. (2019). Distinct binding interactions of α5β1-integrin and proteoglycans with fibronectin. *Biophys. J.* 117, 688–695. doi: 10.1016/j.bpj.2019.07.002

Khatun, Z., Nurunnabi, M., Reeck, G. R., Cho, K. J., and Lee, Y.-K. (2013). Oral delivery of taurocholic acid linked heparin-docetaxel conjugates for cancer therapy. *J. Control. Release* 170, 74–82. doi: 10.1016/j.jconrel.2013.04.024

Kim, H.-P., Han, S.-W., Song, S.-H., Jeong, E.-G., Lee, M.-Y., Hwang, D., et al. (2014). Testican-1-mediated epithelial-mesenchymal transition signaling confers acquired resistance to lapatinib in HER2-positive gastric cancer. *Oncogene* 33, 3334–3341. doi: 10.1038/onc.2013.285

Kim, Y., and Kumar, S. (2014). CD44-mediated adhesion to hyaluronic acid contributes to mechanosensing and invasive motility. *Mol. Cancer Res.* 12, 1416–1429. doi: 10.1158/1541-7786.MCR-13-0629

Kind, S., Merenkow, C., Büscheck, F., Möller, K., Dum, D., Chirico, V., et al. (2019). Prevalence of syndecan-1 (CD138) expression in different kinds of human tumors and normal tissues. *Disease Markers* 2019:4928315. doi: 10.1155/2019/4928315

Kodama, J., Hasengaowa, Kusumoto, T., Seki, N., Matsuo, T., Ojima, Y., et al. (2007). Prognostic significance of stromal versican expression in human endometrial cancer. *Ann. Oncol.* 18, 269–274. doi: 10.1093/annonc/mdl370

Kolset, S. O., and Tveit, H. (2008). Serglycin–structure and biology. *Cell. Mol. Life Sci.* 65, 1073–1085.

Kolseth, I. B. M., Reine, T. M., Vuong, T. T., Meen, A. J., Fan, Q., Jenssen, T. G., et al. (2015). Serglycin is part of the secretory repertoire of LPS-activated monocytes. *Immun. Inflamm. Dis.* 3, 23–31. doi: 10.1002/iid3.47

Kurylo, M. P., Grandfield, K., Marshall, G. W., Altoe, V., Aloni, S., and Ho, S. P. (2016). Effect of proteoglycans at interfaces as related to location, architecture,

and mechanical cues. *Arch. Oral Biol.* 63, 82–92. doi: 10.1016/j.archoralbio.2015.11.021

Laklai, H., Miroshnikova, Y. A., Pickup, M. W., Collisson, E. A., Kim, G. E., Barrett, A. S., et al. (2016). Genotype tunes pancreatic ductal adenocarcinoma tissue tension to induce matricellular fibrosis and tumor progression. *Nat. Med.* 22, 497–505. doi: 10.1038/nm.4082

Lee, C. M., Tanaka, T., Murai, T., Kondo, M., Kimura, J., Su, W., et al. (2002). Novel chondroitin sulfate-binding cationic liposomes loaded with cisplatin efficiently suppress the local growth and liver metastasis of tumor cells in vivo. *Cancer Res.* 62, 4282–4288.

Lee, K. S., Park, G. S., Hong, S. H., Byun, J. H., Woo, I. S., Jeon, H.-M., et al. (2010). Prognostic relevance of collagen XVIII expression in metastatic gastric carcinoma. *Tumour Biol.* 31, 165–170. doi: 10.1007/s13277-010-0022-z

Levental, K. R., Yu, H., Kass, L., Lakins, J. N., Egeblad, M., Erler, J. T., et al. (2009). Matrix crosslinking forces tumor progression by enhancing integrin signaling. *Cell* 139, 891–906. doi: 10.1016/j.cell.2009.10.027

Lewis, J. L., Krawczak, D. A., Oegema, T. R. Jr., and Westendorf, J. J. (2010). Effect of decorin and dermatan sulfate on the mechanical properties of a neocartilage. *Connect. Tissue Res.* 51, 159–170. doi: 10.3109/03008200903174342

Li, K., Li, L., Wu, X., Yu, J., Ma, H., Zhang, R., et al. (2019). Loss of SDC1 expression is associated with poor prognosis of colorectal cancer patients in Northern China. *Dis. Markers* 2019:3768708. doi: 10.1155/2019/3768708

Li, N., Gao, W., Zhang, Y.-F., and Ho, M. (2018). Glypicans as cancer therapeutic targets. *Trends Cancer Res.* 4, 741–754. doi: 10.1016/j.trecan.2018.09.004

Li, R., Li, Y., Wu, Y., Zhao, Y., Chen, H., Yuan, Y., et al. (2018). Heparin-Poloxamer thermosensitive hydrogel loaded with bFGF and NGF enhances peripheral nerve regeneration in diabetic rats. *Biomaterials* 168, 24–37. doi: 10.1016/j.biomaterials.2018.03.044

Li, Y., Sun, C., Yates, E. A., Jiang, C., Wilkinson, M. C., and Fernig, D. G. (2016). Heparin binding preference and structures in the fibroblast growth factor family parallel their evolutionary diversification. *Open Biol.* 6:150275. doi: 10.1098/rsob.150275

Lin, X. (2004). Functions of heparan sulfate proteoglycans in cell signaling during development. *Development* 131, 6009–6021. doi: 10.1242/dev.01522

Lindahl, U., Couchman, J., Kimata, K., and Esko, J. D. (2015). *Proteoglycans and Sulfated Glycosaminoglycans*. Available online at: https://europepmc.org/books/n/glyco3/ch17/?extid=28876832&src=med (accessed April 25, 2020).

Liu, B. P., Cafferty, W. B. J., Budel, S. O., and Strittmatter, S. M. (2006). Extracellular regulators of axonal growth in the adult central nervous system. *Philos. Trans. R. Soc. B Biol. Sci.* 361, 1593–1610. doi: 10.1098/rstb.2006.1891

Liu, C.-Y., Lin, H.-H., Tang, M.-J., and Wang, Y.-K. (2015). Vimentin contributes to epithelial-mesenchymal transition cancer cell mechanics by mediating cytoskeletal organization and focal adhesion maturation. *Oncotarget* 6, 15966–15983. doi: 10.18632/oncotarget.3862

Liu, M., Tolg, C., and Turley, E. (2019). Dissecting the dual nature of hyaluronan in the tumor microenvironment. *Front. Immunol.* 10:947. doi: 10.3389/fimmu.2019.00947

Longmuir, K. J., Haynes, S. M., Baratta, J. L., Kasabwalla, N., and Robertson, R. T. (2009). Liposomal delivery of doxorubicin to hepatocytes in vivo by targeting heparan sulfate. *Int. J. Pharm.* 382, 222–233. doi: 10.1016/j.ijpharm.2009.07.030

Lu, R., Wu, C., Guo, L., Liu, Y., Mo, W., Wang, H., et al. (2012). The role of brevican in glioma: promoting tumor cell motility in vitro and in vivo. *BMC Cancer* 12:607. doi: 10.1186/1471-2407-12-607

Lundström, E., Sahlin, L., Skoog, L., Hägerström, T., Svane, G., Azavedo, E., et al. (2006). Expression of syndecan-1 in histologically normal breast tissue from postmenopausal women with breast cancer according to mammographic density. *Climacteric* 9, 277–282. doi: 10.1080/13697130600865741

Maller, O., Drain, A. P., Barrett, A. S., Borgquist, S., Ruffell, B., Thanh, P. T., et al. (2020). Inflammation promotes tumor aggression by stimulating stromal cell-dependent collagen crosslinking and stromal stiffening. *bioRxiv [Preprint]* doi: 10.1101/2020.02.13.948141

Manou, D., Bouris, P., Kletsas, D., Götte, M., Greve, B., Moustakas, A., et al. (2020). Serglycin activates pro-tumorigenic signaling and controls glioblastoma cell stemness, differentiation and invasive potential. *Matrix Biol. Plus* 6:100033. doi: 10.1016/j.mbplus.2020.100033

Matte, B. F., Kumar, A., Placone, J. K., Zanella, V. G., Martins, M. D., Engler, A. J., et al. (2019). Matrix stiffness mechanically conditions EMT and migratory behavior of oral squamous cell carcinoma. *J. Cell Sci.* 132:jcs224360. doi: 10.1242/jcs.224360

Maurel, P., Rauch, U., Flad, M., Margolis, R. K., and Margolis, R. U. (1994). Phosphacan, a chondroitin sulfate proteoglycan of brain that interacts with neurons and neural cell-adhesion molecules, is an extracellular variant of a receptor-type protein tyrosine phosphatase. *Proc. Natl. Acad. Sci. U.S.A.* 91, 2512–2516. doi: 10.1073/pnas.91.7.2512

Mekhdjian, A. H., Kai, F., Rubashkin, M. G., Prahl, L. S., Przybyla, L. M., McGregor, A. L., et al. (2017). Integrin-mediated traction force enhances paxillin molecular associations and adhesion dynamics that increase the invasiveness of tumor cells into a three-dimensional extracellular matrix. *Mol. Biol. Cell* 28, 1467–1488. doi: 10.1091/mbc.e16-09-0654

Melo, S. A., Luecke, L. B., Kahlert, C., Fernandez, A. F., Gammon, S. T., Kaye, J., et al. (2015). Glypican-1 identifies cancer exosomes and detects early pancreatic cancer. *Nature* 523, 177–182. doi: 10.1038/nature14581

Miao, L., Wang, Y., Xia, H., Yao, C., Cai, H., and Song, Y. (2013). SPOCK1 is a novel transforming growth factor-β target gene that regulates lung cancer cell epithelial-mesenchymal transition. *Biochem. Biophys. Res. Commun.* 440, 792–797. doi: 10.1016/j.bbrc.2013.10.024

Miroshnikova, Y. A., Mouw, J. K., Barnes, J. M., Pickup, M. W., Lakins, J. N., Kim, Y., et al. (2016). Tissue mechanics promote IDH1-dependent HIF1α-tenascin C feedback to regulate glioblastoma aggression. *Nat. Cell Biol.* 18, 1336–1345. doi: 10.1038/ncb3429

Misra, S., Hascall, V. C., Atanelishvili, I., Moreno Rodriguez, R., Markwald, R. R., and Ghatak, S. (2015). Utilization of glycosaminoglycans/proteoglycans as carriers for targeted therapy delivery. *Int. J. Cell Biol.* 2015:537560. doi: 10.1155/2015/537560

Mondal, N., Stolfa, G., Antonopoulos, A., Zhu, Y., Wang, S.-S., Buffone, A., et al. (2016). Glycosphingolipids on human myeloid cells stabilize E-selectin–dependent rolling in the multistep leukocyte adhesion cascadesignificance. *Arterioscler. Thromb. Vasc. Biol.* 36, 718–727. doi: 10.1161/atvbaha.115.306748

Monne, H. M.-S., Danne, R., Róg, T., Ilpo, V., and Gurtovenko, A. (2013). Structure of glycocalyx. *Biophys. J.* 104, 251a.

Moscatello, D. K., Santra, M., Mann, D. M., McQuillan, D. J., Wong, A. J., and Iozzo, R. V. (1998). Decorin suppresses tumor cell growth by activating the epidermal growth factor receptor. *J. Clin. Invest.* 101, 406–412. doi: 10.1172/JCI846

Mulloy, B., and Rider, C. C. (2006). Cytokines and proteoglycans: an introductory overview. *Biochem. Soc. Trans.* 34, 409–413. doi: 10.1042/BST0340409

Mytilinaiou, M., Nikitovic, D., Berdiaki, A., Kostouras, A., Papoutsidakis, A., Tsatsakis, A. M., et al. (2017). Emerging roles of syndecan 2 in epithelial and mesenchymal cancer progression. *IUBMB Life* 69, 824–833. doi: 10.1002/iub.1678

Naso, M. F., Zimmermann, D. R., and Iozzo, R. V. (1994). Characterization of the complete genomic structure of the human versican gene and functional analysis of its promoter. *J. Biol. Chem.* 269, 32999–33008.

Neill, T., Schaefer, L., and Iozzo, R. V. (2016). Decorin as a multivalent therapeutic agent against cancer. *Adv. Drug Deliv. Rev.* 97, 174–185. doi: 10.1016/j.addr.2015.10.016

Newick, K., O'Brien, S., Moon, E., and Albelda, S. M. (2017). CAR T cell therapy for solid tumors. *Annu. Rev. Med.* 68, 139–152. doi: 10.1146/annurev-med-062315-120245

Nia, H. T., Han, L., Bozchalooi, I. S., Roughley, P., Youcef-Toumi, K., Grodzinsky, A. J., et al. (2015). Aggrecan nanoscale solid-fluid interactions are a primary determinant of cartilage dynamic mechanical properties. *ACS Nano* 9, 2614–2625. doi: 10.1021/nn5062707

Nicolosi, P. A., Dallatomasina, A., and Perris, R. (2015). Theranostic impact of NG2/CSPG4 proteoglycan in cancer. *Theranostics* 5, 530–544. doi: 10.7150/thno.10824

Nikitovic, D., Berdiaki, A., Spyridaki, I., Krasanakis, T., Tsatsakis, A., and Tzanakakis, G. N. (2018). Proteoglycans—biomarkers and targets in cancer therapy. *Front. Endocrinol.* 9:69. doi: 10.3389/fendo.2018.00069

Nishida, J., Miyazono, K., and Ehata, S. (2018). Decreased TGFBR3/betaglycan expression enhances the metastatic abilities of renal cell carcinoma cells through TGF-β-dependent and -independent mechanisms. *Oncogene* 37, 2197–2212. doi: 10.1038/s41388-017-0084-0

Njah, K., Chakraborty, S., Qiu, B., Arumugam, S., Raju, A., Pobbati, A. V., et al. (2019). A role of agrin in maintaining the stability of vascular endothelial growth factor receptor-2 during tumor angiogenesis. *Cell Rep.* 28, 949.e7–965.e7. doi: 10.1016/j.celrep.2019.06.036

Noguchi, S., Saito, A., and Nagase, T. (2018). YAP/TAZ signaling as a molecular link between fibrosis and cancer. *Int. J. Mol. Sci.* 19:3674. doi: 10.3390/ijms19113674

Northey, J. J., Przybyla, L., and Weaver, V. M. (2017). Tissue Force programs cell fate and tumor aggression. *Cancer Discov.* 7, 1224–1237. doi: 10.1158/2159-8290.CD-16-0733

Nugent, M. A. (2000). Heparin sequencing brings structure to the function of complex oligosaccharides. *Proc. Natl. Acad. Sci. U. S. A.* 97, 10301–10303. doi: 10.1073/pnas.97.19.10301

Okina, E., Grossi, A., Gopal, S., Multhaupt, H. A. B., and Couchman, J. R. (2012). Alpha-actinin interactions with syndecan-4 are integral to fibroblast-matrix adhesion and regulate cytoskeletal architecture. *Int. J. Biochem. Cell Biol.* 44, 2161–2174. doi: 10.1016/j.biocel.2012.08.017

Ostapoff, K. T., Awasthi, N., Cenik, B. K., Hinz, S., Dredge, K., Schwarz, R. E., et al. (2013). PG545, an angiogenesis and heparanase inhibitor, reduces primary tumor growth and metastasis in experimental pancreatic cancer. *Mol. Cancer Ther.* 12, 1190–1201. doi: 10.1158/1535-7163.MCT-12-1123

Paszek, M. J., DuFort, C. C., Rossier, O., Bainer, R., Mouw, J. K., Godula, K., et al. (2014). The cancer glycocalyx mechanically primes integrin-mediated growth and survival. *Nature* 511, 319–325. doi: 10.1038/nature13535

Paszek, M. J., Zahir, N., Johnson, K. R., Lakins, J. N., Rozenberg, G. I., Gefen, A., et al. (2005). Tensional homeostasis and the malignant phenotype. *Cancer Cell* 8, 241–254. doi: 10.1016/j.ccr.2005.08.010

Peer, D., Karp, J. M., Hong, S., Farokhzad, O. C., Margalit, R., and Langer, R. (2007). Nanocarriers as an emerging platform for cancer therapy. *Nat. Nanotechnol.* 2, 751–760. doi: 10.1038/nnano.2007.387

Pellegatta, S., Savoldo, B., Di Ianni, N., Corbetta, C., Chen, Y., Patané, M., et al. (2018). Constitutive and TNFα-inducible expression of chondroitin sulfate proteoglycan 4 in glioblastoma and neurospheres: implications for CAR-T cell therapy. *Sci. Transl. Med.* 10:eaao2731. doi: 10.1126/scitranslmed.aao2731

Perurena, N., Zandueta, C., Martínez-Canarias, S., Moreno, H., Vicent, S., Almeida, A. S., et al. (2017). EPCR promotes breast cancer progression by altering SPOCK1/testican 1-mediated 3D growth. *J. Hematol. Oncol.* 10:23. doi: 10.1186/s13045-017-0399-x

Pirinen, R., Leinonen, T., Böhm, J., Johansson, R., Ropponen, K., Kumpulainen, E., et al. (2005). Versican in nonsmall cell lung cancer: relation to hyaluronan, clinicopathologic factors, and prognosis. *Hum. Pathol.* 36, 44–50. doi: 10.1016/j.humpath.2004.10.010

Pogoda, K., Bucki, R., Byfield, F. J., Cruz, K., Lee, T., Marcinkiewicz, C., et al. (2017). Soft substrates containing hyaluronan mimic the effects of increased stiffness on morphology, motility, and proliferation of glioma cells. *Biomacromolecules* 18, 3040–3051. doi: 10.1021/acs.biomac.7b00324

Polacheck, W. J., Kutys, M. L., Yang, J., Eyckmans, J., Wu, Y., Vasavada, H., et al. (2017). A non-canonical Notch complex regulates adherens junctions and vascular barrier function. *Nature* 552, 258–262. doi: 10.1038/nature24998

Pomin, V. H., and Mulloy, B. (2018). Glycosaminoglycans and proteoglycans. *Pharmaceuticals* 11:27. doi: 10.3390/ph11010027

Qazi, H., Palomino, R., Shi, Z.-D., Munn, L. L., and Tarbell, J. M. (2013). Cancer cell glycocalyx mediates mechanotransduction and flow-regulated invasion. *Integr. Biol.* 5, 1334–1343. doi: 10.1039/c3ib40057c

Qiao, W., Liu, H., Guo, W., Li, P., and Deng, M. (2019). Prognostic and clinical significance of syndecan-1 expression in breast cancer: a systematic review and meta-analysis. *Eur. J. Surg. Oncol.* 45, 1132–1137. doi: 10.1016/j.ejso.2018.12.019

Ramani, V. C., Purushothaman, A., Stewart, M. D., Thompson, C. A., Vlodavsky, I., Au, J. L.-S., et al. (2013). The heparanase/syndecan-1 axis in cancer: mechanisms and therapies. *FEBS J.* 280, 2294–2306.

Rankin, K. S., and Frankel, D. (2016). Hyaluronan in cancer - from the naked mole rat to nanoparticle therapy. *Soft Matter* 12, 3841–3848. doi: 10.1039/c6sm00513f

Rivera, C., Zandonadi, F. S., Sánchez-Romero, C., Soares, C. D., Granato, D. C., González-Arriagada, W. A., et al. (2018). Agrin has a pathological role in the progression of oral cancer. *Br. J. Cancer* 118, 1628–1638. doi: 10.1038/s41416-018-0135-5

Rizzolio, S., Rabinowicz, N., Rainero, E., Lanzetti, L., Serini, G., Norman, J., et al. (2012). Neuropilin-1-dependent regulation of EGF-receptor signaling. *Cancer Res.* 72, 5801–5811. doi: 10.1158/0008-5472.can-12-0995

Robinson, K. A., Sun, M., Barnum, C. E., Weiss, S. N., Huegel, J., Shetye, S. S., et al. (2017). Decorin and biglycan are necessary for maintaining collagen fibril structure, fiber realignment, and mechanical properties of mature tendons. *Matrix Biol.* 64, 81–93. doi: 10.1016/j.matbio.2017.08.004

Rossi, G. D., De Rossi, G., Evans, A. R., Kay, E., Woodfin, A., McKay, T. R., et al. (2014). Shed syndecan-2 inhibits angiogenesis. *J. Cell Sci.* 127, 4788–4799. doi: 10.1242/jcs.153015

Samuel, M. S., Lopez, J. I., McGhee, E. J., Croft, D. R., Strachan, D., Timpson, P., et al. (2011). Actomyosin-mediated cellular tension drives increased tissue stiffness and β-catenin activation to induce epidermal hyperplasia and tumor growth. *Cancer Cell* 19, 776–791. doi: 10.1016/j.ccr.2011.05.008

Sanz-Moreno, V., Gaggioli, C., Yeo, M., Albrengues, J., Wallberg, F., Viros, A., et al. (2011). ROCK and JAK1 signaling cooperate to control actomyosin contractility in tumor cells and stroma. *Cancer Cell* 20, 229–245. doi: 10.1016/j.ccr.2011.06.018

Sarntinoranont, M., Rooney, F., and Ferrari, M. (2003). Interstitial stress and fluid pressure within a growing tumor. *Ann. Biomed. Eng.* 31, 327–335. doi: 10.1114/1.1554923

Sarrazin, S., Lamanna, W. C., and Esko, J. D. (2011). Heparan sulfate proteoglycans. *Cold Spring Harb. Perspect. Biol.* 3:a004952.

Sasse, P., Malan, D., Fleischmann, M., Roell, W., Gustafsson, E., Bostani, T., et al. (2008). Perlecan is critical for heart stability. *Cardiovasc. Res.* 80, 435–444. doi: 10.1093/cvr/cvn225

Sawada, Y., Tamada, M., Dubin-Thaler, B. J., Cherniavskaya, O., Sakai, R., Tanaka, S., et al. (2006). Force sensing by mechanical extension of the Src family kinase substrate p130Cas. *Cell* 127, 1015–1026. doi: 10.1016/j.cell.2006.09.044

Sayyad, M. R., Puchalapalli, M., Vergara, N. G., Wangensteen, S. M., Moore, M., Mu, L., et al. (2019). Syndecan-1 facilitates breast cancer metastasis to the brain. *Breast Cancer Res. Treat.* 178, 35–49. doi: 10.1007/s10549-019-05347-0

Schedin, P., and Keely, P. J. (2011). Mammary gland ECM remodeling, stiffness, and mechanosignaling in normal development and tumor progression. *Cold Spring Harb. Perspect. Biol.* 3:a003228. doi: 10.1101/cshperspect.a003228

Schick, B. P., Gradowski, J. F., and San Antonio, J. D. (2001). Synthesis, secretion, and subcellular localization of serglycin proteoglycan in human endothelial cells. *Blood* 97, 449–458. doi: 10.1182/blood.v97.2.449

Schnepp, A., Lindgren, P. K., Hulsmann, H., Kroger, S., Paulsson, M., and Hartmann, U. (2005). Mouse testican-2: expression, glycosylation, and effects on neurite outgrowth. *J. Biol. Chem.* 280, 11274–11280. doi: 10.1074/jbc.m414276200

Shawky, M. S., Ricciardelli, C., Lord, M., Whitelock, J., Ferro, V., Britt, K., et al. (2015). Proteoglycans: potential agents in mammographic density and the associated breast cancer risk. *J. Mammary Gland Biol. Neoplasia* 20, 121–131. doi: 10.1007/s10911-015-9346-z

Shen, X.-H., Lin, W.-R., Xu, M.-D., Qi, P., Dong, L., Zhang, Q.-Y., et al. (2015). Prognostic significance of versican expression in gastric adenocarcinoma. *Oncogenesis* 4:e178. doi: 10.1038/oncsis.2015.36

Shi, Z.-D., Wang, H., and Tarbell, J. M. (2011). Heparan sulfate proteoglycans mediate interstitial flow mechanotransduction regulating MMP-13 expression and cell motility via FAK-ERK in 3D collagen. *PLoS One* 6:e15956. doi: 10.1371/journal.pone.0015956

Shimizu, Y., Suzuki, T., Yoshikawa, T., Endo, I., and Nakatsura, T. (2019). Next-generation cancer immunotherapy targeting glypican-3. *Front. Oncol.* 9:248. doi: 10.3389/fonc.2019.00248

Shintani, Y., Takashima, S., Asano, Y., Kato, H., Liao, Y., Yamazaki, S., et al. (2006). Glycosaminoglycan modification of neuropilin-1 modulates VEGFR2 signaling. *EMBO J.* 25, 3045–3055. doi: 10.1038/sj.emboj.7601188

Shriver, Z., Capila, I., Venkataraman, G., and Sasisekharan, R. (2012). Heparin and heparan sulfate: analyzing structure and microheterogeneity. *Handb. Exp. Pharmacol.* 207, 159–176. doi: 10.1007/978-3-642-23056-1_8

Shurer, C. R., Kuo, J. C.-H., Roberts, L. M., Gandhi, J. G., Colville, M. J., Enoki, T. A., et al. (2019). Physical principles of membrane shape regulation by the glycocalyx. *Cell* 177, 1757.e27–1770.e27. doi: 10.1016/j.cell.2019.04.017

Silver, D. J., Siebzehnrubl, F. A., Schildts, M. J., Yachnis, A. T., Smith, G. M., Smith, A. A., et al. (2013). Chondroitin sulfate proteoglycans potently inhibit invasion and serve as a central organizer of the brain tumor microenvironment. *J. Neurosci.* 33, 15603–15617. doi: 10.1523/JNEUROSCI.3004-12.2013

Skandalis, S. S., Karalis, T. T., Chatzopoulos, A., and Karamanos, N. K. (2019). Hyaluronan-CD44 axis orchestrates cancer stem cell functions. *Cell. Signal.* 63:109377. doi: 10.1016/j.cellsig.2019.109377

Soares da Costa, D., Reis, R. L., and Pashkuleva, I. (2017). Sulfation of glycosaminoglycans and its implications in human health and disorders. *Annu. Rev. Biomed. Eng.* 19, 1–26. doi: 10.1146/annurev-bioeng-071516-044610

Su, Z., Kishida, S., Tsubota, S., Sakamoto, K., Cao, D., Kiyonari, S., et al. (2017). Neurocan, an extracellular chondroitin sulfate proteoglycan, stimulates neuroblastoma cells to promote malignant phenotypes. *Oncotarget* 8, 106296–106310. doi: 10.18632/oncotarget.22435

Sulka, B., Lortat-Jacob, H., Terreux, R., Letourneur, F., and Rousselle, P. (2009). Tyrosine dephosphorylation of the syndecan-1 PDZ binding domain regulates syntenin-1 recruitment. *J. Biol. Chem.* 284, 10659–10671. doi: 10.1074/jbc.M807643200

Sun, D., Mcalmon, K. R., Davies, J. A., Bernfield, M., and Hay, E. D. (1998). Simultaneous loss of expression of syndecan-1 and E-cadherin in the embryonic palate during epithelial-mesenchymal transformation. *Int. J. Dev. Biol.* 42, 733–736.

Teixeira, F. C. O. B., Kumar, A. V., Katakam, S. K., Cocola, C., Pelucchi, P., Graf, M., et al. (2020). The heparan sulfate sulfotransferases HS2ST1 and HS3ST2 are novel regulators of breast cancer stem-cell properties. *Front. Cell Dev. Biol.* 8:559554. doi: 10.3389/fcell.2020.559554

Teng, Y. H.-F., Aquino, R. S., and Park, P. W. (2012). Molecular functions of syndecan-1 in disease. *Matrix Biol.* 31, 3–16. doi: 10.1016/j.matbio.2011.10.001

Theocharis, A. D., and Karamanos, N. K. (2019). Proteoglycans remodeling in cancer: underlying molecular mechanisms. *Matrix Biol.* 7, 220–259. doi: 10.1016/j.matbio.2017.10.008

Tian, C., Öhlund, D., Rickelt, S., Lidström, T., and Huang, Y. (2020). Cancer cell–derived matrisome proteins promote metastasis in pancreatic ductal adenocarcinoma. *Cancer Res.* 80, 1461–1474.

Tkachenko, E., Elfenbein, A., Tirziu, D., and Simons, M. (2006). Syndecan-4 clustering induces cell migration in a PDZ-dependent manner. *Circ. Res.* 98, 1398–1404. doi: 10.1161/01.RES.0000225283.71490.5a

Tse, J. M., Cheng, G., Tyrrell, J. A., Wilcox-Adelman, S. A., Boucher, Y., Jain, R. K., et al. (2012). Mechanical compression drives cancer cells toward invasive phenotype. *Proc. Natl. Acad. Sci. U. S. A.* 109, 911–916. doi: 10.1073/pnas.1118910109

Tsen, G., Halfter, W., Kröger, S., and Cole, G. J. (1995). Agrin is a heparan sulfate proteoglycan. *J. Biol. Chem.* 270, 3392–3399. doi: 10.1074/jbc.270.7.3392

Tsoyi, K., Osorio, J. C., Chu, S. G., Fernandez, I. E., De Frias, S. P., Sholl, L., et al. (2019). Lung Adenocarcinoma syndecan-2 potentiates cell invasiveness. *Am. J. Respir. Cell Mol. Biol.* 60, 659–666. doi: 10.1165/rcmb.2018-0118OC

Vachon, C. M., van Gils, C. H., Sellers, T. A., Ghosh, K., Pruthi, S., Brandt, K. R., et al. (2007). Mammographic density, breast cancer risk and risk prediction. *Breast Cancer Res.* 9:217. doi: 10.1186/bcr1829

Varga, I., Hutóczki, G., Szemcsák, C. D., Zahuczky, G., Tóth, J., Adamecz, Z., et al. (2012). Brevican, neurocan, tenascin-C and versican are mainly responsible for the invasiveness of low-grade astrocytoma. *Pathol. Oncol. Res.* 18, 413–420. doi: 10.1007/s12253-011-9461-0

Varki, A., Cummings, R. D., Esko, J. D., Stanley, P., Hart, G. W., Aebi, M., et al. (eds) (2016). *Essentials of Glycobiology*. Cold Spring Harbor, NY: Cold Spring Harbor Laboratory.

Vennin, C., Mélénec, P., Rouet, R., Nobis, M., Cazet, A. S., Murphy, K. J., et al. (2019). CAF hierarchy driven by pancreatic cancer cell p53-status creates a pro-metastatic and chemoresistant environment via perlecan. *Nat. Commun.* 10:3637. doi: 10.1038/s41467-019-10968-6

Vogel, K. G., and Peterson, D. W. (1981). Extracellular, surface, and intracellular proteoglycans produced by human embryo lung fibroblasts in culture (IMR-90). *J. Biol. Chem.* 256, 13235–13242.

Vuoriluoto, K., Högnäs, G., Meller, P., Lehti, K., and Ivaska, J. (2011). Syndecan-1 and -4 differentially regulate oncogenic K-ras dependent cell invasion into collagen through α2β1 integrin and MT1-MMP. *Matrix Biol.* 30, 207–217. doi: 10.1016/j.matbio.2011.03.003

Wang, C., Tong, X., and Yang, F. (2014). Bioengineered 3D brain tumor model to elucidate the effects of matrix stiffness on glioblastoma cell behavior using PEG-based hydrogels. *Mol. Pharm.* 11, 2115–2125. doi: 10.1021/mp5000828

Wang, S., Zhang, X., Wang, G., Cao, B., Yang, H., Jin, L., et al. (2019). Syndecan-1 suppresses cell growth and migration via blocking JAK1/STAT3 and Ras/Raf/MEK/ERK pathways in human colorectal carcinoma cells. *BMC Cancer* 19:1160. doi: 10.1186/s12885-019-6381-y

Wang, X., He, J., Zhao, X., Qi, T., Zhang, T., and Kong, C. (2018). Syndecan-1 suppresses epithelial-mesenchymal transition and migration in human oral cancer cells. *Oncol. Rep.* 39, 1835–1842. doi: 10.3892/or.2018.6271

Wei, S. C., Fattet, L., Tsai, J. H., Guo, Y., Pai, V. H., Majeski, H. E., et al. (2015). Matrix stiffness drives epithelial–mesenchymal transition and tumour metastasis through a TWIST1–G3BP2 mechanotransduction pathway. *Nat. Cell Biol.* 17, 678–688. doi: 10.1038/ncb3157

West, D. C., Rees, C. G., Duchesne, L., Patey, S. J., Terry, C. J., Turnbull, J. E., et al. (2005). Interactions of multiple heparin binding growth factors with neuropilin-1 and potentiation of the activity of fibroblast growth factor-2. *J. Biol. Chem.* 280, 13457–13464. doi: 10.1074/jbc.m410924200

Whitelock, J. M., Graham, L. D., Melrose, J., Murdoch, A. D., Iozzo, R. V., and Underwood, P. A. (1999). Human perlecan immunopurified from different endothelial cell sources has different adhesive properties for vascular cells. *Matrix Biol.* 18, 163–178. doi: 10.1016/s0945-053x(99)00014-1

Whitelock, J. M., Melrose, J., and Iozzo, R. V. (2008). Diverse cell signaling events modulated by perlecan. *Biochemistry* 47, 11174–11183. doi: 10.1021/bi8013938

Wight, T. N., Kang, I., and Merrilees, M. J. (2014). Versican and the control of inflammation. *Matrix Biol.* 35, 152–161. doi: 10.1016/j.matbio.2014.01.015

Wight, T. N., Toole, B. P., and Hascall, V. C. (2011). "Hyaluronan and the aggregating proteoglycans," in *The Extracellular Matrix: an Overview. Biology of Extracellular Matrix*, ed. R. Mecham (Berlin: Springer), 147–195. doi: 10.1007/978-3-642-16555-9_5

Winzen, U., Cole, G. J., and Halfter, W. (2003). Agrin is a chimeric proteoglycan with the attachment sites for heparan sulfate/chondroitin sulfate located in two multiple serine-glycine clusters. *J. Biol. Chem.* 278, 30106–30114. doi: 10.1074/jbc.m212676200

Wolf, K. J., Chen, J., Coombes, J. D., Aghi, M. K., and Kumar, S. (2019). Dissecting and rebuilding the glioblastoma microenvironment with engineered materials. *Nat. Rev. Mater.* 4, 651–668. doi: 10.1038/s41578-019-0135-y

Woods, A., and Couchman, J. R. (2001). Syndecan-4 and focal adhesion function. *Curr. Opin. Cell Biol.* 13, 578–583. doi: 10.1016/s0955-0674(00)00254-4

Woods, E. C., Kai, F., Barnes, J. M., Pedram, K., Pickup, M. W., Hollander, M. J., et al. (2017). A bulky glycocalyx fosters metastasis formation by promoting G1 cell cycle progression. *Elife* 6:e25752. doi: 10.7554/eLife.25752

Xiang, Y. Y., Ladeda, V., and Filmus, J. (2001). Glypican-3 expression is silenced in human breast cancer. *Oncogene* 20, 7408–7412. doi: 10.1038/sj.onc.1204925

Xu, Y., Xu, J., Yang, Y., Zhu, L., Li, X., and Zhao, W. (2018). SRGN promotes colorectal cancer metastasis as a critical downstream target of HIF-1α. *Cell. Physiol. Biochem.* 48, 2429–2440. doi: 10.1159/000492657

Yamada, H., Watanabe, K., Shimonaka, M., and Yamaguchi, Y. (1994). Molecular cloning of brevican, a novel brain proteoglycan of the aggrecan/versican family. *J. Biol. Chem.* 269, 10119–10126.

Yanagishita, M. (1993). Function of proteoglycans in the extracellular matrix. *Pathol. Int.* 43, 283–293. doi: 10.1111/j.1440-1827.1993.tb02569.x

Yang, J., Yang, Q., Yu, J., Li, X., Yu, S., and Zhang, X. (2016). SPOCK1 promotes the proliferation, migration and invasion of glioma cells through PI3K/AKT and Wnt/β-catenin signaling pathways. *Oncol. Rep.* 35, 3566–3576. doi: 10.3892/or.2016.4757

Yang, N., Mosher, R., Seo, S., Beebe, D., and Friedl, A. (2011). Syndecan-1 in breast cancer stroma fibroblasts regulates extracellular matrix fiber organization and carcinoma cell motility. *Am. J. Pathol.* 178, 325–335. doi: 10.1016/j.ajpath.2010.11.039

Zeng, Y., Waters, M., Andrews, A., Honarmandi, P., Ebong, E. E., Rizzo, V., et al. (2013). Fluid shear stress induces the clustering of heparan sulfate via mobility of glypican-1 in lipid rafts. *Am. J. Physiol. Heart Circ. Physiol.* 305, H811–H820. doi: 10.1152/ajpheart.00764.2012

Zhang, G., Ezura, Y., Chervoneva, I., Robinson, P. S., Beason, D. P., Carine, E. T., et al. (2006). Decorin regulates assembly of collagen fibrils and acquisition

of biomechanical properties during tendon development. *J. Cell. Biochem.* 98, 1436–1449. doi: 10.1002/jcb.20776

Zhang, K., Grither, W. R., Van Hove, S., Biswas, H., Ponik, S. M., Eliceiri, K. W., et al. (2016). Mechanical signals regulate and activate SNAIL1 protein to control the fibrogenic response of cancer-associated fibroblasts. *J. Cell Sci.* 129, 1989–2002. doi: 10.1242/jcs.180539

Zhang, Z., Qiu, N., Yin, J., Zhang, J., Liu, H., Guo, W., et al. (2020). SRGN crosstalks with YAP to maintain chemoresistance and stemness in breast cancer cells by modulating HDAC2 expression. *Theranostics* 10, 4290–4307. doi: 10.7150/thno.41008

Zhao, P., Guan, H.-T., Dai, Z.-J., Ma, Y.-G., Liu, X.-X., and Wang, X.-J. (2016). Knockdown of SPOCK1 inhibits the proliferation and invasion in colorectal cancer cells by suppressing the PI3K/Akt pathway. *Oncol. Res.* 24, 437–445. doi: 10.3727/096504016X14685034103554

Zhong, X., Liu, Y., Liu, H., Zhang, Y., Wang, L., and Zhang, H. (2018). Identification of potential prognostic genes for neuroblastoma. *Front. Genet.* 9:589. doi: 10.3389/fgene.2018.00589

Zimmermann, D. R., and Dours-Zimmermann, M. T. (2008). Extracellular matrix of the central nervous system: from neglect to challenge. *Histochem. Cell Biol.* 130, 635–653. doi: 10.1007/s00418-008-0485-9

Zimmermann, D. R., and Ruoslahti, E. (1989). Multiple domains of the large fibroblast proteoglycan, versican. *EMBO J.* 8, 2975–2981. doi: 10.1002/j.1460-2075.1989.tb08447.x

Zoeller, J. J., McQuillan, A., Whitelock, J., Ho, S.-Y., and Iozzo, R. V. (2008). A central function for perlecan in skeletal muscle and cardiovascular development. *J. Cell Biol.* 181, 381–394. doi: 10.1083/jcb.200708022

Zong, Y., and Jin, R. (2013). Structural mechanisms of the agrin-LRP4-MuSK signaling pathway in neuromuscular junction differentiation. *Cell. Mol. Life Sci.* 70, 3077–3088. doi: 10.1007/s00018-012-1209-9

Conflict of Interest: The authors declare that the research was conducted in the absence of any commercial or financial relationships that could be construed as a potential conflict of interest.

frontiers in Cell and Developmental Biology

REVIEW
published: 03 December 2020
doi: 10.3389/fcell.2020.560442

Research and Application of Chondroitin Sulfate/Dermatan Sulfate-Degrading Enzymes

*Wenshuang Wang, Liran Shi, Yong Qin and Fuchuan Li**

National Glycoengineering Research Center and Shandong Provincial Key Laboratory of Carbohydrate Chemistry and Glycobiology, Shandong University, Jinan, China

Chondroitin sulfate (CS) and dermatan sulfate (DS) are widely distributed on the cell surface and in the extracellular matrix in the form of proteoglycan, where they participate in various biological processes. The diverse functions of CS/DS can be mainly attributed to their high structural variability. However, their structural complexity creates a big challenge for structural and functional studies of CS/DS. CS/DS-degrading enzymes with different specific activities are irreplaceable tools that could be used to solve this problem. Depending on the site of action, CS/DS-degrading enzymes can be classified as glycosidic bond-cleaving enzymes and sulfatases from animals and microorganisms. As discussed in this review, a few of the identified enzymes, particularly those from bacteria, have wildly applied to the basic studies and applications of CS/DS, such as disaccharide composition analysis, the preparation of bioactive oligosaccharides, oligosaccharide sequencing, and potential medical application, but these do not fulfill all of the needs in terms of the structural complexity of CS/DS.

Keywords: chondroitin sulfate, dermatan sulfate, structure-function relationships, oligosaccharide, enzymes

OPEN ACCESS

Edited by:
Jeremy Turnbull, University of Liverpool, United Kingdom

Reviewed by:
Shuji Mizumoto, Meijo University, Japan
Herbert M. Geller, National Heart, Lung, and Blood Institute (NHLBI), United States

****Correspondence:***
Fuchuan Li
fuchuanli@sdu.edu.cn

Specialty section:
This article was submitted to Signaling, a section of the journal Frontiers in Cell and Developmental Biology

Received: *08 May 2020*
Accepted: *05 November 2020*
Published: *03 December 2020*

Citation:
Wang W, Shi L, Qin Y and Li F (2020) Research and Application of Chondroitin Sulfate/Dermatan Sulfate-Degrading Enzymes. Front. Cell Dev. Biol. 8:560442. doi: 10.3389/fcell.2020.560442

STRUCTURE AND FUNCTIONS OF CHONDROITIN SULFATE/DERMATAN SULFATE

As a major member of the glycosaminoglycan (GAG) family, chondroitin sulfate (CS)/dermatan sulfate (DS) chains covalently attach to core proteins to form CS/DS proteoglycans (CS/DSPGs), which are widespread on cell surfaces and within extra/pericellular matrices to regulate the extracellular environment, involving in many biological and pathophysiological activities (Sugahara and Kitagawa, 2000). As the side chains of PGs, CS is composed of repeating disaccharides consisting of D-glucuronic acid (GlcA) and *N*-acetylgalactosamine (GalNAc) with different sulfation patterns, once the GlcA residues are isomerized to L-iduronic acid (IdoA) residues CS is converted to DS, also called CS-B, and CS and DS domains are usually detected in one chain as co-hybrid structure CS/DS (Sugahara et al., 2003; **Figure 1**). The sulfated modification of CS/DS chains at C-4 and/or C-6 of GalNAc or/and C-2 of GlcUA/IdoUA by various specific sulfotransferases generates significant structural diversity (Kusche-Gullberg and Kjellen, 2003; **Figure 1**). Monosulfated disaccharide GlcAβ1-3GalNAc(4S) (A unit) and GlcA β1-3GalNAc(6S) (C unit), of which 4S and 6S stand for 4-*O*-sulfate and 6-*O*-sulfate, respectively, are the most common components found in CS from terrestrial animals (Mathews, 1958; **Table 1**). Additionally, some highly sulfated disaccharides, such as GlcA(2S)β1-3GalNAc(6S) (D unit), of which 2S stands for 2-*O*-sulfate, and GlcAβ1-3GalNAc(4S, 6S) (E unit), have been found in CS/DS from mammals,

in which they account a relatively low proportion but play very important roles in various functions of CS/DS chains (Nandini and Sugahara, 2006; **Table 1**). In contrast, DS from mammals is mainly composed of the iA unit (IdoAα1-3GalNAc(4S)) with a small amount of the iB unit (IdoA(2S)α1-3GalNAc(4S)) (Bao et al., 2005; Nandini and Sugahara, 2006). Interestingly, some CS/DS chains from marine animals contain a high proportion of rare highly sulfated disaccharides, such as the D unit in CS from shark fin and the E unit in CS from squid cartilage (Mizumoto et al., 2013a; Ueoka et al., 2000; **Table 1**). Traditionally, CS/DS is named based the main common disaccharide unit or enriched rare disaccharide unit, such as CS-A from mammalian cartilage and sturgeon notochord containing A unit as main disaccharide, CS-C from shark cartilage containing C unit as main disaccharide, CS-D from shark fin containing rare D unit, and CS-E from squid cartilage containing rare E unit. CS/DS chains are widely present in connective tissues of vertebrates and invertebrates, and the polymerization degree and sulfation pattern of CS/DS polysaccharide chains determine the physicochemical properties and physiological and pharmacological activities of CS/DS and CS/DSPGs. The structure complexity of CS/DS leads to its functional diversity. More and more studies have shown that CS/DS is involved in cell division and differentiation (Sugahara et al., 2003; Mizuguchi et al., 2003; Bülow and Hobert, 2006; Izumikawa et al., 2010; Schwartz and Domowicz, 2018; Shida et al., 2019), cell adhesion (Sugahara et al., 2003; Handel et al., 2005; Bülow and Hobert, 2006; Sugahara and Mikami, 2007), morphogenesis (Klüppel et al., 2005; Hayes et al., 2018), inflammation (Li et al., 2020; Campo et al., 2009) and viral infection (Hsiao et al., 1999; Bergefall et al., 2005; Kim et al., 2017). CS/DS chains carry out these functions through interacting with target proteins such as various growth factors fibroblast growth factor (FGF), hepatocyte growth factor (HGF) and pleiotrophin (PTN) (Nandi et al., 2006; Taylor and Gallo, 2006) and cytokines (Hwang et al., 2003; Mizuguchi et al., 2003; Izumikawa et al., 2004; Mizumoto and Sugahara, 2013).

CS/DS BIOSYNTHESIS

The biosynthesis of CS/DS is a complex, multistep and enzymatically accommodated process that occurs in endoplasmic reticulum/Golgi compartments and is initiated by the synthesis of GAG-protein linkage region covalently linked to specific serine residues embedded in different core proteins (Sugahara and Kitagawa, 2000; Silbert and Sugumaran, 2002; Sugahara et al., 2003). The linkage region is a specific tetrasaccharide structure GlcAβ1-3Galβ1-3Galβ1-4Xylβ1, in which Gal and Xyl represent galactose and xylose residues, respectively (**Figure 1**). This structure is catalyzed by the corresponding glycosyltransferase in the tetrasaccharide sequence. Firstly, a Xyl residue is connected to a specific Ser residue of core protein through the catalyzation of xylosyltransferase (Götting et al., 2000, 2007); then, β1,4-galactosyltransferase I (Almeida et al., 1999; Okajima et al., 1999) and β1,3-galactosyltransferase II (Bai et al., 2001) catalyze the connection of two Gal residues in turn; and, finally, β1,3-glucuronyltransferase I (Kitagawa et al., 1998; Bai et al., 1999, 2001) catalyzes the addition of GlcUA residue to form the tetrasaccharide linkage region.

Once the synthesis of the linkage tetrasaccharide is completed, the extension of CS/DS chain will be triggered by the transfer of a GalNAc residue to the nonreducing terminal GlcA residue of the tetrasaccharide linkage region by GalNAc transferase I, and then GlcA and GalNAc residues will be added in turn to form the chondroitin (Chn) skeleton composed of repeating disaccharide GlcA-GlaNAc through alternating catalysis of GalNAc transferase II and GlcA transferase II (Sugahara and Kitagawa, 2000; Silbert and Sugumaran, 2002; Sugahara et al., 2003). During the process of polymerization, some GlcA residues in the Chn skeleton can be transformed into IdoA under the control of two GlcA C-5 epimerases, thereby transforming the corresponding Chn domains into its stereoisomer dermatan domains (Maccarana et al., 2006; Pacheco et al., 2009). Furthermore, some hydroxyl groups of GalNAc or GlcA/IdoA residues in the chains can be site-specifically modified by a variety of sulfotransferases by using 3'-phosphoadenosine 5'-phosphosulfate as a donor substrate (Habuchi, 2000). Under the control of chondroitin 4-*O*-sulfotransferase-1, 2 and 3 (Yamauchi et al., 2000; Hiraoka et al., 2000; Kang et al., 2002), and dermatan 4-*O*-sulfotransferase (Evers et al., 2001; Mikami et al., 2003) the sulfate group is transferred to the hydroxyl group at the C-4 location of GlcA to generate an A unit and an iA unit, respectively. The 6-*O*-sulfation of the C unit is catalyzed by chondroitin 6-*O*-sulfotransferase-1 (Fukuta et al., 1998). The GalNAc 4-sulfate 6-*O*-sulfotransferase transfers sulfate to the C-6 position of the A/iA unit to generate an E/iE unit (Ohtake et al., 2001), and uronyl 2-*O*-sulfotransferase sulfates GlcA in the C-2 position of the C/iA unit to generate a D/iB unit (Kobayashi et al., 1999). The space-time-dependent expression and combined action of these enzymes make the structure of CS/DS chains extremely diverse and complex, which presents significant challenges for the structural and functional studies of CS/DS.

CS/DS-DEGRADING ENZYMES

As a reverse process of CS/DS synthesis, the degradation of CS/DS chains in the organisms also involves various enzymes including glycosidic bond-cleaving enzymes and sulfatases, which correspond to glycosyltransferases and sulfotransferases, respectively. Thus, the CS/DS-degrading enzymes are indispensable tools for analyzing the structure and function of CS/DS chains. Based on the enzymatic mechanism, CS/DS glycosidic bond-cleaving enzymes are accordingly classified as either hydrolases or lyases. According to their similarities of amino acid sequences, hydrolases and lyases are assigned to glycoside hydrolase (GH) families and polysaccharide lyase (PL) families, respectively (Henrissat, 1991). CS/DS hydrolases and lyases are usually found in animals and microorganisms, respectively. CS/DS sulfatases belong to the formylglycine-dependent family that specifically hydrolyzes sulfate esters on poly- and oligosaccharides of CS/DS. These CS/DS-degrading enzymes play key roles in the catabolic metabolism of CS/DS polysaccharides and are widely found in animals and microorganisms.

Hydrolases

In animals, CS/DS glycosidic bond-cleaving enzymes are hydrolases that cleave the β-1,4-glycosidic bond between GalNAc and GlcA residues in CS chains via a hydrolysis mechanism to produce saturated oligosaccharide products (Kreil, 1995). In mammals, the so-called hyaluronidases (EC 3.2.1.35) have been reported to be the only hydrolases that cleave CS chains, and even some hyaluronidases do not degrade hyaluronan (HA) but only degrade CS (Kaneiwa et al., 2010). In fact, most animal-derived hyaluronidases and microorganism-derived CS/DS lyases, which we will introduce later, show both HA- and Chn/CS-degrading activities, which may be due to the very similar structural features of the two GAG polysaccharides. Both HA and CS chains have same types of β-glycosidic bonds in

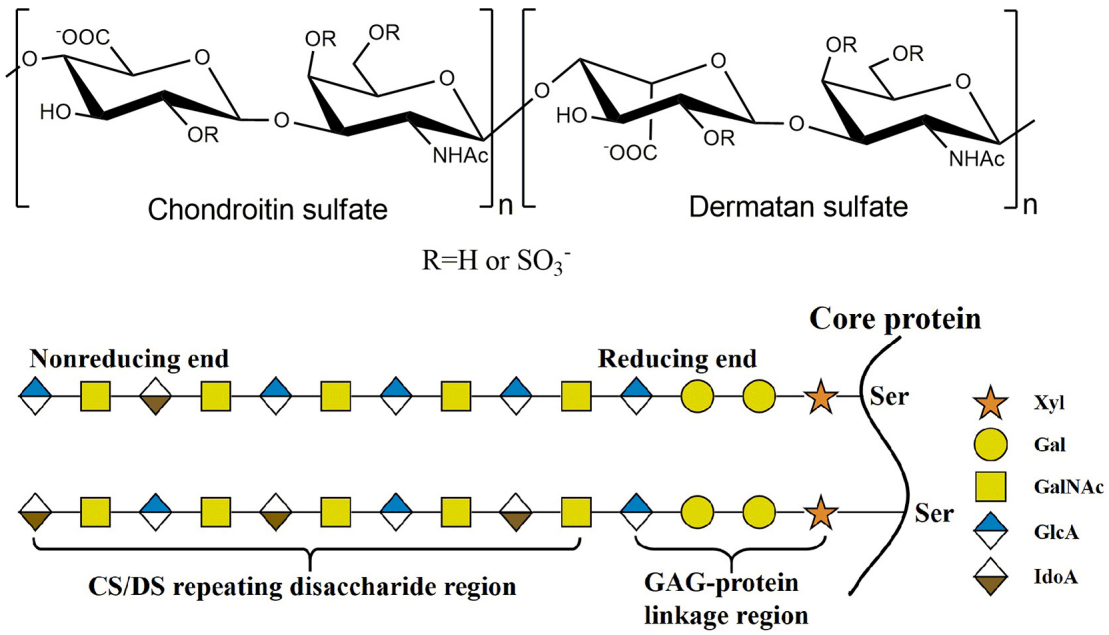

FIGURE 1 | The structure of CS/DS. The CS/DS chain consisting of D-glucuronic acid (GlcA) or L-iduronic (IdoA) acid glycosidically linked to *N*-acetylgalacyosamine (GalNAc) [(-4GlcAβ1-3GalNAcβ1-) or (-4IdoAα1-3GalNAcβ1-). CS/DS chains are covalently attached to the core protein by GAG-protein linkage region tetrasaccharide.

TABLE 1 | The CS/DS disaccharide and unsaturated disaccharide produced by CS/DS lyase.

CS units		DS units		Unsaturated units	
Unit	**Sequence**	**Unit**	**Sequence**	**Unit**	**Sequence**
O unit	GlcAβ1-3GalNAc	**iO unit**	IdoAα1-3GalNAc	**ΔO unit**	ΔHexA-GalNAc
A unit	GlcAβ1-3GalNAc(4S)	**iA unit**	IdoAα1-3GalNAc(4S)	**ΔA unit**	ΔHexA-GalNAc(4S)
B unit	GlcA(2S)β1-3GalNAc(4S)	**iB unit**	IdoA(2S)α1-3GalNAc(4S)	**ΔB unit**	ΔHexA(2S)-GalNAc(4S)
C unit	GlcAβ1-3GalNAc(6S)	**iC unit**	IdoAα1-3GalNAc(6S)	**ΔC unit**	ΔHexA-GalNAc(6S)
D unit	GlcA(2S)β1-3GalNAc(6S)	**iD unit**	IdoA(2S)α1-3GalNAc(6S)	**ΔD unit**	ΔHexA(2S)-GalNAc(6S)
E unit	GlcAβ1-3GalNAc(4S,6S)	**iE(H) unit**	IdoAα1-3GalNAc(4S,6S)	**ΔE unit**	ΔHexA-GalNAc(4S,6S)
F unit	GlcAβ1-3GalNAc(4S) | Fuc(α1-3)	**iK unit**	IdoA(3S)α1-3GalNAc(4S)	**ΔF unit**	ΔHexA-GalNAc(4S) | Fuc(α1-3)
G unit	GlcAβ1-3GalNAc(4S) | Glc(β1-6)	**iL unit**	IdoA(3S)α1-3GalNAc(6S)	**ΔG unit**	ΔHexA-GalNAc(4S) | Glc(β1-6)
K unit	GlcA(3S)β1-3GalNAc(4S)	**iT unit**	IdoA(2S)α1-3GalNAc(4S,6S)	**ΔK unit***	ΔHexA(3S)-GalNAc(4S)
L unit	GlcA(3S)β1-3GalNAc(6S)	**iU unit**	IdoA(2S)α1-3GalNAc	**ΔL unit***	ΔHexA(3S)-GalNAc(6S)
M unit	GlcA(3S)β1-3GalNAc(4S,6S)			**ΔM unit***	ΔHexA(3S)-GalNAc(4S,6S)
T unit	GlcA(2S)β1-3GalNAc(4S,6S)			**ΔT unit**	ΔHexA(2S)-GalNAc(4S,6S)
U unit	GlcA(2S)β1-3GalNAc			**ΔU unit**	ΔHexA(2S)-GalNAc

**The disaccharides containing ΔHexA (3S) are unstable and result in sulfated GalNAc.*

and between repeating disaccharide units consisting of GlcA and hexosamine residues, and the only difference in structure between them is that the acetylated hexosamine GlcNAc in HA is replaced by the GalNAc in the Chn skeleton of CS. In addition, like other glycoside hydrolases, hyaluronidases exhibit certain transglycosidase activities (Hoffman et al., 1956), which can be used for synthesizing of HA (Kobayashi et al., 2003), Chn (Kobayashi et al., 2003), CS (Fujikawa et al., 2005), their derivatives (Ochiai et al., 2007b; Kobayashi et al., 2003), and hybrids of HA-Chn and HA-CS (Ochiai et al., 2007a).

In human genome, six highly homologous genes have been found to encode hyaluronidase-like sequences including five functional hyaluronidases genes (*HYAL1, HYAL2, HYAL3, HYAL4 and SPAM1*) and a pseudogene *HYALP1*(also called *HYAL6P*) that is transcribed in humans but is not translated (Csoka et al., 2001; Stern and Jedrzejas, 2006). *HYAL1, HYAL2,* and *HYAL3* are clustered in the chromosome 3p21.3 locus, whereas the *HYAL4*, *SPAM1*(encodes PH-20) and *HYALP1* genes are found on chromosome 7q31.3 (Csoka et al., 2001; Stern, 2003). Based on the optimal pH, most of these hyaluronidases show their highest activity at an acidic pH (Lokeshwar et al., 2001; Sabeur et al., 1997). As mentioned above, these so-called hyaluronidases from humans also show a certain degree of CS-degrading activity. The sperm-specific enzyme PH-20 shows much higher activity against Chn than CSA and HA at pH 4.5, whereas prefers HA and CS to Chn at pH 4.0 (Honda et al., 2012). In contrast, plasma hyaluronidase HYAL1 prefers to degrade CS-A than HA at pH 4.5 but prefers HA than CS-A at pH 3.5 (Csoka et al., 2001; Honda et al., 2012; Yamada, 2015). Furthermore, C units in CS-C negatively affect the hyaluronidase activity of PH-20. More interestingly, HYAL4 has been shown to be a specific CS-degrading enzyme without any activity toward HA, which means that the name of hyaluronidase is a misnomer for this enzyme (Csoka et al., 2001; Stern, 2003; Jedrzejas and Stern, 2005; Kaneiwa et al., 2010). The HYAL1 and PH-20 with CS-degrading activity cannot cleave the galactosaminidic linkages in -GalNAc-IdoA- and -GalNAc-GlcA(2S)- sequences, which are often found in DS chains and in highly sulfated D unit-containing domains of CS chains, respectively. In contrast, HYAL4 could strongly cleave the galactosaminidic linkages in -GlcA(2S)-GalNAc(6S)-GlcA-GalNAc(4S or 6S)- (Kaneiwa et al., 2010), suggesting that HYAL4 plays an important role in the degradation of CS in mammal. However, the degradation mechanism of DS chains in animals remains to be further investigated. Enzymes HYAL1 and HYAL2 are the main HA-degrading enzymes in somatic tissues. HYAL1 is a lysosomal enzyme and by contrast HYAL2 binds to plasma membrane via a glycosylphosphatidylinositol anchor (Afify et al., 1993; Rai et al., 2001). The traditional HA degradation model is that high molecular weight HA is digested into low molecular weight HA oligosaccharides by extracellular HYAL2, then, the HA oligosaccharides are internalized by interaction with cell surface receptors, and the internalized HA oligosaccharides are further decomposed by lysosomal HYAL1, exoglycosidases β-glucuronidase and β-hexosaminidase (Hex) (Stern, 2003; Stern, 2004; **Figure 2** and **Table 2**). As a dimeric enzyme, human Hex exists in two main isoforms HexA (αβ) and HexB (ββ), of which the α- and β-subunits are encoded by *HexA* and *HexB* genes, respectively (Chiricozzi et al., 2014). Interestingly, HexA can hydrolyze HA and CS chains from their non-reducing ends but HexB cannot (Thompson et al., 1973; Bearpark and Stirling, 1978). Like HA, CS can be internalized by interaction with cell surface receptors and degraded in the lysosome (Wood et al., 1973). Indeed, mice lost both HYAL1 and Hex activity show the accumulation of HA and CS (Gushulak et al., 2012).

Lyases

Unlike the hyaluronidases from animals, CS/DS-lyases from microorganisms cleave the β-1,4-glycosidic linkage between hexosamine and hexuronic acid residues in HA or CS/DS chains through an elimination reaction to yield an unsaturated double bond between C-4 and C-5 on the uronic acid residue $\Delta^{4,5}$hexuronate (ΔHexA) at the nonreducing end of the resulting oligosaccharide products. Conventionally, CD/DS lyases are named as chondroitinases (CSases), although some of them cannot digest CS, such as CSase B, which shows specific activity towards DS only. Moreover, CS/DS lyases can be classified into endolytic and exolytic types according to their substrate-degrading patterns, in which endolyases cleave CS/DS chains initially into larger oligosaccharides and finally to small disaccharides with a random cleavage pattern, whereas exolyases successively release disaccharides from the end of the sugar chains and do not produce any larger oligosaccharides in the process. The unsaturated double bond of oligosaccharides produced by lyases shows specific absorption of ultraviolet light at 232 nm, which is beneficial for the detection of CS/DS oligosaccharide products. In addition, CS/DS lyases have many advantages such as more diversity, better stability and activity and simpler preparation compared with hydrolases. Due to the outstanding features above, lyase has a wide range of applications in the preparation of oligosaccharides (Li et al., 2007; Mizumoto et al., 2013a), treatment of nerve damage (Janzadeh et al., 2017; Mondello et al., 2015; Sarveazad et al., 2017), and other CS structure-activity relationship studies.

Commercialized CS/DS Lyases

Based on their substrate specificity, CS/DS lyases are subdivided into three types CSase ABC, AC and B. The CSase ABC can digest CS, DS and HA, irrespective of their sulfation/C-5-epimerization pattern. Currently, the CSase ABC from *Proteus vulgaris* is widely used for GAG structure analysis. The commercially available CSase ABC comprises a mixture of the CSase ABC I (EC 4.2.2.20) with endolytic activity and the CSase ABC II (EC 4.2.2.21) with exolytic activity (Yamagata et al., 1968; Hamai et al., 1997). The CSase AC (EC 4.2.2.5) is highly sensitive to the 5-epimerization of GlcA residues in GAG chains and can act only on CS, HA and CS domains in CS-DS hybrid chains (Yamagata et al., 1968; Hiyama and Okada, 1975; Linhardt et al., 2006), whereas, the CSase B (EC 4.2.2.19) is specifically cleaves DS and DS domains in CS-DS hybrid chains (Yamagata et al., 1968; Gu et al., 1995). The CSase AC I from *Flavobacterium heparinum* and CSase AC II from *Arthrobacter aurescens* are well-known CS/DS lyases showing endolytic and exolytic activities, respectively (Yamagata et al., 1968; Hiyama and Okada, 1975). The CSase B from *Flavobacterium heparinum* is the only commercialized lyase with specific endolytic activity to DS (Yamagata et al., 1968). Notably, the CSase ABC and CSase AC belong to the polysaccharide

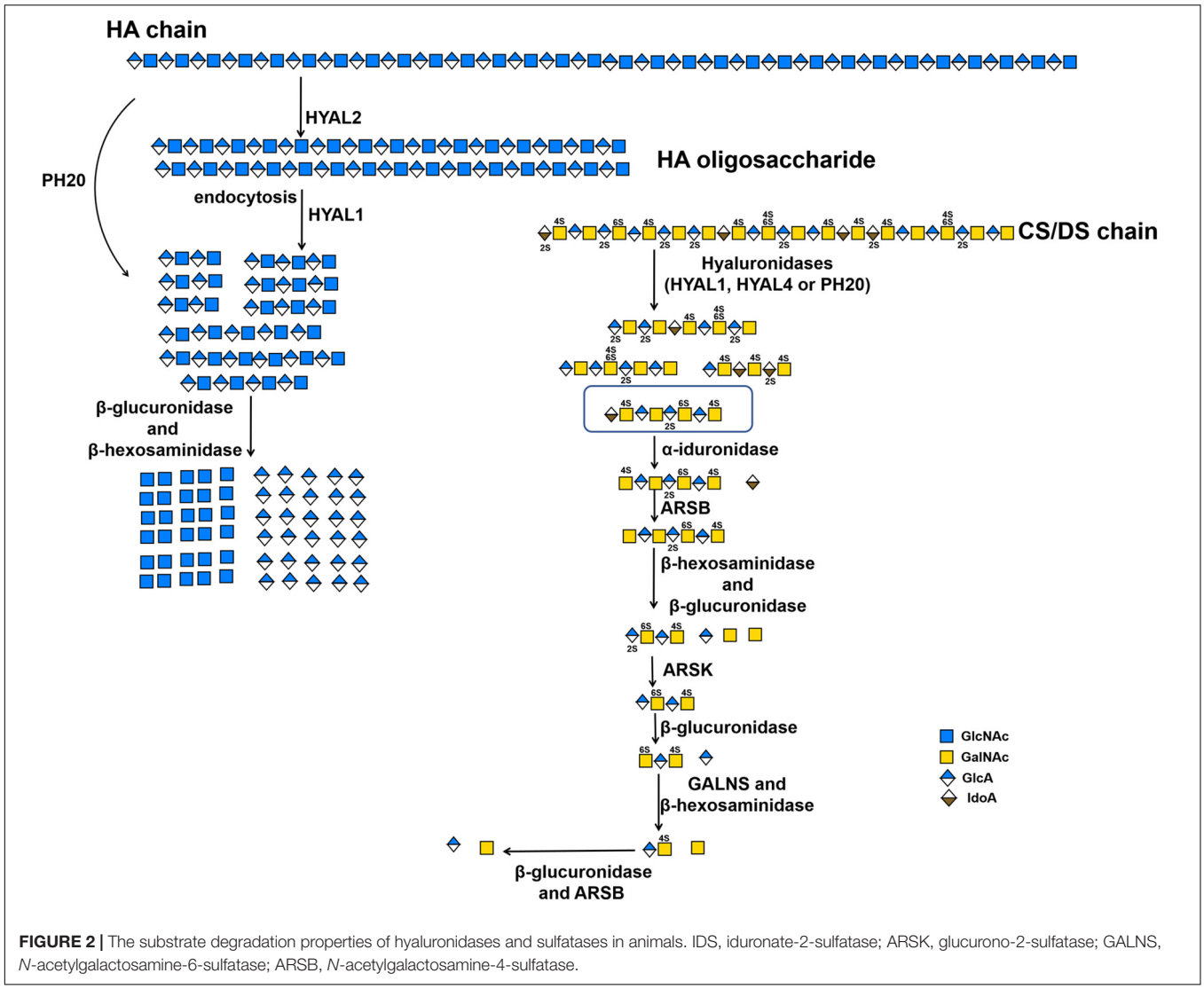

FIGURE 2 | The substrate degradation properties of hyaluronidases and sulfatases in animals. IDS, iduronate-2-sulfatase; ARSK, glucurono-2-sulfatase; GALNS, *N*-acetylgalactosamine-6-sulfatase; ARSB, *N*-acetylgalactosamine-4-sulfatase.

lyase (PL) family 8, but the CSase B belongs to PL family 6, which comprises alginate lyases (www.cazy.org) (**Figure 3** and **Table 2**). Structural heterogeneity has hampered structure-function relationship studies of CS/DS chains. However, there are only a few CS/DS lyases that have been characterized in detail and commercially available, which is far from meeting the needs of CS/DS-related researches and applications.

Newly Identified CS/DS Lyases

Most recently, some unique CS/DS lyases have been identified in various microorganisms (**Table 2**). Most of them are CS and HA lyases. Hyaluronidase-B from *Bacillus* sp. A50 and the hyaluronate lyase BniHL from the deep-sea bacterium *Bacillus niacin* show endolytic activity towards CS and HA at an approximately neutral pH (Guo et al., 2014; Kurata et al., 2015). A Chn lyase ChoA1 from *Arthrobacter* sp. MAT3885 can degrade Chn, CS and HA (Kale et al., 2015). Namburi et al. found a CSase AC from *Helicobacter bizzozeronii* in canine stomach, and this enzyme exhibited specific endolytic activity on HA and various CSs with different sulfation patterns at an optimum low pH between pH 4.0 and pH 5.5 and might represent one of several factors involved in the development of gastritis in dogs (Namburi et al., 2016). The CSase AsChnAC identified from *Arthrobacter* sp. SD-04 displays exolytic activity toward HA and various CSs too (Chen et al., 2019). Sugiura et al. identified two highly homologous occlusion-derived variants of virus envelope protein 66s from *Autographa californica* nucleopolyhedrovirus and *Bombyx mori* nucleopolyhedrovirus, and both of the variants showed specific lyase activity towards non-sulfated and 6-*O*-sulfated CS (Sugiura et al., 2011; Sugiura et al., 2013). BtCDH from the human gut microbe *Bacteroides thetaiotaomicron* belongs to a new PL family (PL29) and shows optimum endolytic activity toward HA and CS, particularly large chains longer than decasaccharide, at a very high temperature of 60 °C (Ndeh et al., 2018). Two novel CS/DS lyases have been found from *Acinetobacter* sp. C26 and *Sphingomonas paucimobilis*, respectively, both of which have lower molecular weights but similar broad-spectrum activities against CS, DS and HA compared with CSase ABC (Zhu et al., 2017; Fu et al., 2018). However, most of these studies have mainly focused on

TABLE 2 | CS/DS-degrading enzymes from bacteria.

Name	Substrate	Source	Degradation mechanism	Action pattern	EC number (Filmay)	References
CSase ABC I	HA, CS or DS	*Proteus vulgaris*	lysis	endo	EC 4.2.2.20 (PL8)	Yamagata et al., 1968; Hamai et al., 1997
CSase ABC II	HA, CS or DS	*Proteus vulgaris*	lysis	exo (from nonreducing end)	EC 4.2.2.20 (PL8)	Yamagata et al., 1968; Hamai et al., 1997
CSase AC I	HA or CS	*Flavobacterium heparinum*	lysis	endo	EC 4.2.2.5 (PL8)	Yamagata et al., 1968; Gu et al., 1995
CSase AC II	HA or CS	*Arthrobacter aurescens*	lysis	exo (from reducing end)	EC 4.2.2.5 (PL8)	Lunin et al., 2004; Yin et al., 2016
CSase AC-III	HA or CS	*Flavobacterium* sp. Hpl02	lysis	endo	EC 4.2.2.5 (PL8)	Miyazono et al., 1990
CSase C	HA or CSC	*Flavobacterium heparinum.*	lysis	endo	EC 4.2.2.-(PL8)	Michelacci and Dietrich, 1976
CSase B	DS	*Flavobacterium heparinum*	lysis	endo	EC 4.2.2.19 (PL6)	Yamagata et al., 1968; Gu et al., 1995
CSase B II	DS	*Flavobacterium* sp. Hpl02	lysis	endo	EC 4.2.2.19 (PL6)	Miyazono et al., 1990
Hyaluronidase-B	HA or CS	*Bacillus* sp. A50	lysis	endo	EC 4.2.2.- (PL8)	Guo et al., 2014
AcODV-E66	HA or CS	*Autographa californica* nucleopolyhedrovirus	lysis	endo	EC 4.2.2.- (PL8)	Sugiura et al., 2011
BmODV-E66	HA or CS	*Bombyx mori nucleopolyhedrovirus*	lysis	endo	EC 4.2.2.- (PL8)	Sugiura et al., 2013
HCLase	HA or CS	*Vibrio* sp. FC509	lysis	endo	EC 4.2.2.- (PL8)	Han et al., 2014
HCDLase	HA, CS or DS	*Vibrio* sp. FC509	lysis	exo (from reducing end)	EC 4.2.2.- (PL8)	Wang et al., 2017
HCLase Er	HA or CS	*Vibrio* sp. FC509	lysis	endo	EC 4.2.2.- (PL8)	(Peng et al., 2018)
BniHL	HA or CS	*Bacillus niacin*	lysis	endo	EC 4.2.2.- (PL8)	Kurata et al., 2015
ChoA1	HA or CS	*Arthrobacter* sp. MAT3885	lysis	endo	EC 4.2.2.- (PL8)	Kale et al., 2015
BtCDH	HA or CS	*Bacteroides thetaiotaomicron*	lysis	endo	EC 4.2.2.-(PL8)	Ndeh et al., 2018
BHCSase AC	HA or CS	*Helicobacter bizzozeronii*	lysis	endo	EC 4.2.2.-(PL8)	Namburi et al., 2016
AsChnAC	HA or CS	*Arthrobacter* sp. SD-04	lysis	exo (undetermined)	EC 4.2.2.- (PL8)	Chen et al., 2019
HYAL	HA	*Streptomyces hyalurolyticus*	lysis	endo	EC 4.2.2.1 (PL8)	Ohya and Kaneko, 1970
HYAL	HA	*Streptococcus dysgalactiae*	lysis	endo	EC 4.2.2.1 (PL8)	Sting et al., 1990
4-*O*-endosulfatase	4-*O*-sulfate on GalNAc of CS and DS	*Vibrio* sp. FC509	sulfatase	endo (from reducing end)	EC 3.1.6.- (S1_27)	Wang et al., 2015; Wang et al., 2019b
BT_3349	4-*O*-sulfate on GalNAc of CS and DS	*Bacteroides thetaiotaomicron*	sulfatase	endo	EC 3.1.6.- (S1_27)	Ulmer et al., 2014
BT_3333	6-*O*-sulfate on GalNAc	*Bacteroides thetaiotaomicron*	sulfatase	exo (nonreducing end)	EC 3.1.6.- (S1_15)	Ulmer et al., 2014
BT_1596	2-*O*-sulfate on ΔHexA of HS/CS degradation products	*Bacteroides thetaiotaomicron*	sulfatase	exo (nonreducing end)	EC 3.1.6.- (S1_9)	Ulmer et al., 2014
chondro-4-sulfatase	4-*O*-sulfate on GalNAc of CS	*Proteus vulgaris*	sulfatase	exo (reducing end)	EC 3.1.6.9 (S1_27)	Yamagata et al., 1968; Sugahara and Kojima, 1996
chondro-6-sulfatase	6-*O*-sulfate on GalNAc of CS	*Proteus vulgaris*	sulfatase	exo (reducing end)	EC 3.1.6.10 (S1_15)	Yamagata et al., 1968; Sugahara and Kojima, 1996
delta-hexuronate-2-sulfatase	2-*O*-sulfate on ΔHexA of HS/CS degradation products	*Flavobacterium heparinum*	sulfatase	exo (nonreducing end)	EC 3.1.6.- (S1_9)	Sugahara and Kojima, 1996; Myette et al., 2003
PB2SF	2-*O*-sulfate on ΔHexA of HS/CS degradation products	*Photobacterium* sp. FC615	sulfatase	exo (reducing end)	EC 3.1.6.- (S1_2)	Wang et al., 2019a
exoPB4SF	4-*O*-sulfate on CS/DS GalNAc	*Photobacterium* sp. FC615	sulfatase	exo (reducing end)	EC 3.1.6.12 (S1_27)	Wang et al., 2019b

PL: Polysaccharide lyase family; S: Sulfatase famlily.

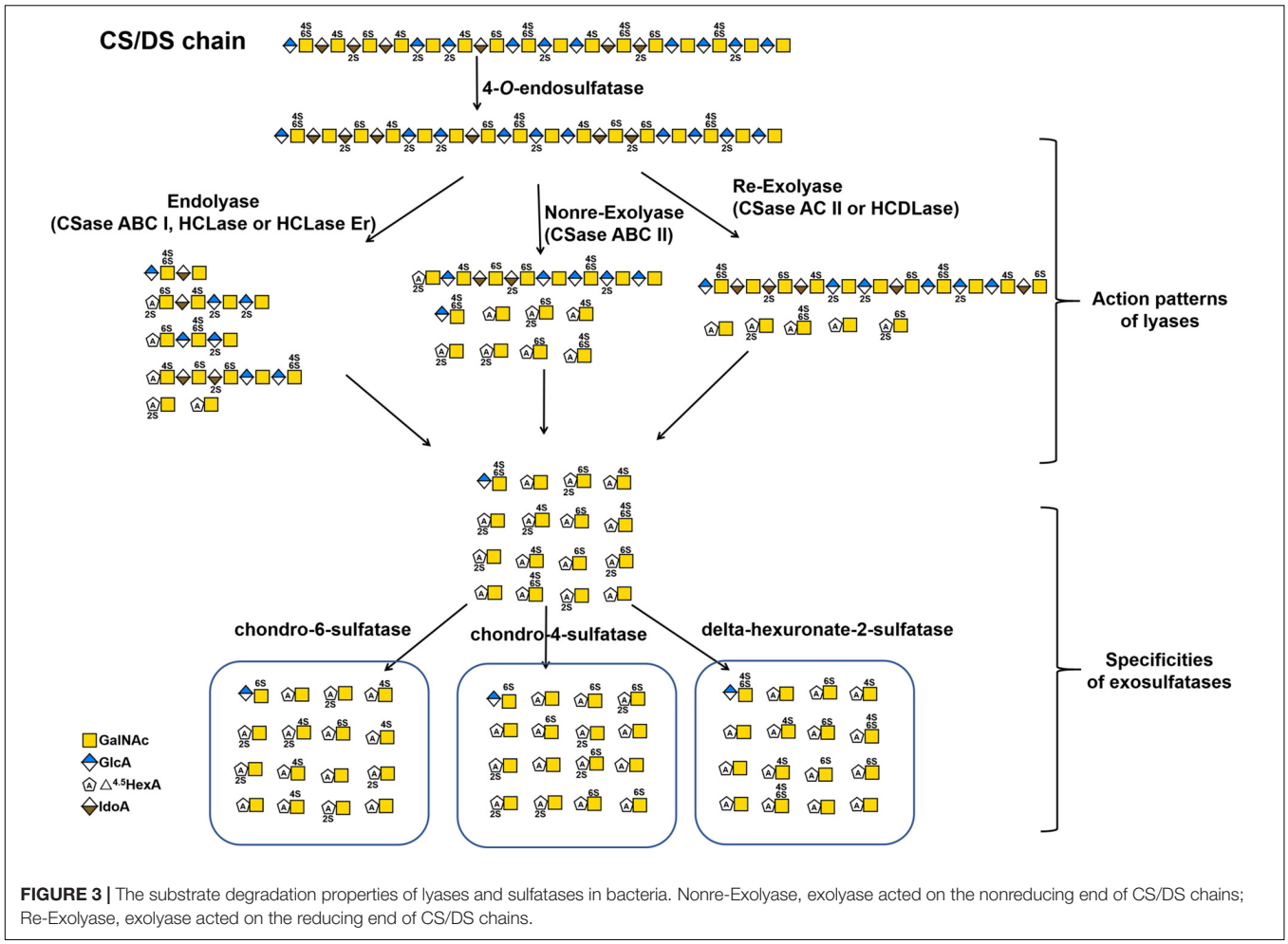

FIGURE 3 | The substrate degradation properties of lyases and sulfatases in bacteria. Nonre-Exolyase, exolyase acted on the nonreducing end of CS/DS chains; Re-Exolyase, exolyase acted on the reducing end of CS/DS chains.

the basic enzymatic properties and rough substrate specificity of these novel CS/DS lyases, and there is a lack of in-depth studies on their substrate-degrading mode and catalytic mechanism of these enzymes.

Marine animals are enriched in CS/DS with unique structures, which indicates that there must be a large number of microorganisms owning corresponding enzymes that would allow them to degrade and utilize these unique CS/DS forms in the ocean. Consistent with our speculation, marine bacteria-derived CS/DS-degrading enzymes show various unique characteristics. HCLase is the first marine-derived CS/DS lyase identified from the bacterium *Vibrio* sp., which is isolated from sea mud. This enzyme has high endolytic activity towards HA and CS with various sulfation patterns at an approximately neutral pH and exhibits excellent biochemical characteristics, such as halophilicity, pH stability and thermal stability. Although HCLase can digest the β-1,4-glycosidic bond between GalNAc and most disaccharide units, it is unable to act on the galactosaminidic linkage between GalNAc and the D unit, suggesting that the 2-*O*-sulfation of GlcA inhibits the action of HCLase, which is similar to the case of CSase AC I (Han et al., 2014). In contrast, HCLase Er from the same strain is the first identified CS lyase that is specifically inhibited by both 4-*O*- and 6-*O*-sulfation of GalNAc, which is very useful for selectively preparing E unit–rich oligosaccharides from CS polysaccharides (Peng et al., 2018). HCDLase is a novel exo-type lyase from the same bacterial strain, which can degrade HA, CS and DS from their reducing end by sequentially releasing unsaturated disaccharides. In particular, it can effectively cleave CS oligosaccharides with reducing ends that are labeled with 2-aminobenzamide (2-AB) to release the 2-AB-labelled reducing-end disaccharides, which is a rare activity useful for the enzymatic sequencing of CS chain (Wang et al., 2017). Taken together, these studies suggest that the ocean is an untapped treasure trove of new CS/DS-degrading enzymes.

CS/DS Sulfatases

The sulfation patterns of CS/DS chains play a key role in various functions of CS/DS. Technically, sulfatases with specific activity that allow them to selectively remove sulfate groups from CS/DS chains should be another important tool for the structural and functional studies of CS/DS. Based on the positions of sulfate groups in CS/DS chains, there are several types of specific sulfatases in animals and bacteria, such as *N*-acetylgalactosamine-4-*O*-sulfatase (Yamagata et al., 1968; Sugahara and Kojima, 1996; Wang et al., 2019b; Baum et al., 1959) and *N*-acetylgalactosamine-6-*O*-sulfatase (Yamagata et al., 1968; Sugahara and Kojima, 1996; Lim and Horwitz, 1981; Singh et al.,

1976), which specifically hydrolyze sulfate groups on the C-4 and C-6 positions of GalNAc residues, respectively, and hexuronate-2-*O*-sulfatase, which specifically removes C-2 sulfate groups from saturated or unsaturated hexuronic acids derived from the digestion of CS/DS by GAG lyases (Sugahara and Kojima, 1996; Myette et al., 2003; Wang et al., 2019a; **Tables 2**, **3**). Based on the sequence similarities, the GAG sulfatases were recently classified in the database SulfAtlas (http://abims.sb-roscoff.fr/sulfatlas/) (Barbeyron et al., 2016). Animal CS/DS sulfatases are lysosomal enzymes responsible for the degradation of endogenous CS/DS, and genetic defects of these enzymes result in the formation of several mucopolysaccharidoses (MPS) in humans, such as MPS II, MPS IVA and MPS VI (Khan et al., 2017). The well-studied animal CS/DS sulfatases are *N*-acetylgalactosamine-4-*O* sulfatase (also named Arylsulfatase B, ARSB) (Baum et al., 1959; Wicker et al., 1991), *N*-acetylgalactosamine-6-*O*-sulfatase (GALNS) (Lim and Horwitz, 1981; Bielicki and Hopwood, 1991; Tomatsu et al., 1991), iduronate-2-*O*-sulfatase (IDS) (Lim et al., 1974; Shaklee et al., 1985; Wilson et al., 1990) and Glucurono-2-sulfatase (Arylsulfatase K, ARSK) (Dhamale et al., 2017), which specifically remove the 4-*O*-sulfate group from sulfated GalNAc residues of CS/DS, 6-*O*-sulfate group from sulfated GalNAc residues of CS/DS and sulfated galactose of keratan sulfate, 2-*O*-sulfate groups of sulfate IdoA residues of DS and heparin (Hep), and 2-*O*-sulfate groups of GlcA residues of heparan sulfate (HS), respectively (Parenti et al., 1997; **Tables 2**, **3**). All these animal CS/DS sulfatases belong to exosulfatases.

In contrast, bacterial CS/DS sulfatases are essential for the biodegradation and utilization of CS/DS from animals, and a large number of potential sulfatase genes have been found in the genomes of various bacteria. However, only a few CS/DS sulfatases have been studied in detail. Three $\Delta^{4,5}$HexA-2-*O*-sulfatases have been identified from *Flavobacterium heparinum*, *Bacteroides thetaiotaomicron* and *Photobacterium* sp. FC615, that can specifically remove 2-*O*-sulfate ester from a ΔHexA residue located at the nonreducing terminus of an unsaturated oligosaccharide (Sugahara and Kojima, 1996; Myette et al., 2003; Ulmer et al., 2014; Wang et al., 2019a). Two *N*-acetylgalactosamine-4-*O*-sulfatases from *Proteus vulgaris* and *Photobacterium* sp. FC615 specifically hydrolyze 4-*O*-sulfate groups on GalNAc residues at the reducing ends of CS/DS chains (Sugahara and Kojima, 1996; Wang et al., 2019b). An *N*-acetylgalactosamine-6-*O*-sulfatase from *Proteus vulgaris* has been shown to specifically act on 6-*O*-sulfates on GalNAc residues at the reducing termini of CS/DS oligosaccharides (Sugahara and Kojima, 1996), and another *N*-acetylgalactosamine-6-*O*-sulfatase from *Bacteroides thetaiotaomicron* can only attack the 6-*O*-sulfate group on monosaccharide GalNAc residues (Ulmer et al., 2014). Notably, most of the identified CS/DS sulfatases are exo-type enzymes, which only remove sulfate esters from the ends of CS/DS poly-/oligosaccharides and thus have very limited applications to structural and functional studies of CS/DS. Recently, two endo-type *N*-acetylgalactosamine-4-*O*-sulfatases were identified from *Bacteroides thetaiotaomicron* (Ulmer et al., 2014) and *Vibrio* sp. FC509 (Wang et al., 2015), which can effectively remove 4-*O*-sulfate groups from GalNAc

TABLE 3 | CS/DS-degrading enzymes from animals.

Name	Substrate	Source	Degradation mechanism	Action pattern	EC number	References
HYAL1	HA or CS	*human*	hydrolysis	endo	EC 3.2.1.35 (GH56)	De Salegui and Pigman, 1967; Csoka et al., 1999
HYAL2	HA	*human*	hydrolysis	endo	EC 3.2.1.35 (GH56)	Rai et al., 2001; Csoka et al., 1999
HYAL3	HA	*human*	hydrolysis	endo	EC 3.2.1.35 (GH56)	Csoka et al., 1999
HYAL4	CS	*human*	hydrolysis	endo	EC 3.2.1.35 (GH56)	Csoka et al., 1999; Kaneiwa et al., 2010
PH-20	HA or CS	*human*	hydrolysis	endo	EC 3.2.1.35 (GH56)	Cherr et al., 2001
Hyaluronidase	HA	*bovine* testis	hydrolysis	endo	EC 3.2.1.35 (GH56)	Freeman et al., 1949
HYAL	HA	*bee venom*	hydrolysis	endo	EC 3.2.1.35 (GH56)	Gmach and Kreil, 1993
***N*-acetylgalactosamine-4-sulfatase (Arylsulfatase B, ARSB)**	4-*O*-sulfate on GalNAc of CS and DS	*human*	sulfatase	exo (reducing end)	EC 3.1.6.12 (S1_2)	Baum et al., 1959; Wicker et al., 1991
***N*-acetylgalactosamine-6-sulfatase (GALNS)**	6-*O*-sulfate on GalNAc of CS and keratan sulfate	*human*	sulfatase	exo (reducing end)	EC 3.1.6.4 (S1_5)	Lim and Horwitz, 1981; Bielicki and Hopwood, 1991; Tomatsu et al., 1991
Iduronate-2-sulfatase (IDS)	2-*O*-sulfate on IdoA of DS and Hep	*human*	sulfatase	exo (nonreducing end)	EC 3.1.6.13 (S1_7)	Lim et al., 1974; Shaklee et al., 1985; Wilson et al., 1990
Glucurono-2-sulfatase (Arylsulfatase K, ARSK)	2-*O*-sulfate on GlcA of HS	*human*	sulfatase	exo (nonreducing end)	EC 3.1.6.18 (S1_7)	Dhamale et al., 2017

GH: Glycoside hydrolase family, S: Sulfatase family.

residues within the CS/DS chains (**Table 2** and **Figures 2**, **3**). Compared with exosulfatases, endosulfatases should be more useful enzymatic tools for CS/DS studies but seem to be very rare in nature. Our recent study has shown that CS/DS sulfatases with similar specificities have common signature sequences and can cluster to form a single branch in the phylogenetic tree, although they descended from separate ancestral genes (Wang et al., 2019a). Based on this finding, a series of $\Delta^{4,5}$HexA-2-*O*-sulfatases have been successfully predicted and verified from sequences in GenBank (Wang et al., 2019a), and we believe that some CS/DS endosulfatases could also be found by using this method. In fact, the existence of endosulfatases facilitates the catabolic metabolism of CS/DS by bacteria, in which the degradation of CS/DS chains by lyases can be significantly promoted via pre-desulfation by endosulfatases (Wang et al., 2015).

APPLICATIONS IN CS/DS STRUCTURE-FUNCTION STUDIES

Their great structural heterogeneity endows CS/DS chains with various functions but also poses a great challenge to the structure-function studies of CS/DS. A growing body of research shows that CS/DS chains function through interacting with target proteins and that some oligosaccharide domains with specific structural features in CS/DS chains are involved in these interactions (Sugahara et al., 2003; Raman et al., 2005; Kastana et al., 2019; Pudelko et al., 2019). Thus, it is key for studying the structure and function of CS/DS to investigate the structural features in particular functional domains of the CS/DS chains involved in an interaction with a specific target protein. CS/DS-degrading enzymes with different specific activities play irreplaceable tools in such studies (Linhardt et al., 2006; Li et al., 2010; Wang et al., 2017).

Compositional Analysis of CS/DS

As a kind of highly heterogeneous polysaccharides, the exact structures of all the chains in CS/DS samples cannot be determined with current technology. Thus, the disaccharide composition is used as a basic parameter to characterize various CS/DS preparations used in basic studies and industrial production. Commercial CS/DS preparations are extracted from terrestrial and marine sources, such as the cartilages from bovine, porcine, chicken, shark and squid, and are wildly used in medicines and health products (Bao et al., 2005; Deepa et al., 2007a; Volpi, 2007, 2009; Valcarcel et al., 2017). However, the biological and pharmacological properties of these CS/DS preparations are seriously affected by the raw materials, manufacturing processes and many other factors impacting their production. Disaccharide analysis has been commonly used to evaluate the quality of CS/DS products. CS/DS lyases play a key role in disaccharide composition assays of CS/DS. In general, the disaccharide compositions of various forms of CS/DS with different sulfation patterns can be easily determined by digestion with the commercial CSase ABC followed by anion-exchange HPLC. However, digestion by CSase ABC causes the conversion of both GlcA and IdoA residues into unsaturated uronic acid and thus CS and DS in the test sample cannot be distinguished by this method. In this case, we can use the substrate specificity of the CSase AC and CSase B to investigate the disaccharide composition and proportions of CS and DS in samples.

For example, to determine the disaccharide composition of CS/DS extracted from shark liver, we used CSases that differed in their specificity (CSase ABC, mixture of CSase AC-I and CSase AC-II or CSase B) to digest the sample, and then the digests were labeled with 2-AB and analyzed by anion exchange HPLC on an amine-bound silica PA-03 column using a solvent system of 16 and 530 mM NaH_2PO_4 over a period of 1 h by fluorescent detection. Although the shark liver-derived CS/DS preparation contained highly heterogenous hybrid chains of CS-DS, the disaccharide composition and contents of CS and DS domains in the hybrid chains could be well determined by this method (Li et al., 2007). In summary, CSases with different substrate specificities play an important role in the disaccharide composition assays of CS/DS.

Preparation of Oligosaccharides With Specific Activity

The various biological functions of CS/DS are thought to be due to their functional domains, some oligosaccharide sequences with specific structural features. For a specific target protein, the functional domains of CS/DS chains are usually not a single specific structure but some oligosaccharide domains with similar characteristics, such as a minimum size requirement and the enrichment of specific oversulfated disaccharide units (Trowbridge and Gallo, 2002; Trowbridge et al., 2002; Sugahara et al., 2003; Sugahara and Mikami, 2007; Li et al., 2010). Therefore, isolation of the functional oligosaccharide domains from CS/DS chains is key to not only structure-function relationship studies of CS/DS but also the preparation of functional oligosaccharides with specific activities. Compared with the harsh conditions of chemical and physical methods, the enzymatic method is mild and biocompatible for degrading CS/DS to prepare the functional domains. In general, functional oligosaccharides with specific activity can be obtained through the partial digestion of CS/DS chains with specific enzymes followed by a series of chromatographic separations, especially affinity chromatography. Various CS/DS glycosidic bond-cleaving enzymes, including hyaluronidases and lyases, have been used to prepare CS/DS oligosaccharides. As mentioned above, the CS/DS oligosaccharides produced by lyases bear an unsaturated 4,5-bond between C-4 and C-5 of ΔHexA at their nonreducing ends, which can be easily detected at 232 nm. Moreover, CS/DS lyases show more flexibility in terms of substrate specificity. Thus, CS/DS lyases, including CSase ABC, AC I and B, have been widely used to partially digest various forms of CS/DS for preparing functional oligosaccharides that specifically bind to certain proteins (Fukui et al., 2002; Bao et al., 2005; Kim et al., 2017; Li et al., 2007). In contrast, glycan arrays have the advantages of low dosage, high sensitivity, high throughput, and rapid analysis, which is suitable for the large-scale

screening and investigation of potential biological functions of various glycans and their conjugates including CS/DS poly- and oligosaccharides (Fukui et al., 2002). By using this technique, E unit-rich polysaccharides and structure-defined tetrasaccharides have been shown to interact with TNF-α (Tully et al., 2006), bFGF (Miyachi et al., 2015), and midkine-derived and brain-derived neurotrophic factor (Gama et al., 2006) with high affinity. Moreover, this method was used to investigate the interaction between DS and its binding proteins (Yamaguchi et al., 2006). Thus, glycan arrays can be very a powerful tool for the identification of novel functions of CS/DS oligosaccharides with different structures derived from the digestion of CS/DS polysaccharides with various degrading enzymes.

The selective degradation of inactive domains is an ideal way to isolate functional oligosaccharides from CS/DS polysaccharides. Technically, this can be achieved by selecting enzymes with a certain substrate specificity. For example, in a previous study we found that shark skin/liver-derived CS/DS could strongly interact with PTN and HGF to promote neurite outgrowth and this activity could be abolished by treatment with the CSase B but not the CSase AC I. Based on this finding, a PTN- and HGF-binding hexasaccharide containing two iB units was eventually isolated from shark skin CS/DS through selective digestion with the CSase AC I followed by pleiotrophin affinity and anion exchange chromatographies (Li et al., 2007, 2010). In addition to the different selectivity of the CSase AC and B toward uronic acid epimers, some enzymes show high sensitivity to specific sulfation patterns of CS/DS chains, which is important for the preparation of oligosaccharides with specific structures, such as E unit-rich oligosaccharides, which play a key role in neuronal cell adhesion and outgrowth (Ueoka et al., 2000; Mikami et al., 2009; Nandini and Sugahara, 2006; Purushothaman et al., 2007), cancer cell metastasis (Li et al., 2008; Mizumoto et al., 2012, 2013b) and virus infections (Bergefall et al., 2005; Kato et al., 2010), and D unit-rich oligosaccharides, which significantly promote hippocampal neurite outgrowth through interacting with various growth factors and other proteins (Nandini and Sugahara, 2006; Clement et al., 1998; Shida et al., 2019). Testicular hyaluronidase can efficiently digest non-sulfated and low sulfated domains but not highly sulfated domains in CS chains, which makes it a good choice for the selective isolation of highly sulfated domains from CS/DS chains, such as the preparation of D unit-rich oligosaccharides from CS-D (Nadanaka and Sugahara, 1997) and E unit-rich oligosaccharides from CS-E (Kinoshita et al., 2001), respectively. Furthermore, our studies have shown that HCLase like CSase AC I cannot cleave the β–1,4–linkage between GalNAc and D unit (Han et al., 2014), and in contrast, HCLase Er cannot efficiently act on the β–1,4–linkage between E unit and GlcA (Peng et al., 2018), which makes these enzymes more specific tools for the selective isolation of D unit-rich domains and E unit-rich domains in CS/DS chains. **Figure 4** shows a schematic diagram of the preparation of various structurally determined hexasaccharides by CS/DS degradation of enzymes with specific activities. In addition, various CS/DS sulfatases combined with sulfotransferases can be potential tools to further edit the sulfation pattern of the obtained oligosaccharides for functional evaluation (Li et al., 2017; Shioiri et al., 2016; Wang et al., 2015; Wang et al., 2019b). Recently, Li et al. developed a method to synthesize CS oligosaccharides using multiple glycosyltransferases and sulfotransferases, and synthesized 15 homogeneous CS oligosaccharide by this method (Li et al., 2017). However, the de novo synthesis of CS/DS oligosaccharides is very cumbersome, heavy workload, time-consuming and costly. By contrast, it can be a relatively simple, efficient and low-cost choice to prepare basic oligosaccharide structures from CS/DS polysaccharides by treatment with various degrading enzymes and further modify these basic structures with specific synthetases to prepare structure-defined oligosaccharides (Cai et al., 2012; Zhang et al., 2019).

In brief, CS/DS-degrading enzymes, including hydrolases, lyases and sulfatases, are very useful tools for preparing functional oligosaccharides with specific structures from CS/DS polysaccharides. With the identification of an increasing number of enzymes with novel substrate specificity, the directional isolation and preparation of oligosaccharides with specific structures from various CS/DS forms will be achieved, which may represent a more feasible and low-cost way to prepare CS/DS oligosaccharides with specific bioactivity compared with synthetic methods.

Sequencing of CS/DS Oligosaccharides

Sequencing of the isolated functional oligosaccharides with special structures is essential for structure-function studies of CS/DS. Various methods, such as NMR and MS, have been used to determine the structures of CS/DS oligosaccharides. Ly et al. reported successful sequencing of bikunin CS chains with up to 43 saccharide units with FT-ICR-MS/MS (Ly et al., 2011). It is still difficult to distinguish different units with the same sulfation degree, such as monosulfated A and C units or disulfated D and E units. Meanwhile, the distinction of hexuronate epimers and the loss of sulfate groups during analysis are also major challenges. In addition, instrument requirements formethods using NMR and MS are more sophisticated, and NMR, in particular, requires a much greater amount of sample. Sugahara lab has developed a method to analyze and monitor CS/DS oligosaccharides with highly sensitively via the fluorescent labelling of reducing ends with 2-AB followed by anion exchange HPLC, and the detection limit for 2-AB-oligosaccharides is as low as 1 pmol (Kinoshita and Sugahara, 1999). However, further study showed that the 2-AB labelling completely inhibited the cleavage of the β-1,4- linkage in the tetrasaccharide at the reducing end of the CS/DS chain by CSase ABC (Kinoshita and Sugahara, 1999). Whereas, in most cases, some exolyases, such as CSase AC II and HCDLase, can effectively degrade 2-AB-labelled CS oligosaccharides to release the 2-AB-labelled reducing-end disaccharides. By taking advantage of these characteristics of enzymes, CS/DS oligosaccharides that are shorter than decasaccharides can be easily sequenced by enzymatic methods (Bao et al., 2005; Deepa et al., 2007b). Recently, we exploited a novel exolyase HCDLase combined with CSase ABC to sequence a complex octasaccharide

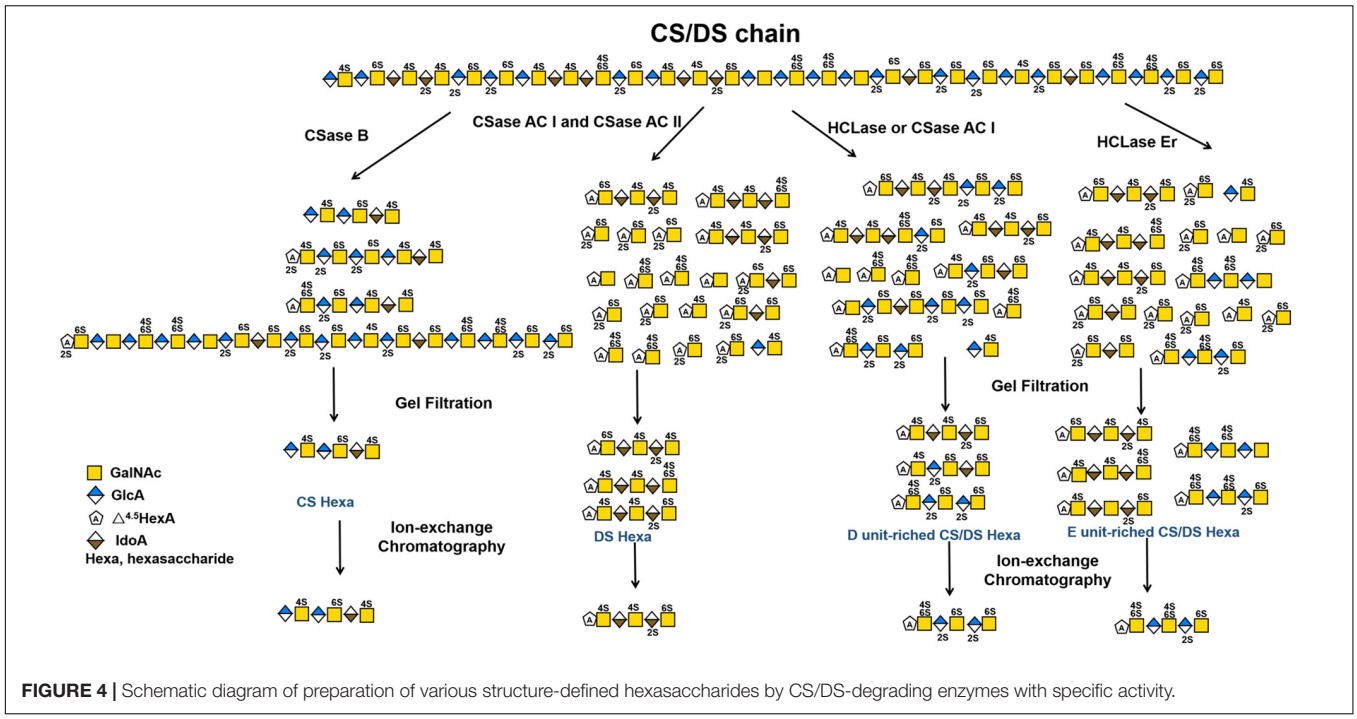

FIGURE 4 | Schematic diagram of preparation of various structure-defined hexasaccharides by CS/DS-degrading enzymes with specific activity.

(ΔC-A-D-C) (Wang et al., 2017). In this method, the disaccharide composition of the octasaccharide was determined by digestion with the CSase ABC followed by 2-AB labelling and HPLC assay. Then, the octasaccharide was labeled with 2-AB and partially digested with CSase ABC to prepare the 2-AB-labelled reducing-end hexasaccharides. The reducing-end C unit can be directly determined through the digestion of the 2-AB-labelled octasaccharide with HCDLase followed by HPLC-fluorescence detection. To determine the first and second disaccharide units from the nonreducing terminus, the 2-AB-labelled octasaccharide and reducing-end hexasaccharide prepared as described above were individually digested by the CSase ABC and analyzed by HPLC after relabelling with 2-AB. This strategy is theoretically feasible for sequencing longer oligosaccharides but is not easy to achieve due to the rapid increase in operating steps with the increase of saccharide chains. Moreover, Shioiri et al. developed an enzymatic method for the sequencing of a synthesized CS dodecasaccharide (C-C-O-A-O-O) by using a strategy involving dual-fluorescence labelling and dual-digestion (Shioiri et al., 2016). This provides a possibility of sequencing longer CS/DS oligosaccharides. However, the inability of testicular hyaluronidase to cleave DS and highly sulfated CS limits the application of this method, and thus, it is necessary to find alternative enzymes with better features.

Potential Medical Applications

The abnormal expression of CS/DS has been shown to be closely related to the occurrence and development of various diseases, such as glial scar formation after brain injury, tumor metastasis, skeletal disorder and viral infection, indicating that the treatment with CS/DS-degrading enzymes should affect the progression of the related diseases and these enzymes might be used as therapeutic agent for the related diseases. In the research of a spinal cord injury (SCI) model, Lemons et al. expounded that CSPGs increased in the lesion and inhibited the growth of axons, that is, inhibited the recovery of the function of the lesion (Lemons et al., 1999; Mondello et al., 2015). Injecting of CSase ABC induces abnormal axon growth or enhance axon regeneration in zebrafish (Bernhardt and Schachner, 2000; Becker and Becker, 2002), adult rats (Bradbury et al., 2002; Janzadeh et al., 2017; Moon et al., 2001), mice (Li et al., 2013), and cats (Mondello et al., 2015). Moreover, CSase ABC combined with other operations such as human adipose derived stem cells (Sarveazad et al., 2017) or low level laser therapy (Janzadeh et al., 2017) can promote the treatment of SCI. Additionally,CSase ABC is used to treat some diseases related to nerve damage, such as glaucoma (Tribble et al., 2018), lumber intervertebral disc (Hoogendoorn et al., 2007; Sugimura et al., 1996; Lü et al., 1997), and to delay the progress of Parkinson's disease (Kauhausen et al., 2015) and Alzheimer's disease (Howell et al., 2015). Overall, these studies suggest that CS/DS-degrading enzymes, in particular CSase ABC with broad substrate spectrum, are very promising therapeutic agents for the treatment of nerve injury-related diseases. Most recently, studies have also found that 4-*O*-sulfated CS GAG chains are increased significantly at the injury site after SCI (Wang et al., 2008) and optic nerve injury (Pearson et al., 2018). ARSB, a mammalian 4-*O*-sulfatase, treatment improves locomotor function recovery after SCI (Yoo et al., 2013) and improves regeneration after optic nerve injury (Pearson et al., 2018). Comparing with the exo-sulfatases, the newly discovered 4-*O*-endosulfatases may show better effect in nerve injury repair, which remains to be investigated.

The abnormal expression of CS/DS or CS/DSPGs in cells and tissues is closely related to many tumorigenic processes including cell growth and survival, adhesion, migaration and invasion (Theocharis et al., 2010; Iozzo and Sanderson, 2011; Li et al., 2008). A series of studies have shown that CSases have potential application value in anti-tumor. For example, CSase ABC and CSase AC could significantly inhibited the growth of tumor while streptomyces hyaluronidase, and β-glucuronidase could not (Takeuchi, 1972), CSase AC and CSase B can inhibits the invasion and proliferation of melanoma (Denholm et al., 2001), CSase ABC can assist temozolomide in the treatment of glioblastoma (Jaime-Ramirez et al., 2017), the adhere ability of squamous tongue carcinoma SCC-9 LN-1 cells can be reduced by treatment with CSaseABC (Kawahara et al., 2014), the metastasis of Lewis lung carcinoma LM66-H11 cells can be effectively inhibited by treatment with CSase ABC (Li et al., 2008), and so on (Sullivan et al., 2018). Moreover, Link et al. found that treatment with CSase ABC enhanced integration of both immature and mature self-assembled articular cartilage to native tissue, indicating that Case ABC has a potential therapeutic target for the integration of neocartilage (Link et al., 2020). In fact, some hyaluronidases, such as ovine testicles hyaluronidase (Vitrase®), bovine testicular hyaluronidase (Hydase™) and recombinant human hyaluronidase PH20 (ENHANZE®), have been clinically used in ophthalmic surgery (Sarvela et al., 1994) and in cosmetic dermatosurgery for the treatment of complications caused by filler injection (Hirsch et al., 2007).

Additionally, the lack of sulfatase leads to the long-term accumulation of highly sulfated oligosaccharides in the lysosome, which cause lysosomal storage disorders MPSs. MPSII (Hunter, OMIM 309900), MPS IVA (Morquio A, OMIM 253000) and MPS VI (Maroteaux-Lamy, OMIM 253200) resulted from the deficiencies of IDS, GALNS and ARSB, respectively (Bondeson et al., 1995; Matalon et al., 1974; Dorfman et al., 1976). Enzyme replacement therapy is the standard treatment option for MPSs, which can start treatment immediately and improve prognosis. Recombinant human IDS (idursulfase and idursulfase beta), GALNS (elosulfase alfa) and ARSB (galsulfase) are clinically used to treat the corresponding MPSs (Whiteman and Kimura, 2017; Sawamoto et al., 2020; Harmatz and Shediac, 2017). Hematopoietic stem cell transplantation is also available for MPSs treatment (Coppa et al., 1995; Mullen et al., 2000). Moreover, gene therapy should be another potential choice for MPSs (Sawamoto et al., 2018; Ponder and Haskins, 2007).

However, the clinical application of CS/DS-degrading enzymes still faces many problems such as immunogenicity, instability and low activity in vivo, which need further study to solve.

CONCLUSION

Undoubtedly, CS/DS-degrading enzymes with various specific activities play indispensable roles in structural and functional studies as well as other applications related to CS/DS, such as disaccharide composition analysis, quality control of products, preparation of bioactive oligosaccharides, and oligosaccharide sequencing. However, the types and numbers of well-characterized enzymes currently are far from meeting the needs of the research and applications of CS/DS. Therefore, it is an urgent task to identify more CS/DS-degrading enzymes with novel specific activity and to carry out re-examination of old enzymes whose action patterns remain to be investigated in detail.

AUTHOR CONTRIBUTIONS

WW, LS, and YQ collected the literature, wrote the manuscript, and made the figures. FL conceptualized, edited and made significant revisions to the manuscript. All authors read and approved the final manuscript.

FUNDING

This work was supported by the National Natural Science Foundation of China (Nos. 31971201, 31570071, and 31800665), the National Natural Science Foundation of Shandong Province (No. ZR2018BC013), the Science and Technology Development Project of Shandong Province (No. 2018GSF121002), the Major Scientific and Technological Innovation Project (MSTIP) of Shandong Province (2019JZZY010817), the General Financial Grant from China Postdoctoral Science Foundation Grant (No. 2019M662343), and the Project of Taishan Industry Leading Talent of Shandong Province (tscy20160311).

REFERENCES

Afify, A. M., Stern, M., Guntenhoener, M., and Stern, R. (1993). Purification and characterization of human serum hyaluronidase. *Arch. Biochem. Biophys.* 305, 434–441. doi: 10.1006/abbi.1993.1443

Almeida, R., Levery, S. B., Mandel, U., Kresse, H., Schwientek, T., Bennett, E. P., et al. (1999). Cloning and expression of a proteoglycan UDP-galactose:beta-xylose beta1,4-galactosyltransferase I. A seventh member of the human beta4-galactosyltransferase gene family. *J. Biol. Chem.* 274, 26165–26171. doi: 10.1074/jbc.274.37.26165

Bai, X., Wei, G., Sinha, A., and Esko, J. D. (1999). Chinese hamster ovary cell mutants defective in glycosaminoglycan assembly and glucuronosyltransferase I. *J. Biol. Chem.* 274, 13017–13024. doi: 10.1074/jbc.274.19.13017

Bai, X., Zhou, D., Brown, J. R., Crawford, B. E., Hennet, T., and Esko, J. D. (2001). Biosynthesis of the linkage region of glycosaminoglycans: cloning and activity of galactosyltransferase II, the sixth member of the beta 1,3-galactosyltransferase family (beta 3GalT6). *J. Biol. Chem.* 276, 48189–48195. doi: 10.1074/jbc.m107339200

Bao, X. F., Muramatsu, T., and Sugahara, K. (2005). Demonstration of the pleiotrophin-binding oligosaccharide sequences isolated from chondroitin sulfate/dermatan sulfate hybrid chains of embryonic pig brains. *J. Biol. Chem.* 280, 35318–35328. doi: 10.1074/jbc.m507304200

Barbeyron, T., Brillet-Guéguen, L., Carré, W., Carrière, C., Caron, C., Czjzek, M., et al. (2016). Matching the diversity of sulfated biomolecules: creation of a classification database for sulfatases reflecting their substrate specificity. *PLoS One* 11:e0164846. doi: 10.1371/journal.pone.0164846

Baum, H., Dodgson, K. S., and Spencer, B. (1959). The assay of arylsulphatases A and B in human urine. *Clin. Chim. Acta* 4, 453–455. doi: 10.1016/0009-8981(59)90119-6

Bearpark, T. M., and Stirling, J. L. (1978). A difference in the specificities of human liver N-acetyl-beta-hexosaminidase A and B detected by their activities towards glycosaminoglycan oligosaccharides. *Biochem. J.* 173, 997–1000. doi: 10.1042/bj1730997

Becker, C. G., and Becker, T. (2002). Repellent guidance of regenerating optic axons by chondroitin sulfate glycosaminoglycans in zebrafish. *J. Neurosci.* 22, 842–853. doi: 10.1523/jneurosci.22-03-00842.2002

Bergefall, K., Trybala, E., Johansson, M., Uyama, T., Naito, S., Yamada, S., et al. (2005). Chondroitin sulfate characterized by the E-disaccharide unit is a potent inhibitor of herpes simplex virus infectivity and provides the virus binding sites on gro2C cells. *J. Biol. Chem.* 280, 32193–32199. doi: 10.1074/jbc.m503645200

Bernhardt, R. R., and Schachner, M. (2000). Chondroitin sulfates affect the formation of the segmental motor nerves in zebrafish embryos. *Dev. Biol.* 221, 206–219. doi: 10.1006/dbio.2000.9673

Bielicki, J., and Hopwood, J. J. (1991). Human liver N-acetylgalactosamine 6-sulphatase. Purification and characterization. *Biochem. J.* 279(Pt 2), 515–520. doi: 10.1042/bj2790515

Bondeson, M. L., Dahl, N., Malmgren, H., Kleijer, W. J., Tönnesen, T., Carlberg, B. M., et al. (1995). Inversion of the IDS gene resulting from recombination with IDS-related sequences is a common cause of the Hunter syndrome. *Hum. Mol. Genet.* 1995, 615–621. doi: 10.1093/hmg/4.4.615

Bradbury, E. J., Moon, L. D., Popat, R. J., King, V. R., Bennett, G. S., Patel, P. N., et al. (2002). Chondroitinase ABC promotes functional recovery after spinal cord injury. *Nature* 416, 636–640.

Bülow, H. E., and Hobert, O. (2006). The molecular diversity of glycosaminoglycans shapes animal development. *Annu. Rev. Cell. Dev. Biol.* 22, 375–407. doi: 10.1146/annurev.cellbio.22.010605.093433

Cai, C., Solakyildirim, K., Yang, B., Beaudet, J. M., Weyer, A., Linhardt, R. J., et al. (2012). Semi-synthesis of chondroitin sulfate-E from chondroitin sulfate-A. *Carbohydr. Polym.* 87, 822–829. doi: 10.1016/j.carbpol.2011.08.075

Campo, G. M., Avenoso, A., Campo, S., D'Ascola, A., Traina, P., Samà, D., et al. (2009). Glycosaminoglycans modulate inflammation and apoptosis in LPS-treated chondrocytes. *J. Cell Biochem.* 106, 83–92. doi: 10.1002/jcb.21981

Chen, L.-Z., Shi, C.-Q., Yin, F.-X., Wang, F.-S., and Sheng, J.-Z. (2019). Cloning and characterization of a chondroitin AC exolyase from Arthrobacter sp. *SD*-04. *Mol. Biotechnol.* 61, 791–800. doi: 10.1007/s12033-019-00208-z

Cherr, G. N., Yudin, A. I., and Overstreet, J. W. (2001). The dual functions of GPI-anchored PH-20: hyaluronidase and intracellular signaling. *Matrix. Biol.* 20, 515–525. doi: 10.1016/s0945-053x(01)00171-8

Chiricozzi, E., Niemir, N., Aureli, M., Magini, A., Loberto, N., Prinetti, A., et al. (2014). Chaperone therapy for GM2 gangliosidosis: effects of pyrimethamine on β-hexosaminidase activity in Sandhoff fibroblasts. *Mol. Neurobiol.* 50, 159–167. doi: 10.1007/s12035-013-8605-5

Clement, A. M., Nadanaka, S., Masayama, K., Mandl, C., Sugahara, K., and Faissner, A. (1998). The DSD-1 carbohydrate epitope depends on sulfation, correlates with chondroitin sulfate D motifs, and is sufficient to promote neurite outgrowth. *J. Biol. Chem.* 273, 28444–28453. doi: 10.1074/jbc.273.43.28444

Coppa, G. V., Gabrielli, O., Zampini, L., Pierani, P., Giorgi, P. L., Jezequel, A. M., et al. (1995). Bone marrow transplantation in Hunter syndrome (mucopolysaccharidosis type II): two-year follow-up of the first Italian patient and review of the literature. *Pediatr. Med. Chir.* 17, 227–235.

Csoka, A. B., Frost, G. I., and Stern, R. (2001). The six hyaluronidase-like genes in the human and mouse genomes. *Matrix. Biol.* 20, 499–508. doi: 10.1016/s0945-053x(01)00172-x

Csoka, A. B., Scherer, S. W., and Stern, R. (1999). Expression analysis of paralogous human hyaluronidase genes clustered on chromosomes 3p21 and 7q31. *Genomics* 60, 356–361. doi: 10.1006/geno.1999.5876

De Salegui, M., and Pigman, W. (1967). The existence of an acid-active hyaluronidase in serum. *Arch. Biochem. Biophys.* 120, 60–67. doi: 10.1016/0003-9861(67)90598-x

Deepa, S. S., Kalayanamitra, K., Ito, Y., Kongtawelert, P., Fukui, S., Yamada, S., et al. (2007a). Novel sulfated octa- and decasaccharides from squid cartilage chondroitin sulfate E: sequencing and application for determination of the epitope structure of the monoclonal antibody MO-225. *Biochemistry* 46, 2453–2465. doi: 10.1021/bi602374m

Deepa, S. S., Yamada, S., Fukui, S., and Sugahara, K. (2007b). Structural determination of novel sulfated octasaccharides isolated from chondroitin sulfate of shark cartilage and their application for characterizing monoclonal antibody epitopes. *Glycobiology* 17, 631–645. doi: 10.1093/glycob/cwm021

Denholm, E. M., Lin, Y. Q., and Silver, P. J. (2001). Anti-tumor activities of chondroitinase AC and chondroitinase B: inhibition of angiogenesis, proliferation and invasion. *Eur. J. Pharmacol.* 416, 213–221. doi: 10.1016/s0014-2999(01)00884-6

Dhamale, O. P., Lawrence, R., Wiegmann, E. M., Shah, B. A., Al-Mafraji, K., Lamanna, W. C., et al. (2017). Arylsulfatase K is the lysosomal 2-sulfoglucuronate sulfatase. *ACS Chem. Biol.* 12, 367–373. doi: 10.1021/acschembio.6b01033

Dorfman, A., Arbogast, B., and Matalon, R. (1976). The enzymic defects in Morquio and Maroteaux-Lamy syndrome. *Adv. Exp. Med. Biol.* 68, 261–276. doi: 10.1007/978-1-4684-7735-1_18

Evers, M. R., Xia, G., Kang, H. G., Schachner, M., and Baenziger, J. U. (2001). Molecular cloning and characterization of a dermatan-specific N-acetylgalactosamine 4-O-sulfotransferase. *J. Biol. Chem.* 276, 36344–36353. doi: 10.1074/jbc.m105848200

Freeman, M. E., Anderson, P., Oberg, M., and Dorfman, A. (1949). Preparation of purified hyaluronidase from bovine testis. *J. Biol. Chem.* 180, 655–662.

Fu, J., Jiang, Z., Chang, J., Han, B., Liu, W., and Peng, Y. (2018). Purification, characterization of Chondroitinase ABC from Sphingomonas paucimobilis and in vitro cardiocytoprotection of the enzymatically degraded CS-A. *Int. J. Biol. Macromol.* 115, 737–745. doi: 10.1016/j.ijbiomac.2018.04.117

Fujikawa, S., Ohmae, M., and Kobayashi, S. (2005). Enzymatic synthesis of chondroitin 4-sulfate with well-defined structure. *Biomacromolecules* 6, 2935–2942. doi: 10.1021/bm050364p

Fukui, S., Feizi, T., Galustian, C., Lawson, A. M., and Chai, W. G. (2002). Oligosaccharide microarrays for high-throughput detection and specificity assignments of carbohydrate-protein interactions. *Nat. Biotechnol.* 20, 1011–1017. doi: 10.1038/nbt735

Fukuta, M., Kobayashi, Y., Uchimura, K., Kimata, K., and Habuchi, O. (1998). Molecular cloning and expression of human chondroitin 6-sulfotransferase. *Biochim. Biophys. Acta* 1399, 57–61. doi: 10.1016/s0167-4781(98)00089-x

Gama, C. I., Tully, S. E., Sotogaku, N., Clark, P. M., Rawat, M., Vaidehi, N., et al. (2006). Sulfation patterns of glycosaminoglycans encode molecular recognition and activity. *Nat. Chem. Biol.* 2, 467–473. doi: 10.1038/nchembio810

Gmach, M., and Kreil, G. (1993). Bee venom hyaluronidase is homologous to a membrane protein of mammalian sperm. *Proc. Natl. Acad. Sci. U.S.A.* 90, 3569–3573. doi: 10.1073/pnas.90.8.3569

Götting, C., Kuhn, J., and Kleesiek, K. (2007). Human xylosyltransferases in health and disease. *Cell. Mol. Life Sci.* 64, 1498–1517. doi: 10.1007/s00018-007-7069-z

Götting, C., Kuhn, J., Zahn, R., Brinkmann, T., and Kleesiek, K. (2000). Molecular cloning and expression of human UDP-D-Xylose:proteoglycan core protein beta-d-xylosyltransferase and its first isoform XT-II. *J. Mol. Biol.* 304, 517–528. doi: 10.1006/jmbi.2000.4261

Gu, K., Linhardt, R. J., Laliberte, M., and Zimmermann, J. (1995). Purification, characterization and specificity of chondroitin lyases and glycuronidase from Flavobacterium heparinum. *Biochem. J.* 312, 569–577. doi: 10.1042/bj3120569

Guo, X., Shi, Y., Sheng, J., and Wang, F. (2014). A novel hyaluronidase produced by *Bacillus* sp. A50. *PLoS One* 9:e94156. doi: 10.1371/journal.pone.0094156

Gushulak, L., Hemming, R., Martin, D., Seyrantepe, V., Pshezhetsky, A., and Triggs-Raine, B. (2012). Hyaluronidase 1 and β-hexosaminidase have redundant functions in hyaluronan and chondroitin sulfate degradation. *J. Biol. Chem.* 287, 16689–16697. doi: 10.1074/jbc.m112.350447

Habuchi, O. (2000). Diversity and functions of glycosaminoglycan sulfotransferases. *Biochim. Biophys. Acta* 1474, 115–127. doi: 10.1016/s0304-4165(00)00016-7

Hamai, A., Hashimoto, N., Mochizuki, H., Kato, F., Makiguchi, Y., Horie, K., et al. (1997). Two distinct chondroitin sulfate ABC lyases an endoeliminase yielding tetrasaccharides and an exoeliminase preferentially acting on oligosaccharides. *J. Biol. Chem.* 272, 9123–9130. doi: 10.1074/jbc.272.14.9123

Han, W., Wang, W., Zhao, M., Sugahara, K., and Li, F. (2014). A Novel eliminase from a marine bacterium that degrades hyaluronan and chondroitin sulfate. *J. Biol. Chem.* 289, 27886–27898. doi: 10.1074/jbc.m114.590752

Handel, T. M., Johnson, Z., Crown, S. E., Lau, E. K., Sweeney, M., and Proudfoot, A. E. (2005). Regulation of protein function by glycosaminoglycans - as

exemplified by chemokines. *Annu. Rev. Biochem.* 74, 385–410. doi: 10.1146/annurev.biochem.72.121801.161747

Harmatz, P., and Shediac, R. (2017). Mucopolysaccharidosis VI: pathophysiology, diagnosis and treatment. *Front Biosci.* 22:385–406. doi: 10.2741/4490

Hayes, A. J., Smith, S. M., Caterson, B., and Melrose, J. (2018). Concise review: Stem/progenitor cell proteoglycans decorated with 7-D-4, 4-C-3, and 3-B-3(-) chondroitin sulfate motifs are morphogenetic markers of tissue development. *Stem Cells* 36, 1475–1486. doi: 10.1002/stem.2860

Henrissat, B. (1991). A classification of glycosyl hydrolases based on amino acid sequence similarities. *Biochem. J.* 280, 309–316. doi: 10.1042/bj2800309

Hiraoka, N., Nakagawa, H., Ong, E., Akama, T. O., Fukuda, M. N., and Fukuda, M. (2000). Molecular cloning and expression of two distinct human chondroitin 4-O-sulfotransferases that belong to the HNK-1 sulfotransferase gene family. *J. Biol. Chem.* 275, 20188–20196. doi: 10.1074/jbc.m002443200

Hirsch, R. J., Brody, H. J., and Carruthers, J. D. (2007). Hyaluronidase in the office: a necessity for every dermasurgeon that injects hyaluronic acid. *J. Cosmet. Laser. Ther.* 9, 182–1855. doi: 10.1080/14764170701291674

Hiyama, K., and Okada, S. (1975). Amino acid composition and physiochemical characterization of chondroitinase from *Arthrobacter aurescens*. *J. Biochem.* 78, 1183–1190. doi: 10.1093/oxfordjournals.jbchem.a131015

Hoffman, P., Meyer, K., and Linker, A. (1956). Transglycosylation during the mixed digestion of hyaluronic acid and chondroitin sulfate by testicular hyaluronidase. *J. Biol. Chem.* 219, 653–663.

Honda, T., Kaneiwa, T., Mizumoto, S., Sugahara, K., and Yamada, S. (2012). Hyaluronidases have strong hydrolytic activity toward chondroitin 4-sulfate comparable to that for hyaluronan. *Biomolecules* 2, 549–563. doi: 10.3390/biom2040549

Hoogendoorn, R. J., Wuisman, P. I., Smit, T. H., Everts, V. E., and Helder, M. N. (2007). Experimental intervertebral disc degeneration induced by chondroitinase ABC in the goat. *Spine* 32, 1816–1825. doi: 10.1097/brs.0b013e31811ebac5

Howell, M. D., Bailey, L. A., Cozart, M. A., Gannon, B. M., and Gottschall, P. E. (2015). Hippocampal administration of chondroitinase ABC increases plaque-adjacent synaptic marker and diminishes amyloid burden in aged APPswe/PS1dE9 mice. *Acta Neuropathol. Commun.* 3:54.

Hsiao, J. C., Chung, C. S., and Chang, W. (1999). Vaccinia virus envelope D8L protein binds to cell surface chondroitin sulfate and mediates the adsorption of intracellular mature virions to cells. *J. Virol.* 73, 8750–8761. doi: 10.1128/jvi.73.10.8750-8761.1999

Hwang, H. Y., Olson, S. K., Esko, J. D., and Horvitz, H. R. (2003). Caenorhabditis elegans early embryogenesis and vulval morphogenesis require chondroitin biosynthesis. *Nature* 423, 439–443. doi: 10.1038/nature01634

Iozzo, R. V., and Sanderson, R. D. (2011). Proteoglycans in cancer biology, tumour microenvironment and angiogenesis. *J. Cell. Mol. Med.* 15, 1013–1031. doi: 10.1111/j.1582-4934.2010.01236.x

Izumikawa, T., Kanagawa, N., Watamoto, Y., Okada, M., Saeki, M., Sakano, M., et al. (2010). Impairment of embryonic cell division and glycosaminoglycan biosynthesis in glucuronyltransferase-I-deficient Mice. *J. Biol. Chem.* 285, 12190–12196. doi: 10.1074/jbc.m110.100941

Izumikawa, T., Kitagawa, H., Mizuguchi, S., Nomura, K. H., Nomura, K., Tamura, J., et al. (2004). Nematode chondroitin polymerizing factor showing cell-/organ-specific expression is indispensable for chondroitin synthesis and embryonic cell division. *J. Biol. Chem.* 279, 53755–53761. doi: 10.1074/jbc.m409615200

Jaime-Ramirez, A. C., Dmitrieva, N., Yoo, J. Y., Banasavadi-Siddegowda, Y., Zhang, J., Relation, T., et al. (2017). Humanized chondroitinase ABC sensitizes glioblastoma cells to temozolomide. *J. Gene Med.* 19:e2942. doi: 10.1002/jgm.2942

Janzadeh, A., Sarveazad, A., Yousefifard, M., Dameni, S., Samani, F. S., Mokhtarian, K., et al. (2017). Combine effect of chondroitinase ABC and low level laser (660nm) on spinal cord injury model in adult male rats. *Neuropeptides* 65, 90–99. doi: 10.1016/j.npep.2017.06.002

Jedrzejas, M. J., and Stern, R. (2005). Structures of vertebrate hyaluronidases and their unique enzymatic mechanism of hydrolysis. *Proteins* 61, 227–238. doi: 10.1002/prot.20592

Kale, V., Friðjónsson, Ó, Jónsson, J. Ó, Kristinsson, H. G., Ómarsdóttir, S., and Hreggviðsson, G. Ó (2015). Chondroitin lyase from a marine Arthrobacter sp. *MAT*3885 for the production of chondroitin sulfate disaccharides. *Mar. Biotechnol.* 17, 479–492. doi: 10.1007/s10126-015-9629-9

Kaneiwa, T., Mizumoto, S., Sugahara, K., and Yamada, S. (2010). Identification of human hyaluronidase-4 as a novel chondroitin sulfate hydrolase that preferentially cleaves the galactosaminidic linkage in the trisulfated tetrasaccharide sequence. *Glycobiology* 20, 300–309. doi: 10.1093/glycob/cwp174

Kang, H. G., Evers, M. R., Xia, G., Baenziger, J. U., and Schachner, M. (2002). Molecular cloning and characterization of chondroitin-4-O-sulfotransferase-3. A novel member of the HNK-1 family of sulfotransferases. *J. Biol. Chem.* 277, 34766–34772. doi: 10.1074/jbc.m204907200

Kastana, P., Choleva, E., Poimenidi, E., Karamanos, N., Sugahara, K., and Papadimitriou, E. (2019). Insight into the role of chondroitin sulfate E in angiogenesis. *FEBS J.* 286, 2921–2936. doi: 10.1111/febs.14830

Kato, D., Era, S., Watanabe, I., Arihara, M., Sugiura, N., Kimata, K., et al. (2010). Antiviral activity of chondroitin sulphate E targeting dengue virus envelope protein. *Antiviral. Res.* 88, 236–243. doi: 10.1016/j.antiviral.2010.09.002

Kauhausen, J. A., Thompson, L. H., and Parish, C. L. (2015). Chondroitinase improves midbrain pathway reconstruction by transplanted dopamine progenitors in Parkinsonian mice. *Mol. Cell. Neurosci.* 69, 22–29. doi: 10.1016/j.mcn.2015.10.002

Kawahara, R., Granato, D. C., Carnielli, C. M., Cervigne, N. K., Oliveria, C. E., Martinez, C. A. R., et al. (2014). Agrin and perlecan mediate tumorigenic processes in oral squamous cell carcinoma. *PLoS One* 9:e115004. doi: 10.1371/journal.pone.0115004

Khan, S. A., Peracha, H., Ballhausen, D., Wiesbauer, A., Rohrbach, M., Gautschi, M., et al. (2017). Epidemiology of mucopolysaccharidoses. *Mol. Genet. Metab.* 121, 227–240.

Kim, S. Y., Zhao, J., Liu, X., Fraser, K., Lin, L., Zhang, X., et al. (2017). Interaction of zika virus envelope protein with glycosaminoglycans. *Biochemistry* 56, 1151–1162. doi: 10.1021/acs.biochem.6b01056

Kinoshita, A., and Sugahara, K. (1999). Microanalysis of glycosaminoglycan-derived oligosaccharides labeled with a fluorophore 2-aminobenzamide by high-performance liquid chromatography: application to disaccharide composition analysis and exosequencing of oligosaccharides. *Anal. Biochem.* 269, 367–378. doi: 10.1006/abio.1999.4027

Kinoshita, A., Yamada, S., Haslam, S. M., Morris, H. R., Dell, A., and Sugahara, K. (2001). Isolation and structural determination of novel sulfated hexasaccharides from squid cartilage chondroitin sulfate E that exhibits neuroregulatory activities. *Biochemistry* 40, 12654–12665. doi: 10.1021/bi015577n

Kitagawa, H., Tone, Y., Tamura, J., Neumann, K. W., Ogawa, T., Oka, S., et al. (1998). Molecular cloning and expression of glucuronyltransferase I involved in the biosynthesis of the glycosaminoglycan-protein linkage region of proteoglycans. *J. Biol. Chem.* 273, 6615–6618. doi: 10.1074/jbc.273.12.6615

Klüppel, M., Wight, T. N., Chan, C., Hinek, A., and Wrana, J. L. (2005). Maintenance of chondroitin sulfation balance by chondroitin-4-sulfotransferase 1 is required for chondrocyte development and growth factor signaling during cartilage morphogenesis. *Development* 132, 3989–4003. doi: 10.1242/dev.01948

Kobayashi, M., Sugumaran, G., Liu, J. A., Shworak, N. W., Silbert, J. E., and Rosenberg, R. D. (1999). Molecular cloning and characterization of a human uronyl 2-sulfotransferase that sulfates iduronyl and glucuronyl residues in dermatan chondroitin sulfate. *J. Biol. Chem.* 274, 10474–10480. doi: 10.1074/jbc.274.15.10474

Kobayashi, S., Fujikawa, S., and Ohmae, M. (2003). Enzymatic synthesis of chondroitin and its derivatives catalyzed by hyaluronidase. *J. Am. Chem. Soc.* 125, 14357–14369. doi: 10.1021/ja036584x

Kreil, G. (1995). Hyaluronidases—a group of neglected enzymes. *Protein Sci.* 4, 1666–1669. doi: 10.1002/pro.5560040902

Kurata, A., Matsumoto, M., Kobayashi, T., Deguchi, S., and Kishimoto, N. (2015). Hyaluronate lyase of a deep-sea *Bacillus niacini*. *Mar. Biotechnol.* 17, 277–284. doi: 10.1007/s10126-015-9618-z

Kusche-Gullberg, M., and Kjellen, L. (2003). Sulfotransferases in glycosaminoglycan biosynthesis. *Curr. Opin. Struct. Biol.* 13, 605–611. doi: 10.1016/j.sbi.2003.08.002

Lemons, M. L., Howland, D. R., and Anderson, D. K. (1999). Chondroitin sulfate proteoglycan immunoreactivity increases following spinal cord injury and transplantation. *Exp. Neuro.* 160, 51–65. doi: 10.1006/exnr.1999.7184

Li, F., Nandini, C. D., Hattori, T., Bao, X., Murayama, D., Nakamura, T., et al. (2010). Structure of pleiotrophin- and hepatocyte growth factor-binding sulfated hexasaccharide determined by biochemical and computational approaches. *J. Biol. Chem.* 285, 27673–27685. doi: 10.1074/jbc.m110.118703

Li, F., Shetty, A. K., and Sugahara, K. (2007). Neuritogenic activity of chondroitin/dermatan sulfate hybrid chains of embryonic pig brain and their mimicry from shark liver. Involvement of the pleiotrophin and hepatocyte growth factor signaling pathways. *J. Biol. Chem.* 282, 2956–2966. doi: 10.1074/jbc.m609296200

Li, F., ten Dam, G. B., Murugan, S., Yamada, S., Hashiguchi, T., Mizumoto, S., et al. (2008). Involvement of highly sulfated chondroitin sulfate in the metastasis of the lewis lung carcinoma cells. *J. Biol. Chem.* 283, 34294–34304. doi: 10.1074/jbc.m806015200

Li, H. P., Komuta, Y., Kimura-Kuroda, J., van Kuppevelt, T. H., and Kawano, H. (2013). Roles of chondroitin sulfate and dermatan sulfate in the formation of a lesion scar and axonal regeneration after traumatic injury of the mouse brain. *J. Neurotraum.* 30, 413–425. doi: 10.1089/neu.2012.2513

Li, J., Sparkenbaugh, E. M., Su, G., Zhang, F., Xu, Y., Xia, K., et al. (2020). Enzymatic synthesis of chondroitin sulfate e to attenuate bacteria lipopolysaccharide-induced organ damage. *ACS Cent. Sci.* 6, 1199–1207. doi: 10.1021/acscentsci.0c00712

Li, J., Su, G., and Liu, J. (2017). Enzymatic synthesis of homogeneous chondroitin sulfate oligosaccharides. *Angew. Chem. Int. Ed. Engl.* 56, 11784–11787. doi: 10.1002/anie.201705638

Lim, C. T., and Horwitz, A. L. (1981). Purification and properties of human Nacetylgalactosamine-6-sulfate sulfatase. *Biochim. Biophys. Acta* 657, 344–355. doi: 10.1016/0005-2744(81)90320-x

Lim, T. W., Leder, I. G., Bach, G., and Neufeld, E. F. (1974). An assay for iduronate sulfatase (Hunter corrective factor). *Carbohydr. Res.* 37, 103–109. doi: 10.1016/s0008-6215(00)87067-6

Linhardt, R. J., Avci, F. Y., Toida, T., Kim, Y. S., and Cygler, M. (2006). CS lyases: structure, activity, and applications in analysis and the treatment of diseases. *Adv. Pharmacol.* 53, 187–215. doi: 10.1016/s1054-3589(05)53009-6

Link, J. M., Hu, J. C., and Athanasiou, K. A. (2020). Chondroitinase ABC enhances integration of self-assembled articular cartilage, but its dosage needs to be moderated based on neocartilage maturity. *Cartilage* [Epub ahead of print] doi: 10.1177/1947603520918653

Lokeshwar, V. B., Rubinowicz, D., Schroeder, G. L., Forgacs, E., Minna, J. D., Block, N. L., et al. (2001). Stromal and epithelial expression of tumor markers hyaluronic acid and HYAL1 hyaluronidase in prostate cancer. *J. Biol. Chem.* 276, 11922–11932. doi: 10.1074/jbc.m008432200

Lü, D. S., Shono, Y., Oda, I., Abumi, K., and Kaneda, K. (1997). Effects of chondroitinase ABC and chymopapain on spinal motion segment biomechanics. An in vivo biomechanical, radiologic, and histologic canine study. *Spine* 22, 1828–1835. doi: 10.1097/00007632-199708150-00006

Lunin, V. V., Li, Y., Linhardt, R. J., Miyazono, H., Kyogashima, M., Kaneko, T., et al. (2004). High-resolution crystal structure of *Arthrobacter aurescens* chondroitin AC lyase: an enzyme–substrate complex defines the catalytic mechanism. *J. Mol. Biol.* 337, 367–386. doi: 10.1016/j.jmb.2003.12.071

Ly, M., Leach, F. E. I. I. I., Laremore, T. N., Toida, T., Amster, I. J., and Linhardt, R. J. (2011). The proteoglycan bikunin has a defined sequence. *Nat. Chem. Biol.* 7, 827–833. doi: 10.1038/nchembio.673

Maccarana, M., Olander, B., Malmstrom, J., Tiedemann, K., Aebersold, R., Lindahl, U., et al. (2006). Biosynthesis of dermatan sulfate: chondroitin-glucuronate C5-epimerase is identical to SART2. *J. Biol. Chem.* 281, 11560–11568. doi: 10.1074/jbc.m513373200

Matalon, R., Arbogast, B., Justice, P., Brandt, I. K., and Dorfman, A. (1974). Morquio's syndrome: deficiency of a chondroitin sulfate N-acetylhexosamine sulfate sulfatase. *Biochem. Biophys. Res. Commun.* 61, 759–765. doi: 10.1016/0006-291x(74)91022-5

Mathews, M. B. (1958). Isomeric chondroitin sulphates. *Nature* 181, 421–422. doi: 10.1038/181421a0

Michelacci, Y. M., and Dietrich, C. P. (1976). Chondroitinase C from *Flavobacterium heparinum*. *J. Biol. Chem.* 251, 1154–1158.

Mikami, T., Mizumoto, S., Kago, N., Kitagawa, H., and Sugahara, K. (2003). Specificities of three distinct human chondroitin/dermatan N-acetylgalactosamine 4-O-sulfotransferases demonstrated using partially desulfated dermatan sulfate as an acceptor: implication of differential roles in dermatan sulfate biosynthesis. *J. Biol. Chem.* 278, 36115–36127. doi: 10.1074/jbc.m306044200

Mikami, T., Yasunaga, D., and Kitagawa, H. (2009). Contactin-1 is a functional receptor for neuroregulatory chondroitin sulfate-E. *J. Biol. Chem.* 284, 4494–4499. doi: 10.1074/jbc.m809227200

Miyachi, K., Wakao, M., and Suda, Y. (2015). Syntheses of chondroitin sulfate tetrasaccharide structures containing 4,6-disulfate patterns and analysis of their interaction with glycosaminoglycan-binding protein. *Bioorg. Med. Chem. Lett.* 25, 1552–1555. doi: 10.1016/j.bmcl.2015.02.011

Miyazono, H., Kikuchi, H., Yoshida, K., Morikawa, K., and Tokuyasu, K. (1990). Purification and properties of three novel chondroitinases. *Glycoconj. J.* 8, 201.

Mizuguchi, S., Uyama, T., Kitagawa, H., Nomura, K. H., Dejima, K., Gengyo-Ando, K., et al. (2003). Chondroitin proteoglycans are involved in cell division of *Caenorhabditis elegans*. *Nature* 423, 443–448. doi: 10.1038/nature01635

Mizumoto, S., Murakoshi, S., Kalayanamitra, K., Deepa, S. S., Fukui, S., Kongtawelert, P., et al. (2013a). Highly sulfated hexasaccharide sequences isolated from chondroitin sulfate of shark fin cartilage: insights into the sugar sequences with bioactivities. *Glycobiology* 23, 155–168. doi: 10.1093/glycob/cws137

Mizumoto, S., Watanabe, M., Yamada, S., and Sugahara, K. (2013b). Expression of N-acetylgalactosamine 4-sulfate 6-O-sulfotransferase involved in chondroitin sulfate synthesis is responsible for pulmonary metastasis. *Biomed. Res. Int.* 2013:656319.

Mizumoto, S., and Sugahara, K. (2013). Glycosaminoglycans are functional ligands for receptor for advanced glycation end-products in tumors. *FEBS J.* 280, 2462–2470. doi: 10.1111/febs.12156

Mizumoto, S., Takahashi, J., and Sugahara, K. (2012). Receptor for advanced glycation end products (RAGE) functions as a receptor for specific sulfated glycosaminoglycans, and anti-RAGE antibody or the sulfated glycosaminoglycans delivered in vivo inhibit pulmonary metastasis of tumor cells. *J. Biol. Chem.* 287, 18985–18994. doi: 10.1074/jbc.m111.313437

Mondello, S. E., Jefferson, S. C., Tester, N. J., and Howland, D. R. (2015). Impact of treatment duration and lesion size on effectiveness of chondroitinase treatment post-SCI. *Exp. Neuro.* 267, 64–77. doi: 10.1016/j.expneurol.2015.02.028

Moon, L. D., Asher, R. A., Rhodes, K. E., and Fawcett, J. W. (2001). Regeneration of CNS axons back to their target following treatment of adult rat brain with chondroitinase ABC. *Nat. Neurosci.* 4, 465–466. doi: 10.1038/87415

Mullen, C. A., Thompson, J. N., Richard, L. A., and Chan, K. W. (2000). Unrelated umbilical cord blood transplantation in infancy for mucopolysaccharidosis type IIB (Hunter syndrome) complicated by autoimmune hemolytic anemia. *Bone Marrow Transpl.* 25, 1093–1097. doi: 10.1038/sj.bmt.1702397

Myette, J. R., Shriver, Z., Claycamp, C., McLean, M. W., Venkataraman, G., and Sasisekharan, R. (2003). The heparin/heparan sulfate 2-O-sulfatase from *Flavobacterium heparinum* - Molecular cloning, recombinant expression, and biochemical characterization. *J. Biol. Chem.* 278, 12157–12166. doi: 10.1074/jbc.m211420200

Nadanaka, S., and Sugahara, K. (1997). The unusual tetrasaccharide sequence GlcA beta 1-3GalNAc(4-sulfate) beta 1-4GlcA(2-sulfate) beta 1-3GalNAc(6-sulfate) found in the hexasaccharides prepared by testicular hyaluronidase digestion of shark cartilage chondroitin sulfate D. *Glycobiology* 7, 253–263. doi: 10.1093/glycob/7.2.253

Namburi, R. B., Berteau, O., Spillmann, D., and Rossi, M. (2016). Chondroitinase AC: a host-associated genetic feature of *Helicobacter bizzozeronii*. *Vet. Microbiol.* 186, 21–27. doi: 10.1016/j.vetmic.2016.02.013

Nandi, S., Akhter, M. P., Seifert, M. F., Dai, X. M., and Stanley, E. R. (2006). Developmental and functional significance of the CSF-1 proteoglycan chondroitin sulfate chain. *Blood* 107, 786–795. doi: 10.1182/blood-2005-05-1822

Nandini, C. D., and Sugahara, K. (2006). Role of the sulfation pattern of chondroitin sulfate in its biological activities and in the binding of growth factors. *Adv. Pharmacol.* 53, 253–279. doi: 10.1016/s1054-3589(05)53012-6

Ndeh, D., Munoz, J. M., Cartmell, A., Bulmer, D., Wills, C., Henrissat, B., et al. (2018). The human gut microbe *Bacteroides thetaiotaomicron* encodes the founding member of a novel glycosaminoglycan-degrading polysaccharide lyase family PL29. *J. Biol. Chem.* 293, 17906–17916. doi: 10.1074/jbc.ra118.004510

Ochiai, H., Fujikawa, S., and Ohmae, M. (2007a). Enzymatic copolymerization to hybrid glycosaminoglycans: a novel strategy for intramolecular hybridization

of polysaccharides. *Biomacromolecules* 8, 1802–1806. doi: 10.1021/bm0700340

Ochiai, H., Ohmae, M., Mori, T., and Kobayashi, S. (2007b). Hyaluronidase-catalyzed copolymerization for the single-step synthesis of functionalized hyaluronan derivatives. *Biomacromolecules* 8, 1327–1332. doi: 10.1021/bm061136d

Ohtake, S., Ito, Y., Fukuta, M., and Habuchi, O. (2001). Human N-acetylgalactosamine 4-sulfate 6-O-sulfotransferase cDNA is related to human B cell recombination activating gene-associated gene. *J. Biol. Chem.* 276, 43894–43900. doi: 10.1074/jbc.m104922200

Ohya, T., and Kaneko, Y. (1970). Novel hyaluronidase from streptomyces. *Biochim. Biophys. Acta.* 198, 607–609. doi: 10.1016/0005-2744(70)90139-7

Okajima, T., Yoshida, K., Kondo, T., and Furukawa, K. (1999). Human homolog of *Caenorhabditis elegans* sqv-3 gene is galactosyltransferase I involved in the biosynthesis of the glycosaminoglycan-protein linkage region of proteoglycans. *J. Biol. Chem.* 274, 22915–22918. doi: 10.1074/jbc.274.33.22915

Pacheco, B., Malmstrom, A., and Maccarana, M. (2009). Two dermatan sulfate epimerases form iduronic acid domains in dermatan sulfate. *J. Biol. Chem.* 284, 9788–9795. doi: 10.1074/jbc.m809339200

Parenti, G., Meroni, G., and Ballabio, A. (1997). The sulfatase gene family. *Curr. Opin. Genet. Dev.* 7, 386–391. doi: 10.1016/s0959-437x(97)80153-0

Pearson, C. S., Mencio, C. P., Barber, A. C., Martin, K. R., and Geller, H. M. (2018). Identification of a critical sulfation in chondroitin that inhibits axonal regeneration. *eLife* 7:e37139.

Peng, C., Wang, Q., Wang, S., Wang, W., Jiao, R., Han, W., et al. (2018). A chondroitin sulfate and hyaluronic acid lyase with poor activity to glucuronyl 4,6-O-disulfated N-acetylgalactosamine (E-type)-containing structures. *J. Biol. Chem.* 293, 4230–4243. doi: 10.1074/jbc.ra117.001238

Ponder, K. P., and Haskins, M. E. (2007). Gene therapy for mucopolysaccharidosis. *Expert Opin. Biol. Ther.* 7, 1333–1345.

Pudelko, A., Wisowski, G., Olczyk, K., and Kozma, E. M. (2019). The dual role of the glycosaminoglycan chondroitin-6-sulfate in the development, progression and metastasis of cancer. *FEBS J.* 286, 1815–1837. doi: 10.1111/febs.14748

Purushothaman, A., Fukuda, J., Mizumoto, S., ten Dam, G. B., van Kuppevelt, T. H., Kitagawa, H., et al. (2007). Functions of chondroitin sulfate/dermatan sulfate chains in brain development. critical roles of E and iE disaccharide units recognized by a single chain antibody GD3G7. *J. Biol. Chem.* 282, 19442–19452. doi: 10.1074/jbc.m700630200

Rai, S. K., Duh, F. M., Vigdorovich, V., Danilkovitch-Miagkova, A., Lerman, M. I., and Millet, A. D. (2001). Candidate tumor suppressor HYAL2 is a glycosylphosphatidylinositol (GPI)-anchored cell-surface receptor for jaagsiekte sheep retrovirus, the envelope protein of which mediates oncogenic transformation. *Proc. Natl. Acad. Sci. U.S.A.* 98, 4443–4448. doi: 10.1073/pnas.071572898

Raman, R., Sasisekharan, V., and Sasisekharan, R. (2005). Structural insights into biological roles of protein-glycosaminoglycan interactions. *Chem. Biol.* 12, 267–277. doi: 10.1016/j.chembiol.2004.11.020

Sabeur, K., Cherr, G. N., Yudin, A. I., Primakoff, P., Li, M. W., and Overstreet, J. W. (1997). The PH-20 protein in human spermatozoa. *J. Androl.* 8, 151–158.

Sarveazad, A., Babahajian, A., Bakhtiari, M., Soleimani, M., Behnam, B., Yari, A., et al. (2017). The combined application of human adipose derived stem cells and Chondroitinase ABC in treatment of a spinal cord injury model. *Neuropeptides* 61, 39–47. doi: 10.1016/j.npep.2016.07.004

Sarvela, P. J., Paloheimo, M. P., and Nikki, P. H. (1994). Comparison of pH-adjusted bupivacaine 0.75 % and a mixture of bupivacaine 0.75% and lidocaine 2 %, both with hyaluronidase, in day-case cataract surgery under regional anesthesia. *Anesth. Analg.* 9, 35–39.

Sawamoto, K., Álvarez González, J. V., Piechnik, M., Otero, F. J., Couce, M. L., Suzuki, Y., et al. (2020). Mucopolysaccharidosis IVA: diagnosis, treatment, and management. *Int. J. Mol. Sci.* 21:1517. doi: 10.3390/ijms21041517

Sawamoto, K., Chen, H. H., Alméciga-Díaz, C. J., Mason, R. W., and Tomatsu, S. (2018). Gene therapy for Mucopolysaccharidoses. *Mol. Genet. Metab.* 123, 59–68. doi: 10.1016/j.ymgme.2017.12.434

Schwartz, N. B., and Domowicz, M. S. (2018). Proteoglycans in brain development and pathogenesis. *FEBS Lett.* 592, 3791–3805. doi: 10.1002/1873-3468.13026

Shaklee, P. N., Glaser, J. H., and Conrad, H. E. (1985). A sulfatase specific for glucuronic acid 2-sulfate residues in glycosaminoglycans. *J. Biol. Chem.* 260, 9146–9149.

Shida, M., Mikami, T., Tamura, J. I., and Kitagawa, H. (2019). Chondroitin sulfate-D promotes neurite outgrowth by acting as an extracellular ligand for neuronal integrin αVβ3. *Biochim. Biophys. Acta Gen. Subj.* 1863, 1319–1331. doi: 10.1016/j.bbagen.2019.06.004

Shioiri, T., Tsuchimoto, J., Watanabe, H., and Sugiura, N. (2016). Sequence determination of synthesized chondroitin sulfate dodecasaccharides. *Glycobiology* 26, 592–606. doi: 10.1093/glycob/cww008

Silbert, J. E., and Sugumaran, G. (2002). Biosynthesis of chondroitin/dermatan sulfate. *IUBMB Life* 54, 177–186.

Singh, J., Di Ferrante, N., Niebes, P., and Tavella, D. (1976). N-acetylgalactosamine-6-sulfate sulfatase in man. Absence of the enzyme in Morquio disease. *J. Clin. Invest.* 57, 1036–1040. doi: 10.1172/jci108345

Stern, R. (2003). Devising a pathway for hyaluronan catabolism: are we there yet? *Glycobiology* 13, 105R–115R.

Stern, R. (2004). Hyaluronan catabolism: a new metabolic pathway. *Eur. J. Cell Biol.* 83, 317–325. doi: 10.1078/0171-9335-00392

Stern, R., and Jedrzejas, M. J. (2006). Hyaluronidases: their genomics, structures, and mechanisms of action. *Chem. Rev.* 106, 818–839. doi: 10.1021/cr050247k

Sting, R., Schaufuss, P., and Blobel, H. (1990). Isolation and characterization of hyaluronidases from *Streptococcus dysgalactiae*, *S. zooepidemicus* and *S. equi*. *Zentralbl. Bakteriology* 272, 276–282. doi: 10.1016/s0934-8840(11)80028-9

Sugahara, K., and Kitagawa, H. (2000). Recent advances in the study of the biosynthesis and functions of sulfated glycosaminoglycans. *Curr. Opin. Struct. Biol.* 10, 518–527. doi: 10.1016/s0959-440x(00)00125-1

Sugahara, K., and Kojima, T. (1996). Specificity studies of bacterial sulfatases by means of structurally defined sulfated oligosaccharides isolated from shark cartilage chondroitin sulfate D. *Eur. J. Biochem.* 239, 865–870. doi: 10.1111/j.1432-1033.1996.0865u.x

Sugahara, K., and Mikami, T. (2007). Chondroitin/dermatan sulfate in the central nervous system. *Curr. Opin. Struct. Biol.* 17, 536–545. doi: 10.1016/j.sbi.2007.08.015

Sugahara, K., Mikami, T., Uyama, T., Mizuguchi, S., Nomura, K., and Kitagawa, H. (2003). Recent advances in the structural biology of chondroitin sulfate and dermatan sulfate. *Curr. Opin. Struct. Biol.* 13, 612–620. doi: 10.1016/j.sbi.2003.09.011

Sugimura, T., Kato, F., Mimatsu, K., Takenaka, O., and Iwata, H. (1996). Experimental chemonucleolysis with chondroitinase ABC in monkeys. *Spine* 21, 161–165. doi: 10.1097/00007632-199601150-00001

Sugiura, N., Ikeda, M., Shioiri, T., Yoshimura, M., Kobayashi, M., and Watanabe, H. (2013). Chondroitinase from baculovirus *Bombyx mori* nucleopolyhedrovirus and chondroitin sulfate from silkworm *Bombyx mori*. *Glycobiology* 23, 1520–1530. doi: 10.1093/glycob/cwt082

Sugiura, N., Setoyama, Y., Chiba, M., Kimata, K., and Watanabe, H. (2011). Baculovirus envelope protein odv-e66 is A novel chondroitinase with distinct substrate specificity. *J. Biol. Chem.* 286, 29026–29034. doi: 10.1074/jbc.m111.251157

Sullivan, W. J., Mullen, P. J., Schmid, E. W., Flores, A. A., Momcilovic, M., Sharpley, M. S., et al. (2018). Extracellular matrix remodeling regulates glucose metabolism through TXNIP destabilization. *Cell* 175, 117–132. doi: 10.1016/j.cell.2018.08.017

Takeuchi, J. (1972). Effect of chondroitinases on the growth of solid Ehrlich ascites tumour. *Br. J. Cancer Suppl.* 26, 115–119. doi: 10.1038/bjc.1972.17

Taylor, K. R., and Gallo, R. L. (2006). Glycosaminoglycans and their proteoglycans: host-associated molecular patterns for initiation and modulation of inflammation. *FASEB J.* 20, 9–22. doi: 10.1096/fj.05-4682rev

Theocharis, A. D., Skandalis, S. S., Tzanakakis, G. N., and Karamanos, N. K. (2010). Proteoglycans in health and disease: novel roles for proteoglycans in malignancy and their pharmacological targeting. *FEBS J.* 277, 3904–3923. doi: 10.1111/j.1742-4658.2010.07800.x

Thompson, J. N., Stoolmiller, A. C., Matalon, R., and Dorfman, A. (1973). N-Acetyl-β-hexosaminidase: role in the degradation of glycosaminoglycans. *Science* 181, 866–867. doi: 10.1126/science.181.4102.866

Tomatsu, S., Fukuda, S., Masue, M., Sukegawa, K., Fukao, T., Yamagishi, A., et al. (1991). Morquio disease: isolation, characterization and expression of full-length cDNA for human N-acetylgalactosamine-6-sulfate sulfatase. *Biochem. Biophys. Res. Commun.* 181, 677–683. doi: 10.1016/0006-291x(91)91244-7

Tribble, J. R., Williams, P. A., Caterson, B., Sengpiel, F., and Morgan, J. E. (2018). Digestion of the glycosaminoglycan extracellular matrix by chondroitinase ABC

supports retinal ganglion cell dendritic preservation in a rodent model of experimental glaucoma. *Mol. Brain* 11:69.

Trowbridge, J. M., and Gallo, R. L. (2002). Dermatan sulfate: new functions from an old glycosaminoglycan. *Glycobiology* 12, 117R–125R.

Trowbridge, J. M., Rudisill, J. A., Ron, D., and Gallo, R. L. (2002). Dermatan sulfate binds and potentiates activity of keratinocyte growth factor (FGF-7). *J. Biol. Chem.* 277, 42815–42820. doi: 10.1074/jbc.m204959200

Tully, S. E., Rawat, M., and Hsieh-Wilson, L. (2006). Discovery of a TNF-α antagonist using chondroitin sulfate microarrays. *J. Am. Chem. Soc.* 128, 7740–7741. doi: 10.1021/ja061906t

Ueoka, C., Kaneda, N., Okazaki, I., Nadanaka, S., Muramatsu, T., and Sugahara, K. (2000). Neuronal cell adhesion, mediated by the heparin-binding neuroregulatory factor midkine, is specifically inhibited by chondroitin sulfate E. Structural ans functional implications of the over-sulfated chondroitin sulfate. *J. Biol. Chem.* 275, 37407–37413. doi: 10.1074/jbc.m002538200

Ulmer, J. E., Vilen, E. M., Namburi, R. B., Benjdia, A., Beneteau, J., Malleron, A., et al. (2014). Characterization of glycosaminoglycan (GAG) sulfatases from the human gut symbiont *Bacteroides thetaiotaomicron* reveals the first gag-specific bacterial endosulfatase. *J. Biol. Chem.* 289, 24289–24303. doi: 10.1074/jbc.m114.573303

Valcarcel, J., Novoa-Carballal, R., Pérez-Martín, R. I., Reis, R. L., and Vázquez, J. A. (2017). Glycosaminoglycans from marine sources as therapeutic agents. *Biotechnol. Adv.* 35, 711–725. doi: 10.1016/j.biotechadv.2017.07.008

Volpi, N. (2007). Analytical aspects of pharmaceutical grade chondroitin sulfates. *J. Pharm. Sci.* 96, 3168–3180. doi: 10.1002/jps.20997

Volpi, N. (2009). Quality of different chondroitin sulfate preparations in relation to their therapeutic activity. *J. Pharm. Pharmacol.* 61, 1271–1280. doi: 10.1211/jpp.61.10.0002

Wang, H., Katagiri, Y., McCann, T. E., Unsworth, E., Goldsmith, P., Yu, Z. X., et al. (2008). Chondroitin-4-sulfation negatively regulates axonal guidance and growth. *J. Cell Sci.* 121, 3083–3091. doi: 10.1242/jcs.032649

Wang, S., Guan, J., Zhang, Q., Chen, X., and Li, F. (2019a). Identification and signature sequences of bacterial delta (4,5) hexuronate-2-O-sulfatases. *Front. Microbiol.* 10:704. doi: 10.3389/fmicb.2019.00704

Wang, S., Su, T., Zhang, Q., Guan, J., He, J., Gu, L., et al. (2019b). Comparative study of two chondroitin sulfate/dermatan sulfate 4-O-sulfatases with high identity. *Front. Microbiol.* 10:1309. doi: 10.3389/fmicb.2019.01309

Wang, W., Cai, X., Han, N., Han, W., Sugahara, K., and Li, F. (2017). Sequencing of chondroitin sulfate oligosaccharides using a novel exolyase from a marine bacterium that degrades hyaluronan and chondroitin sulfate/dermatan sulfate. *Biochem. J.* 474, 3831–3848. doi: 10.1042/bcj20170591

Wang, W., Han, W., Cai, X., Zheng, X., Sugahara, K., and Li, F. (2015). Cloning and characterization of a novel chondroitin sulfate/dermatan sulfate 4-O-endosulfatase from a marine bacterium. *J. Biol. Chem.* 290, 7823–7832. doi: 10.1074/jbc.m114.629154

Whiteman, D. A., and Kimura, A. (2017). Development of idursulfase therapy for mucopolysaccharidosis type II (Hunter syndrome): the past, the present and the future. *Drug Des. Dev. Ther.* 11, 2467–2480. doi: 10.2147/dddt.s139601

Wicker, G., Prill, V., Brooks, D., Gibson, G., Hopwood, J., von Figura, K., et al. (1991). Mucopolysaccharidosis VI (Maroteaux-Lamy syndrome). An intermediate clinical phenotype caused by substitution of valine for glycine at position 137 of arylsulfatase B. *J. Biol. Chem.* 266, 21386–21391.

Wilson, P. J., Morris, C. P., Anson, D. S., Occhiodoro, T., Bielicki, J., Clements, P. R., et al. (1990). Hunter syndrome: isolation of an iduronate-2-sulfatase cDNA clone and analysis of patient DNA. *Proc. Natl. Acad. Sci. U.S.A.* 87, 8531–8535. doi: 10.1073/pnas.87.21.8531

Wood, K. M., Wusteman, F. S., and Curtis, C. G. (1973). The degradation of intravenously injected chondroitin 4-sulfate in the rat. *Biochem. J.* 134, 1009–1013. doi: 10.1042/bj1341009

Yamada, S. (2015). Role of hyaluronidases in the catabolism of chondroitin sulfate. *Adv. Exp. Med. Biol.* 842, 185–197. doi: 10.1007/978-3-319-11280-0_12

Yamagata, T., Saito, H., Habuchi, O., and Suzuki, S. (1968). Purification and properties of bacterial chondroitinases and chondrosulfatases. *J. Biol. Chem.* 243, 1523–1535.

Yamaguchi, K., Tamaki, H., and Fukui, S. (2006). Detection of oligosaccharide ligands for hepatocyte growth factor/scatter factor (HGF/SF), keratinocyte growth factor (KGF/FGF-7), RANTES and heparin cofactor II by neoglycolipid microarrays of glycosaminoglycan-derived oligosaccharide fragments. *Glycoconj. J.* 23, 513–523. doi: 10.1007/s10719-006-7151-z

Yamauchi, S., Mita, S., Matsubara, T., Fukuta, M., Habuchi, H., Kimata, K., et al. (2000). Molecular cloning and expression of chondroitin 4-sulfotransferase. *J. Biol. Chem.* 275, 8975–8981. doi: 10.1074/jbc.275.12.8975

Yin, F.-X., Wang, F.-S., and Sheng, J.-Z. (2016). Uncovering the catalytic direction of chondroitin AC exolyase: from the reducing end towards the non-reducing end. *J. Biol. Chem.* 291, 4399–4406. doi: 10.1074/jbc.c115.708396

Yoo, M., Khaled, M., Gibbs, K. M., Kim, J., Kowalewski, B., Dierks, T., et al. (2013). Arylsulfatase B improves locomotor function after mouse spinal cord injury. *PLoS ONE* 8:e57415. doi: 10.1371/journal.pone.0057415

Zhang, X., Liu, H., Yao, W., Meng, X., and Li, Z. (2019). Semisynthesis of chondroitin sulfate oligosaccharides based on the enzymatic degradation of chondroitin. *J. Org. Chem.* 84, 7418–7425. doi: 10.1021/acs.joc.9b00112

Zhu, C., Zhang, J., Zhang, J., Jiang, Y., Shen, Z., Guan, H., et al. (2017). Purification and characterization of chondroitinase ABC from *Acinetobacter* sp C26. *Int. J. Biol. Macromol.* 95, 80–86. doi: 10.1016/j.ijbiomac.2016.10.044

Conflict of Interest: The authors declare that the research was conducted in the absence of any commercial or financial relationships that could be construed as a potential conflict of interest.

frontiers in Cell and Developmental Biology

PERSPECTIVE
published: 12 January 2021
doi: 10.3389/fcell.2020.567358

Chondroitin Sulfate as a Potential Modulator of the Stem Cell Niche in Cornea

Sean Ashworth[1,2], Jodie Harrington[1,3], Greg M. Hammond[1], Kiranjit K. Bains[1], Elena Koudouna[1], Anthony J. Hayes[2], James R. Ralphs[2], Justyn W. Regini[1], Robert D. Young[1], Ryuhei Hayashi[3,4], Kohji Nishida[4], Clare E. Hughes[2] and Andrew J. Quantock[1]*

[1] Structural Biophysics Group, School of Optometry and Vision Sciences, College of Biomedical and Life Sciences, Cardiff University, Cardiff, United Kingdom, [2] School of Biosciences, College of Biomedical and Life Sciences, Cardiff University, Cardiff, United Kingdom, [3] Department of Stem Cells and Applied Medicine, Osaka University Graduate School of Medicine, Osaka, Japan, [4] Department of Ophthalmology, Osaka University Graduate School of Medicine, Osaka, Japan

OPEN ACCESS

Edited by:
Jeremy Turnbull,
University of Liverpool,
United Kingdom

Reviewed by:
Andreas Faissner,
Ruhr University Bochum, Germany
Shuji Mizumoto,
Meijo University, Japan

***Correspondence:**
Clare E. Hughes
HughesCE1@cf.ac.uk

Specialty section:
This article was submitted to Signaling, a section of the journal Frontiers in Cell and Developmental Biology

Received: 29 May 2020
Accepted: 07 December 2020
Published: 12 January 2021

Citation:
Ashworth S, Harrington J, Hammond GM, Bains KK, Koudouna E, Hayes AJ, Ralphs JR, Regini JW, Young RD, Hayashi R, Nishida K, Hughes CE and Quantock AJ (2021) Chondroitin Sulfate as a Potential Modulator of the Stem Cell Niche in Cornea. Front. Cell Dev. Biol. 8:567358. doi: 10.3389/fcell.2020.567358

Chondroitin sulfate (CS) is an important component of the extracellular matrix in multiple biological tissues. In cornea, the CS glycosaminoglycan (GAG) exists in hybrid form, whereby some of the repeating disaccharides are dermatan sulfate (DS). These CS/DS GAGs in cornea, through their presence on the proteoglycans, decorin and biglycan, help control collagen fibrillogenesis and organization. CS also acts as a regulatory ligand for a spectrum of signaling molecules, including morphogens, cytokines, chemokines, and enzymes during corneal growth and development. There is a growing body of evidence that precise expression of CS or CS/DS with specific sulfation motifs helps define the local extracellular compartment that contributes to maintenance of the stem cell phenotype. Indeed, recent evidence shows that CS sulfation motifs recognized by antibodies 4C3, 7D4, and 3B3 identify stem cell populations and their niches, along with activated progenitor cells and transitional areas of tissue development in the fetal human elbow. Various sulfation motifs identified by some CS antibodies are also specifically located in the limbal region at the edge of the mature cornea, which is widely accepted to represent the corneal epithelial stem cell niche. Emerging data also implicate developmental changes in the distribution of CS during corneal morphogenesis. This article will reflect upon the potential roles of CS and CS/DS in maintenance of the stem cell niche in cornea, and will contemplate the possible involvement of CS in the generation of eye-like tissues from human iPS (induced pluripotent stem) cells.

Keywords: cornea, chondroitin sulfate, proteoglycan, glycosaminoglcyan, stem cell niche, human iPS cells

INTRODUCTION

Proteoglycans form key components of the extracellular matrix, typically consisting of a protein core with one or more covalently attached glycosaminoglycan (GAG) chains. These molecules play vital roles in cell-cell signaling, tissue homeostasis and wound healing. Chondroitin sulfate/dermatan sulfate (CS/DS) and certain sulfation motifs of these GAG species are present in the stem cell niche in various tissues (Hayes et al., 2008, 2016; Caterson, 2012; Melrose et al., 2012),

and reportedly influence progenitor and stem cell function in composite tissue scaffolds (Farrugia et al., 2018). The importance of CS/DS as a structural extracellular matrix component in the cornea is fairly well-established (Lewis et al., 2010; Chen and Birk, 2011; Parfitt et al., 2011; Chen et al., 2014, 2015), but its potential role in the maintenance and development of the stem cell niche in cornea has been little studied until recently.

The cornea is the transparent tissue at the front of the eye. In humans, it is ∼0.5 mm thick and 11–12 mm in diameter, wherein it merges with the white sclera of the eye at an anatomical region known as the limbus. The bulk of the cornea is composed of a collagen-rich extracellular matrix – the corneal stroma – that contains ∼250 stacked and interwoven sheets or lamellae, made up of uniformly thin (∼30 nm diameter), and regularly-spaced, hybrid type I/V collagen fibrils. CS/DS and keratan sulfate (KS) proteoglycans associate with collagen fibrils to maintain the characteristic collagen architecture essential for transparency of the corneal stroma (Kao et al., 2006; Hassell and Birk, 2010; Lewis et al., 2010; Quantock et al., 2010; Meek and Knupp, 2015). The anterior-most region of the corneal stroma in most species is a thin, acellular, disorganized meshwork of collagen fibrils called Bowman's layer, which is integral at its distal limit with a basement membrane that supports the corneal epithelium. An intact and properly stratified corneal epithelium is vital for clear vision. Throughout life, superficial corneal epithelial cells are constantly shed into the tear film, a loss that is counteracted by replenishment by a population of corneal epithelial stem cells at the limbus (Kinoshita et al., 2001).

THE CORNEAL LIMBAL STEM CELL NICHE

The concept of a limbal stem cell niche (**Figure 1**) was first proposed almost 50 years ago, as a regenerative source of epithelial cells migrating centrally from a distinct, pigmented region of the peripheral cornea (Davanger and Evensen, 1971). Further work revealed a distinct side-population of slow-cycling cells within the basal layer of corneal limbal epithelium, which appeared to be responsible for centripetal migration of epithelium and the restoration of the corneal surface in wound healing (Cotsarelis et al., 1989; Dua and Forrester, 1990). These cells were subsequently distinguished by virtue of their small size, characteristically high nucleus to cytoplasmic ratio, and expression of various stem cell markers such as ABCG2 or p63 and its various isoforms (Romano et al., 2003; Watanabe et al., 2004; Di Iorio et al., 2005; Kawakita et al., 2009). Further markers include ABCB5, which is essential for limbal epithelial stem cell maintenance and development; cells isolated using this marker are able to restore the cornea in limbal epithelial stem cell-deficient mouse models (Ksander et al., 2014). A 3D structural analysis has further elucidated the architecture of the limbal stem cell niche, revealing the presence of limbal crypts circumferentially around the eye, interspaced alongside distal invaginations of stromal extracellular matrix, termed the palisades of Vogt (Grieve et al., 2015). The identification of limbal epithelial stem cells has galvanized the study of these cells for therapeutic purposes to treat various corneal epithelial diseases (Pellegrini et al., 1997; Bains et al., 2019; Le et al., 2020).

Damage or loss of resident corneal epithelial stem cells, either through disease or injury, can lead to a limbal stem cell deficiency that ultimately results in corneal blindness, necessitating corneal surgery to restore vision. Transplantation is one treatment option for late-stage corneal pathology, however, this carries the risk of tissue rejection. Moreover, there is a distinct lack of donor tissue, with only one cornea available for every 70 required for transplantation worldwide (Gain et al., 2016). For this reason, other therapies have been investigated, including *ex vivo* expanded limbal epithelial stem cell transplantation (autograft or allograft), and the generation of an epithelial multilayer derived from oral mucosal epithelium (Oie and Nishida, 2016; Bains et al., 2019), or induced pluripotent stem cells (Hayashi et al., 2016, 2017). Whilst these pioneering technologies have shown great clinical promise, they could be further optimized by careful manipulation of culture conditions for these regenerative cells, as well as through their selection. A further potential avenue of exploration from a tissue engineering standpoint might be recreating an extracellular matrix microenvironment of the limbal stem cell niche seeded with isolated corneal limbal epithelial stem cells or induced pluripotent stem (iPS) cell derived-corneal epithelial cells.

The limbal region of the cornea also harbors a population of mesenchymal stem cells, termed corneal stromal stem cells, in the extracellular matrix subjacent to the corneal epithelial stem cell niche (Du et al., 2005). Electron microscopy has provided evidence for direct connections between corneal epithelial and stromal cells at the limbus that traverse the epithelial basement membrane (Higa et al., 2013; Dziasko et al., 2014; Yamada et al., 2015). This, along with the results of studies of the behavior of limbal epithelial and stromal cells in culture, has led to the notion of a multicellular limbal niche complex at the edge of the cornea involving both epithelial and stromal cells (Hertsenberg and Funderburgh, 2015; Dziasko and Daniels, 2016; Funderburgh et al., 2016). Work with bovine cells from the corneal stroma in culture has shown that ^{35}S-labeled CS/DS, when measured by sensitivity to chondroitinase ABC, is increased 3–3.5-fold in activated fibroblasts and myofibroblasts compared with quiescent keratocytes (Funderburgh et al., 2003). To the best of our knowledge, however, the association between corneal stromal stem cells and CS has not been directly investigated. Nevertheless, it is noteworthy that the peripheral human cornea and limbus, where corneal stromal stem cells reside, contain less acidic GAG than the central cornea, primarily because KS levels are decreased (Borcherding et al., 1975). This work also indicated that chondroitin was replaced by CS at the limbus and that DS was present at detectable levels. More recently, immunohistochemistry was conducted to probe the composition of the bovine corneal stroma in which monoclonal antibody 2B6 was utilized after (i) chondroitinase ABC treatment to identify CS and DS, (ii) chondroitinase ACII treatment to identify CS, and (iii) chondroitinase B treatment to identify DS (Ho et al., 2014). This revealed that DS was present throughout the corneal stroma and into the sclera, with CS detected toward the outer periphery of the cornea and the limbus.

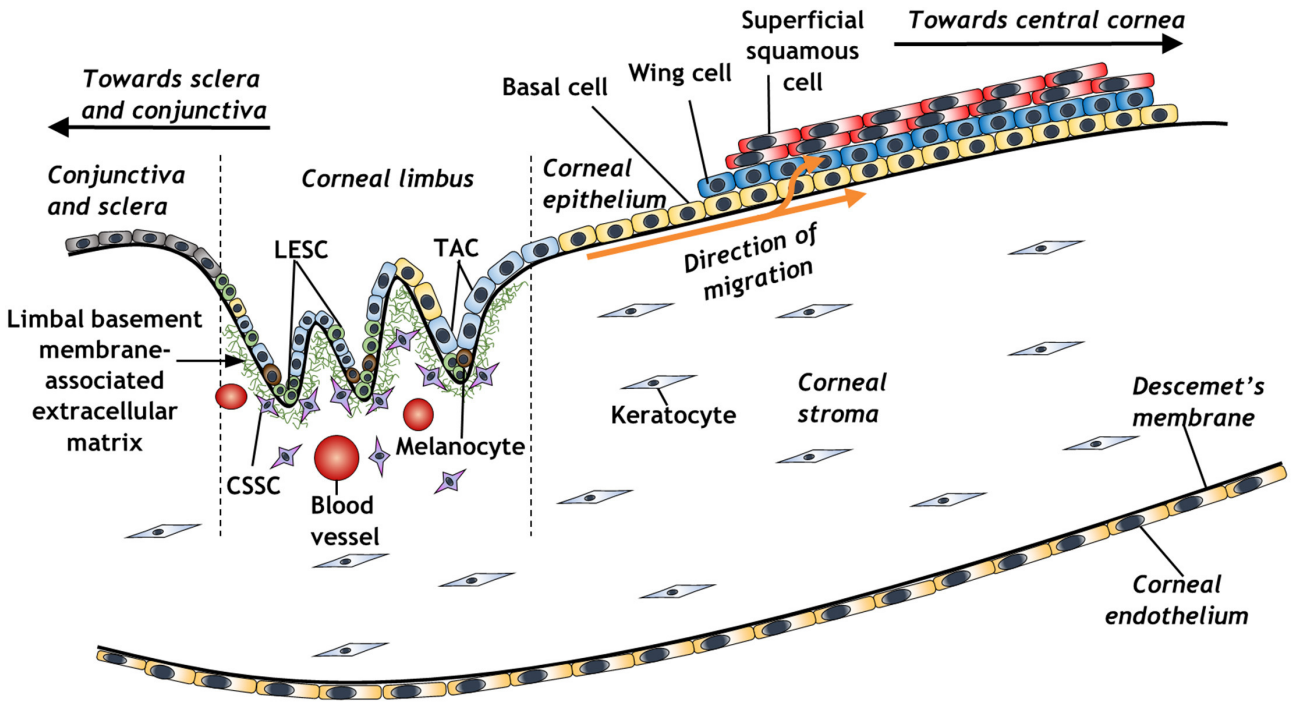

FIGURE 1 | Schematic representation of the corneal limbal stem cell niche and some of its constituent elements (LESC, limbal epithelial stem cell; CSSC, corneal stromal stem cell; TAC, transient amplifying cell).

Investigations enabling us to accurately recreate the microenvironment of the limbal stem cell niche would be of great scientific value, not only in terms of understanding the biological functions of different components of this environment, but also because of the potential in regenerative medicine. To this end, various attempts have been made to elucidate the extracellular matrix molecules and cell-cell interactions that are important for the maintenance of the corneal limbal stem cell niche. Indeed, the corneal limbus has a distinct extracellular matrix profile compared to the central cornea and conjunctiva (Schlötzer-Schrehardt et al., 2007; Mei et al., 2012). CS, amongst other matrix molecules such as laminin isoforms and tenascin-C, are enriched at the corneal limbus where they co-localize with putative stem and progenitor cells in the basal limbal epithelium (Schlötzer-Schrehardt et al., 2007). The importance of tenascin-C in several stem cell niches has been well-documented, particularly within neural and hematopoietic environments (Seiffert et al., 1998; Garcion et al., 2001; Chiquet-Ehrismann et al., 2014). Tenascin-C, as mentioned, has been identified in the corneal limbal stem cell niche (Maseruka et al., 2000), and its spatial and temporal expression during development and wound healing, aligned to its presence in the adult limbus (Maseruka et al., 1997; Ljubimov et al., 1998; Ding et al., 2008) advocate a potential role in the self-renewal and differentiation of stem cells. It is likely that this can be achieved by providing a favorable stem cell microenvironment via interactions with other extracellular matrix components such as fibronectin (Hunt et al., 2012; Singh and Schwarzbauer, 2012) and CS, with an association between tenascin and CS having been reported in experimental models of neural repair (Gates et al., 1996).

CHONDROITIN SULFATE/DERMATAN SULFATE STRUCTURE AND ANTIBODIES

CS and CS/DS GAG structures are typically heterogeneous and polydisperse from molecule to molecule. The disaccharide repeat unit of CS consists of a (hex)uronic acid (glucuronic) and a hexosamine (galactosamine, typically N-acetylated), whilst in DS disaccharides the D-glucuronic acid residue is converted to αL-iduronic acid, yielding DS. Linkage of these CS disaccharide units occurs through ß3-linkage (GlcAß3GalNAc), whilst DS is through ∂3 -linkage (IdoA∂3GalNAc) (Caterson, 2012). CS/DS heterogeneity is further generated through sulfation of hydroxyl groups at positions 2, 4 and C6 on the sugar molecules, giving rise to great structural diversity (Sugahara et al., 2003; Hayes et al., 2018). Indeed, recent estimates from Persson et al. (2020) suggest, with a chain of 50 CS/DS disaccharides, an estimated 16^{50} theoretical variants arise from sixteen possible disaccharide variants. Such structural diversity is believed to be responsible for the ability of CS/DS to interact with a range of growth factors, morphogens, cytokines and chemokines, to potentially help regulate cell proliferation, cell differentiation, and tissue development (Nandini and Sugahara, 2006; Caterson, 2012; Purushothaman et al., 2012; Hayes et al., 2018; Karamanos et al.,

2018). In a number of tissues, cornea included, CS exists as a co-polymer with DS forming CS/DS hybrid GAGs (Habuchi et al., 1973; Inoue and Iwasaki, 1976). An ability to recognize different sulfation patterns on CS or CS/DS is useful for the study of structurally diverse CS/DS isoforms within a tissue, and a range of monoclonal antibodies have been developed to help with this endeavor (Sorrell et al., 1990). For example, antibodies 6C3, 4C3, 7D4, and 3B3 (Caterson et al., 1985), can recognize distinct, native (i.e. non-chondroitinase-digested) and non-native (i.e., chondroitinase-digested) epitopes on CS/DS chains.

Some examples of these antibodies and the location of their respective CS/DS binding sites are shown in **Figure 2** along with a simplified structure of a typical CS/DS hybrid chain, the location of the binding site having been deciphered by sequential enzymatic digestion. Other CS antibodies developed in our lab include 4D3 and 3B5, which also recognize a specific pattern of carbon sulfation on sequential sugar molecules within a polysaccharide chain (Sorrell et al., 1990). Whilst the exact epitope for some of these antibodies remains to be elucidated, other studies of D-type CS antibodies (which bind sites of sulfation on carbon-2 of the glucuronic acid and carbon-6 of the *N*-acetylgalactosamine sugar) have indicated they require at least an hexasaccharide (in the case of 473HD), or octasaccharide (in the case of CS-56 and MO-225), to bind and recognize a specific tetrasaccharide within the chain (Ito et al., 2005). Whilst useful, it is important to note that the flanking regions of the recognized tetrasaccharide can affect antibody affinity and *in vivo* growth factor binding. This results in overlapping oligosaccharide binding regions, termed "wobble motifs," further increasing the complexity of epitope definition and discussed in more detail elsewhere (Caterson, 2012; Purushothaman et al., 2012).

Immunohistochemical investigations using these and other antibodies have disclosed that a number of stem cell niches exhibit specific or preferential sulfation patterns. For example, in human skin, the 6C3 epitope is located just below the basal lamina of the epidermis, adjacent to resident epidermal stem cells (Sorrell et al., 1990). This is of particular interest, given the similarities between epidermal stem cells and limbal epithelial stem cells, which both form a stratified epithelium that expresses the p63 stem cell marker (Pellegrini et al., 2001). Also, of note, is the finding that epidermal stem cells can convert into corneal epithelial-like cells when placed in corneal tissue (Gao et al., 2007). CS GAGs are also present in primordial stem cell populations in fetal tissue, such as hair bulbs and perichondrium (Hayes et al., 2016), allowing us to hypothesize a potential role for CS in maintenance of the corneal limbal stem cell niche.

CHONDROITIN SULFATE IN THE CORNEAL LIMBAL STEM CELL NICHE

Whilst much work has focused on the role of CS in the corneal stroma, less attention has been paid to a potential role for CS in the stem cell niche of the corneal limbus. The main CS proteoglycans present in cornea are decorin and biglycan, which are expressed widely throughout the corneal stroma, with biglycan levels decreasing toward maturity. CS in the cornea helps define stromal architecture, and decorin and biglycan null mice have significantly disrupted collagen ultrastructure (Zhang et al., 2009). Similar effects are seen in biglycan/lumican null mice, which display significant corneal opacity compared to mice with single proteoglycan knockouts (Chen et al., 2014).

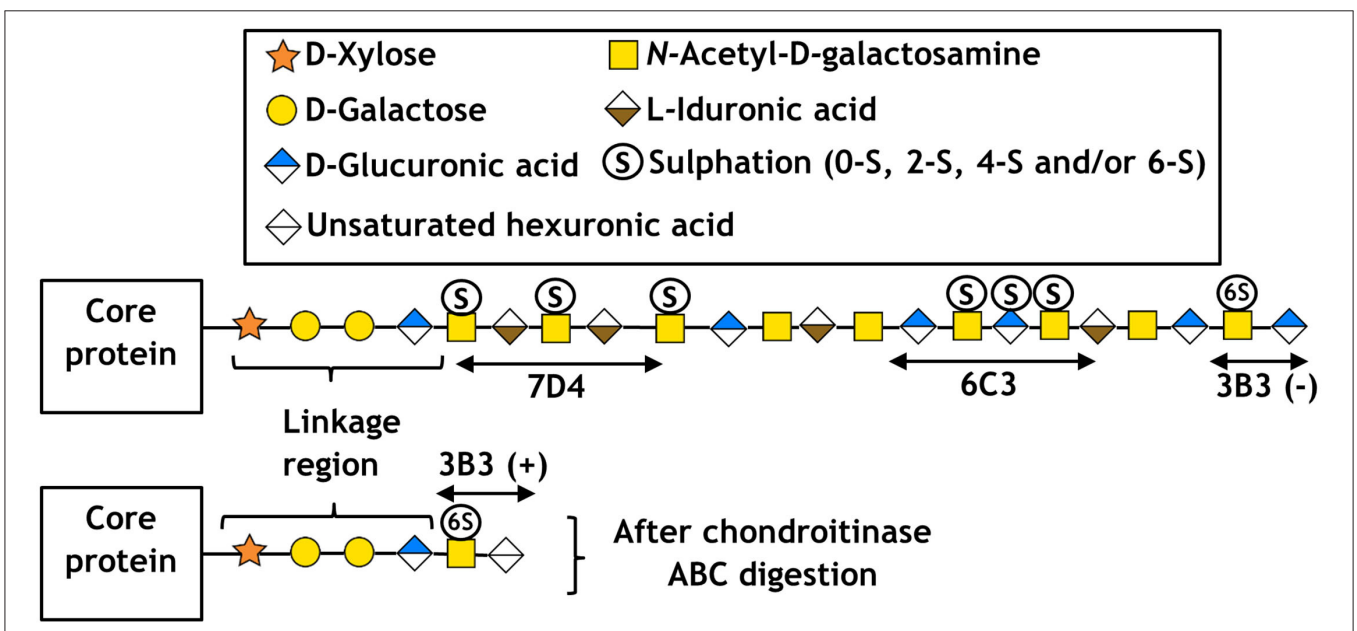

FIGURE 2 | Schematic of CS/DS following the symbol nomenclature for the graphical representation of glycans (Varki et al., 2015), including the approximate location of epitopes for antibodies 7D4, 6C3, and 3B3. Respectively, (+) and (–) indicate with and without chondroitinase ABC digestion.

In terms of overall GAG distribution, the cornea is primarily constituted of KS GAG (both high and low sulfated forms), with CS/DS hybrid GAGs also present in slightly lower quantities, and with CS located preferentially toward the limbus (Ho et al., 2014). Heparan sulfate has also been shown to play a role in maintenance of the corneal epithelium, as its absence results in reduced corneal epithelial wound repair and improper stratification of epithelial cells (Coulson-Thomas et al., 2015).

In order to determine in more detail the specific pattern of CS distribution within the cornea, previous work by our group used the aforementioned panel of CS antibodies to map CS/DS in rabbit corneas (Yamada et al., 2015). The rabbit eye, however, differs in its microanatomy to that of human cornea and lacks a series of limbal epithelial crypts that are located circumferentially around the limbus and which form the palisades of Vogt. Limbal crypts are essentially downward focal projections of epithelial cells into the underlying extracellular matrix and run around the periphery of the cornea. The porcine limbus is believed to have a series of epithelial crypts, which is somewhat analogous to that of the human cornea. However, the positioning of the crypts around the limbal circumference of the pig eye is debated (Notara et al., 2011; Grieve et al., 2015), and new evidence about their size, shape and circumferential extent is adding to this debate (Hammond et al., unpublished results). Porcine corneas are closer in size to human corneas with a similar anatomical structure (Sanchez et al., 2011) and protein composition (Sharifi et al., 2019), thus their obvious value for corneal research. Both porcine and human corneas have a Bowman's layer – a thin, acellular layer of the distal corneal stroma immediately subjacent to the corneal epithelial basement membrane – as demonstrated by recent high-resolution investigations (Hammond et al., 2020). Bowman's layer is often missing in many other species commonly used for corneal research (Hayashi et al., 2002), identifying the pig as a reasonable animal model.

Native CS sulfation motifs identified by the antibodies 7D4 and 6C3 were detected in the porcine cornea (**Figures 3A,C**), specifically at the limbus in the case of 6C3 (**Figure 3C**), as was observed in the presumptive stem cell niche in rabbit cornea (Yamada et al., 2015). 3B3, an antibody recognizing non-native, chondroitinase ABC-digested stubs without digestion of a terminal disaccharide of the CS chain (6-*O*-sulfated *N*-acetylgalactosamine adjacent to the terminal glucuronate), also appeared to label CS structures surrounding the limbal niche (**Figure 3F**). The 6C3 CS epitope also localized in close proximity to putative limbal epithelial stem cells, as identified by two markers, ABCB5 and keratin 19 (**Figures 3G,H**). Although these are preliminary data, such co-localization of an extracellular matrix component and putative stem cell identifiers is an interesting discovery, which invites speculation as to a causal link in terms of the potential for the matrix to define a milieu that favorably sustains stem cell expression. With this in mind and as alluded to earlier, we also note that mesenchymal stem cells have been identified in the corneal stroma, subjacent to the basement membrane at the limbus, and are hypothesized to be supportive of the resident limbal epithelial stem cells (Du et al., 2005; Pinnamaneni and Funderburgh, 2012; Funderburgh et al., 2016). We speculate whether the 6C3 antibody might recognize cell surface-associated CS on corneal stromal stem cells or sub-epithelial stromal melanocytes that, when present within the epithelium, have been shown to be supportive of the limbal epithelial stem cell population (Dziasko et al., 2015). Ongoing studies will serve to better characterize CS in the limbal environment and aim to clarify its involvement as a potential modulator of the stem cell niche.

CHONDROITIN SULFATE AND REGENERATIVE MEDICINE

In recent years, CS has been highlighted as essential for the functional integrity of pluripotent and multipotent stem cells, and as an important factor in the maintenance of pluripotency and differentiation propensity. For example, when CS is depleted through genetic knockout or removed by enzymatic digestion, mouse embryonic stem cells become arrested in a pluripotent state and are unable to differentiate. The addition of exogenous CS, however, recovers the differentiation propensity thus pointing to an influential role for CS in pluripotent stem cell biology (Izumikawa et al., 2014). Accordingly, CS has considerable relevance to both embryological development and stem cell biology and has been shown to be implicated in the differentiation and proliferation of multipotent stem cells from a range of tissues. Many of these studies focus on neural-derived tissue and have indicated that the removal of CS through enzymatic degradation, typically using chondroitinase ABC, can have a marked effect on neural progenitor/stem cell proliferation, differentiation and migration. The mechanism is believed to be mediated by fibroblast growth factor-2 (FGF-2) and epidermal growth factor (EGF) (Sirko et al., 2007, 2010; Gu et al., 2009). Removal of CS can also cause spontaneous differentiation of oligodendrocyte precursor cells (Karus et al., 2016), whilst the disruption of CS/DS in mesenchymal stem cells has been shown to influence osteogenic differentiation (Manton et al., 2007). Owing to the localization of specific CS motifs in corneal limbal stroma, we speculate that these molecules could potentially facilitate maintenance of corneal limbal epithelial stem cells and/or potentiate their differentiation from iPS cells *in vitro*. Various researchers have developed differentiation protocols for generating corneal epithelium from both pluripotent and multipotent stem cells. Initial attempts involved recreating the limbal niche using collagen IV and limbal fibroblast-conditioned medium to differentiate pluripotent stem cells toward a corneal epithelial phenotype. However, the cells generated were not very robust and differed from native corneal epithelium (Ahmad et al., 2007).

Other studies using pluripotent stem cells generated improved corneal epithelial-like cells that displayed corneal epithelial markers (K3/K12 and Pax-6), and showed how the regulation of *PAX6* is critical for *in vitro* differentiation (Hayashi et al., 2012; Shalom-Feuerstein et al., 2012; Brzeszczynska et al., 2014). Whilst promising, these studies failed to take into account the elaborate nature of whole eye development with the

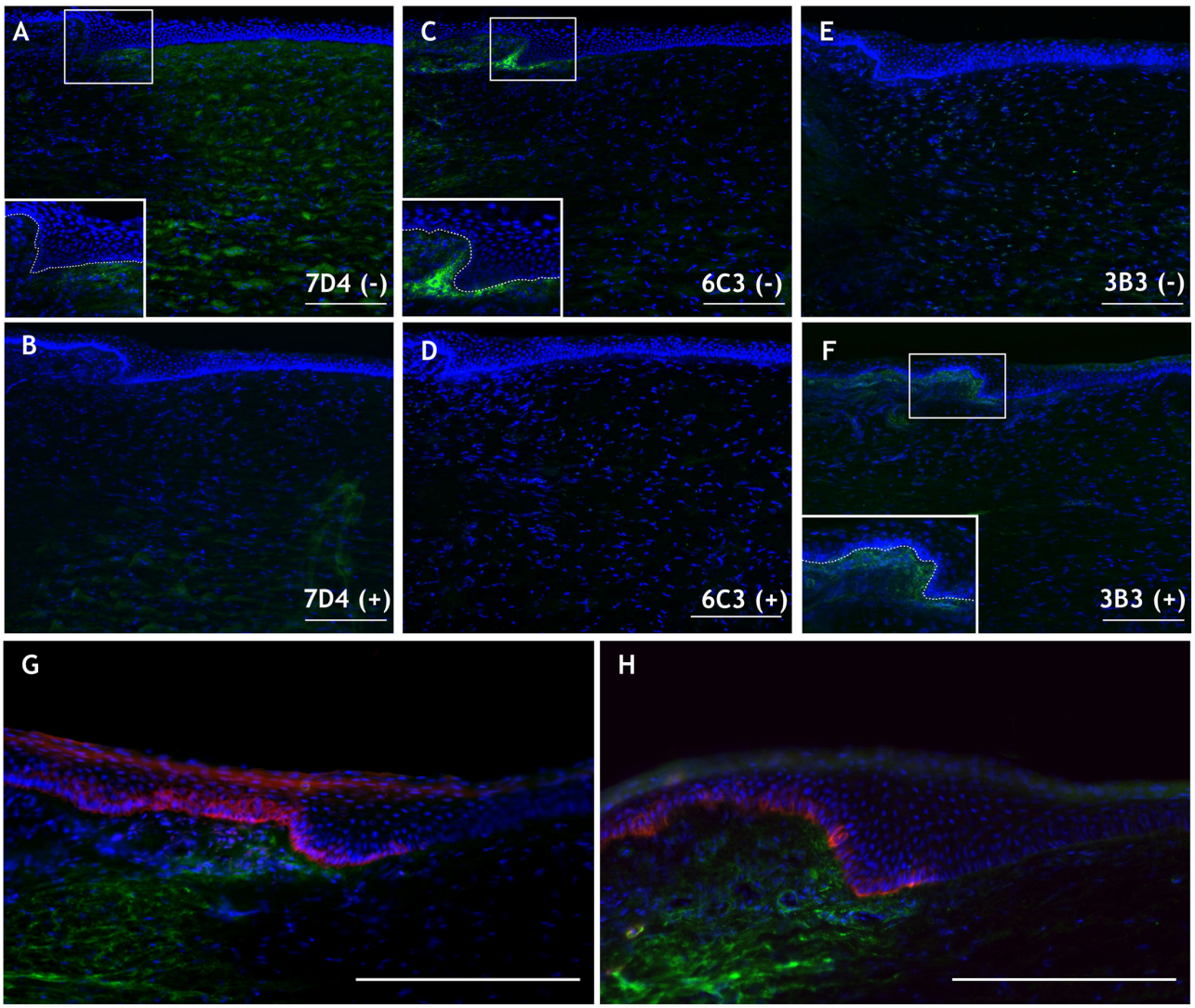

FIGURE 3 | Immunohistochemical images of the peripheral porcine cornea (located to the right in each panel) and limbus. **(A,C,E)** Native 7D4, 6C3, and 3B3 epitope localization is shown in green without [i.e., (–)] chondroitinase ABC pretreatment. **(B,D,F)** Staining with the same antibodies following chondroitinase ABC treatment [i.e., (+)], which removes 7D4 and 6C3 epitopes and exposes the 3B3 epitope. Inlays in **(A,C,F)** magnify the limbal region (white box) and delineate the epithelial basement membrane (dashed line). **(G,H)** 6C3 (green) is localized in close proximity to stem cell markers ABCB5 **(G)** and keratin 19 **(H)** (both red). Scale bars = 200 μm. DAPI is employed as a nuclear stain shown in blue. Methods and negative control images with primary antibodies omitted are provided as **Supplementary Material**.

plethora of spatial and temporal developmental cues that occur between distinct cell types. One recently-developed method demonstrated that human iPS cells can give rise to self-forming ectodermal autonomous multi-zones (SEAMs), representing concentric zones of cells of distinct ocular lineages, including cells that resemble those of the corneal epithelium (Hayashi et al., 2016, 2017; **Supplementary Video**). In the original discovery of SEAM formation (Hayashi et al., 2016), which was modified by other researchers (Li et al., 2019), the cellular zones represented neuronal lineages (innermost zone 1), retina-like and neural crest-like cells (zone 2, more peripherally), ocular surface ectoderm-like cells (zone 3, more peripherally still), and finally non-ocular surface epithelial-like cells in the outermost zone 4. Lens-like cells appeared at the borders of SEAM zones 2 and 3.

Further work involving manipulation within the substrate of laminin, another extracellular matrix molecule present in basement membrane of the corneal limbus, showed that different isoforms differentially influence the differentiation propensity of corneal epithelial cells derived from human iPS cells (Shibata et al., 2018). Laminin can also influence cell phenotype based upon the selective adhesiveness of the

cells toward various substrates (Shibata et al., 2020). We also note, in relation to the eye, that both CS and laminin are temporally and spatially expressed during optic nerve regeneration in fish (Battisti et al., 1992), and more recently have been applied in the expansion of corneal endothelial cells for potential transplantation (Kennedy et al., 2019). In addition, CS and laminin are suggested to have counteractive roles in precursor cell differentiation, due to regulation of the β1-integrin signaling pathway (Sun et al., 2017), which highlights potential impacting interactions (indirect and/or direct) between these ECM molecules. As mentioned, laminin influences SEAM development, and some recent preliminary data indicate that CS, too, is likely involved in the differentiation of human iPS cells in a developing SEAM as it is increasingly deposited from weeks 4–6 (**Figure 4**). Specifically, the CS moiety revealed by 7D4 was detected in SEAM zones 3, outward to zone 4 (**Figures 4A–C**). Furthermore, CS is ubiquitously deposited into the surrounding matrix by week 6 (**Figure 4D**). Thus, facilitating deposition or exogenous supply of CS, could potentially be used to modulate differentiation of human iPS cells in SEAMs.

Whilst the application of CS to bioengineered scaffolds and its use to promote cell differentiation is not new, there are few investigations into defined species of CS and their influence on stem cell differentiation in the context of the corneal epithelium. Also, seldom considered is the fact that commercially prepared CS can often contain significant impurities, for example KS (Santos et al., 2017). Essentially, there has been relatively little detailed exploration into possible modulatory roles for CS, or indeed other GAGs, within the corneal limbal stem cell niche, but emerging knowledge will provide an enhanced understanding of the influence of CS upon the behavior of

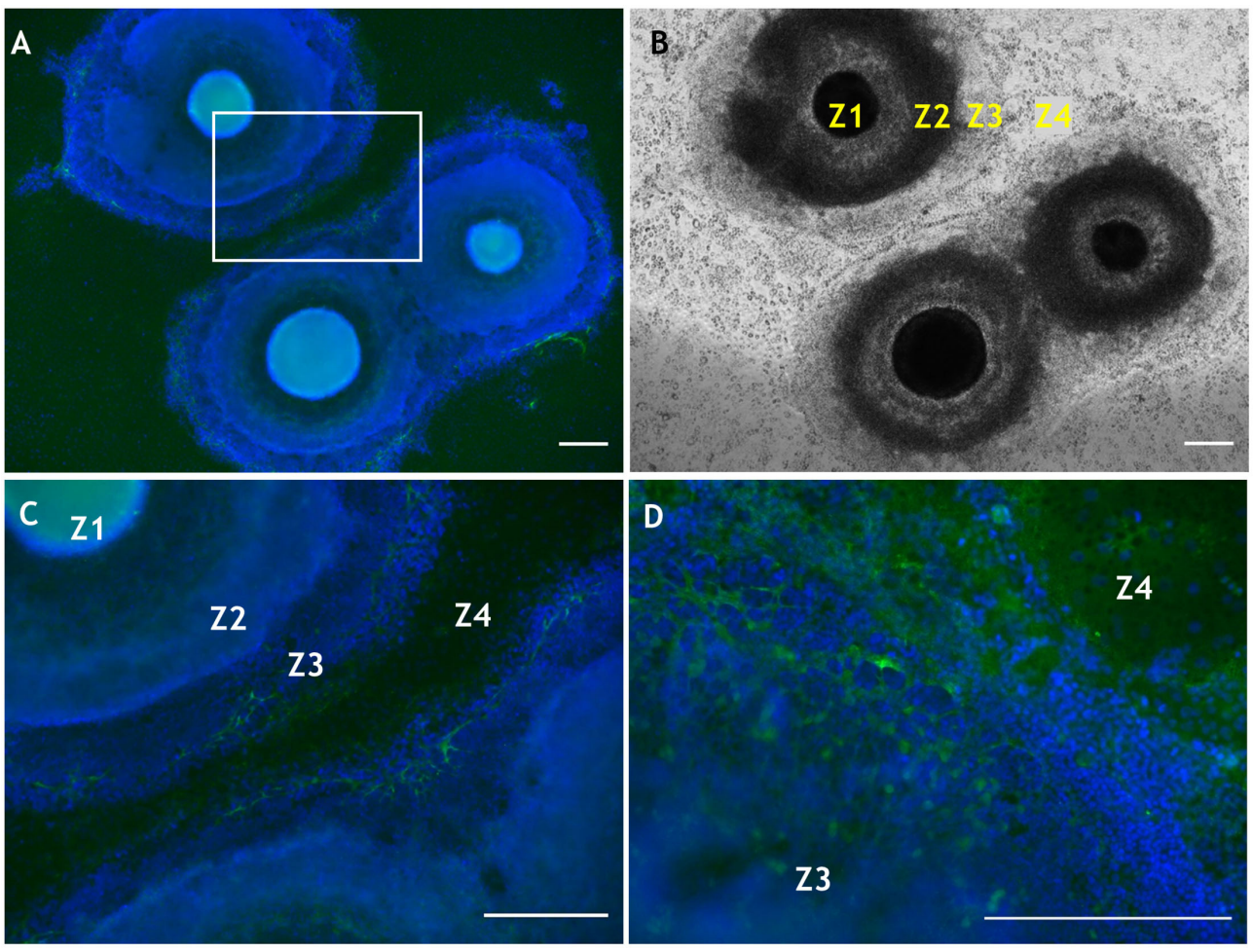

FIGURE 4 | Localization of CS using antibody 7D4 within developing SEAM cultures at weeks 4 and 6 of differentiation. **(A)** Wide-field view of three SEAM colonies at week 4 of differentiation, two of which are beginning to merge (7D4 is shown in green and nuclear Hoechst-334 staining in blue). **(B)** Bright-field image of a SEAM at week 4 of differentiation with each zone (Z) indicated. **(C)** Higher magnification view of CS immunolocalisation in a selected region in **(A)**. **(D)** High magnification of a SEAM at week 6 of differentiation indicating a widespread deposition of CS. Scale bars = 100 μm. Methods and negative control images with primary antibodies omitted are provided as **Supplementary Material**.

human stem cells and their potential involvement in corneal regenerative medicine.

DATA AVAILABILITY STATEMENT

The original contributions presented in the study are included in the article/**Supplementary Materials**, further inquiries can be directed to the corresponding author/s.

AUTHOR CONTRIBUTIONS

AQ, SA, and CH planned the article. SA composed **Figures 1**, **2**. GH and SA obtained the data presented in **Figure 3**. JH, SA, and RH obtained the data presented in **Figure 4**. AQ, JRe, JRa, CH, RH, and KN obtained funding. All authors contributed to the writing of the article.

FUNDING

The research described in this article was funded by BBSRC Responsive Mode Project Grant BB/P017843/1 (to AQ, JRe, and JRa), BBSRC International Partnering Award BB/R021244/1 (to AQ and KN), and Ph.D. studentships for SA and GH from Fight-for-Sight (5069/5070 to AQ and CH) and the BBSRC (South West Biosciences Doctoral Training Partnership, Grant reference BB/M009122/1 to AQ), respectively.

SUPPLEMENTARY MATERIAL

The Supplementary Material for this article can be found online at: https://www.frontiersin.org/articles/10.3389/fcell.2020.567358/full#supplementary-material

REFERENCES

Ahmad, S., Stewart, R., Yung, S., Kolli, S., Armstrong, L., Stojkovic, M., et al. (2007). Differentiation of human embryonic stem cells into corneal epithelial-like cells by *in vitro* replication of the corneal epithelial stem cell niche. *Stem Cells* 25, 1145–1155. doi: 10.1634/stemcells.2006-0516

Bains, K. K., Fukuoka, H., Hammond, G. M., Sotozono, C., and Quantock, A. J. (2019). Recovering vision in corneal epithelial stem cell deficient eyes. *Cont. Lens Anterior Eye* 42, 350–358. doi: 10.1016/j.clae.2019.04.006

Battisti, W. P., Shinar, Y., Schwartz, M., Levitt, P., and Murray, M. (1992). Temporal and spatial patterns of expression of laminin, chondroitin sulphate proteoglycan and HNK-1 immunoreactivity during regeneration in the goldfish optic nerve. *J. Neurocytol.* 21, 557–573. doi: 10.1002/cne.903540211

Borcherding, M. S., Blacik, L. J., Sittig, R. A., Bizzell, J. W., Breen, M., and Weinstein, H. G. (1975). Proteoglycans and collagen fibre organization in human corneoscleral tissue. *Exp. Eye Res.* 21, 59–70. doi: 10.1016/0014-4835(75)90057-3

Brzeszczynska, J., Samuel, K., Greenhough, S., Ramaesh, K., Dhillon, B., Hay, D. C., et al. (2014). Differentiation and molecular profiling of human embryonic stem cell-derived corneal epithelial cells. *Int. J. Mol. Med.* 33, 1597–1606. doi: 10.3892/ijmm.2014.1714

Caterson, B. (2012). Fell-muir lecture: chondroitin sulphate glycosaminoglycans: fun for some and confusion for others. *Int. J. Exp. Pathol.* 93, 1–10. doi: 10.1111/j.1365-2613.2011.00807.x

Caterson, B., Christner, J. E., Baker, J. R., and Couchman, J. R. (1985). Production and characterization of monoclonal antibodies directed against connective tissue proteoglycans. *Fed. Proc.* 44, 386–393.

Chen, S., and Birk, D. E. (2011). Focus on molecules: decorin. *Exp. Eye Res.* 92, 444–445. doi: 10.1016/j.exer.2010.05.008

Chen, S., Mienaltowski, M. J., and Birk, D. E. (2015). Regulation of corneal stroma extracellular matrix assembly. *Exp. Eye Res.* 133, 69–80. doi: 10.1016/j.exer.2014.08.001

Chen, S., Young, M. F., Chakravarti, S., and Birk, D. E. (2014). Interclass small leucine-rich repeat proteoglycan interactions regulate collagen fibrillogenesis and corneal stromal assembly. *Matrix Biol.* 35, 103–111. doi: 10.1016/j.matbio.2014.01.004

Chiquet-Ehrismann, R., Orend, G., Chiquet, M., Tucker, R. P., and Midwood, K. S. (2014). Tenascins in stem cell niches. *Matrix Biol.* 37, 112–123. doi: 10.1016/j.matbio.2014.01.007

Cotsarelis, G., Cheng, S. Z., Dong, G., Sun, T. T., and Lavker, R. M. (1989). Existence of slow-cycling limbal epithelial basal cells that can be preferentially stimulated to proliferate: implications on epithelial stem cells. *Cell* 57, 201–209. doi: 10.1016/0092-8674(89)90958-6

Coulson-Thomas, V. J., Chang, S.-H., Yeh, L.-K., Coulson-Thomas, Y. M., Yamaguchi, Y., Esko, J., et al. (2015). Loss of corneal epithelial heparan sulfate leads to corneal degeneration and impaired wound healing. *Invest. Ophthalmol. Vis. Sci.* 56, 3004–3014. doi: 10.1167/iovs.14-15341

Davanger, M., and Evensen, A. (1971). Role of the pericorneal papillary structure in renewal of corneal epithelium. *Nature* 229, 560–561. doi: 10.1038/229560a0

Di Iorio, E., Barbaro, V., Ruzza, A., Ponzin, D., Pellegrini, G., and De Luca, M. (2005). Isoforms of DeltaNp63 and the migration of ocular limbal cells in human corneal regeneration. *Proc. Natl. Acad. Sci. U.S.A.* 102, 9523–9528. doi: 10.1073/pnas.0503437102

Ding, Z., Dong, J., Liu, J., and Deng, S. X. (2008). Preferential gene expression in the limbus of the vervet monkey. *Mol Vis.* 14, 2031–2041.

Du, Y., Funderburgh, M. L., Mann, M. M., SundarRaj, N., and Funderburgh, J. L. (2005). Multipotent stem cells in human corneal stroma. *Stem Cells* 23, 1266–1275. doi: 10.1634/stemcells.2004-0256

Dua, H. S., and Forrester, J. V. (1990). The corneoscleral limbus in human corneal epithelial wound healing. *Am. J. Ophthalmol.* 110, 646–656. doi: 10.1016/s0002-9394(14)77062-x

Dziasko, M. A., Armer, H. E., Levis, H. J., Shortt, A. J., Tuft, S., and Daniels, J. T. (2014). Localisation of epithelial cells capable of holoclone formation *in vitro* and direct interaction with stromal cells in the native human limbal crypt. *PLoS ONE* 9:e94283. doi: 10.1371/journal.pone.0094283

Dziasko, M. A., and Daniels, J. T. (2016). Anatomical features and cell-cell interactions in the human limbal epithelial stem cell niche. *Ocul. Surf.* 14, 322–330. doi: 10.1016/j.jtos.2016.04.002

Dziasko, M. A., Tuft, S. J., and Daniels, J. T. (2015). Limbal melanocytes support limbal epithelial stem cells in 2D and 3D microenvironments. *Exp. Eye Res.* 138, 70–79. doi: 10.1016/j.exer.2015.06.026

Farrugia, B. L., Lord, M. S., Whitelock, J. M., and Melrose, J. (2018). Harnessing chondroitin sulphate in composite scaffolds to direct progenitor and stem cell function for tissue repair. *Biomater. Sci.* 6, 947–957. doi: 10.1039/C7BM01158J

Funderburgh, J. L., Funderburgh, M. L., and Du, Y. (2016). Stem cells in the limbal stroma. *Ocul. Surf.* 14, 113–120. doi: 10.1016/j.jtos.2015.12.006

Funderburgh, J. L., Mann, M. M., and Funderburgh, M. L. (2003). Keratocyte phenotype mediates proteoglycan structure: a role for fibroblasts in corneal fibrosis. *J. Biol. Chem.* 278, 45629–45637. doi: 10.1074/jbc.M303292200

Gain, P., Jullienne, R., He, Z., Aldossary, M., Acquart, S., Cognasse, F., et al. (2016). Global survey of corneal transplantation and eye banking. *JAMA Ophthalmol.* 134, 167–173. doi: 10.1001/jamaophthalmol.2015.4776

Gao, N., Wang, Z., Huang, B., Ge, J., Lu, R., Zhang, K., et al. (2007). Putative epidermal stem cell convert into corneal epithelium-like cell under corneal tissue *in vitro*. *Sci. China C Life Sci.* 50, 101–110. doi: 10.1007/s11427-007-0006-4

Garcion, E., Faissner, A., and ffrench-Constant, C. (2001). Knockout mice reveal a contribution of the extracellular matrix molecule tenascin-C to neural precursor proliferation and migration. *Development* 128, 2485–2496. Available online at: https://dev.biologists.org/content/128/13/2485

Gates, M. A., Fillmore, H., and Steindler, D. A. (1996). Chondroitin sulfate proteoglycan and tenascin in the wounded adult mouse neostriatum *in vitro*: dopamine neuron attachment and process outgrowth. *J. Neurosci.* 16, 8005–8018. doi: 10.1523/JNEUROSCI.16-24-08005.1996

Grieve, K., Ghoubay, D., Georgeon, C., Thouvenin, O., Bouheraoua, N., Paques, M., et al. (2015). Three-dimensional structure of the mammalian limbal stem cell niche. *Exp. Eye Res.* 140, 75–84. doi: 10.1016/j.exer.2015.08.003

Gu, W. L., Fu, S. L., Wang, Y. X., Li, Y., Lu, H. Z., Xu, X. M., et al. (2009). Chondroitin sulfate proteoglycans regulate the growth, differentiation and migration of multipotent neural precursor cells through the integrin signaling pathway. *BMC Neurosci.* 10:128. doi: 10.1186/1471-2202-10-128

Habuchi, H., Yamagata, T., Iwata, H., and Suzuki, S. (1973). The occurrence of a wide variety of dermatan sulfate-chondroitin sulfate copolymers in fibrous cartilage. *J. Biol. Chem.* 248, 6019–6028.

Hammond, G. M., Young, R. D., Muir, D. D., and Quantock, A. J. (2020). The microanatomy of Bowman's layer in the cornea of the pig: changes in collagen fibril structure at the corneoscleral limbus. *Eur. J. Anat.* 24, 399–406. Available online at: http://www.eurjanat.com/web/paper.php?id=200195gh

Hassell, J. R., and Birk, D. E. (2010). The molecular basis of corneal transparency. *Exp. Eye Res.* 91, 326–335. doi: 10.1016/j.exer.2010.06.021

Hayashi, R., Ishikawa, Y., Ito, M., Kageyama, T., Takashiba, K., Fujioka, T., et al. (2012). Generation of corneal epithelial cells from induced pluripotent stem cells derived from human dermal fibroblast and corneal limbal epithelium. *PLoS ONE* 7:e45435. doi: 10.1371/journal.pone.0045435

Hayashi, R., Ishikawa, Y., Katori, R., Sasamoto, Y., Taniwaki, Y., Takayanagi, H., et al. (2017). Coordinated generation of multiple ocular-like cell lineages and fabrication of functional corneal epithelial cell sheets from human iPS cells. *Nat. Protoc.* 12, 683–696. doi: 10.1038/nprot.2017.007

Hayashi, R., Ishikawa, Y., Sasamoto, Y., Katori, R., Nomura, N., Ichikawa, T., et al. (2016). Co-ordinated ocular development from human iPS cells and recovery of corneal function. *Nature* 531, 376–380. doi: 10.1038/nature17000

Hayashi, S., Osawa, T., and Tohyama, K. (2002). Comparative observations on corneas, with special reference to Bowman's layer and Descemet's membrane in mammals and amphibians. *J. Morphol.* 254, 247–258. doi: 10.1002/jmor.10030

Hayes, A., Sugahara, K., Farrugia, B., Whitelock, J. M., Caterson, B., and Melrose, J. (2018). Biodiversity of CS–proteoglycan sulphation motifs: chemical messenger recognition modules with roles in information transfer, control of cellular behaviour and tissue morphogenesis. *Biochem. J.* 475, 587–620. doi: 10.1042/BCJ20170820

Hayes, A. J., Hughes, C. E., Smith, S. M., Caterson, B., Little, C. B., and Melrose, J. (2016). The CS sulfation motifs 4C3, 7D4, 3B3[–]; and perlecan identify stem cell populations and their niches, activated progenitor cells and transitional areas of tissue development in the fetal human elbow. *Stem Cells Dev.* 25, 836–847. doi: 10.1089/scd.2016.0054

Hayes, A. J., Tudor, D., Nowell, M. A., Caterson, B., and Hughes, C. E. (2008). Chondroitin sulfate sulfation motifs as putative biomarkers for isolation of articular cartilage progenitor cells. *J. Histochem. Cytochem.* 56, 125–138. doi: 10.1369/jhc.7A7320.2007

Hertsenberg, A. J., and Funderburgh, J. L. (2015). Stem cells in the cornea. *Prog. Mol. Biol. Transl. Sci.* 134, 25–41. doi: 10.1016/bs.pmbts.2015.04.002

Higa, K., Kato, N., Yoshida, S., Ogawa, Y., Shimazaki, J., Tsubota, K., et al. (2013). Aquaporin 1-positive stromal niche-like cells directly interact with N-cadherin-positive clusters in the basal limbal epithelium. *Stem Cell Res.* 10, 147–155. doi: 10.1016/j.scr.2012.11.001

Ho, L. T. Y., Harris, A. M., Tanioka, H., Yagi, N., Kinoshita, S., Caterson, B., et al. (2014). A comparison of glycosaminoglycan distributions, keratan sulphate sulphation patterns and collagen fibril architecture from central to peripheral regions of the bovine cornea. *Matrix Biol.* 38, 59–68. doi: 10.1016/j.matbio.2014.06.004

Hunt, G. C., Singh, P., and Schwarzbauer, J. E. (2012). Endogenous production of fibronectin is required for self-renewal of cultured mouse embryonic stem cells. *Exp. Cell Res.* 318, 1820–1831. doi: 10.1016/j.yexcr.2012.06.009

Inoue, S., and Iwasaki, M. (1976). Dermatan sulfate-chondroitin sulfate copolymers from ambilical cord isolation and characterization. *J. Biochem.* 80, 513–524. doi: 10.1093/oxfordjournals.jbchem.a131306

Ito, Y., Hikino, M., Yajima, Y., Mikami, T., Sirko, S., von Holst, A., et al. (2005). Structural characterization of the epitopes of the monoclonal antibodies 473HD, CS-56, and MO-225 specific for chondroitin sulfate D-type using the oligosaccharide library. *Glycobiology* 15, 593–603. doi: 10.1093/glycob/cwi036

Izumikawa, T., Sato, B., and Kitagawa, H. (2014). Chondroitin sulfate is indispensable for pluripotency and differentiation of mouse embryonic stem cells. *Sci. Rep.* 4:3701. doi: 10.1038/srep03701

Kao, W. W., Funderburgh, J. L., Xia, Y., Liu, C. Y., and Conrad, G. W. (2006). Focus on molecules: lumican. *Exp. Eye Res.* 82, 3–4. doi: 10.1016/j.exer.2005.08.012

Karamanos, N. K., Piperigkou, Z., Theocharis, A. D., Watanabe, H., Franchi, M., Baud, S., et al. (2018). Proteoglycan chemical diversity drives multifunctional cell regulation and therapeutics. *Chem. Rev.* 118, 9152–9232. doi: 10.1021/acs.chemrev.8b00354

Karus, M., Ulc, A., Ehrlich, M., Czopka, T., Hennen, E., Fischer, J., et al. (2016). Regulation of oligodendrocyte precursor maintenance by chondroitin sulphate glycosaminoglycans. *Glia* 64, 270–286. doi: 10.1002/glia.22928

Kawakita, T., Shimmura, S., Higa, K., Espana, E. M., He, H., Shimazaki, J., et al. (2009). Greater growth potential of p63-positive epithelial cell clusters maintained in human limbal epithelial sheets. *Invest. Ophthalmol. Vis. Sci.* 50, 4611–4617. doi: 10.1167/iovs.08-2586

Kennedy, S., Lace, R., Carserides, C., Gallagher, A. G., Wellings, D. A., Williams, R. L., et al. (2019). Poly-ε-lysine based hydrogels as synthetic substrates for the expansion of corneal endothelial cells for transplantation. *J. Mater. Sci. Mater. Med.* 30:102. doi: 10.1007/s10856-019-6303-1

Kinoshita, S., Adachi, W., Sotozono, C., Nishida, K., Yokoi, N., Quantock, A. J., et al. (2001). Characteristics of the human ocular surface epithelium. *Prog. Retin. Eye Res.* 20, 639–673. doi: 10.1016/s1350-9462(01)00007-6

Ksander, B. R., Kolovou, P. E., Wilson, B. J., Saab, K. R., Guo, Q., Ma, J., et al. (2014). ABCB5 is a limbal stem cell gene required for corneal development and repair. *Nature* 511, 353–357. doi: 10.1038/nature13426

Le, Q., Chauhan, T., Yung, M., Tseng, C. H., and Deng, S. X. (2020). Outcomes of limbal stem cell transplant: a meta-analysis. *JAMA Ophthalmol.* 138, 660–670. doi: 10.1001/jamaophthalmol.2020.1120

Lewis, P. N., Pinali, C., Young, R. D., Meek, K. M., Quantock, A. J., and Knupp, C. (2010). Structural interactions between collagen and proteoglycans are elucidated by three-dimensional electron tomography of bovine cornea. *Structure* 18, 239–245. doi: 10.1016/j.str.2009.11.013

Li, Z., Duan, H., Li, W., Hu, X., Jia, Y., Zhao, C., et al. (2019). Rapid differentiation of multi-zone ocular cells from human induced pluripotent stem cells and generation of corneal epithelial and endothelial cells. *Stem Cells Dev.* 28, 454–463. doi: 10.1089/scd.2018.0176

Ljubimov, A. V., Saghizadeh, M., Spirin, K. S., Mecham, R. P., Sakai, L. Y., and Kenney, M. C. (1998). Increased expression of fibrillin-1 in human corneas with bullous keratopathy. *Cornea* 17, 309–314.

Manton, K. J., Leong, D. F. M., Cool, S. M., and Nurcombe, V. (2007). Disruption of heparan and chondroitin sulfate signaling enhances mesenchymal stem cell-derived osteogenic differentiation via bone morphogenetic protein signaling pathways'. *Stem Cells* 25, 2845–2854. doi: 10.1634/stemcells.2007-0065

Maseruka, H., Bonshek, R. E., and Tullo, A. B. (1997). Tenascin-C expression in normal, inflamed, and scarred human corneas. *Br. J. Ophthalmol.* 81, 677–682. doi: 10.1136/bjo.81.8.677

Maseruka, H., Ridgway, A., Tullo, A., and Bonshek, R. (2000). Developmental changes in patterns of expression of tenascin-C variants in the human cornea. *Invest. Ophthalmol. Vis. Sci.* 41, 4101–4107. Available online at: https://iovs.arvojournals.org/article.aspx?articleid=2162675

Meek, K. M., and Knupp, C. (2015). Corneal structure and transparency. *Prog. Retin. Eye Res.* 49, 1–16. doi: 10.1016/j.preteyeres.2015.07.001

Mei, H., Gonzalez, S., and Deng, S. X. (2012). Extracellular matrix is an important component of limbal stem cell niche. *J. Funct. Biomater.* 3, 879–894. doi: 10.3390/jfb3040879

Melrose, J., Isaacs, M. D., Smith, S. M., Hughes, C. E., Little, C. B., Caterson, B., et al. (2012). Chondroitin sulphate and heparan sulphate sulphation motifs and their proteoglycans are involved in articular cartilage formation during human foetal knee joint development. *Histochem. Cell Biol.* 138, 461–475. doi: 10.1007/s00418-012-0968-6

Nandini, C. D., and Sugahara, K. (2006). Role of the sulfation pattern of chondroitin sulfate in its biological activities and in the binding of growth factors. *Adv. Pharmacol.* 53, 253–279. doi: 10.1016/S1054-3589(05)53012-6

Notara, M., Schrader, S., and Daniels, J. T. (2011). The porcine limbal epithelial stem cell niche as a new model for the study of transplanted tissue-engineered human limbal epithelial cells. *Tissue Eng. Part A* 17, 741–750. doi: 10.1089/ten.TEA.2010.0343

Oie, Y., and Nishida, K. (2016). Corneal regenerative medicine. *Regen. Ther*. 5, 40–45. doi: 10.1016/j.reth.2016.06.002

Parfitt, G. J., Pinali, C., Akama, T. O., Young, R. D., Nishida, K., Quantock, A. J., et al. (2011). Electron tomography reveals multiple self-association of chondroitin sulphate/dermatan sulphate proteoglycans in Chst5-null mouse corneas. *J. Struct. Biol.* 174, 536–541. doi: 10.1016/j.jsb.2011.03.015

Pellegrini, G., Dellambra, E., Golisano, O., Martinelli, E., Fantozzi, I., Bondanza, S., et al. (2001). P63 identifies keratinocyte stem cells. *Proc. Natl. Acad. Sci. U.S.A.* 98, 3156–3161. doi: 10.1073/pnas.061032098

Pellegrini, G., Traverso, C. E., Franzi, A. T., Zingirian, M., Cancedda, R., and De Luca, M. (1997). Long-term restoration of damaged corneal surfaces with autologous cultivated corneal epithelium. *Lancet* 349, 990–993. doi: 10.1016/S0140-6736(96)11188-0

Persson, A., Vorontsov, E., Larson, G., and Nilsson, J. (2020). Glycosaminoglycan domain mapping of cellular chondroitin/dermatan sulfates. *Sci. Rep*. 10:3506. doi: 10.1038/s41598-020-60526-0

Pinnamaneni, N., and Funderburgh, J. L. (2012). Concise review: stem cells in the corneal stroma. *Stem Cells* 30, 1059–1063. doi: 10.1002/stem.1100

Purushothaman, A., Sugahara, K., and Faissner, A. (2012). Chondroitin sulfate "wobble motifs" modulate maintenance and differentiation of neural stem cells and their progeny. *J. Biol. Chem*. 287, 2935–2942. doi: 10.1074/jbc.R111.298430

Quantock, A. J., Young, R. D., and Akama, T. O. (2010). Structural and biochemical aspects of keratan sulphate in the cornea. *Cell. Mol. Life Sci*. 67, 891–906. doi: 10.1007/s00018-009-0228-7

Romano, A. C., Espana, E. M., Yoo, S. H., Budak, M. T., Wolosin, J. M., and Tseng, S. C. G. (2003). Different cell sizes in human limbal and central corneal basal epithelia measured by confocal microscopy and flow cytometry. *Invest. Ophthalmol. Vis. Sci*. 44, 5125–5129. doi: 10.1167/iovs.03-0628

Sanchez, I., Martin, R., Ussa, F., and Fernandez-Bueno, I. (2011). The parameters of the porcine eyeball. *Graefes Arch. Clin. Exp. Ophthalmol*. 249, 475–482. doi: 10.1007/s00417-011-1617-9

Santos, G. R. C., Piquet, A. A., Glauser, B. F., Tovar, A. M. F., Pereira, M. S., Vilanova, E., et al. (2017). Systematic analysis of pharmaceutical preparations of chondroitin sulfate combined with glucosamine. *Pharmaceuticals* 10:38. doi: 10.3390/ph10020038

Schlötzer-Schrehardt, U., Dietrich, T., Saito, K., Sorokin, L., Sasaki, T., Paulsson, M., et al. (2007). Characterization of extracellular matrix components in the limbal epithelial stem cell compartment. *Exp. Eye Res*. 85, 845–860. doi: 10.1016/j.exer.2007.08.020

Seiffert, M., Beck, S. C., Schermutzki, F., Müller, C. A., Erickson, H. P., and Klein, G. (1998). Mitogenic and adhesive effects of tenascin-C on human hematopoietic cells are mediated by various functional domains. *Matrix Biol*. 17, 47–63. doi: 10.1016/s0945-053x(98)90124-x

Shalom-Feuerstein, R., Serror, L., De La Forest Divonne, S., Petit, I., Aberdam, E., Camargo, L., et al. (2012). Pluripotent stem cell model reveals essential roles for miR-450b-5p and miR-184 in embryonic corneal lineage specification. *Stem Cells* 30, 898–909. doi: 10.1002/stem.1068

Sharifi, R., Yang, Y., Adibnia, Y., Dohlman, C. H., Chodosh, J., and Gonzalez-Andrades, M. (2019). Finding an optimal corneal xenograft using comparative analysis of corneal matrix proteins across species. *Sci. Rep*. 9:1876. doi: 10.1038/s41598-018-38342-4

Shibata, S., Hayashi, R., Kudo, Y., Okubo, T., Imaizumi, T., Katayama, T., et al. (2020). Cell-type-specific adhesiveness and proliferation propensity on laminin isoforms enable purification of iPSC-derived corneal epithelium. *Stem Cell Rep*. 14, 663–676. doi: 10.1016/j.stemcr.2020.02.008

Shibata, S., Hayashi, R., Okubo, T., Kudo, Y., Katayama, T., Ishikawa, Y., et al. (2018). Selective laminin-directed differentiation of human induced pluripotent stem cells into distinct ocular lineages. *Cell Rep*. 25, 1668–1679. doi: 10.1016/j.celrep.2018.10.032

Singh, P., and Schwarzbauer, J. E. (2012). Fibronectin and stem cell differentiation - lessons from chondrogenesis. *J. Cell Sci*. 125, 3703–3712. doi: 10.1242/jcs.095786

Sirko, S., von Holst, A., Weber, A., Wizenmann, A., Theocharidis, U., Götz, M., et al. (2010). Chondroitin sulfates are required for fibroblast growth factor-2-dependent proliferation and maintenance in neural stem cells and for epidermal growth factor-dependent migration of their progeny. *Stem Cells* 28, 775–787. doi: 10.1002/stem.309

Sirko, S., von Holst, A., Wizenmann, A., Götz, M., and Faissner, A. (2007). Chondroitin sulfate glycosaminoglycans control proliferation, radial glia cell differentiation and neurogenesis in neural stem/progenitor cells. *Development* 134, 2727–2738. doi: 10.1242/dev.02871

Sorrell, J. M., Mahmoodian, F., Schafer, I. A., Davis, B., and Caterson, B. (1990). Identification of monoclonal antibodies that recognize novel epitopes in native chondroitin/dermatan sulfate glycosaminoglycan chains: their use in mapping functionally distinct domains of human skin. *J. Histochem. Cytochem*. 38, 393–402. doi: 10.1177/38.3.1689338

Sugahara, K., Mikami, T., Uyama, T., Mizuguchi, S., Nomura, K., and Kitagawa, H. (2003). Recent advances in the structural biology of chondroitin sulfate and dermatan sulfate. *Curr. Opin. Struct. Biol*. 13, 612–620. doi: 10.1016/j.sbi.2003.09.011

Sun, Y., Deng, Y., Xiao, M., Hu, L., Li, Z., and Chen, C. (2017). Chondroitin sulfate proteoglycans inhibit the migration and differentiation of oligodendrocyte precursor cells and its counteractive interaction with laminin. *Int. J. Mol. Med*. 40, 1657–1668. doi: 10.3892/ijmm.2017.3153

Varki, A., Cummings, R. D., Aebi, M., Packer, N. H., Seeberger, P. H., Esko, J. D., et al. (2015). Symbol nomenclature for graphical representations of glycans. *Glycobiology* 25, 1323–1324. doi: 10.1093/glycob/cwv091

Watanabe, K., Nishida, K., Yamato, M., Umemoto, T., Sumide, T., Yamamoto, K., et al. (2004). Human limbal epithelium contains side population cells expressing the ATP-binding cassette transporter ABCG2. *FEBS Lett*. 565, 6–10. doi: 10.1016/j.febslet.2004.03.064

Yamada, K., Young, R. D., Lewis, P. N., Shinomiya, K., Meek, K. M., Kinoshita, S., et al. (2015). Mesenchymal–epithelial cell interactions and proteoglycan matrix composition in the presumptive stem cell niche of the rabbit corneal limbus. Mol. *Vis*. 21, 1328–1339.

Zhang, G., Chen, S., Goldoni, S., Calder, B. W., Simpson, H. C., Owens, R. T., et al. (2009). Genetic evidence for the coordinated regulation of collagen fibrillogenesis in the cornea by decorin and biglycan. *J. Biol. Chem*. 284, 8888–8897. doi: 10.1074/jbc.M806590200

Conflict of Interest: The authors declare that the research was conducted in the absence of any commercial or financial relationships that could be construed as a potential conflict of interest.

Advantages of publishing in Frontiers

OPEN ACCESS
Articles are free to read for greatest visibility and readership

FAST PUBLICATION
Around 90 days from submission to decision

HIGH QUALITY PEER-REVIEW
Rigorous, collaborative, and constructive peer-review

TRANSPARENT PEER-REVIEW
Editors and reviewers acknowledged by name on published articles

Frontiers
Avenue du Tribunal-Fédéral 34
1005 Lausanne | Switzerland

Visit us: www.frontiersin.org
Contact us: frontiersin.org/about/contact

REPRODUCIBILITY OF RESEARCH
Support open data and methods to enhance research reproducibility

DIGITAL PUBLISHING
Articles designed for optimal readership across devices

FOLLOW US
@frontiersin

IMPACT METRICS
Advanced article metrics track visibility across digital media

EXTENSIVE PROMOTION
Marketing and promotion of impactful research

LOOP RESEARCH NETWORK
Our network increases your article's readership